LOW-CRACKING HIGH-PERFORMANCE CONCRETE (LC-HPC) BRIDGE DECKS: SHRINKAGE-REDUCING ADMIXTURES, INTERNAL CURING, AND CRACKING PERFORMANCE

BY

Benjamin Pendergrass

Submitted to the graduate degree program in Civil Engineering
and the Graduate Faculty of the University of Kansas in partial fulfillment
of the requirements for the degree of Doctor of Philosophy.

_____
Chairperson

_____

_____

_____

_____
Committee Members

Date Defended:_____

The Dissertation Committee for Benjamin Pendergrass
certifies that this is the approved version of the following dissertation:

LOW-CRACKING HIGH-PERFORMANCE CONCRETE (LC-HPC) BRIDGE DECKS: SHRINKAGE-REDUCING ADMIXTURES, INTERNAL CURING, AND CRACKING PERFORMANCE

_____
Chairperson

Date approved:_____

ABSTRACT

The development, construction, and evaluation of low-cracking high-performance concrete (LC-HPC) bridge decks is described based on laboratory tests of mixtures containing shrinkage-reducing admixtures and mineral admixtures in conjunction with internal curing and experiences gained during the construction of decks bid in accordance with LC-HPC specifications and control decks constructed in accordance with standard specifications in Kansas.

The laboratory portion of the study involves the 53 concrete mixtures evaluated based on free shrinkage, freeze-thaw durability, scaling resistance, compressive strength, and air-void system stability. The study includes mixtures containing different dosages of two shrinkage-reducing admixtures (SRAs) in combination with surfactant-based and polymer-based air-entraining admixtures (AEAs) and air contents ranging from 3.5 to 9 percent. Mixtures containing different combinations of pre-wetted lightweight aggregate (LWA), Grade 100 slag cement, and silica fume are also evaluated. The majority of shrinkage occurs at early ages. Higher dosages of SRA reduce both early-age and long-term shrinkage, with these reductions in shrinkage concentrated within the first 90 days. Higher SRA dosages contribute to larger air-void spacing factors and greater losses in air content from plastic to hardened concrete, leading to decreased freeze-thaw durability and scaling resistance. The detrimental effects on freeze-thaw durability and scaling resistance caused by SRAs can be mitigated by the use of air contents of 7 percent or more. When used with an SRA, mixtures containing the polymer-based AEA exhibit significantly lower freeze-thaw durability and scaling resistance than mixtures containing the surfactant-based AEA. This lower durability is likely due to the larger air-void spacing factors that are observed in the mixtures containing the polymer-based AEA. The replacement of a portion of total aggregate with an equal volume of

pre-wetted LWA reduces both early-age and long-term shrinkage. Shrinkage is reduced additionally as slag cement is used as a partial replacement (30 percent by volume) for portland cement in conjunction with LWA, and again as silica fume is used a partial replacement (nominally 3 percent by volume) for portland cement in conjunction with LWA and slag cement. The additions of slag and silica fume contribute to reduced shrinkage primarily within the first 30 days of drying. The use of LWA, slag, or silica fume do not significantly affect freeze-thaw durability, scaling resistance, or strength; slag and silica fume, however, were observed to decrease scaling resistance to a degree.

The second portion of the study involves the construction and evaluation of 16 LC-HPC and 11 control bridge decks, the latter constructed in accordance with standard specifications for state bridge construction, in Kansas, as well as another deck bid under but not constructed in accordance with the LC-HPC specifications. Experiences and lessons learned during construction are described, as is the cracking performance of each deck. The results indicate that the degree of compliance with LC-HPC specifications corresponds to the degree of reduction in cracking. The LC-HPC decks exhibit lower early-age cracking and a slower increase in cracking over time than do the other decks, with LC-HPC decks exhibiting approximately one-third of the cracking of the control decks at similar ages. Factors observed to increase cracking include the use of overlays, increased paste content, slump, compressive strength, and air temperature range on the day of construction, increases in concrete temperature relative to air temperature on the day of construction, and decreased air content. Techniques used by individual contractors also influence cracking.

Keywords: air-void system, bridge deck construction, compressive strength, cracking, free shrinkage, freeze-thaw durability, high-performance concrete, internal curing, lightweight aggregate, scaling resistance, shrinkage-reducing admixture, silica fume, slag cement

ACKNOWLEDGEMENTS

I would like to sincerely thank Dr. David Darwin and Dr. JoAnn Browning for their support and guidance during my graduate studies at the University of Kansas. I would also like to thank the other members of my committee, Dr. Adolfo Matamoros, Dr. Caroline Bennett, Dr. Ron Barrett, and Dr. Richard Hale. I am grateful for the support I received during laboratory testing from Jim Weaver, Matt Maksimowicz, Dr. Matt O'Reilly, and Dr. Mark Ewing.

Most importantly, I would like to thank my wife, Callie, and son, Elijah, for their endless support and patience during the past four years of my graduate work. I will be forever grateful to Callie for allowing me to leave my job and enroll as a full-time student, placing the financial burden of our family solely on her shoulders.

Funding for this research was provided by the Kansas Department of Transportation serving as the lead agency for the "Construction of Crack-Free Bridge Decks, Phase II" Transportation Pooled Fund Study, Project No. TPF-5(174). The Federal High Administration (FHWA) of the U.S. Department of Transportation (DOT), Colorado DOT, Idaho Transportation Department, Indiana DOT, Michigan DOT, Minnesota DOT, Mississippi DOT, New Hampshire DOT, New York DOT, North Dakota DOT, Ohio DOT, Oklahoma DOT, Texas DOT, Wisconsin DOT, the University of Kansas Transportation Research Institute, BASF Construction Chemicals, and the Silica Fume Association provided funding to the pooled fund. Representatives from each sponsor served on a Technical Advisory Committee that provided advice and oversight to the project.

Midwest Concrete Materials, Geiger Ready Mix, Ash Grove Cement, Lafarge North America, BASF Construction Chemicals, Miracon Technologies, Buildex, Inc., Holcim, Inc., and Euclid Chemical Company provided concrete materials.

TABLE OF CONTENTS

LIST OF TABLES

LIST OF FIGURES

LIST OF SYMBOLS & ACRONYMS

$\boldsymbol{\alpha}$ = level of significance determined from Student's t-test, indicates the probability that a t-test will identify a statistically significant difference in sample means when, in fact, there is no difference

$\propto_{max}$ = maximum degree of cement hydration (Eq. 1.2)

$\boldsymbol{\beta}$ = coefficient corresponding to each contractor in dummy variables regression analysis (Chapter 6)

γ = free surface energy of water (Eq. 1.1) or coefficient corresponding to each independent factor in dummy variables regression analysis (Chapter 6)

μ = mean of crack densities in a given age range (Eq. 6.1)

$\boldsymbol{\rho}$ = density of water (62.4 lb/ft^3) (Eq. 1.2)

$\boldsymbol{\sigma}$ = standard deviation (Eq. 6.1)

$\boldsymbol{\phi}$ = porosity of lightweight aggregate (Eq. 1.3)

AADT = average annual daily traffic

AAS = alkali activated slag

ACI = American Concrete Institute

AEA = air-entraining agent, air-entraining admixture

ASTM = American Society for Testing and Materials

$\boldsymbol{C}$ = cement content (Eq. 1.2) or 1083.6 m^{-1}, a constant based on specimen shape and Poisson's ratio found in ASTM C125 (Eq. 2.1)

$\boldsymbol{CD_{42-month}}$ = crack density at 42 months (Eq. 6.2)

CH = calcium hydroxide

C-MONO = conventional monolithic

CO = conventional high-density overlay

CRA = crack-reducing admixture

$\boldsymbol{CS}$ = volume change due to autogenous shrinkage of cementitious materials at complete hydration (Eq. 1.2)

C_2S = dicalcium silicate

C-S-H = calcium silicate hydrate

DF = Durability Factor

$\boldsymbol{Dyn.E}$ = dynamic modulus of elasticity (Eq. 2.1)

F-test = probability that an observed correlation between dependent and independent variables in a dummy variables regression analysis occurs by chance (Chapter 6)

GGBFS = ground granulated blast-furnace slag

ITZ = interfacial transition zone

KDOT = Kansas Department of Transportation

KU = University of Kansas

LC-HPC = low-cracking high-performance concrete

LWA = lightweight aggregate

M = mixture containing Micro Air

$\boldsymbol{M}$ = specimen mass (Eq. 2.1) or 300 cycles (Eq. 2.2)

MONO = monolithic

$\boldsymbol{n}$ = fundamental transverse frequency (Eq. 2.1) or number of crack densities in a given age range (Eq. 6.1)

$\boldsymbol{N}$ = number of cycles at which P reached 60 percent or 300 cycles (whichever is less) (Eq. 2.2)

$\boldsymbol{P}$ = percentage of dynamic modulus of elasticity remaining at N cycles (Eq. 2.2)

$\boldsymbol{PC}$ = paste content (Eq. 6.2)

$\boldsymbol{P_{cap}}$ = hydrostatic tension within cement paste capillaries (Eq. 1.1)

PS = prestressed

PSD = Particle Size Determination

$\boldsymbol{r}$ = capillary pore radius (Eq. 1.1)

$\mathbf{R^2}$ = coefficient of determination

RH = relative humidity

$\boldsymbol{S}$ = degree of saturation of aggregate (Eq. 1.3)

SF = silica fume

SFO = silica fume overlay

SRA = shrinkage-reducing admixture

SSA = specific surface area

SSD = saturated surface-dry

T = mixture containing Tough Air

$\boldsymbol{V_{LWA}}$ = volume fraction of LWA necessary to offset autogenous shrinkage (Eq. 1.3)

$\boldsymbol{V_{wat}}$ = volume fraction of water needed in internal curing medium to offset autogenous shrinkage (Eq. 1.2)

$\boldsymbol{w/c}$ = water-cement ratio

$\boldsymbol{w/cm}$ = water-cementitious material ratio

$\boldsymbol{X}$ = individual crack density (Eq. 6.1) or independent factor in dummy variables regression analysis (Eq. 6.2)

XRF = X-Ray Fluorescence

$\boldsymbol{Y}$ = dependent variable in dummy variables regression analysis, crack density at 42 months (Eq. 6.2)

Z = dummy variable assigned to contractor in dummy variables regression analysis (Eq. 6.2)

CHAPTER 1: INTRODUCTION

1.1 GENERAL

Concrete bridge deck deterioration caused by corrosion of reinforcing steel is a serious problem that can considerably reduce structure service life and introduce numerous maintenance problems. Cracking of bridge decks accelerates this deterioration by allowing water and corrosive deicing chemicals to more easily penetrate the deck and reach the reinforcement. Cracks can extend entirely through the deck and also accelerate corrosion of structural members below. As chlorides in the deicing chemicals reach and corrode the reinforcing steel, the expansive corrosion products cause delamination and spalling within the deck. Chlorides can also degrade the epoxy coating that is used on most reinforcing steel to improve corrosion performance (Darwin et al. 2011). These problems have worsened within the past 50 years due to the increased use of deicing salts on bridge decks starting in the 1960s and 1970s from the "bare pavements" policy introduced by many state transportation departments (Transportation Research Board 1979). According to the Transportation Research Board – National Research Council, the usage of deicing salt in the United States ranges from 8 to 12 million tons per year for the purpose of pavement ice removal (Transportation Research Board 1991).

Transportation agencies are aware of the financial and safety issues brought on by deck durability concerns. Deck deterioration in the form of concrete distress and reinforcement corrosion is one of the leading causes of structural deficiency listed in the National Bridge Inventory (Russell 2004). In 1978, it was reported that nearly one-third of all highway bridge decks in the United States were seriously deteriorated due to corrosion of reinforcing steel, and the cost of restoring these decks was estimated at $6.3 billion (Transportation Research Board 1979). In 2005, the average annual direct cost of corrosion for bridges in the United States was estimated at $8.3

billion (Yunovich et al. 2005), with associated costs from traffic delays and lost productivity approximated at 10 times the direct costs (Thompson et al. 2005).

Transportation agencies consider bridge deck cracking a primary cause of these durability problems. The National Cooperative Highway Research Program (NCHRP) sent surveys to all United States transportation departments and several foreign transportation agencies to better understand the scope of bridge deck cracking. Of the 52 respondents, 62 percent considered transverse cracking at early ages to be a problem. The remaining respondents acknowledged the existence of transverse cracking, but did not label it as a durability problem (Krauss and Rogalla 1996).

The principal mechanisms of bridge deck cracking involve shrinkage and thermal stresses developed in the concrete. Many studies have determined concrete material properties to be a main cause of these induced stresses, with construction procedures, environmental conditions, and design details also contributing. Deck deterioration also exists in the form of scaling, spalling, and pop outs due to repeated cycles of freezing and thawing on the deck surface. Tensile stresses and cracks develop as water and deicing chemicals penetrate the concrete and as water expands when frozen.

Since the 1960s, transportation agencies have put much effort into minimizing bridge deck cracking through improvements to material, design, and construction specifications. Concrete mixtures deemed as "high-performance" have been developed in an effort to improve cracking tendency and corrosion, although in most cases "high-performance" leads to high strength, which actually results in increased cracking. A number of additional materials are currently being used to improve both plastic and hardened concrete properties, including lightweight aggregates and other materials to provide internal curing, mineral admixtures, and shrinkage-reducing admixtures (SRA), for improved cracking performance. Many field and laboratory

studies have been completed to determine the mechanisms of concrete cracking. The general conclusion is that cracking will inevitably occur in bridge decks, but certain measures can be taken to diminish its incidence.

Low-cracking high-performance concrete (LC-HPC) specifications have been developed through this study to improve cracking performance and overall durability of bridge decks. Sixteen bridge decks constructed throughout Kansas in accordance with the LC-HPC specifications have exhibited improved cracking performance compared to control decks constructed in accordance with the standard Kansas Department of Transportation (KDOT) specifications. The improved performance results from modifications to mixture proportions and construction procedures. The LC-HPC specifications, however, have yet to include new technologies, such as internal curing and the use of mineral and shrinkage-reducing admixtures.

This report examines the cracking performance of the bridge decks constructed in accordance with the LC-HPC specifications. Relationships are established between cracking performance and material properties, environmental conditions during placement, and construction procedures for LC-HPC decks and associated control decks. In addition, the free shrinkage performance, freeze-thaw durability, and scaling resistance of mixtures that employ new technologies, such as internal curing with lightweight aggregate and the use of mineral and shrinkage-reducing admixtures, are examined through laboratory tests to verify their potential effectiveness for use in future LC-HPC bridge decks.

This chapter focuses on findings from previous studies, summarizes causes and actions that can be taken to minimize shrinkage and cracking and improve overall durability, and presents the objective and scope of the study.

1.2 MECHANISMS OF CRACKING

Concrete bridge decks develop cracks when tensile stresses in the deck exceed the concrete tensile strength. These tensile stresses can be caused by a multitude of

factors, including settlement of plastic concrete, concrete shrinkage, temperature changes, and external loading. The majority of cracking is attributed to shrinkage and thermal strains, but strains alone will not cause cracking in decks. Unrestrained concrete expands when heated, contracts when cooled, and shrinks when dried with no development of stresses. In bridges, however, restraint is provided by the composite action between the girders and deck and stresses develop in the deck concrete due to shrinkage and thermal strains. The largest stresses develop when the difference in strain is greatest between the deck and girders. Restraint is typically higher for steel girders than for precast, prestressed concrete girders because steel does not shrink and concrete and steel have different coefficients of thermal expansion (Krauss and Rogalla 1996). This section summarizes the factors that cause concrete tensile stresses and cracking.

1.2.1 Concrete Shrinkage

Shrinkage is a general term in that a number of different internal and external mechanisms can lead to the shrinkage of concrete. Shrinkage can be categorized into two groups: shrinkage that occurs while the concrete is still plastic and shrinkage that occurs after the concrete has hardened. Each type of shrinkage can lead to significant cracking and must be controlled in a unique way.

1.2.1.1 Plastic Shrinkage

Plastic shrinkage cracking occurs in fresh concrete as the rate of surface water evaporation exceeds the rate at which bleed water reaches the surface. As water is lost from cement paste, negative capillary pressures develop and cause the volume of the paste to shrink. Tensile stresses and cracking develop due to differential shrinkage between the surface and concrete at greater depth. Structures with large surface area to volume ratios, such as bridge decks, are more susceptible to plastic shrinkage cracking due to the greater exposure of bleed water to the environment

(Mora-Ruacho 2009). Plastic cracks are short, can occur in any direction, and are typically wide at the surface but narrow considerably with depth, rarely exceeding a depth of 2 to 3 in. (Krauss and Rogalla 1996). Plastic shrinkage cracking in bridge decks can be controlled if certain precautions are taken to minimize the evaporation of bleed water.

The risk of plastic shrinkage cracking increases with decreases in bleeding rate or increases in evaporation rate. The addition of silica fume or finely-ground cement, both of which increase the surface area of the particles in cement paste, decrease the bleeding rate and increase the potential for plastic shrinkage cracking. An increase in the hydration rate of cement can cause plastic shrinkage cracking by requiring more water during the hydration process in the plastic condition, leaving less available bleed water. Entrained air and a reduction in water content can also decrease bleed water and promote plastic shrinkage cracking. The use of high-range water reducers typically leads to decreases in water content and bleeding capacity. In addition, these high-range water reducers are often used in conjunction with silica fume to compensate for the fineness of the material, which further increases the potential for plastic shrinkage cracking by both reducing the bleeding capacity and the rate at which bleed water can reach the surface (Krauss and Rogalla 1996).

The rate of evaporation in concrete is increased with high air temperature, low relative humidity, high concrete temperature, and high wind velocity and is often determined using the nomograph shown in Figure 1.1. Evaporation rates above 0.2 $lb/ft^2/hr$ (1.0 $kg/m^2/h$) generally require protective actions during placement and curing. Concretes containing pozzolans may require protective actions even at evaporation rates as low as 0.1 $lb/ft^2/hr$ (0.5 $kg/m^2/h$) (Mindess et al. 2003).

Plastic shrinkage can be controlled by reducing the concrete temperature and wind velocity, and maintaining a wet concrete surface during the plastic condition. Concrete temperatures are best controlled by controlling the temperature of each

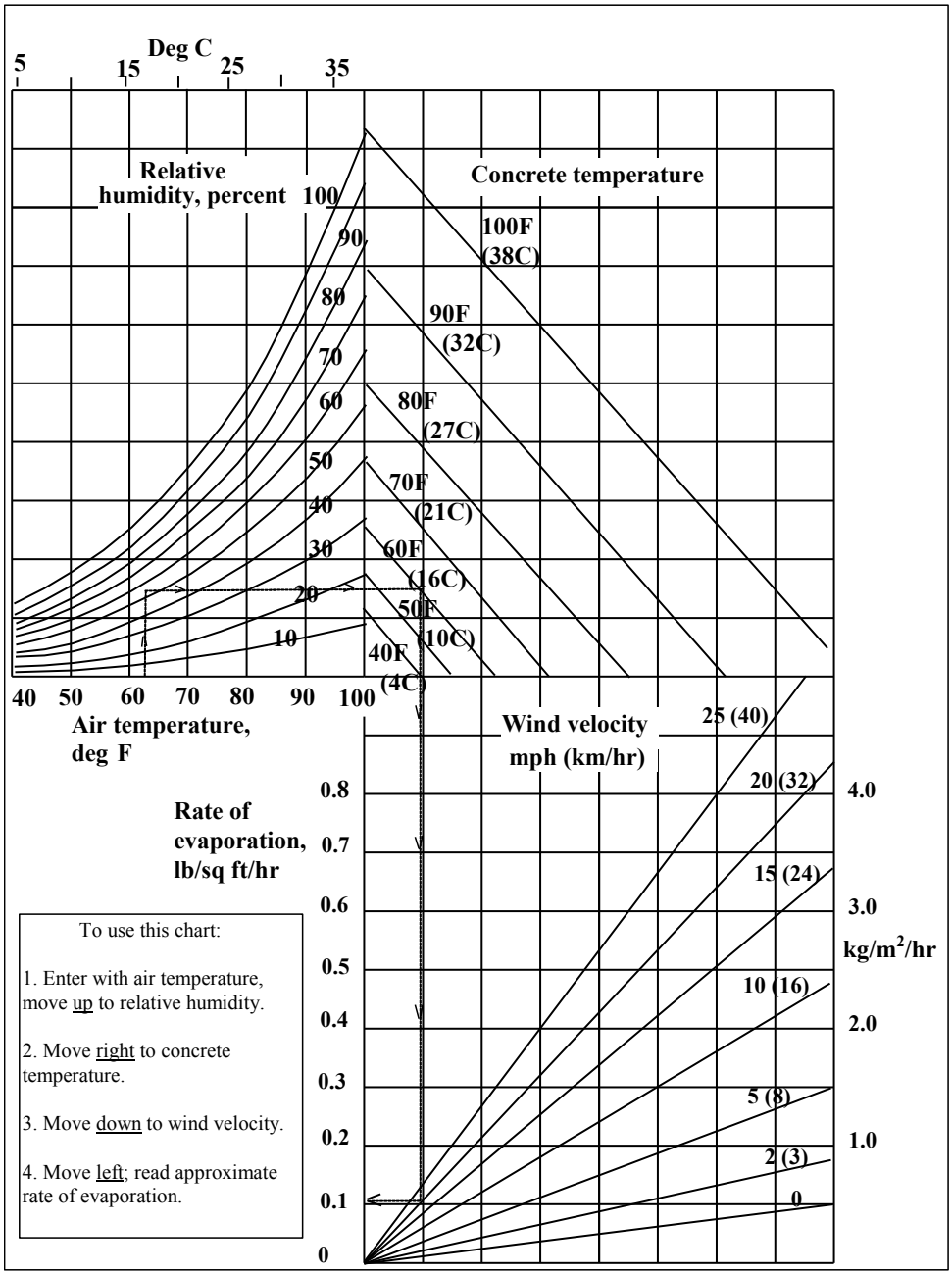

Effect of concrete and air temperatures, relative humidity, and wind velocity on the rate of evaporation of surface moisture from concrete. This chart provides a graphic method of estimating the loss of surface moisture for various weather conditions. To use the chart, follow the four steps outlined above. When the evaporation rate exceeds 0.2 lb/ft^2/hr (1.0 kg/ m^2/hr), measures shall be taken to prevent excessive moisture loss from the surface of unhardened concrete; when the rate is less than 0.2 lb/ft^2/hr (1.0 kg/m^2/hr) such measures may be needed. When excessive moisture loss is not prevented, plastic cracking is likely to occur.

Figure 1.1 Evaporation rate nomograph (ACI Committee 308)

constituent. Due to a high specific heat, water is useful in controlling concrete temperatures. Replacing a portion of the mixture water with ice is effective in lowering concrete temperature since heat is absorbed during the melting process. Wind velocity can be decreased by using windbreaks. Placement of a wet, plastic cover or wet burlap immediately after finishing of the surface and the use of soaker hoses or fog spray for the entire curing period are beneficial in reducing the evaporation rate. Wetting the forms and reinforcing steel before placement minimizes moisture loss from absorption and evaporation (Mindess et al. 2003). Water-reducing admixtures containing hydroxylated carboxylic acid are known to increase the concrete bleeding capacity (Krauss and Rogalla 1996). Plastic shrinkage cracking has also been combated with the use of fiber reinforcement in concrete by supplying some tensile capacity and increasing the cohesiveness of the plastic concrete and minimizing the crack widths (Padron and Zollo 1990).

The evaporation of bleed water occurs in both warm and cool weather environments. Plastic shrinkage cracking due to evaporation in cold weather conditions can be more detrimental since the cooler temperatures will cause the concrete to be in a plastic condition for a longer period. The placement of warm concrete in a cold environment can increase the potential for plastic shrinkage cracking as the warm concrete heats the air directly above the surface, lowering the relative humidity (Krauss and Rogalla 1996).

1.2.1.2 Drying Shrinkage

Drying shrinkage is caused by a volume change produced by the loss of water in hardened concrete and is the most substantial shrinkage mechanism in bridge decks. Drying shrinkage typically occurs over a much longer time period than other types of shrinkage, but the great majority of the shrinkage occurs at an early age. Holt (2001) stated that approximately 80 percent of total drying shrinkage occurs within the first three months. Much of the shrinkage that occurs with early age drying

is irreversible, meaning that any volume increase with rewetting is smaller than the initial shrinkage. Pickett (1956) and Helmuth and Turk (1967) determined that irreversible shrinkage can be as large as 60 percent of the volume change on first drying. Structures and structural members with a large surface-to-volume ratio will experience increased early age drying shrinkage, which is a major concern for bridge decks due to the large surface exposed to a drying environment. Concrete creep, explained at greater length in Section 1.4.1, can lessen the effect of drying shrinkage by minimizing tensile stresses developed in the deck surface. Drying shrinkage cracking typically occurs directly above reinforcing steel due to a weakened plane created by the combination of restraint from the reinforcement and settlement of plastic concrete (see Section 1.2.3), making the steel particularly susceptible to corrosion.

Drying shrinkage in bridge decks can also induce tensile stresses internally without an external restraint due to a nonlinear drying gradient that forms between the exterior and interior of the deck. Drying and shrinkage increase at the concrete surface from exposure to the environment, while the interior concrete maintains a more constant moisture content and volume. The shrinkage of the surface concrete is restrained by the inner concrete, causing tensile stresses and possibly cracking. The tensile stresses develop parallel to the surface, causing cracks to initiate perpendicular to the surface (Bisschop and Van Mier 2000). The use of stay-in-place forms prevents drying from occurring on the bottom deck surface, doubling the drying gradient through the deck depth and increasing stresses and cracking.

Concrete material properties have been established as the major factor contributing to drying shrinkage. Cement paste has the highest shrinkage potential of all concrete constituents, and therefore, is known as the main source of drying shrinkage. Aggregates provide stiffness to the concrete and maintain dimensional stability with loss of moisture. An increase in the aggregate volume fraction of

concrete reduces drying shrinkage. Increased cement fineness increases drying shrinkage by decreasing the pore size of the paste capillaries and increasing capillary stresses. Reynolds et al. (2009) determined that additions of pre-wetted lightweight aggregate in conjunction with ground granulated blast furnace slag (GGBFS) reduced drying shrinkage. Yuan et al. (2011) found that additions of fly ash lead to increased drying shrinkage up to one year for shorter curing periods. Both Reynolds et al. (2009) and Yuan et al. (2011) determined that increased curing periods led to reduced drying shrinkage.

The primary cause of drying shrinkage is evaporation of free water from the cement paste capillaries, although adsorbed water is also lost from hardened calcium silicate (C-S-H) gel and solid surfaces. As water is lost from the cement paste, internal pressures develop from three phenomena: capillary stresses, disjoining pressures, and surface free energy.

Capillary Stress

Capillary stresses develop due to the evaporation of pore water near the concrete surface. The relative humidity (RH) at which pore water evaporates is dependent on the pore radius and surface free energy (surface tension) of the water. When capillary pores lose moisture, the surface tension of the pore water forms a meniscus at the interface between the air and water. The surface tension begins to pull the pore water inward, shrinking the adjacent paste. The amount of hydrostatic pressure that develops within the capillaries is a function of the pore radius and surface free energy, and can be expressed as:

$$P_{cap} = \frac{2\gamma}{r} \tag{1.1}$$

where P_{cap} is the hydrostatic tension, γ is the surface free energy of the water, and r is the capillary pore radius. Large capillaries empty at RH values down to 95 percent and develop low stresses, and shrinkage, due to the large pore radius. Water in

smaller capillaries evaporates as the RH continues to drop, increasing both the hydrostatic stresses and shrinkage. Capillary stresses cannot develop below 45 percent RH because the menisci are no longer stable (Mindess et al. 2003). This shrinkage mechanism only occurs in pores between 2.5 to 50 nm (8×10^{-8} to 2×10^{-6} in.) in diameter. In pores larger than 50 nm (2×10^{-6} in.), the hydrostatic tension is too low to cause significant shrinkage. A meniscus will not form to pull water inward in pores smaller than 2.5 nm (8×10^{-8} in.) (Larrard 1997).

Disjoining Pressure

The relief of disjoining pressure between C-S-H gel particles is another mechanism that contributes to drying shrinkage. Disjoining pressure is caused by the buildup of adsorbed water on the surface of adjacent C-S-H particles. Adjacent C-S-H particles are mutually attracted to one another by van der Waals' forces, bringing the particles in close contact. As the particles come in contact with water, adsorbed water accumulates on the particles and thickens with increasing RH. Disjoining pressures develop as the thickness of the adsorbed water between adjacent particles increases sufficiently and separation occurs between particles as the disjoining pressure increases above van der Waals' attractions.

A reduction in RH leads to evaporation of a portion of the adsorbed water and a decrease in disjoining pressures. The C-S-H particles are once again drawn together as van der Waals' attraction exceeds the disjoining pressures, decreasing the total volume of the concrete. As with capillary stresses, the effect of decreased disjoining pressure on shrinkage is only significant for RH above 45 percent (Mindess et al. 2003).

Free Surface Energy

Free surface energy can be blamed for any drying shrinkage of concrete at RH below 45 percent. The surface free energy of the solid increases considerably as the most strongly adsorbed water is removed from the C-S-H particles. Compression

pressures develop within the gel particles as a function of the surface energy and particle specific surface area, decreasing the solid volume (Mindess et al. 2003).

Autogenous Shrinkage

Autogenous shrinkage is a unique type of drying shrinkage that occurs without the loss of moisture to the environment. It is associated with cement hydration and is often referred to as chemical shrinkage. The process involves self-desiccation that occurs when insufficient water is available in the paste for continued hydration of the cement. Water is then drawn out of capillary pores between the cement particles as hydration progresses, leading to shrinkage (Holt 2001).

Autogenous shrinkage occurs at low water-cement ratios and in dense concrete where external curing water cannot easily penetrate the concrete. Powers and Brownyard (1948) suggested that complete cement hydration (i.e., no autogenous shrinkage) occurs at water-cement ratios above 0.42, but this value can change depending on gel porosity. Concretes containing silica fume may experience autogenous shrinkage at higher water-cement ratios due the decreased concrete permeability. Autogenous shrinkage has more recently become a concern as modern admixtures are used to produce high-strength concretes with very low water-cementitious material ratios. Even at low water-cement ratios, autogenous shrinkage can be limited by the addition of adequate water during curing, for example through the use of pre-wetted lightweight aggregate as a source of internal curing water (Bentur et al. 2001, Cusson and Hoogeveen 2008, Bentz and Snyder 1999, Pyc et al. 2008).

1.2.2 Thermal Cracking

Thermal cracking in bridge decks is caused by stresses from thermally-induced volume changes in the concrete deck. Concrete expands and contracts as internal temperatures increase and decrease. The restraint placed on the concrete from the girders, abutments, and reinforcing steel prohibits the concrete from

expanding and contracting and stresses develop. After deck placement, the concrete temperature quickly rises for a few hours due to the heat of hydration. During this time, the concrete has relatively low stiffness and does not develop significant stresses due to thermally-induced expansion. After reaching a peak temperature, the hydration rate slows and the concrete begins to contract as it cools down to ambient temperature. The concrete has sufficient stiffness by this time to develop tensile stresses that may be high enough to cause cracking, as the contraction is restrained by the girders, abutments, and reinforcement (Babaei and Fouladgar 1997). The higher the initial concrete temperature compared to the girders, the greater the potential for thermal cracking.

Nonlinear temperature changes within concrete may induce stresses without any external restraint. Internal thermal cracking may occur in thick concrete sections due to a significant internal thermal gradient. Although not the case for bridge decks, concrete sections with low surface to volume ratios cannot adequately dissipate the internal heat generated from the hydration reaction. The high internal temperatures cause expansion of the inner concrete at early ages when insufficient stiffness has been gained to induce compressive stresses. As the outer concrete begins to cool and contract, the sufficiently-stiff inner concrete provides restraint and induces tensile stresses on the surface. High-early-strength cements with a high heat of hydration are more susceptible to thermal cracking due to the increased heat evolution that causes greater initial expansion. The use of Type IV cement can reduce thermal expansion by decreasing the amount of heat produced during hydration (Mindess et al. 2003).

Differences in coefficients of thermal expansion between materials (for example, deck and girders) may cause thermal cracking. A constant temperature change can still induce stresses when the deck and girders consist of two materials with different thermal coefficients (for example, concrete and steel) because the

materials are unable to freely expand to different degrees where joined (Krauss and Rogalla 1996).

1.2.3 Settlement Cracking

Settlement, or subsidence, cracking occurs as fresh concrete continues to settle after consolidation. The settlement creates a weakened concrete zone above the reinforcement as fixed objects, such as reinforcing steel, resist the movement of the concrete. Tensile stresses develop directly above the reinforcement as the concrete settles on either side of a bar. Because concrete has little tensile strength in the plastic condition, these stresses often initiate settlement cracks. Even if settlement cracking does not occur in the plastic concrete, the weakened concrete zone due to the settlement can provide a prime location for cracks to form after the concrete has hardened (Babaei and Purvis 1995). Research by Dakhil, Cady, and Carrier (1975) found that increased slump and bar size and decreased top cover resulted in increased settlement cracking – this study is discussed in greater length in Section 1.4.3. Insufficient consolidation also increases the settlement of plastic concrete around reinforcement. Suprenant and Malisch (1999) completed a study similar to that of Dakhil, Cady, and Carrier and determined that the use of polypropylene fibers significantly decreases settlement cracking, presumably by making the concrete more cohesive and by providing tensile strength to the plastic concrete matrix to counteract the restraint provided by the reinforcement.

1.2.4 External Loading

External loads applied to bridge decks, including self weight, dead loads from barriers and medians, and live loads from traffic, cause flexural tensile stresses that can initiate flexural cracking. Girder and deck stiffness and span length are factors contributing to the magnitude of tensile stresses developed in the deck. Krauss and

Rogalla (1996) suggested, however, that stresses caused by external loads are minimal compared to those caused by thermal or shrinkage strains.

1.3 BRIDGE DECK CRACKING ORIENTATION

Cracking in bridge decks is often categorized based on the orientation with respect to the longitudinal axis of the bridge. The orientation of the reinforcing steel with respect to a crack affects the exposure of the steel to the environment. When a crack is perpendicular to the reinforcement, only localized corrosion will likely occur. Research has suggested that corrosion occurs between three and thirteen bar-diameters away from an intersecting crack (Krauss and Rogalla 1996). Deck cracking, however, commonly appears directly above and parallel to reinforcing steel due to the weakened plane developed above the bars caused by settlement, which increases the risk of corrosion of reinforcing steel because a large percentage of the bar area is exposed by the crack. The Portland Cement Association (Durability 1970) divided cracking into six categories: transverse, longitudinal, diagonal, pattern or map, D-cracking, and random cracking. Each type of cracking is caused by different mechanisms and will typically develop at specific locations in a bridge deck.

Transverse cracks are oriented perpendicular to the longitudinal axis of the deck and are the primary type of cracking found in bridge decks. The cracks typically form early in the deck life, directly above the transverse reinforcement, creating a direct path for oxygen, moisture, and deicing chemicals to the steel. These cracks may be full depth (Krauss and Rogalla 1996) and are located 3 to 10 ft (1 to 3 m) apart along the span length (Durability 1970).

Longitudinal cracking develops parallel to the bridge centerline and is typically found in solid and hollow slab-bridges. These cracks usually extend above the longitudinal reinforcing steel in solid slab-bridges and above the void tubes in hollow slab-bridges. A primary cause of longitudinal cracking is the longitudinal reinforcement, which restrains the settlement of the surrounding plastic concrete.

Longitudinal cracks are also commonly found propagating at the end of the bridge decks for decks that are integral with the abutment (Schmitt and Darwin 1995, Miller and Darwin 2000, Lindquist et al. 2005, Pendergrass et al. 2011).

Diagonal cracking is observed near integral abutments, skewed bridge ends, and over single-column piers. This cracking generally does not develop in any pattern and is caused by flexural stresses and drying shrinkage.

Pattern, or map, cracks are found on all types of bridges and are typically much shorter and shallower than other crack types. These cracks typically interconnect and can occur at any location on a deck. Map cracks can be attributed to rapid evaporation of the surface moisture from improper curing at early ages (Durability 1970). Overfinishing of the deck surface can bring excess cement paste to the surface and can also lead to increased map cracking. Map cracking has not been found to cause significant long-term durability problems in bridge decks.

D-cracking consists of cracks parallel to joints and edges of concrete slabs. This cracking is primarily caused by freeze-thaw damage of saturated aggregates and occurs most frequently in slabs on grade, not in bridge decks.

Random cracks are categorized as any cracks that do not fit another category. These cracks can have a variety of orientations and can be attributed to a range of factors.

1.4 FACTORS AFFECTING BRIDGE DECK CRACKING

The large number of variables involved in bridge design and construction has, in the past, made it difficult for researchers to agree upon the primary causes of bridge deck cracking. Bridge deck cracking is affected by a complicated interaction of many factors, some of which are not fully understood, and cannot be pinpointed to a single cause. Concrete shrinkage is generally responsible for many of the factors that promote cracking, but is not the sole cause of cracking. A number of investigations have come to similar conclusions on the factors primarily responsible

for cracking. Generally, the accepted factors are functions of concrete material properties, construction methods, environmental conditions, and structural design. Four studies that focus on the causes and remedies of bridge deck cracking are reviewed in Section 1.5 and the factors concluded to most affect cracking in each study are summarized. This section summarizes the factors affecting deck cracking that are generally accepted among researchers.

1.4.1 Concrete Material Properties

Many studies suggest that concrete material properties have the greatest effect on cracking tendency. Fortunately, these material properties can be controlled by the engineer without much dependency on other characteristics of a bridge design. Since restrained shrinkage is accountable for much of concrete cracking, much of cracking can be tied to the shrinkage potential of each individual concrete constituent. It is accepted among researchers that a primary factor contributing to shrinkage is the cement paste (water and cementitious materials) content. This means that increasing quantities of water, cementitious material, or both can contribute to greater shrinkage. In an evaluation of 32 monolithic bridge deck placements, Schmitt and Darwin (1999) determined that concrete decks with a paste volume greater than 27 percent had significantly greater cracking than decks with paste volumes below this value. Deshpande et al. (2007) examined factors thought to affect concrete shrinkage, including paste content, water-cement ratio, and cement type, and found that paste content was the primary cause of shrinkage. The researchers observed that free shrinkage of concrete specimens at 180 drying days increased by 150 με as the paste content increased from 20 to 30 percent of total concrete volume and an additional 100 με as the paste content increased from 30 to 40 percent. Yuan et al. (2011) conducted restrained ring tests on concrete specimens and monitored time to cracking using compressive strain readings in the restrained rings and visual observation. For mixtures with a water-cement ratio of 0.45, the researchers noted cracking 9 days

earlier based on compressive strain readings and 32 days earlier based on the appearance of cracks as paste contents increased from 24 to 33 percent.

A number of studies have associated high cement contents with high shrinkage and cracking. A reduction in cement content results in a reduced paste content, minimizing the potential for concrete shrinkage and improving cracking performance. A reduction in cement content also improves cracking performance through decreased heat of hydration and thermal stresses (Brown et al. 2001). Increased cement fineness increases the potential for cracking by increasing the heat of hydration and the resulting thermal stresses and capillary stresses that induce drying shrinkage (Chariton and Weiss 2002). Krauss and Rogalla (1996) concluded that cement content is a major factor contributing to early-age cracking in bridge decks. They conducted restrained and free shrinkage tests for mixtures with varying cement contents, water contents, paste contents, and water-cement ratios. While conducting the restrained shrinkage tests, the researchers observed that the mixture with the highest cement content, 846 lb/yd^3 (502 kg/m^3), was the first to crack while the mixture with the lowest cement content, 470 lb/yd^3 (279 kg/m^3), was the last to crack. The researchers observed a minor link between increased paste content and cracking tendency in the restraint tests. The relationship between paste content and free shrinkage was more apparent than that between paste content or free shrinkage and cracking tendency. In a study of the cracking performance of 21 concrete bridge decks, French et al. (1999) observed greater cracking with higher paste and cement contents.

Changes in concrete properties that occur with both increasingly high and low water-cementitious material ratios have conflicting negative effects on concrete durability and cracking. A decrease in water-cementitious material ratio for a given set of concrete constituent materials decreases concrete permeability and increases compressive strength. The decreased permeability improves concrete durability, but

the higher compressive strength reduces concrete creep. Over time, the decreased creep limits the mitigation of tensile stresses in the deck (Krauss and Rogalla 1996). Tia et al. (2005) investigated the effects of water-cementitious material ratio and the addition of mineral admixtures on creep. They observed reduced creep for mixtures with lower water-cementitious material ratios. Reduced creep was also observed for mixtures containing slag compared to mixtures containing fly ash at comparable water-cementitious material ratios.

Lindquist et al. (2008) examined the free shrinkage performance of concrete specimens as a function of paste content and water-cement ratio. Paste content was reduced by decreasing the water content while maintaining a cement content of 535 lb/yd^3 (317 kg/m^3). As the water-cement ratio was reduced from 0.45 to 0.41, the paste content was reduced from 24.4 to 23.1 percent of the total concrete volume. Lindquist et al. observed decreased free shrinkage for concrete with lower paste contents. The effect of water-cement ratio on free shrinkage is difficult to determine from these observations due to the relationship between water-cement ratio and paste content. The researchers, however, also examined the free shrinkage performance of mixtures as a function of water-cement ratio, while maintaining a constant paste content. Lindquist et al. observed no significant difference in shrinkage performance between mixtures with water-cement ratios of 0.36, 0.38, 0.40, and 0.42 after 365 days of drying, demonstrating that paste content, rather than water-cement ratio, is the primary variable affecting shrinkage.

Odman (1968) analyzed the free shrinkage performance of concrete specimens as a function of water-cement ratio and aggregate content and observed increased free shrinkage at higher water-cement ratios and lower aggregate contents. A decrease in aggregate content is directly comparable to an increase in paste content at a given air content. The effect of water-cement ratio on free shrinkage was more pronounced at lower aggregate contents. At a 70 percent aggregate content (70

percent of concrete volume), an increase in water-cement ratio from 0.40 to 0.50 resulted in an increase in shrinkage of approximately 200 με. At a 60 percent aggregate content, a similar increase in water-cement ratio resulted in an increase in shrinkage of approximately 360 με.

Deshpande et al. (2007) and West et al. (2010) examined the free shrinkage performance of non-air-entrained concrete mixtures that had been cured for 3 days and observed increased shrinkage in mixtures with decreased aggregate contents. They also observed that the effect of aggregate content on shrinkage increased with time. For example, the difference in free shrinkage at 180 days of drying between mixtures containing 60 percent and 70 percent aggregate content was 139 με, while the difference at 365 drying days between the same mixtures was 183 με. In contrast to Odman (1968), Deshpande et al. (2007) and West et al. (2010) observed a small decrease in shrinkage with an increase in water-cement ratio for mixtures with the same aggregate content. Hansen and Almudaiheem (1987) examined the free shrinkage performance of concrete as a function of aggregate content and, similarly to Odman (1968), Deshpande et al. (2007), and West et al. (2010), found an increase in aggregate content in this case from 65 to 70 percent, resulted in a decrease (18 percent) in drying shrinkage. French et al. (1999) observed that maximizing the aggregate volume reduces cracking.

Research by the Portland Cement Association (1970) determined that use of a larger maximum-size and low-shrinkage aggregate reduced shrinkage and cracking. Imamoto and Arai (2008) found that an increased aggregate specific surface area (SSA) for concretes with the same cement content and water-cement ratio resulted in increased shrinkage. Krauss and Rogalla (1996) observed that the use of aggregates with a high modulus of elasticity, low shrinkage, and low coefficient of thermal expansion resulted in lower shrinkage. Russell et al. (2003) suggested one negative effect of using an aggregate with a high modulus of elasticity is that it can provide

added restraint and internal stress concentrations that can lead to internal microcracking. The development of surface macrocracks, however, have a considerably greater impact on the corrosion of reinforcing steel than do internal microcracks, and the benefits of using an aggregate with a high modulus of elasticity seem to outweigh any associated negative effects when overall shrinkage is restrained, as it is for bridge decks.

Slump is a plastic concrete property that is affected by the proportions of the concrete constituents and can influence cracking tendency. Increased cracking is observed directly above reinforcing steel for concretes with increased slump due to settlement cracking (see Section 1.2.3). Darwin et al. (2004) and Lindquist et al. (2005) examined 31 bridge decks and observed an increase in crack density of 0.11 m/m^2 as the average slump increased from 1.5 to 3 in. (40 to 75 mm). Similarly, McLeod et al. (2009) and Yuan et al. (2011) observed decreased overall cracking for concretes with lower slumps in bridge decks that were constructed in accordance with the low-cracking high-performance concrete (LC-HPC) specifications in Kansas compared to decks constructed following the standard Kansas Department of Transportation specifications.

1.4.2 Construction Methods and Environmental Conditions

It is generally accepted that construction procedures and environmental conditions during and after construction affect bridge deck cracking. Krauss and Rogalla (1996) compiled and ranked a list of construction-related factors that contribute to cracking, which include weather, time of casting, curing period and method, finishing procedures, vibration of fresh concrete, and pour length and sequence. They concluded that weather, time of casting, curing, and finishing are the factors with the greatest contribution to cracking. A study by the California Department of Transportation concluded that adverse weather conditions during placement, such as strong winds, high ambient temperatures, and low humidity, had a

greater effect on cracking performance than any construction factor examined (Poppe 1981).

1.4.2.1 Weather and Time of Casting

Weather conditions during and immediately after placement affect the cracking performance of bridge decks. Environmental conditions have a considerable effect on the development of drying and thermal shrinkage stresses within a deck. Drying and shrinkage at the deck surface increase with an increased evaporation rate, which is a function of ambient and concrete temperature, relative humidity, and wind speed. Bridge deck cracking performance is affected by both the concrete temperature and the relative temperature difference between the deck and girders. Thermal stresses develop within the deck as ambient temperatures contribute to large temperature differences within the deck and between the deck and girders. Krauss and Rogalla (1996) observed that deck placement during early evening or night helped reduce cracking. Concrete placed in cold weather exhibits a decreased rate of hydration and strength development and precautions should be considered to maintain concrete temperatures during curing. When warm concrete is placed in a cold environment, the air is heated directly above the concrete surface, lowering the relative humidity. This reduction in relative humidity can cause increased evaporation and plastic shrinkage cracking (Krauss and Rogalla 1996).

French et al. (1999) examined the cracking performance of 10 prestressed and 8 steel girder bridges as a function of high and low temperature on the day of placement. Incomplete construction records prevented correlations from being made between differences between ambient and concrete temperatures and cracking performance. The researchers determined that decks with the lowest cracking tendency were cast on days in which the air temperature was between a high of 65° to 70° F (18° to 21° C) and a low of 45° to 50° F (7° to 10° C). Three of the four lowest-performing prestressed girder decks had low air temperatures during deck

placement at or below 35° F (2° C) and the other low-performing prestressed girder deck experienced considerably high air temperatures, approximately 90° F (32° C), during placement. A wide temperature range on the placement date also contributed to increased cracking. A slight trend of increased cracking was observed for both prestressed and steel girder bridges as high temperatures decreased on the placement date.

In contrast to French et al., Lindquist et al. (2005) observed decreased cracking in conventional overlay decks as high temperatures decreased on the placement date. The conflicting observations may be a result of neither analysis considering the effect of ambient and concrete temperature differences during placement. Both Lindquist et al. and French et al. observed that increased air temperature range on the placement date did increase the cracking tendency. Yuan et al. (2011) examined the relationship between cracking performance and ambient temperature on the casting date for 40 monolithic bridge decks in Kansas using a dummy variables analysis (Draper and Smith 1981). In the analysis, the researchers observed a trend similar to that observed by Lindquist et al. (2005) finding increased cracking with an increase in maximum air temperature on the placement date. Similar to trends observed by French et al. (1999) and Lindquist et al. (2005), Yuan et al. (2011) also observed increased cracking with an increase in temperature range on the placement date.

As discussed in Section 1.2.2, the thermal interaction between the concrete deck and the girders can induce thermal stresses and cracking due to the restraint provided by the girders. Placement of higher-temperature concrete on lower-temperature girders can lead to increased cracking due to the thermal stresses developed by the large initial temperature difference between the concrete and the girders as the temperatures of the concrete and girders return to ambient conditions over time. The concrete temperatures can increase above that of the girders due to the

heat generated by hydration at early ages, resulting in greater expansion of the deck compared to the girders. As the heat of hydration decreases, the concrete cools and contracts just as sufficient strength has been gained to develop tensile stresses.

Subramaniam and Agrawal (2009) monitored the temperatures and strains of the concrete decks and steel girders of newly-constructed bridges to examine the development of early-age tensile stresses in the decks and observed a rapid increase in concrete temperature within the first 48 hours, followed by a cooling period to ambient temperature. After 48 hours, the measured temperatures of the steel girders and concrete deck remained near the ambient temperature. Temperature-controlled concrete placed in cold environments can experience the problems associated with temperature differences between the deck and girders if precautions are not taken. As the low ambient temperature eventually increases, the girders expand more than the concrete and tensile stresses develop. Studies have recommended heating of the air below the deck to increase girder temperatures in cold weather (Durability 1970, Babaei and Fouladgar 1997).

Babaei and Purvis (1996) conducted a field analysis of eight bridge decks under construction. Ambient and concrete temperatures were recorded throughout the curing process and concrete samples were taken to determine thermal and drying shrinkage. Thermal shrinkage was estimated using the maximum temperature difference between the concrete and ambient air for a period up to 8.5 hours after casting. The ambient air temperature was assumed to be equivalent to the steel girder temperature for this timeframe. The researchers recommended that to maintain a transverse crack spacing greater than 30 ft (9 m), the 4-month drying shrinkage should be less than 700 με and the thermal contraction should be limited to 150 με by keeping the temperature difference between the concrete deck and steel girders to within 22° F (12° C).

The construction specifications for low-cracking high-performance concrete (LC-HPC) bridge decks in Kansas require decks be cast within a concrete temperature range of 55 to 70° F (13 to 21° C) with a 5° F (3° C) adjustment outside of the range if approved by the Engineer. The specifications prohibit placing concrete if there is a probability of the air temperature dropping more than 25° F (14° C) below the concrete temperature during the first 24 hours after placement unless insulation is provided for the deck and girders (Kansas Department of Transportation 2007c). This requirement reduces the influence of thermal stresses that results from a large temperature difference between the deck and girders.

1.4.2.2 Curing

The immediate implementation of curing techniques after finishing is important for preventing plastic and early-age drying shrinkage cracking. Proper curing is critical on bridge decks due to the large surface area exposed to the environment. The construction specifications for low-cracking high-performance concrete (LC-HPC) bridge decks in Kansas require that wet burlap be placed within 10 minutes of strikeoff and a second burlap layer be placed within an additional five minutes (Lindquist et al. 2008, McLeod et al. 2009, Yuan et al. 2011, Pendergrass et al. 2011).

Research by Holt (2001) illustrated the importance of proper curing on early-age concrete shrinkage. Figure 1.2 displays the effect of curing method on shrinkage to an age of 70 days. Specimens were placed in three environments during the first 24 hours after casting, including exposure to 4.5 mph (2 m/s) wind, 40 percent relative humidity, and 100 percent relative humidity conditions. As shown in the figure, early-age shrinkage was found to increase significantly for concrete exposed to 4.5 mph (2 m/s) wind during curing. Concrete cured in a 40 percent relative humidity environment exhibited lower shrinkage, and wet-cured concrete subjected to

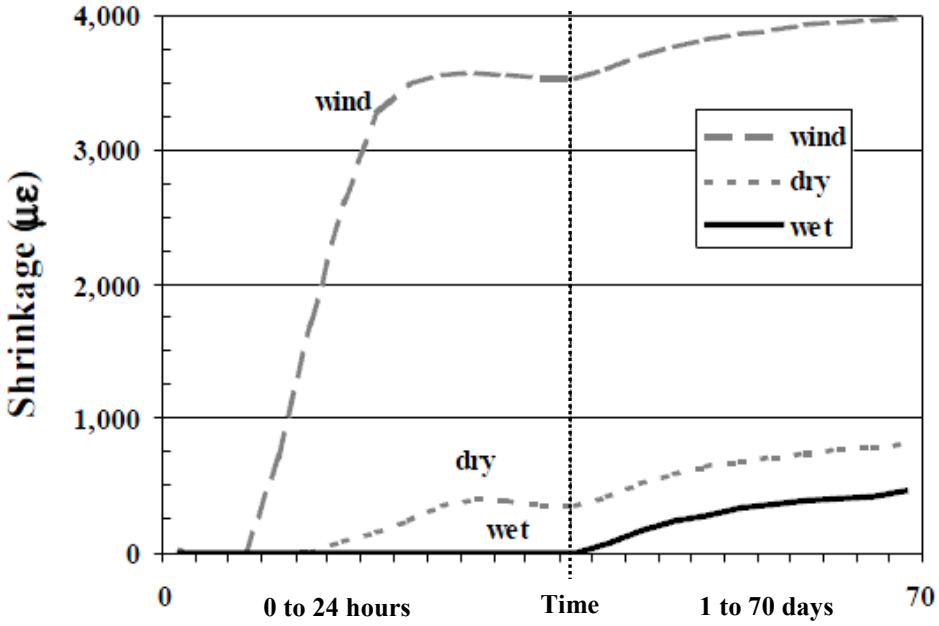

Figure 1.2 Effect of curing environments on shrinkage (Holt 2001)

100 percent relative humidity exhibited the lowest shrinkage of all. The wet-cured concrete did not experience any shrinkage during curing.

Therrien et al. (2000) measured the ultimate moisture loss of concrete specimens as a function of curing time and relative humidity (Figure 1.3). The researchers determined that at 53 percent relative humidity, moisture loss increased as curing time decreased. They concluded this relationship was due to increased moisture loss from the larger paste capillary pores in the specimens cured for the shorter periods. The researchers believed that the longer curing allows concrete to develop smaller pores as a result of ongoing hydration that can be emptied only at a lower relative humidity (< 53 percent). They concluded that concrete exhibits decreased moisture loss when cured longer due to a greater amount of internal water being consumed by the increased cement hydration. As shown in Figure 1.3, at the high relative humidity (97 percent), similar moisture losses were observed for all concretes, regardless of the length of curing. They concluded that this was due to the

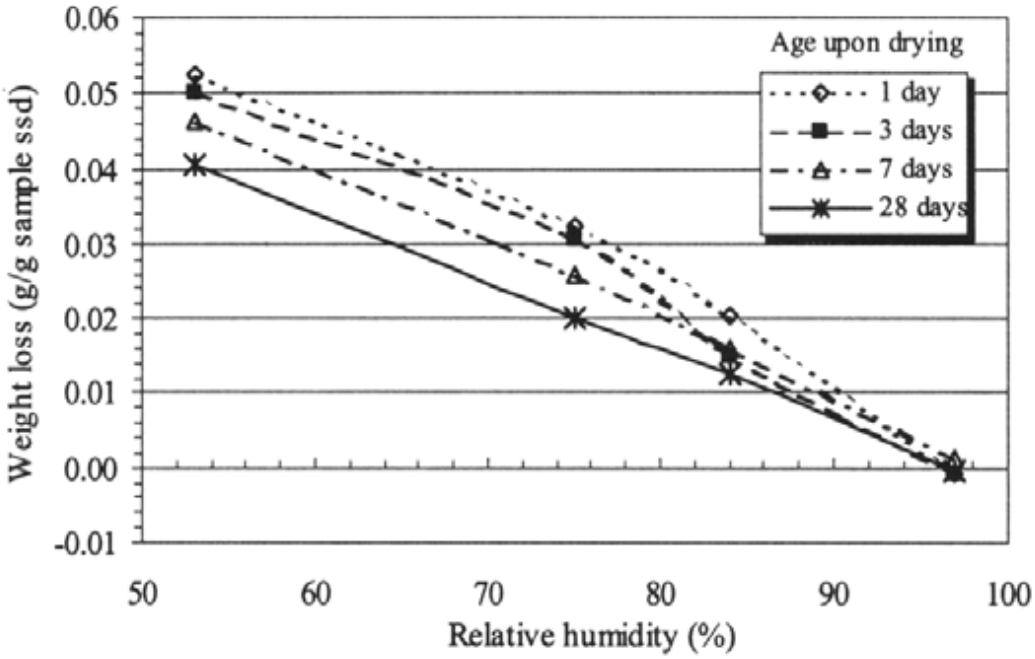

Figure 1.3 Moisture loss versus curing time and relative humidity (Therrien et al. 2000)

relative humidity being too high to empty either large or small pores. The behavior of the specimens stored at the lowest relative humidity in the test is of particular importance since this humidity is more indicative of typical bridge deck environments.

Nassif and Suksawang (2002) examined the effect of curing procedure on concrete shrinkage. The researchers subjected specimens to six different curing procedures, including moist curing at 95 percent relative humidity, dry curing, application of a curing compound, and curing under a wet burlap cover for 3, 7, and 14 days. The concrete that was moist cured at 95 percent relative humidity experienced the least shrinkage, while the dry-cured, curing compound, and 3-day wet-burlap-cover concrete experienced the greatest shrinkage at 28 days of drying. Increasing burlap cover time was observed to reduce shrinkage.

Yuan et al. (2011) analyzed the free shrinkage performance of 100 percent cement and cement and fly ash combination mixtures at constant paste contents. They observed decreased free shrinkage for the mixtures with both cement and fly ash when subjected to increasing curing periods of 7, 14, 28, and 56 days. The researchers also noted that mixtures containing fly ash exhibited more pronounced free-shrinkage benefits with increased curing periods than the 100 percent cement mixtures. A mixture containing a 40 percent replacement by volume of cement with fly ash experienced 33 με greater shrinkage after 30 days of drying than a corresponding mixture with 100 percent cement when cured for 7 days, while the same fly ash mixture experienced equal shrinkage to the cement mixture after 30 days of drying when cured for 14 days. When cured for 28 and 56 days, the mixture containing 40 percent fly ash exhibited 21 and 56 με less shrinkage, respectively, than the corresponding mixture with 100 percent cement after 30 days of drying. Tia et al. (2005) analyzed the free shrinkage of mixtures containing replacements of cement with fly ash and slag cement. They observed decreased shrinkage as the curing period was increased from 7 to 14 days for mixtures containing a 20 percent replacement by weight of cement with fly ash. No reduction in shrinkage was observed as the curing period was increased from 7 to 14 days for mixtures containing 50 to 70 percent weight replacements of cement with slag cement.

Lindquist et al. (2008) observed decreased shrinkage with an increase in curing period from 7 to 14 days in mixtures with a given water-cement ratio and paste content. They also observed that increasing the curing period from 7 to 21 days had a more pronounced effect on reducing shrinkage than decreasing the paste content from 23.3 to 21.6 percent. Reynolds et al. (2009) analyzed the shrinkage performance of mixtures containing 9 to 14 percent volume replacements of normalweight aggregate with pre-wetted, intermediate-sized lightweight aggregate and 30 to 60 percent

volume fraction replacements of cement with slag cement. They observed a reduction in free shrinkage as the curing period was increased from 7 to 14 days.

1.4.2.3 Finishing

Concrete finishing procedures also affect bridge deck cracking. Overfinishing and overwetting of the deck surface promote increased spalling (Larson et al. 1967) and scaling (Klieger 1955). Overfinishing of the surface pushes coarse aggregate lower into the deck and brings excess cement paste to the surface, contributing to durability problems. Lindquist et al. (2005) noted that roller screeds, which are commonly used in contemporary construction, bring more paste to the surface than vibrating screeds, which were typically used in the 1980s. Concrete that is finished at a slower rate is exposed to the environment for a longer period of time and is at risk of plastic shrinkage cracking due to delays in the initiation of curing.

1.4.3 Structural Design

Details of structural design can have an effect on cracking tendency, although this study focuses on the influences of material properties and construction techniques on cracking. Krauss and Rogalla (1996) determined that degree of restraint had the greatest design-related effect on cracking. As discussed in Section 1.2, increased stresses develop when the degree of restraint is greatest between the deck and girders. A fully-restrained deck does not allow any concrete shrinkage or expansion without the development of stresses, while a partially-restrained deck allows a portion of concrete strain to occur before stresses develop. The elimination of the composite action between the deck and girders would reduce the restraint provided to the deck, although isolating the deck from the girders is not normally economically practical and an amount of restraint will always exist from the friction between the deck and girders (Krauss and Rogalla 1996).

A number of reports suggest that continuous spans exhibit increased cracking compared to simply-supported spans (Krauss and Rogalla 1996, Ramey et al. 1996, and Ramey and Wright 1994). Some studies suggest that much of the cracking in continuous spans occurs directly above the piers in the negative moment region of the deck (Ramey et al. 1996, Ramey and Wright 1994) since this is the location in which the top deck surface is placed in tension. Other studies have found no increased incidence of cracking in negative moment regions (Lindquist et al. 2005, Pendergrass et al. 2011, Yuan et al. 2011). Studies by the Portland Cement Association (Durability 1970), Ramey et al. (1996), and Ramey and Wright (1994) reported increased cracking with use of steel girders compared to concrete girders. This increased cracking is likely due to the greater flexibility, longer possible spans, difference in coefficients of thermal expansion, and lack of creep (to relieve induced tensile stress) in steel girders.

Babaei and Purvis (1994a) determined that the use of larger reinforcement bars increased the probability of a weakened plane forming above the bars, increasing the risk of cracking. Babaei and Hawkins (1987) recommended the use of smaller-diameter reinforcement to reduce cracking. Schmitt and Darwin (1995) similarly observed increased cracking with the use of No. 6 (19 mm) top reinforcing bars compared to No. 5 (16 mm) or a combination of No. 4 and No. 5 (13 and 16 mm) bars.

Dakhil, Cady, and Carrier (1975) determined that decreased depth of cover and increased bar size increased cracking directly above the reinforcement (Figure 1.4). Decreased cover compounds any corrosion problems since cracking tendency is increased and the corrosive agents have a shorter distance of travel to reach the reinforcement (Lindquist et al. 2006). This increased cracking is thought to occur with decreased cover because less concrete is available to counteract the weakened

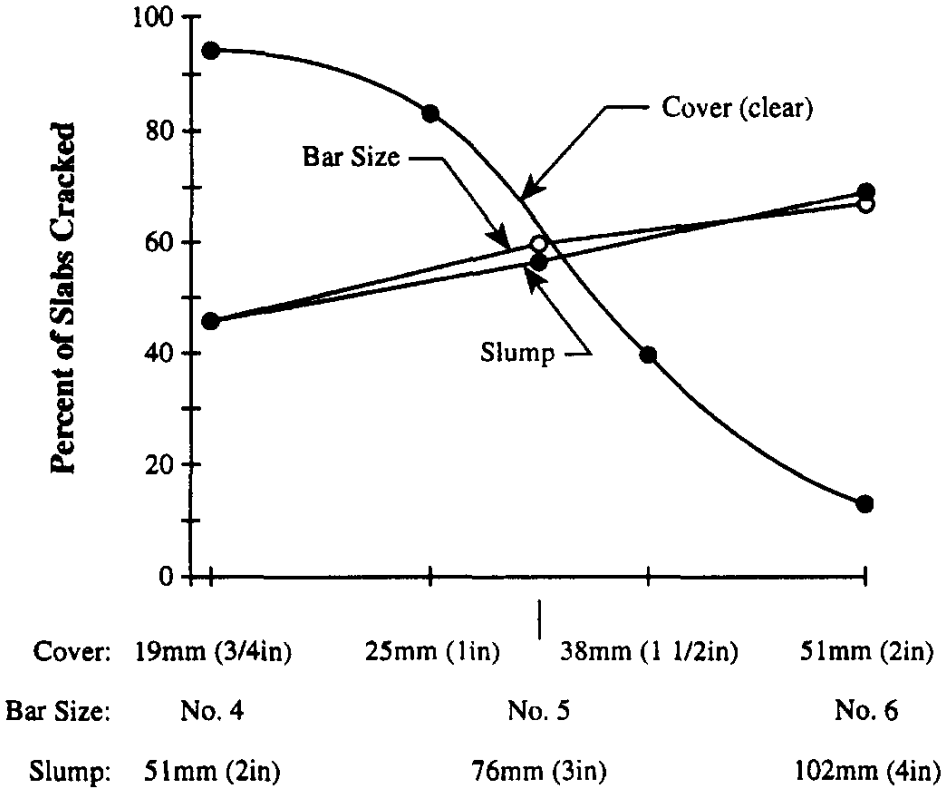

Figure 1.4 Settlement cracking as a function of bar size, cover, and slump (Dakhil et al. 1975)

plane developed above the reinforcement from subsidence of fresh concrete (Durability 1965).

Perragaux and Brewster (1992) and Meyers (1982) reported trends that conflict with the observations of Dakhil et al. (1975) by observing greater cracking with concrete covers above 3 in. (75 mm), although Dakhil et al. (1975) did not test covers above 2 in. (51 mm). An outside consultant (Wilbur Smith Associates) recommended that the Pennsylvania Department of Transportation place the top transverse reinforcement below the top longitudinal reinforcement to reduce transverse cracking (Babaei and Purvis 1994b). The reversal of transverse and longitudinal reinforcement was also recommended by the American Concrete Institute (ACI) (ACI Committee 345).

Krauss and Rogalla (1996) observed that larger girders at closer spacing provide greater restraint and cause increased shrinkage and thermal stresses in the deck. They determined that any increase in cracking observed from larger span lengths is likely due to the larger girder size that must be used. Schmitt and Darwin (1995), Miller and Darwin (2000), and Lindquist et al. (2005) found no significant connection between span length and cracking. Horn et al. (1972) observed that increasing the deck thickness from 6.4 in. (162 mm) to 8.6 in. (218 mm) reduced cracking.

1.5 LITERATURE REVIEW

This section reviews four studies focused on the primary causes of and means to prevent cracking on bridge decks. Three of the studies were completed at the University of Kansas and provide background information that serves as the basis of this report. The fourth study, by Krauss and Rogalla (1996), provides analytical, field, and laboratory examinations of cracking mechanisms and has notably contributed to advances in the subject of bridge deck cracking.

Schmitt and Darwin (1995)

Schmitt and Darwin (1995) completed a study of continuous steel girder bridges throughout northeastern Kansas in an effort to determine the primary causes of bridge deck cracking. A total of 40 steel girder bridges were analyzed in the study, consisting of 37 composite and 3 non-composite decks. Of the 37 composite decks, 15 decks were monolithic, 20 decks had a high-density (conventional) concrete overlay, and 2 decks had a silica fume overlay. The bridges represented a wide range of ages, traffic loads, and levels of deterioration, so a greater variation in cracking existed to better establish relationships between cracking performance and each considered variable. Design and construction data for each bridge was collected from project files, construction field books, as-built plans, and weather data logs. From this data, 31 variables were then compared to the cracking observed on each deck to

determine correlations with cracking. Due to the wide range of deck types analyzed, comparisons were made primarily between decks of similar type. The thirty-one variables considered in the study were divided into four categories: material properties, site conditions, construction procedures, and design specifications.

Field surveys were conducted to determine the degree of cracking on each deck. All cracks were located and marked by surveyors and then transposed to a scaled diagram of the deck, producing a crack map. The crack maps were scanned and crack densities in linear meter of crack per square meters of deck were calculated with use of computer programs. Crack densities were calculated for each entire deck, separate spans, separate placements, and the first and last 3 m (10 ft) of each deck.

Schmitt and Darwin (1995) came to several conclusions dealing with crack performance. The mean crack densities for monolithic and overlay decks (both conventional and silica fume) were found to be nearly identical, suggesting that deck type has little effect on cracking performance. The overlay decks, however, were generally younger than the monolithic decks; a factor that affected this comparison (see discussion of work by Lindquist, Darwin, and Browning 2005). Bridge type was also determined to have little influence on cracking, but increased bridge length was found to increase cracking for both deck types. Bridges with fixed-end (integral) abutments had approximately 2 to 3 times greater cracking within 10 ft (3 m) of the abutments than bridges with pinned-end girders. An increase in cracks extending from the abutments in the longitudinal direction occurred as the length of deck increased along the fixed-end abutments. A slight increase in cracking was evident with increases in average annual daily traffic (AADT). It was also determined that bridges built prior to 1988 exhibited less cracking than newer bridges of both deck types.

Several factors were observed to influence cracking on monolithic decks. The examination of material properties revealed that cracking increased with increasing

slump, percent volume of water and cement (cement paste), water content, cement content, and compressive strength. Cracking also appeared to increase with increasing water-cement ratios, but it was difficult to arrive at a definitive conclusion since three similar water-cement ratios were all that were used in the decks (0.40, 0.42, and 0.44). Cracking in monolithic decks increased with decreasing air contents, with a significant increase in cracking on decks with air contents below 6.0 percent. The environmental site conditions found to increase cracking included increased maximum daily air temperature and daily air temperature range on the casting date.

A number of conclusions were also established for cracking performance of decks with overlays. Overlays placed with zero-slump concrete consistently exhibited high crack densities. Overlays containing silica fume, a water reducer, and an air entraining agent (AEA) had more cracking than overlays containing only an AEA. As with monolithic decks, overlay decks had increased cracking with increases in high air temperature and daily temperature range on the day of casting. Overlay decks also exhibited increased cracking with an increase in average air temperature on the day of casting. Cracking was found to increase with increases in placement length and, to some extent, bridge skew. Increases in cracking occurred with increased transverse reinforcing bar size, illustrated by greater cracking with the use of No. 6 (19 mm) top reinforcing bars compared to No. 5 (16 mm) or a combination of No. 4 and No. 5 (13 and 16 mm) bars. Cracking was found to be more severe as the transverse reinforcing bar spacing increased above 6.0 in. (150 mm).

Schmitt and Darwin (1995) made three principal recommendations based on their findings to reduce bridge deck cracking. First, the volume of water and cement (cement paste) should not exceed 27.0 percent of the total concrete volume for monolithic deck placements or for the subdeck (lower layer) of overlay deck placements. Second, the minimum air content of concrete used in monolithic bridge decks should be 6.0 percent. Lastly, concrete should not be placed with a zero slump

in bridge deck overlays. Schmitt and Darwin (1995) recommended that several other general practices be considered for design and construction of concrete bridge decks. First, designers should be aware that the use of fixed-end girders, as opposed to pinned-end girders, will significantly increase cracking near the bridge abutments. Second, the effects of high air temperatures and large changes in air temperatures during casting should be considered when scheduling deck placements. Third, the lowest possible slump that will still allow sufficient placement and consolidation should be used on monolithic decks, with an upper limit of approximately 2.0 in. (50 mm). In addition, the use of shorter placement lengths, especially for overlays, and a limit on the size of top transverse reinforcing steel (No. 4 or No. 5 bars (13 or 16 mm)) spaced at 6.0 in. (150 mm) or less should be considered. Finally, the use of fog sprays should be specified for silica fume overlays to lessen the risk for plastic shrinkage cracking.

Miller and Darwin (2000)

Miller and Darwin (2000) completed a follow-up to the study by Schmitt and Darwin (1995, 1999). As with the previous study, the effects of material properties and construction practices on the cracking performance of concrete bridge decks throughout northeastern Kansas were evaluated. A comparison of bridge decks containing silica fume overlays and conventional high-density overlays was emphasized in this study due to the increased usage of silica fume overlays at this time in Kansas. In the study, 40 composite continuous steel girder bridges were evaluated, 11 of which were also investigated in the previous study by Schmitt and Darwin (1995, 1999). Of the 40 decks, 20 had silica fume overlays, 16 had conventional high-density overlays, and 4 were monolithic.

The same procedures were used for field surveys and crack density analysis as used by Schmitt and Darwin (1995, 1999). Twenty-seven variables were considered, including bridge age, material properties, construction procedures, design

specifications, and traffic volume. Comparisons were made based on overlay properties and properties of the subdeck for the overlay bridges.

Several conclusions were made based on the analysis completed in the study. Crack densities were found to be similar for decks of the same age with conventional and silica fume overlays. It was determined that crack density increased with age for decks with silica fume overlays. The study could not confirm that this behavior was due to improved construction procedures or low age. Conversely, increased cracking was observed in younger conventional overlay and monolithic decks constructed between 1989 and 1995 compared to older decks of the same type.

Cracking was compared based on concrete properties for each deck type. Cracking was found to increase with increased slump, cement paste content, water content, cement content, and compressive strength for monolithic decks and overlay subdecks, regardless of overlay type and quality. Conventional overlays were also observed to have increased cracking with increasing compressive strength. Cracking increased for monolithic decks with increased water-cement ratios, but this relationship was not found for overlays or subdecks. Silica fume overlays with slumps greater than 3.5 in. (90 mm) and conventional overlays with zero slumps exhibited greater cracking. No connection was observed between air content and cracking for conventional overlays, but cracking was observed to be significantly lower for monolithic decks with air contents above 6 percent.

Several environmental effects on cracking were observed by the researchers. Decks with conventional overlays exhibited increased cracking with increasing average air temperature on the day of the overlay placement. For silica fume overlays, cracking decreased with increases in relative humidity on the day of the overlay placement and with use of fogging and precure materials after placement. For conventional overlays and subdecks, cracking increased with increasing maximum air temperature on the placement date of the overlay or subdeck,

respectively. Cracking increased for silica fume overlay, conventional overlay, and monolithic decks as the daily air temperature range increased on the date of the overlay or monolithic concrete placement.

Relationships were established between design considerations and cracking tendency. Generally, steel structure type, bridge length, span type, and bridge skew appeared to have no link to cracking. This observation conflicts with findings by Schmitt and Darwin (1995) where bridge length and, to some extent, bridge skew were found to influence cracking performance. Increased cracking was observed on decks with increased transverse bar size and spacing. The crack density within 10 ft (3 m) of the abutments was observed to be nearly three times greater for overlay decks with fixed-end girders compared to pinned-end girders.

A number of recommendations were made by the researchers based on the findings. No conclusions could be made on the cracking performance of the decks with silica fume overlays because of the young age of these decks compared to the conventional overlay and monolithic decks. Miller and Darwin (2000) recommended that construction records be maintained for the lifetime of each bridge so that deck performance could be compared with construction data in an effort to improve construction procedures. They recommended limitations on the maximum cementitious material content and/or compressive strength in the provisions for both subdeck and overlay concrete. The use of precure material and fogging immediately after finishing was recommended for all deck types.

Lindquist, Darwin, and Browning (2005)

A study by Lindquist, Darwin, and Browning (2005) was the final of three for the Kansas Department of Transportation to determine factors contributing to bridge deck cracking in Kansas. In the study, 59 steel girder bridge decks were analyzed, that included 49 of the bridges investigated by Schmitt and Darwin (1995, 1999), Miller and Darwin (2000), or both. Of the 59 bridges, 13 had monolithic decks, 16

had conventional overlay decks, and 30 had silica fume overlay decks. Of the 30 decks with silica fume overlays, 19 had 5 percent of the cement replaced by silica fume and 11 had 7 percent of the cement replaced by silica fume.

As with the studies by Schmitt and Darwin (1995) and Miller and Darwin (2000), field surveys were completed on the bridge decks and crack densities were calculated. In total, 27 variables were evaluated, comprising bridge age, construction practices, material properties, site conditions, bridge design, and traffic volume. A main objective of the study was to compare the performance of silica fume overlay (SFO) decks with conventional overlay (CO) and monolithic (MONO) decks due to the increasing use of silica fume overlays in Kansas.

Lindquist et al. calculated age-corrected crack densities for each deck to remove the variable of age from the analysis. They observed that crack densities were higher for overlay decks (0.51 m/m^2 for a 7 percent SFO, 0.49 m/m^2 for a 5 percent SFO, and 0.44 m/m^2 for a CO) than for monolithic decks (0.33 m/m^2) and that cracking in silica fume overlay decks was higher than for conventional overlay decks. These observations are of interest since crack surveys of the same decks by Schmitt and Darwin (1995) found similar cracking performance for all deck types. Lindquist et al. also observed that direct relationships exist between the construction contractor and cracking performance. Cracking was determined to increase with age, although a significant percentage of the cracking occurred within the first three years.

Similar to the findings by Schmitt and Darwin (1995) and Miller and Darwin (2000), monolithic and conventional overlay decks constructed in the 1980s exhibited less cracking than similar decks constructed in the 1990s. The opposite trend was found for silica fume overlay decks, as a decrease in cracking was observed in the 1990s. Lindquist et al. determined this was likely the result of increased efforts to limit evaporation, a cause of plastic shrinkage cracking, prior to application of wet curing. The newest silica fume overlay decks were found to have slightly higher

crack densities than decks constructed in the 1990s, likely due to an increase in the silica fume content used in the decks from 5 to 7 percent.

Relationships between material properties and cracking performance were found to be consistent with the findings of Schmitt and Darwin (1995) and Miller and Darwin (2000). Cracking increased with increases in water content, cement content, cement paste volume, compressive strength, and slump for monolithic decks and overlay subdecks. Decreased cracking was observed in decks with air contents greater than 6 percent. For conventional overlay decks, significantly higher cracking was observed in overlays placed with zero-slump concrete. Increased cracking was also observed as the average and minimum air temperatures on the date of casting increased. For conventional overlay and monolithic decks, cracking increased as the maximum air temperature and daily air temperature range on the date of casting increased. Increased cracking was observed in overlay decks with larger transverse reinforcement and spacing in the subdeck, similar to findings by Schmitt and Darwin (1995).

Lindquist, Darwin, and Browning (2005) made several recommendations based on their findings. Conventional high-density overlays were recommended in place of silica fume overlays due to better cracking performance. The use of high-density concrete overlays was recommended to be limited to resurfacing applications since monolithic decks exhibited less cracking than overlay decks. The process of selecting a contractor was recommended to be based on the quality of previous work since a clear relationship was found between contractor and cracking performance. Other recommendations were consistent with previous recommendations by Schmitt and Darwin (1995), including use of a cement paste volume below 27 percent, concrete placement at the lowest slump that will allow proper placement and consolidation, and design of pinned-end girders as opposed to fixed-end girders.

Krauss and Rogalla (1996)

Krauss and Rogalla completed a multipart study to determine the primary factors that contribute to transverse cracking in bridge decks. They identified contributing factors in three categories: construction methods, concrete materials, and design details. The study included an analytical examination of variables thought to effect cracking tendency, field instrumentation of a newly constructed bridge deck, and laboratory testing.

The analytical study evaluated the impact of different factors on tensile stresses and cracking. Equations were derived based on these factors to calculate stresses in a composite reinforced concrete bridge subjected to temperature and shrinkage conditions. Shrinkage and thermal stresses were calculated for approximately 18,000 combinations of concrete material properties and bridge geometry. The analysis determined that concrete material properties influenced shrinkage stresses more than design parameters. Modulus of elasticity was found to have the greatest effect of any physical concrete property on shrinkage and thermal stresses. Shrinkage and diurnal thermal stresses were found to be linearly proportional to concrete shrinkage and the concrete coefficient of thermal expansion, respectively. Their analysis indicated that aggregates with a low modulus of elasticity were found to decrease shrinkage and thermal stresses by decreasing the overall concrete stiffness, although in practice, low modulus aggregates have been found to increase total shrinkage (Pickett 1956, Hansen and Almudaiheem 1987). Aggregates with a greater thermal conductivity were determined to reduce thermal gradients within the deck and lower thermal stresses.

The design factors that most greatly increased deck stresses included increased girder depth, decreased girder spacing, and decreased deck thickness. Deck reinforcement was observed to have a minimal effect on stresses. Steel studs or channels were found to locally increase deck stresses. Stay-in-place steel forms were

found to cause non-uniform shrinkage in the deck that produced greater stresses at the surface.

A field study was completed through instrumentation during deck replacement of the Portland-Columbia Bridge, located between Pennsylvania and New Jersey. Strain and temperature sensors installed on the deck and girders were monitored from deck replacement until several months after construction to measure the shrinkage and thermal behavior of the bridge at early ages. Environmental conditions were also monitored throughout the study. The combined measurements of deck strain, temperature, environment, concrete properties, and cracking tendency provided important information to better understand the general shrinkage and thermal behavior of the bridge. The recorded data from the bridge instrumentation was then compared with the equations derived from the analytical study. The stresses based on the measured strains in the field study were found to be similar to the stresses determined in the analytical study. While the field data did not necessarily reflect the behavior of all bridge decks, it verified that the analytical approach could predict actual behavior.

A laboratory test procedure was developed by Krauss and Rogalla to compare the cracking tendency of different concrete mixtures. Concrete mixtures with different material properties were the focus of the laboratory testing since the analytical study determined these factors to have the greatest effect on cracking performance. Thirty-nine different mixtures were examined using a restrained ring test, which consisted of a concrete ring cast around a section of steel tubing. This test promoted the development of tensile stresses and cracking as the restrained concrete began to shrink. Gages on the steel tubing measured strains to determine the initiation of cracks, and the concrete rings were visually inspected for cracking. Strength cylinders and free-shrinkage specimens were also cast from each mixture to determine relationships between cracking and shrinkage, development of strength and

modulus of elasticity, and creep. The effects of a number of factors were investigated and, ranked in order of importance, were water-cement ratio; cement content; aggregate type and size; the use of high-range water reducers, silica fume, set accelerators, and retarders; air-entrainment; freeze-thaw cycles; evaporation rate; curing; and shrinkage-compensating cement. Each factor was placed in one of three categories, materials, design, or construction, to investigate the effect of each category on cracking.

A number of trends were observed based on the laboratory testing. Krauss and Rogalla determined aggregate type to be the most significant factor affecting the cracking of concrete. Concretes with aggregates that had greater angularity cracked later than did concretes with more rounded aggregates, and aggregates with a high coefficient of thermal expansion and high modulus of elasticity were found to initiate more cracking. An increase in cement content and decrease in water-cement ratio were observed to increase cracking tendency. The researchers did not find any correlation between water content and cracking performance from the restrained ring data, although increased water content was found to increase shrinkage as a result of an increase in paste content. They suggested that any tendency to increase cracking as the result of a higher water content was offset by the increased creep that occurred in mixtures with higher water contents. The researchers did not observe any relationship between paste content or free shrinkage and time of cracking in the restrained ring tests. They, however, believed that paste content is a primary contributor to drying shrinkage cracking. Slump was not found to have a significant effect on cracking in the laboratory tests, but mixtures with virtually no slump, a low cement content, and a low water-cement ratio exhibited the best performance by taking the longest to crack of all restrained ring specimens. Slump was not expected to contribute to cracking in the restrained ring test since cracking due to slump is a result of restrained settlement, not restrained shrinkage. Cracking was delayed with

the use of shrinkage-compensating cement, and the addition of fly ash was found to slightly delay cracking in the restrained ring test. Entrained air was not found to play a role in cracking tendency. Silica fume was found to increase cracking tendency. The use of a high-range water reducer delayed cracking, except when used with a zero-slump concrete. Concretes with set accelerators or retarders, on average, cracked slightly earlier than comparable control mixtures, but the effect was not significant enough to draw a conclusion. Concretes subjected to longer curing periods experienced lower cracking. Benefits of longer curing on cracking were more pronounced for concretes with a high cement and low water-cement ratio.

Several recommendations dealing with materials and construction were made by the researchers to minimize cracking. Concrete with a high creep capability, low modulus of elasticity, and low coefficient of thermal expansion should be used to minimize thermal and shrinkage stresses and cracking. Cement contents should be limited to reduce shrinkage, decrease early strength, modulus of elasticity, and heat of hydration, and increase creep. Krauss and Rogalla suggested that 56 or 90-day design strengths be considered to promote low heat of hydration. Fly ash was recommended for use due to its reduction in early strength. The largest possible maximum size aggregate was recommended for use to allow for a low paste content mixture while maintaining workability.

Krauss and Rogalla suggested placing concrete during early or mid-evening to minimize ambient temperatures and lower the heat of hydration. Maintaining lower concrete temperatures during placement was suggested as a way to lower early hydration temperatures and thermal stresses. The placement of concrete much warmer than the ambient temperature was found to decrease the relative humidity above the surface and promote plastic shrinkage cracking. The study recommended that concrete be cast 10 to 20° F (5 to 10° C) cooler than ambient temperature at ambient temperatures above 60° F (16° C). They recommended casting at ambient

temperature for temperatures below 60° F (16° C). Concrete should not be placed in windy conditions, and wet curing techniques, including misting, curing compound, and wet blanket procedures, should be implemented quickly after placement and maintained for at least 7 days, and preferably 14 days, to minimize surface drying. Windbreaks and concrete misting procedures should be used during placement when the evaporation rate exceeds 0.2 lb/ft^2/hr (1 kg/m^2/hr) to avoid plastic shrinkage cracking. Mechanical grooving of hardened concrete was recommended in place of rake tining of plastic concrete because of the decreased damage applied to the deck surface and the ability to more rapidly initiate curing.

1.6 FREEZE-THAW DURABILITY

The penetration of water and chemicals through cracks not only initiates corrosion of the reinforcing steel, but also promotes durability problems of the concrete itself. The environmental conditions to which bridge decks are subjected place the concrete at high risk for the development of durability problems. The nearly horizontal surface of most decks slows the removal of water and other chemicals, alternating wetting and drying cycles are much more damaging than constant submersion, and freezing and thawing cycles can lead to fracture and spalling problems (Transportation Research Board 1979). The development of cracks can contribute to damage under repeated freeze-thaw cycles. This study examines the freeze-thaw durability performance and scaling resistance, as well as the shrinkage and cracking performance, of concrete mixtures to more effectively extend the lifespan of bridge decks. The following sections discuss the freeze-thaw damage mechanisms in both the cement paste and aggregates and reports measures that can be taken to alleviate freeze-thaw problems.

1.6.1 Cement Paste Freeze-Thaw Damage Mechanism

The high porosity and fine particle size of hardened cement paste causes the material to be susceptible to freeze-thaw damage. Capillaries within the cement paste are primary locations for water to freeze in saturated, non-air-entrained oncrete. Powers and Helmuth (1953) observed that a significant increase in volume occurs in non-air-entrained, saturated cement paste when subjected to freezing conditions. This volume increase from the expansive formation of ice leads to internal tensile stresses and cracking. In air-entrained cement paste, very little volume increase and significant shrinkage is observed upon freezing.

The freeze-thaw behavior within cement paste is caused by several processes, including hydraulic pressure, osmotic pressure, and desorption of water. Studies by Powers (1945, 1949) initially concluded that hydraulic pressure was the primary contributor to the damaging increase in volume. Powers proposed that a volume increase due to ice formation inside a paste capillary causes compression of unfrozen, residual water. This hydraulic pressure can only be relieved by the water escaping to an open space by diffusion through unfrozen pores. Volume increases and stresses in the capillary will occur if the distance is too great for the residual water to escape (Mindess et al. 2003).

Further analysis by Powers and Helmuth (1953), however, demonstrated that processes other than hydraulic pressure were the key contributors to the freeze-thaw damage in the paste. The researchers observed that partially-dry, non-air-entrained cement paste would initially shrink and then expand when frozen. The partially-dry paste had a sufficiently empty pore volume to accommodate the increase in volume from the water turning to ice. Freezing damage was also observed with liquids that do not expand when frozen. These observations suggest that water is moving towards the frozen locations, rather than away. Significant dilation occurs as water travels to the freezing sites, subjecting the surrounding paste to tensile stresses.

Powers and Helmuth (1953) suggested that this behavior was due to osmosis. Ice in a pore nucleates from the pore solution, leading to an increased solute concentration in the liquid near the ice. Through the process of osmosis, the solution with a lower concentration is drawn towards the solution with a higher concentration. The movement of this water causes osmotic pressure that can lead to stresses and cracking in the surrounding paste.

Another explanation stems from the desorption of water. The freezing temperature of water in paste capillaries is based on the diameter of the pore neck. This causes water in smaller diameter pores to freeze at lower temperatures than water in larger diameter pores. As the temperature drops below 32° F (0° C), water in smaller diameter pores supercools rather than freezes. The chemical potential of ice is lower than that of supercooled water, leading to a higher vapor pressure in the smaller, unfrozen pores. This lowers the relative humidity near the frozen areas and promotes the movement of water towards these frozen sites. The paste away from the frozen regions shrinks and significant volume increases and stresses occur at the frozen locations in the paste.

1.6.1.1 Durability Effects of Air Entrainment

Air entrainment is a proven method of minimizing freeze-thaw damage in cement paste (Transportation Research Board 1979). The addition of entrained air provides empty space within the cement paste for water to move and freeze, lessening damage. Water inside of the air voids begins to freeze at higher temperatures than capillary water due to the larger size of the air voids. The processes of osmosis and desorption reduce the saturation of the surrounding cement paste as nearby water is drawn into the air voids (Mindess et al. 2003).

Higher air content alone, however, does not provide improved freeze-thaw durability to the concrete. It is necessary to evenly distribute the air voids throughout the concrete to allow the majority of the capillary water to be drawn into the voids.

The osmotic and vapor pressures developed within the concrete are not great enough to draw water into the air voids if the distance to these voids is too great. For this reason, air-void spacing, described in terms of the air-void spacing factor, is an important component in determining the freeze-thaw durability of concrete. An air-void spacing factor of no greater than 0.008 in. (0.20 mm) is suggested to provide sufficient freeze-thaw protection to the concrete (Russell 2004). The volume of air recommended by American Concrete Institute (ACI) Committee 201 to achieve satisfactory frost protection is between 5 and 6 percent for mixtures with a maximum size aggregate of 1 in. (25.4 mm). The construction specifications for low-cracking high-performance concrete (LC-HPC) bridge decks in Kansas require air contents within the range of 6.5 to 9.5 percent for concrete to be accepted for placement (Kansas Department of Transportation 2007b). The lower limit of the LC-HPC specifications require air contents above that recommended by ACI Committee 201 based on observations by Schmitt and Darwin (1995), Miller and Darwin (2000), and Lindquist et al. (2005) that bridge decks placed with concretes with air contents above 6 percent exhibit a drop in cracking. The upper limit of the specifications helps ensure that adequate concrete strength is achieved.

1.6.1.2 Durability Effects of Water-Cementitious Material Ratio

The water-cementitious material ratio of concrete has a great effect on freeze-thaw durability due to its relationship with total capillary porosity (Powers and Brownyard 1947) and pore size distribution (Parrott 1989). Powers and Brownyard (1947) determined that in fully hydrated portland cement paste, a reduction in water-cement ratio from 0.6 to 0.4 decreased the pore volume (capillary and gel pores) fraction from 50 to 30 percent. A lower water-cementitious ratio and porosity result in fewer large pores within the cement paste and a lower maximum potential water content. Lower water-cementitious material ratios also reduce permeability, which increases durability by lessening the penetration of water into the concrete. ACI

Committee 201 recommends that a maximum water-cementitious material ratio of 0.45 be used for bridge deck concrete to maintain adequate freeze-thaw durability.

1.6.2 Aggregate Freeze-Thaw Damage Mechanism

Aggregates generally have larger pores that can be more easily saturated than the smaller capillary pores of cement paste. Hydraulic pressure due to the formation of ice within pores is the main factor that contributes to the freeze-thaw damage in aggregates (Transportation Research Board 1979). Freezing damage occurs when the distance for the pore water to travel within the aggregate is too great for the water to escape and relieve hydraulic pressure before fracture occurs. This distance, which establishes the critical aggregate size, is based on freezing rate, degree of saturation, permeability, and tensile strength of the aggregate. Freezing damage may occur in aggregates with fine pores, high absorption, and low permeability. Even if an aggregate with a high absorption is not damaged by freezing, the water that is forced out of the pores of the aggregate by the hydraulic pressure can damage the surrounding cement paste (Mindess et al. 2003). The benefit of entrained air is minimal in lessening the damage due to freezing within aggregates (ACI Committee 201).

1.6.3 Scaling

Even properly air-entrained concrete with durable aggregates can be damaged in the presence of deicing salts due to scaling. Scaling is defined as the loss of surface mortar and often occurs in conjunction with a loosening of surface aggregates. Salt solutions have a lower vapor pressure than pure water, and concretes exposed to salt exhibit a lower rate of evaporation and a higher degree of saturation than concretes not exposed to salt. The use of salt has safety benefits for pavements by decreasing ice accumulation through a reduction of the freezing temperature of water, which also contributes to the increased saturation at the concrete surface. The

increased moisture at the surface can promote the formation of ice lenses that can fracture the concrete. It has also been suggested that heat is removed from the subsurface concrete to melt the ice at the surface when salt is used, causing a rapid temperature drop below the surface. Significant freezing in the subsurface from the temperature drop results in tensile stresses and cracking from thermal strains (Mindess et al. 2003).

Valenza and Scherer (2006) suggested that the glue spall mechanism is the primary cause of salt scaling, named after a similar phenomena that occurs with epoxy-covered glass. As a salt solution freezes on a concrete surface, an ice/concrete composite material forms. As the temperature decreases below the melting point of the salt solution, the ice layer on the concrete surface tends to contract five times the amount of the underlying concrete, placing tensile stresses in the surface of the concrete.

The salt concentration in the solution affects the level of damage to the concrete. Verbeck and Klieger (1956) found that scaling of the concrete is greatest at low to intermediate concentrations (2 to 4 percent) of both calcium chloride and sodium chloride. Scaling problems commonly occur in overvibrated and overfinished concrete where increased paste and inadequate air voids exist on the surface (Mindess et al. 2003). The use of proper air-entrainment and low-permeability concrete provides the best protection from scaling. Air voids relieve differences in vapor pressure between water and ice and low permeability reduces the penetration of liquid into the concrete. Proper air-entrainment reduces scaling in the same manner as it reduces freeze-thaw damage, by providing a freezing location for water outside of the cement paste capillaries.

1.7 DURABILITY EFFECTS OF ALTERNATIVE AGGREGATES, SUPPLEMENTARY CEMENTITIOUS MATERIALS, AND SHRINKAGE-REDUCING ADMIXTURES

Alternative aggregates, supplementary cementitious materials, and shrinkage-reducing admixtures are added to concrete to improve performance, reduce cost, or improve environmental sustainability. Studies conducted at the University of Kansas have addressed the effect on the free shrinkage of additions of pre-wetted lightweight aggregate for internal curing, the use of slag cement, fly ash, and silica fume as portland cement replacements, and the use of shrinkage-reducing admixtures (Lindquist et al. 2008, Reynolds et al. 2009, Browning et al. 2011, Yuan et al. 2011). The effect of these materials on the freeze-thaw durability and scaling resistance of concrete, however, was not examined. As with any modification in mixture proportions, it is important to understand the effect of these materials on overall durability. The unique contributions to the performance of concrete provided by each material must be understood before they are acceptable for use in bridge decks. This study examines the freeze-thaw durability and scaling resistance, as well as reaffirms the benefits to free shrinkage of a number of materials. The following sections summarize the benefits and drawbacks to concrete performance of the materials that are examined in this study.

1.7.1 Internal Curing with Lightweight Aggregate

The use of lightweight aggregate as a source of internal curing water in concrete bridge decks is increasing as the benefits become better known. In terminology currently being considered by ACI Committee 308, internal curing is the process of cement hydration by the use of additional internal water that is not part of the mixing water. This additional internal water can be provided by the use of small amounts of pre-wetted, fine or intermediate-sized lightweight aggregate (LWA) that has a high porosity. The benefits of internal curing include reduced autogenous shrinkage and cracking, increased hydration and strength, reduced permeability, and

increased durability (Roberts 2004, Geiker et al. 2004). The American Society for Testing and Materials (ASTM) has developed the Standard Specification for Lightweight Aggregate for Internal Curing of Concrete (ASTM C1761) as a result of the increased use of internal curing with lightweight aggregate.

As discussed in Section 1.2.1.2, autogenous shrinkage is caused by a drop in the internal relative humidity of concrete. The humidity drops as insufficient water is available to supply that lost from the capillary pores during hydration, leading to self-desiccation of the cement paste. This self-desiccation occurs at low water-cement ratios, below 0.42, where there is not enough water to hydrate the cement unless water is added during curing (Mindess et al. 2003). External wet-curing cannot supply enough water to eliminate autogenous shrinkage for mixtures with low permeability (Mindess et al. 2003). The addition of pre-wetted, porous lightweight aggregate can provide the internal curing water needed to fill the empty pore space in the paste. Although autogenous shrinkage is not a problem for concrete with the water-cement ratios used in LC-HPC bridge decks (0.42 to 0.45), previous research at the University of Kansas has shown that internal curing also helps with the reduction of drying shrinkage at these higher water-cement ratios (Browning et al. 2011). The lightweight aggregate aids in alleviating drying shrinkage by providing internal water to fill capillary pores as the hardened concrete loses water to the environment. The internal water also improves the efficiency of the curing process.

The volume of internal curing water needed to offset autogenous shrinkage is a function of cement content, maximum expected degree of saturation of the cement, and autogenous shrinkage. As reported by Bentz and Snyder (1999), the necessary internal curing water is determined by the following equation:

$$V_{wat} = \frac{C \times \propto_{max} \times CS}{\rho} \tag{1.2}$$

where V_{wat} is the volume fraction of water (ft^3 water/ft^3 concrete) needed in the internal curing medium (for example, lightweight aggregate) to offset autogenous shrinkage, C is the cement content (lb cement/ft^3 concrete), $\propto_{max}$ is the maximum degree of cement hydration (from 0 to 1), ρ is the density of water (62.4 lb/ft^3), and CS is the volume change due to autogenous shrinkage of the cementitious materials at complete (100 percent) hydration (lb water/lb cement hydrated). A typical conservative value for CS is 0.07 lb water/lb cement hydrated. For concrete with a water-cement ratio (*w/c*) below 0.40, complete hydration cannot be achieved, and the maximum degree of cement hydration ($\propto_{max}$) can be estimated as (*w/c*)/0.40. The volume fraction of LWA (ft^3 LWA/ft^3 concrete) necessary to offset autogenous shrinkage can be determined by the following equation:

$$V_{LWA} = \frac{V_{wat}}{\phi \times S} \tag{1.3}$$

where V_{LWA} is the volume fraction of LWA necessary (ft^3 LWA/ft^3 concrete), ϕ is the porosity of the LWA, and *S* is the degree of saturation of the aggregate (from 0 to 1). Zhutovsky et al. (2002) determined that the amount of absorbed water in the LWA must be greater than the amount of internal curing water required for preventing autogenous shrinkage since not all absorbed water is desorbed from the aggregate. The amount of desorption water available in the aggregate for use in the cement paste is a function of pore size and aggregate spacing. A small aggregate with a large pore structure will most efficiently release water into the paste. Zhutovsky et al. reported an equation similar to that of Equation 1.3 that included an efficiency factor (η) in the denominator. The efficiency factor is based on the amount of absorbed water that is desorbed into the paste. Bentz and Snyder (1999) determined that the level of dispersion of the LWA within the cement paste can influence the effectiveness of the internal curing. Concretes with an even dispersion of LWA throughout the paste matrix are able to more effectively distribute internal curing water through the entire

paste. Similar to entrained air, the LWA distribution will influence how effectively the desorbed water will reach the empty capillary pores in the cement.

Browning et al. (2011) evaluated the effectiveness of vacuum pre-wetted, intermediate-sized lightweight aggregate as a source of internal curing. The study focused on three replacement levels (8.9, 11.3, and 13.8 percent by total aggregate volume) of normalweight aggregate with lightweight aggregate. Browning et al. concluded that for mixtures with *w/c* = 0.44, increasing replacement levels of lightweight aggregate substantially decreased shrinkage after both 30 and 365 days of drying. Considerable swelling was observed in the mixtures with lightweight aggregate during the wet-curing period. An increase in swelling has potential benefits in bridge deck applications by placing the restrained concrete in compression. Less shrinkage was observed for the mixtures with lightweight aggregate compared to those without lightweight aggregate even when the swelling was neglected. The moisture contents of the vacuum pre-wetted lightweight aggregates used in the study ranged from 25 to 30 percent. Typical wetting methods in field applications are less effective than vacuum pre-wetting methods, resulting in the use of lightweight aggregates containing lower moisture contents than their absorption capacity. The New York State Department of Transportation requires that lightweight aggregate be wetted using soaker hoses or sprinklers for 48 hours or until the moisture content is at least 15 percent by weight. Fine lightweight aggregates are typically delivered in the air-dry condition and wetted just prior to batching because the fine particles are able to become highly saturated in a short period of time. It is important to understand that the saturation level of the lightweight aggregate affects the amount of internal water available in the concrete. Merikallio et al. (1996) examined the effect of dry lightweight aggregate on the internal relative humidity and evaporation rate of concrete specimens. They observed a decrease in internal relative humidity and evaporation rate in concrete specimens containing dry lightweight

aggregates due to the aggregate absorbing a portion of the mixing water. The decreased evaporation resulted from internal water being absorbed by the lightweight aggregate instead of evaporating.

Other researchers have observed early-age expansion (swelling) similar to that observed by Browning et al. (2011) in mixtures containing pre-wetted lightweight aggregate. Bentz et al. (2001) concluded that this swelling may be related to ettringite formation or swelling of the gel hydration products. The initial expansion benefits the cracking performance of concrete by delaying the onset of tensile stresses to a time when the concrete has a higher tensile strength (Cusson and Hoogeveen 2008). Lura and van Breugel (2000) analyzed the effectiveness of different sizes of lightweight aggregate on swelling performance. They compared mixtures with similar volumes of lightweight aggregate with three different sizes, fine – to 4 mm (0 to 0.16 in.), intermediate – 4 to 8 mm (0.16 to 0.31 in.), and coarse – 8 to 16 mm (0.31 to 0.63 in.). At 144 hours after casting, 40 percent greater swelling was observed in the fine lightweight aggregate mixture than in the coarse mixture.

Decreased permeability, improved cement hydration, and increased strength have been observed in concretes that incorporate internal curing. Bentz (2009) observed a reduction in the chloride diffusion coefficient from 25 to 45 percent in mortar specimens with a water-cement ratio of 0.40 as a 24 percent replacement by weight of sand with pre-wetted lightweight aggregate was included. The decreased permeability was attributed to a reduction in percolation through the paste at the interfacial transition zone around the lightweight aggregate particles and improved long-term cement hydration, both resulting from the internal curing. Cusson and Margeson (2010) observed that cement hydration in air-entrained concrete with a water-cement ratio of 0.35 was enhanced (20 percent higher C-S-H content) by internal curing. The improved hydration of the cement led to a 10 percent increase in 28-day compressive strength, a 20 percent decrease in water permeability, and a 25

percent decrease in chloride ion penetrability. The researchers also observed a 60 percent reduction in autogenous shrinkage after 28 days of drying for internally-cured specimens.

Recent field examinations of structures that incorporated internal curing showed that 7-day flexural strengths reached 90 to 100 percent of the required 28-day flexural strength due to an improved cement hydration. Compressive strengths of air-cured cylinders were found to be similar to those of wet-cured cylinders at all ages, suggesting that internal curing provides adequate water for cement hydration (Villarreal and Crocker 2007).

Few studies have considered the freeze-thaw durability of concrete containing LWA. The increased internal water available with use of LWA has raised concerns over freeze-thaw performance because it may allow more water to freeze and expand within the cement paste. In addition, if the internal curing is inadequate, the porous characteristics of LWAs can contribute to lower strength. Contrary to these concerns, Cusson and Margeson (2010) observed that internally-cured concrete performed better than non-internally-cured concrete when subjected to 300 rapid freeze-thaw cycles in water and 50 slow freeze-thaw cycles in a solution of deicing chemicals (4 percent calcium chloride). Holm et al. (2003) observed decreased permeability with additions of LWA due to the improved interfacial transition zone (ITZ) between the LWA and cement paste matrix. Lam and Hooton (2005) determined that higher replacements of normalweight aggregate with pre-wetted LWA resulted in a lower chloride diffusivity. The researchers observed that the use of finer LWA resulted in a greater decrease in chloride diffusivity than coarser LWA.

1.7.2 Mineral Admixtures

1.7.2.1 Slag Cement

Blast furnace slag is a by-product of the production of pig iron. Slow, air-cooled slag crystallizes to form inert aluminum magnesium and calcium magnesium silicates and exhibits no pozzolanic or cementitious properties, even if ground to a high fineness. When slag is cooled quickly, or quenched, and then ground, however, a hydraulically active calcium aluminosilicate glass is formed that has cementitious properties (Mindess et al. 2003). The quenching process is called granulation, and the final product is ground granulated blast furnace slag (Ramachandran 1997), commonly known as slag cement.

Blast furnace slags are rich in lime, silica, and alumina and have relatively more silica and less calcium than portland cement. Of all by-product mineral admixtures, slags are the closest in chemical composition to portland cement. Impervious coatings of amorphous silica and alumina form around slag particles early in the hydration process and cause the slag to react slowly with water. Alkalis and sulfates provided by portland cement are able to break down these impervious coatings and initiate hydration. A 10 to 20 percent portland cement content is all that is needed to activate a slag-cement blend, though these blends typically contain much more cement than this. Typically, slag is ground to a fineness exceeding that of portland cement to attain increased activity at early ages. As the percentage of slag increases in a slag-cement blend, a slower rate of strength should be expected, particularly at early ages (ACI Committee 233).

Several compounds, such as alkalis, gypsum, and lime, can also serve as activators for slag hydration. The addition of alkalis produces alkali activated slag (AAS), which sets more rapidly than portland cement. Alkali activated slag also has a more rapid rate of strength gain, higher ultimate strength, and lower permeability than typical slag-cement blends. Because slag has a lower lime content than portland

cement, it produces calcium silicate hydrate (C-S-H) that has a lower C/S ratio than pure cement during the hydration process. The increased silica content leads to pozzolanic behavior, as calcium hydroxide, one of the hydration products of cement, reacts with the silica (Mindess et al. 2003).

Slag is classified into three grades (80, 100, and 120) per ASTM C989 based on a slag-activity index. The slag-activity index is dependent on mortar strengths produced by slag when blended with an equal weight of portland cement, and compared to that of pure portland cement mortar. The slag-activity index is measured at both 7 and 28 days and increases with increasing grades of slag. Increased fineness contributes to increased activity and higher early strength (ACI Committee 233).

Concrete containing a slag-cement blend typically has greater workability and easier consolidation than concrete containing 100 percent portland cement, allowing a lower cement paste content to be used. Wood (1981) has suggested that this improved workability is due to smooth slip planes created in the paste by the slag. The water demand for a given slump may be 3 to 5 percent lower for a concrete with a slag-cement blend than for a 100 percent portland cement concrete (Meusel and Rose 1983). An increased set time can generally be expected for concrete with the addition of slag. The degree to which setting time is affected is dependent on concrete temperature, quantity of slag, water-cementitious material ratio, and the characteristics of the portland cement (Fulton 1974). The compressive strength of concrete containing slag is dependent on the grade and amount of slag used in the mixture. Greater long-term strength gain (beyond 20 years), compared to pure portland cement concrete, has been observed for concrete containing slag (Wood 1992). Fulton (1974) and Hogan and Meusel (1981) observed increased strength in concrete containing slag compared to concrete containing only portland cement when subjected to elevated temperature conditions during curing. Fulton (1974) reported that concrete containing slag is more sensitive to poor curing conditions than concrete

containing only portland cement if slag is used in proportions higher than 30 percent of cementitious material volume. He attributed this to the relative reduction in hydration of the slag compared to that attained by portland cement due to the lack of water at early ages, which contributes to more water not being consumed in the hydration process and available for evaporation. The use of slag is known to reduce the rise of temperatures in mass concrete.

The permeability of concrete containing slag is greatly reduced compared to concrete containing only portland cement (Rose 1987), with decreased permeability as the proportion of slag is increased. This lower permeability is due to a change in the pore structure of the cement paste matrix. The excess silica in slag reacts with the calcium hydroxide (CH) and alkalis released during the cement hydration, leading to C-S-H filling concrete pores (Bakker 1980, Roy and Idorn 1983). A reduction in pore size has been observed for slag mixtures in the first 28 days after mixing (Mehta 1980). This reduction in permeability has been found to significantly reduce the penetration of chlorides to all depths within the concrete, enhancing the resistance to corrosion of the reinforcing steel (Bakker 1980; Fulton 1974; Mehta 1980).

Previous studies have reported conflicting findings on the freeze-thaw durability and scaling resistance of mixtures containing slag-cement blends. Fulton (1974), Klieger and Isberner (1967), and Mather (1957) reported similar freeze-thaw durability in mixtures with slag-cement blends or 100 percent portland cement. Malhotra et al. (1987), however, found that while different combinations of portland cement, slag, and fly ash provided concrete properties similar to that of concrete with 100 percent cement, mixtures containing slag and/or fly ash did not perform as well as concrete with 100 percent cement when subjected to freeze-thaw cycles. Malhotra et al. recommended a minimum cement content of 200 kg/m^3 (337 lb/yd^3) to provide adequate freeze-thaw durability. Gunter, Bier, and Hilsdorf (1987) observed that concretes containing slag that were exposed to carbonation exhibited a significant

reduction in durability when subjected to a 3 percent sodium chloride solution and freeze-thaw cycles. Concretes with 100 percent cement exhibited increased freeze-thaw durability when exposed to the same conditions. Stark and Ludwig (1997) reported similar findings to Gunter et al. (1987) and determined that, in concretes containing slag, carbonation creates a coarser surface microstructure compared to the denser subsurface, which contributes to decreased durability on the surface. Bilodeau and Ludwig (1992) reported decreased scaling resistance for concretes containing 25 and 50 percent replacements of cement with slag by weight when exposed to sodium chloride and cycles of freezing and thawing.

1.7.2.2 Fly Ash

Fly ash is a finely divided residue created from the combustion of ground or powdered coal. During the combustion process, the fly ash is transported by flue gases into a particle removal system (ACI Committee 232). Fly ash is the most widely used supplementary cementitious material due to its desirable effects on concrete properties and low cost (less than half the cost of cement). Fly ash particles are mostly spherical, with a mean particle diameter similar to that of portland cement (10 to 15 μm). The specific surface area of fly ash (1 to 2 m^2/g) is greater than that of portland cement (less than 1 m^2/g) (Mindess et al. 2003).

Due to the great variety in the properties of coal used in the power industry, the chemical composition and properties of fly ash can vary considerably. For this reason, ASTM C618 has separated fly ash into two classes, F and C. Class F fly ashes are produced from bituminous and anthracite coals, which are found in the eastern United States and typically have a high heat energy. Bituminous and anthracite coals rarely contain more than 15 percent calcium oxide. ASTM C618 specifies that the content of acidic oxides (SiO_2, Al_2O_3, and Fe_2O_3) must exceed 70 percent for fly ash to be classified as a Class F. Class C fly ashes are a product of the combustion of lignitic coals from the western United States (Mindess et al. 2003).

Class C fly ashes, also known as high-lime ashes, have an acidic oxide content between 50 and 70 percent and generally contain more than 20 percent calcium oxide. The silica (SiO_2) content in fly ash is mainly accredited to the clay minerals and quartz in the coal. Bitiminous and anthracite coals contain more clay minerals and a higher silica content than lignite coals. Class C fly ashes often exhibit a higher rate of reaction at early ages than do Class F fly ashes. Concretes containing certain Class C fly ashes, however, may not experience the same level of long-term strength gain as concretes containing Class F fly ash (ACI Committee 232).

Fly ash is a pozzolan and the siliceous and aluminous material in the fly ash alone possesses little cementitious value. The material reacts with the calcium hydroxide produced during cement hydration to form calcium silicate and aluminate hydrates, which, like those formed in cement hydration, have cementitious properties (ACI Committee 232). The calcium oxide in Class C fly ash can give the material some cementitious properties. The reaction of fly ash with calcium hydroxide occurs at a much slower rate than the corresponding reaction for silica fume, leading to a slower rate of strength gain. The slower reaction of fly ash is due to its smaller specific surface area and lower silica content. The rate of hydration that occurs with fly ash is similar to that of C_2S in cement, which occurs at a slower rate than other cement components. The addition of fly ash has a similar effect to that of increasing the C_2S content in cement, which decreases the early heat evolution and lowers early strength, but increases long-term strength. For this reason, it is necessary to wet-cure concrete containing fly ash for a sufficient length of time to achieve the full benefits. Without sufficient wet-curing, the unreacted portion of the fly ash will act as a noncementitious filler.

Fly ash provides benefits to both plastic and hardened concrete properties. The pozzolanic reaction leads to both a decrease in the rate of reaction and a decrease in the total heat of hydration, allowing for greater control of temperature and

decreased thermal effects. Due to the spherical shape of the particles, the addition of fly ash allows a mixture to maintain workability and pumpability with a decreased water content (Mindess et al. 2003). Fly ash also benefits plastic concrete by increasing cohesiveness, reducing segregation and bleeding, and improving finishability (Russell 2004). The addition of a sufficient amount of fly ash can be used to reduce the effects of the alkali-silica reaction in concrete (Mindess et al. 2003). Other benefits of fly ash on hardened concrete include reduced permeability, reduced chloride diffusivity, increased resistivity, and increased resistance to sulfate attack (Russell 2004). Yuan et al. (2011) examined the free shrinkage of mixtures with a 40 percent volume replacement of cement with Class F fly ash. They observed that mixtures with 100 percent portland cement experienced lower free shrinkage than mixtures with fly ash when cured for 7 and 14 days. As the curing period increased to 28 and 56 days, however, the mixtures containing fly ash exhibited lower shrinkage compared to the mixtures with only cement, illustrating that longer curing periods improve the shrinkage performance of mixtures with fly ash more than for mixtures without fly ash.

1.7.2.3 Silica Fume

Silica fume is a by-product of the production of silicon metal or ferrosilicon alloys and consists of very fine spherical particles having diameters 100 times finer than portland cement. The fine silica fume particles have a high specific surface area and tend to adsorb more water, causing an increase in the water demand of a mixture (ACI Committee 234). This increased water demand can be offset with a water reducer. The extremely small size and spherical shape of silica fume particles makes it a highly reactive pozzolan (Ramachandran 1997). When mixing water comes in contact with silica fume, a silica-rich gel is formed that collects between and coats the cement particles. A pozzolanic reaction between the gel and calcium hydroxide generated by the hydration of cement creates calcium-silicate hydrate (C-S-H) that

forms in the voids between other C-S-H that forms during cement hydration, producing a dense cement matrix. Silica fume particles also increase the denseness of the cement paste by filling in the spaces between the larger cement particles. This increased packing is especially of interest near the paste-aggregate interface where the concrete is weakest and has the highest permeability. Researchers have come to conflicting conclusions on the reason concrete containing silica fume experiences higher compressive strength. Mindess (1988) concluded that silica fume increases concrete strength mainly due to an increased bond between the cement paste and aggregate particles. Conversely, Cong et al. (1992), supported by work by Darwin and Slate (1970), determined that silica fume increases concrete strength due to an increase in the cement paste strength and changes in the properties of the paste-aggregate interface have little effect on strength. The increase in strength with the addition of silica fume is minimal after 28 days.

The addition of silica fume results in a reduction in concrete permeability of approximately one order of magnitude (Maage 1984; Maage and Sellevold 1987), which can be of great benefit for corrosion protection of reinforcing steel. Silica fume creates a more discontinuous pore structure by decreasing the number of large pores while also densifying the interfacial transition zone (Mindess et al. 2003). As reported by Bentur et al. (1988), this effect of pore structure causes a slower rate of water loss during drying since water evaporates more rapidly from larger pores. The small particle size and high specific surface of silica fume, however, causes a reduction in bleed water flow which can lead to plastic shrinkage cracking if insufficient curing water is available.

An abundance of testing has been performed to determine the resistance of silica fume concrete to chloride ion penetration. This penetration resistance is important to bridge deck concrete by providing protection to the reinforcing steel from deicing agents. Byfors (1987) observed a considerable reduction in chloride ion

penetration with the addition of silica fume up to 20 percent by volume of cementitious material. This penetration resistance decreased at higher water-cementitious material ratios. The effect of silica fume on chloride penetration was measured by Whiting and Detwiler (1998) for a range of silica fume contents and water-cementitious material ratios. They observed that an increase in the silica fume content up to approximately 6 percent of total cementitious materials reduced chloride diffusivity. At silica fume contents above 6 percent, much more silica fume was needed to achieve the same incremental benefit**.** The permeability and chloride ion penetration resistance of concrete containing silica fume is greatly dependent on the length and method of curing. During curing, the dense cement paste matrix containing silica fume requires enough water to be available for a sufficient length of time to adequately hydrate the cement and allow the pozzolanic reaction to proceed (Whiting and Khulman 1987).

Studies of the freeze-thaw durability of concrete containing silica fume have produced conflicting results. Sorensen (1983), Aitcin and Vezina (1984), and Malhotra (1986) observed that for properly air-entrained concrete, the addition of silica fume does not have a significant effect on freeze-thaw durability and scaling resistance. Conversely, Pigeon et al. (1987) observed a reduction in scaling resistance as the silica fume replacement exceeded five percent by volume of cementitious material. Pigeon et al. (1986) reported that the critical air-void spacing factor to achieve adequate freeze-thaw protection is smaller for concretes containing silica fume. This is likely due to the greater length of time needed for pore water to reach an air void in the less permeable material. Sellevold et al. (1982) observed increases in the dynamic modulus of elasticity with increasing silica fume contents. Sabir and Kouyiali (1991) found that replacing cement with increasing amounts of silica fume by weight results in more rapid decreases in the dynamic modulus of elasticity when exposed to freeze-thaw cycles.

A number of state departments of transportation have used silica fume concrete as a bridge deck overlay material in an effort to achieve better surface abrasion resistance, good bond strength with the base deck, and increased strength (Luther 1988). Investigators, however, have observed increased bridge deck cracking with use of silica fume overlays (Popovic et al. 1988, McDonald 1991, Lindquist et al. 2005). Lindquist et al. (2008) observed increased cracking on bridge decks with silica fume overlays. This observation is likely due to the added restraint provided to the concrete deck by the overlay. Concrete containing silica fume typically experiences a higher early heat of hydration that can cause increased thermal stresses (Huang and Feldman 1985, Krauss and Rogalla 1996), but the amount of silica fume needed to produce a significantly higher early heat of hydration (20 to 30 percent replacement of cement by volume) is not used in bridge deck overlays and is highly unlikely to be used in most concrete structures. As mentioned previously, increased plastic shrinkage cracking can occur as bleed water slowly moves through the low-permeability concrete (Krauss and Rogalla 1996). Krauss and Rogalla (1996) observed that concrete containing 7.5 percent silica fume experienced cracking 5 to 6 days earlier in restrained ring tests than concrete containing no silica fume, likely due to the higher early-age strength and stiffness of concrete containing silica fume

1.7.3 Shrinkage-Reducing Admixtures

Advances in admixture technology within the past 20 years have resulted in an increased usage of shrinkage-reducing admixtures (SRAs) to improve concrete shrinkage performance. Reductions in drying shrinkage achieved with SRAs are greater than what can be achieved with optimal material properties, construction procedures, environmental conditions, and design considerations. The admixture is available in both liquid and solid forms, with the liquid form dispersed within the mixing water and the solid form dispersed within the cementitious material prior to mixing for better distribution throughout the concrete. The internal mechanism that

promotes improved shrinkage performance is considerably different for liquid and solid SRAs. Liquid SRAs are more commonly used and are the focus of this section.

As discussed in Section 1.2.1.2, much of drying shrinkage stems from capillary stresses that develop within the cement paste pores due to the surface tension of the pore solution. Liquid SRAs function by reducing the surface tension of the pore solution, minimizing capillary stresses and drying shrinkage. The admixture remains in the pore system after the concrete has hardened and continues to reduce surface tension. The primary purpose of the admixture is to reduce drying shrinkage, but it has other effects on the fresh and hardened concrete properties. Mora-Ruacho et al. (2009) found that the use of shrinkage-reducing admixtures also reduces plastic shrinkage cracking. The researchers determined that a reduction in the surface tension of the pore solution lowers the evaporation rate and delays the onset of peak capillary pressures within the concrete.

The use of an SRA can have a slight retarding effect on the rate of cement hydration and may extend the setting time up to an hour. A reduction in thermal cracking can occur with SRAs due to this retardation and a related reduction in peak temperature. The use of an SRA also decreases the air content of concrete, requiring a higher dosage of air-entraining admixture to achieve a specific air content. The possibility of strength reduction must also be considered with the use of SRAs. Previous work has shown that a 2 percent addition of SRA by weight of cement will reduce the 28-day compressive strength by as much as 15 percent (Berke et al. 1994). The strength reduction is generally less in concretes with lower water-cement ratios and can be offset by the use of superplasticizers. SRAs affect the stability of the air-void system within the concrete as the result of the reduction in the surface tension of water. Lindquist et al. (2008) observed a more stable air-void system with an SRA dosage of 1 percent by weight of cement than with a 2 percent dosage. The researchers tested the air content of mixtures at five-minute increments after mixing

until the change in air content from one test to the next was less than 1 percent. The mixture with 1 percent SRA maintained a more constant air content for a longer time period than the mixture with 2 percent SRA.

The use of a shrinkage-reducing admixture will also change the shape of the drying profile within fresh cement pastes. Typically, the top 3/8 to 3/4 in. (10 to 20 mm) of exposed cement paste will dry out uniformly as the largest pores are emptied first. With the addition of an SRA, the decreased surface tension of the pore water allows much smaller pores at the surface to be emptied, resulting in a steep drying gradient beginning at the concrete surface. Although the evaporation rate increases, the decreased surface tension does not allow pore solution to wick to the surface from deep within the concrete, decreasing the drying rate (Bentz 2005).

Studies suggest that liquid SRAs are most effective at dosages of 1.5 to 2.0 percent by weight of cement (Balogh 1996, Tomita 1992). The shrinkage reduction provided by the use of SRAs will be more significant for mixtures with lower water-cement ratios. Longer periods of wet curing have been found to increase the effectiveness of an SRA, especially at early ages. Lindquist et al. (2008) investigated the effect of SRAs in concrete at dosages of 0, 1, and 2 percent by weight of cement. The addition of increasing amounts of SRA resulted in a reduction in both early-age and long-term shrinkage. Lindquist et al. found that increasing the curing period from 7 to 14 days did not have a significant effect on the free shrinkage of the mixtures containing an SRA. Like Lindquist et al., Yuan et al. (2011) observed decreased free shrinkage with increasing dosages of SRA. Yuan et al. observed decreased free shrinkage for mixtures containing an SRA, but similar values of water loss for mixtures with and without SRAs.

1.8 OBJECTIVE AND SCOPE

The factors responsible for bridge deck cracking and freeze-thaw damage are generally recognized. Cement paste is the concrete constituent that contains the

highest shrinkage potential and contributes to cracking. Concretes with increasingly high water-cement ratios exhibit increased permeability, while concretes with increasingly low water-cement ratios exhibit increased compressive strength and stiffness and reduced effects from creep. Increased slump and reinforcing bar size and decreased top concrete cover contribute to increased settlement cracking. High ambient and concrete temperatures, high wind speeds, and low humidity all contribute to an increased evaporation rate and plastic shrinkage cracking. Concrete temperatures during placement that are significantly above that of the steel girders can induce thermal stresses that can lead to thermal cracking. Improper curing allows internal moisture to be lost to the environment prior to its consumption in the hydration process, contributing to drying shrinkage and cracking. Mixtures containing low air contents experience freeze-thaw damage by allowing water to freeze and expand within the cement paste rather than in the air-voids.

The actions needed to alleviate cracking and freeze-thaw damage are becoming better understood due to a range of field, analytical, and laboratory studies completed on the subject. Few studies, however, have taken the step to implement these findings in the construction of low-cracking bridge decks. This report is part of a long-term pooled-fund study that includes two separate objectives.

1.8.1 Objective #1 – Laboratory Evaluations of Innovative Mixtures for Improved Cracking and Durability Performance

Laboratory evaluations are performed on mixtures employing new technologies to further improve shrinkage and cracking performance, including the addition of lightweight aggregate to provide internal curing and the use of mineral and shrinkage-reducing admixtures. The freeze-thaw durability and scaling resistance of each mixture is evaluated to determine overall durability performance. Fifty-three batches of concrete are evaluated using the following six laboratory tests. Detailed descriptions of the test procedures are provided in Chapter 2.

- ASTM C157 – Standard Test Method for Length Change of Hardened Hydraulic Cement Mortar and Concrete. Three specimens per mixture were tested.
- ASTM C666 – Procedure B – Standard Test Method for Resistance of Concrete to Rapid Freezing and Thawing. Three specimens per mixture were tested.
- ASTM C215 – Standard Test Method for Fundamental Transverse, Longitudinal, and Torsional Frequencies of Concrete Specimens. Three specimens per mixture were tested.
- BNQ NQ 2621-900 – Bétons de Masse Volumique Normale et Constituants (Quebec standard test equivalent to ASTM C672). Three specimens per mixture were tested.
- ASTM C39 – Standard Test Method for Compressive Strength of Cylindrical Concrete Specimens. Three specimens per mixture were tested.
- ASTM C457 – Standard Test Method for Microscopical Determination of Parameters of the Air-Void System in Hardened Concrete. Two specimens per mixture were tested.

The study involves three testing programs summarized below:

1.8.1.1 Evaluation of Mixtures Containing Two Air-Entraining Admixtures Used in Conjunction with Shrinkage-Reducing Admixtures

The free shrinkage performance, freeze-thaw durability, scaling resistance, compressive strength, and air-void system characteristics of concrete mixtures containing a surfactant-based or a polymer-based air-entraining admixture in conjunction with shrinkage-reducing admixtures are examined. Surfactant-based air-entraining admixtures function by reducing the surface tension of water to promote the formation of air-voids through agitation during mixing (Mindess et al. 2003). As described in Section 1.7.3, shrinkage-reducing admixtures function through a similar reduction in pore water surface tension. This additional reduction in surface tension can decrease the stability of the air-void system, contributing to reduced freeze-thaw

protection. Mixtures containing a polymer-based air-entraining admixture, presumably not to be influenced by pore water surface tension, are evaluated alongside mixtures containing a surfactant-based air-entraining admixture to determine their behavior when used in conjunction with shrinkage-reducing admixtures. It is hypothesized that the mixtures containing the polymer-based admixture will provide improved air-void stability and freeze-thaw protection compared to the mixtures containing the surfactant-based admixture. Twenty-four batches containing two shrinkage-reducing admixtures with varying dosages (0, 0.5, 1.0, and 2.0 percent by weight of cement) and two air-entraining admixtures (surfactant-based and polymer-based) are tested in this program. The results of the program are discussed in Chapter 3.

1.8.1.2 Durability Evaluation of Mixtures Containing Shrinkage-Reducing Admixtures with Air Contents below LC-HPC Requirements

The freeze-thaw durability and scaling resistance of mixtures containing varying dosages of shrinkage-reducing admixture with air contents below that required by the low-cracking high-performance concrete (LC-HPC) specifications are examined. The reduction in pore water surface tension that occurs with the use of shrinkage-reducing admixtures affects the air-void system stability of concrete, which can contribute to freeze-thaw damage. The LC-HPC specifications require a minimum air content of 6.5 percent based on observations of decreased cracking in bridge decks containing air contents above 6 percent (Schmitt and Darwin 1995, Miller and Darwin 2000, and Lindquist et al. 2005). The variability in concrete properties and the need for continuous placement of concrete in the field can lead to the occasional placement of concrete with air contents below the specified minimum, which may result in poor freeze-thaw and cracking performance – performance that may be further degraded due to the lower stability of the air-void system when shrinkage-reducing admixtures are used. This program examines the freeze-thaw

durability and scaling resistance of 16 batches containing varying dosages (0, 0.5, 1.0, and 2.0 percent by weight of cement) of a shrinkage-reducing admixture with air contents ranging from 3.5 to 9 percent to determine their behavior in bridge deck construction applications. A goal of this program is to determine a lower allowable limit for air content that could be used for mixtures containing shrinkage-reducing admixtures that would still exhibit adequate freeze-thaw durability. This lower allowable limit could then be translated into air content restrictions for bridge deck placements with concretes containing shrinkage-reducing admixtures. The results of the program are discussed in Chapter 3.

1.8.1.3 Evaluation of Mixtures Containing Mineral Admixtures Used in Conjunction with Internal Curing

The free shrinkage performance, freeze-thaw durability, scaling resistance, compressive strength, and air-void system characteristics of mixtures containing varying combinations of pre-wetted lightweight aggregate, slag cement, and silica fume are examined. A previous study at the University of Kansas (Reynolds et al. 2009) determined that small additions of pre-wetted lightweight aggregate provide internal curing water that contributes to reduced free shrinkage. In addition, the researchers observed an additional reduction in free shrinkage as lightweight aggregate was used in conjunction with increasing amounts of slag cement.

It is well understood that concretes containing silica fume and slag exhibit a reduction in permeability and improved resistance to chloride ion penetration. Research at the University of Kansas (McLeod et al. 2009) determined that additions of slag cement and silica fume contribute to a reduction in chloride ingress. This reduced permeability could improve the durability of bridge decks as long as the addition of the silica fume does not contribute to increased cracking and decreased freeze-thaw durability performance. In addition, research by Bentur et al. (1988) observed a slower rate of water loss during drying in concrete containing silica fume

as a result of the reduced permeability. If sufficient internal curing water is supplied to the concrete through the use of pre-wetted lightweight aggregate, the reduced permeability provided by the silica fume could reduce drying shrinkage as the internal water is unable to quickly reach the evaporative conditions of the surface.

Twenty-one batches containing different combinations of volume replacements of total aggregate with lightweight aggregate (0, 8, and 10 percent), portland cement with slag cement (0 and 30 percent), and portland cement with silica fume (0, 3, and 6 percent) are examined. A number of studies have observed reduced freeze-thaw durability and scaling resistance in mixtures containing slag (Gunter, Bier, and Hilsdorf 1987, Malhotra et al. 1987, Bilodeau and Ludwig 1992, Stark and Ludwig 1997) and silica fume (Pigeon et al. 1987, Sabir and Kouyiali 1991). The freeze-thaw durability and scaling resistance of these mixtures are examined to verify their overall durability for use in bridge deck construction. Relationships are developed between the air-void system characteristics and overall durability for each mixture. The results of the program are discussed in Chapter 4.

1.8.2 Objective #2 – Construction and Evaluation of Low-Cracking High-Performance Concrete Bridge Decks

This study evaluates the effectiveness of modifications in mixture proportions and construction procedures on the cracking performance of bridge decks constructed in accordance with the low-cracking high-performance concrete (LC-HPC) specifications. Annual field surveys are completed on 16 LC-HPC bridge decks and 13 associated control decks constructed in accordance with the standard Kansas Department of Transportation (KDOT) specifications. The cracking performance of each deck is quantified in terms of a crack density. Direct comparisons are made between the cracking performance of the LC-HPC and the control decks. Relationships are established between cracking performance and the material properties, environmental conditions during placement, and construction procedures

of these two deck types and additional decks examined in previous studies at the University of Kansas.

1.8.3 Report

The following chapters describe the experimental and field research used to satisfy the objectives of this study.

CHAPTER 2: EXPERIMENTAL PROGRAM AND FIELD EVALUATION TECHNIQUES

2.1 GENERAL

This chapter describes the experimental program and field evaluation techniques. Laboratory tests were performed on 53 batches of concrete employing new technologies, such as the use of lightweight aggregate to provide internal curing in conjunction with mineral admixtures and shrinkage-reducing admixtures, to verify their potential effectiveness for use in future low-cracking high-performance concrete (LC-HPC) bridge decks. The laboratory portion of this study includes three test programs. The properties of the materials used in the concrete mixtures, including cement, fine and coarse aggregates, lightweight aggregate, and mineral and chemical admixtures, are reported. Laboratory methods used to proportion and prepare the concrete are described. The procedures for the tests used to analyze the mixtures, including free shrinkage, freeze-thaw durability, scaling resistance, compressive strength, and hardened concrete air-void analysis, are summarized. Concrete mixture proportions and plastic concrete properties of the mixtures are reported.

The field work in this study includes the construction and evaluation of LC-HPC bridge decks throughout Kansas. This chapter describes the method of data collection and type of data collected during deck construction. On-site crack surveys have been completed annually on each deck to quantitatively establish cracking performance through determination of crack density. Control decks constructed in accordance with the standard Kansas Department of Transportation (KDOT) specifications were selected and also surveyed to provide comparisons to determine the effect of the LC-HPC specification on cracking performance. The crack survey procedure and method to determine crack density are summarized in this chapter.

2.2 MATERIALS

This section describes the materials used in the mixtures evaluated in the laboratory study.

2.2.1 Cement

Type I/II portland cement complying with the requirements of ASTM C150 for both Type I normal portland cement and Type II modified portland cement was used in this study. The Type I/II portland cement was obtained in seven portions over a span of 3-1/2 years and was analyzed by the Ash Grove Cement Company Technical Center in Overland Park, KS. The tests completed on the cement include ASTM C204 – "Standard Test Method for Fineness of Hydraulic Cement by Air-Permeability Apparatus" to determine Blaine fineness, an X-Ray Fluorescence (XRF) elemental analysis followed by a Bogue composition analysis based on the elemental analysis, and a Particle Size Determination (PSD) using a laser particle size analyzer. The results of the cement analysis are listed in Table A.1 in Appendix A.

2.2.2 Fine Aggregates

Kansas River sand and pea gravel were used as the fine aggregates in the concrete mixtures. Twelve samples of sand and five samples of pea gravel were obtained over a span of 3-1/2 years. The sand complies with the requirements of the Kansas Department of Transportation (KDOT) and was obtained from Builder's Choice Aggregates in Topeka, KS. The pea gravel is classified as UD-1 in the KDOT material specifications and was obtained from Midwest Concrete Materials in Lawrence, KS. The properties of the sand and pea gravel are reported in Table A.2 in Appendix A.

2.2.3 Coarse Aggregates

Granite was used as the coarse aggregate. Nineteen samples of granite were obtained over a span of 3-1/2 years. The granite complies with KDOT material specifications and was obtained from Geiger Ready Mix in Olathe, KS (samples G-1 to G-18) and Midwest Concrete Materials in Lawrence, KS (sample G-19). Granite samples with maximum sizes of 1 and 3/4 in. (25 and 19 mm) were blended in 49 of the mixtures to achieve optimized gradations. Granite sample G-19 was separated into two portions (G-19A and G-19B) and reblended to obtain the desired gradation in four of the mixtures. The properties of the granite are reported in Table A.3 in Appendix A.

2.2.4 Lightweight Aggregate – Buildex, Inc.

An expanded shale lightweight aggregate (Haydite) was used as a partial replacement of the pea gravel to provide internal curing in some of the mixtures. The lightweight aggregate was vacuum pre-wetted prior to mixing. The expanded shale was intermediate-sized (1/4 to 1/8 in.) and obtained from Buildex, Inc. in Marquette, KS. The properties of the lightweight aggregate, as reported by Buildex, are given in Table A.4 in Appendix A. The specific gravity values of the lightweight aggregate in the vacuum pre-wetted condition vary from the values reported by Buildex because of variations in the aggregate moisture content. The specific gravity and absorption values reported by Buildex are based on a 24-hour immersion of the aggregate in water prior to testing in accordance with ASTM C127 / C128. The lightweight aggregate properties after vacuum pre-wetting are reported along with information on the concrete mixtures in Program 3 that incorporate the aggregate in Table A.13 in Appendix A.

2.2.5 Mineral Admixtures

Grade 100 ground granulated blast-furnace slag (GGBFS) and silica fume were used as partial replacements of cement in some mixtures. The properties of these admixtures are reported in Table A.5 in Appendix A. The Grade 100 ground granulated blast-furnace slag (trade name GranCem®) was obtained from Holcim in Theodore, AL and the silica fume (trade name Eucon MSA) was obtained from Euclid Chemical Company.

2.2.6 Chemical Admixtures

Air-entraining admixtures, shrinkage-reducing admixtures, and superplasticizers were used in the study. The air-entraining admixtures include Micro Air®, by BASF Construction Chemicals, LLC, and Tough Air™, by Miracon™ Technologies. Micro Air® is a tall oil-based surfactant and functions by lowering the surface tension of water to promote the formation of air bubbles during concrete mixing. The solids content and specific gravity for Micro Air® are 13 percent and 1.01, respectively. Tough Air™ is synthetic and polymer-based and consists of a foam, generated using aeration equipment, which is dispersed throughout the concrete during mixing.

The shrinkage-reducing admixtures include two products produced by BASF Construction Chemicals, Tetraguard® AS20 and MasterLIFE CRA 007. Both admixtures function by minimizing cement paste capillary stresses through a reduction in the surface tension of the pore water. The specific gravity for both admixtures is 0.99.

The superplasticizer used throughout the study, Glenium® 3030NS, is produced by BASF Construction Chemicals. The superplasticizer was used when necessary to achieve desired concrete slumps. The solids content and specific gravity of Glenium® 3030NS are 20 percent and 1.05, respectively.

2.3 LABORATORY METHODS

The methods employed to design and produce the concrete used in the laboratory studies are described in this section.

2.3.1 Mixture Proportioning

The aggregate gradation of the mixtures was optimized using KU Mix, a mix design program developed at the University of Kansas. Optimized aggregate gradations were used to produce workable concrete at the low cement paste contents used in the prototype low-cracking high-performance mixtures in the study. Four separate aggregates with unique gradations were used in the optimization process. A complete discussion of aggregate optimization using KU Mix is presented by Lindquist et al. (2008). KU Mix can be downloaded from http://www.iri.ku.edu/projects/concrete/phase2.html.

Dosages of shrinkage-reducing admixture were calculated based on a percent weight of cement in the mixtures; however, the dosages were converted to a volume when measured and added to the mixtures. These dosages are reported by volume in the tables that provide information on the concrete mixtures in Program 1 and 2 that incorporate the admixtures (Tables A.7 and A.10, respectively, in Appendix A). Dosages of Micro Air and Tough Air were established through trial batches to achieve a desired air content. The dosages of Micro Air and the Tough Air foam were measured by volume when added to the mixtures. The Tough Air foam was dispensed into a container and deposited manually throughout the mixing concrete.

2.3.2 Mixing Procedure

Prior to mixing, the coarse aggregate was soaked for a minimum of 24 hours and then prepared to a saturated surface-dry (SSD) condition in accordance with ASTM C127. Fine aggregate was added to the mixer in a partially wet condition. The free surface moisture of the fine aggregate was determined in accordance with

ASTM C70 and a correction was made to the mixing water to accommodate excess surface moisture. Lightweight aggregate, if used, was vacuum pre-wetted and prepared to a wetted surface-dry condition. The vacuum pre-wetting process is described in Section 2.3.3. A sample of the lightweight aggregate in the wetted surface-dry condition was obtained to determine moisture content in accordance with ASTM C128.

A counter-current pan mixer was used in accordance with ASTM C192. The pan surface and blades were dampened prior to mixing. The coarse aggregate and 80 percent of the water were first added to the mixer as the mixer began rotating. If used, silica fume was then added to the mixer and mixed for 1-1/2 minutes. Cement and any other mineral admixtures were then added to the mixer and mixed for an additional 1-1/2 minutes. The fine aggregate was then added to the mixer and mixed for 2 minutes. Lightweight aggregate was added with the other fine aggregates.

The materials continued to mix for another 5 minutes. Within the 5 minutes, the water reducer, if used, combined with 10 percent of the mixing water was added and mixed for 1 minute. If used, the shrinkage-reducing admixture (SRA) was added next. The air-entraining admixture, combined with the final 10 percent of the mixing water, was added and the concrete mixed for 1 minute. If the Tough Air air-entraining admixture was used, the foam was generated using aeration equipment and dispersed manually throughout the mixing concrete at this time. After the completion of the 5 minute mixing period, mixing was stopped for 5 minutes. During this rest period, damp towels were placed over the concrete to prevent evaporation and the concrete temperature was checked. The concrete was then mixed for an additional 3 minutes. After the final 3 minutes of mixing, the concrete was ready for casting. If the concrete contained an SRA, an additional 30 minute rest period was carried out before casting to allow for stabilization of the air content. If necessary, liquid nitrogen was added to the concrete during mixing to achieve temperatures below 75°

F (24° C). Slump (ASTM C143), air content (ASTM C173), temperature (ASTM C1064), and unit weight (ASTM C138) measurements were taken on the concrete prior to casting. The casting, demolding, and curing procedures were dependent on the specific test being completed and are described in the following sections.

2.3.3 Casting

Different casting procedures were followed for prismatic specimens (including specimens for free shrinkage, freeze-thaw durability, and scaling resistance tests) and cylindrical specimens (including specimens for compressive strength tests and hardened air-void analyses).

Prismatic Specimens

Concrete was placed within each mold in two layers of approximately equal depth. Each layer was consolidated on a vibrating table with an amplitude of 0.006 in. (0.15 mm) and a frequency of 60 Hz for 15 to 30 seconds. Care was taken to overfill the second layer to produce specimens with the proper dimensions (filled to the mold top) after consolidation. The surfaces of the specimens were then struck off with a 2 × 5-1/2 in. (50 × 135 mm) steel screed (for free shrinkage and freeze-thaw durability specimens) or a 4 × 1 in. (102 × 25 mm) wooden screed (for scaling resistance specimens) to produce an even surface. The specimens were covered with 6-mil (152-µm) Marlex® strips and then wrapped on the surface and sides with 3.5-mil (89-µm) plastic sheets secured with rubber bands to prevent moisture loss. A 1/2-in. thick piece of Plexiglas® was placed over each set of three covered molds. The specimens were maintained in this condition for 23-1/2 ± 1/2 hour after casting.

Cylindrical Specimens

Cylindrical specimens were cast in accordance with ASTM C31. The 4 × 8 in. (102 × 203 mm) cylinders were consolidated by rodding and cast in steel molds. After casting, the specimens were covered with 3.5-mil (89-µm) plastic sheets

secured with rubber bands to prevent moisture loss. The specimens were maintained in this condition for 23-1/2 ± 1/2 hour after casting.

2.3.4 Lightweight Aggregate Vacuum Pre-Wetting

Vacuum pre-wetting equipment, shown in Figure 2.1, was fabricated to achieve rapid absorption of the lightweight aggregate. The equipment includes a Gast Rotary Vane air compressor/vacuum pump, a 19 × 28 in. (48 × 53 cm) steel barrel, and a five gallon bucket. Plastic tubes with a 1/4-in. (6-mm) inner diameter connected the steel barrel to the vacuum pump and five gallon bucket. The lid for the steel barrel is designed to attain an air-tight seal and includes a pressure gage, a pressure release valve, and valves for the vacuum pump and five gallon bucket tube connections.

The lightweight aggregate to be pre-wetted was placed in the steel barrel, followed by placement of the lid. The five gallon bucket was filled with water to a designated level. The end of one plastic tube was submerged in the five gallon bucket, connecting the steel barrel lid to the bucket. The valve for that tube was closed. The valve on the tube connecting the vacuum pump to the barrel lid was opened and the pump was turned on. The decrease in air pressure within the barrel was monitored using the pressure gage. The valve to the water bucket was opened as the pressure reached 5.9 psi (12 in. Hg). The negative pressure pulled water into the barrel. The water valve was closed when the water within the bucket dropped to a predetermined level. Care was taken to maintain the vacuum pressure within the barrel by not allowing the bucket to be fully emptied. The vacuum pressure was maintained for a minimum of 10 minutes. The pressure was then released, wetting the aggregate. Additional information regarding the vacuum pre-wetting process is presented by Reynolds et al. (2009).

Figure 2.1 Vacuum pre-wetting equipment

2.4 TESTING PROCEDURES

The procedures used for the laboratory tests are described in this section. Demolding and curing procedures were unique to each test and are described within each test procedure. The tests include free shrinkage, freeze-thaw durability and fundamental transverse frequency, scaling resistance, compressive strength, and a hardened concrete air-void analysis. Three specimens per batch were evaluated for all tests except for the air-void analysis (two specimens per batch). Specimens not handled in accordance with their respective test procedures were omitted from the analysis. These omitted specimens are identified in the presentation of the raw data in Appendix C.

2.4.1 Free Shrinkage

Free shrinkage tests were performed in accordance with ASTM C157 – Standard Test Method for Length Change of Hardened Hydraulic-Cement Mortar and Concrete. Three 11-1/4 × 3 × 3 in. (286 × 76 × 76 mm) free shrinkage specimens were prepared for each batch of concrete in accordance with ASTM C192. Cold-

rolled steel molds were used to produce the specimens. Gage studs were embedded at the ends of the specimens, creating a testing gage length of 10 in. (254 mm) (Figure 2.2).

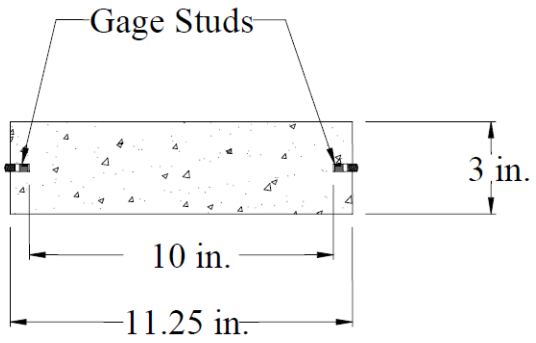

Figure 2.2 Free shrinkage specimens (Tritsch et al. 2005)

Demolding, Curing, and Drying

The specimens were demolded 23-1/2 ± 1/2 hour after casting, labeled, immediately wrapped in wet towels, and placed under running water to prevent moisture loss. Initial length readings were taken, and the specimens were cured in lime-saturated water in accordance with ASTM C511 for 13 days (14 total curing days from casting date). A number of studies have demonstrated that increasing the curing from 7 to 14 days reduces the free shrinkage of concrete (Lindquist et al. 2008, Browning et al. 2011, Yuan et al. 2011). After curing, the specimens were placed in a low air flow, environmentally-controlled room with a relative humidity of 50 percent ± 4 percent and a temperature of 73° ± 3° F (23° ± 2° C).

Data Collection

Free shrinkage measurements were taken using a mechanical dial gage length comparator (Figure 2.3) with an accuracy of 0.0001 in. (0.00254 mm) and a total

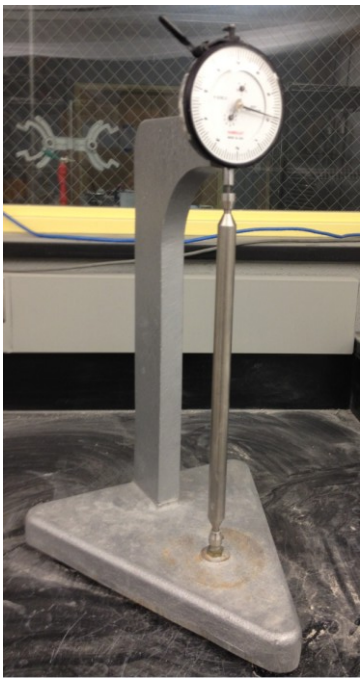

Figure 2.3 Mechanical dial gage length comparator

and C490 prior to every six measurements to provide a consistent reference point for readings. Readings were taken by slowly rotating the specimens in the clockwise direction and recording the minimum (shortest) dial gage reading. Free shrinkage readings were taken daily for the first 30 days, every other day for Days 31 to 90, weekly for Days 91 to 180, and monthly thereafter through 365 days.

2.4.2 Freeze-Thaw Durability and Fundamental Transverse Frequency

Freeze-thaw durability and fundamental transverse frequency tests were performed in accordance with Procedure B of ASTM C666 – Standard Test Method for Resistance of Concrete to Rapid Freezing and Thawing and ASTM C215 – Standard Test Method for Fundamental Transverse, Longitudinal, and Torsional Frequencies of Concrete Specimens, respectively. Three 16 × 3 × 4 in. (406 × 76 × 102 mm) specimens were prepared for each batch of concrete in accordance with ASTM C192. Steel molds were used.

Demolding and Curing

The specimens were demolded 23-1/2 ± 1/2 hour after casting, labeled, and immediately placed in lime-saturated water. In accordance with Kansas Department of Transportation (KDOT) Test Method KTMR-22, the specimens were wet-cured in the lime-saturated water for 67 days, placed in an environmentally-controlled room at 50 percent ± 4 percent relative humidity and 73° ± 3° F (23° ± 2° C) for 21 days, placed in a water-filled, tempering tank maintained at 70° F (21° C) for 24 hours, and placed in a water-filled, insulated cooler maintained at 40° F (4.4° C) for 24 hours. The initial mass and fundamental transverse frequency of each specimen were measured to determine its dynamic modulus of elasticity. The procedures for determining mass, fundamental transverse frequency, and the dynamic modulus of elasticity are described following a description of the freeze-thaw testing regime.

Freezing and Thawing

The specimens were subjected to three-hour freeze-thaw cycles in accordance with ASTM C666 – Procedure B using a ScienTemp^{TM} 20-Block Concrete Freeze-Thaw Machine (Figure 2.4). The temperature was alternately lowered from 40 to 0° F (4 to -18° C) in air and raised from 0 to 40° F (-18 to 4° C) in water for a single freeze-thaw cycle. The specimens were removed from the machine in the thawed condition at intervals ranging from 4 to 48 cycles for determination of mass and fundamental transverse frequency. Testing continued until specimens were subjected to at least 300 freeze-thaw cycles or until the average dynamic modulus of elasticity of the specimens dropped to 60 percent of the initial dynamic modulus. ASTM C666 requires the mass and transverse frequency to be measured at intervals of no greater than 36 cycles. In 32 of 45 mixtures tested per ASTM C666, a portion of the measurements needed to complete testing were taken at intervals exceeding 36 cycles. On average, these 32 mixtures each had three of the intervals needed to complete testing exceed 36 cycles.

Figure 2.4 Freeze-thaw machine

To determine the dynamic modulus of elasticity, specimens were dried to a surface-dry condition and weighed after removal from the freeze-thaw machine. The specimens were immediately placed in an enclosed, storage cooler to prevent further moisture loss. The fundamental transverse frequency of each specimen was then determined in accordance with ASTM C215 – Impact Resonance Method (Figure 2.5) using the following equipment:

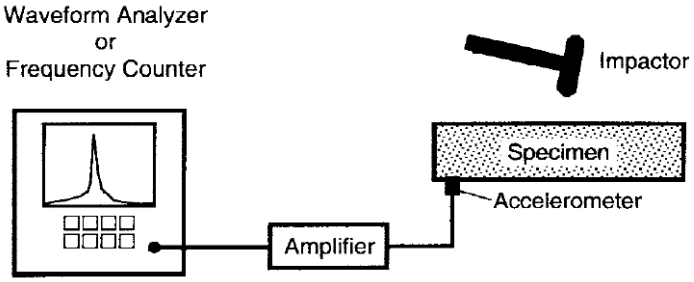

Figure 2.5 Schematic of impact resonance test (ASTM C215)

- National Instruments Impact Hammer
- Instron Accelerometer
- Data Physics SignalCalc Dynamic Signal Analyzer (Waveform Analyzer)
- Data Physics Signal Conditioner (Amplifier)

The fundamental transverse frequency, in Hz, was determined using a fast Fourier transform completed by the signal analyzer. Outside vibrations were damped out during testing by placing the specimens on a pedestal made of rubber and foam that supported the specimens at two points (Figure 2.6).

Figure 2.6 Impact resonance test – specimen setup

The dynamic modulus of elasticity was determined for each specimen using Eq. (2.1), which is based on the transverse frequency and specimen mass in accordance with ASTM C215.

$$Dyn.E = C \times M \times n^2 \tag{2.1}$$

In Eq. (2.1), $Dyn.E$ is the dynamic modulus of elasticity (Pa), C = 1083.6 m^{-1} and is a constant based on specimen shape and Poisson's ratio found in ASTM C125, M is the specimen mass (kg), and n is the fundamental transverse frequency (Hz). Specimens not handled in accordance with ASTM C666 were not included in the calculations. These specimens are identified along with the testing data in Appendix C. The

freeze-thaw performance of the mixtures was based on the percentage of the dynamic modulus of elasticity remaining at the test completion. The freeze-thaw performance was quantified by a Durability Factor (DF), determined for each mixture using Eq. (2.2).

$$DF = \frac{P \times N}{M} \tag{2.2}$$

In Eq. (2.2), DF is the Durability Factor, P is the percentage of the dynamic modulus of elasticity remaining at N cycles, N is either the number of cycles at which P reached 60 percent or 300 cycles (whichever is less), and M is 300 cycles.

2.4.3 Scaling Resistance

Scaling resistance tests were performed in accordance with Canadian Test BNQ NQ 2621-900 Annex B, with minor modifications, including different freeze-thaw cycle temperatures, a lower NaCl solution concentration, and a smaller screen size to determine mass loss. The Canadian Test was used in place of ASTM C672 due to observations by Bickley et al. (2006) that the Canadian Test provided a better correlation with field performance than ASTM C672. Three 9 × 16 × 3 in. (229 × 406 × 76 mm) specimens were cast in accordance with ASTM C192 using steel molds.

Demolding, Curing, and Specimen Preparation

The specimens were demolded 23-1/2 ± 1/2 hour after casting, labeled, and immediately placed in lime-saturated water to cure in accordance with ASTM C511 for 13 days (14 total curing days from casting date). After curing, the specimens were placed in an environmentally-controlled room with a relative humidity of 50 percent ± 4 percent and temperature of 73° ± 3° F (23° ± 2° C) for 14 days (Days 15 to 28 after casting). Twenty-one days after casting, a Styrofoam™ dike was attached

to the finished surface of the specimen using a polyurethane sealant (Figure 2.7). Twenty-eight days after casting, a 1/4-in. (6 mm) deep layer of 2.5 percent NaCl solution was placed within the dike of each specimen for a seven-day period at room temperature. The 2.5 percent NaCl solution value was selected in place of the BNQ NQ 2621-900 Annex B specified value of 3.0 percent based on work by Verbeck and Klieger (1957), who observed greater scaling with a 2.5 percent NaCl solution.

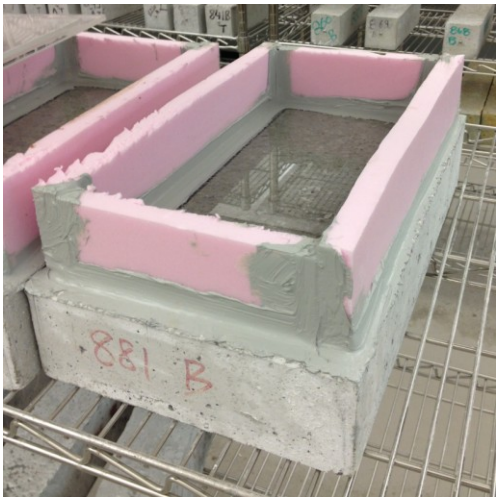

Figure 2.7 Scaling resistance test specimen

Freezing and Thawing and Determination of Mass Loss

The specimens were subjected to freeze-thaw cycles (beginning 35 days after casting), consisting of a 16 ± 1 hour freezing phase at 0° ± 5° F (–18° ± 3° C) followed by an 8 ± 1 hour thawing phase at 73° ± 3° F (23° ± 2° C). The freezing phase was performed each night in a walk-in freezer. The thawing phase was performed each day in the environmentally-controlled room used after curing. Specimens remained in the freezing phase during weekends. The temperatures used in the testing (described above) vary slightly from those specified by BNQ NQ 2621-900 Annex B. The BNQ NQ 2621-900 procedure requires a –0.4° ± 5.4° F (–18° ±

3° C) freezing phase followed by a 77° ± 5.4° F (25° ± 3° C) thawing phase. To determine mass loss of the specimens after 7, 21, 35, and 56 cycles, the loose material produced by scaling of the top surface of the specimen was wet-sieved over a No. 200 (75-µm) sieve instead of the BNQ NQ 2621-900 specified 80-µm sieve. Specimens not handled in accordance with BNQ NQ 2621-900 were not included in the determination of cumulative mass loss. These specimens are identified along with the testing data in Appendix C. BNQ NQ 2621-900 allows a maximum average cumulative mass loss limit of 0.31 lb/ft^2 (1500 g/m^2) at test completion.

2.4.4 Compressive Strength

Compressive strength was measured in accordance with ASTM C39 – Standard Test Method for Compressive Strength of Cylindrical Concrete Specimens. Three 4 × 8 in. (102 × 203 mm) cylindrical specimens were prepared for each batch of concrete in accordance with ASTM C192 and ASTM C31. The specimens were cast in steel molds.

Demolding, Curing, and Testing

The specimens were demolded 23-1/2 ± 1/2 hour after casting, labeled, and immediately placed in lime-saturated water to cure in accordance with ASTM C511 for 27 days (28 total curing days from casting date). The cylinders were tested for strength 28 days after casting in accordance with ASTM C39.

2.4.5 Hardened Concrete Air-Void Analysis

A hardened concrete air-void analysis was completed on cylindrical specimens in accordance with ASTM C457 – Standard Test Method for Microscopical Determination of Parameters of the Air-Void System in Hardened Concrete – Procedure A – Linear Traverse Method. Two 4 × 8 in. (102 × 203 mm) cylindrical specimens were prepared for each batch of concrete in accordance with ASTM C192 and ASTM C31. The specimens were cast in steel molds.

Demolding, Curing, and Analysis

The specimens were demolded 23-1/2 ± 1/2 hour after casting, labeled, and immediately placed in an environmentally-controlled, moist-curing room with a minimum relative humidity of 95 percent and a temperature of 73° ± 3° F (23° ± 2° C) for a minimum of 14 days. The cylinders were then transferred to the Kansas Department of Transportation Materials Laboratory for testing. The hardened concrete air content and air-void spacing factor of each cylinder was determined from the analysis.

2.5 TEST PROGRAMS

Fifty-three concrete batches, including twenty-nine unique types of mixtures, were evaluated that employ technologies to improve shrinkage and cracking performance. The mixtures incorporated either shrinkage-reducing admixtures or lightweight aggregate as a source of internal curing in conjunction with mineral admixtures. The freeze-thaw durability and scaling resistance of each batch was evaluated to determine overall durability performance. A hardened air-void analysis was performed on a portion of the batches to determine the effect of the material additions on the air-void system and relationships between the air-void system and durability performance. Correlations between compressive strength and shrinkage and durability performance were also evaluated.

The concrete was prepared in accordance with the methods described in this chapter. Plastic concrete was tested for slump (ASTM C143), air content (ASTM C173 – volumetric method), and temperature (ASTM C1064). The mixtures containing only portland cement as a cementitious material were proportioned using either 520 lb/yd^3 (308 kg/m^3) or 540 lb/yd^3 (320 kg/m^3) of Type I/II portland cement, a 0.44 or 0.45 water-cement ratio, and a target slump of 3 in. (75 mm). A small range of cement paste contents was used throughout the study to more clearly observe the effects of differences in materials (not the effects of paste content) on concrete

performance. The cement contents, water-cement ratios, and target slump were chosen to coincide with those required in the low-cracking high-performance concrete (LC-HPC) bridge deck specifications (Kansas Department of Transportation 2007b). Mixtures designated as "control" were designed and produced in accordance with the current LC-HPC specifications and used for comparison with mixtures incorporating the new technologies with LC-HPC. The numbers used to designate concrete batches represent the sequential order in which the concrete was batched.

The study involved three testing programs. A summary is provided explaining the purpose and scope of each program.

2.5.1 Program 1: Evaluation of Mixtures Containing Two Air-Entraining Admixtures Used in Conjunction with Shrinkage-Reducing Admixtures

Program 1 examined the free shrinkage performance, freeze-thaw durability, scaling resistance, compressive strength, and air-void system characteristics of concrete mixtures containing a surfactant-based or a polymer-based air-entraining admixture in conjunction with shrinkage-reducing admixtures. Air-entraining admixtures aid in the formation and stabilization of air-voids in concrete, providing improved freeze-thaw protection. Most air-entraining agents are surfactant-based and function by reducing the surface tension of water to promote the formation of air-voids through agitation during mixing (Mindess et al. 2003). Shrinkage-reducing admixtures provide improved concrete shrinkage and cracking performance by way of a similar reduction in pore water surface tension (Bentz 2005). This additional reduction in surface tension can decrease the stability of the air-void system by increasing the size and spacing of the air bubbles, thus, contributing to reduced freeze-thaw protection. A polymer-based air-entraining agent, presumably not influenced by the effects on pore water surface tension, has been developed in an effort to improve air-void system stability and freeze-thaw protection. The polymer-

based admixture generates a foam through use of aeration equipment. The foam is then dispersed throughout the concrete during mixing (Welker and Watson 2007).

Twenty-four batches containing dosages of 0, 0.5, 1.0, and 2.0 percent by weight of cement of two shrinkage-reducing admixtures, Tetraguard AS20 (referred to as SRA in specimen designations) and MasterLIFE CRA 007 (referred to as CRA for "crack-reducing admixture" in specimen designations) and surfactant-based (Micro Air) and polymer-based (Tough Air) air-entraining agents were examined. Compressive strengths were measured for 20 of the batches in accordance with ASTM C39. A hardened concrete air-void analysis was performed on 20 of the batches in accordance with ASTM C457. Comparisons were made between hardened concrete and plastic concrete air contents to observe any effects of the shrinkage-reducing admixtures on the air-void systems. Relationships were determined between the air-void spacing factor and freeze-thaw durability and scaling resistance. Powers (1949) observed that the air-void spacing factor was important in determining freeze-thaw durability. An air-void spacing factor of 0.008 in. (0.20 mm) was empirically established by Philleo (1986) as an upper limit to provide adequate freeze-thaw protection.

The mixture matrix for this program is shown in Table 2.1. The material samples (summarized in Section 2.2) used in each mixture are identified in Table A.6 in Appendix A. The mixture proportions are summarized in Table A.7 in Appendix A. The mixtures are designated by percentage of SRA/CRA by weight of cement (0, 0.5, 1.0, and 2.0 percent) and whether Micro Air (designated with an "M") or Tough Air (designated with a "T") was used. Duplicate batches were tested for a number of mixtures to evaluate repeatability and are referred to with a #2 or #3 throughout the program. Ultimately, 14 distinct mixtures were investigated within the 24 batches. The mixtures containing 520 lb/yd^3 (308 kg/m^3) of cement were proportioned using a water-cement ratio of 0.45, except for one mixture containing Tough Air and no

Table 2.1 Program 1: Mixture matrix

	Batch Description	Mixture Designation	Batch Number
Control & Micro Air	Control w/ MicroAir	0% SRA-M	730
	Control w/ MicroAir	0% SRA-M #2	754
	Control w/ MicroAir	0% SRA-M #3	796
SRA & Micro Air	0.5% SRA w/ MicroAir	0.5% SRA-M	769
	0.5% SRA w/ MicroAir	0.5% SRA-M #2	834
	1% SRA w/ MicroAir	1.0% SRA-M	722
	1% SRA w/ MicroAir	1.0% SRA-M #2	816
	2% SRA w/ MicroAir	2.0% SRA-M	727
	2% SRA w/ MicroAir	2.0% SRA-M #2	820
CRA & Micro Air	0.5% CRA w/ MicroAir	0.5% CRA-M	732
	1% CRA w/ MicroAir	1.0% CRA-M	735
	1% CRA w/ MicroAir	1.0% CRA-M #2	843
	2% CRA w/ MicroAir	2.0% CRA-M	845
Control & Tough Air	Control w/ ToughAir	0% SRA-T	772
	Control w/ ToughAir	0% SRA-T #2	807
SRA & Tough Air	0.5% SRA w/ ToughAir	0.5% SRA-T	781
	0.5% SRA w/ ToughAir	0.5% SRA-T #2	808
	1% SRA w/ ToughAir	1.0% SRA-T	782
	1% SRA w/ ToughAir	1.0% SRA-T #2	810
	2% SRA w/ ToughAir	2.0% SRA-T	786
	2% SRA w/ ToughAir	2.0% SRA-T #2	811
CRA & Tough Air	0.5% CRA w/ ToughAir	0.5% CRA-T	789
	1% CRA w/ Tough Air	1.0% CRA-T	790
	2% CRA w/ ToughAir	2.0% CRA-T	794

SRA (designated as 0% SRA-T #2), which had a water-cement ratio of 0.44. The mixtures containing 540 lb/yd^3 (320 kg/m^3) of cement were proportioned using a water-cement ratio of 0.44. Cement paste contents ranged from 23.7 to 24.3 percent by volume, except for one batch with a 23.4 percent paste content (0% SRA-T #2). The measured air contents were considered when determining the percentage of the total concrete volume that was cement paste (water and cement). The test matrix is shown in Table 2.2.

The properties of the concrete batches, including slump, air content, batching temperature, unit weight, and 28-day compressive strength, are summarized in Table

Table 2.2 Program 1: Test matrix*

Mixture Designation	Free Shrinkage	Thaw Durability	Scaling Resistance	Compressive Strength	Air-Void Analysis
0% SRA-M			X	X	X
0% SRA-M #2		X	X	X	
0% SRA-M #3	X	X	X		X
0.5% SRA-M		X	X	X	X
0.5% SRA-M #2	X	X	X	X	X
1.0% SRA-M			X	X	X
1.0% SRA-M #2	X	X	X		X
2.0% SRA-M			X	X	
2.0% SRA-M #2	X	X	X	X	X
0.5% CRA-M			X	X	
1.0% CRA-M		X	X	X	
1.0% CRA-M #2	X			X	X
2.0% CRA-M	X			X	X
0% SRA-T		X	X		X
0% SRA-T #2	X	X	X	X	X
0.5% SRA-T		X	X	X	X
0.5% SRA-T #2	X	X	X	X	X
1.0% SRA-T		X	X	X	X
1.0% SRA-T #2	X	X	X	X	X
2.0% SRA-T		X	X	X	X
2.0% SRA-T #2	X	X	X	X	X
0.5% CRA-T		X	X		X
1.0% CRA-T		X	X	X	X
2.0% CRA-T		X	X	X	X

*X = test performed

A.8 in Appendix A. The mixtures were proportioned using a target air content of 8 percent to achieve compliance with LC-HPC specifications. The volume of air used in LC-HPC mixtures (6.5 to 9.5 percent) is greater than the 5 to 6 percent recommended by the American Concrete Institute (ACI) to achieve satisfactory frost protection for concrete with 1 in. (25 mm) maximum-size aggregate (ACI Committee 201). The lower limit of air content required by the LC-HPC specifications is based on observations by Schmitt and Darwin (1995), Miller and Darwin (2000), and Lindquist et al. (2005) that bridge decks placed with concretes with air contents above

6 percent exhibit reduced cracking. The upper limit of the specifications helps ensure that adequate concrete strength is achieved.

Measured concrete slumps ranged from 1.75 to 5 in. (44 to 127 mm), measured air contents ranged from 7.5 to 9.5 percent, batching temperatures ranged from 65 to 76° F (18 to 24° C), and 28-day compressive strengths ranged from 3390 to 5270 psi (23.4 to 36.4 MPa). One batch containing a 2.0 percent dosage of SRA by weight of cement with Tough Air (designated as 2.0% SRA-T #2) had a compressive strength of 5420 psi (37.3 MPa), but was tested at 37 days.

2.5.2 Program 2: Durability Evaluation of Mixtures Containing Shrinkage-Reducing Admixtures with Air Contents below LC-HPC Requirements

Program 2 examined the freeze-thaw durability and scaling resistance of mixtures containing varying dosages of shrinkage-reducing admixture with air contents below that required by the low-cracking high-performance concrete (LC-HPC) specifications. The reduction in pore water surface tension that occurs with the use of shrinkage-reducing admixtures affects the stability of the air-void system, which can contribute to freeze-thaw damage. The LC-HPC specifications require a minimum air content of 6.5 percent. The variability in batch plant concrete production during continuous concrete placement in the field contributes to the occasional batch of concrete containing air contents below the specified value, which may result in poor freeze-thaw and cracking performance – performance that may be further degraded due to the lower stability of the air-void system when shrinkage-reducing admixtures are used.

This program examined the freeze-thaw durability and scaling resistance of 16 batches, including 16 distinct mixtures, to determine their behavior in bridge deck construction applications. Six of these sixteen batches, identified as Batch Numbers 722, 754, 769, 796, 816, and 820, were also included in the evaluation of Program 1. The mixtures contained 0, 0.5, 1.0, and 2.0 percent by weight of cement of the

shrinkage-reducing admixture Tetraguard AS20 (SRA in specimen designations) and air contents ranging from 3.5 to 9 percent. The range of air contents was obtained using varying dosages of Micro Air. Compressive strengths were measured for 12 of the batches in accordance with ASTM C39. A hardened concrete air-void analysis was completed on 14 of the mixtures in accordance with ASTM C457 A goal of this program was to determine a lower allowable limit for air content that could be used for mixtures containing shrinkage-reducing admixtures that would still exhibit adequate freeze-thaw durability. This lower allowable limit could then be translated into air-content restrictions for bridge deck placements with concretes containing shrinkage-reducing admixtures.

The list of mixtures and the test matrix are shown in Table 2.3. The material samples used in each mixture are identified in Table A.9 in Appendix A. The mixture proportions are summarized in Table A.10 in Appendix A. The mixtures are designated by percentage of SRA by weight of cement (0, 0.5, 1.0, and 2.0 percent) and air content. The mixtures containing 520 lb/yd^3 (308 kg/m^3) of cement were proportioned using a water-cement ratio of 0.45 and the mixtures containing 540 lb/yd^3 (320 kg/m^3) of cement were proportioned using a water-cement ratio of 0.44. The batches in this program contain a wider range of cement paste contents (23.0 to 25.4 percent by volume) than the other two programs due to the wide range of air contents that were tested (concretes with lower air contents have less volume being taken up by air voids).

The properties of the concrete batches are summarized in Table A.11 in Appendix A, which includes slump, air content, batching temperature, unit weight, and 28-day compressive strength. Five of the sixteen mixtures contained air contents below that recommended by ACI to achieve satisfactory frost protection for concrete with 1 in. (25 mm) maximum-size aggregate (5 to 6 percent) (ACI Committee 201).

Table 2.3 Program 2: Mixture and test matrix*

	Mixture Designation	Batch Number	Freeze-Thaw Durability	Scaling Resistance	Compressive Strength	Air-Void Analysis
Control	Control w/ 3.5% air	828	X	X	X	X
	Control w/ 6% air	839	X	X	X	X
	Control w/ 8.75% air	754	X	X	X	
	Control w/ 9% air	796	X	X		X
0.5% SRA	0.5% SRA w/ 4% air	832	X	X	X	X
	0.5% SRA w/ 7% air	833	X	X	X	X
	0.5% SRA w/ 8% air	769	X	X	X	X
1% SRA	1% SRA w/ 5.25% air	830	X	X	X	X
	1% SRA w/ 6.75% air	814	X	X		X
	1% SRA w/ 7.75% air	816	X	X		X
	1% SRA w/ 8.75% air	722		X	X	X
2% SRA	2% SRA w/ 3.5% air	817	X	X		
	2% SRA w/ 3.75% air	831	X	X	X	X
	2% SRA w/ 4.75% air	838	X	X	X	X
	2% SRA w/ 7% air	836	X	X	X	X
	2% SRA w/ 8.25% air	820	X	X	X	X

*X = test performed

Measured concrete slumps ranged from 1.5 to 3 in. (38 to 76 mm), measured air contents ranged from 3.5 to 9 percent, batching temperatures ranged from 64 to 75° F (18 to 24° C), and 28-day compressive strengths ranged from 4350 to 6700 psi (30.0 to 46.2 MPa). Four of the sixteen batches had compressive strengths exceeding the upper strength limit of 5500 psi (37.9 MPa) permitted by the LC-HPC bridge deck specifications. The high strengths resulted from the low air contents. Concretes containing low air contents will not only experience reduced freeze-thaw durability, but because of their high strength will also experience reduced creep effects, which decreases concrete stresses and cracking.

2.5.3 Program 3: Evaluation of Mixtures Containing Mineral Admixtures Used in Conjunction with Internal Curing

Program 3 examined the free shrinkage performance, freeze-thaw durability, scaling resistance, compressive strength, and air-void system characteristics of mixtures containing different combinations of pre-wetted lightweight aggregate, slag

cement, and silica fume. A previous study at the University of Kansas (Reynolds et al. 2009, Browning et al. 2011) determined that small additions of pre-wetted lightweight aggregate, which provide internal curing water, contribute to reduced free shrinkage in concretes with water-cement ratios above that at which internal curing is used to control autogenous shrinkage. The researchers observed additional reduction in free shrinkage as lightweight aggregate was used in conjunction with increasing amounts of slag cement.

It is well understood that concretes containing silica fume exhibit a reduction in permeability and improved resistance to chloride ion penetration. Research at the University of Kansas (McLeod et al. 2009) determined that additions of slag cement and silica fume contribute to a reduction in chloride ingress. This reduced permeability could improve the durability of bridge decks as long as the addition of the silica fume does not contribute to increased cracking and decreased freeze-thaw durability performance. In addition, Bentur et al. (1988) explained that concrete containing silica fume experiences a slower rate of water loss during drying as a result of the reduced permeability. If sufficient internal curing water is supplied to the concrete through pre-wetted lightweight aggregate, the reduced permeability provided by the silica fume could reduce drying shrinkage because the internal water is unable to quickly reach the surface, and thus evaporate.

Twenty-one batches containing different combinations of replacements of total aggregate with lightweight aggregate (0, 8, and 10 percent by volume), replacements of portland cement with slag cement (0 and 30 percent by volume), and replacements of portland cement with silica fume (0, 3, and 6 percent by volume) were examined. A number of studies have observed reduced freeze-thaw durability and scaling resistance in mixtures containing slag (Gunter, Bier, and Hilsdorf 1987, Malhotra et al. 1987, Bilodeau and Ludwig 1992, Stark and Ludwig 1997) and silica fume (Pigeon et al. 1987, Sabir and Kouyiali 1991). The freeze-thaw durability and

scaling resistance of the mixtures in the study were examined to verify their overall durability for use in bridge deck construction. Relationships were developed between the air-void system characteristics and the durability of each mixture.

The batches within this program were examined based on free shrinkage, freeze-thaw durability, scaling resistance, compressive strength, and a hardened air-void analysis. Compressive strengths were measured for 19 of the batches in accordance with ASTM C39. These compressive strengths are summarized in Table A.14 of Appendix A. Tables 2.4 through 2.7 show the batches (with mixture designations) that were examined in the tests. Two of the twenty-one batches examined in Program 3 were also examined in Programs 1 and 2 (Batch Numbers 754 and 796). Duplicate batches were examined for the mixtures evaluated in each test to determine repeatability of the results. The duplicate batches were organized into different series for each test (for example, Series 2 and Series 3). Six distinct mixture designs were evaluated in the program, including:

- no lightweight aggregate or mineral admixtures (designated as Control),
- an 8 percent replacement of total aggregate by volume with lightweight aggregate (designated as 8% LWA),
- a 10 percent replacement of total aggregate by volume with lightweight aggregate (designated as 10% LWA),
- a 10 percent replacement of total aggregate by volume with lightweight aggregate and a 30 percent replacement of portland cement by volume with slag cement (designated as 10% LWA, 30% slag),
- a 10 percent replacement of total aggregate by volume with lightweight aggregate, a 30 percent replacement of portland cement by volume with slag cement, and a 3 percent replacement of portland cement by volume with silica fume (designated as 10% LWA, 30% slag, 3% SF),

Table 2.4 Program 3: Free shrinkage test mixtures

	Mixture Designation	Batch Number
Series 1	Control	796
	8% LWA	827
	10% LWA	826
	10% LWA, 30% Slag	821
	10% LWA, 30% Slag, 3% SF	823
	10% LWA, 30% Slag, 6% SF	822
Series 2	Control	876
	10% LWA	873
	10% LWA, 30% Slag, 3% SF	869
	10% LWA, 30% Slag, 6% SF	870

Table 2.5 Program 3: Freeze-thaw durability test mixtures

	Mixture Designation	Batch Number
Series 1	Control	754
	8% LWA	756
	10% LWA	758
	10% LWA, 30% Slag	759
	10% LWA, 30% Slag, 3% SF	764
	10% LWA, 30% Slag, 6% SF	767
Series 2	Control	796
	8% LWA	798
	10% LWA	799
	10% LWA, 30% Slag	801
	10% LWA, 30% Slag, 3% SF	802
	10% LWA, 30% Slag, 6% SF	803

Table 2.6 Program 3: Scaling resistance test mixtures

	Mixture Designation	Batch Number
Series 1	Control	754
	8% LWA	756
	10% LWA	758
	10% LWA, 30% Slag	759
	10% LWA, 30% Slag, 3% SF	764
	10% LWA, 30% Slag, 6% SF	767
Series 2	Control	796
	8% LWA	798
	10% LWA	799
	10% LWA, 30% Slag	801
	10% LWA, 30% Slag, 3% SF	802
	10% LWA, 30% Slag, 6% SF	803
Series 3	Control	796
	8% LWA	827
	10% LWA	826
	10% LWA, 30% Slag	821
	10% LWA, 30% Slag, 3% SF	823
	10% LWA, 30% Slag, 6% SF	822

Table 2.7 Program 3: Hardened air-void analysis mixtures

	Mixture Designation	Batch Number
Series 1	8% LWA	756
	10% LWA	758
	10% LWA, 30% Slag	759
	10% LWA, 30% Slag, 3% SF	764
	10% LWA, 30% Slag, 6% SF	767
Series 2	Control	796
	8% LWA	798
	10% LWA	799
	10% LWA, 30% Slag	801
	10% LWA, 30% Slag, 3% SF	802
	10% LWA, 30% Slag, 6% SF	803
Series 3	Control	796
	8% LWA	827
	10% LWA	826
	10% LWA, 30% Slag	821
	10% LWA, 30% Slag, 3% SF	823
	10% LWA, 30% Slag, 6% SF	822

- a 10 percent replacement of total aggregate by volume with lightweight aggregate, a 30 percent replacement of portland cement by volume with slag cement, and a 6 percent replacement of portland cement by volume with silica fume (designated as 10% LWA, 30% slag, 6% SF).

The material samples used in each batch are identified in Table A.12 in Appendix A. The constituent proportions of the mixtures are summarized in Table A.13 in Appendix A. Cement paste contents ranged from 23.4 to 24.0 percent of total volume. The mixtures were designed to remain within a small range of paste contents by volume rather than a small range of cementitious material contents by weight, causing the mixtures containing slag and slag and silica fume to have lower cementitious material contents by weight than the mixtures containing only portland cement as a cementitious material.

Moisture contents of the vacuum pre-wetted lightweight aggregate used in the batches ranged from 20.3 to 28.4 percent. The moisture contents, in fact, exceeded the absorption value of 16 percent reported by Buildex in Table A.4 of Appendix A. The range of lightweight aggregate moisture contents stems from variability in the vacuum pre-wetting process. A large amount of water is held within lightweight aggregate compared to the other aggregates used in the batches (> 20 percent vs. < 1 percent of total aggregate weight), resulting in a large increase in available internal curing water. The water held by the aggregate in 10 of the batches is shown in Table A.13 in Appendix A. The mixtures that contain a 10 percent replacement by volume of total aggregate with lightweight aggregate hold, on average, nearly three times as much water in the aggregate as the mixtures that contain no lightweight aggregate [66.0 vs. 23.1 lb/yd^3 (39.2 vs. 13.7 kg/m^3)]. Each mixture was proportioned using a target air content of 8 percent to achieve compliance with LC-HPC specifications.

The properties of the concrete batches are summarized in Table A.14 of Appendix A (slump, air content, batching temperature, unit weight, and 28-day

compressive strength). Measured concrete slumps ranged from 1.5 to 3.25 in. (38 to 83 mm), measured air contents ranged from 7.0 to 9.0 percent, batching temperatures ranged from 61 to 77° F (16 to 25° C), and 28-day compressive strengths ranged from 3620 to 5660 psi (25.0 to 39.0 MPa). One batch, containing a 10 percent replacement of total aggregate by volume with lightweight aggregate, a 30 percent replacement of portland cement by volume with slag cement, and a 3 percent replacement of portland cement by volume with silica fume, exhibited a compressive strength of 5660 psi (39.0 MPa), which is out of the range of 3500 to 5500 psi (24.1 to 37.9 MPa) required by the LC-HPC specifications (Kansas Department of Transportation 2007b).

2.6 DATA COLLECTION DURING BRIDGE DECK CONSTRUCTION

Representatives from the University of Kansas were in attendance during the construction of each LC-HPC bridge deck to accomplish two objectives. First, the representatives provided guidance to the contractors to better achieve compliance with the LC-HPC specifications (Kansas Department of Transportation 2007a,b,c). Second, the representatives collected data throughout construction to determine the level of compliance that was achieved with respect to the LC-HPC specifications. The data was then used in the evaluation of cracking performance of the decks to aide in determining the parameters that affect cracking. A description of the type of data collected and method of data collection is presented in this section. In addition to the data collected during construction described in this section, trip tickets for the concrete, dates of form removal, and concrete cylinder strengths were measured after construction.

2.6.1 Environmental Conditions

The evaporation rate prior to and during placement was determined and recorded at least once per hour using the nomograph displayed in Figure 1.1. As explained in Section 1.2.1.1, high evaporation rates during construction contribute to

drying of the concrete surface and the formation of plastic shrinkage cracks. The evaporation rate is a function of air temperature, wind speed, relative humidity, and concrete temperature. The LC-HPC specifications require actions to be taken, such as cooling the concrete or the installation of wind breaks, if the evaporation rate exceeds 0.2 lb/ft^2/hr (1.0 kg/m^2/hr).

The temperatures of the steel girder flanges and web are checked and recorded on occasion during construction. As explained in Section 1.2.2, warm concrete placed on cool girders can induce thermal stresses in the deck as the concrete and girders return to ambient temperatures.

2.6.2 Plastic Concrete Properties

Plastic concrete properties were tested by Kansas Department of Transportation (KDOT) personnel and recorded by University of Kansas representatives during construction. The concrete slump, air content, unit weight, and temperature were measured at a frequency required by the LC-HPC specifications. The location at which the concrete was tested (from the truck or pump discharge) was recorded. Truck identification number, discharge time, and concrete volume were recorded to approximate the placement location of the truckload on the bridge deck and to determine delivery and placement rates. The trucks from which compressive strength cylinders were cast were identified and recorded. General notes of interest were recorded as events occurred that could affect the cracking performance of the bridge deck, such as delivery and placement delays, placement of out-of-specification concrete, or concrete testing methods that did not comply with the specifications.

2.6.3 Burlap Placement

Time periods between concrete finishing and burlap placement were determined by recording “time of concrete finish” and “time of burlap placement” at predetermined increments along the bridge. Average times to burlap placement were

calculated from the data. The LC-HPC specifications require placement of a first layer of saturated burlap within ten minutes of strikeoff, followed by a second layer within another five minutes. The placement of the first layer was recorded as the time of burlap placement. The degree of burlap saturation was monitored throughout construction. Causes of delays in burlap placement and improper placement were observed and noted. General observations, such as improper finishing techniques and over or under-wetting of the already-placed burlap, were noted.

2.7 EVALUATION OF LOW-CRACKING HIGH-PERFORMANCE CONCRETE (LC-HPC) BRIDGE DECKS

2.7.1 Crack Surveys

Crack surveys were completed annually on each LC-HPC and associated control deck to quantitatively evaluate cracking performance through determination of a crack density. A standard procedure, summarized below, is followed for each crack survey to provide an accurate comparison of results. The full bridge deck survey specifications are provided in Appendix B.

Surveys are conducted between sunrise and sunset on days that are mostly sunny. Regardless of weather conditions, the bridge decks must be completely dry before the survey can begin, and the air temperature must be 60° F (16° C) or above.

A scaled plan of the deck is created for each bridge deck to serve as a template for indicating locations and lengths of cracks on the actual deck. The plan is created at a scale of 1 in. = 10 ft (25.4 mm = 3.048 m) and should include compass and traffic directions, deck stationing, and a 5 × 5 ft (1.524 × 1.524 m) grid. A scaled grid is placed underneath the deck plan to allow for accurate transfer of data from the deck to the plan.

After traffic has been closed, grid markings are placed on the deck at 5-ft (1.524-m) increments in the longitudinal and transverse directions using sidewalk chalk, corresponding with the scaled bridge deck plan. The survey process consists

of surveyors marking visible cracks with sidewalk chalk as they walk over the entire deck. Surveyors bend at the waist and mark cracks that can be seen from this position. After a crack has been located from this position, the surveyor is allowed to get a closer view of the crack to complete the trace to the end of the crack. At least one other surveyor will then recheck the marked portion of the deck for additional cracks. This method has been shown to provide a consistent measure of cracking from bridge to bridge (Lindquist et al. 2005, 2008). Another surveyor will transfer the marked cracks on the deck to the scaled crack map, using the scaled grid to accurately represent crack locations and lengths.

Once a survey is complete, the crack maps are scanned and prepared for computer analysis. Each scanned map is edited so that pixels are darkened to the proper shade and crack lines are continuous from beginning to end. All non-crack lines on the scanned crack map, including deck boundaries, stationing, and compass direction, must be erased in the scanned image so that only the pixels from the cracks are analyzed. Nonlinear cracks are broken into shorter linear segments by removing single pixels so the analysis program, which measures between end points, can accurately calculate total crack lengths. The analysis program tracks the number of adjacent pixels (that are sufficiently dark) (Lindquist et al. 2005). Crack densities for the entire deck, as well as various portions of the deck, are measured and reported. The crack densities are used in the evaluation of the LC-HPC and control decks in Chapter 6.

CHAPTER 3: FREE-SHRINKAGE AND DURABILITY EVALUATION OF MIXTURES CONTAINING SHRINKAGE-REDUCING ADMIXTURES

3.1 OVERVIEW

This chapter presents evaluations of mixtures containing shrinkage-reducing admixtures. The objective of these evaluations was to identify concrete mixtures that exhibit low shrinkage characteristics while maintaining high freeze-thaw durability and scaling resistance for use in bridge deck field applications. The evaluations included two programs (1 and 2), described in Chapters 1 and 2. In addition to free shrinkage, Program 1 examined the effects of two air-entraining admixtures on the freeze-thaw durability, scaling resistance, compressive strength, and air-void system stability of mixtures containing one of two shrinkage-reducing admixtures. Similar evaluations were performed in Program 2 but on mixtures with air contents below that required by the low-cracking high-performance concrete (LC-HPC) specifications. The results of the two programs are discussed in the Sections 3.2 and 3.3.

3.1.1 Statistical Analysis

The Student's t-test was used to determine the statistical significance of differences in the performance of individual mixtures. The Student's t-test is a parametric analysis that verifies whether the difference in the means of two samples, X_1 and X_2, represent a difference in the population means, μ_1 and μ_2, at a specified level of significance α. The t-test is frequently used when sample sizes are small and population characteristics are unknown, such as with the evaluations in this study. The t-test depends on the means of two sample groups, the size of the samples, and the standard deviation of each group to determine the level of statistical significance. The degree of statistical significance between the differences is represented by the level of significance for which the difference does not occur by chance. For example,

a significance level of $\alpha = 0.02$ indicates that there is a 2 percent probability that the test will incorrectly identify (or a 98 percent probability that the test will correctly identify) a statistically significant difference in sample means when, in fact, there is no difference (a difference). A two-sided test was used in the analyses, meaning that there was a probability of $\alpha/2$ of finding that $\mu_1 > \mu_2$ and a probability of $\alpha/2$ of finding that $\mu_1 < \mu_2$ when, in fact, μ_1 and μ_2 were equal. The results of the Student's t-test are presented in tables in the following format: Significance levels of at least $\alpha = 0.02$ (at least a 98 percent probability) and less than $\alpha = 0.20$ (less than an 80 percent probability) are represented by "Y" and "N", respectively. In addition, significance levels α of at least = 0.05, 0.10, and 0.20 are represented by "95%", "90%", and "80%", respectively.

3.2 EVALUATION OF MIXTURES CONTAINING TWO AIR-ENTRAINING ADMIXTURES USED IN CONJUNCTION WITH SHRINKAGE-REDUCING ADMIXTURES (PROGRAM 1)

3.2.1 General

The results from Program 1, described in Sections 1.8.1.1 and 2.5.1, are presented in this section. The program examined the effects of surfactant-based and polymer-based air-entraining admixtures on the air-void system stability, freeze-thaw durability, scaling resistance, and compressive strength of concrete mixtures containing different dosages of two shrinkage-reducing admixtures. In addition, the free shrinkage performance of mixtures containing the two shrinkage-reducing admixtures was evaluated as a function of dosage. As explained in Sections 1.8.1.1 and 2.5.1, surfactant-based air-entraining admixtures and shrinkage-reducing admixtures function similarly by reducing the surface tension of water. When these admixtures are used together, a sizeable reduction in surface tension takes place that can decrease the stability of the air-void system and contribute to reduced freeze-thaw protection. Concrete containing a polymer-based air-entraining admixture,

presumably not influenced by surface tension, was compared with concrete containing a surfactant-based air-entraining admixture based on the air-void stability and freeze-thaw durability of mixtures that contained a shrinkage-reducing admixture.

Three factors, dosage and type of shrinkage-reducing admixture and type of air-entraining admixture, were examined to determine their effect on free shrinkage, freeze-thaw durability, scaling resistance, compressive strength, and air-void system characteristics. Twenty-four batches of concrete containing dosages of 0, 0.5, 1.0, and 2.0 percent by weight of cement of shrinkage-reducing admixtures Tetraguard AS20 (referred to as SRA in specimen designations) and MasterLIFE CRA 007 (referred to as CRA for "crack-reducing admixture" in specimen designations), and a surfactant-based (Micro Air) or polymer-based (Tough Air) air-entraining admixture were examined. The 24 batches included 10 duplicate batches to determine test repeatability. Detailed information regarding the test program is provided in Section 2.5.1. The mixtures examined in each test, including descriptions, batch numbering, and name designations, are shown in Tables 2.1 and 2.2. The mixture proportions, concrete properties, and compressive strengths of each batch are summarized in Tables A.7 and A.8 in Appendix A. The mixture proportions were selected to comply with the LC-HPC specifications. The mixtures had cement contents of 520 or 540 lb/yd^3 (308 or 320 kg/m^3) and water-cement ratios of 0.44 or 0.45, resulting in cement paste contents ranging from 23.4 to 24.3 percent by volume. The mixtures were proportioned using a target air content of 8 percent and a target slump of 2.25 ± 0.75 in. (55 ± 20 mm).

The mixtures are evaluated for free shrinkage per ASTM C157, freeze-thaw durability in accordance with ASTM C666 – Procedure B with modifications per Kansas Department of Transportation Test Method KTMR-22, and scaling resistance per Canadian Test BNQ NQ 2621-900 Annex B with some modifications. Compressive strengths were measured in accordance with ASTM C39 and a hardened

air-void analysis was completed in accordance with ASTM C457. The results of these evaluations are presented in the following sections. Detailed information regarding the procedures of the tests is provided in Chapter 2.

3.2.2 Free Shrinkage

A number of studies have observed progressively lower free shrinkage in concrete with increased dosages of shrinkage-reducing admixture. Lindquist et al. (2008) investigated the effect of shrinkage-reducing admixtures at dosages of 0, 1, and 2 percent by weight of cement and observed a reduction in both early-age and long-term shrinkage with increasing dosages. Yuan et al. (2011) also observed decreased free shrinkage as dosages of shrinkage-reducing admixture were increased from 0 to 0.5 percent and again to 1.0 percent by weight of cement. Balogh (1996) and Tomita (1992) observed shrinkage-reducing admixtures to be most effective at dosages of 1.5 to 2.0 percent by weight of cement.

In Program 1, 10 concrete mixtures were examined evaluating the effects of dosage and type of shrinkage-reducing admixture on free shrinkage. The ten mixtures included six that contained the surfactant-based air-entraining admixture (Micro Air) and four that contained the polymer-based admixture (Tough Air). Four dosages of the SRA (0, 0.5, 1.0, and 2.0 percent by weight of cement) were tested for mixtures containing both the Micro Air and Tough Air. In addition, mixtures containing two dosages of the CRA (1.0 and 2.0 percent by weight of cement) were tested with Micro Air. The type of air-entraining admixture used in the mixtures was not expected to have an effect on the free shrinkage performance. All specimens were wet-cured for 14 days and then subjected to drying, as described in Section 2.4.1.

The average free shrinkage of three specimens from each mixture is plotted as a function of drying period for 30, 90, 180, and 365 days in Figures 3.1 through 3.4,

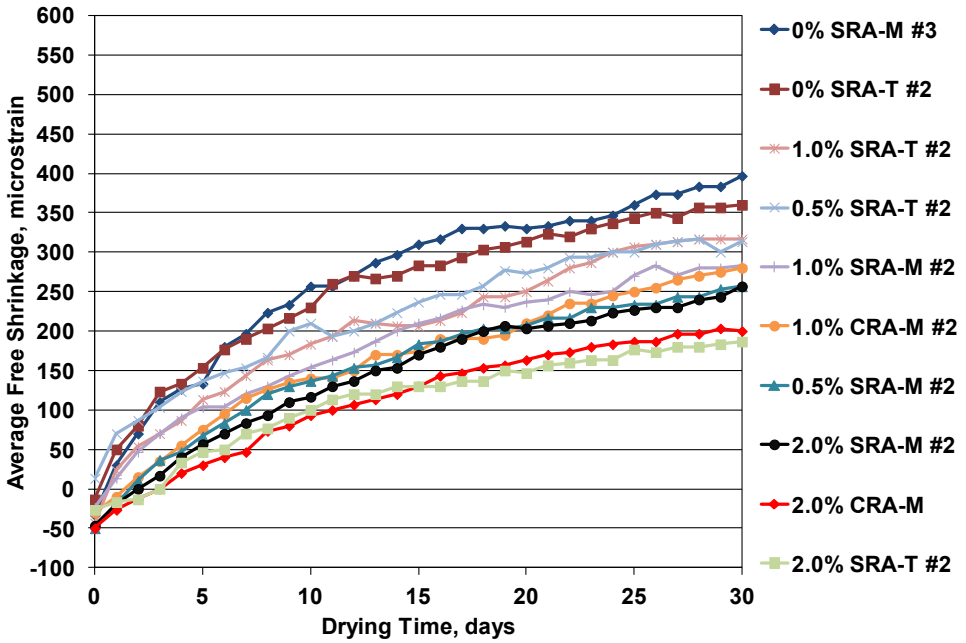

Note: Notation used for mixture designations explained in Section 2.5.1

Figure 3.1 Average free shrinkage versus drying time through 30 days for mixtures in Program 1

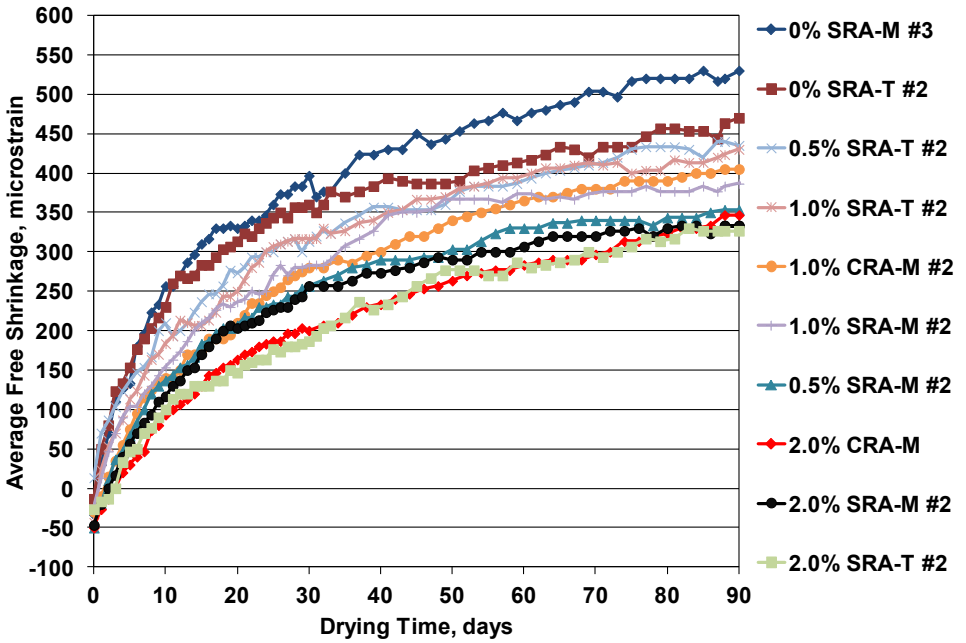

Note: Notation used for mixture designations explained in Section 2.5.1

Figure 3.2 Average free shrinkage versus drying time through 90 days for mixtures in Program 1

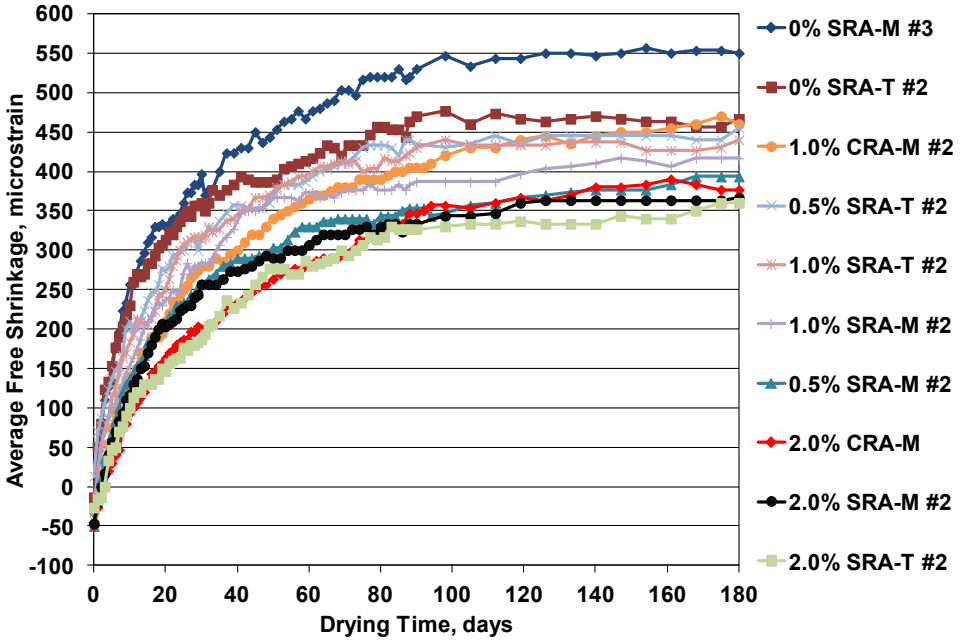

Note: Notation used for mixture designations explained in Section 2.5.1

Figure 3.3 Average free shrinkage versus drying time through 180 days for mixtures in Program 1

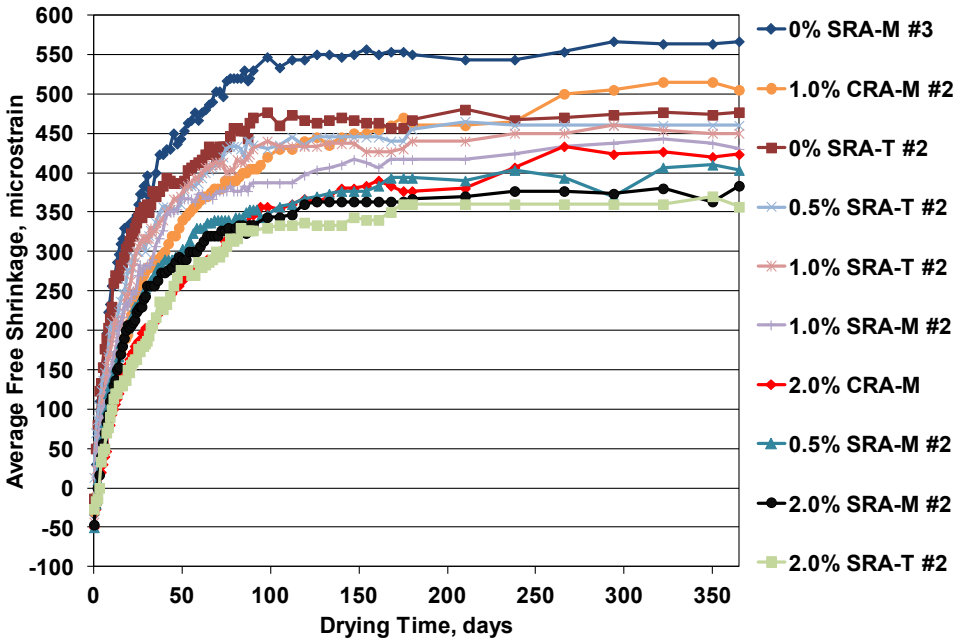

Note: Notation used for mixture designations explained in Section 2.5.1

Figure 3.4 Average free shrinkage versus drying time through 365 days for mixtures in Program 1

respectively. The mixtures in the figures are compared based on dosage and type of shrinkage-reducing admixture and type of air-entraining admixture. In the figure legends, the mixtures are listed in the order of descending shrinkage at the end of the period shown. The average shrinkage strains for drying periods of 0, 30, 90, 180, and 365 days are summarized in Table 3.1. Early-age shrinkage (out to 90 days) is of particular importance for structures with restrained dimensional change, such as concrete bridge decks, due to the large percentage of the total shrinkage that occurs during this time and the moderately short period available for creep to reduce tensile stresses. The negative shrinkage shown in Table 3.1 indicates that swelling occurred during the 14-day wet-curing period. The statistical significance of the differences in free shrinkage determined from the Student's t-test are shown in Tables 3.2 through 3.5. The mixtures are compared based on two variables (dosage of SRA and type of air-entraining admixture) in Tables 3.2 and 3.4 and one variable (type of shrinkage-reducing admixture) in Tables 3.3 and 3.5. Shrinkage values after 30 days of drying are evaluated in Tables 3.2 and 3.3, while the values after 365 days are evaluated in Tables 3.4 and 3.5. The free shrinkage values used in the t-test are shown in the tables.

As shown in Figures 3.1 through 3.4 and Table 3.1, the shrinkage for the 10 mixtures ranged from 187 to 397 microstrain after 30 days, 327 to 530 microstrain after 90 days, 360 to 550 microstrain after 180 days, and 357 to 567 microstrain after 365 days. After each drying period, the mixture with Micro Air and no shrinkage-reducing admixture (0% SRA-M #3) had the highest shrinkage, while the mixture with Tough Air and a 2.0 percent dosage of SRA (2.0% SRA-T #2) had the lowest shrinkage.

The figures and table show that the addition of SRA or CRA reduces both early-age and long-term shrinkage for concrete containing either Micro Air or Tough Air. A mixture containing Micro Air and no SRA (0% SRA-M #3) had 140, 113, and

Table 3.1 Average free shrinkage in microstrain versus drying time at different lengths of drying for mixtures in Program 1

Days of Drying	0	30	90	180	365
Mixture	Free Shrinkage at Day of Drying (με)*				
0% SRA-M #3	-33	397	530	550	567
0.5% SRA-M #2	-50	257	353	393	403
1.0% SRA-M #2	-23	283	387	417	430
2.0% SRA-M #2	-47	257	337	367	383
1.0% CRA-M #2	-30	280	405	460	505
2.0% CRA-M	-50	200	347	377	423
0% SRA-T #2	-13	360	470	467	477
0.5% SRA-T #2	13	313	435	455	460
1.0% SRA-T #2	-43	317	430	440	450
2.0% SRA-T #2	-27	187	327	360	357

*Negative values indicate swelling during wet-curing period
Note: Notation used for mixture designations explained in Section 2.5.1
Three specimens tested per mixture

Table 3.2 Student's t-test results displaying statistical significance of SRA dosage and air-entraining admixture type on 30-day free shrinkage for mixtures in Program 1

Mixture	30-Day Free Shrinkage*	0% SRA-M #3	0% SRA-T #2	0.5% SRA-M #2	0.5% SRA-T #2	1.0% SRA-M #2	1.0% SRA-T #2	2.0% SRA-M #2	2.0% SRA-T #2
		397	360	257	313	283	317	257	187
0% SRA-M #3	397		N	Y	90%	Y	90%	Y	Y
0% SRA-T #2	360			Y	N	95%	N	90%	95%
0.5% SRA-M #2	257				N	N	80%	N	N
0.5% SRA-T #2	313					N	N	N	80%
1.0% SRA-M #2	283						N	N	80%
1.0% SRA-T #2	317							N	80%
2.0% SRA-M #2	257								N
2.0% SRA-T #2	187								

*The 30-day free shrinkage for each mixture was determined by averaging the shrinkage values of each specimen.
Note: "Y" indicates a statistical difference between the two datum at a significance level of $\alpha = 0.02$ (98%). "N" indicates that these is no statistical significance at a significance level of $\alpha = 0.20$ (80%). Statistical differences at significance levels at, but not exceeding, $\alpha = 0.05$, 0.10, and 0.20 are represented by "95%", "90%", and "80%".
Notation used for mixture designations explained in Section 2.5.1.

Table 3.3 Student's t-test results displaying statistical significance of shrinkage-reducing admixture type on 30-day free shrinkage for mixtures in Program 1

Mixture	30-Day Free Shrinkage*	1.0% CRA-M #2	2.0% CRA-M
		280	200
0% SRA-M #3	397	Y	Y
1.0% SRA-M #2	283	N	90%
1.0% CRA-M #2	280		90%
2.0% SRA-M #2	257	N	N

*The 30-day free shrinkage for each mixture was determined by averaging the shrinkage values of each specimen.
Note: "Y" indicates a statistical difference between the two datum at a significance level of $\alpha = 0.02$ (98%). "N" indicates that these is no statistical significance at a significance level of $\alpha = 0.20$ (80%). Statistical differences at significance levels at, but not exceeding, $\alpha = 0.05$, 0.10, and 0.20 are represented by "95%", "90%", and "80%".
Notation used for mixture designations explained in Section 2.5.1.

Table 3.4 Student's t-test results displaying statistical significance of SRA dosage and air-entraining admixture type on 365-day free shrinkage for mixtures in Program 1

Mixture	365-Day Free Shrinkage*	0% SRA-M #3	0% SRA-T #2	0.5% SRA-M #2	0.5% SRA-T #2	1.0% SRA-M #2	1.0% SRA-T #2	2.0% SRA-M #2	2.0% SRA-T #2
		567	477	403	460	430	450	383	357
0% SRA-M #3	567		90%	95%	90%	Y	80%	Y	Y
0% SRA-T #2	477			N	N	N	N	80%	80%
0.5% SRA-M #2	403				N	N	N	N	N
0.5% SRA-T #2	460					N	N	N	80%
1.0% SRA-M #2	430						N	N	N
1.0% SRA-T #2	450							N	N
2.0% SRA-M #2	383								N
2.0% SRA-T #2	357								

*The 365-day free shrinkage for each mixture was determined by averaging the shrinkage values of each specimen.
Note: "Y" indicates a statistical difference between the two datum at a significance level of $\alpha = 0.02$ (98%). "N" indicates that these is no statistical significance at a significance level of $\alpha = 0.20$ (80%). Statistical differences at significance levels at, but not exceeding, $\alpha = 0.05$, 0.10, and 0.20 are represented by "95%", "90%", and "80%".
Notation used for mixture designations explained in Section 2.5.1.

Table 3.5 Student's t-test results displaying statistical significance of shrinkage-reducing admixture type on 365-day free shrinkage for mixtures in Program 1

Mixture	365-Day Free Shrinkage*	1.0% CRA-M #2	2.0% CRA-M
		505	423
0% SRA-M #3	567	Y	Y
1.0% SRA-M #2	430	95%	N
1.0% CRA-M #2	505		90%
2.0% SRA-M #2	383	95%	N

*The 365-day free shrinkage for each mixture was determined by averaging the shrinkage values of each specimen.
Note: "Y" indicates a statistical difference between the two datum at a significance level of $\alpha = 0.02$ (98%). "N" indicates that these is no statistical significance at a significance level of $\alpha = 0.20$ (80%). Statistical differences at significance levels at, but not exceeding, $\alpha = 0.05$, 0.10, and 0.20 are represented by "95%", "90%", and "80%".
Notation used for mixture designations explained in Section 2.5.1.

140 microstrain greater shrinkage after 30 days of drying and 163, 137, and 183 microstrain greater shrinkage after 365 days of drying than mixtures containing Micro Air and SRA dosages of 0.5, 1.0, and 2.0 percent (0.5% SRA-M #2, 1.0% SRA-M #2, and 2.0% SRA-M #2), respectively. In addition, the mixture containing Micro Air and no SRA had 117 and 197 microstrain greater shrinkage after 30 days and 62 and 143 microstrain greater shrinkage after 365 days than mixtures with Micro Air and CRA dosages of 1.0 and 2.0 percent (1.0% CRA-M #2 and 2.0% CRA-M), respectively. The differences in free shrinkage after 30 days are statistically significant at the highest significance level ($\alpha = 0.02$) as SRA or CRA was added to the mixtures containing Micro Air (Tables 3.2 and 3.3). After 365 days, the difference in shrinkage is statistically significant at $\alpha = 0.05$ as the SRA dosage increased from 0 to 0.5 percent, while the shrinkage differences are statistically significant at $\alpha = 0.02$ as the dosages of SRA or CRA increased from 0 to 1.0 percent and from 0 to 2.0 percent (Tables 3.4 and 3.5). A mixture containing Tough Air and no SRA (0% SRA-T #2) had 47, 43, and 173 microstrain greater shrinkage after 30

days and 17, 27, and 120 microstrain greater shrinkage after 365 days than mixtures containing Tough Air and SRA dosages of 0.5, 1.0, and 2.0 percent (0.5% SRA-T #2, 1.0% SRA-T #2, and 2.0% SRA-T #2), respectively. The differences in free shrinkage after 30 and 365 days are statistically significant at $\alpha = 0.05$ and $\alpha = 0.20$, respectively, as the SRA dosage increased from 0 to 2.0 percent in the mixtures containing Tough Air (Tables 3.2 and 3.4). Conversely, the differences in free shrinkage after 365 days are not statistically significant as the SRA dosages increased from 0 to 0.5 percent and from 0 to 1.0 percent in the Tough Air mixtures (Table 3.4).

Figures 3.1 through 3.3 and Table 3.1 show that the three mixtures with a dosage of 2.0 percent SRA or CRA by weight of cement (2.0% SRA-M #2, 2.0% CRA-M, and 2.0% SRA-T #2) had the lowest shrinkage after 30, 90, and 180 days. Two of these mixtures (2.0% CRA-M and 2.0% SRA-T #2) had shrinkage of 200 microstrain or less after 30 days (200 and 187 microstrain, respectively). As shown in Figure 3.1, the two mixtures with the lowest shrinkage after 30 days (2.0% CRA-M and 2.0% SRA-T #2) had at least 50 microstrain less shrinkage than the next-closest mixture. After 90 days of drying (Figure 3.2), this gap closed as four different mixtures had free shrinkage of approximately 325 to 350 microstrain. After 365 days (Figure 3.4), 2.0% SRA-M #2 and 2.0% SRA-T #2 had the lowest shrinkage (383 and 357 microstrain, respectively). The two mixtures with no SRA (0% SRA-M #3 and 0% SRA-T #2) had the highest shrinkage after 30, 90, and 180 days of drying. After 30 days, these two mixtures had 160 to 210 microstrain greater shrinkage, respectively, than the corresponding mixtures with the lowest shrinkage, 2.0% CRA-M and 2.0% SRA-T #2. One of the two mixtures with no SRA (0% SRA-M #3) also had the highest shrinkage after 365 days (567 microstrain).

The addition of increasing dosages of SRA did not produce consistent results. No clear distinction in shrinkage was observed between mixtures containing 0.5 and 1.0 percent SRA by weight of cement. In fact, as shown in Table 3.1, a mixture with

0.5 percent SRA and Micro Air (0.5% SRA-M #2) had lower shrinkage than each of the three Micro Air mixtures with 1.0 percent SRA or CRA throughout the testing. As shown in Tables 3.2 and 3.4, these differences in free shrinkage after either 30 or 365 days are not statistically significant. An increase in SRA dosage from 0.5 to 2.0 percent had only a minimal effect on shrinkage. A mixture with Micro Air and 2.0 percent SRA (2.0% SRA-M #2) had shrinkage equal to the mixture with Micro Air and 0.5 percent SRA (0.5% SRA-M #2) after 30 days. After 365 days, the mixture with 2.0 percent SRA had 20 microstrain less shrinkage than the mixture with 0.5 percent SRA. A mixture with 2.0 percent CRA (2.0% CRA-M) had 20 microstrain greater shrinkage after 365 days than the mixture with 0.5 percent SRA. The differences in free shrinkage after either 30 or 365 days are not statistically significant as the dosage of SRA increased from 0.5 to 2.0 percent (Tables 3.2 and 3.4). Decreased shrinkage was observed as the SRA dosage increased from 1.0 to 2.0 percent in the mixtures containing Micro Air. As shown in Table 3.1, a mixture with Micro Air and a 1.0 percent dosage of SRA (1.0% SRA-M #2) had 26 and 47 microstrain greater shrinkage after 30 and 365 days, respectively, than the mixture with Micro Air and 2.0 percent SRA. These differences in free shrinkage after either 30 or 365 days, however, are not statistically significant (Tables 3.2 and 3.4).

For the mixtures containing Tough Air, substantial reductions in shrinkage were observed as the SRA dosage increased from either 0.5 to 2.0 percent or from 1.0 to 2.0 percent. A mixture with Tough Air and a 0.5 percent dosage of SRA (0.5% SRA-T #2) had 127 microstrain greater shrinkage after 30 days and 108 microstrain greater shrinkage after 365 days than a mixture with Tough Air and 2.0 percent SRA (2.0% SRA-T #2); these differences are statistically significant at $\alpha = 0.20$. A mixture with Tough Air and a 1.0 percent SRA dosage (1.0% SRA-T #2) had 129 microstrain greater shrinkage after 30 days and 89 microstrain greater shrinkage after 365 days than the mixture with Tough Air and 2.0 percent SRA. The difference after

30 days is statistically significant at $\alpha = 0.20$, but the difference after 365 days is not significant.

Decreased shrinkage was observed after 30 and 365 days as the dosage of CRA increased from 1.0 to 2.0 percent. A mixture containing 1.0 percent CRA (1.0% CRA-M #2) had 80 microstrain greater shrinkage after 30 days and 82 microstrain greater shrinkage after 365 days than a mixture with 2.0 percent CRA (2.0% CRA-M); these differences in free shrinkage are statistically significant at $\alpha = 0.10$.

Figures 3.1 through 3.4 and Table 3.1 show that the two types of shrinkage-reducing admixture had similar effects on free shrinkage at early ages (after 30 and 90 days of drying). As shown in Table 3.3, the differences in free shrinkage obtained with the two admixtures after 30 days are not statistically significant. After 365 days of drying, however, the mixtures containing CRA had greater shrinkage the corresponding mixtures with SRA (Figure 3.4). As shown in Table 3.1, the mixture 1.0% CRA-M had only 18 microstrain greater shrinkage than the mixture 1.0% SRA-M #2 after 90 days, but had 75 microstrain greater shrinkage after 365 days. This difference after 365 days is statistically significant at $\alpha = 0.05$ (Table 3.5). Additionally, the mixture 2.0% CRA-M had only 10 microstrain greater shrinkage than the mixture 2.0% SRA-M #2 after 90 days, but had 40 microstrain greater shrinkage after 365 days (Table 3.1). This difference in shrinkage after 365 days, however, is not statistically significant.

No significant relationship is apparent, nor is one expected, between type of air-entraining admixture and free shrinkage performance in the mixtures containing SRA. The mixture containing Tough Air and no SRA (0% SRA-T #2), however, had 90 microstrain less shrinkage than the mixture containing Micro Air and no SRA (0% SRA-M #3) after 365 days (477 vs. 567 microstrain). This difference in free shrinkage is, in fact, statistically significant at $\alpha = 0.10$ (Table 3.4).

The free shrinkage of each mixture is separated into two drying periods, early-age (0 to 90 days) and long-term (90 to 365 days), in Table 3.6. In addition, the table shows the percentage of total shrinkage after 365 days observed during the first 90 days. As shown in the table, the mixtures containing CRA experienced more shrinkage than all other mixtures, including those with no SRA or CRA, between 90 and 365 days. The mixtures 1.0% CRA-M #2 and 2.0% CRA-M experienced shrinkage of 100 and 76 microstrain, respectively, during this period, while no other mixture experienced more than 50 microstrain.

As shown in Table 3.6, each mixture had more than 80 percent of the shrinkage at one year occur during the first 90 days. The mixtures without CRA, which includes the mixtures with SRA, had a greater percentage of the total shrinkage at one year occur during the first 90 days than the mixtures with CRA. The two mixtures with CRA, 1.0% CRA-M #2 and 2.0% CRA-M, had 81.3 and 83.9 percent, respectively, of their total shrinkage at one year occur during the first 90 days, while the eight mixtures without CRA (including mixtures with SRA) had at least 89 percent of their one-year shrinkage occur within 90 days. Delaying shrinkage to a later age may reduce the potential for cracking as strength and modulus of elasticity increase at about the same rate and additional time is provided for tensile stresses to be mitigated by the effects of creep. Although the mixtures with CRA had a greater percentage of shrinkage at later ages than the corresponding SRA mixtures, the CRA mixtures experienced similar early-age shrinkage and more total shrinkage than the SRA mixtures.

Of the 10 mixtures shown in Table 3.6, three of the four mixtures that had the greatest percentage of total shrinkage at one year occur during the first 90 days contained Tough Air; all exceeding 94 percent. In fact, the mixture containing Tough Air with no SRA had 98.6 percent of the one-year shrinkage occur during the first 90 days.

Table 3.6 Free shrinkage in microstrain during two periods of drying time (0 to 90 days and 90 to 365 days) for mixtures in Program 1

Mixture	Drying Period (days)		% of total shrinkage occurring in first 90 days†
	0-90	90-365	
0% SRA-M #3	563	37	93.8%
0.5% SRA-M #2	403	50	89.0%
1.0% SRA-M #2	410	43	90.5%
2.0% SRA-M #2	384	46	89.3%
1.0% CRA-M #2	435	100	81.3%
2.0% CRA-M	397	76	83.9%
0% SRA-T #2	483	7	98.6%
0.5% SRA-T #2	422	25	94.4%
1.0% SRA-T #2	473	20	95.9%
2.0% SRA-T #2	354	30	92.2%

†Shrinkage during first 90 days divided by total shrinkage after 365 days
Note: The shrinkage values for each drying period represent total shrinkage and do not take into account swelling during wet-curing.
Notation used for mixture designations explained in Section 2.5.1.
Note: Three specimens tested per mixture.

The free shrinkage of the mixtures during four periods of drying (0 to 30 days, 30 to 90 days, 90 to 180 days, and 180 to 365 days) are shown in Figures 3.5 through 3.7. Mixtures containing Micro Air and SRA, Micro Air and CRA, and Tough Air and SRA are displayed in Figures 3.5, 3.6, and 3.7, respectively. The data shown in the figures are tabulated in Table 3.7. As shown in the figures and table, a majority of shrinkage for all mixtures occurred during the first 30 days of drying. Shrinkage during the first 30 days for the mixtures in Figures 3.5, 3.6, and 3.7, respectively, ranged from 304 to 430 microstrain, 250 to 430 microstrain, and 214 to 373 microstrain. The mixtures experienced less shrinkage between 30 and 90 days and again between 90 and 180 days. Between 30 and 90 days, the shrinkage of the mixtures in Figures 3.5, 3.6, and 3.7 ranged from 80 to 133 microstrain, 126 to 147 microstrain, and 110 to 140 microstrain, respectively; much lower values than observed during the first 30 days. Most mixtures also had less shrinkage in each

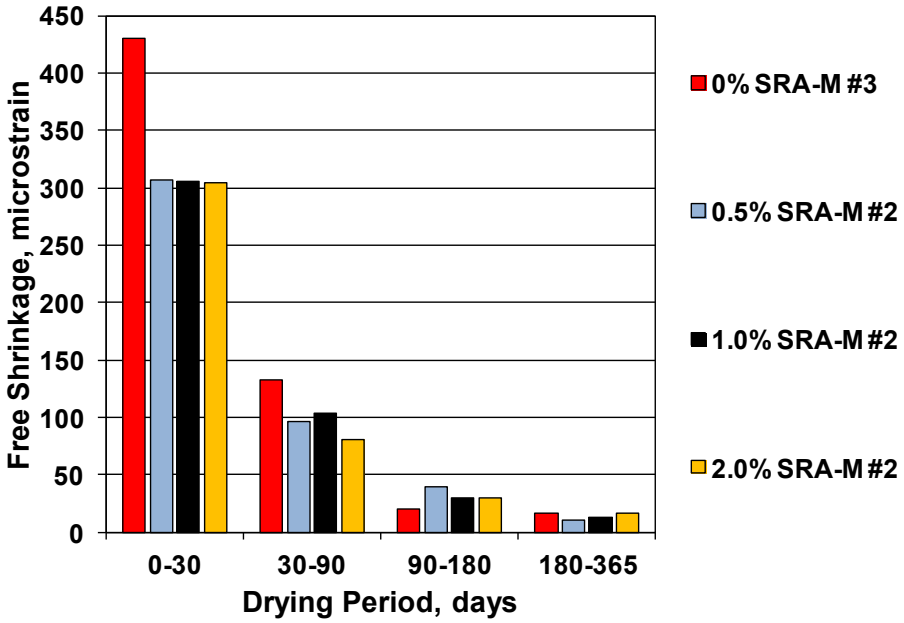

Note: Notation used for mixture designations explained in Section 2.5.1

Figure 3.5 Free shrinkage during four periods of drying (0 to 30 days, 30 to 90 days, 90 to 180 days, and 180 to 365 days) for mixtures containing Micro Air and a dosage of SRA

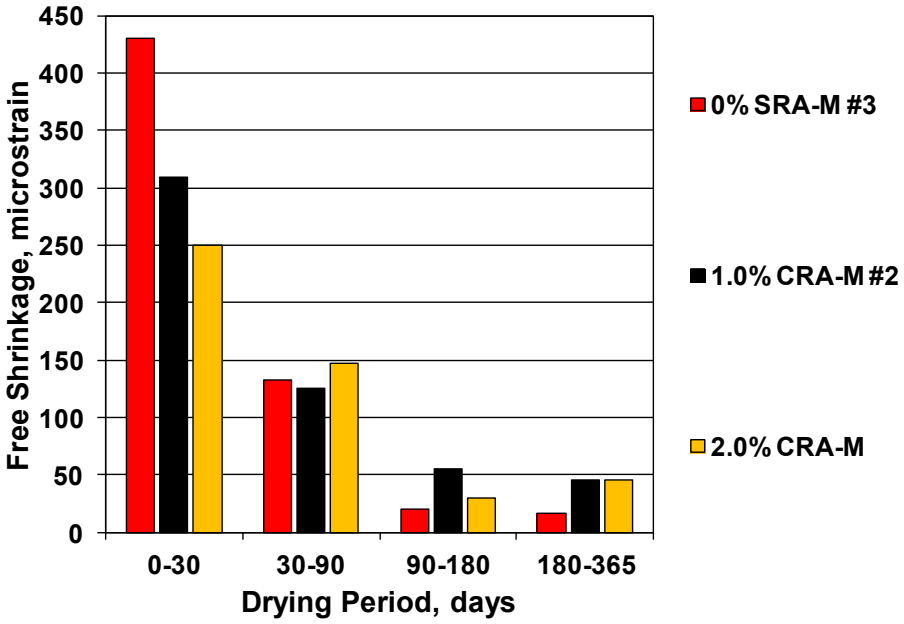

Note: Notation used for mixture designations explained in Section 2.5.1

Figure 3.6 Free shrinkage during four periods of drying (0 to 30 days, 30 to 90 days, 90 to 180 days, and 180 to 365 days) for mixtures containing Micro Air and a dosage of CRA

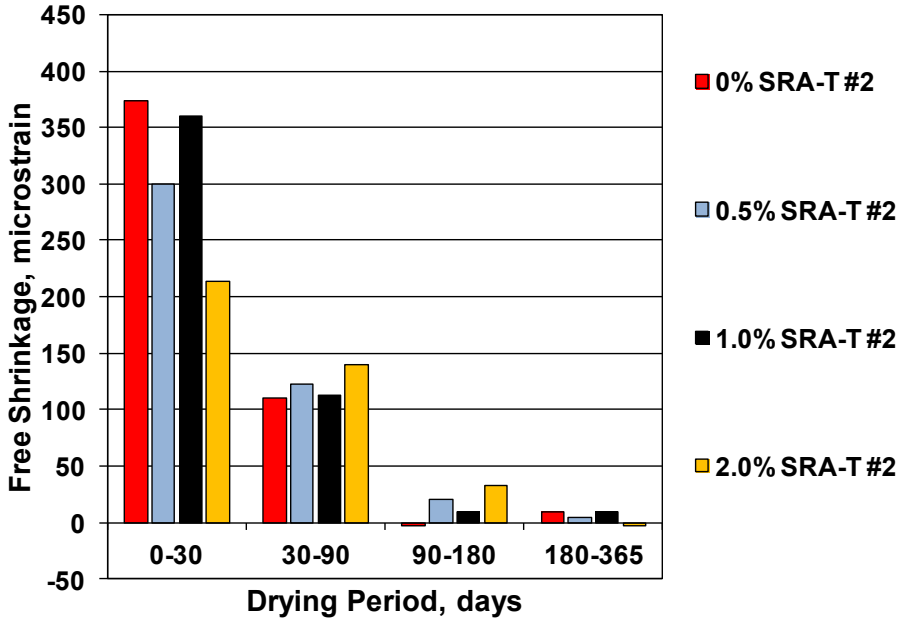

Note: Notation used for mixture designations explained in Section 2.5.1

Figure 3.7 Free shrinkage during four periods of drying (0 to 30 days, 30 to 90 days, 90 to 180 days, and 180 to 365 days) for mixtures containing Tough Air and a dosage of SRA

Table 3.7 Free shrinkage in microstrain during four periods of drying (0 to 30 days, 30 to 90 days, 90 to 180 days, and 180 to 365 days) for mixtures in Program 1

Drying Period (days)	0-30	30-90	90-180	180-365
Mixture	Free Shrinkage in Drying Period (με)			
0% SRA-M #3	430	133	20	17
0.5% SRA-M #2	307	96	40	10
1.0% SRA-M #2	306	104	30	13
2.0% SRA-M #2	304	80	30	16
1.0% CRA-M #2	310	125	55	45
2.0% CRA-M	250	147	30	46
0% SRA-T #2	373	110	-3	10
0.5% SRA-T #2	300	122	20	5
1.0% SRA-T #2	360	113	10	10
2.0% SRA-T #2	214	140	33	-3

Note: Notation used for mixture designations explained in Section 2.5.1.
Three specimens tested per mixture.

subsequent drying period. Three of the ten mixtures (2.0% CRA-M, 0% SRA-T #2, and 1.0% SRA-T #2), however, had the same or more shrinkage between 180 and 365 days compared to the period between 90 and 180 days, but the differences are under 20 microstrain.

Figure 3.5 indicates that the addition of SRA to mixtures containing Micro Air contributed to reduced shrinkage, primarily during the first 90 days of drying. Conversely, the mixture with no SRA had slightly less shrinkage than the mixtures with SRA in the drying period between 90 and 365 days. Figures 3.6 and 3.7 show that the addition of CRA to mixtures containing Micro Air and the addition of SRA to mixtures containing Tough Air contributed to reduced shrinkage only during the first 30 days of drying. In a number of cases, more shrinkage occurred between 30 and 90 days, 90 and 180 days, and 180 and 365 days for the mixtures with the shrinkage-reducing admixture than for mixtures with no SRA. The shrinkage observed between 90 and 365 days, however, was much lower than the shrinkage during the first 30 days for all mixtures.

The average rate of shrinkage in microstrain per day (με/day) during each drying period is shown in Table 3.8. The average shrinkage rates during the first 30 days of drying were significantly higher than during any other drying period. The rates ranged from 7.1 to 14.3 με/day during the first 30 days of drying. The mixtures with the two lowest rates during the first 30 days had 2.0 percent SRA or CRA by weight of cement (2.0% SRA-T #2 and 2.0% CRA-M). Surprisingly, these two mixtures also had the two highest average shrinkage rates between 30 and 90 days. The two mixtures with no SRA (0% SRA-M #3 and 0% SRA-T #2) had the two highest rates during the first 30 days. Between 30 and 90 days, the average shrinkage rates decreased considerably, with values ranging from 1.3 to 2.5 με/day. The rates dropped below 0.1 με/day between 180 and 365 days for all mixtures, except for the

Table 3.8 Average rate of free shrinkage during four periods of drying (0 to 30 days, 30 to 90 days, 90 to 180 days, and 180 to 365 days) for mixtures in Program 1

Drying Period (days)	0-30	30-90	90-180	180-365
Mixture	Shrinkage Rate in Drying Period (με/day)			
0% SRA-M #3	14.3	2.2	0.2	0.1
0.5% SRA-M #2	10.2	1.6	0.4	0.1
1.0% SRA-M #2	10.2	1.7	0.3	0.1
2.0% SRA-M #2	10.1	1.3	0.3	0.1
1.0% CRA-M #2	10.3	2.1	0.6	0.2
2.0% CRA-M	8.3	2.5	0.3	0.2
0% SRA-T #2	12.4	1.8	0.0	0.1
0.5% SRA-T #2	10.0	2.0	0.2	0.0
1.0% SRA-T #2	12.0	1.9	0.1	0.1
2.0% SRA-T #2	7.1	2.3	0.4	0.0

Note: Notation used for mixture designations explained in Section 2.5.1.
Three specimens tested per mixture.

two mixtures containing CRA, 1.0% CRA-M #2 and 2.0% CRA-M, which each had an average shrinkage rate of 0.2 με/day between 180 and 365 days.

3.2.3 Freeze-Thaw Durability

As discussed in Section 1.6, freeze-thaw damage in concrete with inadequate air entrainment is primarily caused by water moving to the freezing sites, leading to internal tensile stresses and cracking. The principal method of controlling freeze-thaw damage is through the addition of entrained air. Properly-spaced air voids provide sites for water to freeze while drawing water from the surrounding paste, and thus, protecting the cement paste from damage. The amount of entrained air (percentage of total volume of concrete) and spacing of the air voids play important roles in the effectiveness of the air-void system in protecting the concrete from freeze-thaw damage.

As discussed previously, the use of a shrinkage-reducing admixture in conjunction with a surfactant-based air entraining admixture can potentially decrease the stability the air-void system through a reduction in the surface tension of the pore

water. This decreased surface tension reduces the stability of the air-void barriers and promotes the formation of larger, wider-spaced air voids. Lindquist et al. (2008) observed a reduction in the stability of the air-void system as the dosage of SRA increased from 1 to 2 percent by weight of cement. In making this observation, Lindquist et al. measured the air content of mixtures at five-minute intervals after mixing until the change in air content between subsequent measurements was less than 1 percent. The mixture with a 1 percent dosage of SRA maintained a more constant air content for a longer time period than the 2 percent SRA mixture.

The evaluation of freeze-thaw durability in Program 1 included tests of 18 batches of concrete to examine the effects of dosage and type of shrinkage-reducing admixture and type of air-entraining admixture on freeze-thaw durability. The batches included twelve distinct mixtures, of which six were duplicated. The eighteen batches included seven containing Micro Air and eleven containing Tough Air. Because these batches were designed to meet the requirements of low-cracking high-performance concrete (LC-HPC), the air contents ranged between 7.5 and 9.5 percent (Table A.8 in Appendix A). Similar to the free-shrinkage analysis, four dosages of SRA (0, 0.5, 1.0, and 2.0 percent by weight of cement) were tested in conjunction with Micro Air and Tough Air. In addition, one dosage of CRA (1.0 percent by weight of cement) was tested in mixtures containing Micro Air and three CRA dosages (0.5, 1.0, and 2.0 percent by weight of cement) were tested in mixtures containing Tough Air. Duplicate batches with SRA dosages of 0 and 0.5 percent and Micro Air and SRA dosages of 0, 0.5, 1.0, and 2.0 percent and Tough Air were tested to determine test repeatability.

Three specimens were tested for each batch in accordance with ASTM C666 – Procedure B and Kansas Department of Transportation (KDOT) Test KTMR-22. Detailed information regarding the procedures is provided in Section 2.4.2. As explained in Section 2.4.2, testing stopped when specimens were subjected to a

minimum of 300 freeze-thaw cycles or when the average dynamic modulus of elasticity of the three specimens from a batch dropped to 60 percent or less of the initial dynamic modulus of elasticity. A Durability Factor (DF, see Section 2.4.2) is used to quantify the freeze-thaw performance of the mixtures. The DF represents the percentage of the initial dynamic modulus of elasticity remaining after the specimens are subjected to 300 cycles. For the batches in which the dynamic modulus dropped to 60 percent or less of the initial value prior to completing 300 cycles, the DF represents the estimated percentage of the initial dynamic modulus of elasticity if the specimens had been subjected to 300 cycles (see Section 2.4.2). The Kansas Department of Transportation (KDOT) requires a minimum DF of 95 (95 percent of initial dynamic modulus of elasticity maintained at test completion) for concretes placed on-grade (Kansas Department of Transportation 2007d) and represents the standard for acceptable durability in this evaluation. The raw data from the tests are provided in Appendix C.

The average dynamic modulus of elasticity for the three specimens from each batch is plotted as a function of the number of freeze-thaw cycles in Figures 3.8 and 3.9 for the Micro Air and Tough Air mixtures, respectively. In the figure legends, the mixtures are listed in the order of descending DF. Table 3.9 shows the DFs of the mixtures and, where applicable, the number of freeze-thaw cycles completed prior to reaching 60 percent of the initial dynamic modulus. Linear interpolation between dynamic modulus and freeze-thaw cycle was used to determine the number of freeze-thaw cycles corresponding to 60 percent of the initial dynamic modulus for the specimens that did not reach 300 cycles and the average dynamic modulus at 300 cycles for the specimens that extended beyond 300 cycles.

As shown in Figures 3.8 and 3.9 and Table 3.9, the mixtures containing Tough Air exhibited a greater decrease in dynamic modulus of elasticity than the mixtures

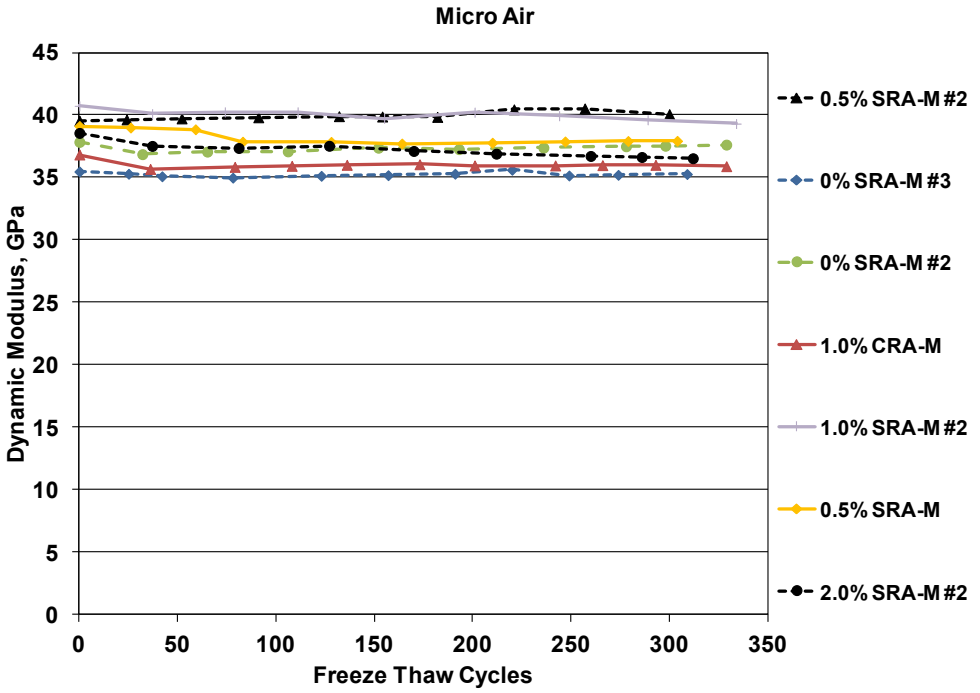

Note: Notation used for mixture designations explained in Section 2.5.1

Figure 3.8 Average dynamic modulus of elasticity versus freeze-thaw cycles for mixtures containing Micro Air in Program 1

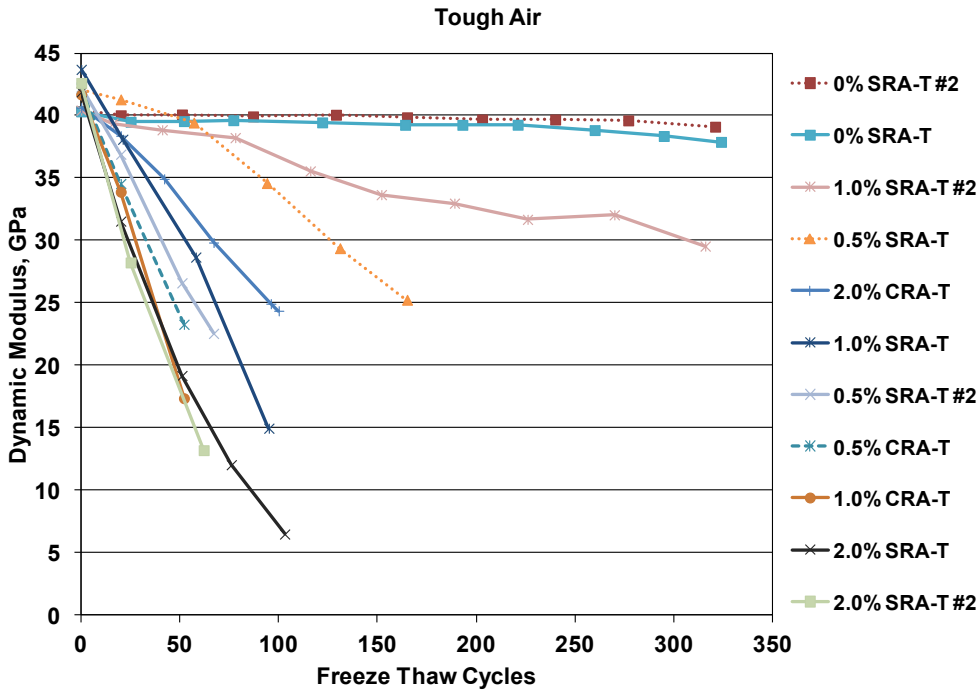

Note: Notation used for mixture designations explained in Section 2.5.1

Figure 3.9 Average dynamic modulus of elasticity versus freeze-thaw cycles for mixtures containing Tough Air in Program 1

Table 3.9 Summary of average dynamic modulus of elasticity versus freeze-thaw cycles for mixtures in Program 1

Mixture	Durability Factor[#]	Cycles Completed at 60% of Initial Dynamic Modulus[†]
0% SRA-M #2	99	-
0% SRA-M #3	99	-
0.5% SRA-M	97	-
0.5% SRA-M #2	101	-
1.0% SRA-M #2	97	-
2.0% SRA-M #2	95	-
1.0% CRA-M	98	-
0% SRA-T	95	-
0% SRA-T #2	98	-
0.5% SRA-T	33	165
0.5% SRA-T #2	11	56
1.0% SRA-T	13	65
1.0% SRA-T #2	75	-
2.0% SRA-T	7	36
2.0% SRA-T #2	6	32
0.5% CRA-T	9	46
1.0% CRA-T	7	37
2.0% CRA-T	20	100

[#] *Durability Factor (DF) = (P × N) / 300 cycles*,
where *P* is the percentage of the initial dynamic modulus remaining at *N* cycles, *N* is either the number of cycles at which *P* reached 60 percent or 300 cycles (whichever is smaller).
†Number of freeze-thaw cycles completed prior to reaching 60 percent of the initial dynamic modulus.
"-" denotes mixture reached 300 cycles prior to dropping to 60 percent of initial dynamic modulus.
Note: Notation used for mixture designations explained in Section 2.5.1.
Three specimens tested per mixture

with Micro Air, especially for the mixtures containing a shrinkage-reducing admixture. All seven mixtures containing Micro Air had a DF of 95 or greater at 300 cycles. The lowest DF of the Micro Air mixtures (95) was experienced by mixture 2.0% SRA-M #2. Only two of the eleven mixtures containing Tough Air had a DF of 95 or greater at 300 cycles (0% SRA-T and 0% SRA-T #2). These two mixtures had DFs of 95 and 98, respectively. Only one mixture containing Tough Air and SRA or CRA (1.0% SRA-T #2) reached 300 cycles before dropping below 60 percent of the initial dynamic modulus – this mixture had a DF of 75 at 300 cycles.

The addition of an SRA to the mixtures containing Micro Air had little effect on freeze-thaw durability; although, the mixture with the SRA dosage of 2.0 percent had the lowest DF among these Micro Air mixtures (95). The mixtures containing

Tough Air exhibited decreased freeze-thaw durability as the SRA dosage increased from 0 to 0.5 percent and again from 1.0 to 2.0 percent. The effect on freeze-thaw durability of increasing dosage of CRA was not clear in the mixtures containing Tough Air. For example, Tough Air mixtures containing CRA dosages of 0.5 and 1.0 percent exhibited lower DFs than a Tough Air mixture with a 2.0 percent dosage of CRA. The single mixture tested containing Micro Air and CRA (1.0% CRA-M) had a DF of 98. Mixtures with a 2.0 percent dosage of SRA had the lowest DFs of the mixtures containing either Micro Air or Tough Air; however, these values were significantly lower for the Tough Air mixtures. The two Tough Air mixtures with the lowest DFs (2.0% SRA-T and 2.0% SRA-T #2) dropped to 60 percent of the initial dynamic modulus of elasticity after only 36 and 32 freeze-thaw cycles, respectively, corresponding to DFs of 7 and 6. An increased dosage of SRA would be expected to reduce freeze-thaw durability due to the effect of reduced pore water surface tension on the air-void system. The two Micro Air mixtures containing a 0.5 percent dosage of SRA exhibited the highest (0.5% SRA-M #2) and second lowest (0.5% SRA-M) freeze-thaw durability of the Micro Air mixtures. Even so, these two mixtures had similar DFs, with values of 101 and 97, respectively. The mixture with the DF of 101 completed 300 cycles with a dynamic modulus greater than its initial value. Ultimately, the Micro Air mixtures, regardless of SRA dosage, had a DF of at least 95. Due to the narrow range of the values (ranging from 95 to 101), the order of descending DFs for these mixtures containing Micro Air has little or no significance.

3.2.4 Scaling Resistance

The mechanisms that contribute to scaling in concrete are similar to those responsible for freeze-thaw damage; therefore, proper air entrainment is the primary method of improving scaling resistance. Thus, the effects of the shrinkage-reducing admixtures on the stability of the air-void system are expected to influence the scaling resistance of the examined mixtures.

The evaluation of scaling resistance included tests of twenty-two batches of concrete that included thirteen distinct mixtures plus nine duplicates. As with the evaluation of freeze-thaw durability, the effects of dosage and type of shrinkage-reducing admixture and type of air-entraining admixture on scaling resistance were examined. The 22 batches included 11 each containing Micro Air and Tough Air. Two dosages of CRA (0.5 and 1.0 percent by weight of cement) were tested with the Micro Air mixtures while three CRA dosages (0.5, 1.0, and 2.0 percent by weight of cement) were tested with the Tough Air mixtures. Duplicate batches containing the four dosages of SRA (0, 0.5, 1.0, and 2.0 percent by weight of cement) were tested in conjunction with both Micro Air and Tough Air. Two duplicate batches containing Micro Air and no SRA were tested.

Three specimens from each batch were tested for scaling resistance in accordance with Canadian Test BNQ NQ 2621-900 Annex B. The test is somewhat more severe than the BNQ test because a 2.5 percent NaCl solution was used in place of the specified 3.0 percent solution based on work by Verbeck and Klieger (1957), who observed greater scaling while using the solution with 2.5 percent NaCl. Detailed information regarding the test procedures is provided in Section 2.4.3. As explained in Section 2.4.3, surface mass loss of the specimens was determined after 7, 21, 35, and 56 freeze-thaw cycles. The Canadian Test sets a limit of 0.31 lb/ft^2 (1500 g/m^2) for the maximum average cumulative mass loss for the three specimens at test completion. The raw data from the tests are provided in Appendix C.

The average cumulative mass loss for the three specimens from each batch is plotted as a function of freeze-thaw cycles in Figures 3.10 and 3.11 for the Micro Air and Tough Air mixtures, respectively. In the figure legends, the mixtures are listed in the order of descending cumulative mass loss after 56 freeze-thaw cycles. Mixtures that did not reach 56 cycles are listed in the order of ascending number of freeze-thaw

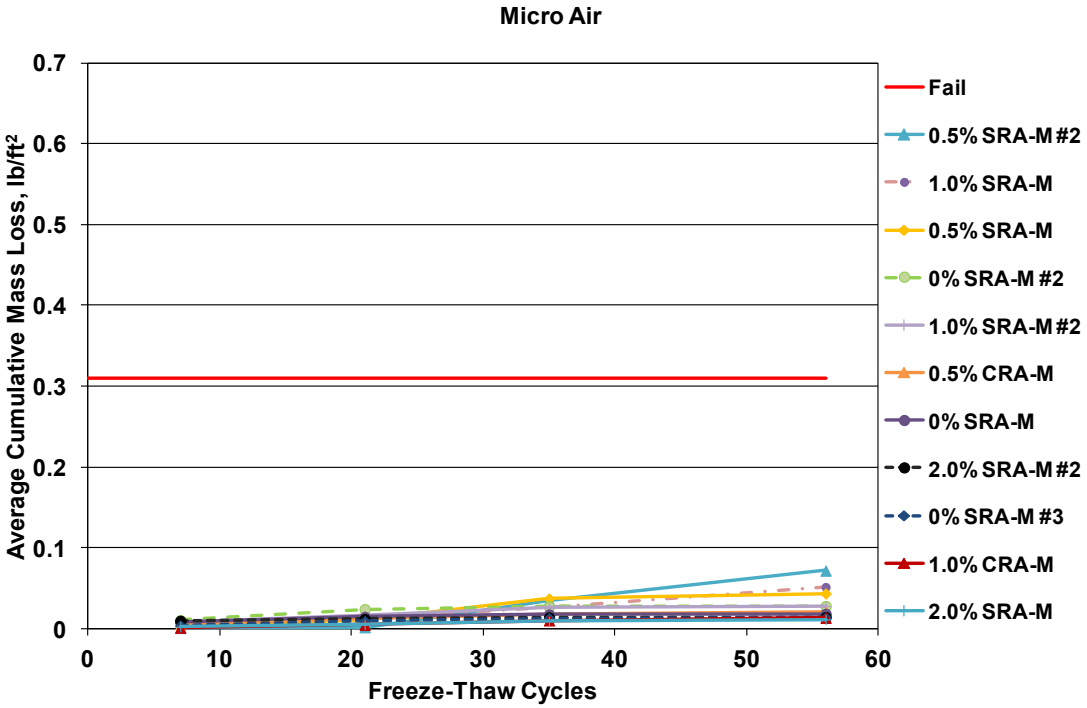

Note: Notation used for mixture designations explained in Section 2.5.1

Figure 3.10 Average cumulative mass loss versus freeze-thaw cycles for mixtures containing Micro Air in Program 1

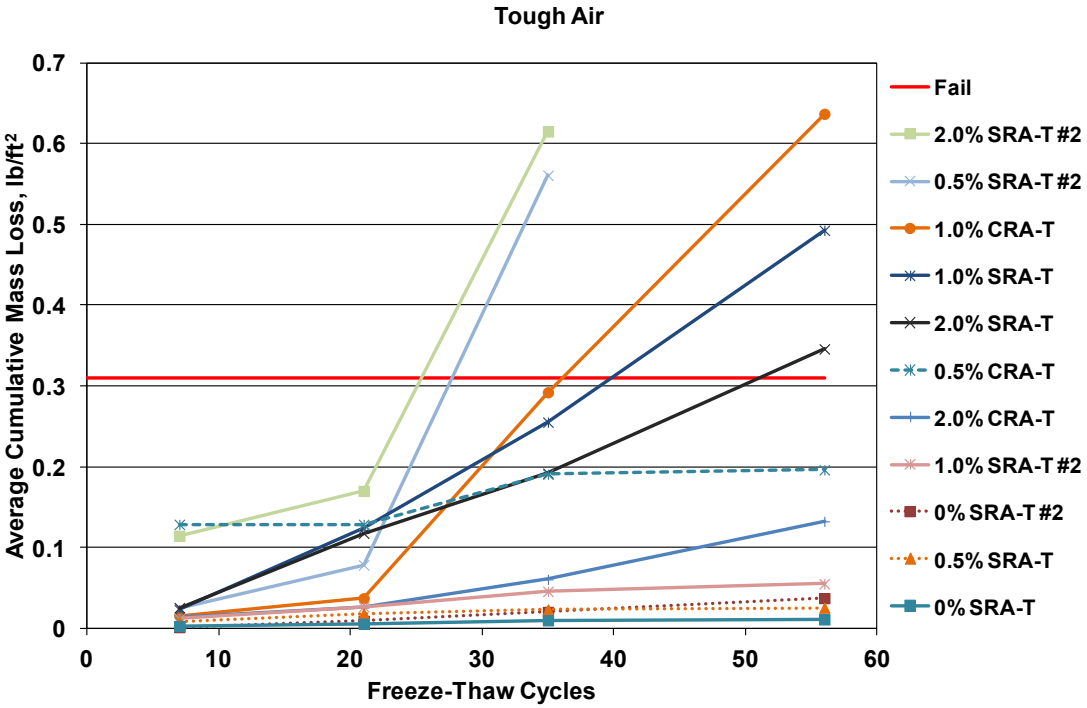

Note: Notation used for mixture designations explained in Section 2.5.1

Figure 3.11 Average cumulative mass loss versus freeze-thaw cycles for mixtures containing Tough Air in Program 1

cycles to failure. Table 3.10 summarizes the average cumulative mass losses for the mixtures at 7, 21, 35, and 56 cycles.

As shown in Figures 3.10 and 3.11 and Table 3.10, the mixtures containing Tough Air exhibited greater scaling losses than the mixtures containing Micro Air. This observation is similar to the findings of the freeze-thaw durability tests described in Section 3.2.3. All mixtures containing Micro Air had a cumulative mass loss below the specified failure limit [0.31 lb/ft^2 (1500 g/m^2)] at test completion. In contrast, only six of the eleven mixtures containing Tough Air, including both mixtures with no SRA, had a cumulative mass loss below the failure limit at test completion. Because the Micro Air and Tough Air mixtures containing no SRA performed similarly, the tests demonstrate that mixtures containing Tough Air are affected more, not less, by a shrinkage-reducing admixture than the mixtures containing Micro Air. Two mixtures containing Tough Air and an SRA (2.0% SRA-T #2 and 0.5% SRA-T #2) exceeded the specified failure limit for mass loss after only 35 cycles.

For the Micro Air and Tough Air mixtures containing an SRA, no clear trend can be established between dosage and scaling resistance, although an increased dosage of shrinkage-reducing admixture would be expected to decrease scaling resistance due to the effect of the reduced pore water surface tension on the air-void system. Two mixtures with a 0.5 percent addition of SRA by weight of cement exhibited the second lowest (0.5% SRA-T) and second highest (0.5% SRA-T #2) scaling mass loss of the Tough Air mixtures. For the Micro Air mixtures, a mixture containing a 2.0 percent dosage of SRA (2.0% SRA-M) exhibited the lowest scaling loss, while a mixture with a dosage of 0.5 percent SRA (0.5% SRA-M #2) exhibited the highest scaling loss; however, the mass losses of the Micro Air mixtures fall within a narrow range of values [11.8 to 72.0 $\times$ 10^{-3} lb/ft^2 (60 to 350 g/m^2)]. Because of this narrow range, the order of decreasing cumulative mass loss for the Micro Air

Table 3.10 Summary of average cumulative mass loss versus freeze-thaw cycles for mixtures in Program 1

Mixture	Average Cumulative Mass Loss 10^{-3} lb/ft^2			
	7 cycles	21 cycles	35 cycles	56 cycles
0% SRA-M	8.2	14.7	17.7	18.6
0% SRA-M #2	10.6	24.3	27.6	28.1
0% SRA-M #3	4.1	9.6	13.2	14.2
0.5% SRA-M	3.2	11.6	37.6	43.7
0.5% SRA-M #2	1.1	2.0	35.5	72.0
1.0% SRA-M	3.1	13.3	26.3	51.8
1.0% SRA-M #2	7.8	16.4	26.8	28.0
2.0% SRA-M	2.6	5.6	9.3	11.8
2.0% SRA-M #2	10.0	12.1	14.1	14.5
0.5% CRA-M	5.5	13.0	17.6	20.6
1.0% CRA-M	1.5	5.0	10.5	13.6
0% SRA-T	3.1	5.9	10.1	11.3
0% SRA-T #2	1.7	9.5	20.5	37.6
0.5% SRA-T	8.7	18.5	23.7	25.8
0.5% SRA-T #2	25	78.7	560.7	‡
1.0% SRA-T	23.2	124.0	255.3	492.7
1.0% SRA-T #2	12.2	26.9	45.9	55.5
2.0% SRA-T	25.7	117.9	192.1	345.9
2.0% SRA-T #2	114.8	170.2	614.9	‡
0.5% CRA-T	128.8	-	190.9	196.4
1.0% CRA-T	16.0	37.5	292.3	636.7
2.0% CRA-T	13.4	26.0	60.8	132.6

‡Mixture exceeded cumulative mass loss exceeded fail limit of 0.31 lb/ft^2 (1500 g/m^2) prior to 56 cycles
Note: Notation used for mixture designations explained in Section 2.5.1.
Three specimens tested per mixture.
10^{-3} lb/ft^2 = 4.884 g/m^2

mixtures has little or no significance. The mixtures containing Micro Air and a CRA had lower mass losses than the Micro Air mixtures with a similar dosage of SRA. The Micro Air mixtures with 0.5 and 1.0 percent CRA (0.5% CRA-M and 1.0% CRA-M) had less than half the mass losses at 56 cycles of the mixtures with matching SRA dosages (0.5% SRA-M, 0.5% SRA-M #2, 1.0% SRA-M, and 1.0% SRA-M #2). For the mixtures containing Tough Air, however, the type of shrinkage-reducing admixture did not appear to affect scaling resistance.

The results indicate that the addition of a shrinkage-reducing admixture decreases the freeze-thaw durability and scaling resistance of mixtures containing Tough Air; possibly due to the effect of reduced pore water surface tension within the

foam. In contrast, the addition of a shrinkage-reducing admixture did not have a significant effect on the freeze-thaw durability or scaling resistance of mixtures containing Micro Air, keeping in mind that these mixtures had an air content of at least 7.5 percent (shown in Table A.8 in Appendix A).

3.2.5 Compressive Strength

The average 28-day compressive strengths of mixtures containing similar dosages of shrinkage-reducing admixture are shown as a function of shrinkage-reducing admixture dosage and air-entraining admixture type in Figure 3.12. The data from the figure are tabulated in Table 3.11. In the figure and table, "SRA" is used to identify the mixtures even though those containing either type of shrinkage-reducing admixture (SRA and CRA) are included in the calculations of average compressive strength. Strengths for the SRA and CRA mixtures are combined to allow for larger sample sizes when determining average compressive strengths. The individual results are presented in Table A.8 in Appendix A. The number of batches included in the average strength (three cylinders per batch) is shown in the figure. The range of compressive strengths for the batches for each dosage are represented in the figure with error bars. The average air contents measured in the plastic concrete are shown in Table 3.11 for the mixtures associated with each average compressive strength to identify any possible influences of air content on strength. The air contents for the mixtures containing Micro Air range from 8.33 to 8.75 percent, while the values for the mixtures containing Tough Air range from 7.67 to 8.83 percent. Although the Micro Air and Tough Air mixtures fell within a narrow range of air contents in the plastic concrete, results from the hardened air-void analysis (discussed in Section 3.2.6) indicate that many of the Tough Air mixtures had lower air contents than the Micro Air mixtures when measured in the hardened concrete.

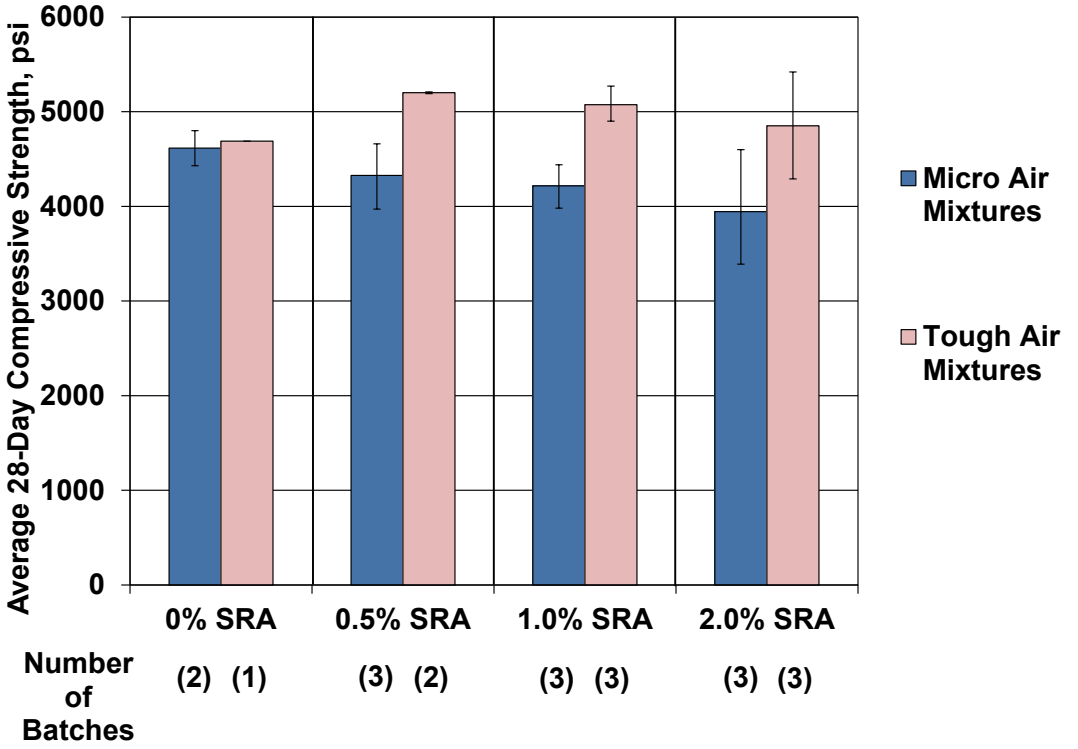

Note: 1 psi = 0.0069 MPa

Figure 3.12 Average 28-day compressive strength versus dosage of SRA and type of air-entraining admixture for mixtures in Program 1

Table 3.11 Average 28-day compressive strength and average air content versus dosage of SRA and type of air-entraining admixture for mixtures in Program 1

SRA Dosage	Micro Air Mixtures			Tough Air Mixtures		
	Average 28-Day Compressive Strength (psi)	Percent change in Strength vs. 0% SRA (%)	Average Air Content* (%)	Average 28-Day Compressive Strength (psi)	Percent change in Strength vs. 0% SRA (%)	Average Air Content* (%)
0% SRA	4620	-	8.75	4690	-	7.75
0.5% SRA	4330	-6.3%	8.33	5200	+10.9%	8.50
1.0% SRA	4220	-8.7%	8.75	5070	+8.1%	7.67
2.0% SRA	3940	-14.7%	8.75	4850	+3.4%	8.83

*Plastic concrete
Note: 1 psi = 0.0069 MPa

The mixtures containing Micro Air with 0, 0.5, 1.0, and 2.0 percent dosages of shrinkage-reducing admixture had compressive strengths ranging from 4430 to 4800 psi (30.6 to 33.1 MPa), 3970 to 4660 psi (27.4 to 32.2 MPa), 3980 to 4440 psi (27.5 to 30.6 MPa), and 3390 to 4600 psi (23.4 to 31.7 MPa), respectively. The mixtures containing Tough Air with dosages of shrinkage-reducing admixture of 0.5, 1.0, and 2.0 percent had compressive strengths ranging from 5190 to 5210 psi (35.8 to 35.9 MPa), 4900 to 5270 psi (33.8 to 36.4 MPa), and 4290 to 5420 psi (29.6 to 37.4 MPa), respectively. In addition, a single batch containing Tough Air and no shrinkage-reducing admixture had a compressive strength of 4690 psi (32.4 MPa). In a previous study with a different shrinkage-reducing admixture, Berke et al. (1994) observed a 15 percent reduction in strength for mixtures containing a 2.0 percent dosage of shrinkage-reducing admixture by weight of cement compared to those with no shrinkage-reducing admixture. The average compressive strength for each dosage of SRA (or CRA) and the percent change in strength compared to the mixtures with no SRA are tabulated in Table 3.11. The statistical significance of the differences in compressive strength determined from the Student's t-test are shown in Table 3.12. This statistical analysis evaluates the effects of dosage of shrinkage-reducing admixture and type of air-entraining admixture on compressive strength.

Figure 3.12 and Table 3.11 show that mixtures containing Micro Air exhibited decreased compressive strength as the dosage of shrinkage-reducing admixture was increased. The mixtures containing Micro Air and a 2.0 percent dosage of shrinkage-reducing admixture had an average compressive strength approximately 15 percent lower than the mixtures containing no shrinkage-reducing admixture [3940 vs. 4620 psi (27.2 vs. 31.9 MPa)], supporting the findings by Berke et al. (1994). The mixtures with 2.0 percent SRA had an average air content equal to that of the mixtures with no SRA (8.75 percent), indicating that air content of the plastic concrete had no effect on this difference in compressive strength. Table 3.12 shows

Table 3.12 Student's t-test results displaying statistical significance of SRA or CRA dosage and air-entraining admixture type on compressive strength for mixtures in Program 1

			Micro Air				Tough Air			
Air Entrainer Type	**Mixture**	**Average 28-Day Compressive Strength (psi)**	**0% SRA**	**0.5% SRA**	**1.0% SRA**	**2.0% SRA**	**0% SRA**	**0.5% SRA**	**1.0% SRA**	**2.0% SRA**
			4620	4330	4220	3940	4690	5200	5070	4850
Micro Air	**0% SRA**	4620		N	90%	95%	N	90%	90%	N
	0.5% SRA	4330			N	80%	Y	Y	95%	90%
	1.0% SRA	4220				N	Y	Y	95%	95%
	2.0% SRA	3940					Y	Y	Y	95%
Tough Air	**0% SRA**	4690						N	N	N
	0.5% SRA	5200							N	N
	1.0% SRA	5070								N
	2.0% SRA	4850								

Note: "Y" indicates a statistical difference between the two datum at a significance level of $\alpha = 0.02$ (98%). "N" indicates that these is no statistical significance at a significance level of $\alpha = 0.20$ (80%). Statistical differences at significance levels at, but not exceeding, $\alpha = 0.05$, 0.10, and 0.20 are represented by "95%", "90%", and "80%".
Notation used for mixture designations explained in Section 2.5.1.

that the differences in compressive strength are statistically significant at $\alpha = 0.10$ and $\alpha = 0.05$ as the dosage of shrinkage-reducing admixture increased from 0 to 1.0 percent and from 0 to 2.0 percent, respectively, in the mixtures containing Micro Air. No relationship can be established between dosage of shrinkage-reducing admixture and compressive strength for the mixtures containing Tough Air. For the mixtures with Tough Air, those with no shrinkage-reducing admixture had the lowest average compressive strength [4690 psi (32.4 MPa)], while the mixtures with a 0.5 percent dosage of shrinkage-reducing admixture had the highest average compressive strength [5200 psi (35.9 MPa)]. The compressive strengths of the Tough Air mixtures do not appear to have been affected by differences in the air content of the plastic concrete. As shown in Table 3.12, the differences in compressive strength for the Tough Air mixtures are not statistically significant.

The mixtures containing Tough Air and an SRA had average compressive strengths approximately 20 percent higher than the corresponding mixtures

containing Micro Air. The difference in compressive strength is statistically significant at $\alpha = 0.02$ when the mixtures containing Micro Air or Tough Air are compared at a 0.5 percent dosage of shrinkage-reducing admixture. In addition, the differences in compressive strength are statistically significant at $\alpha = 0.05$ when the mixtures containing Micro Air or Tough Air are compared at dosages of 1.0 and 2.0 percent SRA. Welker and Watson (2007) similarly observed higher compressive strengths in concrete containing a polymer-based air-entraining admixture compared to a surfactant-based air-entraining admixture in mixtures with similar air contents. The mixtures containing Micro Air and Tough Air and no SRA had similar compressive strengths (the difference is not statistically significant, Table 3.12). As shown in Table 3.11, the Micro Air mixtures with SRA dosages of 0 and 1.0 percent had average air contents in the plastic concrete approximately one percent above the corresponding Tough Air mixtures, while the Micro Air and Tough Air mixtures with SRA dosages of 0.5 and 2.0 percent had similar air contents. The lower air contents in the plastic concrete of the Tough Air mixtures with SRA dosages of 0 and 1.0 percent could have contributed to the higher compressive strengths. Conversely, the air content in the plastic concrete did not appear to influence the relative strengths of the Micro Air and Tough Air mixtures with SRA dosages of 0.5 and 2.0 percent. As stated previously, results from the hardened air-void analysis discussed in Section 3.2.6 indicate that many of the Tough Air mixtures had lower air contents than the Micro Air mixtures when measured in the hardened concrete. This drop in air content in the hardened concrete is sure to have contributed to the higher compressive strengths in the mixtures containing Tough Air.

3.2.6 Hardened Concrete Air-Void Analysis

As discussed in Section 3.2.3, the quantity and spacing of entrained air voids in concrete greatly influences the effectiveness of the air-void system in protecting the concrete from freeze-thaw damage. The spacing of the air voids is represented by

an air-void spacing factor, defined as the average distance from any point in the cement paste to the edge of the nearest void. Powers (1954) suggested that air-void spacing contributes more to frost protection than actual air content. As discussed in Section 1.6.1, an air-void spacing factor of no greater than 8×10^{-3} in. (0.20 mm) is suggested to provide sufficient freeze-thaw protection to the concrete (Russell 2004). In addition, the volume of air recommended by American Concrete Institute (ACI) Committee 201 to achieve satisfactory frost protection is between 5 and 6 percent for mixtures with a maximum aggregate size of 1 in. (25.4 mm). The LC-HPC specifications require air contents within the range of 6.5 to 9.5 percent for concrete to be accepted for placement (Kansas Department of Transportation 2007b), a requirement that is based on producing practical concrete mixtures that exhibit low cracking on bridge decks.

In this study, air contents in plastic concrete were determined using the Volumetric Air Content Method (ASTM C173), while air contents in hardened concrete were determined for two cylindrical specimens per mixture using the hardened concrete air-void analysis (ASTM C457). The air contents measured in the plastic and hardened concrete for mixtures containing Micro Air or Tough Air are shown in Figure 3.13. In the figure, the mixtures are categorized based on SRA dosages (0, 0.5, 1.0, and 2.0 percent by weight of cement). The air contents are tabulated in Table 3.13 and include the percentage difference in air content between those measured in the plastic and hardened concrete. The data in the figure and table represent the average plastic and hardened air contents of the mixtures for each SRA dosage. The number of batches used to calculate the average air content for each dosage is shown in parentheses in the figure and table.

As shown in Figure 3.13 and Table 3.13, both the Micro Air and Tough Air mixtures with no SRA exhibited only slightly lower air contents in the hardened concrete than in the plastic concrete. Between measurements in the plastic and

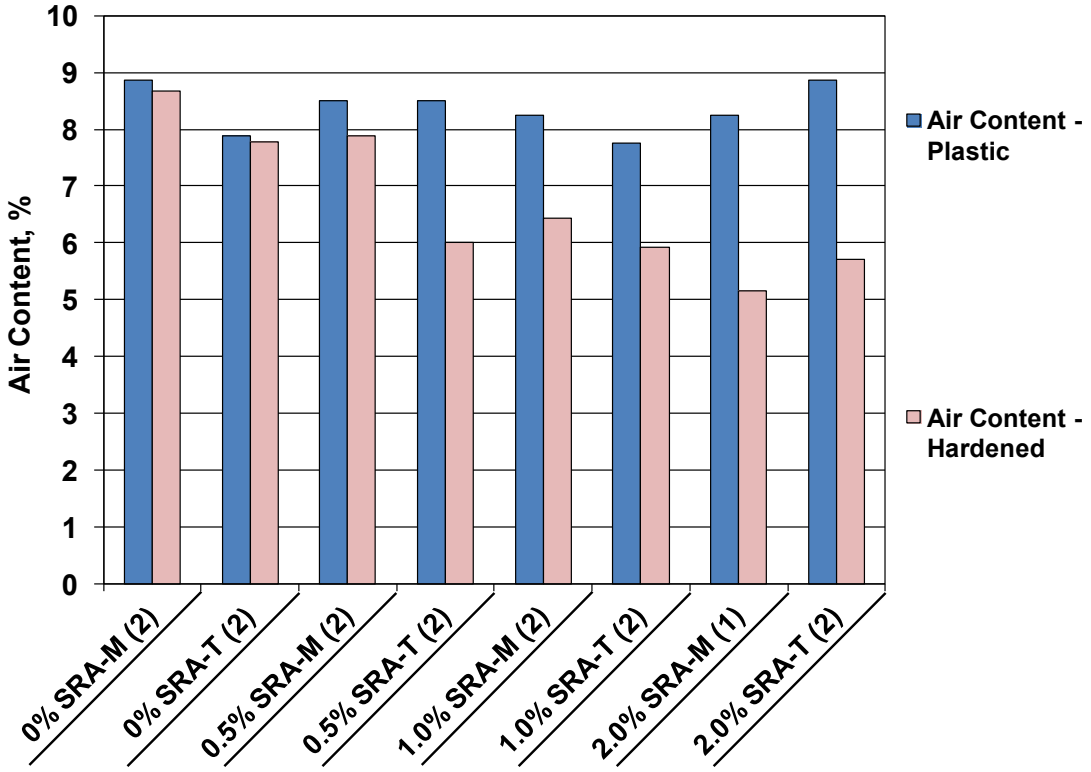

Note: Plastic and hardened air contents determined through ASTM C173 and C457, respectively. Number of mixtures used to calculate average air contents shown in parentheses, two specimens tested per mixture.

Figure 3.13 Air content in plastic and hardened concrete for mixtures in Program 1

Table 3.13 Air content values and percentage difference in air content between those measured in plastic and hardened concrete for mixtures in Program 1

Mixture*	Air Content		
	Plastic (%)	Hardened (%)	Percentage Difference†
0% SRA-M (2)	8.88	8.68	-2.3%
0% SRA-T (2)	7.88	7.78	-1.3%
0.5% SRA-M (2)	8.50	7.88	-7.4%
0.5% SRA-T (2)	8.50	6.00	-29.4%
1.0% SRA-M (2)	8.25	6.43	-22.1%
1.0% SRA-T (2)	7.75	5.93	-23.5%
2.0% SRA-M (1)	8.25	5.15	-37.6%
2.0% SRA-T (2)	8.88	5.70	-35.8%

*Number of batches used to calculate average air contents shown in parentheses, two specimens tested per mixture

†Percentage difference in air content between values measured in plastic and hardened concrete

Note: Plastic and hardened air contents determined through ASTM C173 and C457, respectively

Notation used for mixture designations explained in Section 2.5.1

hardened concrete, the Micro Air mixtures with no SRA (0% SRA-M) experienced a decrease in air content from 8.88 to 8.68 percent (a 2.3 percent reduction), while the Tough Air mixtures with no SRA (0% SRA-T) experienced a similar decrease from 7.88 to 7.78 percent (a 1.3 percent reduction). In contrast, the Micro Air and Tough Air mixtures containing an SRA experienced, in general, progressively greater reductions in air content between measurements in the plastic and hardened concrete, suggesting that the decreased surface tension of the water caused by the SRA reduced the stability of the air-void system as the specimens were placed and consolidated. The mixtures with Tough Air and SRA dosages of 0.5 and 1.0 percent experienced greater losses in air content than the corresponding mixtures with Micro Air. For the mixtures with a dosage of 0.5 percent shrinkage-reducing admixture (SRA) by weight of cement, the air content decreased from 8.5 percent in the plastic concrete to 7.88 percent in the hardened concrete for the Micro Air mixtures (a 7.4 percent reduction), but from 8.5 percent to 6.0 percent for the Tough Air mixtures (a 29.4 percent reduction). For the mixtures containing a 1.0 percent dosage of SRA, the air content decreased from 8.25 percent in the plastic concrete to 6.43 percent in the hardened concrete for the Micro Air mixtures (a 22.1 percent reduction), and from 7.75 percent to 5.93 percent for the Tough Air mixtures (a 23.5 percent reduction). Both the Micro Air and Tough Air mixtures generally experienced greater losses in air content from the plastic to the hardened concrete as the dosage of SRA was increased. The greatest loss in air content for both the Micro Air and Tough Air mixtures occurred when a 2.0 percent dosage of SRA was added to the mixtures, with reductions in air content of 37.6 and 35.8 percent, respectively, from the plastic to hardened condition.

The average air-void spacing factors in the hardened concrete (ASTM C457) are shown in Figure 3.14. As discussed previously, an air-void spacing factor of no greater than 8×10^{-3} in. (0.20 mm) is suggested to provide adequate freeze-thaw protection to the concrete (Russell 2004). Figure 3.14 shows that the air-void spacing

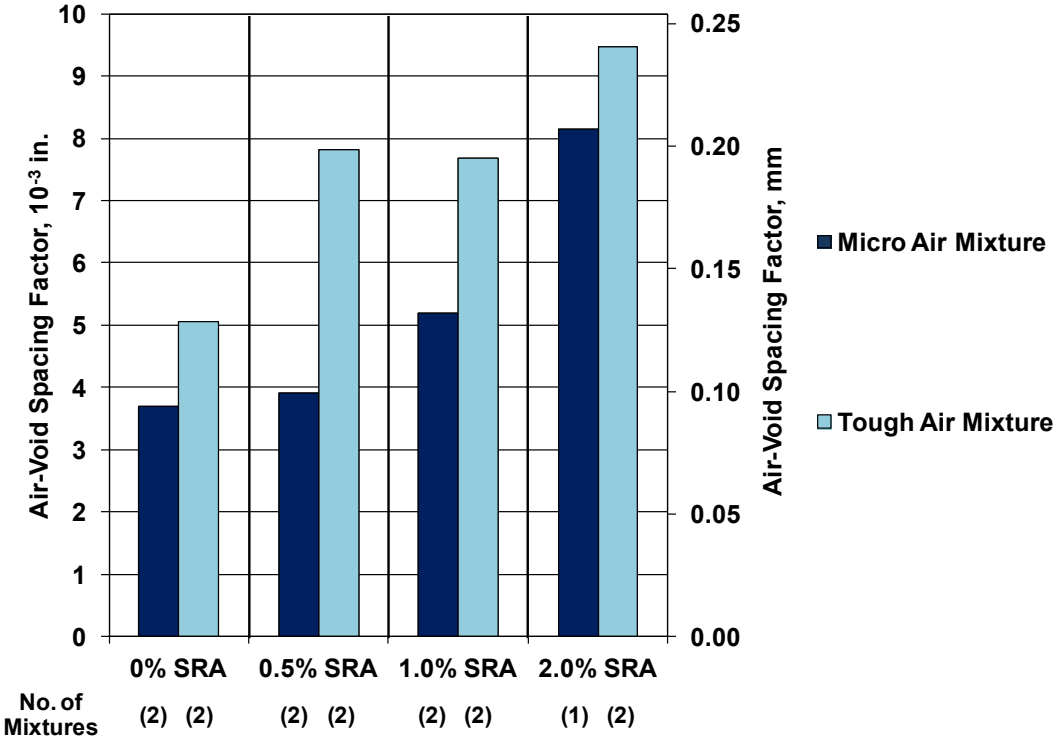

Note: Air-void spacing factor determined through ASTM C457

Figure 3.14 Average air-void spacing factor for Micro Air and Tough Air mixtures with different dosages of SRA (0, 0.5, 1.0, and 2.0 percent by weight of cement)

factor increased as the SRA dosage increased for both the Micro Air and Tough Air mixtures, but the factor is consistently lower for the Micro Air than for the Tough Air mixtures, even for the mixtures with no SRA. The highest air-void spacing factors correspond with the highest dosage of SRA (2.0 percent). In fact, the air-void spacing factors for both the Micro Air and Tough Air mixtures containing a dosage of 2.0 percent SRA exceed 8×10^{-3} in. (0.20 mm). The figure also shows that the Tough Air mixtures had a greater air-void spacing factor than the Micro Air mixtures at each dosage of SRA. The largest difference in air-void spacing factor occurs in the mixtures containing 0.5 percent SRA, for which the Micro Air and Tough Air mixtures have average spacing factors of 3.91×10^{-3} in. (0.10 mm) and 7.82×10^{-3} in. (0.20 mm), respectively. The spacing factor for each Tough Air mixture with SRA

approaches or exceeds 8×10^{-3} in. (0.20 mm) even though each of these mixtures had a plastic air content of at least 7.5 percent.

The average air-void spacing factors are shown as a function of the Durability Factor (DF) per ASTM C666 in Figure 3.15 and the average cumulative mass loss after 56 freeze-thaw cycles in Figure 3.16. The symbols used in the figures represent dosages of shrinkage-reducing admixture of 0, 0.5, 1.0, and 2.0 percent by weight of cement. The dosages are labeled "SRA" in the legends, but represent mixtures containing both the SRA and the CRA. Mixtures containing Micro Air and Tough Air are designated by "M" and "T," respectively, in the legends. Lines representing a DF of 95 and a mass loss limit of 0.31 lb/ft^2 (1500 g/m^2) are shown in Figures 3.15 and 3.16, respectively, to display the limits for acceptable freeze-thaw durability and scaling resistance. Air-void spacing factors, DFs, and values of mass loss after 56 freeze-thaw cycles are also shown in Table 3.14. Four of the twenty mixtures subjected to the hardened concrete air-void analyses (0% SRA-M, 1.0% SRA-M, 1.0% CRA-M #2, and 2.0% CRA-M) were not subjected to freeze-thaw testing and are not included in Figure 3.15. In addition, three of these mixtures (0% SRA-M, 1.0% CRA-M #2, and 2.0% CRA-M) were not tested for scaling resistance and are not included in Figure 3.16.

A clear relationship can be established between an increased air-void spacing factor and decreased freeze-thaw durability and scaling resistance, a relationship that is consistent with the findings from previous studies. As shown in Figure 3.15, six of the seven mixtures with a DF of 95 or greater had an air-void spacing factor less than or equal to 6×10^{-3} in. (0.15 mm). The seventh mixture, with a DF of 95, had a spacing factor of 8×10^{-3} in. (0.20 mm), meeting the suggested limit for adequate freeze-thaw durability. Four mixtures (1.0% SRA-T #2, 0.5% SRA-T, 2.0% CRA-T, and 2.0% SRA-T) with spacing factors between 6 and 8×10^{-3} in. (0.15 and 0.20

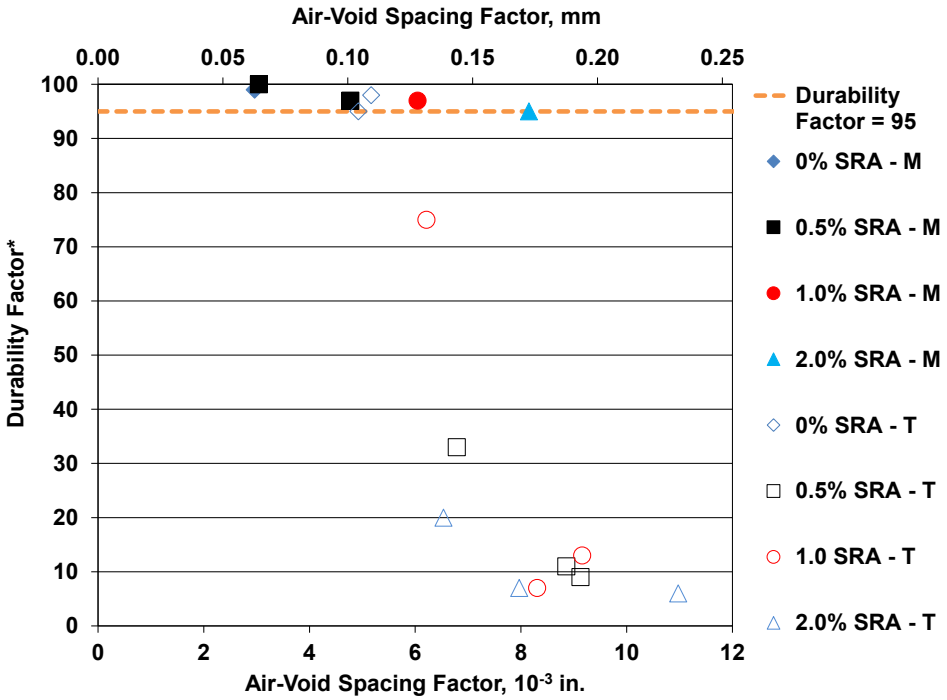

**Durability Factor (DF) = (P × N) / 300 cycles*, where *P* is the percentage of the initial dynamic modulus remaining at *N* cycles, *N* is either the number of cycles at which *P* reached 60 percent or 300 cycles (whichever is smaller)

Note: Air-void spacing factor determined through ASTM C457

Micro Air and Tough Air mixtures designated in legend by "M" and "T," respectively

Figure 3.15 Durability Factor versus air-void spacing factor for mixtures in Program 1

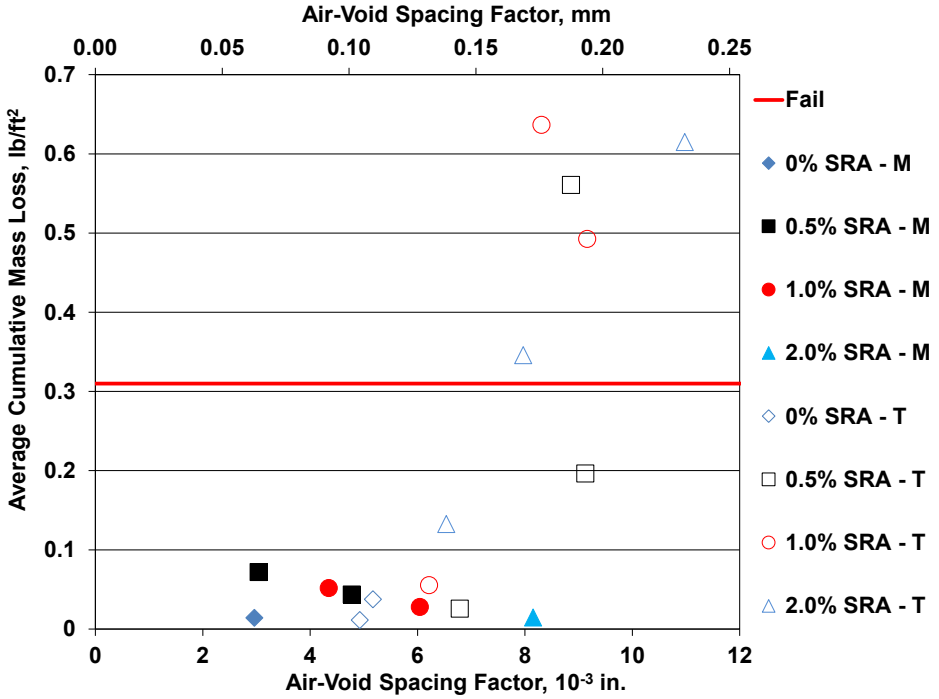

Note: Air-void spacing factor determined through ASTM C457

Micro Air and Tough Air mixtures designated in legend by "M" and "T," respectively

Figure 3.16 Average cumulative mass loss at 56 freeze-thaw cycles versus air-void spacing factor for mixtures in Program 1

Table 3.14 Summary of average cumulative mass loss at 56 freeze-thaw cycles and freeze-thaw cycles to test completion versus air-void spacing factor for mixtures in Program 1

Mixture	Air-Void Spacing Factor		Durability Factor*	Cumulative Mass Loss @ 56 cycles
	(mm)	(10^{-3} in.)		(10^{-3} lb/ft^2)
0% SRA-M	0.11	4.44	†	18.6
0% SRA-M #3	0.08	2.96	99	14.2
0.5% SRA-M	0.12	4.77	97	43.7
0.5% SRA-M #2	0.08	3.04	101	72
1.0% SRA-M	0.11	4.34	†	51.8
1.0% SRA-M #2	0.15	6.04	97	28
2.0% SRA-M #2	0.21	8.15	95	14.5
1.0% CRA-M #2	0.08	3.18	†	†
2.0% CRA-M	0.09	3.66	†	†
0% SRA-T	0.13	4.93	95.0	11.3
0% SRA-T #2	0.13	5.17	98	37.6
0.5% SRA-T	0.17	6.79	33	25.8
0.5% SRA-T #2	0.22	8.86	11	560.7‡
1.0% SRA-T	0.23	9.16	13	492.7
1.0% SRA-T #2	0.16	6.21	75	55.5
2.0% SRA-T	0.20	7.97	7	345.9
2.0% SRA-T #2	0.28	10.98	6	614.9‡
0.5% CRA-T	0.23	9.13	9	196.4
1.0% CRA-T	0.21	8.31	7	636.7
2.0% CRA-T	0.17	6.53	20	132.6

**Durability Factor (DF) = (P × N) / 300 cycles*, where *P* is the percentage of the initial dynamic modulus remaining at *N* cycles, *N* is either the number of cycles at which *P* reached 60 percent or 300 cycles (whichever is smaller).
†Mixture not subjected to testing
‡Testing completed at 35 cycles
Note: 10^{-3} lb/ft^2 = 4.884 g/m^2
Notation used for mixture designations explained in Section 2.5.1

mm), however, had DFs between 7 and 75. The two mixtures with the highest DFs (0% SRA-M #3 and 0.5% SRA-M #2) also had the lowest spacing factors. Conversely, the six mixtures with DFs below 20 each had a spacing factor greater than or equal to 8×10^{-3} in. (0.20 mm).

Scaling loss increased significantly as the air-void spacing factor approached or exceeded 8×10^{-3} in. (0.20 mm). Five of the seven mixtures with spacing factors equal to or greater than 8×10^{-3} in. (0.20 mm) (0.5% SRA-T #2, 1.0% SRA-T,

2.0% SRA-T, 2.0% SRA-T #2, and 1.0% CRA-T) experienced scaling losses above the failure limit of 0.31 lb/ft^2 (1500 g/m^2) specified in BNQ NQ 2621-900. Two mixtures with spacing factors above 8×10^{-3} in. (0.20 mm) (2.0% SRA-M #2 and 0.5% CRA-T), however, exhibited scaling losses of only 0.01 and 0.20 lb/ft^2 (50 and 975 g/m^2), respectively. The four mixtures with the greatest mass loss (1.0% CRA-T, 1.0% SRA-T, 2.0% SRA-T #2, and 0.5% SRA-T #2) had air-void spacing factors of greater than 8×10^{-3} in. (0.20 mm). The three mixtures with no SRA (0% SRA-M #3, 0% SRA-M, and 0% SRA-T) had spacing factors of less than 5.5×10^{-3} in. (0.14 mm) and exhibited low mass losses. The eight mixtures with spacing factors below 6.5×10^{-3} in. (0.17 mm) exhibited scaling losses below 0.10 lb/ft^2 (488 g/m^2), approximately one-third of the failure limit. In addition, two mixtures with spacing factors between 6.5 and 8×10^{-3} in. (0.17 and 0.20 mm) (0.5% SRA-T and 2.0% CRA-T) exhibited mass losses of 0.03 and 0.13 lb/ft^2 (145 and 635 g/m^2), respectively.

3.2.7 Program 1 Summary

The results from Program 1 show that the addition of SRA or CRA reduces both early-age (0 to 90 days) and long-term (90 to 365 days) shrinkage for concrete containing either Micro Air or Tough Air. The mixtures with a 2.0 percent dosage of shrinkage-reducing admixture by weight of cement exhibited the lowest shrinkage after 30, 90, 180, and 365 days of drying. No significant differences in shrinkage were observed between the mixtures with 0.5 and 1.0 percent dosages of shrinkage-reducing admixture. The type of shrinkage-reducing admixture had no significant effect on early-age shrinkage; however, the mixtures containing SRA (Tetraguard AS20) experienced lower long-term shrinkage than the mixtures containing similar dosages of CRA (MasterLIFE CRA 007). As expected, the type of air-entraining admixture used in the mixtures did not affect free shrinkage. A majority of the total shrinkage occurred during the first 30 days of drying. In addition, more than 80

percent of the total shrinkage after one year occurred during the first 90 days of drying for all mixtures. Mixtures containing CRA had a smaller percentage of the shrinkage after one year occur during the first 90 days than mixtures without CRA (including mixtures with SRA). The addition of an SRA or CRA had the greatest effect on shrinkage during the first 90 days of drying. Between 90 and 365 days, mixtures with and without a shrinkage-reducing admixture experienced similar increases in shrinkage.

When a shrinkage-reducing admixture was used, mixtures containing Tough Air exhibited significantly lower freeze-thaw durability and scaling resistance than mixtures containing Micro Air. When a shrinkage-reducing admixture was not included, the Tough Air mixtures exhibited slightly lower freeze-thaw durability and similar scaling resistance to the Micro Air mixtures. Mixtures with a 2.0 percent dosage of SRA had the lowest freeze-thaw durability of the mixtures containing either Micro Air or Tough Air and the lowest scaling resistance of the mixtures containing Tough Air; however, these values were significantly lower for the Tough Air mixtures. The type of shrinkage-reducing admixture did not appear to significantly affect freeze-thaw durability or scaling resistance.

Mixtures containing Micro Air experienced progressive reductions in compressive strength as the dosage of SRA or CRA was increased. For a 2.0 percent dosage of SRA or CRA, the compressive strength of the Micro Air mixtures decreased by approximately 15 percent, supporting findings by Berke et al. (1994). Tough Air mixtures exhibited higher strengths than Micro Air mixtures at similar air contents in the plastic concrete at 0.5 and 2.0 percent dosages of shrinkage-reducing admixture. Mixtures containing Tough Air with a 1.0 percent dosage of shrinkage-reducing admixture also exhibited higher strengths than the corresponding mixtures containing Micro Air; however, these Tough Air mixtures had slightly lower air contents than the Micro Air mixtures, possibly contributing to the difference in

compressive strength. Mixtures containing Micro Air or Tough Air and no SRA exhibited similar compressive strengths.

Micro Air and Tough Air mixtures containing an SRA experienced greater losses in air content from the plastic to the hardened concrete than mixtures without an SRA, with losses increasing as the SRA dosage increased. Increased dosages of SRA also contributed to increased air-void spacing factors for both Micro Air and Tough Air mixtures. These observations suggest that the decreased surface tension of the water caused by the SRA affected the air-void stability. In addition, the air-void spacing factors of the Tough Air mixtures were consistently greater than those of the Micro Air mixtures, even for the mixtures without an SRA. The mixtures with an increased air-void spacing factor experienced decreased freeze-thaw durability and scaling resistance, with the greatest effect for mixtures with air-void spacing factors above 8×10^{-3} in. (0.20 mm).

Ultimately, the polymer-based air-entraining admixture (Tough Air) did not, as originally expected, improve the stability of the air-void system with the addition of a shrinkage-reducing admixture. In fact, the polymer-based air void system seemed to exhibit less stability than the surfactant-based system (Micro Air) when a shrinkage-reducing admixture was added to the concrete. The reduction in surface tension provided by the shrinkage-reducing admixture clearly affected the stability of the foam bubbles in the polymer-based air-void system.

3.3 DURABILITY EVALUATION OF MIXTURES CONTAINING SHRINKAGE-REDUCING ADMIXTURES WITH AIR CONTENTS BELOW LC-HPC REQUIREMENTS (PROGRAM 2)

3.3.1 General

As described in Sections 1.8.1.2 and 2.5.2, Program 2 examined the freeze-thaw durability, scaling resistance, compressive strength, and air-void system characteristics of mixtures containing a shrinkage-reducing admixture with air

contents below that required by the low-cracking high-performance concrete (LC-HPC) specifications. As explained in Section 1.6.1.1, proper volume and spacing of air voids are needed to provide adequate freeze-thaw durability and scaling resistance to concrete. A uniform distribution of small, closely-spaced air voids protects the concrete against freeze-thaw damage by providing locations for internal water to freeze and expand, protecting the cement paste from tensile stresses and cracking. The LC-HPC specifications require concrete to contain a minimum air content of 6.5 percent (Kansas Department of Transportation 2007b).

As discussed in Sections 1.7.3 and 3.2.1, shrinkage-reducing admixtures function by reducing the surface tension of the pore water, minimizing capillary stresses and, thus, drying shrinkage, a principal factor contributing to cracking. The reduced surface tension, however, can affect the stability of the air-void system, causing larger, more widely-spaced air-voids. As shown in the analysis in Program 1, the addition of a shrinkage-reducing admixture can decrease the freeze-thaw durability and scaling resistance of concrete.

Program 2 advanced the findings of Program 1 by examining the freeze-thaw performance of mixtures containing a shrinkage-reducing admixture with air contents below 6.5 percent. The reason for concern is that, although the LC-HPC specifications require a minimum air content of 6.5 percent, the variability in concrete properties and the need for continuous placement of concrete in the field can lead to the occasional placement of concrete with air contents below the specified minimum. In addition, the freeze-thaw durability and scaling performance of the concrete with low air content may be further degraded if the stability of the air-void system is reduced by a shrinkage-reducing admixture. The objective of this program was to determine a lower limit for air content for mixtures containing shrinkage-reducing admixtures that would still provide adequate freeze-thaw durability. This lower limit

could then be translated into air-content restrictions for bridge deck placements with concretes containing shrinkage-reducing admixtures.

Program 2 examined the effects of dosage of shrinkage-reducing admixture and air content on freeze-thaw durability, scaling resistance, compressive strength, and air-void system characteristics. The program included 16 batches with SRA (Tetraguard AS20) dosages of 0, 0.5, 1.0, and 2.0 percent by weight of cement and air contents ranging from 3.5 to 9 percent. Six of these sixteen batches, identified in Tables 2.1 and 2.3 as Batch Numbers 722, 754, 769, 796, 816, and 820, were also included in the evaluation of Program 1. The surfactant-based air-entraining admixture used in Program 1, Micro Air, was used in all mixtures. Detailed information regarding the test program is provided in Section 2.5.2. Mixture descriptions, name designations, batch numbering, and testing information are provided in Table 2.3. The mixture proportions, concrete properties, and compressive strengths are summarized in Tables A.10 and A.11 in Appendix A. The mixtures had cement contents of 520 or 540 lb/yd^3 (308 or 320 kg/m^3) and water-cement ratios of 0.44 or 0.45, complying with the requirements of the LC-HPC specifications. The range of cement paste contents (23.0 to 25.4 percent) was somewhat greater for Program 2 than for Program 1 because of the wide range in air contents (mixtures with lower air contents have less volume occupied by air). The mixtures were designed for a target slump of 2.25 ± 0.75 in. (55 ± 20 mm).

The mixtures are evaluated for freeze-thaw durability in accordance with ASTM C666 – Procedure B (with modifications per KDOT Test KTMR-22) and scaling resistance per Canadian Test BNQ NQ 2621-900 Annex B. Compressive strengths were measured in accordance with ASTM C39 and hardened air-void analyses were completed in accordance with ASTM C457. The results of the evaluations are provided in the following sections. Detailed information regarding the procedures of the tests is provided in Chapter 2.

3.3.2 Freeze-Thaw Durability

The evaluation of freeze-thaw durability in Program 2 included tests of 15 batches (15 different mixtures), examining the effects of shrinkage-reducing admixture dosage and air content on freeze-thaw durability. The mixtures include four with no SRA (air contents ranging from 3.5 to 9 percent), three with a 0.5 percent dosage (by weight of cement) of SRA (air contents from 4 to 8 percent), three with a 1.0 percent dosage of SRA (air contents from 5.25 to 7.75 percent), and five with a 2.0 percent dosage of SRA (air contents from 3.5 to 8.25 percent). The mixtures are shown in Table 2.3. Similar to Program 1, three specimens from each batch were tested in accordance with ASTM C666 and KDOT Test KTMR-22. Detailed test procedures are described in Section 2.4.2. Testing was completed once the specimens had completed 300 freeze-thaw cycles or when the average dynamic modulus of elasticity of the three specimens dropped to 60 percent or less of the initial average dynamic modulus of elasticity. As with Program 1, the Durability Factor (DF, Section 2.4.2) was used to quantify the freeze-thaw performance of the mixtures. In accordance with the KDOT requirements for concrete placed on-grade (Kansas Department of Transportation 2007d), a DF of 95 is the minimum acceptable value in this evaluation. The raw data from the tests are provided in Appendix C.

The average dynamic modulus of elasticity for the three specimens from each batch is plotted as a function of the number of freeze-thaw cycles in Figures 3.17, 3.18, and 3.19, respectively, for mixtures containing air contents of less than 4.5 percent, 4.5 to 6.75 percent, and greater than or equal to 7 percent. In the figure legends, the mixtures are listed in the order of descending DF. Table 3.15 shows the DFs of the mixtures and, where applicable, the number of freeze-thaw cycles completed prior to reaching 60 percent of the initial dynamic modulus. Interpolation between dynamic modulus and freeze-thaw cycle is used to determine the number of freeze-thaw cycles corresponding to 60 percent of the initial dynamic modulus for the

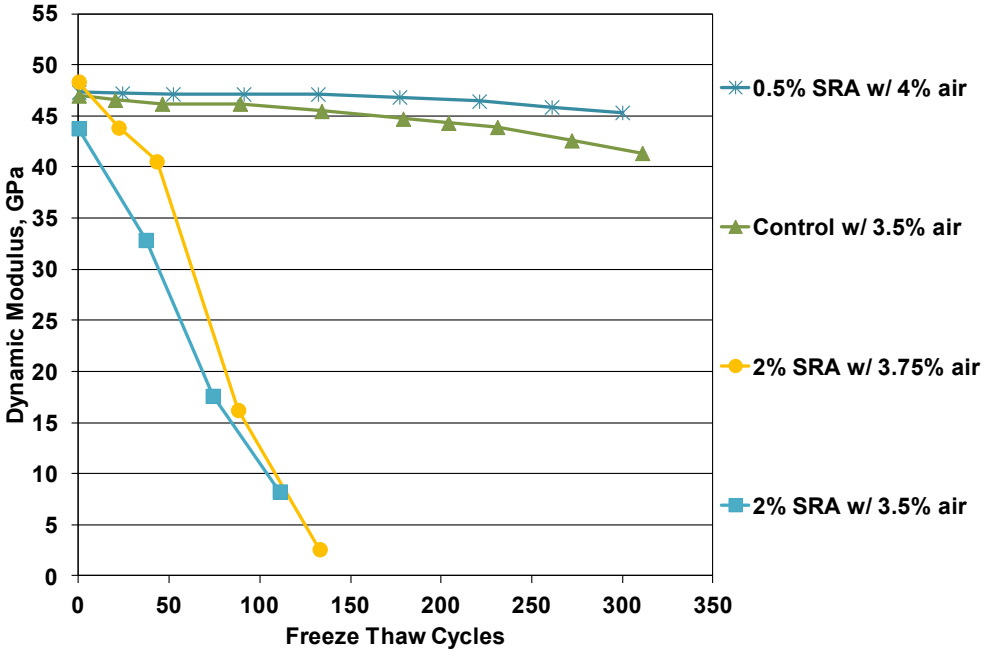

Figure 3.17 Average dynamic modulus of elasticity versus freeze-thaw cycles for mixtures containing air contents of less than 4.5 percent in Program 2

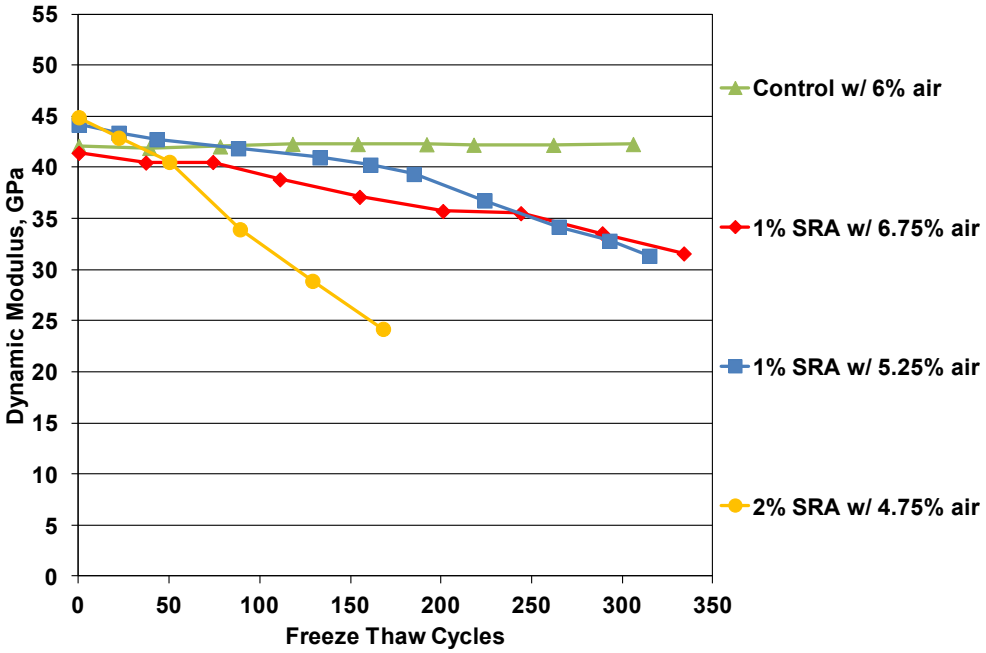

Figure 3.18 Average dynamic modulus of elasticity versus freeze-thaw cycles for mixtures containing air contents between 4.5 and 6.75 percent in Program 2

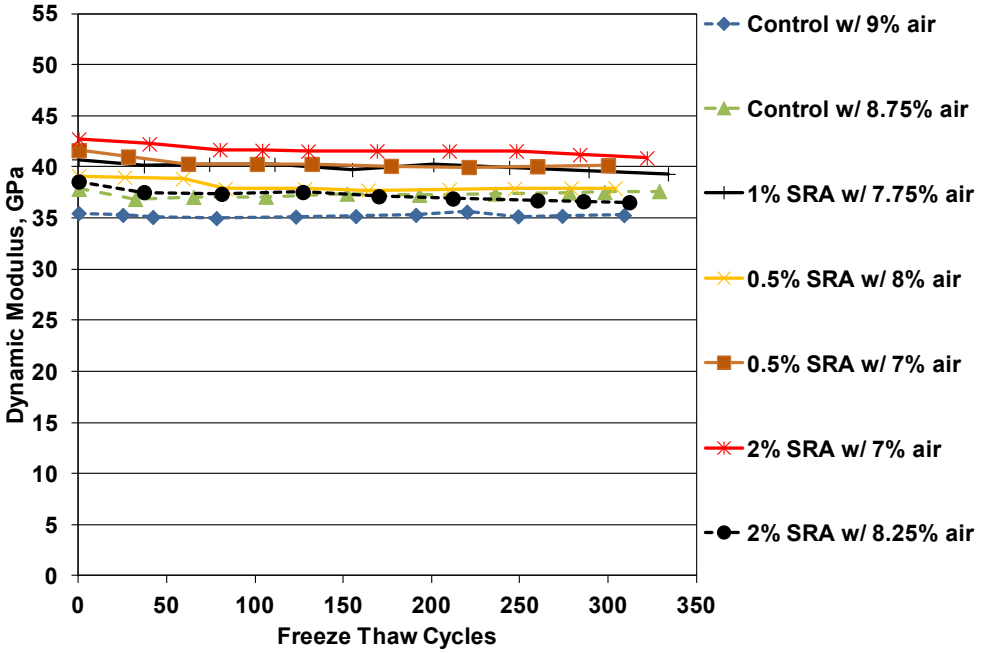

Figure 3.19 Average dynamic modulus of elasticity versus freeze-thaw cycles for mixtures containing air contents greater than or equal to 7 percent in Program 2

Table 3.15 Summary of average dynamic modulus of elasticity versus freeze-thaw cycles for mixtures in Program 2

Air Content	Mixture	Durability Factor[#]	Cycles Completed at 60% of Initial Dynamic Modulus[†]
< 4.5%	0.5% SRA w/ 4% air	96	-
	Control w/ 3.5% air	89	-
	2% SRA w/ 3.75% air	13	64
	2% SRA w/ 3.5% air	11	53
4.5 to 6.75%	Control w/ 6% air	100	-
	1% SRA w/ 6.75% air	80	-
	1% SRA w/ 5.25% air	73	-
	2% SRA w/ 4.75% air	29	145
≥ 7%	Control w/ 9% air	99	-
	Control w/ 8.75% air	99	-
	1% SRA w/ 7.75% air	97	-
	0.5% SRA w/ 8% air	97	-
	0.5% SRA w/ 7% air	96	-
	2% SRA w/ 7% air	96	-
	2% SRA w/ 8.25% air	95	-

[#] *Durability Factor (DF) = (P × N) / 300 cycles*,
where *P* is the percentage of the initial dynamic modulus remaining at *N* cycles, *N* is either the number of cycles at which *P* reached 60 percent or 300 cycles (whichever is smaller).
†Number of freeze-thaw cycles completed prior to reaching 60 percent of the initial dynamic modulus.
"-" denotes mixture reached 300 cycles prior to dropping to 60 percent of initial dynamic modulus.
Note: Three specimens tested per mixture

specimens that did not reach 300 cycles and the average dynamic modulus at 300 cycles for the specimens subjected to more than 300 cycles. The figures and table show that the mixtures with air contents of less than 4.5 percent, 4.5 to 6.75 percent, and greater than or equal to 7 percent had, respectively, DFs ranging from 11 to 96, 29 to 100, and 95 to 99.

As shown in the figures and table, increased air content contributed to increased freeze-thaw durability. This observation supports the understanding that an increased availability of air-voids protects the concrete from freeze-thaw damage by providing closely-spaced locations for internal water to freeze and expand. Only one of the four mixtures with an air content below 4.5 percent (0.5% SRA w/ 4% air) had a DF above 95 after 300 freeze-thaw cycles (Figure 3.17). A mixture with no SRA and an air content of 3.5 percent (Control w/ 3.5% air) had a DF of only 89. Regardless of SRA dosage, mixtures with an air content above 5 percent had a DF of greater than 70 and mixtures with an air content above 7 percent had a DF of 95 or greater.

The mixtures exhibited decreased freeze-thaw durability as the dosage of SRA was increased. The decrease in durability was most pronounced for an SRA dosage above 1.0 percent. Decreased freeze-thaw durability would be expected for mixtures with increased dosages of SRA due to the effect of reduced pore water surface tension on the stability of the air-void system. The three mixtures with DFs below 60 contained a 2.0 percent dosage of SRA. At lower air contents, the effect of SRA dosage on durability was more pronounced. At air contents below 7 percent (Figures 3.17 and 3.18), the freeze-thaw durability decreased significantly as the SRA dosage increased from 0 to 1.0 percent and again to 2.0 percent. In contrast, two mixtures with a 2.0 percent dosage of SRA and an air content above 7 percent (2% SRA w/ 7% air and 2% SRA w/ 8.25% air) had DFs of 95 or greater (Figure 3.19). Three mixtures with 0.5 percent SRA had similar DFs as mixtures with comparable air

contents and no SRA. In fact, a mixture containing a 0.5 percent dosage of SRA with an air content of 4 percent had a higher DF than a mixture with no SRA dosage and an air content of 3.5 percent (96 vs. 89). Three mixtures with no SRA (Control w/ 6% air, Control w/ 9% air, and Control w/ 8.75% air) had the highest DFs (100, 99, and 99, respectively).

Figure 3.20 shows the DFs of the mixtures as a function of air content. The symbols used in the figure depict the four SRA dosages. A line representing a DF of 95 is shown in the figure to display the limit for acceptable durability is this study. The figure indicates that nine of the fifteen mixtures had a DF of 95 or greater. Three mixtures with a dosage of 2.0 percent SRA and air contents below 5 percent had significantly lower durability than the other mixtures, each with a DF of less than 30. As discussed previously, all mixtures with an air content of 7 percent or greater, regardless of SRA dosage, had a DF of 95 or greater. The figure shows that the mixtures with SRA dosages of 0 and 0.5 percent were not significantly affected by changes in air content; the one exception was a mixture with no SRA and an air content of just 3.5 percent, which had a DF of 89. The mixtures with SRA dosages of 1.0 and 2.0 percent experienced considerable reductions in durability at air contents below 7 percent.

3.3.3 Scaling Resistance

The evaluation of scaling resistance in Program 2 included the tests of 16 batches (16 different mixtures), examining the effects of SRA dosage and air content on scaling resistance. The 16 mixtures included the 15 mixtures that were evaluated for freeze-thaw durability in Section 3.3.2 and an additional mixture with a 1.0 percent dosage of SRA by weight of cement and an air content of 8.75 percent (designated as 1% SRA w/ 8.75% air).

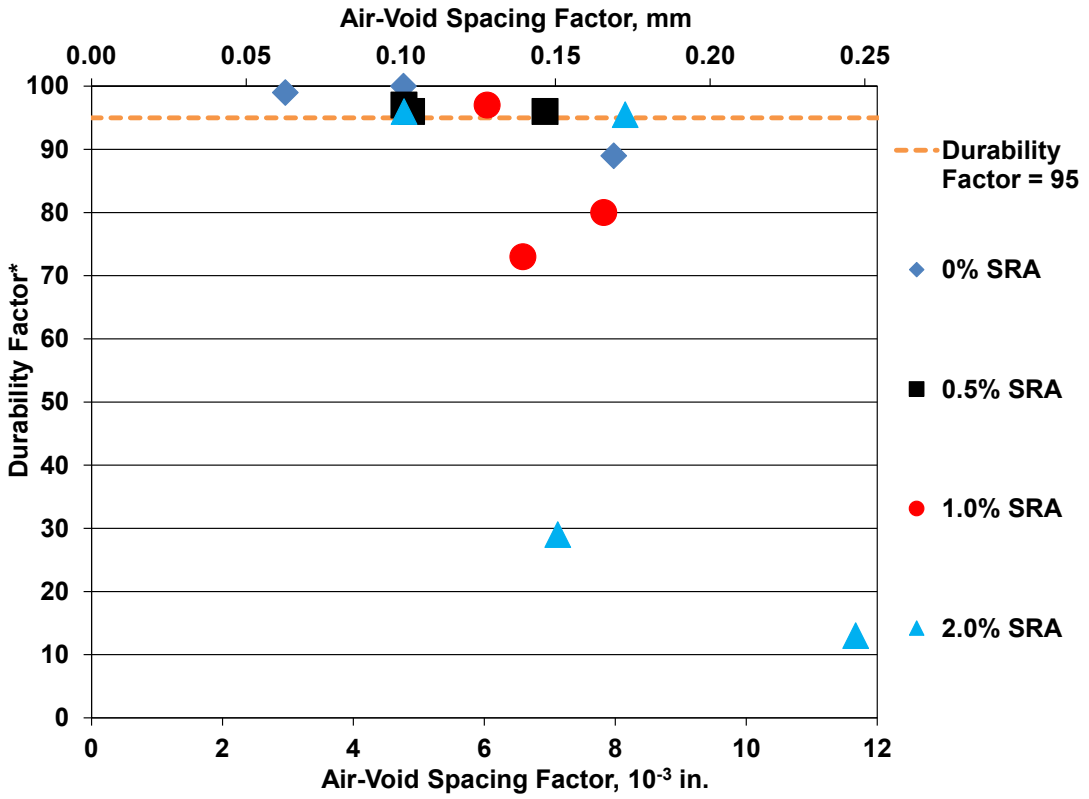

* *Durability Factor (DF) = (P × N) / 300 cycles*,
where *P* is the percentage of the initial dynamic modulus remaining at *N* cycles, *N* is either the number of cycles at which *P* reached 60 percent or 300 cycles (whichever is smaller).

Figure 3.20 Durability Factor versus air content for mixtures in Program 2

Three specimens from each batch were tested for scaling resistance in accordance with Canadian Test BNQ NQ 2621-900 Annex B. The test procedures are described in Section 2.4.3. As explained in Section 2.4.3, surface mass loss of the specimens is determined after 7, 21, 35, and 56 freeze-thaw cycles, and the specified limit for average cumulative mass loss for the three specimens at the test completion is 0.31 lb/ft^2 (1500 g/m^2). The raw data from the tests are provided in Appendix C.

The average cumulative mass loss for the three specimens per batch is plotted as a function of freeze-thaw cycles in Figures 3.21, 3.22, and 3.23, respectively, for mixtures with air contents of less than 4.5 percent, 4.5 to 6.75 percent, and greater than or equal to 7 percent. In the figure legends, the mixtures are listed in the order of

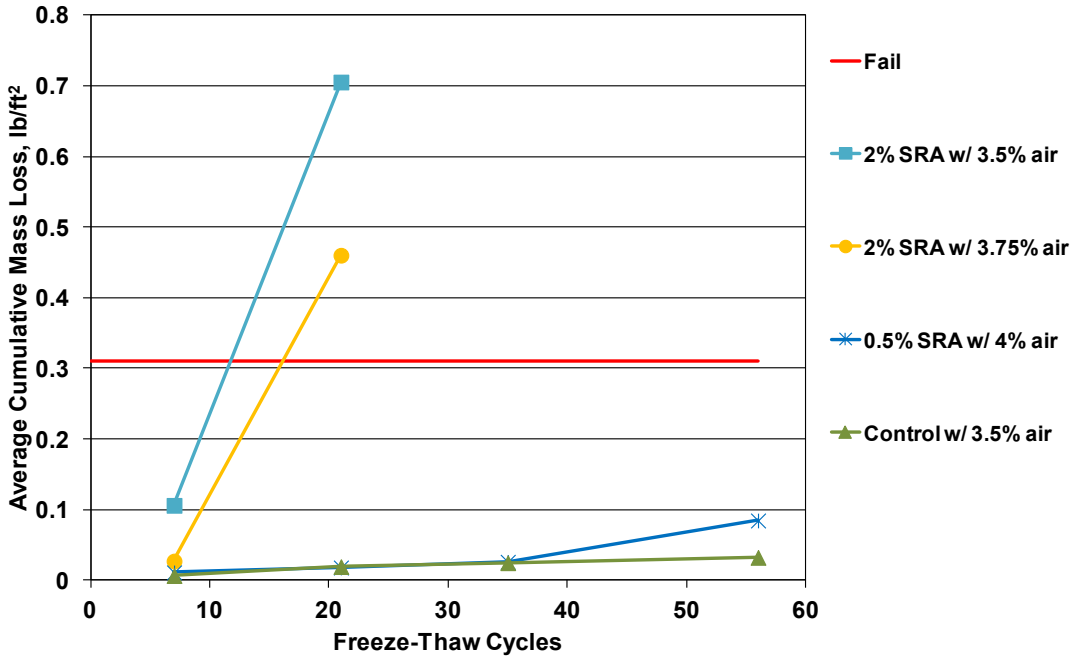

Figure 3.21 Average cumulative mass loss versus freeze-thaw cycles for mixtures containing air contents less than 4.5 percent in Program 2

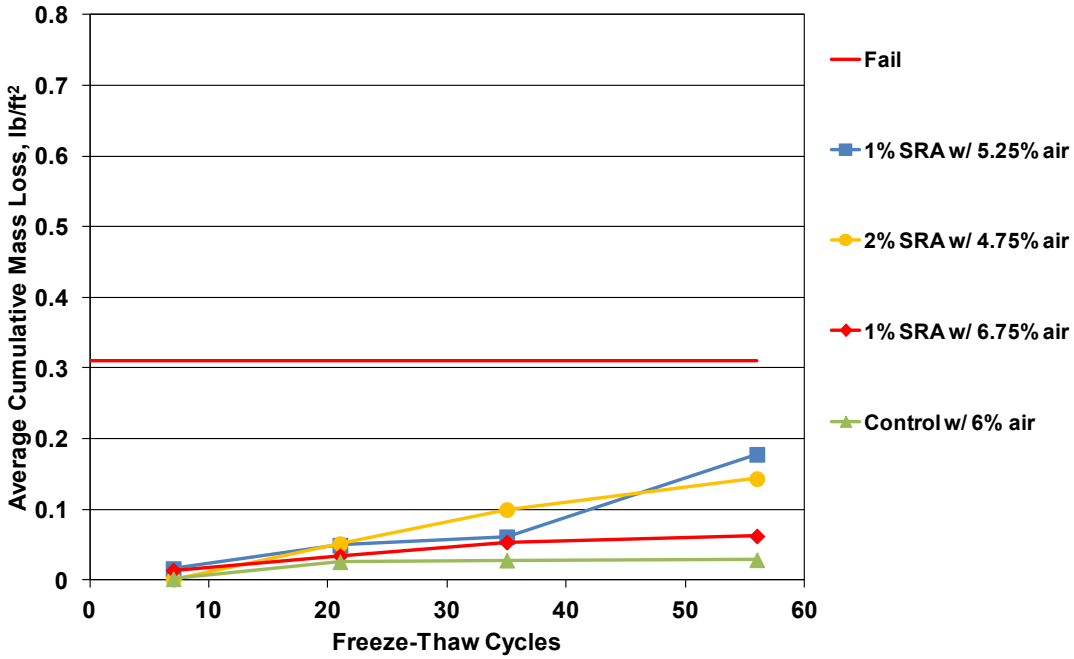

Figure 3.22 Average cumulative mass loss versus freeze-thaw cycles for mixtures containing air contents between 4.5 and 6.75 percent in Program 2

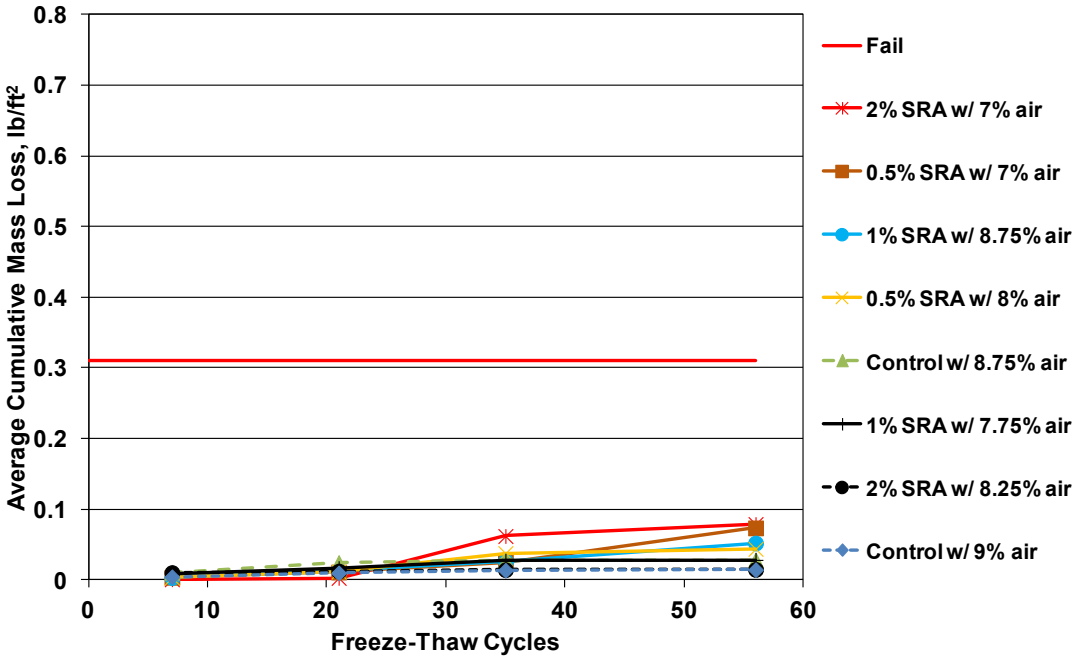

Figure 3.23 Average cumulative mass loss versus freeze-thaw cycles for mixtures containing air contents greater than or equal to 7 percent in Program 2

descending cumulative mass loss after 56 freeze-thaw cycles. Mixtures that did not reach 56 cycles are listed in the order of ascending number of freeze-thaw cycles to failure. The losses for the mixtures at 7, 21, 35, and 56 cycles are summarized in Table 3.16. The figures and table show that the mixtures with air contents of less than 4.5 percent, 4.5 to 6.75 percent, and greater than or equal to 7 percent had average mass losses at completion of the test ranging from 0.03 to 0.71 lb/ft^2 (155 to 3445 g/m^2), 0.03 to 0.18 lb/ft^2 (140 to 870 g/m^2), and 0.01 to 0.08 lb/ft^2 (70 to 385 g/m^2), respectively.

As shown in the figures and table, both decreasing air content and increasing dosage of SRA reduce scaling resistance. This observation is similar to the findings of the freeze-thaw durability tests in Section 3.3.2. The two mixtures that exceeded the limit of cumulative mass loss [0.31 lb/ft^2 (1500 g/m^2)] prior to 56 cycles contained a 2.0 percent dosage of SRA and an air content below 4 percent (2% SRA w/ 3.5% air and 2% SRA w/ 3.75% air). These two mixtures had, in fact, exceeded

Table 3.16 Summary of average cumulative mass loss versus freeze-thaw cycles for mixtures in Program 2

Air Content	Mixture	Average Cumulative Mass Loss 10^{-3} lb/ft^2			
		7 cycles	21 cycles	35 cycles	56 cycles
< 4.5%	Control w/ 3.5% air	6.3	19.0	24.4	32.1
	0.5% SRA w/ 4% air	10.8	17.7	25.8	84.4
	2% SRA w/ 3.75% air	26.9	460.1	‡	‡
	2% SRA w/ 3.5% air	105.8	705.5	‡	‡
4.5 to 6.75%	Control w/ 6% air	1.7	25.7	27.9	28.5
	1% SRA w/ 6.75% air	13.7	34.3	53.4	62.1
	1% SRA w/ 5.25% air	15.9	49.1	61.0	177.7
	2% SRA w/ 4.75% air	0.9	51.2	99.5	143.2
≥ 7%	Control w/ 9% air	4.1	9.6	13.2	14.2
	Control w/ 8.75% air	10.6	24.3	27.6	28.1
	0.5% SRA w/ 8% air	3.1	11.6	37.6	43.7
	0.5% SRA w/ 7% air	3.3	10.8	24.7	73.3
	1% SRA w/ 8.75% air	3.1	13.3	26.3	51.8
	1% SRA w/ 7.75% air	7.8	16.4	26.8	28.0
	2% SRA w/ 8.25% air	10.0	12.1	14.1	14.5
	2% SRA w/ 7% air	0.5	2.5	61.8	78.7

‡Mixture exceeded failure limit of 0.31 lb/ft^2 (1500 g/m^2) prior to 56 cycles
Note: 10^{-3} lb/ft^2 = 4.884 g/m^2
Three specimens tested per mixture

the mass loss limit after only 21 cycles. Two other mixtures with air contents of 4 percent or less (0.5% SRA w/ 4% air and Control w/ 3.5% air) had cumulative mass losses below 0.10 lb/ft^2 (488 g/m^2), approximately one-third of the failure limit, after 56 freeze-thaw cycles. Apart from the two mixtures with a 2.0 percent SRA dosage and air contents below 4 percent, only two other mixtures experienced cumulative mass losses greater than 0.10 lb/ft^2 (488 g/m^2) (approximately one-third of the failure limit) after 56 freeze-thaw cycles – these mixtures contained dosages of 1.0 and 2.0 percent SRA with air contents of 5.25 and 4.75 percent, respectively. No mixture with an air content above 7 percent, regardless of SRA dosage, experienced a cumulative mass loss greater than 0.10 lb/ft^2 (488 g/m^2). For mixtures with similar air contents, increased dosages of SRA generally contributed to increased mass loss. This trend is more pronounced when comparing mixtures at lower air contents. Mixtures containing increased dosages of SRA would be expected to experience

reduced scaling resistance due to the effect of the reduced pore water surface tension on the air-void system. Mixtures with no SRA experienced the lowest mass loss in each of the three ranges of air content (less than 4.5 percent, between 4.5 and 6.75 percent, and 7 percent or greater). Because the cumulative mass losses at test completion for the mixtures with air contents of 7 percent or greater fell within a narrow range of values, 0.01 to 0.08 lb/ft^2 (70 to 385 g/m^2), the order of decreasing mass loss for these mixtures is of limited or no significance.

Figure 3.24 shows the cumulative mass loss of the mixtures at test completion as a function of air content. As discussed previously, testing was completed either after 56 freeze-thaw cycles or when the average cumulative mass loss of the three specimens per mixture exceeded the specified limit of 0.31 lb/ft^2 (1500 g/m^2). The symbols used in the figures represent the four SRA dosages. The figure indicates that mixtures with increased air contents exhibited decreased mass losses. SRA dosage did not greatly affect the scaling resistance of mixtures with air contents of 7 percent or more. At air contents below 7 percent, mixtures with increased dosages of SRA exhibited increased mass losses. The two mixtures with a 2.0 percent SRA dosage with air contents below 4 percent exhibited more than twice the mass loss of any other mixture. The scaling resistance of a mixture with a 2.0 percent SRA dosage and an air content of 4.75 percent was significantly better than the two mixtures with a 2.0 percent SRA dosage and air contents below 4 percent, suggesting that the relationship between scaling resistance and air content is non-linear. Reduced air contents did not affect the scaling resistance of mixtures with no SRA. In addition, the scaling resistance of mixtures with a 0.5 percent dosage of SRA was only slightly affected by reduced air contents.

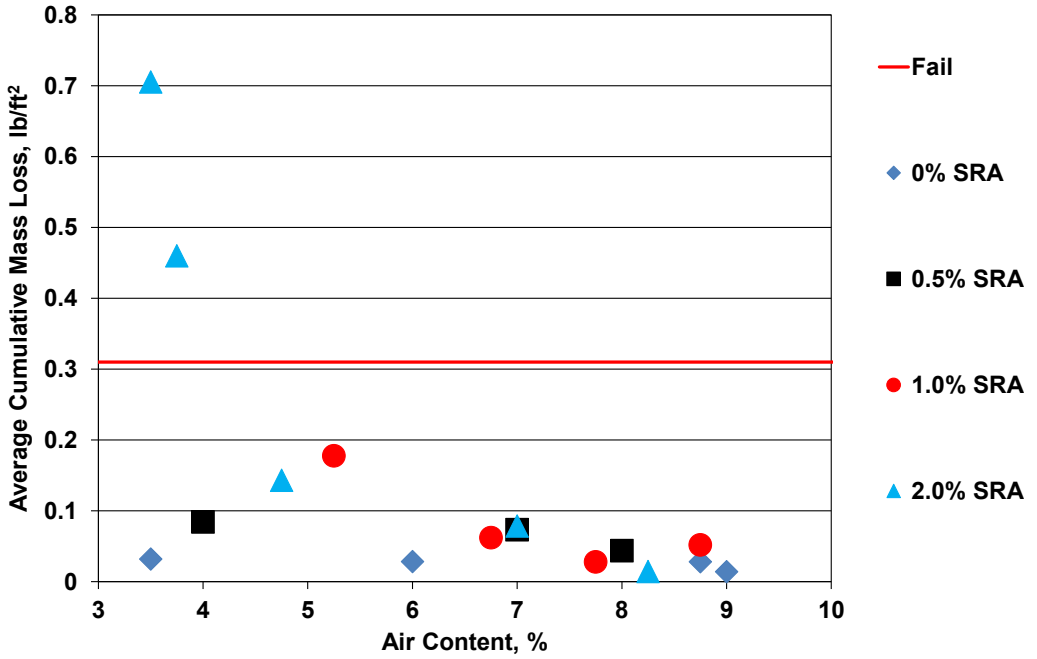

Note: Testing was completed either after 56 freeze-thaw cycles or when the average cumulative mass loss of the three specimens per mixture exceeded the fail limit of 0.31 lb/ft^2 (1500 g/m^2).

Figure 3.24 Average cumulative mass loss at test completion versus air content for mixtures in Program 2

3.3.4 Compressive Strength

Compressive strengths at 28 days were measured for 10 of the batches in Program 2 and are shown in Table A.11 in Appendix A. Concretes with low air contents generally exhibit higher compressive strengths because of the lower volume taken up by air – the component that provides no strength to the constituent matrix. As discussed in Section 1.4.1, higher compressive strengths increase the potential for cracking in bridge decks by reducing the mitigation of tensile stresses provided by the effects of creep.

Figure 3.25 shows the 28-day compressive strengths of the 10 batches as a function of air content. The upper and lower limits for 28-day compressive strength required by the LC-HPC specifications, 5500 and 3500 psi (37.9 and 24.1 MPa), are also shown in the figure. As expected, the figure indicates that compressive strengths

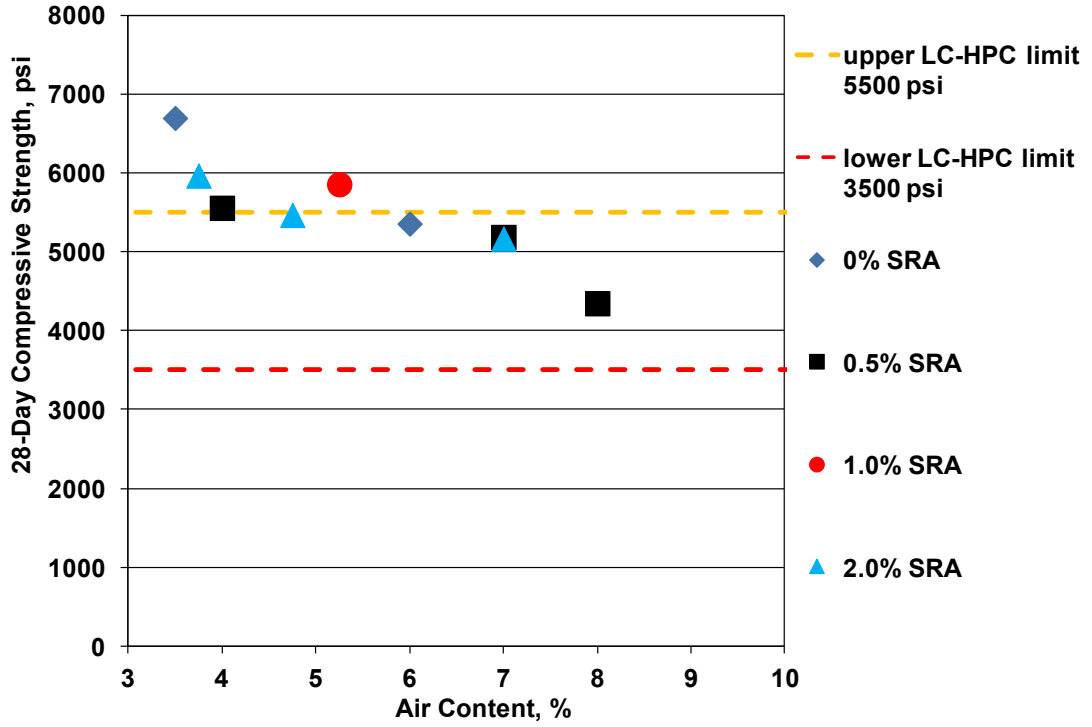

Note: Upper and lower limits for compressive strength required by the LC-HPC specifications (Kansas Department of Transportation 2007b) are shown in the figure.
1 psi = 0.0069 MPa.

Figure 3.25 Compressive strength at 28 days versus air content for mixtures in Program 2

increased for mixtures with lower air contents. The five mixtures with air contents of 6 percent or greater had compressive strengths below the upper limit in the LC-HPC specifications, 5500 psi (37.9 MPa). A mixture with a 2.0 percent dosage of SRA and an air content of 4.75 percent also exhibited a strength below the limit of 5500 psi (37.9 MPa) [5470 psi (37.7 MPa)]. All other mixtures with air contents below 6 percent had compressive strengths above the allowable limit. The single mixture with an air content of at least 8 percent was the only mixture with a strength below 5000 psi (34.5 MPa).

The mixture with no SRA and an air content of 3.5 percent had a strength of 6700 psi (46.2 MPa), the highest strength in this series of mixtures. The mixture with

a 2.0 percent dosage of SRA and an air content of 3.75 percent, close to the air content of the mixture with no SRA, had a strength of 5970 psi (41.2 MPa), considerably lower than the mixture with no SRA. The decrease in strength observed as the SRA dosage increased from 0 to 2.0 percent supports the findings from Program 1 and earlier findings by Berke et al. (1994), both discussed in Section 3.2.5, that noted reductions in strength for mixtures containing a 2.0 percent dosage of a shrinkage-reducing admixture compared to mixtures with no SRA.

The results shown in Figure 3.25 introduce additional problems associated with the use of low-air concrete in bridge deck applications. Not only does concrete with low air contents experience reduced freeze-thaw durability and scaling resistance, but the increased strength of the low-air concrete increases the potential for cracking by reducing the beneficial effects of creep.

3.3.5 Hardened Concrete Air-Void Analysis

The average air-void spacing factors of 14 mixtures in Program 2 are plotted as a function of air content in the plastic concrete in Figure 3.26. The symbols in the figure represent the four dosages of SRA used in the mixtures. The air-void spacing factors of the mixtures are tabulated in Table 3.17. A linear relationship between air content and air-void spacing factor would be expected for mixtures with a constant air-void size. As explained previously, mixtures containing an SRA can have an increased air-void size and spacing because the surface tension at the air-void boundary is decreased.

The figure indicates that, at similar air contents, mixtures with increased dosages of SRA had increased air-void spacing factors. For mixtures with no SRA, the air-void spacing factors increased linearly as the air content decreased; this observation suggests that the air voids maintained a constant size as the air content decreased. Mixtures containing a 0.5 percent dosage of SRA by weight of cement experienced a relatively linear relationship between air content and spacing factor; for

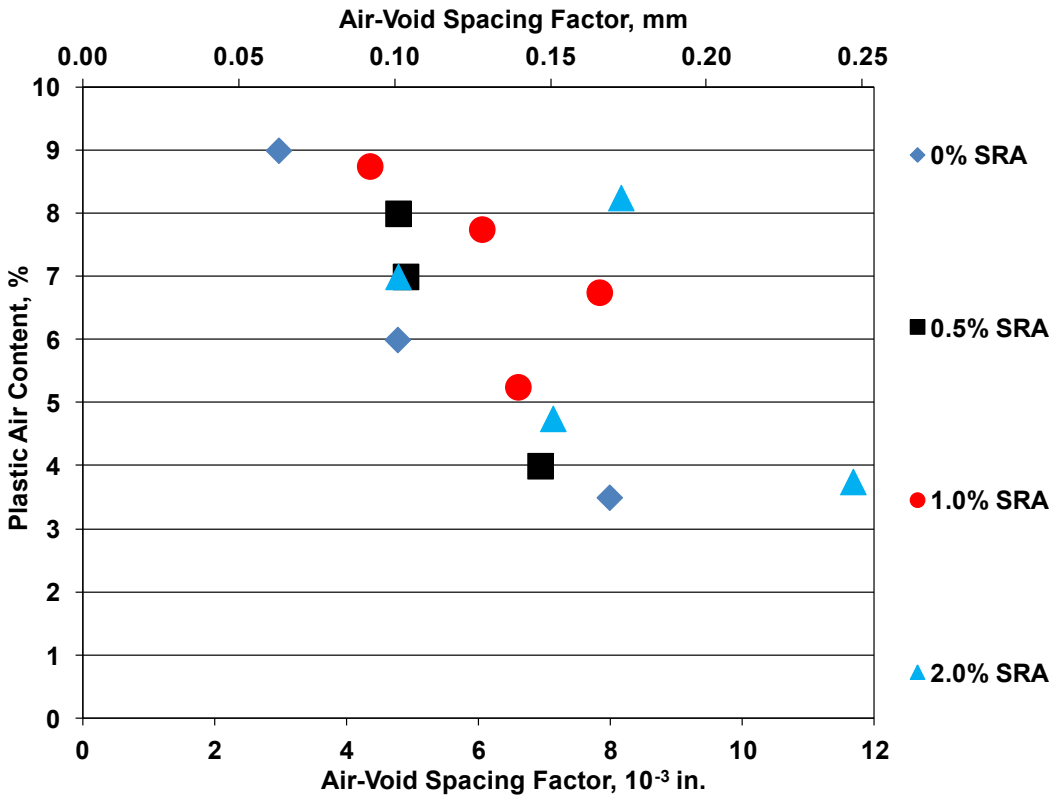

Figure 3.26 Air content in the plastic concrete versus air-void spacing factor for mixtures in Program 2

Table 3.17 Summary of average cumulative mass loss at 56 freeze-thaw cycles and freeze-thaw cycles to test completion versus air-void spacing factor for mixtures in Program 2

Mixture	Air-Void Spacing Factor		Durability Factor[#]	Cumulative Mass Loss @ 56 cycles
	(mm)	(10^{-3} in.)		(10^{-3} lb/ft^2)
0.5% SRA w/ 4% air	0.18	6.93	96	84.4
Control w/ 3.5% air	0.20	7.98	89	32.1
2% SRA w/ 3.75% air	0.30	11.67	13	460.1*
Control w/ 6% air	0.12	4.76	100	28.5
1% SRA w/ 6.75% air	0.20	7.82	80	62.1
1% SRA w/ 5.25% air	0.17	6.59	73	177.7
2% SRA w/ 4.75% air	0.18	7.12	29	143.2
Control w/ 9% air	0.08	2.96	99	14.2
1% SRA w/ 7.75% air	0.15	6.04	97	28
1% SRA w/ 8.75% air	0.11	4.34	†	51.8
0.5% SRA w/ 8% air	0.12	4.77	97	43.7
0.5% SRA w/ 7% air	0.12	4.89	96	73.3
2% SRA w/ 7% air	0.12	4.77	96	78.7
2% SRA w/ 8.25% air	0.21	8.15	95	14.5

#*Durability Factor (DF) = (P × N) / 300 cycles*, where *P* is the percentage of the initial dynamic modulus remaining at *N* cycles, *N* is either the number of cycles at which *P* reached 60 percent or 300 cycles (whichever is smaller).
†Freeze-thaw testing not completed
*Testing completed at 21 cycles
Note: 10^{-3} lb/ft^2 = 4.884 g/m^2

these mixtures, the mixture with the highest air content (8 percent) had the lowest spacing factor [4.77 × 10^{-3} in. (0.12 mm)], while the mixture with the lowest air content (4 percent) had the highest spacing factor [6.93 × 10^{-3} in. (0.18 mm)].

The relationship between air content and air-void spacing factor is not well-defined for mixtures with dosages of 1.0 and 2.0 percent SRA. For the mixtures with a 1.0 percent dosage of SRA, the mixture with an air content of 6.75 percent exhibited a greater spacing factor than the mixture with an air content of 5.25 percent [7.82 × 10^{-3} in. (0.20 mm) vs. 6.59 × 10^{-3} in. (0.17 mm)]. This observation suggests that the air-void size was larger, rather than smaller, for the mixture with the higher air content. The mixtures containing a 2.0 percent dosage of SRA experienced the greatest instability in the relationship between air content and spacing factor; for these

mixtures, the mixture with an air content of 8.25 percent had a larger air-void spacing factor than the mixture with an air content of only 4.75 percent [8.15×10^{-3} in. (0.21 mm) vs. 7.12×10^{-3} in. (0.18 mm)]. In fact, the spacing factor of the mixture with an air content of 8.25 percent exceeded the suggested limit for adequate freeze-thaw durability, 8×10^{-3} in. (0.20 mm) (Russell 2004). These observations suggest that the influence on the air-void stability caused by the addition of a 2.0 percent dosage of SRA cannot be easily predicted.

The average air-void spacing factors are plotted as functions of Durability Factor (DF) and average cumulative mass loss after 56 freeze-thaw cycles in Figures 3.27 and 3.28, respectively. Lines representing a DF of 95 and a mass loss limit of 0.31 lb/ft^2 (1500 g/m^2) are provided in the figures to display the limits for acceptable freeze-thaw durability and scaling resistance in this study. The air-void spacing factors, DFs, and values of mass loss after 56 freeze-thaw cycles for each mixture are shown in Table 3.17.

The figures and table show that the mixtures with large air-void spacing factors generally experienced reduced freeze-thaw durability and scaling resistance. The mixture with the largest spacing factor (2% SRA w/ 3.75% air) experienced both the lowest DF (13) and the highest mass loss [0.46 lb/ft^2 (2290 g/m^2)]. Each mixture with a spacing factor of 6×10^{-3} in. (0.15 mm) or less, regardless of SRA dosage, maintained a DF of greater than 95. Four mixtures with air-void spacing factors less than 8×10^{-3} in. (0.20 mm) had DFs below 95 (Control w/ 3.5% air, 1% SRA w/ 5.25% air, 1% SRA w/ 6.75% air, and 2% SRA w/ 4.75% air). These four mixtures each had air contents below 7 percent, suggesting that both air content and spacing factor influenced freeze-thaw durability. The mixtures with spacing factors of 6×10^{-3} in. (0.15 mm) or less exhibited mass losses of no greater than 0.10 lb/ft^2 (488 g/m^2), approximately one-third of the mass loss limit of 0.31 lb/ft^2 (1500 g/m^2). The mixture with an SRA dosage of 2.0 percent and a spacing factor of 8.15×10^{-3} in. (0.21 mm)

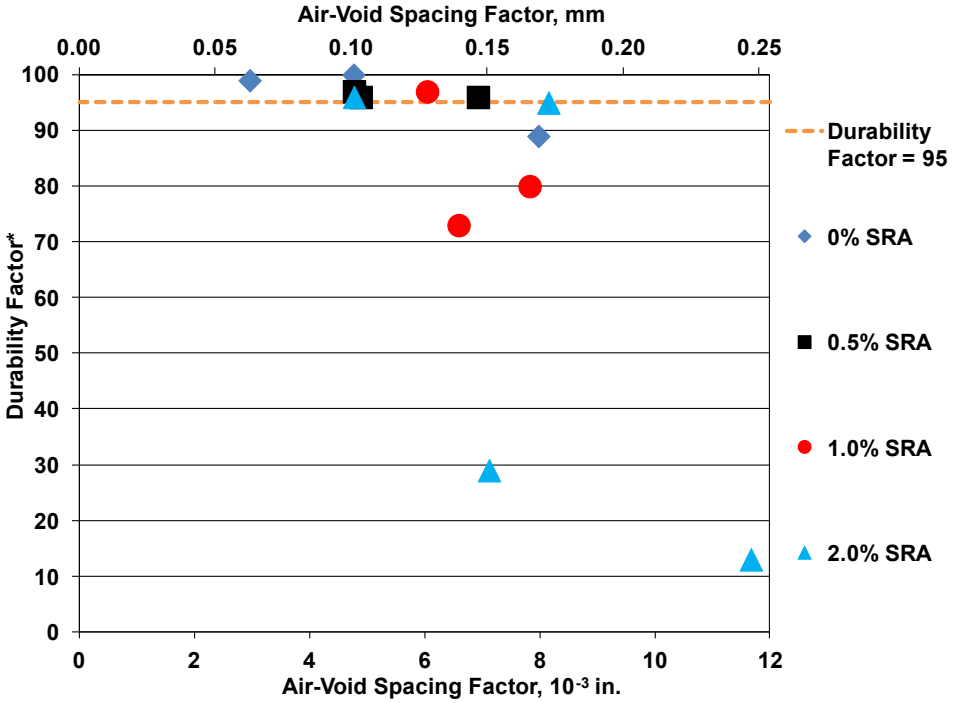

Durability Factor (DF) = (P × N) / 300 cycles, where *P* is the percentage of the initial dynamic modulus remaining at *N* cycles, *N* is either the number of cycles at which *P* reached 60 percent or 300 cycles (whichever is smaller).

Note: Air-void spacing factor determined through ASTM C457.

Figure 3.27 Durability Factor versus air-void spacing factor for mixtures in Program 2

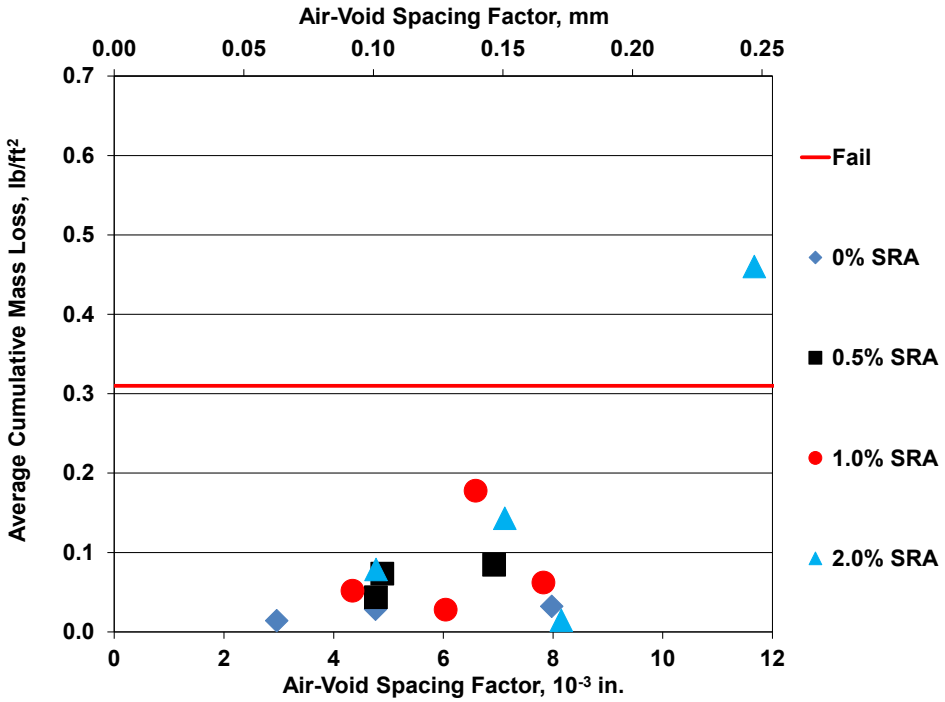

Note: Air-void spacing factor determined through ASTM C457.

Figure 3.28 Average cumulative mass loss at test completion versus air-void spacing factor for mixtures in Program 2

(2.0% SRA w/ 8.25% air) exhibited a mass loss of only 0.01 lb/ft^2 (50 g/m^2); however, this mixture had an air content of 8.25 percent.

3.3.6 Program 2 Summary

The results demonstrate that increased air content contributes to increased freeze-thaw durability and scaling resistance. Mixtures with air contents of 7 percent or more experienced acceptable freeze-thaw durability and scaling resistance, regardless of SRA dosage. Increased dosages of SRA contributed to decreased freeze-thaw durability and scaling resistance. The freeze-thaw durability and scaling resistance of mixtures with SRA dosages of 0 and 0.5 percent by weight of cement were not greatly affected by changes in air content. The reduction in freeze-thaw durability for mixtures with an SRA was most pronounced for the SRA dosages greater than 1.0 percent by weight of cement. Dosage of SRA had a greater effect on freeze-thaw durability and scaling resistance in mixtures with air contents below 7 percent. Mixtures with no SRA experienced the lowest mass losses and highest Durability Factors throughout testing.

As expected, mixtures with lower air contents had higher compressive strengths. All mixtures with air contents below 6 percent had 28-day compressive strengths approaching or exceeding the limit of 5500 psi (37.9 MPa) allowed by the LC-HPC specifications. The only mixture with a 28-day compressive strength below 5000 psi (34.5 MPa) was also the only mixture with an air content of 8 percent or higher. High strengths increase the potential for cracking in bridge decks by decreasing the mitigation of tensile stresses that occur through concrete creep.

Increased dosages of SRA contributed to increased air-void spacing factors in mixtures with similar air contents. In addition, the linear relationship that was observed between air content and air-void spacing factor for mixtures without an SRA became less clear as the dosage of SRA increased. These observations suggest that SRAs influence the size and spacing of the air voids. Mixtures with large air-

void spacing factors exhibited decreased freeze-thaw durability and scaling resistance.

Based on the results, it appears that shrinkage-reducing admixtures can be used safely in bridge deck field applications if there is assurance that only concrete with air contents of 7 percent or above would be placed in the deck. Restrictions on air content could be relaxed when low dosages of SRA (for example, 0.5 percent by weight of cement) are used. When selecting an optimal dosage of SRA, it is important to consider the relationship between increased dosage and reduced air-void system stability, freeze-thaw durability, and scaling resistance. The shrinkage benefits associated with selecting a high SRA dosage (1.0 or 2.0 percent by weight of cement) must be weighed against the potential durability problems.

CHAPTER 4: EVALUATION OF MIXTURES CONTAINING MINERAL ADMIXTURES USED IN CONJUNCTION WITH INTERNAL CURING

4.1 OVERVIEW

The results from Program 3, discussed in Sections 1.8.1.3 and 2.5.3, are presented in this chapter. The program examined the free shrinkage performance, freeze-thaw durability, scaling resistance, compressive strength, and air-void system characteristics of mixtures containing different combinations of pre-wetted, intermediate-sized lightweight aggregate, Grade 100 slag cement, and silica fume. As explained in Section 1.7.1, pre-wetted lightweight aggregate provides a source of internal curing water in concrete. This additional water reduces drying shrinkage by increasing the degree of hydration and by replenishing water lost in the capillary pores due to evaporation. The results of this evaluation built upon the findings of Reynolds et al. (2009) and Browning et al. (2011), which determined that small additions of pre-wetted lightweight aggregate contribute to reduced free shrinkage in concretes with water-cement ratios within the requirements of the LC-HPC specifications. This observation has particular relevance since the water-cement ratio evaluated by the researchers (0.44) was above that at which internal curing is used to control autogenous shrinkage, demonstrating that internal curing contributed to reduced drying shrinkage – a primary concern for bridge decks. The researchers observed an additional reduction in free shrinkage when lightweight aggregate was used in conjunction with slag cement.

Program 3 investigated the free-shrinkage performance of mixtures containing small amounts of silica fume used in conjunction with pre-wetted lightweight aggregate and slag. As discussed in Sections 1.2.1.1 and 1.7.2, additions of slag and silica fume provide concrete with reduced permeability. This reduced permeability can actually increase plastic shrinkage cracking as water that evaporates from the

surface is unable to be replenished by slow-moving internal bleed water. In fact, a number of studies have noted increased cracking in bridge decks with silica fume overlays (Krauss and Rogalla 1996, Lindquist et al. 2008). Drying shrinkage, a major concern for bridge decks, occurs over a longer period of time than plastic shrinkage and is caused by an insufficient availability of water in the capillary pores of the hardened cement paste as water is lost to the environment. Bentur et al. (1988) explained that concrete containing silica fume experiences a slower rate of water loss during drying as a result of the reduced permeability. If sufficient internal curing water is supplied to the concrete through pre-wetted lightweight aggregate, the reduced permeability provided by the silica fume could reduce drying shrinkage because the internal water is unable to quickly reach the surface, and thus evaporate. Over time, this internal water becomes tied up in the hydration process of the cementitious materials and is no longer available to evaporate.

Program 3 also evaluated the freeze-thaw durability and scaling resistance of the mixtures containing lightweight aggregate, Grade 100 slag, and silica fume. A number of studies have observed reduced freeze-thaw durability and scaling resistance in mixtures containing slag (Gunter, Bier, and Hilsdorf 1987, Malhotra et al. 1987, Bilodeau and Ludwig 1992, Stark and Ludwig 1997) and silica fume (Pigeon et al. 1987, Sabir and Kouyiali 1991). Conversely, Hooton (1993) observed non-air-entrained concrete specimens cured for 14 days with 10, 15, and 20 percent additions of silica fume and a water-cementitious material ratio of 0.35 have Durability Factors (DFs) above 90 when tested in accordance with ASTM C666, Procedure A. The mixtures containing lightweight aggregate and slag evaluated by Reynolds et al. (2009) and Browning et al. (2011) were not subjected to tests for freeze-thaw durability or scaling resistance. Therefore, free shrinkage, freeze-thaw durability, and scaling resistance were evaluated in this program to verify the overall performance of the mixtures for use in bridge deck field applications.

Twenty-one batches covering six distinct mixtures with different combinations of replacements of total aggregate with pre-wetted lightweight aggregate (0, 8, and 10 percent by volume), replacements of portland cement with slag cement (0 and 30 percent by volume), and replacements of portland cement with silica fume (0, 3, and 6 percent by volume) were evaluated. Two of these twenty-one batches, identified in Tables 2.1 through 2.7 as Batch Numbers 754 and 796, were also evaluated in Programs 1 and 2. The test program, including batch numbering and mixture descriptions and designations, is described in Section 2.5.3. The batches examined using each test are summarized in Tables 2.4 through 2.7. The mixture proportions, concrete properties, and compressive strengths of the concrete are summarized in Tables A.13 and A.14 in Appendix A. The mixtures had water-cementitious material ratios of 0.44 or 0.45 and paste contents between 23.4 and 24.0 percent of total volume. Moisture contents of the vacuum pre-wetted lightweight aggregate used in the batches ranged from 20.3 to 28.4 percent. The total water contained in the aggregate of 10 of the batches is shown in Table A.13 of Appendix A. This value represents the amount of internal water, beyond the mixture water, available for internal curing. Mixtures were proportioned using a target air content of 8 percent and a target slump of 2.25 ± 0.75 in. (55 ± 20 mm). The surfactant-based air-entraining admixture evaluated in Programs 1 and 2 (Micro Air) was used in the mixtures.

The mixtures are evaluated for free shrinkage in accordance with ASTM C157, freeze-thaw durability per ASTM C666 – Procedure B with modifications per Kansas Department of Transportation Test Method KTMR-22, and scaling resistance per Canadian Test BNQ NQ 2621-900 Annex B. Compressive strengths were measured in accordance with ASTM C39, and a hardened air-void analysis was completed in accordance with ASTM C457. The results of these evaluations are

provided in the following sections. Detailed information regarding the procedures of the tests is provided in Chapter 2.

Similar to the analysis of Program 1 described in Chapter 3, the Student's t-test was used in the analysis of Program 3 to determine the statistical significance of differences in the performance. Detailed information regarding the Student's t-test is provided in Section 3.1.1. Significance levels of at least $\alpha = 0.02$ (at least 98 percent certainty that the differences in results do not occur by chance) and less than $\alpha = 0.20$ (less than 80 percent certainty that the differences in results do not occur by chance) are represented by "Y" and "N", respectively. In addition, significance levels of at least $\alpha = 0.05$, 0.10, and 0.20 are represented by "95%", "90%", and "80%", respectively.

4.1.1 Free Shrinkage

The examination of free shrinkage in Program 3 included tests of 10 batches of concrete, evaluating different combinations and replacement levels of lightweight aggregate, slag, and silica fume. The 10 batches are listed in Table 2.4. The percentage values shown in the mixture designations in Table 2.4 represent the percent replacements of total aggregate by volume with lightweight aggregate (LWA) and the percent replacements of portland cement by volume with slag cement (Slag) or silica fume (SF). The mixtures designated as "Control" contain no lightweight aggregate or mineral admixtures. Six distinct mixtures are included in the ten batches. These six mixtures are designated as:

- Control
- 8% LWA
- 10% LWA
- 10% LWA, 30% Slag
- 10% LWA, 30% Slag, 3% SF
- 10% LWA, 30% Slag, 6% SF

An initial set of one batch for each mixture constitutes Series 1. Duplicate batches of four of these mixtures, including "Control;" "10% LWA;" "10% LWA, 30% Slag 3% SF;" and "10% LWA, 30% Slag, 6% SF," are evaluated in a second series (Series 2) to determine test repeatability. All specimens were wet-cured for 14 days and then subjected to drying, as described in Section 2.4.1.

4.1.1.1 Series 1

The average free shrinkage of three specimens from each mixture in Series 1 is plotted as a function of drying period for 30, 90, 180, and 365 days in Figures 4.1 through 4.4. In the figure legends, the mixtures are listed in the order of descending shrinkage at the end of the period shown. The average shrinkage strains for the drying periods of 0, 30, 90, 180, and 365 days are summarized in Table 4.1. Table 4.1 also shows the percentage of the shrinkage at both 180 and 365 days of drying observed during the first 30 days. The shrinkage values used to calculate the percentages in Table 4.1 are based on the total shrinkage after demolding, and therefore, the effect of swelling during curing is included. As discussed previously, early-age shrinkage (out to 90 days) is a principal concern for bridge decks due to the large percentage of the total shrinkage that occurs during this time and the relatively short period available for creep to mitigate tensile stresses. The negative shrinkage shown in Table 4.1 indicates that swelling occurred during the 14-day wet-curing period. As discussed in Section 1.7.1, swelling has potential benefits in bridge decks because it places the restrained concrete in compression. Thus, more subsequent shrinkage is required to induce tensile stresses and cracking in concrete that is initially placed in compression than in concrete that is initially unstressed. The average values of free shrinkage and the statistical significance of the differences in free shrinkage after 30 and 365 days of drying based on the Student's t-test are shown in Tables 4.2 and 4.3, respectively.

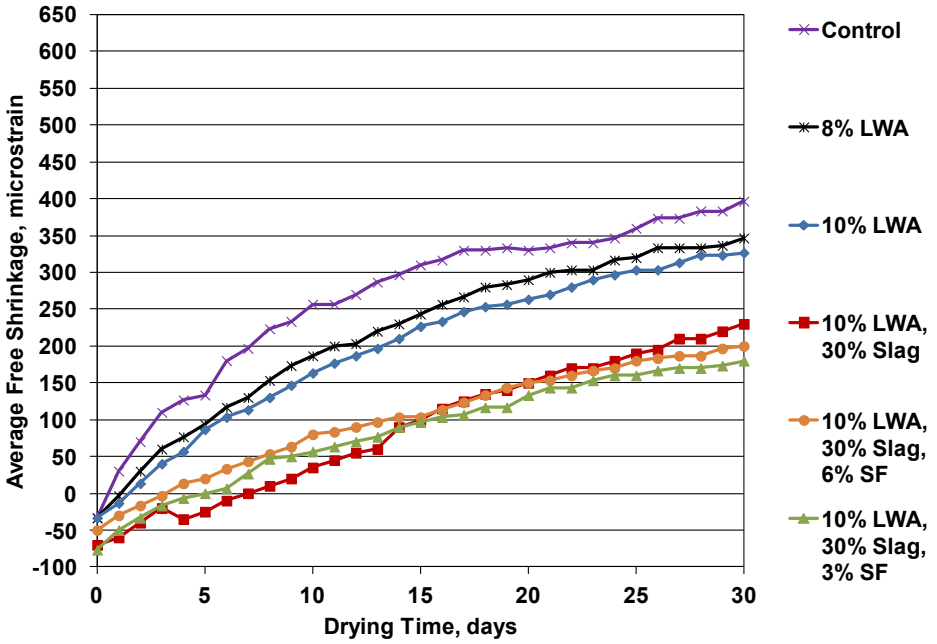

Figure 4.1 Average free shrinkage versus drying time through 30 days for mixtures in Program 3, Series 1

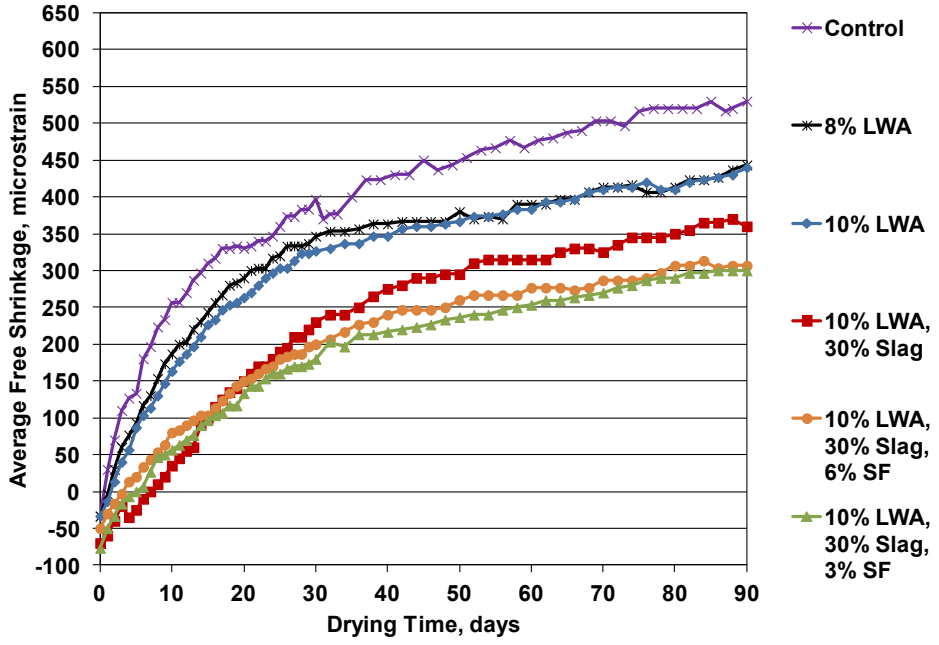

Figure 4.2 Average free shrinkage versus drying time through 90 days for mixtures in Program 3, Series 1

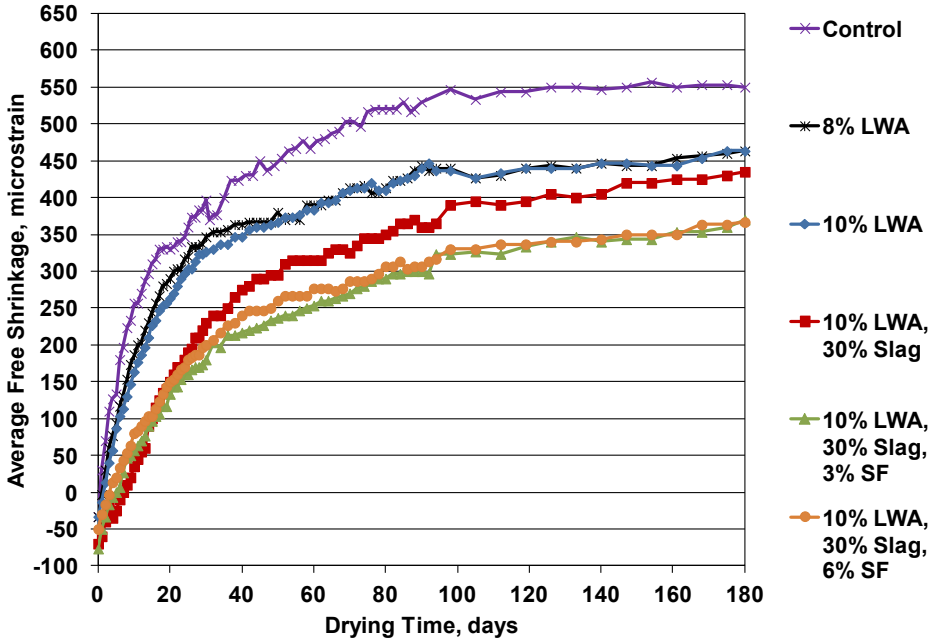

Figure 4.3 Average free shrinkage versus drying time through 180 days for mixtures in Program 3, Series 1

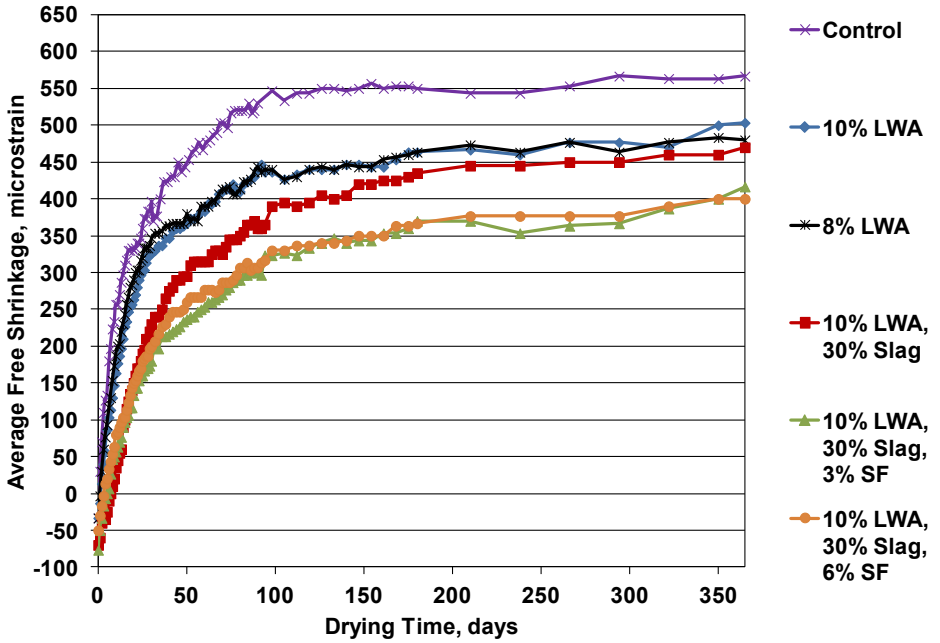

Figure 4.4 Average free shrinkage versus drying time through 365 days for mixtures in Program 3, Series 1

Table 4.1 Average free shrinkage versus drying time after different lengths of drying for mixtures in Program 3, Series 1

Drying Period (days)	0	30	90	180	365	FS_{30}/FS_{180}†	FS_{30}/FS_{365}†
Mixture	Free Shrinkage at Day of Drying (με)*						
Control	-33	397	530	550	567	72.2%	70.0%
8% LWA	-33	347	443	463	480	74.9%	72.3%
10% LWA	-33	327	440	463	503	70.6%	65.0%
10% LWA, 30% Slag	-70	230	360	435	470	52.9%	48.9%
10% LWA, 30% Slag, 3% SF	-77	180	300	370	417	48.6%	43.2%
10% LWA, 30% Slag, 6% SF	-50	200	307	367	400	54.5%	50.0%

*Negative values indicate swelling during wet-curing period
†Free shrinkage after 30 days of drying (FS_{30}) divided by free shrinkage after 180 days (FS_{180}) or 365 days of drying (FS_{365}).
Note: Three specimens tested per mixture

Table 4.2 Student's t-test results displaying statistical significance of differences in 30-day free shrinkage for mixtures in Program 3, Series 1

Mixture	30-Day Free Shrinkage*	Control	8% LWA	10% LWA	10% LWA, 30% Slag	10% LWA, 30% Slag, 3% SF	10% LWA, 30% Slag, 6% SF
		397	347	327	230	180	200
Control	397		80%	95%	Y	Y	Y
8% LWA	347			N	Y	Y	Y
10% LWA	327				95%	Y	Y
10% LWA, 30% Slag	230					95%	N
10% LWA, 30% Slag, 3% SF	180						N
10% LWA, 30% Slag, 6% SF	200						

*The 30-day free shrinkage for each mixture was determined by averaging the shrinkage values of each specimen.
Note: "Y" indicates a statistical difference between the two datum at a significance level of $\alpha = 0.02$ (98%). "N" indicates that these is no statistical significance at a significance level of $\alpha = 0.20$ (80%). Statistical differences at significance levels at, but not exceeding, $\alpha = 0.05$, 0.10, and 0.20 are represented by "95%", "90%", and "80%".

Table 4.3 Student's t-test results displaying statistical significance of differences in 365-day free shrinkage for mixtures in Program 3, Series 1

Mixture	365-Day Free Shrinkage*	Control	8% LWA	10% LWA	10% LWA, 30% Slag	10% LWA, 30% Slag, 3% SF	10% LWA, 30% Slag, 6% SF
		567	480	503	470	417	400
Control	567		90%	80%	Y	Y	Y
8% LWA	480			N	N	80%	80%
10% LWA	503				N	80%	80%
10% LWA, 30% Slag	470					Y	90%
10% LWA, 30% Slag, 3% SF	417						N
10% LWA, 30% Slag, 6% SF	400						

*The 365-day free shrinkage for each mixture was determined by averaging the shrinkage values of each specimen.
Note: "Y" indicates a statistical difference between the two datum at a significance level of $\alpha = 0.02$ (98%). "N" indicates that these is no statistical significance at a significance level of $\alpha = 0.20$ (80%). Statistical differences at significance levels at, but not exceeding, $\alpha = 0.05$, 0.10, and 0.20 are represented by "95%", "90%", and "80%".

Based on shrinkage after 30 days (Figure 4.1 and Table 4.1), the mixtures can be separated into three groups with descending values of shrinkage, the Control mixture, the two mixtures with lightweight aggregate but no mineral admixtures, and the three mixtures with lightweight aggregate and slag, or slag and silica fume. After 365 days (Figure 4.4 and Table 4.1), the mixtures can still be separated into these three groups, but with the mixture containing lightweight aggregate and slag but no silica fume exhibiting shrinkage similar to the two mixtures with lightweight aggregate but no mineral admixtures.

The figures and tables show that the replacement of a portion of total aggregate with pre-wetted lightweight aggregate reduced both early-age (0 to 90 days of drying) and long-term (90 to 365 days of drying) shrinkage. The addition of slag in conjunction with lightweight aggregate contributed to an additional reduction in free shrinkage. These observations support the findings of Reynolds et al. (2009) and Browning et al. (2011). Free shrinkage was reduced even further as silica fume was added in conjunction with the lightweight aggregate and slag.

After 30 days of drying (Figure 4.1), the shrinkage values of the six mixtures ranged from 180 to 397 microstrain. The Control mixture (no lightweight aggregate or mineral admixtures) had the highest shrinkage, while the mixture with lightweight aggregate, slag, and a 3 percent replacement of cement with silica fume (10% LWA, 30% Slag, 3% SF) had the lowest shrinkage. As shown in the figure, the addition of pre-wetted lightweight aggregate reduced shrinkage during this drying period. The mixtures with 8 and 10 percent volume replacement levels of lightweight aggregate (8% LWA and 10% LWA) had 50 and 70 microstrain less shrinkage, respectively, after 30 days than the Control mixture. As shown in Table 4.2, these differences in free shrinkage after 30 days are statistically significant at $\alpha = 0.20$ and $\alpha = 0.05$ as the replacement level of lightweight aggregate increased from 0 to 8 percent and from 0 to 10 percent, respectively. Figure 4.1 also shows that the mixtures with lightweight aggregate and slag, or slag and silica fume (10% LWA, 30% Slag; 10% LWA, 30% Slag, 3% SF; 10% LWA, 30% Slag, 6% SF) had significantly lower shrinkage than those containing lightweight aggregate without slag or silica fume during the first 30 days of drying. In fact, the three mixtures containing lightweight aggregate and slag, or slag and silica fume had more than 100 microstrain less shrinkage than those containing lightweight aggregate without mineral admixtures (8% LWA and 10% LWA) and more than 200 microstrain less shrinkage than the Control mixture, which contained neither lightweight aggregate or mineral admixtures, after only 15 days of drying. After 30 days of drying, the mixture with volume replacement levels of 10 percent lightweight aggregate and 30 percent slag (10% LWA, 30% Slag) had 97 microstrain less shrinkage than the mixture with 10 percent lightweight aggregate without slag (10% LWA). This difference in free shrinkage is statistically significant at $\alpha = 0.05$ (Table 4.2). The mixture with lightweight aggregate and slag without silica fume had 167 microstrain less shrinkage than the Control mixture after 30 days of drying, a difference that is statistically significant at $\alpha = 0.02$. The mixtures with

volume replacement levels of 3 and 6 percent silica fume (10% LWA, 30% Slag, 3% SF and 10% LWA, 30% Slag, 6% SF) had 50 and 30 microstrain less shrinkage, respectively, after 30 days than the mixture with lightweight aggregate and slag without silica fume, differences that are, respectively, statistically significant at $\alpha = 0.05$ and not significant. The mixtures with 3 and 6 percent silica fume had 217 and 197 microstrain less shrinkage, respectively, than the Control mixture after 30 days of drying; these differences are significant at $\alpha = 0.02$.

As shown in Figure 4.1, the addition of silica fume in conjunction with lightweight aggregate and slag did not contribute to reduced shrinkage within the first 20 days of drying. The mixture with lightweight aggregate and slag without silica fume (10% LWA, 30% Slag) had shrinkage similar to that of the two mixtures with lightweight aggregate, slag, and silica fume (10% LWA, 30% Slag, 3% SF and 10% LWA, 30% Slag, 6% SF) through 20 days. This observation suggests that the addition of slag, not silica fume, in conjunction with the lightweight aggregate contributed to the reduced shrinkage during the first 20 days. Figures 4.1 through 4.4 show that after 20 days, however, the two mixtures with lightweight aggregate, slag, and silica fume experienced less shrinkage than the mixture with lightweight aggregate and slag but without silica fume, suggesting that the addition of silica fume contributed to reduced shrinkage after the initial period of drying. After 30 days of drying, no effect on free shrinkage was observed as the volume replacement of cement with silica fume was increased from 3 to 6 percent.

Twenty microstrain less shrinkage was noted at 30 days as the replacement of total aggregate with lightweight aggregate increased from 8 to 10 percent by volume; this decrease in shrinkage, however, is not statistically significant. Swelling during curing increased as slag was added to the mixtures. No increase in swelling was observed with the addition of lightweight aggregate.

After 90 and 180 days of drying (Figures 4.2 and 4.3, respectively), the shrinkage values of the six mixtures ranged from 300 to 530 microstrain and from 367 to 550 microstrain, respectively. Similar to the observations after 30 days of drying, the Control mixture (no lightweight aggregate or mineral admixtures) had the highest shrinkage after both 90 and 180 days. The mixture with lightweight aggregate, slag, and 3 percent silica fume (10% LWA, 30% Slag, 3% SF) had the lowest shrinkage after 90 days, while the mixture with lightweight aggregate, slag, and 6 percent silica fume (10% LWA, 30% Slag, 6% SF) had the lowest shrinkage after 180 days.

After both 90 and 180 days of drying, the mixtures with 8 and 10 percent lightweight aggregate (8% LWA and 10% LWA) had approximately 85 microstrain less shrinkage than the Control mixture (Figures 4.2 and 4.3). As for 30 days of drying, the three mixtures with lightweight aggregate and slag, or slag and silica fume (10% LWA, 30% Slag; 10% LWA, 30% Slag, 3% SF; 10% LWA, 30% Slag, 6% SF) had lower shrinkage than the three without slag or silica fume (Control, 8% LWA, and 10% LWA) after both 90 and 180 days of drying (Figures 4.2 and 4.3). After 90 days, the three mixtures with lightweight aggregate and slag, or slag and silica fume had shrinkage values ranging from 307 to 360 microstrain, while the three without slag or silica fume had values ranging from 440 to 530 microstrain. After 180 days, the mixtures with lightweight aggregate and slag, or slag and silica fume had shrinkage values ranging from 367 to 435 microstrain, while the mixtures without slag or silica fume had values ranging from 463 to 550 microstrain (Table 4.1).

After 90 days of drying (Figure 4.2), the mixture with 10 percent lightweight aggregate and 30 percent slag (10% LWA, 30% Slag) had 80 microstrain less shrinkage than the mixture with 10 percent lightweight aggregate without slag (10% LWA). After 180 days, however, the difference in shrinkage between these two mixtures decreased to only 28 microstrain, indicating that the mixture with

lightweight aggregate and slag experienced greater shrinkage between 90 and 180 days of drying than the mixture with lightweight aggregate and no slag. The two mixtures with lightweight aggregate, slag, and silica fume (10% LWA, 30% Slag, 3% SF and 10% LWA, 30% Slag, 6% SF) had an average of 57 and 67 microstrain less shrinkage than the mixture with lightweight aggregate and slag without silica fume (10% LWA, 30% Slag) after 90 and 180 days, respectively. The mixtures with lightweight aggregate, slag, and silica fume had an average of 137 microstrain less shrinkage after 90 days than the mixtures with lightweight aggregate without slag or silica fume (8% LWA and 10% LWA). After 180 days, however, the mixtures with lightweight aggregate, slag, and silica fume had an average of 95 microstrain less shrinkage than the mixture with lightweight aggregate without slag or silica fume, indicating that the mixtures with lightweight aggregate, slag, and silica fume experienced greater shrinkage between 90 and 180 days than the mixtures with lightweight aggregate without slag or silica fume. Overall, between 90 and 180 days, the three mixtures without slag or silica fume, including the Control mixture, experienced lower shrinkage (approximately 20 microstrain each) than the three mixtures with slag or silica fume (60 to 75 microstrain).

After 365 days of drying (Figure 4.4), the shrinkage values of the six mixtures ranged from 400 to 567 microstrain. This spread of 167 microstrain is the smallest range of shrinkage values for the four drying periods (30, 90, 180, and 365 days). The Control mixture continued to have the highest shrinkage after 365 days of drying, while the mixture with lightweight aggregate, slag, and 6 percent silica fume had the lowest shrinkage.

As shown in the Figure 4.4, the replacement of a portion of total aggregate with pre-wetted lightweight aggregate continued to reduce shrinkage. The mixtures with 8 and 10 percent lightweight aggregate without mineral admixtures (8% LWA and 10% LWA) had 87 and 64 microstrain less shrinkage, respectively, after 365 days

than the Control mixture. As shown in Table 4.3, the differences in free shrinkage after 365 days are statistically significant at $\alpha = 0.10$ and $\alpha = 0.20$ as the replacement level of lightweight aggregate increased from 0 to 8 percent and from 0 to 10 percent, respectively.

Figure 4.4 shows that the three mixtures with lightweight aggregate and slag, or slag and silica fume (10% LWA, 30% Slag; 10% LWA, 30% Slag, 3% SF; 10% LWA, 30% Slag, 6% SF) had lower shrinkage than the three mixtures without slag or silica fume (Control, 8% LWA, 10% LWA), but the difference in shrinkage between the mixtures was less pronounced after 365 days than after 30 days. After 365 days, the mixture with lightweight aggregate and slag but no silica fume (10% LWA, 30% Slag) had only 10 and 33 microstrain less shrinkage, respectively, than the mixtures with 8 and 10 percent lightweight aggregate without slag or silica fume (8% LWA and 10% LWA), differences that are not statistically significant. As discussed previously, the respective differences in shrinkage had been 117 and 97 microstrain at 30 days. At 30 days, the respective differences in shrinkage were statistically significant at $\alpha = 0.02$ and $\alpha = 0.05$.

The mixtures with lightweight aggregate, slag, and silica fume had the lowest shrinkage after 365 days of drying. The mixtures with 3 and 6 percent silica fume (10% LWA, 30% Slag 3% SF and 10% LWA, 30% Slag, 6% SF) had 60 to 100 microstrain less shrinkage than the mixtures with 8 and 10 percent lightweight aggregate without slag or silica fume (8% LWA and 10% LWA), differences that are statistically significant at $\alpha = 0.20$ (Table 4.3). The mixtures with lightweight aggregate, slag, and 3 and 6 percent replacement levels of silica fume had 53 and 70 microstrain less shrinkage, respectively, after 365 days than the mixture with lightweight aggregate and slag without silica fume. These differences in free shrinkage are statistically significant at $\alpha = 0.02$ and $\alpha = 0.10$, respectively (Table 4.3).

At 365 days, shrinkage was essentially the same for the mixtures containing 8 and 10 percent lightweight aggregate by volume of total aggregate. In fact, the mixture with 8 percent lightweight aggregate exhibited 23 microstrain less shrinkage than the mixture with 10 percent lightweight aggregate after 365 days of drying, a difference that is not statistically significant. In addition, shrinkage was not significantly affected by the volume replacement level of portland cement with silica fume. At 365 days, although the mixture with 6 percent silica fume had 17 microstrain less shrinkage than the mixture with 3 percent silica fume (this difference is not statistically significant), the mixture with 3 percent silica fume generally exhibited equal or lower shrinkage than the mixture with 6 percent silica fume during all but the last 30 days of the drying period.

Table 4.1 indicates that a greater percentage of the shrinkage at 365 days occurred during the first 30 days for the three mixtures without slag, 65 to 72 percent, than for the three mixtures with slag, 43 to 50 percent. Additionally, the three mixtures without slag had a greater percentage of the shrinkage at 180 days occur during the first 30 days (70 to 75 percent vs. 49 to 55 percent, respectively). Thus, a portion of the reduced shrinkage at early ages was, in fact, delayed shrinkage. This delayed shrinkage, however, reduces the potential for cracking because additional time is available for creep to mitigate tensile stresses resulting from restrained volume change.

Free shrinkage of the mixtures after 30 and 365 days of drying is shown, respectively, in Figures 4.5 and 4.6. The figures include the shrinkage observed both after demolding (including swelling) and after curing (neglecting swelling). As shown in the figures, all mixtures with lightweight aggregate experienced lower shrinkage than the Control mixture after 30 and 365 days of drying with swelling both considered and neglected. Considering and neglecting swelling, the mixtures with 8 and 10 percent lightweight aggregate (8% LWA and 10% LWA) had, respectively, 50

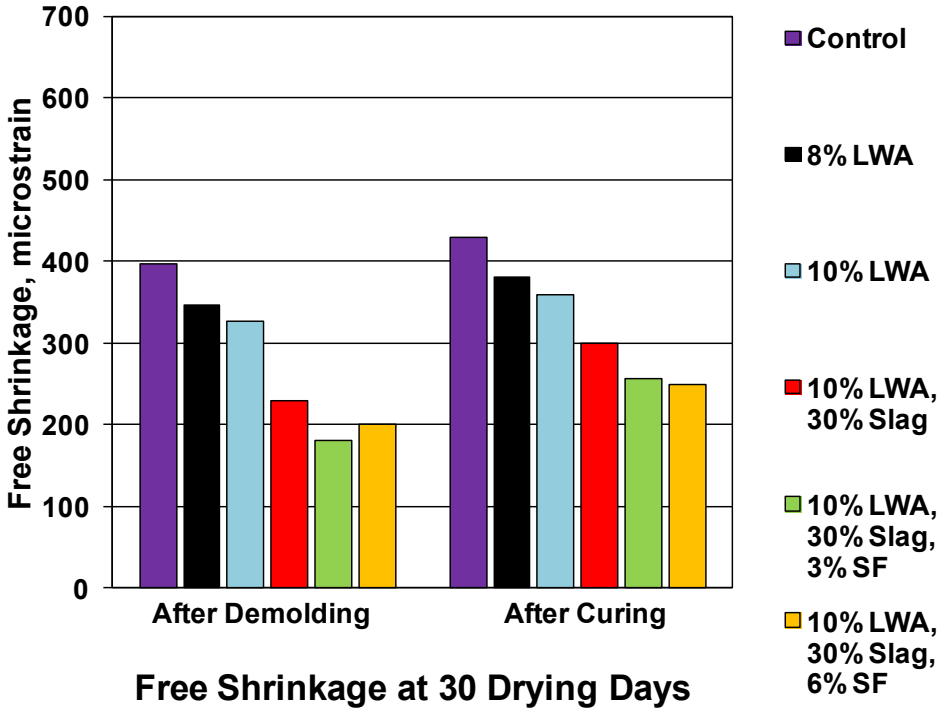

Figure 4.5 Average free shrinkage after 30 days of drying for mixtures in Program 3, Series 1

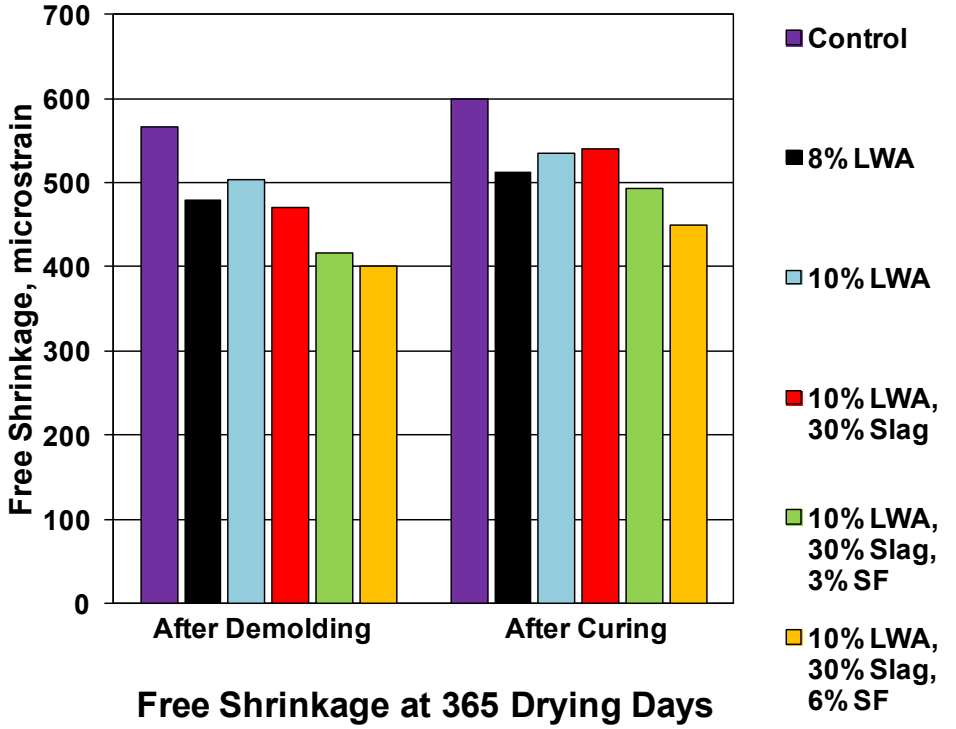

Figure 4.6 Average free shrinkage after 365 days of drying for mixtures in Program 3, Series 1

and 70 microstrain less shrinkage after 30 days and 87 and 64 microstrain less shrinkage after 365 days than the Control mixture. Figure 4.5 indicates that, when swelling is considered, the mixtures containing lightweight aggregate and slag, or slag and silica fume (10% LWA, 30% Slag; 10% LWA, 30% Slag, 3% SF; 10% LWA, 30% Slag, 6% SF) exhibited approximately half the shrinkage of the Control mixture after 30 days of drying. The mixtures with lightweight aggregate and slag, or slag and silica fume had values of shrinkage ranging from 180 to 230 microstrain after 30 days, while Control mixture had a shrinkage of 397 microstrain. The three mixtures also had less shrinkage than the two mixtures with lightweight aggregate without slag or silica fume (8% LWA and 10% LWA), when swelling is considered. Mixtures 8% LWA and 10% LWA had values of shrinkage of 347 and 327 microstrain, respectively.

When swelling is neglected, the mixtures containing lightweight aggregate and slag, or slag and silica fume still exhibited considerably lower shrinkage than the three without slag or silica fume, with values after 30 days ranging from 250 to 300 microstrain compared to values ranging from 360 to 430 microstrain for the mixtures without slag or silica fume.

After 365 days (Figure 4.6), when swelling is considered, the two mixtures with lightweight aggregate, slag, and silica fume (10% LWA, 30% Slag, 3% SF and 10% LWA, 30% Slag, 6% SF) still exhibited the lowest shrinkage, with values of 417 and 400 microstrain, respectively. The mixture with lightweight aggregate and slag had the next-lowest shrinkage, with a value of 470 microstrain. Even so, the absolute reductions in shrinkage resulting from the use of slag or slag and silica fume were less pronounced after 365 days of drying than after 30 days. When swelling is considered, the mixtures with 8 and 10 percent lightweight aggregate but no mineral admixtures had respective shrinkage values of 480 and 503 microstrain after 365 days – on average, only 83 microstrain more than the mixtures with lightweight aggregate,

slag, and silica fume and only 22 microstrain more than the mixture with lightweight aggregate and slag. The Control mixture had a shrinkage of 567 microstrain after 365 days with swelling considered.

When swelling is neglected, the reductions in shrinkage resulting from the use of slag or slag and silica fume were even less pronounced. With swelling neglected, the two mixtures with lightweight aggregate, slag, and 3 and 6 percent silica fume still had the lowest shrinkage (494 and 450 microstrain, respectively); however, the mixture containing lightweight aggregate and slag without silica fume had greater shrinkage after 365 days (540 microstrain) than the mixtures with 8 and 10 percent lightweight aggregate without slag or silica fume (513 and 536 microstrain, respectively). The Control mixture still had the highest shrinkage after 365 days with swelling neglected (600 microstrain).

Table 4.4 shows the free shrinkage observed during four drying periods, 0 to 30 days, 30 to 90 days, 90 to 180 days, and 180 to 365 days. Figures 4.7 through 4.9 show the shrinkage during the first and second drying periods, 0 to 30 days and 30 to 90 days, and the combination of the third and fourth drying periods, 90 to 365 days. During the four drying periods, shrinkage for the six mixtures ranged from 250 to 430 microstrain, 96 to 133 microstrain, 20 to 75 microstrain, and 17 to 47 microstrain, respectively. As shown in Table 4.4 and Figure 4.7, the mixtures with lightweight aggregate and slag, or slag and silica fume had the lowest shrinkage between 0 and 30 days, ranging from 250 to 300 microstrain. The Control mixture had the highest shrinkage over the same period, with a value of 430 microstrain. The mixtures with 8 and 10 percent lightweight aggregate had shrinkage values of 380 and 360 microstrain, respectively.

The table and figures confirm that the use of the mineral admixtures contributed to a reduction in shrinkage only during the first 30 days of drying. As shown in Table 4.4 and Figure 4.8, all six mixtures had similar shrinkage between 30

Table 4.4 Average free shrinkage following curing during four drying periods (0 to 30 days, 30 to 90 days, 90 to 180 days, and 180 to 365 days) for mixtures in Program 3, Series 1

Drying Period (days)	0-30	30-90	90-180	180-365	Total Free Shrinkage at 365 days after curing
Mixture	Free Shrinkage in Drying Period (με)				(με)
Control	430	133	20	17	600
8% LWA	380	96	20	17	513
10% LWA	360	113	23	40	536
10% LWA, 30% Slag	300	130	75	35	540
10% LWA, 30% Slag, 3% SF	257	120	70	47	494
10% LWA, 30% Slag, 6% SF	250	107	60	33	450

Note: Three specimens tested per mixture

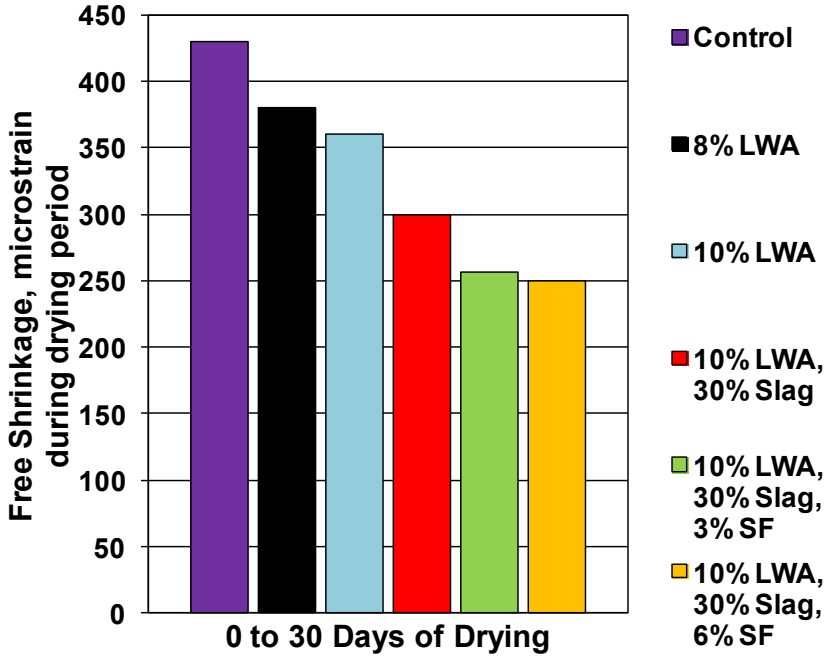

Figure 4.7 Average free shrinkage during the drying period of 0 to 30 days for mixtures in Program 3, Series 1

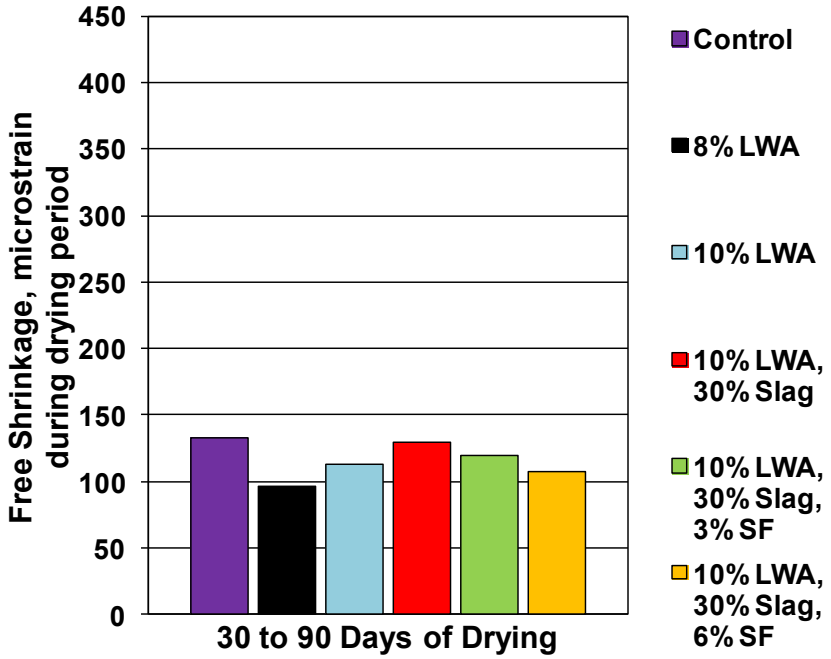

Figure 4.8 Average free shrinkage during the drying period of 30 to 90 days for mixtures in Program 3, Series 1

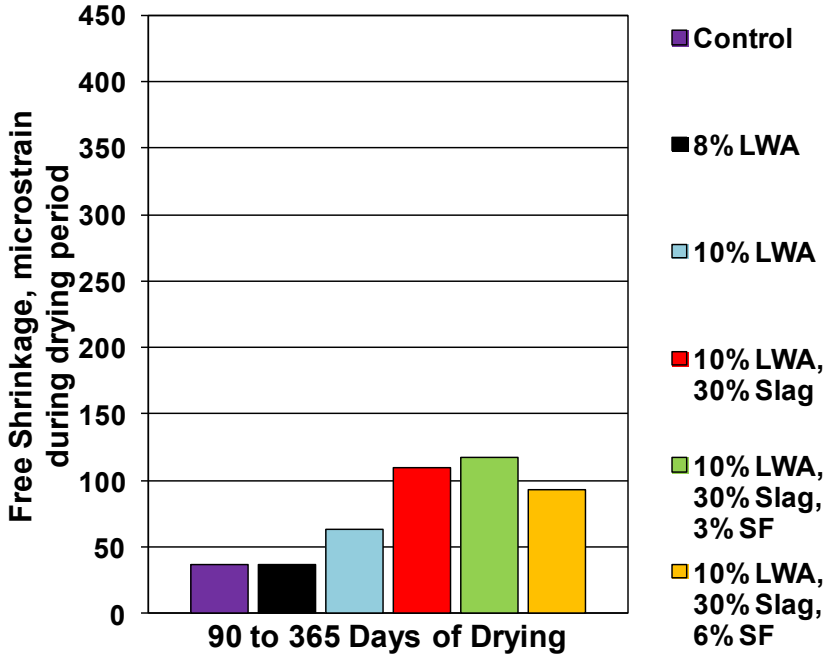

Figure 4.9 Average free shrinkage during the drying period of 90 to 365 days for mixtures in Program 3, Series 1

and 90 days, with the lowest exhibited by the mixture with 8 percent lightweight aggregate and no slag or silica fume (96 microstrain). The Control mixture still experienced the greatest shrinkage between 30 and 90 days (133 microstrain), but the mixture with lightweight aggregate and slag without silica fume (10% LWA, 30% Slag) exhibited only 3 microstrain less shrinkage than the Control mixture over the same period. For the drying period 90 to 180 days, the mixtures with slag experienced substantially greater shrinkage than those without slag. Table 4.4 shows that the three mixtures with slag exhibited three times the shrinkage of the three without slag during the drying period of 90 to 180 days. Over this period, the mixtures with slag had shrinkage ranging from 60 to 75 microstrain, while the mixtures without slag had values from 20 to 23 microstrain. For the drying period 180 to 365 days, the three mixtures with slag had higher shrinkage than the Control mixture and the mixture with 8 percent lightweight aggregate. The mixture with 10 percent lightweight aggregate without slag or silica fume (10% LWA), however, had a level of shrinkage similar to the mixtures with slag. Total shrinkage for the drying period of 90 to 365 days is illustrated in Figure 4.9.

Table 4.5 shows the average rate of shrinkage in microstrain per day (με/day) during the four drying periods shown in Table 4.4. The table indicates that the average shrinkage rates during the first 30 days of drying were significantly greater than in the later drying periods, with values ranging from 8.3 to 14.3 με/day. The two mixtures with lightweight aggregate, slag, and silica fume were the only mixtures with average shrinkage rates below 10 με/day during this period. Conversely, the Control mixture experienced the highest average shrinkage rate (14.3 με/day) during the first 30 days. As expected based on total shrinkage, all six mixtures experienced similar shrinkage rates between 30 and 90 days, with values ranging from 1.6 to 2.2 με/day. From 90 to 180 days, the three mixtures containing slag experienced much higher average shrinkage rates (ranging from 0.7 to 0.8 με/day) than the three without

Table 4.5 Average rates of free shrinkage during four periods of drying (0 to 30 days, 30 to 90 days, 90 to 180 days, and 180 to 365 days) for mixtures in Program 3, Series 1

Drying Period (days)	0-30	30-90	90-180	180-365
Mixture	Shrinkage Rate in Drying Period (με/day)			
Control	14.3	2.2	0.2	0.1
8% LWA	12.7	1.6	0.2	0.1
10% LWA	12.0	1.9	0.3	0.2
10% LWA, 30% Slag	10.0	2.2	0.8	0.2
10% LWA, 30% Slag, 3% SF	8.6	2.0	0.8	0.3
10% LWA, 30% Slag, 6% SF	8.3	1.8	0.7	0.2

Note: Three specimens tested per mixture

slag (ranging from 0.2 to 0.3 με/day). The rates for all mixtures between 90 and 180 days, however, were significantly lower than the values during the first 30 days. The Control mixture and the mixture with 8 percent lightweight aggregate with no slag or silica fume (8% LWA) experienced the lowest rates (0.1 με/day each) during the drying period of 180 to 365 days.

4.1.1.2 Series 2

Series 2 included duplicate batches of four of the six mixtures examined in Series 1 to determine the repeatability of the results. The average free shrinkage of three specimens from each mixture in Series 2 is plotted as a function of drying period for 30, 90, and 180 days in Figures 4.10 through 4.12. The tests are still underway as this report is being written. In the figure legends, the mixtures are listed in the order of descending shrinkage at the end of the period shown. The average shrinkage strains for the drying periods of 0, 30, 90, and 180 days are summarized in Table 4.6. The percentage of the shrinkage at 180 days of drying observed during the first 30 days is shown for the mixtures in Table 4.6. The statistical significance of the differences in free shrinkage after 30 and 180 days of drying determined from the Student's t-test are shown in Tables 4.7 and 4.8, respectively.

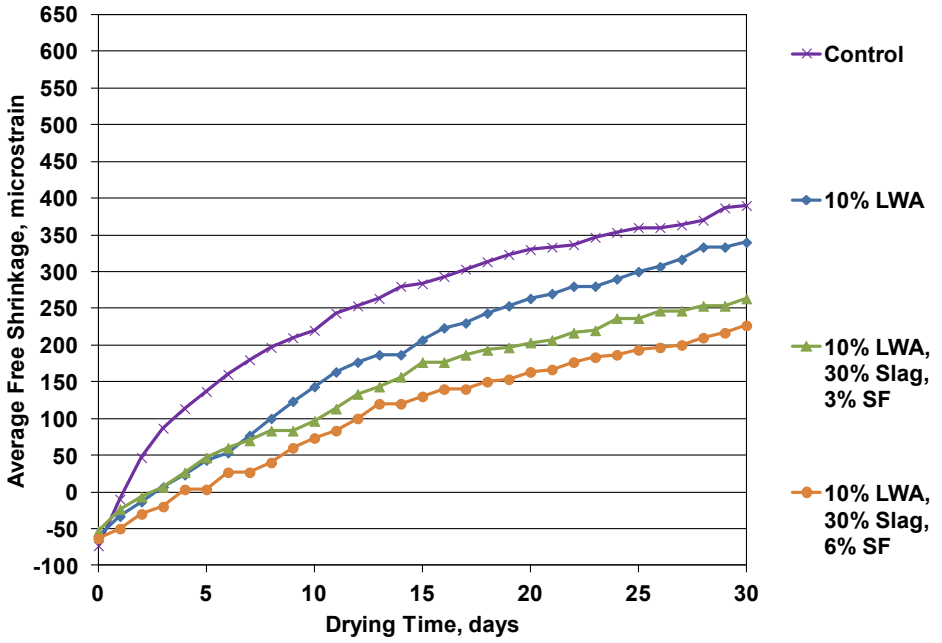

Figure 4.10 Average free shrinkage versus drying time through 30 days for mixtures in Program 3, Series 2

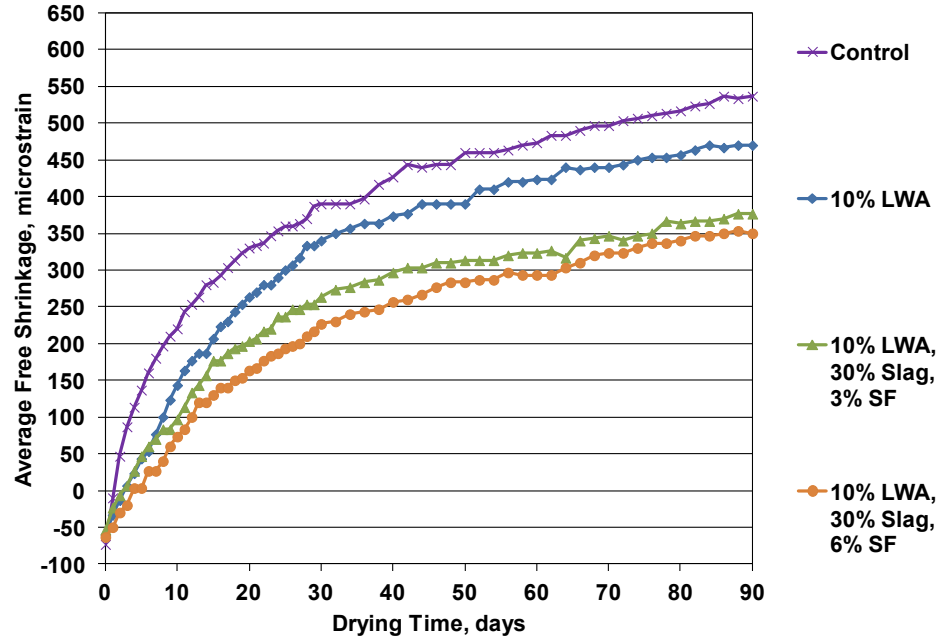

Figure 4.11 Average free shrinkage versus drying time through 90 days for mixtures in Program 3, Series 2

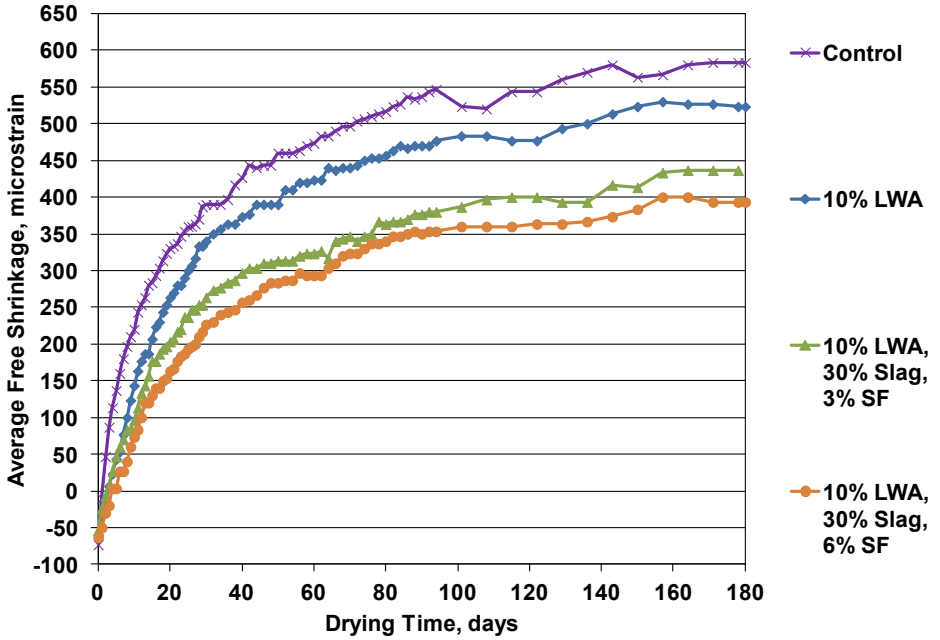

Figure 4.12 Average free shrinkage versus drying time through 180 days for mixtures in Program 3, Series 2

Table 4.6 Average free shrinkage versus drying time after different lengths of drying for mixtures in Program 3, Series 2

Days of Drying	0	30	90	180	FS_{30}/FS_{180} †
Mixture	Free Shrinkage at Day of Drying (με)*				
Control	-73	390	537	583	66.9%
10% LWA	-60	340	470	523	65.0%
10% LWA, 30% Slag, 3% SF	-53	263	377	437	60.2%
10% LWA, 30% Slag, 6% SF	-63	227	350	393	57.8%

*Negative values indicate swelling during wet-curing period

†Free shrinkage after 30 days of drying (FS_{30}) divided by free shrinkage after 180 days of drying (FS_{180}).

Note: Three specimens tested per mixture

Table 4.7 Student's t-test results displaying statistical significance of differences in 30-day free shrinkage for mixtures in Program 3, Series 2

Mixture	30-Day Free Shrinkage*	Control	10% LWA	10% LWA, 30% Slag, 3% SF	10% LWA, 30% Slag, 6% SF
		390	340	263	227
Control	390		90%	Y	Y
10% LWA	340			95%	Y
10% LWA, 30% Slag, 3% SF	263				80%
10% LWA, 30% Slag, 6% SF	227				

*The 30-day free shrinkage for each mixture was determined by averaging the shrinkage values of each specimen.
Note: "Y" indicates a statistical difference between the two datum at a significance level of $\alpha = 0.02$ (98%). "N" indicates that these is no statistical significance at a significance level of $\alpha = 0.20$ (80%). Statistical differences at significance levels at, but not exceeding, $\alpha = 0.05$, 0.10, and 0.20 are represented by "95%", "90%", and "80%".

Table 4.8 Student's t-test results displaying statistical significance of differences in 180-day free shrinkage for mixtures in Program 3, Series 2

Mixture	180-Day Free Shrinkage*	Control	10% LWA	10% LWA, 30% Slag, 3% SF	10% LWA, 30% Slag, 6% SF
		583	523	437	393
Control	583		80%	Y	Y
10% LWA	523			80%	95%
10% LWA, 30% Slag, 3% SF	437				N
10% LWA, 30% Slag, 6% SF	393				

*The 180-day free shrinkage for each mixture was determined by averaging the shrinkage values of each specimen.
Note: "Y" indicates a statistical difference between the two datum at a significance level of $\alpha = 0.02$ (98%). "N" indicates that these is no statistical significance at a significance level of $\alpha = 0.20$ (80%). Statistical differences at significance levels at, but not exceeding, $\alpha = 0.05$, 0.10, and 0.20 are represented by "95%", "90%", and "80%".

As shown in Figures 4.10 through 4.12 and Table 4.6, the shrinkage values of the four mixtures ranged from 227 to 390 microstrain after 30 days, 350 to 537 microstrain after 90 days, and 393 to 583 microstrain after 180 days. Similar to the observations for Series 1, the Control mixture with no lightweight aggregate or mineral admixtures had the highest shrinkage throughout the test. The mixture with lightweight aggregate, slag, and 6 percent silica fume (10% LWA, 30% Slag, 6% SF) had the lowest shrinkage after each drying period. The figures and table confirm that the addition of lightweight aggregate reduced shrinkage, supporting the findings from Series 1 and also those of Reynolds et al. (2009) and Browning et al. (2011). As with Series 1, the addition of slag and silica fume in conjunction with lightweight aggregate contributed to an additional reduction in free shrinkage.

Similar to Series 1, the 10 percent volume replacement of total aggregate with pre-wetted lightweight aggregate contributed to a reduction in shrinkage after 30 days of drying (Figure 4.10). The mixture with 10 percent lightweight aggregate had 50 microstrain less shrinkage after 30 days than the Control mixture, a difference that is statistically significant at $\alpha = 0.10$ (Table 4.7). This mixture (10% LWA) had a shrinkage of 340 microstrain after 30 days compared to 327 microstrain for the corresponding mixture in Series 1 over the same period. The Control mixtures for the two series also had similar shrinkage during the first 30 days (397 microstrain for Series 1 vs. 390 microstrain for Series 2).

Similar to Series 1, the mixtures in Series 2 containing lightweight aggregate, slag, and silica fume had significantly lower shrinkage during the first 30 days of drying than the mixtures without slag or silica fume (Figure 4.10). After 30 days, the mixtures with lightweight aggregate, slag, and 3 and 6 percent silica fume had 77 and 113 microstrain less shrinkage respectively, than the mixture with 10 percent lightweight aggregate (10% LWA) and 127 and 163 microstrain less shrinkage, respectively, than the Control mixture. As shown in Table 4.7, the differences in

shrinkage are statistically significant at $\alpha = 0.05$ and $\alpha = 0.02$ when comparing the mixtures with 3 and 6 percent silica fume (10% LWA, 30% Slag, 3% SF and 10% LWA, 30% Slag, 6% SF), respectively, to the mixture with 10 percent lightweight aggregate (10% LWA). The differences in shrinkage after 30 days are statistically significant at $\alpha = 0.02$ when comparing the mixtures with silica fume to the Control mixture. The mixtures in Series 2 with lightweight aggregate, slag, and silica fume experienced greater shrinkage during the first 30 days than the corresponding mixtures in Series 1. For example, the mixtures with 3 and 6 percent silica fume (10% LWA, 30% Slag, 3% SF and 10% LWA, 30% Slag, 6% SF) in Series 2 had 83 and 27 microstrain more shrinkage after 30 days, respectively, than the corresponding mixtures in Series 1.

As the volume replacement of cement with silica fume increased from 3 to 6 percent in the mixtures in Series 2, free shrinkage after 30 days decreased from 263 to 227 microstrain. This difference is statistically significant at $\alpha = 0.20$. A similar decrease in shrinkage was not observed in Series 1 with increased silica fume content. No increase in swelling during wet-curing was observed in Series 2 with the addition of slag and silica fume, in contrast to the observations in Series 1. In fact, the Control mixture experienced 10 to 20 microstrain greater swelling during wet-curing than the other mixtures.

Figures 4.11 and 4.12 and Table 4.6 show that the mixture containing 10 percent lightweight aggregate without slag or silica fume (10% LWA) had 67 and 60 microstrain less shrinkage than the Control mixture after 90 and 180 days, respectively. This difference after 180 days is statistically significant at $\alpha = 0.20$ (Table 4.8). The mixtures with lightweight aggregate, slag, and 3 and 6 percent silica fume had, respectively, 93 and 120 microstrain less shrinkage after 90 days and 86 and 130 microstrain less shrinkage after 180 days than the mixture with 10 percent lightweight aggregate and no slag or silica fume, supporting the observations in

Series 1. As shown in Table 4.8, the differences in shrinkage after 180 days are statistically significant at $\alpha = 0.20$ and $\alpha = 0.05$ when comparing the mixtures with 3 and 6 percent silica fume (10% LWA, 30% Slag, 3% SF and 10% LWA, 30% Slag, 6% SF), respectively, to the mixture with 10 percent lightweight aggregate (10% LWA).

Unlike the observations in Series 1, the mixture with the 6 percent volume replacement of cement with silica fume had less shrinkage than the mixture with the 3 percent replacement after both 90 (27 microstrain) and 180 days (44 microstrain). The difference after 180 days is, however, not statistically significant.

Table 4.6 indicates that a greater percentage of total shrinkage at 180 days was observed during the first 30 days for the mixtures without slag or silica fume, supporting the observations in Series 1. The mixtures with 3 and 6 percent silica fume (10% LWA, 30% Slag, 3% SF and 10% LWA, 30% Slag, 6% SF) experienced 60 and 58 percent, respectively, of the shrinkage at 180 days during the first 30 days; higher than the values of 49 and 55 percent observed for the corresponding mixtures in Series 1. The Control mixture and the mixture with 10 percent lightweight aggregate but no slag or silica fume (10% LWA) experienced 67 and 65 percent, respectively, of the shrinkage at 180 days during the first 30 days; lower than the values of 72 and 71 percent observed for the corresponding mixtures in Series 1.

Table 4.9 and Figures 4.13 through 4.15 show the free shrinkage observed during three drying periods, 0 to 30 days, 30 to 90 days, and 90 to 180 days. During these drying periods, shrinkage of the four mixtures ranged from 290 to 463 microstrain, 114 to 147 microstrain, and 43 to 60 microstrain, respectively, indicating that shrinkage decreased over time. Similar to Series 1, the addition of slag and silica fume contributed to decreased shrinkage primarily within the first 30 days of drying. During the first 30 days, the two mixtures with lightweight aggregate, slag, and silica fume had shrinkage values of 316 and 290 microstrain, while the two without slag or

Table 4.9 Average free shrinkage following curing during three drying periods (0 to 30 days, 30 to 90 days, and 90 to 180 days) for mixtures in Program 3, Series 2

Drying Period (days)	0-30	30-90	90-180	Total Free Shrinkage at 180 days after curing
Mixture	Free Shrinkage in Drying Period (με)			(με)
Control	463	147	46	656
10% LWA	400	130	53	583
10% LWA, 30% Slag, 3% SF	316	114	60	490
10% LWA, 30% Slag, 6% SF	290	123	43	456

Note: Three specimens tested per mixture

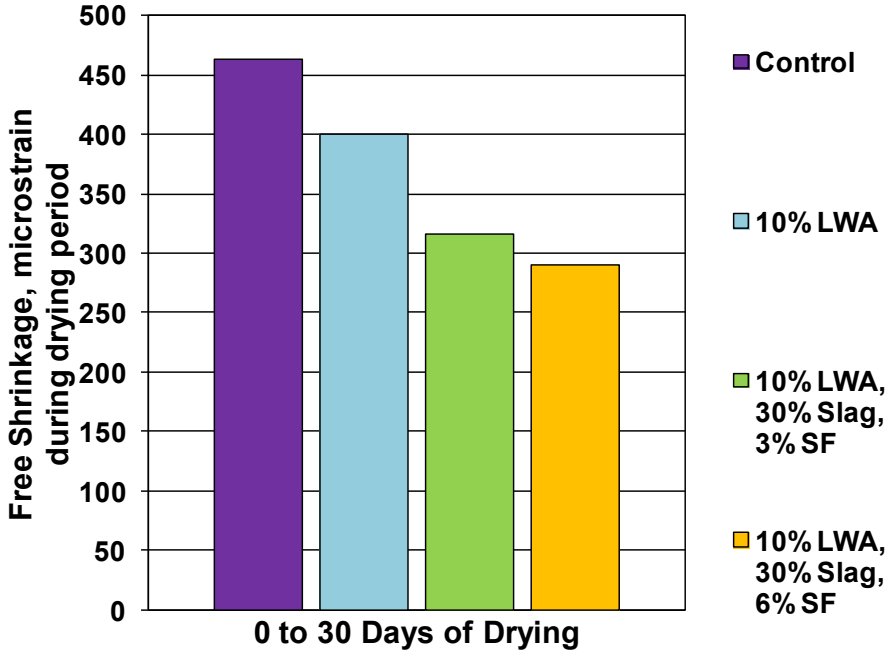

Figure 4.13 Average free shrinkage during the drying period of 0 to 30 days for mixtures in Program 3, Series 2

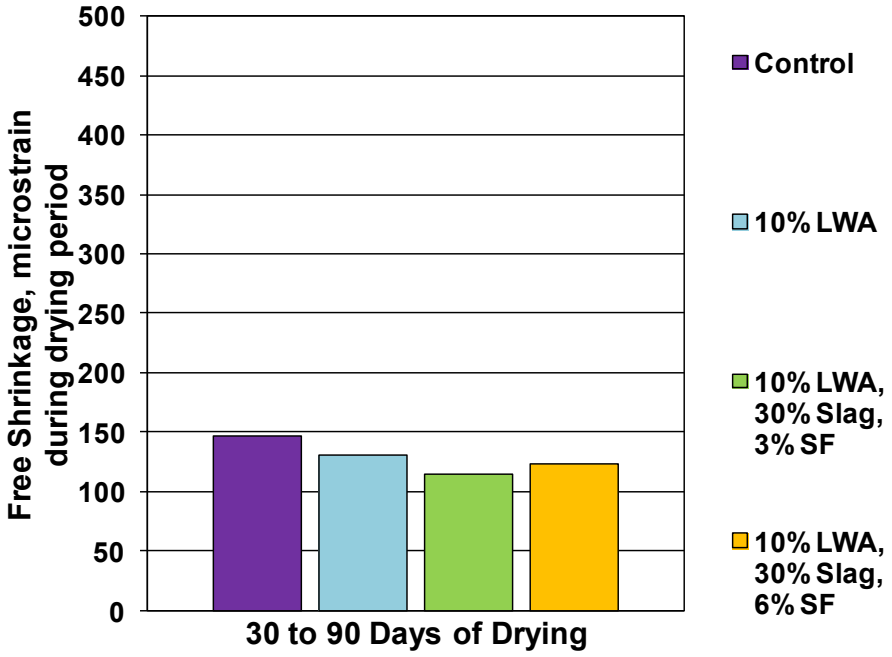

Figure 4.14 Average free shrinkage during the drying period of 30 to 90 days for mixtures in Program 3, Series 2

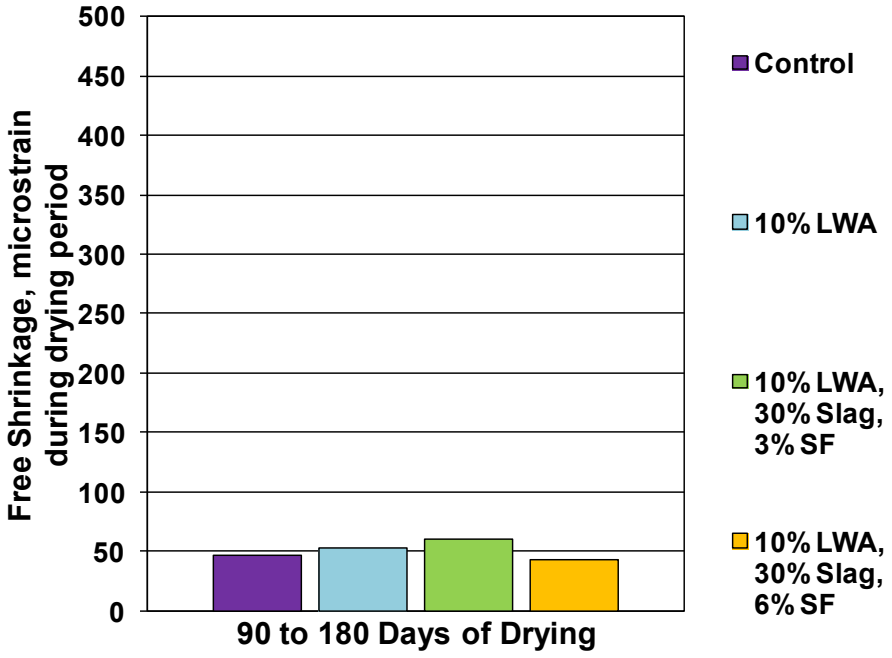

Figure 4.15 Average free shrinkage during the drying period of 90 to 180 days for mixtures in Program 3, Series 2

silica fume had values of 463 and 400 microstrain (Table 4.9 and Figure 4.13). Between 30 and 90 days, the mixtures with lightweight aggregate, slag, and silica fume had slightly less shrinkage than the two mixtures without slag or silica fume, with shrinkage values of 114 and 123 microstrain, respectively, for the mixtures with 3 and 6 percent silica fume compared to 147 and 130 microstrain, respectively, for the Control and 10% LWA mixtures. Between 90 and 180 days, all four mixtures had similar shrinkage, ranging from 43 to 60 microstrain. The mixture with 3 percent silica fume (10% LWA, 30% Slag, 3% SF) had the greatest shrinkage during this drying period. Unlike the observations in Series 1, a substantially higher shrinkage was not observed in the mixtures with slag and silica fume compared with the Control and 10% LWA mixtures in Series 2 between 90 and 180 days.

4.1.2 Freeze-Thaw Durability

The evaluation of freeze-thaw durability in Program 3 included the tests of 12 batches containing the different combinations and replacement levels of lightweight aggregate, slag cement, and silica fume. The twelve batches, shown in Table 2.5, included duplicate batches of the six mixtures examined in the free shrinkage evaluation. The two sets of six mixtures constitute two series (Series 1 and 2).

Three specimens for each batch were tested in accordance with ASTM C666 – Procedure B and KDOT Test KTMR-22. Detailed information regarding the test procedures is provided in Section 2.4.2. As explained in Section 2.4.2, testing stopped when the specimens in the batch were subjected to a minimum of 300 freeze-thaw cycles or when the average dynamic modulus of elasticity of the three specimens from each mixture dropped to 60 percent or less of the initial dynamic modulus of elasticity. As with Programs 1 and 2, the freeze-thaw performance of the mixtures is quantified with a Durability Factor (DF, see Section 2.4.2). As explained in Chapters 2 and 3, the DF represents the percentage of the initial dynamic modulus of elasticity remaining (actual or estimated, depending on when testing is stopped)

after the specimens were subjected to 300 freeze-thaw cycles. As discussed in Chapter 3, the Kansas Department of Transportation (KDOT) requires a minimum DF of 95 (95 percent of initial dynamic modulus of elasticity maintained at test completion) for concretes placed on-grade (Kansas Department of Transportation 2007d); a DF of 95 also represents the standard for acceptable durability in this evaluation. The raw data from the testing are provided in Appendix C.

4.1.2.1 Series 1

The average dynamic modulus of elasticity for the three specimens from each mixture in Series 1 is plotted as a function of the number of freeze-thaw cycles in Figure 4.16. In the figure legends, the mixtures are listed in the order of descending DF. Table 4.10 lists the DFs of the mixtures.

The figure and table show that all mixtures maintained a DF of greater than 95 after 300 freeze-thaw cycles. The addition of lightweight aggregate to the mixtures had no negative effect on freeze-thaw durability. In fact, the mixture with an 8 percent volume replacement of total aggregate with lightweight aggregate (8% LWA) had the highest DF (102). The additions of slag and silica fume also did not have a significant effect on freeze-thaw durability. The three mixtures containing a 30 percent volume replacement of cement with slag (10% LWA, 30% Slag; 10% LWA, 30% Slag, 3% SF; 10% LWA, 30% Slag, 6% SF) had DFs of 97, 98, and 98, respectively, while the three mixtures without slag (Control, 8% LWA, 10% LWA) had DFs of 99, 102, and 99, respectively. In addition, the two mixtures with lightweight aggregate, slag, and silica fume had slightly higher DFs than the mixture with lightweight aggregate and slag without silica fume (98 vs. 97).

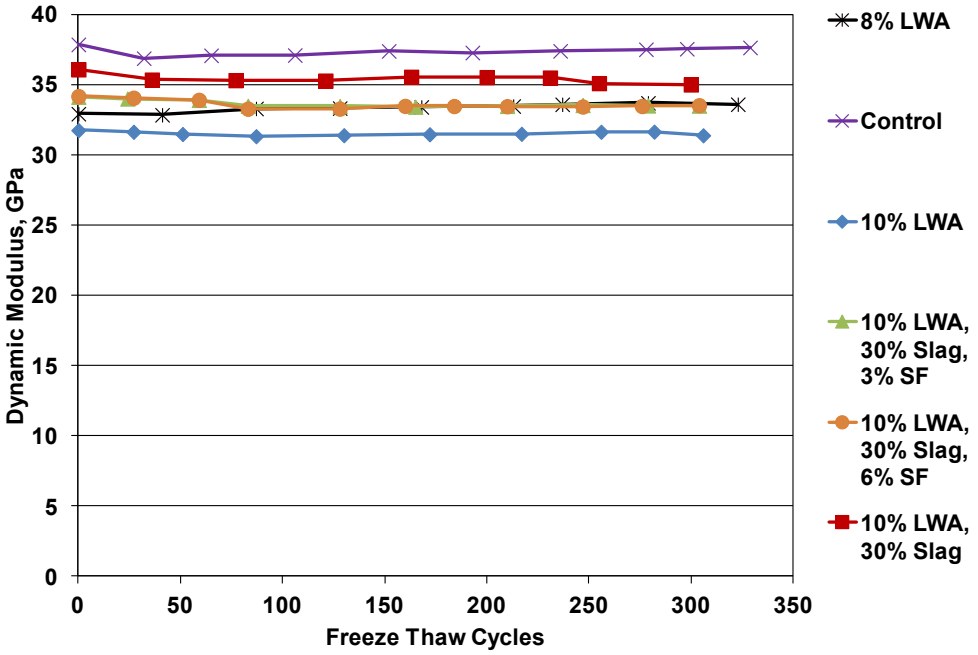

Figure 4.16 Average dynamic modulus of elasticity versus freeze-thaw cycles for mixtures in Program 3, Series 1

Table 4.10 Summary of dynamic modulus of elasticity versus freeze-thaw cycles for mixtures in Program 3, Series 1

Mixture	Durability Factor[#]
Control	99
8% LWA	102
10% LWA	99
10% LWA, 30% Slag	97
10% LWA, 30% Slag, 3% SF	98
10% LWA, 30% Slag, 6% SF	98

[#] *Durability Factor (DF) = (P × N) / 300 cycles*,
where *P* is the percentage of the initial dynamic modulus remaining at *N* cycles, *N* is either the number of cycles at which *P* reached 60 percent or 300 cycles (whichever is smaller).
Note: Three specimens tested per mixture

4.1.2.2 Series 2

The average dynamic modulus of elasticity for the three specimens from each mixture in Series 2 is plotted as a function of the number of freeze-thaw cycles in Figure 4.17. The DFs of the mixtures are listed in Table 4.11. Similar to the findings from Series 1, the figure and table indicate that all mixtures in Series 2 maintained a DF of greater than 95 after 300 freeze-thaw cycles. In fact, no mixture in Series 2 had a DF below 99. The addition of lightweight aggregate, slag, or silica fume did not affect freeze-thaw durability. The three mixtures with the highest DF (101) contained lightweight aggregate. One of these three mixtures also contained slag. Ultimately, the 12 batches evaluated in Program 3 exhibited acceptable freeze-thaw durability.

4.1.3 Scaling Resistance

Seventeen batches containing the different combinations and replacement levels of lightweight aggregate, slag cement, and silica fume were evaluated based on scaling resistance in Program 3. The seventeen batches, shown in Table 2.6, included three matching batches of five mixtures and two matching batches of another mixture. The mixture with only two matching batches contained no lightweight aggregate or mineral admixtures and served as the Control. The six mixtures were separated into three series (Series 1, 2, and 3). Because only two batches of the Control mixture were evaluated, one of the Control batches is included in both Series 2 and 3.

Three specimens for each mixture were tested for scaling resistance in accordance with Canadian Test BNQ NQ 2621-900 Annex B modified as described in Section 2.4.3. As explained in Section 2.4.3, surface mass loss of the specimens was determined after 7, 21, 35, and 56 freeze-thaw cycles. The Canadian Test has a limit of 0.31 lb/ft^2 (1500 g/m^2) for the maximum average cumulative mass loss for the three specimens at the completion of the test. The data from the tests are provided in Appendix C.

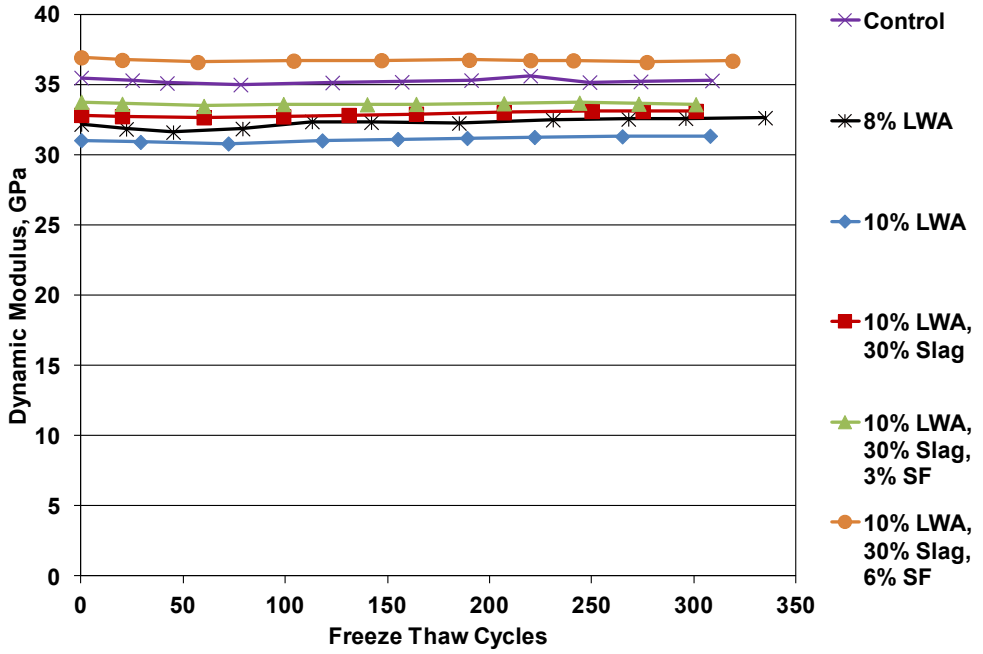

Figure 4.17 Average dynamic modulus of elasticity versus freeze-thaw cycles for mixtures in Program 3, Series 2

Table 4.11 Summary of dynamic modulus of elasticity versus freeze-thaw cycles for mixtures in Program 3, Series 2

Mixture	Durability Factor[#]
Control	99
8% LWA	101
10% LWA	101
10% LWA, 30% Slag	101
10% LWA, 30% Slag, 3% SF	99
10% LWA, 30% Slag, 6% SF	99

[#] *Durability Factor (DF) = (P × N) / 300 cycles*,
where *P* is the percentage of the initial dynamic modulus remaining at *N* cycles, *N* is either the number of cycles at which *P* reached 60 percent or 300 cycles (whichever is smaller).
Note: Three specimens tested per mixture

4.1.3.1 Series 1

The average cumulative mass losses for the mixtures in Series 1 are plotted as a function of the number of freeze-thaw cycles in Figure 4.18. In the figure legends, the mixtures are listed in the order of descending cumulative mass loss after 56 freeze-thaw cycles. Table 4.12 summarizes the cumulative mass loss for each mixture at 7, 21, 35, and 56 cycles.

As shown in the figure and table, mass losses were not increased as the result of the addition of lightweight aggregate. In fact, the mixtures containing 8 and 10 percent volume replacements of total aggregate with lightweight aggregate (8% LWA and 10% LWA) had lower mass losses after 56 freeze-thaw cycles than the Control mixture. Mass loss increased, however, as slag was added in conjunction with lightweight aggregate and again as silica fume was added in conjunction with slag and lightweight aggregate. After 56 freeze-thaw cycles, the mixture with 10 and 30 percent volume replacements, respectively, of total aggregate with lightweight aggregate and cement with slag (10% LWA, 30% Slag) experienced nearly eight times the mass loss of the mixture with a 10 percent volume replacement of total aggregate with lightweight aggregate and no slag (10% LWA). Mixtures with replacement levels of 10 percent lightweight aggregate and 30 percent slag with 3 and 6 percent silica fume (10% LWA, 30% Slag, 3% SF and 10% LWA, 30% Slag, 6% SF) had more than twice the mass loss of the mixture with 10 percent lightweight aggregate and 30 percent slag, but no silica fume (10% LWA, 30% Slag). The losses for the two mixtures containing silica fume were similar, with the 3% SF mixture exhibiting about 3 percent more mass loss than the 6% SF mixture. All six mixtures had mass losses below the failure limit of 0.31 lb/ft^2 (1500 g/m^2) specified in BNQ NQ 2621-900; however, the mixtures containing silica fume had mass losses that approached this limit.

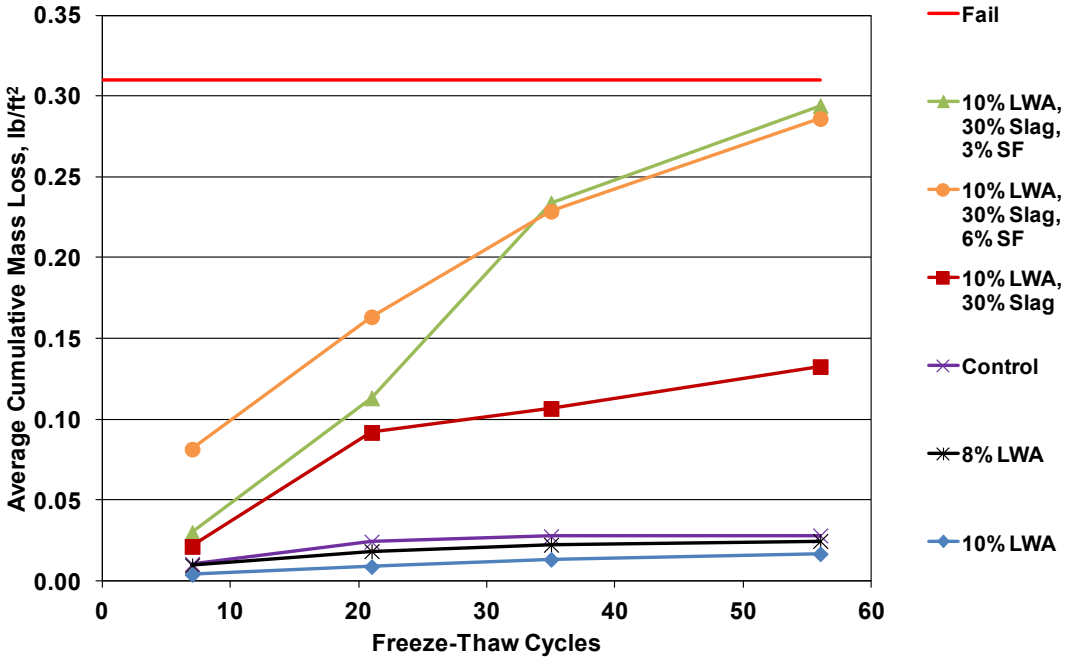

Figure 4.18 Average cumulative mass loss versus freeze-thaw cycles for mixtures in Program 3, Series 1

Table 4.12 Summary of average cumulative mass loss versus freeze-thaw cycles for mixtures in Program 3, Series 1

Mixture	Average Cumulative Mass Loss 10^{-3} lb/ft^2			
	7 cycles	21 cycles	35 cycles	56 cycles
Control	10.6	24.3	27.6	28.1
8% LWA	9.6	18.4	22.4	24.7
10% LWA	4.0	8.9	13.3	16.8
10% LWA, 30% Slag	21.3	91.8	106.7	132.6
10% LWA, 30% Slag, 3% SF	30.0	113.2	233.8	294.0
10% LWA, 30% Slag, 6% SF	81.5	163.4	228.7	286.0

Note: Three specimens tested per mixture
10^{-3} lb/ft^2 = 4.884 g/m^2

4.1.3.2 Series 2

The average cumulative mass losses for the mixtures in Series 2 are plotted as a function of freeze-thaw cycles in Figure 4.19. The cumulative mass losses are summarized in Table 4.13.

Trends similar to Series 1 were observed in Series 2, with the exception of differences in the performance of the mixtures containing 3 and 6 percent replacements of cement with silica fume. In general, the mass losses of the mixtures without mineral admixtures were about the same or slightly lower than in Series 1, while the mass losses for mixtures with mineral admixtures were significantly lower. Mass loss was not affected by the addition of lightweight aggregate. As with Series 1, mass loss increased as slag was added in combination with lightweight aggregate and again as silica fume was added in combination with lightweight aggregate and slag. Unlike Series 1, however, the mass losses of the mixtures containing silica fume differed. After 56 freeze-thaw cycles, the mixture with 6 percent silica fume exhibited a 56 percent higher mass loss than the mixture with 3 percent silica fume. As with Series 1, all six mixtures had mass losses below the failure limit of 0.31 lb/ft^2 (1500 g/m^2) specified in BNQ NQ 2621-900.

4.1.3.3 Series 3

The average cumulative mass losses for the mixtures in Series 3 are plotted as a function of freeze-thaw cycles in Figure 4.20. The cumulative mass losses are summarized in Table 4.14.

The trends observed in Figure 4.20 are similar to those observed for Series 1 and 2, with the losses of the mixtures without mineral admixtures being about the same as in the first two series. As with Series 2, mass loss was highest for the mixture with 6 percent silica fume. The mixtures with slag and slag and silica fume exhibited lower mass losses in Series 3 than in Series 1 or 2, and therefore, all six

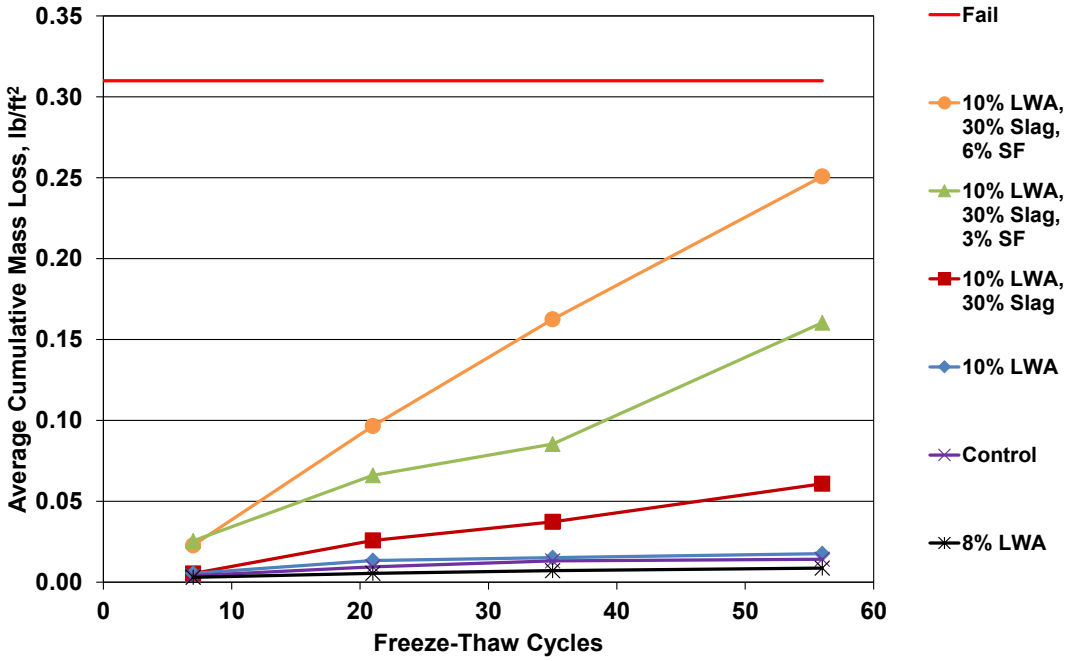

Figure 4.19 Average cumulative mass loss versus freeze-thaw cycles for mixtures in Program 3, Series 2

Table 4.13 Summary of average cumulative mass loss versus freeze-thaw cycles for mixtures in Program 3, Series 2

Mixture	Average Cumulative Mass Loss 10^{-3} lb/ft^2			
	7 cycles	21 cycles	35 cycles	56 cycles
Control	4.1	9.6	13.2	14.2
8% LWA	3.0	5.6	7.2	8.8
10% LWA	5.6	13.5	15.2	17.7
10% LWA, 30% Slag	5.4	25.8	37.3	60.9
10% LWA, 30% Slag, 3% SF	25.6	66.2	85.4	160.4
10% LWA, 30% Slag, 6% SF	22.8	96.6	162.5	250.8

Note: Three specimens tested per mixture
10^{-3} lb/ft^2 = 4.884 g/m^2

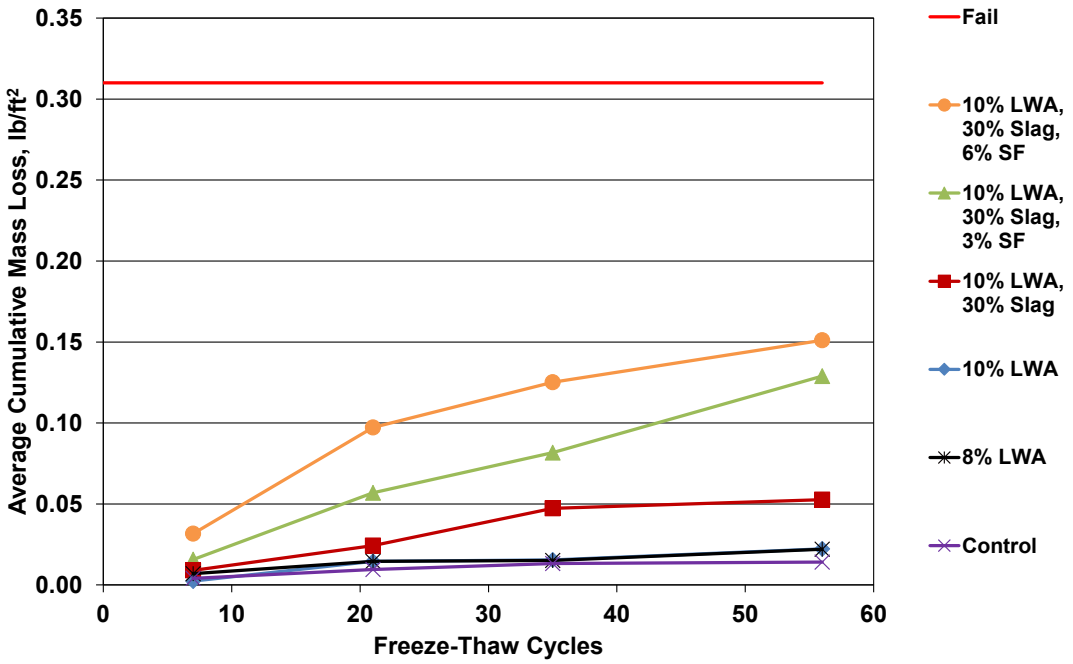

Figure 4.20 Average cumulative mass loss versus freeze-thaw cycles for mixtures in Program 3, Series 3

Table 4.14 Summary of average cumulative mass loss versus freeze-thaw cycles for mixtures in Program 3, Series 3

Mixture	Average Cumulative Mass Loss 10^{-3} lb/ft^2			
	7 cycles	21 cycles	35 cycles	56 cycles
Control	4.1	9.6	13.2	14.2
8% LWA	7.0	14.6	15.2	22.0
10% LWA	2.4	14.6	15.5	22.2
10% LWA, 30% Slag	9.0	24.3	47.3	52.7
10% LWA, 30% Slag, 3% SF	15.6	57.0	81.7	128.9
10% LWA, 30% Slag, 6% SF	31.6	97.3	125.2	151.1

Note: Three specimens tested per mixture
10^{-3} lb/ft^2 = 4.884 g/m^2

mixtures maintained mass losses below the failure limit of 0.31 lb/ft^2 (1500 g/m^2) specified in BNQ NQ 2621-900.

4.1.3.4 Statistical Analysis

The Student's t-test was used to determine the statistical significance of differences in average mass losses for the seventeen batches that comprised the three sets of the six mixtures. Average values of mass loss were calculated for the six mixtures by averaging the cumulative mass losses of all specimens for that mixture at 56 freeze-thaw cycles. Table 4.15 shows the statistical significance for the differences in mass losses of the six mixtures.

As expected, the table shows that the addition of lightweight aggregate did not significantly affect mass loss. Conversely, the increase in mass loss observed with the addition of slag is significant at a significance level of $\alpha = 0.02$. The increase in mass loss is also significant at $\alpha = 0.02$ as silica fume is added in conjunction with lightweight aggregate and slag. Although an increase in mass loss was observed in two of the three series as the replacement level of silica fume increased from 3 to 6 percent, this increase is not statistically significant.

4.1.4 Compressive Strength

The average 28-day compressive strengths of the mixtures containing the different combinations and replacement levels of lightweight aggregate, slag cement, and silica fume are shown in Figure 4.21. The number of batches included in the average strengths (three cylinders per batch) is shown in the figure. The range of compressive strengths for each mixture type is shown in the figure using error bars. The compressive strengths are tabulated in Table 4.16.

The figure and table show that the compressive strengths of the six mixtures fell within a small range, 4320 to 4830 psi (29.8 to 33.3 MPa). All six mixtures had compressive strengths within the limits required by the LC-HPC specifications, 3500

Table 4.15 Student's t-test results displaying statistical significance of differences in mass loss after 56 freeze-thaw cycles for the combined mixtures from Series 1, 2, and 3 of Program 3

Mixture	Average mass loss after 56 freeze-thaw cycles*	Control	8% LWA	10% LWA	10% LWA, 30% Slag	10% LWA, 30% Slag, 3% SF	10% LWA, 30% Slag, 6% SF
		21.1	18.5	18.9	82.1	186.1	229.3
Control	21.1		N	N	Y	Y	Y
8% LWA	18.5			N	Y	Y	Y
10% LWA	18.9				Y	Y	Y
10% LWA, 30% Slag	82.1					Y	Y
10% LWA, 30% Slag, 3% SF	186.1						N
10% LWA, 30% Slag, 6% SF	229.3						

*Average mass losses after 56 freeze-thaw cycles are determined by averaging the mass losses of the nine specimens from the three series for each mixture. Only six specimens are tested to determine the average mass loss for the Control mixture.

Note: "Y" indicates a statistical difference between the two datum at a significance level of $\alpha = 0.02$ (98%). "N" indicates that these is no statistical significance at a significance level of $\alpha = 0.20$ (80%). Statistical differences at significance levels at, but not exceeding, $\alpha = 0.05$, 0.10, and 0.20 are represented by "95%," "90%," and "80%", but were not obtained in this analysis.

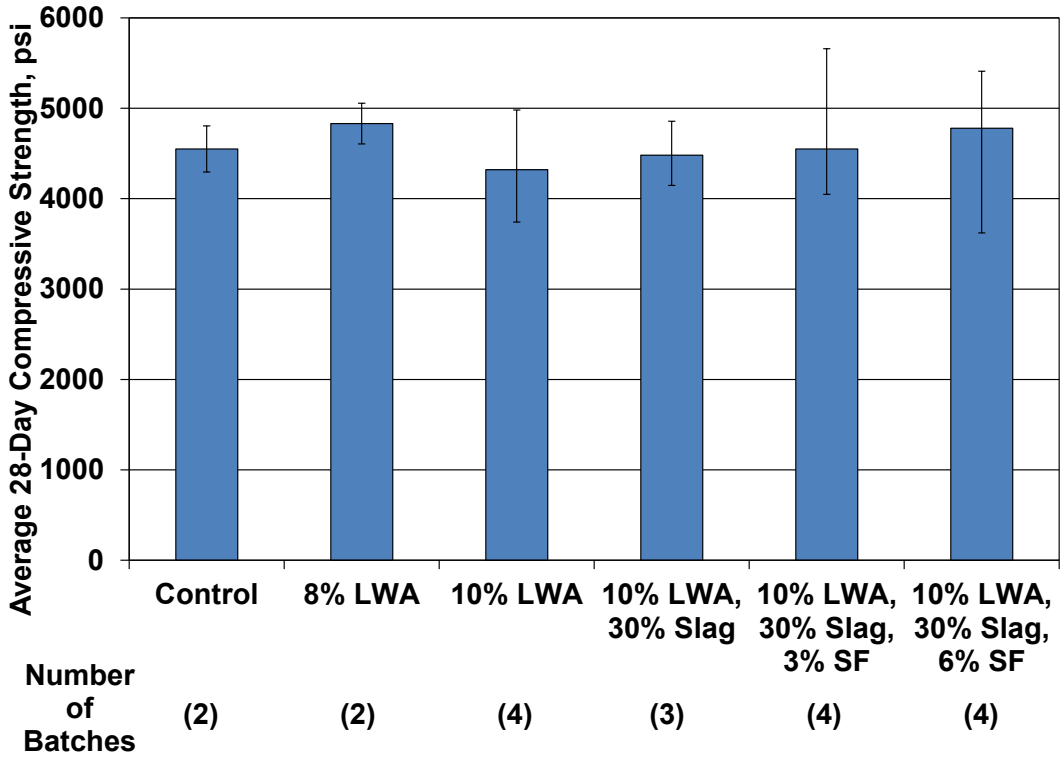

Note: 1 psi = 0.0069 MPa

Figure 4.21 Average 28-day compressive strengths for mixtures in Program 3

Table 4.16 Average 28-day compressive strengths and average air contents for mixtures in Program 3

Mixture	Avg. 28-Day Compressive Strength (psi)	Avg. Air Content (%)
Control	4550	7.88
8% LWA	4830	8.25
10% LWA	4320	8.69
10% LWA, 30% Slag	4480	8.42
10% LWA, 30% Slag, 3% SF	4550	8.38
10% LWA, 30% Slag, 6% SF	4780	8.06

Note: 1 psi = 0.0069 MPa

to 5500 psi (24.1 to 37.9 MPa) (Kansas Department of Transportation 2007b). The effect on strength of replacing a volume of total aggregate with lightweight aggregate is not completely clear since mixtures with 8 and 10 percent volume replacements had the highest and lowest strengths, respectively, of those tested. The effect, however, is small. In previous research by Roberts (2004), Geiker et al. (2004), and Cusson and Margeson (2010), increased strength was observed in high-strength mixtures containing pre-wetted lightweight aggregate with water-cement ratios below 0.40 (significantly lower than the ratios used in this study) due to the increased hydration provided by the internal curing. Conversely, the porous nature of lightweight aggregate can lead to reduced strength. As discussed previously, additional strength is not a desired characteristic of low-cracking concrete because of the reduced creep that is experienced by higher-strength concretes. Based on the results shown in the Figure 4.21 and Table 4.16, the addition of the amounts of lightweight aggregate examined in this study does not appear to significantly affect strength.

The volume replacements of cement with 30 percent slag and 3 or 6 percent silica fume also did not significantly affect strength. The mixture with lightweight aggregate, slag, and a 3 percent volume replacement of cement with silica fume (10%

LWA, 30% Slag, 3% SF) had the same average compressive strength as the Control mixture with no lightweight aggregate, slag, or silica fume, 4550 psi (31.4 MPa). The two mixtures with lightweight aggregate, slag, and silica fume had slightly higher strengths than the mixture with lightweight aggregate and slag with no silica fume. As shown in Table 4.16, all mixtures had average air contents between 7.75 and 8.75 percent, and therefore, air content likely did not influence the strengths.

4.1.5 Hardened Concrete Air-Void Analysis

The air-void analysis of hardened concrete included specimens from sixteen batches, containing the six different combinations and replacement levels of lightweight aggregate, slag cement, and silica fume. In the analysis, the air content in hardened concrete and the air-void spacing factor were determined for two cylinders per batch. The average air contents measured in the plastic (based on ASTM C173) and hardened concrete are shown for the six mixtures in Figure 4.22. The figure shows that the addition of lightweight aggregate, slag, or silica fume did not affect the air content as the concrete was placed and consolidated. The average air contents in the plastic concrete were nearly identical to the average values in the hardened concrete. These observations were as expected since, unlike shrinkage-reducing admixtures, lightweight aggregate, slag, and silica fume are not known to affect the air-void system of concrete. Figure 4.23 shows the average air-void spacing factors for the six mixtures. The batches had a small range of plastic air contents (8 to 9 percent) and, as a result, any effect of air content on the spacing factors was minor. The figure suggests that the addition of lightweight aggregate, slag, or silica fume does not affect the air-void spacing factor. All six mixtures have spacing factors below 4×10^{-3} in. (0.10 mm). As discussed in Section 1.6.1.1, an air-void spacing factor below 8×10^{-3} in. (0.20 mm) is suggested to provide sufficient freeze-thaw protection to the concrete (Russell 2004). Unlike the addition of shrinkage-reducing admixtures, the addition of lightweight aggregate, slag, and silica fume provide

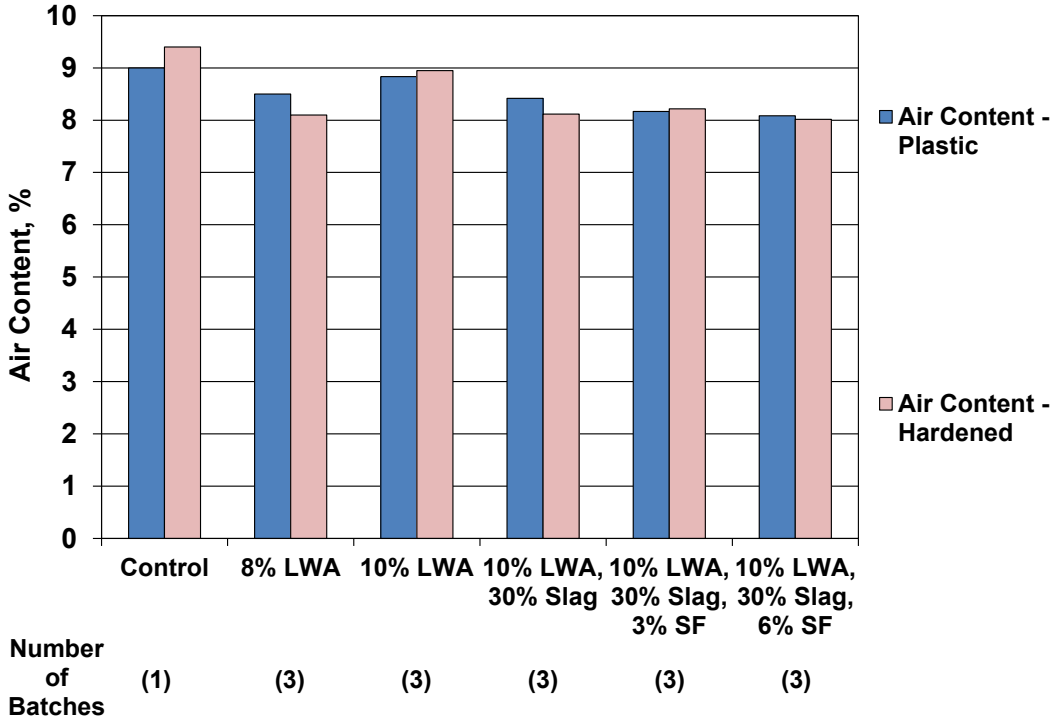

Note: Plastic and hardened air content determined through ASTM C173 and C457, respectively.

Figure 4.22 Air content in the plastic and hardened concrete for mixtures in Program 3

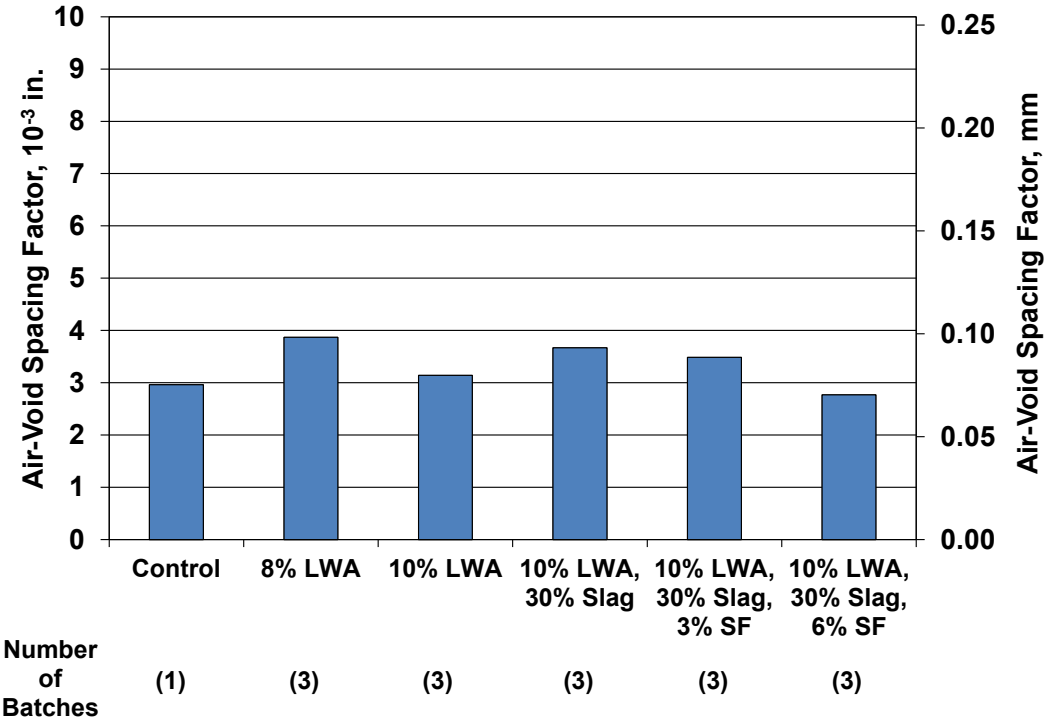

Note: Air-void spacing factor determined through ASTM C457.

Figure 4.23 Average air-void spacing factor for mixtures in Program 3

improved shrinkage performance to concrete without affecting the stability of the air-void system. The increased scaling observed in Section 4.1.3 for mixtures containing slag and silica fume likely resulted from changes in the cement paste constituent of the concrete due to the addition of the mineral admixtures, not a change in the air-void system.

4.1.6 Program 3 Summary

The replacement of a portion of total aggregate with pre-wetted lightweight aggregate reduced both early-age (0 to 90 days) and long-term (90 to 365 days) shrinkage by providing a source of internal curing water. Shrinkage was reduced further as slag was added in conjunction with lightweight aggregate. These observations support the findings of Reynolds et al. (2009) and Browning et al. (2011). An additional reduction in shrinkage was observed as silica fume was added in conjunction with the lightweight aggregate and slag. No differences in shrinkage were observed for volume replacements of lightweight aggregate of 8 and 10 percent. The mixtures in Series 1 containing slag exhibited increased swelling compared to the mixtures without slag during the 14-day wet-curing period, while the mixtures in Series 2 with slag did not. Any effect on shrinkage of increasing the replacement level of silica fume from 3 to 6 percent does not appear to be significant.

The mixtures without slag or silica fume experienced a greater percentage of the 365-day shrinkage during the first 30 days than the mixtures with slag or slag and silica fume. As a result, the difference in shrinkage for mixtures with and without these mineral admixtures was less pronounced after 365 days than after 30 days. The addition of slag contributed to reduced shrinkage only during the first 30 days of drying. In fact, the mixtures in Series 1 with slag experienced greater shrinkage than those without slag during the drying period of 90 to 365 days. As stated previously, however, reducing shrinkage at an early age is the primary concern for bridge decks due to the large percentage of the total shrinkage that occurs during this period and

the relatively short period available for creep to mitigate tensile stresses, and although the mixtures with slag experienced greater shrinkage than those without slag from 90 to 365 days, the amount of shrinkage that occurred during this period was minimal compared to the early-age shrinkage.

The mixtures were examined for freeze-thaw durability and scaling resistance in Program 3. The addition of lightweight aggregate, slag, or silica fume had little impact on freeze-thaw durability, as all mixtures maintained a Durability Factor (DF) of at least 97 after 300 freeze-thaw cycles. The addition of lightweight aggregate did not contribute to increased mass loss in the scaling test. Mass losses did increase, however, as slag was added in conjunction with lightweight aggregate and again as silica fume was added in conjunction with lightweight aggregate and slag. In two of the three series, a higher mass loss was observed for mixtures with a 6 percent volume replacement of cement with silica fume than for mixtures with a 3 percent replacement. These influences on scaling resistance from the addition of slag and silica fume are likely the result of changes in the cement paste constituent of the concrete, not effects on the air-void system. All mixtures had a mass loss below the failure limit of 0.31 lb/ft^2 (1500 g/m^2) specified in BNQ NQ 2621-900.

The replacement levels of lightweight aggregate, slag, and silica fume examined in this study do not appear to significantly affect strength, and all mixtures had compressive strengths within the requirements of the LC-HPC specifications, 3500 to 5500 psi (24.1 to 37.9 MPa).

The addition of lightweight aggregate, slag, or silica fume did not affect the air-void system of the concrete. The air contents of the mixtures in plastic concrete were nearly identical to the those in hardened concrete, indicating that the addition of the lightweight aggregate and these mineral admixtures did not have an effect on air content as the concrete was placed and consolidated. The addition of lightweight aggregate, slag, and silica fume also did not affect the air-void spacing factor, as the

mixtures had spacing factors below 4×10^{-3} in. (0.10 mm) – half the value suggested to attain acceptable freeze-thaw durability. These observations were expected since, unlike surfactant-based shrinkage-reducing admixtures, lightweight aggregate, slag, and silica fume do not provide a reduction in shrinkage through a reduction in the surface tension of pore water – a mechanism that affects the air-void system.

Ultimately, the addition of silica fume in conjunction with the pre-wetted lightweight aggregate and slag did provide reduced shrinkage, primarily during the first 30 days of drying. Reducing shrinkage during the first 30 days is essential for reducing cracking in bridge decks because of the great percentage of total shrinkage that occurs during this time and the short period available for creep to reduce tensile stresses. The reduced permeability attained with the addition of small amounts of silica fume likely slowed the drying process, allowing the pre-wetted lightweight aggregate to provide internal curing water to the cementitious materials. This reduced permeability slowed the movement of internal water to the surface of the concrete, allowing it to be used in the hydration process and preventing it from contributing to shrinkage through evaporation. The increased shrinkage observed in the mixtures with slag and slag and silica fume after 90 days, an amount that is small compared to the early-age shrinkage, could be a result of portions of internal water eventually reaching the surface. The replacement level of silica fume must be regulated since the addition of increasing amounts of the material contributed to increased scaling. Since shrinkage was not significantly reduced as the volume replacement level of silica fume was increased from 3 to 6 percent, it appears that small amounts of the material could be added to provide reduced shrinkage while not substantially reducing scaling resistance. Furthermore, the small quantities of silica fume used in these mixtures resulted in a minimal, if any, increase in strength, a desirable characteristic of low-cracking, high-performance concrete. As a result of the high performance observed for the mixtures containing lightweight aggregate,

slag, and silica fume, an updated version of the LC-HPC specifications, provided in Appendix G, has been created that allows partial replacements of portland cement with slag and silica fume if used in conjunction with internal curing techniques.

CHAPTER 5: CONSTRUCTION OF LOW-CRACKING HIGH-PERFORMANCE CONCRETE (LC-HPC) AND CONTROL BRIDGE DECKS

5.1 GENERAL

This chapter describes the construction of 16 bridge decks constructed under the provisions of low-cracking high-performance concrete (LC-HPC) specifications and 11 associated control bridge decks in Kansas. The 16 LC-HPC decks are numbered in the order they were let and are designated as LC-HPC-1 through LC-HPC-13 and LC-HPC-15 through LC-HPC-17. The construction of another deck which was bid under the LC-HPC specifications, but not constructed following those specifications, is also described. The LC-HPC decks in Kansas were constructed in accordance with the standard Kansas Department of Transportation (KDOT) specifications with special provisions for the aggregate, concrete, and construction. The special provisions included materials and procedures known to minimize cracking and are summarized in Section 5.2. The special provisions for LC-HPC deck construction have been modified over time based on construction experience and laboratory findings. Section 5.3 summarizes the lessons learned during the construction of the bridge decks and proposes methods to improve construction. The control decks were constructed in accordance with the standard KDOT specifications. Control decks were selected based on similarities in design, traffic and environmental conditions, and age. The similarities between the LC-HPC and control decks provide a clear determination of the effects of the special provisions on cracking performance.

As described in Section 2.6, data were collected and observations were made during the construction of each bridge deck. The data collected from each deck are reported in Section 5.3 and include mixture design information, environmental conditions during placement, plastic concrete properties, concrete compressive strength data, and rates of burlap placement.

Crack surveys (described in Section 2.7 and Appendix B) have been completed annually on each bridge deck to quantitatively evaluate the cracking performance in terms of a crack density. Crack maps, which display the distribution of cracks on the deck surface, are produced for each survey. A comparison of the cracking performance of the LC-HPC and associated control decks is reported in Chapter 6. In addition, a crack map from the most recent crack survey of each deck is provided. The data collected for each deck during construction are combined with the crack density information to evaluate the factors that affect cracking performance, reported in Chapter 6.

5.2 LOW-CRACKING HIGH-PERFORMANCE CONCRETE (LC-HPC) SPECIFICATIONS

The LC-HPC special provisions to the standard KDOT specifications (known as the LC-HPC specifications) include three separate sections, on aggregate, concrete, and construction. Aspects of LC-HPC bridge decks that did not involve the LC-HPC special provisions were completed in accordance with the standard KDOT specifications. The 1990 version of the standard KDOT specifications was used for construction of all LC-HPC decks, except for the three decks most recently constructed (LC-HPC-15, 16, and 17), which used the 2007 version of the specifications. Revisions to the LC-HPC specifications have been made over the duration of the study as the field and laboratory evaluations revealed potential improvements to the specifications. The current version of the LC-HPC specifications and the background of the specification revisions are summarized in this section. The latest version of the LC-HPC specifications is presented in Appendix D.

5.2.1 Aggregates

The LC-HPC special provisions require a nominal maximum-size aggregate of 1 in. (25 mm) and an optimized combined aggregate gradation to provide increased

workability in the concrete. A proven optimization method, such as the Shilstone (1990) or KU Mix Method (Lindquist et al. 2008), must be used for the proportioning the combined aggregate gradation. Precautions must be taken to minimize coarse and fine aggregate segregation during transportation and stockpiling. The allowable limits on the combined aggregate gradation are shown in Table 5.1.

The coarse aggregate must be a gravel, chat, or crushed stone with a minimum soundness of 0.9 and maximum absorption of 0.7 percent. In contrast, the standard KDOT specifications permit a maximum absorption of 2.0 percent for coarse aggregate. Limitations on deleterious substances for coarse aggregate are summarized in Table 5.2. The fine aggregate must consist of either natural sand (Type FA-A) or chat (Type FA-B). The provisions governing deleterious substances for both types of fine aggregate are shown in Table 5.3.

Table 5.1 LC-HPC combined gradation limits

Usage	Percent Retained on Individual Sieves - Square Mesh Sieves									
	1" (25.0 mm)	3/4" (19.0 mm)	1/2" (12.5 mm)	3/8" (9.5 mm)	No. 4 (4.75 mm)	No. 8 (2.39 mm)	No. 16 (1.18 mm)	No. 30 (600 µm)	No. 50 (300 µm)	No. 100 (150 µm)
Optimized for LC-HPC Bridge Decks	2 to 6	5 to 18	8 to 18	8 to 18	8 to 18	8 to 18	8 to 18	8 to 15	5 to 15	0 to 5

Table 5.2 Deleterious substance requirements for coarse aggregate

Substance	Maximum Allowable % by Weight
Material passing No. 200 sieve	2.5%
Shale or shale-like material	0.5%
Clay lumps and friable particles	1.0%
Sticks (including absorbed water)	0.1%
Coal	0.5%

Table 5.3 Deleterious substance requirements for fine aggregate

Natural Sand	
Substance	**Maximum Allowable % by Weight**
Material passing No. 200 sieve	2.0%
Shale or shale-like material	0.5%
Clay lumps and friable particles	1.0%
Sticks (including absorbed water)	0.1%
Chat	
Substance	**Maximum Allowable % by Weight**
Material passing No. 200 sieve	2.0%
Clay lumps and friable particles	0.25%

5.2.2 Concrete

The current LC-HPC specifications for concrete require a cement content between 500 and 540 lb/yd^3 (297 and 320 kg/m^3) with a water-cement ratio (by weight) between 0.44 and 0.45. The water-cement ratio can be reduced to 0.43 at the construction site with approval from the Engineer. The specifications for the first seven LC-HPC bridge decks let (designated as LC-HPC-1 through LC-HPC-7) permitted a cement content between 522 and 563 lb/yd^3 (310 and 334 kg/m^3) with a maximum water-cement ratio (by weight) of 0.45. The specifications for the eighth through thirteenth LC-HPC bridge decks let (designated as LC-HPC-8 through LC-HPC-13) permitted a cement content between 500 and 535 lb/yd^3 (297 and 317 kg/m^3) with a maximum water-cement ratio (by weight) of 0.42, although this water-cement ratio is, in fact, too low and, for that reason was used for only some of these decks. Other than LC-HPC-15 and 16, all LC-HPC decks described in this report had concrete with a cement content of 535 or 540 lb/yd^3 (317 or 320 kg/m^3). LC-HPC-15 had a cement content of 500 lb/yd^3 (297 kg/m^3) and LC-HPC-16 was cast using cement contents ranging from 520 to 540 lb/yd^3 (308 to 320 kg/m^3). The LC-HPC specifications require air contents (by volume) between 7.0 and 9.0 percent with an allowable range of 6.5 to 9.5 percent. The designated concrete slump range at the

point of placement is between 1.5 and 3.0 in. (40 and 75 mm). For LC-HPC decks 1 through 13, the specifications stated that the Engineer must reject any concrete with a slump greater than 4.0 in. (100 mm) at the truck discharge. In the current specifications (used for LC-HPC-15 through LC-HPC-17), the Engineer must reject any concrete with a slump greater than 3.5 in. (90 mm). The slump was reduced from 4.0 to 3.5 in. (100 to 90 mm) in the current specifications because the upper slump limit was often used by concrete suppliers as a target slump instead of a maximum allowable slump – examples are provided in this chapter. The specifications require that concrete samples for air content and slump tests must be obtained at the discharge end of the conveyor, bucket, or pump piping. As described in Section 5.3, samples were taken at the truck discharge for some decks. The current specifications (used for LC-HPC-15 through LC-HPC-17) state that concrete compressive strengths must range between 3500 and 5500 psi (24.1 and 37.9 MPa). No upper limit on concrete compressive strength was included in the specifications for LC-HPC decks 1 through 13. The temperature of the concrete immediately before placement must range between 55° and 70° F (13° and 21° C). The concrete temperature can be 5° F (3° C) below or above this range with Engineer approval. For LC-HPC decks 1 and 2, the specifications stated that the concrete temperature immediately before placement must range between 50° and 75° F (10° and 24° C) with no adjustment by the Engineer.

In the specifications for LC-HPC-12, 13, 15, 16, and 17, mineral, set retarding, and accelerating admixtures were prohibited from use in LC-HPC. A Type A water reducer or dual-rated Type A water reducer – Type F high-range water reducer was permitted when necessary to comply with specified fresh and hardened concrete properties. The specifications for LC-HPC decks 1 through 11 allowed the use of a Type C or E accelerating admixture if approved by the Engineer. The specifications for LC-HPC decks 1 through 11 also allowed the use of both water

reducing and set retarding admixtures if deemed necessary by the Engineer. Accelerating and retarding admixtures, however, were not used on any LC-HPC decks. Slump control was permitted at the construction site only by redosing with a water-reducing admixture.

A qualification batch must be completed by the concrete supplier before actual bridge construction to demonstrate the ability to meet all concrete specifications. The expected concrete haul time must be simulated prior to discharge of the qualification batch for testing and the qualification batch must meet the specifications for air content, slump, plastic concrete temperature, compressive strength, and unit weight to be qualified for use in the LC-HPC bridge deck.

5.2.3 Construction

After completion of the qualification batch, a qualification slab must be constructed by the contractor prior to bridge deck construction to demonstrate the ability to handle, place, finish, and cure the LC-HPC bridge deck. The qualification slab must be constructed using the same personnel, construction methods, and equipment as to be used for the actual bridge deck. As with the qualification batch, the concrete delivered to the qualification slab must meet the specifications.

Environmental evaporation rates during deck construction must remain below 0.2 $lb/ft^2/hr$ (1.0 $kg/m^2/hr$). The Engineer must measure and record the air temperature, wind speed, and relative humidity 12 in. (305 mm) above the deck surface as well as the concrete temperature at least once per hour during placement to determine evaporation rates using a nomograph (see Figure 1.1 and Appendix D). Any fogging used on the deck will not be considered in the estimation of evaporation rate. When the evaporation rate is greater than or equal to 0.2 $lb/ft^2/hr$ (1.0 $kg/m^2/hr$), actions must be taken, such as cooling the concrete or installing a wind break, to lower the evaporation rate below the limit level.

Concrete may be placed by conveyor belt or concrete bucket. Concrete may also be placed with a pump if the contractor can demonstrate the ability to pump the approved mixture (using the same equipment as to be used on the deck) prior to deck construction. To minimize the loss of air, a maximum drop height of 5 ft (1.5 m) is allowed from the end of a conveyor or concrete bucket and all pumps must be fitted with an air cuff or bladder valve.

Concrete consolidation must be performed using machine-mounted internal gang vibrators wherever possible on the deck surface and hand-held vibrators where necessary. Each vibrator must have a head diameter between 1.75 and 2.5 in. (45 and 65 mm), loaded vibration frequency between 8,000 and 12,000 vibrations per minute, and an average vibration amplitude of 0.025 to 0.05 in. (0.635 to 1.27 mm). Vibrators must be inserted vertically, spaced at 12 in. (305 mm), and held in the concrete between 3 and 15 seconds. Vibrators must be extracted vertically at a rate that is slow enough so that no voids are left.

Strikeoff of the bridge deck surface must be completed using a vibrating or single-drum roller screed. Tamping devices are not allowed to be mounted on roller screeds. The surface should be finished by a burlap drag, metal pan, or both, mounted to the finishing equipment. Irregularities in the surface may be removed, as necessary, using a bullfloat or hand float. Finishing aids, including water, and tining of the plastic concrete, are prohibited.

To provide curing, one layer of presoaked burlap must cover the LC-HPC within 10 minutes of strikeoff. A second layer of burlap must be applied within 5 minutes. The burlap must be presoaked a minimum of 12 hours prior to placement, and must remain wet throughout the 14-day curing period. Misting hoses or fogging equipment may be used before the concrete has set to maintain the burlap in a saturated condition. After the concrete has set, soaker hoses must be placed on the burlap, and the deck must be covered with white plastic to maintain the burlap in a

wet condition for the duration of the curing period. Water application must be checked every six hours.

5.3 BRIDGE DECK CONSTRUCTION EXPERIENCES

This section describes the experiences and lessons learned during construction of the 16 LC-HPC bridge decks. In addition, methods to improve construction are proposed. The LC-HPC decks were constructed in Kansas from 2005 to 2011 and are numbered in the order they were let, designated as LC-HPC-1 through LC-HPC-13 and LC-HPC-15 through LC-HPC-17. Another deck that was bid as the fourteenth LC-HPC deck but not constructed following the LC-HPC specifications, designated as "OP Bridge" (constructed in Overland Park, KS), is also described. Although representatives from the University of Kansas (KU) were not in attendance during the construction of the 11 control decks, data obtained by KDOT personnel are provided in this section. Control decks were selected for comparison with an LC-HPC deck. General descriptions are given for each LC-HPC and control deck. The LC-HPC decks are described in the order in which they were constructed, although decks constructed within a single contract are presented together. Concrete material information and construction details are described for each qualification batch and slab and LC-HPC bridge deck. Results of the plastic concrete testing for each truckload tested are provided in Appendix E. Detailed information regarding the mixtures as designed for the LC-HPC and control decks, including selected constituent proportions and aggregate designations, is also presented in Appendix E. Occasionally, modifications were made to the mixtures during construction – these modifications are explained in the descriptions of the decks. The bridge identification numbers, project let dates, construction dates, construction contractors, and ready-mix suppliers for the LC-HPC and control decks are provided in Table 5.4.

Table 5.4 Bridge construction information

Bridge Number	Project Let Date	Construction Date	Contractor	Concrete Supplier
LC-HPC-1 p1	9/15/2004	10/14/2005	Clarkson	Fordyce
LC-HPC-1 p2	9/15/2004	11/2/2005	Clarkson	Fordyce
LC-HPC-2	9/15/2005	9/13/2006	Clarkson	Fordyce
Control 1/2 p1	9/15/2004	10/10/2008	Clarkson	Fordyce
Control 1/2 p2	9/15/2005	10/28/2005	Clarkson	Fordyce
LC-HPC-3	8/17/2005	11/13/2007	Clarkson	Fordyce
Control 3	8/17/2005	7/17/2007	Clarkson	Fordyce
LC-HPC-4 p1	8/17/2005	9/29/2007	Clarkson	Fordyce
LC-HPC-4 p2	8/17/2005	10/2/2007	Clarkson	Fordyce
Control 4	8/17/2005	11/16/2007	Clarkson	Fordyce
LC-HPC-5	8/17/2005	11/14/2007	Clarkson	Fordyce
Control 5	8/17/2005	11/25/2007	Clarkson	Fordyce
LC-HPC-6	8/17/2005	11/3/2007	Clarkson	Fordyce
Control 6	8/17/2005	10/20/2008	Clarkson	Fordyce
LC-HPC-7	10/19/2005	6/24/2006	Capital	Concrete Supply of Topeka
Control 7 p1	8/17/2005	3/29/2006	Clarkson	Fordyce
Control 7 p2	8/17/2005	9/15/2006	Clarkson	Fordyce
LC-HPC-8	7/19/2006	10/13/2007	AM Cohron	O'Brien
Control 8/10	7/19/2006	4/6/2007	AM Cohron	O'Brien
LC-HPC-9	7/19/2006	4/15/2009	United	O'Brien
Control 9 p1	7/19/2006	5/21/2008	United	O'Brien
Control 9 p2	7/19/2006	5/29/2008	United	O'Brien
LC-HPC-10	7/19/2006	5/17/2007	AM Cohron	O'Brien
LC-HPC-11	8/16/2006	6/9/2007	King	Mid-America
Control 11	1/19/2005	3/28/2006	AM Cohron	Builders Choice
LC-HPC-12 p1	11/15/2006	4/4/2008	AM Cohron	Builders Choice
LC-HPC-12 p2	11/15/2006	3/18/2009	AM Cohron	Builders Choice
Control 12 p1	11/15/2006	4/1/2008	AM Cohron	Builders Choice
Control 12 p2	11/15/2006	4/14/2009	AM Cohron	Builders Choice
LC-HPC-13	1/17/2007	4/29/2008	Beachner	O'Brien
Control 13	1/17/2007	7/25/2008	Beachner	O'Brien
OP p1	3/26/2007	12/19/2007	Pyramid	Fordyce
OP p2	3/26/2007	5/2/2008	Pyramid	Fordyce
OP p3	3/26/2007	5/21/2008	Pyramid	Fordyce
LC-HPC-15	12/16/2009	11/10/2010	RA Knapp	Geiger
LC-HPC-16	12/16/2009	10/28/2010	RA Knapp	Geiger
LC-HPC-17	12/16/2009	9/28/2011	RA Knapp	Geiger

5.3.1 LC-HPC Bridge 1

The first LC-HPC bridge deck let and constructed in Kansas (designated as LC-HPC-1) is the eastbound deck along Parallel Parkway over I-635 in Kansas City, KS. The westbound deck along the same corridor is the associated control deck for both LC-HPC-1 and LC-HPC-2, is designated as Control 1/2 and discussed later. A single contract was awarded for the construction of LC-HPC-1, LC-HPC-2, and Control 1/2 to W. A. Ellis Construction, who then subcontracted construction of the bridges to Clarkson Construction. The ready-mix concrete for all three decks in the contract was provided by Fordyce Concrete. Parallel Parkway over I-635 includes two separate bridges, LC-HPC-1 and Control 1/2, acting as a single, connected roadway. To accommodate traffic capacity and roadway design requirements, the two bridges have smaller length-to-width ratios than most LC-HPC bridges. LC-HPC-1 has a width of 75.1 ft (22.9 m) and a length of 155.2 ft (47.3 m), with two 77.6-ft (23.7-m) spans. The bridge has steel girders, integral abutments, and was constructed at a 5 degree skew.

Construction of the LC-HPC-1 deck was completed in two full-length, partial-width placements with the first (south portion) and second (north portion) placements completed on October 14 and November 2, 2005, respectively. Placement 1 has a width of 36.3 ft (11.0 m), while Placement 2 has a width of 38.9 ft (11.9 m). Due to the traffic lane geometry, a large portion of the first placement does not handle traffic and the three eastbound traffic lanes are located entirely on the second placement.

5.3.1.1 Concrete

The concrete provided by Fordyce Concrete was designed for a cement content of 540 lb/yd^3 (320 kg/m^3) and a water-cement ratio of 0.45, resulting in a paste content of 24.6 percent. Several studies that were influential to the development of the LC-HPC specifications, including Schmitt and Darwin (1995, 1999) and Lindquist, Darwin, and Browning (2005), recommend a maximum paste

content of 27 percent for improved cracking performance. The concrete specifications required a cement content between 522 and 563 lb/yd^3 (310 and 334 kg/m^3) and a maximum water-cement ratio of 0.45. The aggregates consisted of three granite coarse aggregates and natural river sand as the fine aggregate.

5.3.1.2 Qualification Batch

A qualification batch was produced on June 20, 2005 with no KU personnel in attendance. In early versions of the specifications, this was called a "trial batch" but later changed to the more appropriate title of qualification batch. The concrete met the requirements for slump and air content, but did not meet the temperature requirement. No adjustments were made to control the concrete temperature, resulting in a temperature of 89° F (32° C), greatly exceeding the maximum specified value of 75° F (24° C). The qualification batch was accepted, even with the out-of-specification temperature, because it was decided that the concrete temperature could be controlled without difficulty during construction.

5.3.1.3 Qualification Slab

A first attempt at placing the qualification slab on July 12, 2005 reaffirmed the importance of an in-specification qualification batch. Like the qualification batch, the qualification slab was originally called a "trial slab." The approach taken by the concrete suppliers and contractors on the early decks led to the change in terminology, substituting "qualification" for "trial." The air temperatures on the date of the attempted placement were typical for that time of year in Kansas, ranging from 70° to 89° F (21° to 32° C) and exceeding 90° F (32° C) during the previous week. The concrete supplier attempted to control the temperature with chilled water, but was unsuccessful in reducing the temperature below 78° F (26° C). The placement was cancelled after two truckloads were rejected due to inadequate concrete temperatures. This incident may have been avoided had the concrete supplier been

required to resolve the problem with the high concrete temperature during the qualification batch.

The qualification slab was successfully completed on the second attempt on September 8, 2005. The slab was placed using a conveyor belt with a drop height of approximately 15 ft (4.6 m). The concrete temperature was controlled with chilled water, sustaining a maximum temperature of 71° F (22° C). Plastic concrete properties were tested at the truck discharge and were within the specifications with an average slump of 3.0 in. (75 mm) and an average air content of 8.4 percent. Finishing was completed with a single-drum roller screed (Figure 5.1) followed by a metal pan drag and occasional use of a bullfloat. Three work bridges and a finishing equipment bridge were used for finishing and burlap placement. A fogging system consisted of both machine-mounted and hand-held equipment. Wet burlap placement was generally slow, with an average placement time of 21 minutes after concrete strikeoff. The LC-HPC specification requires that wet burlap be placed over the concrete within 10 minutes of strikeoff.

After completion of the qualification slab, the contractor felt that the concrete could be pumped for the actual bridge deck placement. On September, 30, 2005, approximately two weeks before bridge deck construction, the contractor successfully pumped 1 yd^3 (0.75 m^3) of the mixture to be used in the deck. The LC-HPC specifications for construction of LC-HPC-1 stated that placement by pumping would only be allowed with prior approval from KDOT. Pumping was allowed by KDOT because the contractor displayed the ability to pump the concrete. The current LC-HPC specifications require the contractor to demonstrate the ability to pump the approved concrete during construction of the qualification slab using the same pump as will be used on the deck placement. Placement by pump may also be approved by the Engineer contingent on successful placement of the approved mixture with the

Figure 5.1 Single-drum roller screed – LC-HPC-1 qualification slab

same pump that will be used for the deck placement, at least 15 days prior to the construction of the deck.

5.3.1.4 LC-HPC-1 Placement 1

The first placement for LC-HPC-1 began at the east abutment and was completed between 6:30 and 9:30 a.m. on October 14, 2005. No measures were taken to control the concrete temperature due to an air temperature range of 52° to 59° F (11° to 15° C) during construction. Concrete temperatures were maintained within a range of 61° to 72° F (16° to 22° C) during placement. Plastic concrete tests were completed at the pump discharge, with the exception of the first truck, which was tested at the truck discharge. A bladder valve was used to minimize air losses, although no determination was made for slump and air losses through the pump. Test results indicated that slump measurements ranged from 2.5 to 6.5 in. (65 to 165 mm) with an average of 3.75 in. (95 mm). Air contents ranged from 6.0 to 11.5 percent with an average of 7.9 percent. A single, out-of-specification truckload with a slump of 6.5 in. (165 mm) and an air content of 11.5 percent was placed in the deck approximately 50 ft (15 m) from the east abutment. Crack surveys, discussed later in Section 6.2.1, indicated that the placement of this out-of-specification concrete did

not appear to increase cracking in this region. The specifications for construction of LC-HPC-1 required a slump range of 1.5 to 3.0 in. (35 to 75 mm) with a maximum allowable slump of 4.0 in. (100 mm) to provide leeway for the contractor to minimize construction delays. Seven of the eight slump measurements taken (88 percent) were greater than the required 3.0 in. (75 mm) maximum slump. Five of the eight slump readings (63 percent) were greater than 3.5 in. (90 mm) and one of the eight slump measurements (13 percent) exceeded the maximum allowable slump of 4.0 in. (100 mm). This trend has been common on many LC-HPC bridge decks and shows the tendency of the contractor to use concrete near the maximum allowable slump. The average 28-day concrete compressive strengths of lab and field-cured cylinders were 5210 and 4900 psi (35.9 and 33.8 MPa), respectively. The initial LC-HPC specifications did not include a maximum allowable strength, but subsequent specification revisions limit strength to 5500 psi. The concrete test results for Placement 1 are summarized in Table 5.5.

Pumping of Placement 1 was completed efficiently with no major problems. Slight delays during finishing occurred early on when the metal pan drag tore portions of the concrete surface, requiring additional bullfloating. The pan drag was removed approximately 50 ft (15.2 m) into the placement and finishing was completed with a single-drum roller screed and bullfloat. A fogging system consisting of two spray nozzles was mounted to a platform on the screed. The nozzles provided a mist into the air, but also resulted in water droplets accumulating on the deck surface. The droplets were worked into the concrete surface during bullfloating. As a result, it was decided that future fogging should be completed after bullfloating.

The placement of burlap was slowed primarily due to excess bullfloating. Bullfloating was completed from a work bridge that followed the screed, while the burlap was placed from two additional work bridges that followed the bullfloating

Table 5.5 Concrete test results† – LC-HPC-1 Placement 1

KU Bridge Number	Slump	Air Content	Unit Weight	Concrete Temperature	28-Day Compressive Strength
LC-HPC-1 Placement 1	in. (mm)	%	lb/ft^3 (kg/m^3)	° F (° C)	psi (MPa)
Average	3.75 (95)	7.9	140.5 (2251)	67 (20)	5210 (35.9)*
Minimum	2.50 (65)	6.0	136.6 (2188)	61 (16)	4900 (33.8)**
Maximum	6.50 (165)	11.5	142.1 (2276)	72 (22)	

Percentage of Slump Measurements			Percentage of Air Content Measurements	
≥ 3.0 in. (75 mm)	≥ 3.5 in. (90 mm)	≥ 4.0 in. (100 mm)	≤ 6.5%	≥ 9.5%
88%	63%	13%	0%	13%

* Lab-cured specimens
** Field-cured specimens
†Concrete tested at pump discharge

work bridge. The presence of the bullfloating work bridge caused a significant gap between screeding and burlap placement, and it appeared that the burlap could have been placed much more quickly if not for the additional space required for the bullfloating work bridge. Finishing procedures slowed considerably due to the removal of the metal pan drag. Burlap placement times ranged from 11 to 29 minutes after strikeoff, with an average placement time of 16 minutes. The specified 10-minute time limit for burlap placement after strikeoff was not met throughout construction. Placement of partially-dry burlap was discovered within the first quarter of deck. The contractor corrected the problem by spraying the dry burlap. As discussed later in Section 6.2.1, a grouping of map cracks have been observed in the first quarter of Placement 1, likely a result of plastic shrinkage cracking due to delays in curing, inadequate curing techniques, and overfinishing. Soaker hoses were placed on the deck immediately after the burlap placement. On occasion, the soaker hoses were placed before the concrete had set (Figure 5.2), resulting in indentions in the

Figure 5.2 Soaker hoses placed on burlap – LC-HPC-1 Placement 1

deck. It was discovered after curing that certain areas of the deck had not been kept completely wet by the soaker hoses. These dry areas were scattered throughout the deck, but were generally found near the west end. The evaporation rate remained below 0.2 lb/ft^2/hr throughout placement.

5.3.1.5 LC-HPC-1 Placement 2

The second placement for LC-HPC-1 was completed on November, 2, 2005, with construction between 7:15 and 10:30 a.m. As with Placement 1, concrete placement began at the east abutment. All concrete was sampled at the pump discharge and air losses through the pump were not determined. Slump ranged from 2.5 to 4.25 in. (65 to 110 mm) with an average of 3.25 in. (85 mm). As with Placement 1, the majority of slumps (60 percent) exceeded the upper specified limit of 3.0 in. (75 mm). All of the slumps that exceeded 3.0 in. (75 mm) also exceeded 3.5 in. (90 mm). A single truckload exceeded the maximum allowed slump of 4.0 in. (100 mm) with a value of 4.25 in. (110 mm). Air contents ranged from 3.0 to 9.0 percent with an average of 7.7 percent, with one truckload having an air content

below the specified range of 6.5 to 9.5 percent. Concrete temperatures ranged from 66° to 70° F (19° to 21° C) during construction with an average of 68° F (20° C). The average 28-day compressive strengths of lab and field-cured cylinders were 4980 and 4030 psi (34.4 and 27.8 MPa), respectively. The concrete test results for Placement 2 are summarized in Table 5.6.

Placement, consolidation, and finishing of Placement 2 were completed without any major problems. Fogging equipment was turned off after approximately 45 ft (13.7 m) of placement due to excess paste visible on the surface. Additional paste on the deck surface can lead to increased plastic shrinkage cracking. Crack surveys, discussed later in Section 6.2.1, have observed map cracks in Placement 2 – the type of cracking commonly associated with plastic shrinkage cracking. The fogging equipment was briefly turned on again for a 15-ft (4.6-m) section at 80 ft (24.4 m) from the east abutment as the contractor's attempt to deal with an increasingly rough finish. The contractor was directed to turn off the fogging equipment because the fogging water was worked into the deck with excess bullfloating, and it remained off for the rest of the construction. Placement 2 was given a smoother finish than Placement 1.

The experience gained from Placement 1 helped the contractors more efficiently place the burlap on Placement 2. Unlike on Placement 1, the first and second work bridges, directly following the screed, were used for burlap placement (Figure 5.3). The workers were able to place the burlap approximately 10 ft (3 m) behind the screed. The time to burlap placement ranged from 7 to 17 minutes after strikeoff, with an average of 11 minutes. The burlap was placed more efficiently as construction progressed. Any delays in burlap placement were the result of the use of hand vibration or the removal of equipment near the abutments. Soaker hoses were not placed on the burlap-covered concrete before it had set because of the indentions

Table 5.6 Concrete test results† – LC-HPC-1 Placement 2

KU Bridge Number	Slump	Air Content	Unit Weight	Concrete Temperature	28-Day Compressive Strength
LC-HPC-1 Placement 2	in. (mm)	%	lb/ft^3 (kg/m^3)	° F (° C)	psi (MPa)
Average	3.25 (85)	7.8	139.7 (2238)	68 (20)	4980 (34.4)*
Minimum	2.50 (65)	3.0	136.9 (2193)	66 (19)	4030 (27.8)**
Maximum	4.25 (110)	9.0	146.9 (2354)	70 (21)	

Percentage of Slump Measurements			Percentage of Air Content Measurements	
≥ 3.0 in. (75 mm)	≥ 3.5 in. (90 mm)	≥ 4.0 in. (100 mm)	< 6.5%	> 9.5%
60%	60%	20%	10%	0%

* Lab-cured specimens
** Field-cured specimens
†Concrete tested at pump discharge

Figure 5.3 Burlap placement – LC-HPC-1 Placement 2

that were created on Placement 1 due to early placement of the hoses. The contractor instead used a garden hose with a spray nozzle to maintain the burlap in a wet condition, which worked well. The temperature dropped below freezing during days 13 and 14 of the curing period and no additional protection was used during this time. As with Placement 1, the evaporation rate remained below 0.2 lb/ft^2/hr throughout placement.

5.3.2 LC-HPC Bridge 2

The second LC-HPC bridge let in Kansas, LC-HPC-2, is the 34th Street bridge over I-635 in Kansas City, KS. As previously stated, a single contract was awarded for the construction of LC-HPC-1, LC-HPC-2, and Control 1/2 to W. A. Ellis Construction, who then subcontracted the work to Clarkson Construction. Although LC-HPC-2 was the second LC-HPC bridge let, it was the third LC-HPC deck constructed in Kansas. Construction of the bridge was completed on September 13, 2006.

The 34th Street bridge is a two-span, steel girder bridge with integral abutments and no skew. The bridge connects a residential neighborhood that was divided by construction of I-635 and carries a low volume of residential traffic. Construction was completed in a single placement. The bridge has two equal 87.6-ft (26.7-m) spans and a width of 40.0 ft (12.2 m), with a 34.1-ft (10.4-m) wide driving surface.

5.3.2.1 Concrete

As with LC-HPC-1, the concrete provided by Fordyce Concrete was designed for a cement content of 540 lb/yd^3 (320 kg/m^3) and a water-cement ratio of 0.45.

5.3.2.2 Qualification Batch

The qualification batch for LC-HPC-1 served as the qualification batch requirements for LC-HPC-2 since the same contractor, concrete supplier, and mixture design were used on both bridge decks.

5.3.2.3 Qualification Slab

The qualification slab for LC-HPC-2 was completed on May 24, 2006. Due to high air temperatures during placement, in the range of 70° to 91° F (21° to 33° C), chilled water and ice were used to control the concrete temperature. The evaporation rate remained low (0.02 lb/ft^2/hr), even with the high air temperatures. The concrete producer did not initially account for the contribution of the ice to the water content, and the first truckload of concrete was rejected. Ice was accounted for in the water content of the following three truckloads, but these truckloads exhibited high slumps ranging from 4.0 to 5.5 in. (100 to 140 mm). The concrete air contents remained within the specifications with a range of 7.0 to 8.5 percent. The concrete temperatures ranged from 66° to 72° F (19° to 22° C), with an average of 70° F (21° C).

The same construction crew that placed LC-HPC-1 was used for the LC-HPC-2 qualification slab and deck. The entire qualification slab placement went smoothly, including pumping, placement, consolidation, and finishing. The concrete was finished with a single-drum roller screed and a bullfloat. No fogging was necessary during placement due to high humidity. The bullfloating was completed quickly after passage of the screed, likely with the help of the high concrete slump. Burlap placement was completed within 10 minutes of strikeoff throughout construction due to the experienced crew and rapid finishing. Burlap placed over the barrier reinforcement was not initially tucked in to cover the concrete near the reinforcing bars (Figure 5.4). The contractor was notified and all burlap was subsequently tucked in. Placement stopped approximately 3 ft (1 m) short of completion because the

Figure 5.4 Burlap improperly tucked near barrier reinforcement – LC-HPC-2 qualification slab

contractor ran out of concrete. At this point, the concrete plant had begun to produce a different mixture and could not supply the concrete necessary to complete the slab.

5.3.2.4 LC-HPC-2 Placement

Deck construction of LC-HPC-2 was completed in a single placement on September 13, 2006. Placement took place between 6:00 a.m. and 9:30 a.m., beginning at the east abutment. Air temperatures during placement ranged from 56° to 70° F (13° to 21° C). Chilled water and ice replaced a portion of the mixture water to control the concrete temperature. As with LC-HPC-1, a bladder valve was used at the pump discharge to limit air loss. Concrete samples were taken from the pump discharge for testing. Improper testing procedures were followed throughout the construction, including incomplete consolidation, jerking of the cone prior to lift, tilting of the slump cone during lift, and disposal of concrete samples into the deck prior to placement. The final three truckloads were not tested and several truckloads were not retested after re-mixing with added water-reducer. Halfway through placement, the visual inspection of two truckloads indicated concrete with

approximately a 6.0 in. (150 mm) slump was placed in the deck. Crack survey results, described in Section 6.2.2, indicate that long, transverse cracks have been formed at the approximate location of this high-slump concrete.

Slump test results indicated that all concrete remained within the specification requirements, ranging from 1.5 to 4.0 in. (35 to 110 mm) with an average of 3.0 in. (75 mm). A majority of the recorded slumps (71 percent) exceeded 3.0 in. (75 mm), 29 percent equaled or exceeded 3.5 in. (90 mm), and 14 percent were equal to 4.0 in. (100 mm). The air contents ranged from 7.0 to 8.5 percent with an average of 7.7 percent. The concrete temperature ranged from 61° to 69° F (16° to 21° C) with an average of 67° F (19° C). The average 28-day compressive strengths of lab and field-cured cylinders were 4600 and 4450 psi (31.7 and 30.7 MPa), respectively. The concrete test results are summarized in Table 5.7.

The experienced construction crew placed the deck with no major problems. At times, concrete with a slump as low as 1.5 in. (35 mm) was pumped and placed without problem. As with LC-HPC-1, finishing was completed with a single-drum roller screed followed by bullfloating. Portions of the deck near protruding barrier reinforcing bars were consolidated with hand vibrators (Figure 5.5). The concrete became stiffer approximately two-thirds through the placement, requiring the contractor to increase bullfloating to attain a smooth surface. The contractor began spraying water on the surface about 15 ft (4.6 m) before deck completion to aid in finishing (Figure 5.6), but was forced to stop this action immediately. Crack survey results, described in Section 6.2.2, suggest that this additional water did not contribute to cracking. Fogging was not needed during placement due to low evaporation rates. Delays in finishing occurred on two occasions due to a lack of concrete. Another delay occurred as the concrete pump was repositioned to the opposite side of the bridge.

Table 5.7 Concrete test results† – LC-HPC-2

KU Bridge Number	Slump	Air Content	Unit Weight	Concrete Temperature	28-Day Compressive Strength
LC-HPC-2	in. (mm)	%	lb/ft^3 (kg/m^3)	° F (° C)	psi (MPa)
Average	3.0 (75)	7.7	Not Obtained	67 (19)	4600 (31.7)*
Minimum	1.5 (35)	7.0	Not Obtained	61 (16)	4450 (30.7)**
Maximum	4.0 (100)	8.5	Not Obtained	69 (21)	

Percentage of Slump Measurements			Percentage of Air Content Measurements	
≥ 3.0 in. (75 mm)	≥ 3.5 in. (90 mm)	≥ 4.0 in. (100 mm)	< 6.5%	> 9.5%
71%	29%	14%	0%	0%

* Lab-cured specimens
** Field-cured specimens
†Concrete tested from pump discharge and improper testing procedures were followed throughout construction

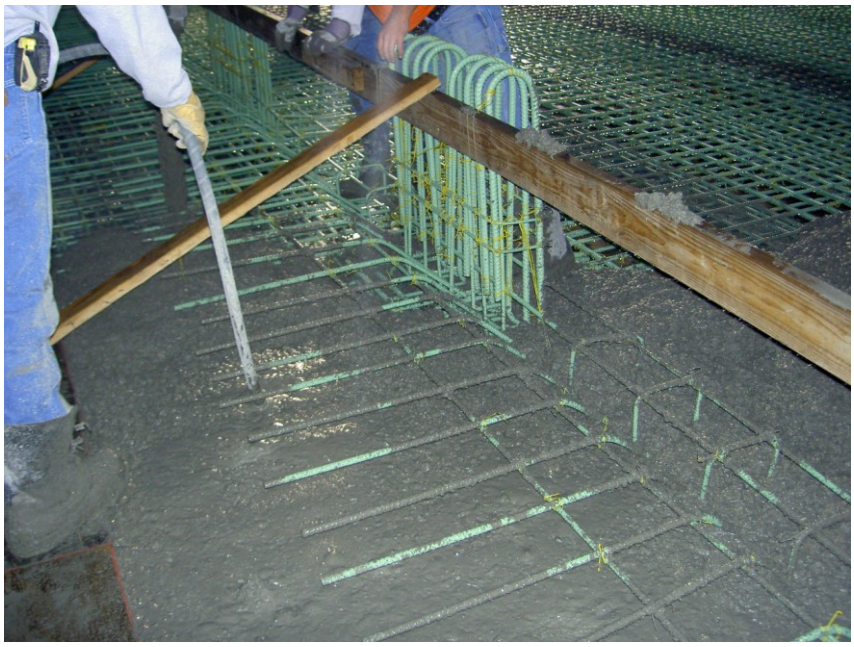

Figure 5.5 Hand-vibration near reinforcement bars – LC-HPC-2

Figure 5.6 Contractor used sprayed water as a finishing aide – LC-HPC-2

The placement of burlap was slow, ranging from 10 to 28 minutes with an average placement time of 15 minutes. Dry spots were observed as the burlap was laid out on a work bridge and soaker hoses were used for rewetting. As with the qualification slab, the burlap was not adequately tucked in near the barrier reinforcement, leaving a portion of concrete uncovered. The contractor was required to correct this problem.

5.3.3 Control Bridge 1/2

Control 1/2 is the westbound bridge along Parallel Parkway over I-635 in Kansas City, KS and is the control deck for LC-HPC-1 and LC-HPC-2. LC-HPC-1 and Control 1/2 are separate structures, but together make up the Parallel Parkway bridge over I-635. Like LC-HPC-1 and LC-HPC-2, Control 1/2 was constructed by Clarkson Construction. The same concrete supplier was also used. Control 1/2 was constructed per Kansas Department of Transportation (KDOT) standard bridge

specifications. It is a steel girder bridge with a skew of 5 degrees, integral abutments, two equal spans of 77.6 ft (23.7 m), and a width of 66.8 ft (20.4 m).

Control 1/2 was constructed in four phases, including two subdecks and two overlays that contained silica fume, hereafter referred to as silica fume overlays (SFO). The placement dates are shown in Table 5.8. The first subdeck and overlay were placed along the north edge of the deck and are designated as Placement 1. Similar to LC-HPC-1 Placement 1, the lane geometry of Control 1/2 results in a large portion of the first (north) placement that does not handle traffic. The second subdeck and overlay (designated as Placement 2) were located directly south of Control 1/2 Placement 1 and adjoin with the north edge of LC-HPC-1 Placement 2. The majority of westbound traffic along Parallel Parkway travels on Control 1/2 Placement 2.

5.3.3.1 Concrete

The subdeck and overlay concrete mixtures for Control 1/2 were designed per KDOT standard specifications. Concrete mixture designs for each subdeck and overlay are summarized in Table 5.8. Both subdecks of Control 1/2 had a higher cement content, 602 lb/yd^3 (357 kg/m^3) for Placement 1 and 605 lb/yd^3 (359 kg/m^3) for Placement 2, and a lower water-cement ratio, 0.40, than LC-HPC-1 and 2, which had 540 lb/yd^3 (320 kg/m^3) of cement and a 0.45 water-cement ratio. Both Control 1/2 subdecks also had a higher cement paste content, 25.6 percent for Placement 1 and 25.7 percent for Placement 2, than LC-HPC-1 and 2, which had a paste content of 24.6 percent. A limestone coarse aggregate was used in the subdeck concrete, while a granite coarse aggregate was used in the LC-HPC decks. The silica fume overlay concrete included a 7 percent replacement of cement by weight with silica fume, a 627 lb/yd^3 (372 kg/m^3) cementitious material content, a water-cementitious material ratio (*w/cm*) of 0.37, a paste content of 26.0 percent, and a granite coarse aggregate.

Table 5.8 Placement dates and concrete mixture information – Control 1/2

Placement Designation	Deck Section	Placement Date	Cement Content	Water Content	Silica Fume Content	*w/cm**	Paste Content	Design Air Content	Coarse Agg. Type
			lb/yd^3 (kg/m^3)	lb/yd^3 (kg/m^3)	lb/yd^3 (kg/m^3)		%	%	
Placement 1	North Subdeck	9/30/2005	602 (357)	241 (143)	-	0.40	25.6%	6.5%	Limestone
	North Overlay	10/10/2005	583 (346)	233 (138)	44 (26)	0.37	26.0%	6.5%	Granite
Placement 2	South Subdeck	10/18/2005	605 (359)	241 (143)	-	0.40	25.7%	6.5%	Limestone
	South Overlay	10/28/2005	583 (346)	233 (138)	44 (26)	0.37	26.0%	6.5%	Granite

* *w/cm* = water-cementitious material ratio

5.3.3.2 Control 1/2 Placement

Construction of Control 1/2 was not observed by KU personnel. Concrete properties were recorded by KDOT personnel and are presented in Table 5.9. Concrete for the control placements, particularly the overlay concrete, generally had higher slump, lower air content, and higher compressive strength than LC-HPC decks 1 and 2. The average slumps for the two subdeck placements [4.25 and 3.25 in. (110 and 80 mm), respectively] were lower than for most other control subdecks. The two subdecks had average air contents of 5.3 and 6.5 percent and average 28-day compressive strengths of 5670 and 5090 psi (39.1 and 35.1 MPa), respectively. Concrete for the two SFO placements had average slumps of 5.0 and 4.5 in. (125 and 115 mm), average air contents of 5.5 and 7.0 percent, and average compressive strengths of 5810 and 8060 psi (40.1 and 55.6 MPa), respectively.

5.3.4 LC-HPC Bridge 7

The second LC-HPC bridge constructed and seventh let in Kansas, designated as LC-HPC-7, is located along County Road 150 over US-75 in Jackson County. The contract was awarded to Koss Construction, who then subcontracted bridge construction to Capital Construction. The deck was constructed in a single placement on June 24, 2006. LC-HPC-7 is a steel plate-girder bridge with two equal spans of

Table 5.9 Concrete test results – Control 1/2

Placement Designation	Deck Section	Average Slump	Average Air Content	Average Unit Weight	Average Concrete Temperature	Average 28-Day Compressive Strength
		in. (mm)	%	lb/ft^3 (kg/m^3)	° F (° C)	psi (MPa)
Placement 1	North Subdeck	4.25 (110)	5.3	144.7 (2318)	66 (19)	5670 (39.1)
	North Overlay	5.00 (125)	5.5	142.4 (2281)	64 (18)	5810 (40.1)
Placement 2	South Subdeck	3.25 (80)	6.5	142.4 (2274)	76 (25)	5090 (35.1)
	South Overlay	4.50 (115)	7.0	140.7 (2254)	68 (20)	8060 (55.6)

139.4 ft (42.5 m), a width of 52.2 ft (15.9 m), integral abutments and no skew. The bridge is located in a rural area north of Topeka and carries low traffic volumes.

5.3.4.1 Concrete

The concrete for LC-HPC-7 was provided by Concrete Supply of Topeka and was based on the mixture design from LC-HPC-1 and 2 with minor differences. As with LC-HPC-1 and 2, a cement content of 540 lb/yd^3 (320 kg/m^3) and water-cement ratio of 0.45 (corresponding to a paste content of 24.6 percent) were used in the qualification batch and deck. The concrete supplier varied the water-cement ratio of the qualification slab from 0.45, 0.43, and 0.41 to provide flexibility on the job site if additional water was needed for slump adjustments. Two granite coarse aggregates were included in the mixture design, deviating from the three granite coarse aggregates used in LC-HPC-1 and 2. Unlike LC-HPC-1 and 2, a water reducer was not required to attain slumps within the LC-HPC specified range.

5.3.4.2 Qualification Batch

The qualification batch for LC-HPC-7 was produced on May 31, 2006 at the plant of the concrete supplier in Topeka, KS with KU and KDOT personnel in attendance. The concrete supplier used the qualification batch to both practice and qualify the mixture and did not attempt any trial batches prior to the qualification

batch. Three batches were necessary for the mixture to meet specifications and be qualified. A partial replacement of water with ice was necessary for the qualification batch to meet the temperature requirements. The concrete met specifications with a slump of 3.75 in. (95 mm), an air content of 6.5 percent, and a concrete temperature of 73° F (23° C).

5.3.4.3 Qualification Slab

The qualification slab for LC-HPC-7 was completed on June 8, 2006 per the specifications, but with a number of delivery delays. Delays resulted from modifications to the water-cement ratio by the concrete supplier on two occasions (0.45 to 0.41, then to 0.43) to provide flexibility on the job site if additional water was needed for slump adjustments. It was determined that there was little benefit in qualifying a mixture that had a varying water-cement ratio and this practice was prohibited in future revisions to the specifications. Additional delays were blamed on insufficient ice available at the mixing plant. The delivery delays caused subsequent delays in concrete placement, finishing, and burlap placement. The slumps met the specifications, ranging from 2.0 to 3.25 in. (50 to 85 mm) with an average of 2.75 in. (70 mm). The air contents also remained within the specifications, ranging from 8.0 to 9.0 percent with an average of 8.5 percent. An "S-Hook" apparatus was attached at the pump discharge to minimize air losses and a test verified a 1.0 percent loss in air from pumping. Full concrete temperature records are unavailable, but the first two truckloads had temperatures of 68° and 75° F (20° and 24° C), respectively.

Finishing was completed with a double-drum roller screed with one roller removed, followed by a metal pan drag. The contractor had difficulty finishing portions of the deck due to the delivery delays. A single work bridge was used for burlap placement, slowing the placement process. The contractor was advised to use two bridges for burlap placement during the deck construction. Fogging nozzles were initially attached to the finishing bridge near the drum roller, spraying water on the

unfinished concrete. The drum roller then worked the sprayed water into the concrete. The contractor was notified of the issue and the fogging system was relocated behind the pan drag (Figure 5.7).

The lack of preparation of the concrete supplier and contractor was evident throughout the trial batch and slab process. The use of the trial batch and slab as a means of practice was unique to this bridge at that time. These observations from the trial batch and slab prompted the replacement of the terms "trial batch" and "trial slab" with "qualification batch" and "qualification slab" to reinforce the importance of qualifying the mixture and construction process by adhering to the specifications.

5.3.4.4 LC-HPC-7 Placement

LC-HPC-7 was constructed in a single placement on June 24, 2006 by pumping. Placement was conducted from east to west, beginning at 2:00 a.m. and lasting for approximately 6.5 hours. A water-cement ratio of 0.45 was used throughout construction, matching the qualification batch. A portion of the mixture water was replaced with ice for concrete temperature control. All concrete samples were taken at the pump discharge other than the first four truckloads. Plastic concrete properties are shown in Table 5.10. Concrete slump remained consistently high during construction, ranging from 2.25 to 6.0 in. (55 to 150 mm) with an average of 3.75 in. (95 mm). The majority of the measured slumps (61 percent) exceeded 3.5 in. (75 mm) and 52 percent of the values exceeded the maximum allowable value of 4.0 in. (100 mm). The air contents ranged from 6.5 to 10.5 percent with an average of 8.0 percent. A single measured air content of 10.5 percent exceeded the specified range of 6.5 to 9.5 percent. The concrete temperatures remained within the specifications, ranging from 68° to 75° F (20° to 24° C) with an average of 71° F (22° C). The average compressive strength of lab-cured cylinders at 31 days was 3790 psi (26.1 MPa), the lowest of any LC-HPC deck.

Figure 5.7 Fogging system placed on pan drag – LC-HPC-7 qualification slab

Table 5.10 Concrete test results† – LC-HPC-7

KU Bridge Number	Slump	Air Content	Unit Weight	Concrete Temperature	31-Day Compressive Strength*
LC-HPC-7	in. (mm)	%	lb/ft^3 (kg/m^3)	° F (° C)	psi (MPa)
Average	3.75 (95)	8.0	138.6 (2221)	71 (22)	3790 (26.1)
Minimum	2.25 (55)	6.5	134.1 (2148)	68 (20)	
Maximum	6.00 (150)	10.5	143.1 (2292)	75 (24)	

Percentage of Slump Measurements			Percentage of Air Content Measurements	
≥ 3.0 in. (75 mm)	≥ 3.5 in. (90 mm)	≥ 4.0 in. (100 mm)	≤ 6.5%	> 9.5%
61%	61%	52%	14%	7%

* Lab-cured specimens, no data obtained for field-cured specimens
†Concrete tested at pump discharge. Trucks 1-4 tested prior to pumping.

The concrete was finished with a double-drum roller screed with one roller removed, followed by a pan drag and burlap drag attached behind the roller screed. Bullfloating was used for additional finishing. The fogging system consisted of plastic nozzles connected to plastic piping and was required to be turned off due to leaking problems. No fogging system was used for the remainder of the placement. Burlap placement was slow throughout construction and was completed by a different crew than was used on the trial slab. The burlap was pre-rolled and often became twisted during placement. The presoaked burlap became heavy for the workers to unroll on the work bridge. The rate of burlap placement slowed as the six workers became fatigued during construction. A delay at the end of construction due to backordered concrete left approximately 15 to 20 ft (4.6 to 6.1 m) of finished concrete exposed near the west abutment for about 1 hour and 15 minutes. Crack survey results discussed later in Section 6.2.5 show an increased incidence of cracking near the west abutment at the location of this exposed concrete.

After burlap placement, lawn sprinklers and garden hoses were used to maintain the wet burlap. The burlap was kept adequately wet, but the process resulted in excess water running off the side of the deck (Figure 5.8). This became a problem due to potential damage of the deck and because the roadway below was open to traffic during construction. The contractor was instructed to stop use of the sprinklers and use only the garden hoses to wet the burlap.

5.3.5 Control Bridge 7

Control 7 is the northbound bridge on Antioch Road over I-435 in Overland Park, KS. The bridge is a two-span, steel girder bridge with integral abutments and a three degree skew. Control 7 is 192.9 ft (58.8 m) long and 51.2 ft (15.6 m) wide with span lengths of 89.9 and 103.0 ft (27.4 and 31.4 m). The bridge was constructed by Clarkson Construction Company in four phases, consisting of two subdecks and two silica fume overlays. The placement dates are shown in Table 5.11. The subdeck and

Figure 5.8 Water runoff due to over-wetting of the burlap – LC-HPC-7

Table 5.11 Placement dates and concrete mixture information – Control 7

Placement Designation	Deck Section	Placement Date	Cement Content	Water Content	Silica Fume Content	Class F Fly Ash Content	*w/cm**	Paste Content	Design Air Content	Coarse Agg. Type
			lb/yd^3 (kg/m^3)	lb/yd^3 (kg/m^3)	lb/yd^3 (kg/m^3)	lb/yd^3 (kg/m^3)		%	%	
Placement 1	East Subdeck	3/15/2006	536 (318)	268 (159)	-	133 (79)	0.40	29.0%	6.5%	Granite
	East Overlay	3/29/2006	583 (346)	233 (138)	44 (26)	-	0.37	26.0%	6.5%	Granite
Placement 2	West Subdeck	8/16/2006	536 (318)	268 (159)	-	133 (79)	0.40	29.0%	6.5%	Granite
	West Overlay	9/15/2006	583 (346)	233 (138)	44 (26)	-	0.37	26.0%	6.5%	Granite

* *w/cm* = water-cementitious material ratio

overlay on the east portion (designated as Placement 1) were constructed on March 15 and 29, 2006, respectively, while the subdeck and overlay on the west portion (designated as Placement 2) were constructed, respectively, on August 16 and September 15, 2006. The bridge construction was completed in two stages. The first stage included the eastern, northbound section with a width of 43.0 ft (13.1 m). A majority of the second stage included the western, southbound section that is not included in this study. A small portion of the second stage of construction, approximately 19.0 ft (5.8 m) of deck width, is included in this study.

5.3.5.1 Concrete

The subdeck and overlay concrete mixtures for Control 7 were designed per KDOT standard specifications and meet the material requirements of the Kansas City Metro Materials Board. The mixture information for each subdeck and overlay are shown in Table 5.11. The subdeck consisted of a binary mixture with a 20 percent replacement by weight of cement with Class F fly ash, a 667 lb yd^3 cementitious material content, and a 0.40 water-cementitious material ratio (*w/cm*). The cementitious material content was higher and the water-cementitious material ratio was lower than permitted by the LC-HPC specifications. The silica fume overlay concrete included a 7 percent replacement by weight of cement with silica fume, a 626 lb/yd^3 cementitious material content, and a 0.37 water-cementitious material ratio. A granite coarse aggregate was used in both the subdeck and overlay.

5.3.5.2 Control 7 Placement

Concrete properties were recorded by KDOT personnel and are presented in Table 5.12. The recorded slumps were significantly high throughout construction, all above 7.0 in. (180 mm). The average air contents for the four placements ranged from 5.9 to 7.4 percent. The average 28-day compressive strengths for the east and west subdecks (Placements 1 and 2) were 5540 and 5500 psi (38.2 and 37.9 MPa), respectively, while the compressive strength for the west overlay (Placement 2) was 7370 psi (50.8 MPa). Compressive strength was not measured for the overlay of Placement 1. Following construction of the second subdeck, the truck supplying curing water ran out of water overnight and the burlap was found to be dry the next morning.

5.3.6 LC-HPC Bridge 10

LC-HPC-10 was the fourth LC-HPC deck constructed and seventh let in Kansas and, along with LC-HPC-8, is one of two LC-HPC decks constructed on prestressed

Table 5.12 Concrete test results – Control 7

Placement Designation	Deck Section	Average Slump	Average Air Content	Average Unit Weight	Average Concrete Temperature	Average 28-Day Compressive Strength
		in. (mm)	%	lb/ft^3 (kg/m^3)	° F (° C)	psi (MPa)
Placement 1	East Subdeck	9.25 (235)	5.9	139.8 (2239)	80 (27)	5540 (38.2)
	East Overlay	7.50 (190)	7.4	139.8 (2239)	73 (23)	not obtained
Placement 2	West Subdeck	7.75 (195)	7.3	139.0 (2226)	70 (21)	5500 (37.9)
	West Overlay	7.00 (180)	6.4	140.6 (2252)	64 (18)	7370 (50.8)

girders. A single contract was awarded to Koss Construction for the construction of LC-HPC-8, 9, and 10. The construction of LC-HPC-8 and LC-HPC-10 was then subcontracted to A. M. Cohron Construction. LC-HPC-10 is located on E 1800 Rd over US-69 in Linn County, KS. It is a precast-prestressed concrete girder bridge with integral abutments, and a 21 degree skew. The bridge is 36.1 ft (11.0 m) wide and 335.0 ft (102.1 m) long with four spans, 75.5, 97.8, 97.8, and 63.9 ft (23.0, 29.8, 29.8, and 19.5 m), respectively. The deck was constructed in a single placement on May, 17, 2007.

5.3.6.1 Concrete

The concrete was supplied by O'Brien Ready-Mix with use of a mobile ready-mix plant located 10.5 mi (16.9 km) from the bridge. LC-HPC-10 was the first deck cast under new specifications that required a lower paste content than the previously-constructed decks. The concrete had a cement content of 535 lb/yd^3 (317 kg/m^3) and a water-cement ratio of 0.42. The resulting paste content of 23.4 percent is lower than the 24.6 percent paste by volume contained in LC-HPC-1, 2, and 7. Two granite coarse aggregates were used.

5.3.6.2 Qualification Batch

The qualification batch for LC-HPC-10 and LC-HPC-8 was produced on April 11, 2007 at the mobile ready-mix plant. The batch met the requirements with a slump of 1.5 in. (40 mm), an air content of 8.6 percent, and a concrete temperature of 65° F (18° C). A total of 1.0 gal/yd^3 (5.0 L/m^3) of mixture water was withheld from the original mixture design to achieve the desired slump. The concrete supplier planned to continue to withhold this amount of mixture water and increase the water-reducer dosage for the qualification slab and deck placement. No measures were taken to control the concrete temperature due to a low air temperature of 47° F (8° C) during the qualification batch. The concrete supplier anticipated the need for a partial replacement of mixture water with ice during the deck placement.

5.3.6.3 Qualification Slab

The qualification slab for LC-HPC-10 was placed on April 26, 2007 at a farm with a 15 minute haul time. Four truckloads were needed and the placement was completed in approximately 1.75 hours. The delivery of the concrete was slow because each truck was initially tested at the batch plant. The concrete supplier did not batch new loads until the previous load was accepted at the slab. Water was withheld at the plant and added, as necessary, on site for slump adjustments. The concrete appeared to be more difficult to pump than previous LC-HPC mixtures, likely due to the reduced paste content. All concrete, except for the third truckload, met the specifications. The third truckload initially had a slump of 2.5 in. (65 mm), but the pump operator insisted that the concrete would not pump. The attempt to pump the concrete was not observed by KU personnel. Additional water reducer was added to the concrete, causing the slump to increase to 5.0 in. (125 mm). The air content and concrete temperature of the third truckload met the specifications. The average slump, air content, and temperature for the concrete were 3.5 in. (90 mm), 8.7 percent, and 70° F (21° C), respectively.

Consolidation was completed with use of a manually operated gang vibration system that included four hand vibrators mounted on a rolling frame. Hand vibration was used for the first 8 ft (2.4 m) of the slab. A single-drum roller screed and a pan drag were used to finish the slab. The slow concrete delivery ultimately slowed the placement, consolidation, finishing, and curing. During delays in concrete delivery, the screed continued to pass over already-finished areas of the slab. The roller screed passed over portions of the slab up to six times. The contractor was notified of this occurrence and the remainder of the slab was not overfinished.

The fogging equipment caused some accumulation of water on the surface and was turned off early in the placement. The wet burlap was rolled and became difficult for the contractors to handle on the narrow work bridges (Figure 5.9). Sections of the burlap did not overlap at all locations and thin strips of the slab were not covered. The contractor was notified and the exposed areas were covered. Due to the troubles with the burlap placement, the contractor decided to fold the burlap accordion-style and deliver the burlap to the deck with a crane during the deck placement.

5.3.6.4 LC-HPC-10 Placement

Construction of LC-HPC-10 was completed in a single placement on May 17, 2007 in a total of 9 hours. Placement began at the east abutment at 3:15 a.m. and was completed by 12:15 p.m. Adjustments to the water content were made on site for nearly every truck, resulting in concrete with water-cement ratios ranging from 0.40 to 0.42. This adjustment resulted in differences between the design and actual water-cement ratio and paste content for the concrete. The specifications allowed up to 2 gal/yd^3 (10 L/m^3) of mixture water to be withheld at the plant and added as needed.

All concrete was tested at the pump discharge. The concrete properties are provided in Table 5.13. The concrete slump values ranged from 1.75 to 5.0 in. (45 to 125 mm) with an average of 3.25 in. (80 mm). A majority of the recorded slumps (60

Figure 5.9 Contractors experienced difficulties placing folded burlap – LC-HPC-10 qualification slab

Table 5.13 Concrete test results† – LC-HPC-10

KU Bridge Number	Slump	Air Content	Unit Weight	Concrete Temperature	28-Day Compressive Strength
LC-HPC-10	**in. (mm)**	**%**	**lb/ft^3 (kg/m^3)**	**° F (° C)**	**psi (MPa)**
Average	3.25 (80)	7.5	138.1 (2212)	66 (19)	4580 (31.6)*
Minimum	1.75 (45)	6.1	134.2 (2149)	60 (16)	4580 (31.6)**
Maximum	5.0 (125)	9.2	142.1 (2276)	72 (22)	

Percentage of Slump Measurements			Percentage of Air Content Measurements	
≥ 3.0 in. (75 mm)	**≥ 3.5 in. (90 mm)**	**≥ 4.0 in. (100 mm)**	**≤ 6.5%**	**> 9.5%**
60%	33%	13%	20%	0%

* Lab-cured specimens
** Field-cured specimens
†Concrete tested at pump discharge

percent) exceeded 3.0 in. (75 mm), 33 percent were greater than or equal to 3.5 in. (90 mm), and 13 percent were greater than or equal to the maximum allowable slump of 4.0 in. (100 mm). This, again, displays the tendency of the concrete supplier to provide concrete with slumps near the upper allowable limit. The third truckload had a slump of 5.0 in. (125 mm) and was set aside, but was not retested before being placed in the deck. Crack survey results shown later in Section 6.2.8 suggest that this untested concrete did not affect cracking. Another truckload with a slump of 4.25 in. (110 mm) was placed in the deck.

The concrete supplier faced difficulty in meeting the air content requirements for the first three truckloads. The first two truckloads had air contents around 5 percent and the concrete was placed in the abutment. The third truckload that contained an air content of 11 percent was set aside and retested after 20 minutes. The retested air content decreased to 8.0 percent and the concrete was placed in the abutment. The air-entraining admixture dosage was adjusted and most of the subsequent truckloads had proper air contents, although two truckloads were placed in the deck with air contents below the requirements. Three of the truckloads that were placed in the deck (23 percent of those tested) had air contents below 7 percent. The concrete temperature throughout the placement ranged from 60° to 72° F (16° to 22° C) with an average of 66° F (20° C). The average 28-day compressive strength of both lab and field-cured cylinders was 4580 psi (31.6 MPa).

A single pump was used for placement. After placing the first 140 ft (43 m) from the west abutment, the pump was relocated to adequately reach the remaining deck, which delayed placement, finishing, and curing. Crack survey results, shown in Section 6.2.8, indicate that no increase in cracking is apparent at the location of the delay. The pump became clogged while placing the west pier cap and an unknown quantity of water was added to the hopper to clear the clog. The concrete with extra water was placed in the pier cap, not in the deck.

The concrete was finished with a single-drum roller screed, followed by a pan drag. Bullfloating was used only at the beginning of the placement. Burlap placement was slow, averaging 17 minutes after finishing. The slow burlap placement was the result of the slow progression of the screed/finishing bridge and a low number of workers placing the burlap. The burlap was soaked improperly by only a brief submersion (about 2 minutes) in a water tank. The improperly-soaked burlap dried out quickly and needed to be rewetted in less than 20 minutes after placement. The majority of the burlap was never properly rewetted after drying out. Figure 5.10 shows dry burlap near the east end of the deck. Crack survey results discussed later in Section 6.2.8 show no incidence of map cracking in LC-HPC-10, a type of cracking associated with the drying out of the concrete surface due to improper curing techniques. Leaking was observed in the fogging system attached to the finishing bridge and it was required to be shut off. Hand-fogging was used on occasion during delays, but was stopped when it was used as a finishing aide in the third pier cap.

5.3.7 LC-HPC Bridge 8

LC-HPC-8 was the second precast-prestressed concrete girder bridge constructed and was part of the same contract as LC-HPC-8, 9, and 10 awarded to Koss Construction. As with LC-HPC-10, the construction of LC-HPC-8 was subcontracted to A. M. Cohron Construction. LC-HPC-8 is located on E 1350 Road over US-69 in Linn County, KS, just south of LC-HPC-10. The prestressed concrete girder bridge has integral abutments and no skew. The bridge is 36.1 ft (11.0 m) wide and 303.0 ft (92.4 m) long with four spans of 60.3, 91.2, 91.2, and 60.3 ft (18.4, 27.8, 27.8, and 18.4 m), respectively. The deck was constructed in a single placement on October 3, 2007.

Figure 5.10 Dry burlap covering deck – LC-HPC-10

5.3.7.1 Concrete

O'Brien Ready-Mix supplied the concrete for LC-HPC-8 with use of the same mobile ready-mix plant as used for LC-HPC-10, located 5 mi (8 km) from the bridge. The same mixture was used for LC-HPC-8 and LC-HPC-10, with a cement content of 535 lb/yd^3 (317 kg/m^3) and a water-cement ratio of 0.42. Adjustments to the slump were made, if needed, by withholding a portion of the mixture water at the plant and adding it at the construction site.

5.3.7.2 Qualification Batch

The qualification batch provided for LC-HPC-10 also served as the qualification batch for LC-HPC-8.

5.3.7.3 Qualification Slab

A separate qualification slab was required for LC-HPC-8 as a result of the problems associated with the construction of LC-HPC-10. The qualification slab for

LC-HPC-8 was completed on September 26, 2007 at a location near the bridge. The concrete was placed with a pump and consolidated with the same gang vibration system as used for LC-HPC-10. Finishing was completed with a single-drum roller screed and metal pan drag, followed by bullfloating from a work bridge.

Similar issues were observed in the qualification slab as were observed in the construction of LC-HPC-10. The burlap was again observed to be dry and was required to be rewetted with a spray hose. The workers appeared to not know how to properly place the burlap, even though the supervisor said that they practiced the previous day. Large holes were observed in the burlap. The fogging system deposited excessive water onto the slab surface, which was then worked into the surface with a bullfloat (Figure 5.11). It was determined that the fogging system was working at a low pressure [400 psi (2.75 MPa)] that was unable to atomize the water. The contractor was required to pressurize the fogging system to 1000 psi (6.9 MPa) during the deck construction.

5.3.7.4 LC-HPC-8 Placement

Construction for LC-HPC-8 was completed in a single placement on October 3, 2007; one week after construction of the qualification slab. Placement began at the west abutment at 7:30 a.m. and was completed by 2:30 p.m. A portion of the mixture water was withheld to control the slump, causing the water-cement ratio to vary between 0.40 and 0.41. All concrete placed in the deck had water-cement ratios below that required in the LC-HPC specifications (0.42). Future revisions of the concrete specifications prohibit mixture water from being withheld from the mixture.

All tested concrete samples were taken at the pump discharge. The concrete properties are provided in Table 5.14. All tested truckloads met the requirements for slump, with values ranging from 1.0 to 3.0 in. (25 to 75 mm) with an average of 2.0 in. (50 mm). Air contents ranged from 5.7 to 10.2 percent with an average of 7.9 percent. Of the 23 tested truckloads, one had an air content below (5.7 percent) and

Figure 5.11 Fogging system deposited excessive water on slab – LC-HPC-8

Table 5.14 Concrete test results† – LC-HPC-8

KU Bridge Number	Slump	Air Content	Unit Weight	Concrete Temperature	28-Day Compressive Strength
LC-HPC-8	**in. (mm)**	**%**	**lb/ft^3 (kg/m^3)**	**° F (° C)**	**psi (MPa)**
Average	2.0 (50)	7.9	141.2 (2264)	67 (20)	4590 (31.7)*
Minimum	1.0 (25)	5.7	137.0 (2194)	59 (15)	4340 (29.9)**
Maximum	3.0 (75)	10.2	144.9 (2321)	73 (23)	

Percentage of Slump Measurements			Percentage of Air Content Measurements	
> 3.0 in. (75 mm)	**≥ 3.5 in. (90 mm)**	**≥ 4.0 in. (100 mm)**	**< 6.5%**	**> 9.5%**
0%	0%	0%	7%	11%

* Lab-cured specimens
** Field-cured specimens
†Concrete tested at pump discharge

two had air contents above (9.7 and 10.2 percent) the range permitted in the LC-HPC specifications (6.5 to 9.5 percent). Concrete temperatures ranged from 59° to 73° F (15° to 23° C), with an average of 67° F (19° C). A portion of the mixture water was replaced with ice to control the concrete temperature. The average 28-day compressive strengths of lab and field-cured cylinders were 4590 and 4340 psi (31.7 and 29.9 MPa), respectively.

The placement of LC-HPC-8 went very well. This deck was the fourth LC-HPC placement completed by the contractor. The requirement of the second qualification slab for this contract helped the contractor understand the problems that occurred during the previous placements. Minimal delays in concrete delivery occurred during placement due to traffic control on the construction zone.

The concrete was placed using two pumps positioned at opposite ends of the deck to eliminate delays caused by repositioning. The concrete finished well with a single-drum roller screed followed by a metal pan drag. Bullfloating was used on rare occasions. Burlap was placed efficiently throughout construction with an average placement time of 12 minutes. A hand-held spray hose was used to keep the burlap wet throughout placement. The burlap was placed by a crew of five workers and one supervisor. The addition of a supervisor was beneficial in improving the burlap placement process.

Fogging was seldom needed since the burlap placement was completed relatively quickly. The fogging system was pressurized to 1050 psi (724 MPa) and was effective in creating a mist without depositing water on the surface. Fogging was only used near the end of the placement during a delay in concrete delivery. Crack survey results shown later in Section 6.2.9 have identified a number of longitudinal cracks extending from the east abutment, the portion of the deck that was exposed during the delivery delay.

5.3.8 Control Bridge 8/10

Control 8/10 is located on K-52 over US-69 in Linn County, KS and acts as the control deck for LC-HPC-8 and 10. The deck is monolithic and constructed on prestressed concrete girders. Control 8/10 was let in the same contract as LC-HPC-8, 9, and 10. Control 8/10 was subcontracted to A. M. Cohron Construction.

The bridge has four spans, with lengths of 72.2, 91.2, 91.2, and 60.7 ft (22.0, 27.8, 27.8, and 18.5 m), and is 75.1 ft (22.9 m) wide. The prestressed concrete girder bridge has integral abutments and no skew. The deck was constructed in a single phase on April 16, 2007.

5.3.8.1 Concrete

The concrete mixture design met the KDOT specifications for this type of structure. The monolithic deck had a cement content of 612 lb/yd^3 (363 kg/m^3) and a water-cement ratio (*w/c*) of 0.40. Limestone was used as the coarse aggregate. The concrete mixture information is shown in Table 5.15.

5.3.8.2 Control 8/10 Placement

The placement was not observed by KU personnel. Concrete properties were recorded by KDOT personnel and are presented in Table 5.16. The concrete had an average slump of 5.25 in. (135 mm), an average air content of 7.4 percent, and an average temperature of 70° F (21° C). The average 28-day compressive strength was 4830 psi (33.3 MPa). The concrete was placed with a pump and construction lasted approximately seven hours.

5.3.9 LC-HPC Bridge 11

LC-HPC-11 is the eastbound bridge on US-50 over the K&O railroad in Hutchinson, KS. The contract was awarded to Koss Construction with the bridge subcontracted to King Construction. The westbound bridge at the same location was

Table 5.15 Placement date and concrete mixture information – Control 8/10

Placement Date	Cement Content	Water Content	Silica Fume Content	Class F Fly Ash Content	*w/c*	Paste Content	Design Air Content	Coarse Agg. Type
	lb/yd^3 (kg/m^3)	lb/yd^3 (kg/m^3)	lb/yd^3 (kg/m^3)	lb/yd^3 (kg/m^3)		%	%	
4/16/2007	612 (363)	244 (145)	-	-	0.40	26.0%	6.5%	Limestone

Table 5.16 Concrete test results – Control 8/10

Average Slump	Average Air Content	Average Unit Weight	Average Concrete Temperature	Average 28-Day Compressive Strength
in. (mm)	%	lb/ft^3 (kg/m^3)	° F (° C)	psi (MPa)
5.25 (135)	7.4	139.4 (2234)	70 (21)	4830 (33.3)

not used as the control deck because it was a haunched slab and did not match the other decks in the study. Placement of the deck was completed on June, 9, 2007.

LC-HPC-11 has three spans with lengths of 35.9, 45.9, and 35.9 ft (11.0, 14.0, 11.0 m), respectively, and a width of 40.0 ft (12.2 m). It is a steel girder bridge with integral abutments and a skew of 0.7 degrees. The deck was completed in one phase.

5.3.9.1 Concrete

The concrete was supplied by Mid-America Redi-Mix. The mixture had a cement content of 535 lb/yd^3 (317 kg/m^3) and a water-cement ratio of 0.42. The mixture design was completed by KDOT representatives due to the inexperience of the ready-mix supplier in working with optimized aggregate gradations. The mixture included three granite coarse aggregates and one natural fine aggregate.

5.3.9.2 First and Second Qualification Batches

An initial qualification batch was produced on May 22, 2007 to serve as a trial batch to determine proper admixture dosage rates. The trial batch met temperature requirements through the use of a partial replacement of mixture water with ice, but exhibited a high slump, 8.5 in. (215 mm), and a low air content, 6.3 percent. A second trial batch was produced the following day, May 23, 2007. The second batch met the requirements for slump and air content, but did not temperature. Unlike the first trial batch, ice was not used as a partial replacement of mixture water in the second trial batch to aid in temperature control. Placement of the qualification slab was allowed to move forward even though neither qualification batch met the specifications.

5.3.9.3 Qualification Slab

The qualification slab was placed on May 25, 2007, two days after production of the second qualification batch. The concrete supplier had difficulty producing concrete within the specifications throughout placement, reinforcing the importance of producing a qualification batch that meets specifications prior to placement of the qualification slab. No delivered concrete met the specifications for both slump and air content. High slumps and/or low air contents were common throughout the placement. Delays in concrete delivery resulted in a slow placement process that lasted for over four hours. The extended delays between deliveries of concrete made it difficult for the workers to practice the placement process in an efficient manner.

At times, the contractor had difficulty pumping the concrete. The pump became clogged at one point as elongated aggregates, measuring approximately 3 in. (75 mm) in length, were discovered in the concrete. Finishing was completed using a single-drum roller screed followed by bullfloating. During delays in placement, the roller screed continuously finished single areas on the surface for extended periods of time. Excessive finishing of the surface can bring a greater amount of paste to the

surface and contribute to cracking. Fogging of the slab worked well during placement. The fogging system produced a large amount of mist with no dripping.

During burlap placement, some workers utilized areas of the ground around the slab, not realistically representing the area accessible during deck construction (Figure 5.12). This method of burlap placement had to be modified for the deck construction to accommodate the working conditions.

5.3.9.4 Third and Fourth Qualification Batches

After completion of the qualification slab, a new mixture design was required that contained less of the coarsest aggregate to minimize the risk of clogging the pump with large aggregate particles. The modification to the mixture design required another qualification batch to be completed. The third qualification batch was produced on June, 6, 2007 and did not meet the specifications. The concrete had high slump, air content, and temperature. A fourth qualification batch produced the following day, however, did meet the specifications. Ultimately, a conveyor belt was chosen for the deck placement to avoid pumping problems.

5.3.9.5 LC-HPC-11 Placement

Placement of LC-HPC-11 was completed on June 9, 2007 in approximately five hours. Placement began from the west abutment at around 6:00 a.m. using a conveyor belt. The concrete was tested at the truck discharge, except for one batch which was tested at the truck and at the end of the conveyor. The plastic concrete test results are shown in Table 5.17. Measured slumps ranged from 2.25 to 4.0 in. (55 to 100 mm) with an average of 3.0 in. (75 mm). Air contents ranged from 6.0 to 9.2 percent with an average of 7.7 percent. Six of the thirteen truckloads tested (46 percent) had slumps greater than 3.0 in. (75 mm), while five truckloads (38 percent) had slumps greater than 3.5 in. (90 mm). One of the thirteen truckloads (8 percent)

Figure 5.12 Improper use of areas near qualification slab for burlap placement – LC-HPC-11 qualification slab

Table 5.17 Concrete test results† – LC-HPC-11

KU Bridge Number	Slump	Air Content	Unit Weight	Concrete Temperature	27-Day Compressive Strength*
LC-HPC-11	**in. (mm)**	**%**	**lb/ft^3 (kg/m^3)**	**° F (° C)**	**psi (MPa)**
Average	3.0 (75)	7.7	142.2 (2278)	60 (16)	4680 (32.3)
Minimum	2.25 (55)	6.0	139.5 (2235)	59 (15)	
Maximum	4.0 (100)	9.2	144.6 (2317)	64 (18)	

Percentage of Slump Measurements			Percentage of Air Content Measurements	
> 3.0 in. (75 mm)	**≥ 3.5 in. (90 mm)**	**= 4.0 in. (100 mm)**	**< 6.5%**	**> 9.5%**
46%	38%	31%	7%	0%

* Lab-cured specimens, no data obtained for field-cured specimens
†Concrete tested from truck discharge

had an air content below 6.5 percent. An air loss of 2.4 percent was measured for the concrete tested at the truck and at the end of the conveyor. This large loss of air was likely a result of a 12 to 15-ft (3.7 to 4.6-m) drop height at the end of the conveyor (Figure 5.13). The current LC-HPC specifications require a maximum drop height of 5 ft (1.5 m) from the end of the conveyor. The concrete temperatures ranged from 59° to 64° F (15° to 18° C) with an average of 60° F (16° C). Ice was used to control concrete temperatures. The average compressive strength of lab-cured cylinders tested at 27 days was 4680 psi (32.3 MPa). Compressive strengths of field-cured cylinders were not measured.

Similar to placement of the qualification slab, large pieces of aggregate were found in the concrete during deck placement (Figure 5.14). A grate with 4-in. (100-mm) openings was placed over the loading hopper to the conveyor.

Finishing was completed using a single-drum roller screed followed by a metal pan drag. Bullfloating was not used until the last few feet of placement when the finishing bridges were removed. The burlap was carried by workers to the deck throughout placement instead of being delivered by crane as was typically done for other deck placements. The burlap was unrolled on the side of the deck and carried to two work bridges. The times from strikeoff to burlap placement ranged from 4 to 19 minutes, with an average of 14 minutes. Hand-held fogging equipment was used to keep the burlap wet after placement. As with the qualification slab, the fogging system worked well in producing a fine mist without dripping on the surface.

5.3.10 Control Bridge 11

Control 11 is located on US-50 over the BNSF railroad in Emporia, KS. Construction was completed by A. M. Cohron Construction and the concrete was supplied by Builders Choice Concrete in Emporia, KS.

The bridge is a three-span, steel plate-girder bridge with integral abutments and a skew of 24.3 degrees. Control 11 is 284.9 ft (86.8 m) long with spans of 83.3,

Figure 5.13 Typical height of concrete drop from conveyor for placement of LC-HPC-11

Figure 5.14 Large pieces of aggregate found in concrete during placement of LC-HPC-11

105.0, and 83.3 ft (25.4, 36.0, and 25.4 m). The bridge has a width of 66.8 ft (20.4 m). The deck was constructed in three phases, comprising of two subdecks and one silica fume overlay. The placement dates are shown in Table 5.18.

5.3.10.1 Concrete

The concrete mixture designs for the subdecks and overlay met the KDOT specifications for this type of structure. The subdecks had a cement content of 600 lb/yd^3 (357 kg/m^3) and a water-cement ratio (*w/c*) of 0.40, resulting in a paste content of 25.6 percent. Limestone was used in the subdecks. The silica fume overlay had a 7 percent replacement of portland cement with silica fume, resulting in 44 lb/yd^3 (26 kg/m^3) of silica fume. The overlay had 581 lb/yd^3 (346 kg/m^3) of Type I/II cement, a water-cementitious material ratio (*w/cm*) of 0.37, and a paste content of 26.0 percent. Quartzite was used as the coarse aggregate in the overlay. Neither the subdecks nor overlay concrete met the LC-HPC specifications for cement content or water-cement ratio. The concrete mixture information is shown in Table 5.18.

5.3.10.2 Control 11 Placement

Construction of Control 11 was not observed by KU personnel. The concrete properties were recorded by KDOT personnel and are presented in Table 5.19. The north subdeck had an average slump of 3.5 in. (90 mm) and air content 6.8 percent. The south subdeck had an average slump of 5.25 in. (135 mm) and air content of 7.0 percent. The silica fume overlay had an average slump and air content of 3.0 in. (75 mm) and 6.0 percent, respectively. The compressive strengths for the north and south subdecks and overlay were 5890, 5440, and 7640 psi (40.6, 37.5, and 52.7 MPa), respectively. Construction diaries indicate that blankets and a heating system were used during curing of the subdeck placements due to cold weather conditions.

Table 5.18 Placement dates and concrete mixture information – Control 11

Deck Section	Placement Date	Cement Content	Water Content	Silica Fume Content	*w/cm**	Paste Content	Design Air Content	Coarse Agg. Type
		lb/yd^3 (kg/m^3)	lb/yd^3 (kg/m^3)	lb/yd^3 (kg/m^3)		%	%	
North Subdeck	2/3/2006	602 (357)	241 (143)	-	0.40	25.6%	6.5%	Limestone
South Subdeck	2/14/2006	602 (357)	241 (143)	-	0.40	25.6%	6.5%	Limestone
Overlay	3/28/2006	583 (346)	233 (138)	44 (26)	0.37	26.0%	6.5%	Quartzite

* *w/cm* = water-cementitious material ratio

Table 5.19 Concrete test results – Control 11

Deck Section	Average Slump	Average Air Content	Average Unit Weight	Average Concrete Temperature	Average 28-Day Compressive Strength
	in. (mm)	%	lb/ft^3 (kg/m^3)	° F (° C)	psi (MPa)
North Subdeck	3.50 (90)	6.8	141.3 (2263)	72 (22)	5890 (40.6)
South Subdeck	5.25 (135)	7.0	140.6 (2252)	73 (23)	5440 (37.5)
Overlay	3.00 (75)	6.0	142.1 (2277)	60 (16)	7640 (52.7)

5.3.11 LC-HPC Bridge 4

A single contract included the construction of LC-HPC-3, 4, 5, and 6 and Control 3, 4, 5, and 6. LC-HPC-4 was the first LC-HPC bridge constructed in the contract and is discussed first. Clarkson Construction was the contractor and Fordyce Concrete supplied the concrete for the eight bridges. Clarkson and Fordyce had successfully worked together in the construction of LC-HPC-1 and 2 in 2005 and 2006, respectively.

LC-HPC-4 is the first (north) unit of the southbound bridge on US-69, immediately preceding the eastbound and westbound flyover bridges to I-435 in Overland Park, KS. The entire bridge is comprised of two units due to the unique geometry needed to connect to the flyover bridges. LC-HPC-4 (Unit 1) is a four-

span, steel plate-girder bridge with non-integral abutments and no skew. LC-HPC-4 is connected to Unit 2 (south unit) by a finger joint. Unit 2 connects LC-HPC-4 (Unit 1) to the flyover bridges and was not constructed in accordance with the LC-HPC specifications.

LC-HPC-4 is 377.3 ft (115.0 m) long with four spans of 82.0, 105.0, 105.0, and 85.3 ft (25.0, 32.0, 32.0, and 26.0 m), respectively. The width of LC-HPC-4 varies from 38.1 ft (11.6 m) at the north end to 40.0 ft (12.2 m) at the south end.

5.3.11.1 Concrete

The initial concrete mixture design used for LC-HPC-3 through 6 was a modified version of the design Fordyce used for LC-HPC-1 and 2. The modifications included a reduction in cement content from 540 to 535 lb/yd^3 (320 to 317 kg/m^3) and a reduction in water-cement ratio from 0.45 to 0.42. These reductions lowered the paste content from 24.6 to 23.4 percent. A similar mixture design had recently been used for LC-HPC-8, 10, and 11 with favorable results. Although not required by the most recent LC-HPC specifications, the contractor agreed to the changes.

The aggregate gradation was optimized by blending two coarse aggregates, a coarse manufactured sand, and a natural sand. The coarse manufactured sand was used to fill the intermediate aggregate sizes. An initial mixture design was completed using KU Mix with 33.1 percent by volume of the total aggregate consisting of the manufactured sand. The contractor had concerns over the pumpability and finishability of a mixture with a high proportion of manufactured sand due to the angular nature of the material. As a result, an alternate mixture design was completed by the concrete supplier that contained less manufactured sand (13.0 percent of the total aggregate by volume). Both mixtures were tested for the qualification batch and qualification slab. The combined gradations of the two mixture designs are reported by Lindquist et al. (2008).

5.3.11.2 Qualification Batch

Qualification batches for the KU Mix and alternate mixture designs were produced on June 7, 2007. In an attempt to compare the workability of the two mixtures, similar dosages of water reducer and air-entraining admixture and a constant simulated haul time (27 minutes) were used for both batches. The KU mix mixture (containing 33.1 percent manufactured sand) had a slump of 4.0 in. (100 mm), an air content of 9.6 percent, and a temperature of 71° F (22° C), while the alternate mixture (containing 13.0 percent manufactured sand) had a slump of 5.0 in. (125 mm), an air content of 9.5 percent, and a temperature of 72° F (22° C). The concrete supplier and KDOT officials were satisfied with the performance of the two mixtures and both were chosen to be tested in the qualification slab.

5.3.11.3 Qualification Slab

A qualification slab for LC-HPC-3, 4, 5, and 6 was constructed on September 14, 2007. A single slab was allowed for the four bridge decks as a result of the contractor having experience successfully completing five placements of LC-HPC concrete. Four truckloads were used, including two truckloads of each mixture (KU Mix and alternate mixture). The two truckloads using the alternate mixture were placed first and had slumps of 2.75 and 2.25 in. (70 and 55 mm), air contents of 7.0 and 7.0 percent, and concrete temperatures of 65° and 63° F (19° and 17° C), respectively. The two truckloads using the KU Mix mixture had slumps of 1.5 and 1.25 in (40 and 35 mm), air contents of 6.9 and 5.6 percent, and concrete temperatures of 63 and 62° F (17 and 17° C), respectively. Both mixtures were pumped and finished without difficulty. The increased proportion of manufactured sand did not appear to adversely affect the performance of the concrete. As a result, the KU Mix mixture was chosen for the deck placement.

Placement and finishing of the slab progressed slowly. A single-drum roller screed and bullfloat were used for finishing. The finishing did not provide a smooth

surface at many locations. On one occasion, a worker used a hand-held water sprayer on the surface to aid in finishing. This action was stopped immediately. Fogging equipment was attached to back side of the finishing bridge. At the beginning of placement, the fogging nozzles were pointed downward and sprayed water directly on the concrete surface. The nozzles were eventually pointed upward. As placement began, the pre-soaked burlap was observed to be partially dry. A portion of the wet burlap dripped water on the surface during placement. The water, however, was not worked into the surface.

5.3.11.4 LC-HPC-4 Placement 1

Construction of LC-HPC-4 was originally scheduled to be completed in one placement on September 29, 2007. The concrete was placed beginning from the south end. An electrical outage at the ready-mix plant caused construction to be halted with only one-quarter of the deck cast. The placement began at 2:00 a.m. and was stopped at 6:00 a.m. for a total construction time of 4 hours. A header was placed between placements and the remaining deck was cast in a second placement on October 2, 2007.

Prior to the electrical outage, the concrete supplier had difficulty consistently producing concrete that met the LC-HPC specifications. Concrete from the first two truckloads had low slumps [1.25 and 0.75 in. (30 and 20 mm), respectively] and was difficult to pump and finish. The third truckload contained an increased dosage of water reducer to improve pumability and finishability. The increased water reducer successfully increased the slump to 4.0 in. (100 mm), but also increased the air content above the allowable range, causing the truckload to be rejected. Low-slump concrete was delivered throughout the placement. During the placement, the decision was made to begin using the alternate mixture that contained a smaller proportion of manufactured sand; however, the electrical outage occurred at the ready-mix plant before the alternate mixture could be used in the deck. After the power outage, no

new concrete could be produced and concrete that did not meet specifications had to be used in the deck to reach the header location.

The concrete test results are summarized in Table 5.20. The slumps ranged from 0.75 to 4.25 in. (20 to 105 mm) with an average of 2.0 in. (50 mm). Two of the nine truckloads tested for slump (22 percent) had values that exceeded 3.5 in. (90 mm). One of the nine truckloads (11 percent) had a slump that exceeded 4.0 in. (100 mm). Concretes with slumps above the required range were from the last two truckloads and were only used when production at the ready-mix plant was halted due to the power outage and the header location had to be reached. The average slump of the first seven tested truckloads was 1.25 in. (30 mm). Air contents ranged from 6.8 to 11.6 percent with an average of 8.7 percent. An air cuff was used at the pump discharge to limit air loss. Two of the seven truckloads tested for air content (29 percent) had values above 9.5 percent. A portion of the mixture water was replaced with ice for temperature control; however, concrete temperature was not recorded during placement. No cylinders were made during placement to determine strength.

An overestimation of the free-surface moisture of the manufactured sand likely contributed to the difficulty in producing concrete within the specifications. The concrete supplier stockpiled the manufactured sand next to a lightweight aggregate bin that was continuously saturated, making it difficult to achieve a uniform moisture content throughout the sand. Free-surface moisture contents of 7.1 and 6.5 percent were used for the moisture corrections for the manufactured sand throughout the first placement, while a value of 4.0 percent was used for the second placement, three days later. If the free-surface moisture content of the manufactured sand throughout the first placement had been, in fact, 4.0 percent, the actual water-cement ratio of the concrete would have been 0.37 instead of 0.42.

A larger pump was used for the first placement than was used for the qualification slab. Larger pumps operate at lower pressures than smaller pumps and

Table 5.20 Concrete test results† – LC-HPC-4 – Placement 1

KU Bridge Number	Slump	Air Content	Unit Weight	Concrete Temperature	28-Day Compressive Strength
LC-HPC-4 Placement 1	in. (mm)	%	lb/ft^3 (kg/m^3)	° F (° C)	psi (MPa)
Average	2.0 (50)	8.7	137.4 (2202)	Not Recorded	Not Tested
Minimum	0.75 (20)	6.8	132.4 (2116)		
Maximum	4.25 (105)	11.6	140.8 (2255)		

Percentage of Slump Measurements			Percentage of Air Content Measurements	
> 3.0 in. (75 mm)	≥ 3.5 in. (90 mm)	≥ 4.0 in. (100 mm)	< 6.5%	> 9.5%
22%	22%	11%	0%	29%

†Concrete tested from truck discharge

can have greater difficulty pumping low slump, low paste content concrete, such as LC-HPC. This reinforces the importance of using the same equipment for the qualification slab and the bridge.

Concrete placement progressed slowly due to the problems with pumping and producing in-specification concrete. The concrete was finished with a single-drum roller screed and bullfloat, with occasional use of a wooden float. Long delays and the use of stiff concrete caused the workers difficulty in adequately finishing portions of the deck. The delays in delivering the concrete occasionally caused long periods between concrete placement and burlap cover. After long delays in placement, finished concrete that was not yet covered with burlap was refinished with a bullfloat. Fogging was extensively used throughout the first placement to maintain low evaporation during the delays.

The process of burlap placement was completed as well as possible, considering the significant delays in placement and finishing. The average time to burlap placement was 9 minutes, not including three delays of 15, 35, and 40 minutes. After placement, the placed burlap was kept wet during the delays with a spray hose.

Crack survey results shown later in Section 6.2.15 indicate that the numerous problems associated with construction of Placement 1, including pumping difficulties and continual placement of out-of-specification concrete, likely contributed to cracking.

5.3.11.5 LC-HPC-4 Placement 2

The remaining portion of LC-HPC-4 was completed in a second placement on October, 2, 2007, three days after the first placement. Placement was completed from south to north, beginning at the header. Construction began at 1:30 a.m. and was completed by 6:00 a.m. for a total time of 4.5 hours. The alternate mixture that contained 13.0 percent manufactured sand was used. As previously stated, a lower free-surface moisture content was used for the manufactured sand when calculating the moisture correction for this placement. The concrete was tested and successfully pumped on October, 1, 2007 using the same pump that was to be used for the first placement.

The concrete test results for the second placement are shown in Table 5.21. All tested concrete met the requirements for slump, with values ranging from 1.5 to 4.0 in. (35 to 100 mm) and an average of 3.0 in. (75 mm). However, a majority of the concrete had slumps near the upper allowable limit, with 63 percent of the measured slumps exceeding 3.0 in. (75 mm), 58 percent exceeding or equal to 3.5 in. (90 mm), and 26 percent equal to 4.0 in. (100 mm). The air contents ranged from 7.4 to 10.4 percent with an average of 8.8 percent. One truckload tested after pumping had an air content of 6.8 percent. Unlike Placement 1, the pump used for the second placement did not use a bladder valve to limit air loss. The first truckload was tested for air content before and after pumping and a 2.0 percent air loss from pumping was observed. Concrete tested at the truck with air contents exceeding the allowable limit was accepted because it was assumed that a 2.0 percent air loss would occur due to

Table 5.21 Concrete test results† – LC-HPC-4 – Placement 2

KU Bridge Number	Slump	Air Content	Unit Weight	Concrete Temperature	28-Day Compressive Strength*
LC-HPC-4 Placement 2	in. (mm)	%	lb/ft^3 (kg/m^3)	° F (° C)	psi (MPa)
Average	3.0 (75)	8.8	137.9 (2210)	64 (18)	4790 (33.1)
Minimum	1.5 (35)	7.2	135.1 (2164)	59 (15)	
Maximum	4.0 (100)	10.4	141.1 (2260)	71 (22)	

Percentage of Slump Measurements			Percentage of Air Content Measurements	
> 3.0 in. (75 mm)	≥ 3.5 in. (90 mm)	= 4.0 in. (100 mm)	< 6.5%	≥ 9.5%
63%	58%	26%	0%	36%

* Lab-cured specimens, no data obtained for field-cured specimens
†Concrete tested from truck discharge

pumping. The concrete temperatures ranged from 59° to 71° F (15° to 22° C) with an average of 64° F (18° C). Chilled water and ice were used to control the concrete temperature. The average 28-day compressive strength for lab-cured cylinders was 4790 psi (33.1 MPa). Compressive strengths of field-cured cylinders were not measured.

Placement of the deck went smoothly with only minor delays at the beginning and end of construction. The concrete was pumped more efficiently than for the first placement. Finishing was completed with a single-drum roller screed followed by a bullfloat. Fogging was not used during placement due to a low evaporation rate of 0.008 lb/ft^2/hr (0.04 kg/m^2/hr). Burlap placement began slowly, but consistently maintained 10 to 15 minutes behind strikeoff for the remainder of construction. The burlap was kept wet with a spray hose after placement. Concrete placement, finishing, and burlap placement were delayed in the last 25 ft (8 m) of construction due to a delay in the delivery of concrete. This portion of the deck was exposed with no fogging for about 40 minutes during the delay. Crack survey results discussed later in Section 6.2.15 indicate that this delay did not appear to affect cracking.

5.3.12 LC-HPC Bridge 6

LC-HPC-6 was the second LC-HPC bridge constructed in the contract that included LC-HPC-3, 4, 5, and 6. This bridge and LC-HPC-5 make up the flyover bridge connecting southbound US-69 to westbound I-435 in Overland Park, KS. LC-HPC-6 is the northeast unit of the flyover bridge and connects to Unit 2 of the LC-HPC-4 bridge on the north end and LC-HPC-5 on the southwest end. LC-HPC-6 is the portion of the bridge that connects to southbound US-69 and LC-HPC-5 is the portion that connects to westbound I-435.

LC-HPC-6 is a four-span, steel-plate girder bridge with non-integral end conditions. The bridge has no skew, but is located within a horizontal curve. The southeast side of the deck is superelevated. The entire bridge, comprising of LC-HPC-5 and 6, is 1150.8 ft (350.85 m) long, with LC-HPC-5 spanning 554.5 ft (169.0 m) and LC-HPC-6 spanning 593.8 ft (181.0 m). LC-HPC-6 has span lengths of 128.0, 167.3, 167.3, and 131.2 ft (39.0, 51.0, 51.0, and 40.0 m) and a width of 25.9 ft (7.9 m).

5.3.12.1 Concrete

The mixture used in LC-HPC-4 Placement 2 (containing 13.0 percent manufactured sand by volume of total aggregate) was also used in LC-HPC-6, with two significant modifications. The modifications included an increase in water-cement ratio from 0.42 to 0.45 and the use of a high-range instead of a mid-range water reducer. The cement content remained at 535 lb/yd^3 (317 kg/m^3). The modifications were made to ensure that no pumping difficulties would be encountered.

5.3.12.2 Qualification Batch

The qualification batches produced prior to placement of LC-HPC-4 served as the qualification batches for LC-HPC-6. The qualified batches, however, had

different mixture proportions than the concrete used for LC-HPC-6. Thus, the LC-HPC-6 mixture was not tested in a qualification batch prior to deck placement.

5.3.12.3 Qualification Slab

The qualification slab placed prior to construction of LC-HPC-4 served as the qualification slab for LC-HPC-6.

5.3.12.4 LC-HPC-6 Placement

The placement of LC-HPC-6 began from the southwest end at 5:30 a.m. on November 3, 2007 and lasted for approximately 7 hours. Air temperatures ranged from 35° to 65° F (2° to 18° C) during construction and, as a result, no measures were taken to limit the concrete temperature.

The concrete supplier had difficulty producing concrete within the specifications throughout construction and KDOT personnel allowed a significant amount of this out-of-specification concrete to be placed in the deck. The placement of this large quantity of out-of-specification concrete likely contributed to LC-HPC-6 being one of the highest cracking LC-HPC decks in the study, discussed later in Section 6.2.18. The concrete test results are summarized in Table 5.22. Measured slumps ranged from 2.25 to 6.0 in. (60 to 150 mm) with an average of 4.0 in. (100 mm). Although 85 percent of the measured slumps exceeded 3.0 in. (75 mm), with 69 percent greater than or equal to 3.5 in. (90 mm) and 50 percent greater than or equal to 4.0 in. (100 mm), only one truckload was rejected due to out-of-specification concrete. Air contents measured from the truck ranged from 7.5 to 11.5 percent with an average of 9.5 percent. The air contents remained high throughout construction, with 73 percent exceeding 9 percent and 60 percent exceeding 9.5 percent. Only three of nine truckloads (33 percent) with air contents exceeding 9.5 percent at the truck were retested on the deck. Concrete temperatures ranged from 52° to 64° F

Table 5.22 Concrete test results – LC-HPC-6

KU Bridge Number	Slump	Air Content	Unit Weight	Concrete Temperature	28-Day Compressive Strength*
LC-HPC-6	in. (mm)	%	lb/ft^3 (kg/m^3)	° F (° C)	psi (MPa)
Average	4.0 (100)	9.5	Not Tested	60 (15)	5840 (40.3)
Minimum	2.25 (60)	7.5		52 (11)	
Maximum	6.0 (150)	11.5		64 (18)	

Percentage of Slump Measurements			Percentage of Air Content Measurements	
> 3.0 in. (75 mm)	≥ 3.5 in. (90 mm)	≥ 4.0 in. (100 mm)	< 6.5%	> 9.5%
85%	69%	50%	0%	60%

* Lab-cured specimens, no data obtained for field-cured specimens
†Concrete tested at truck discharge

(11° to 18° C) with an average of 60° F (15° C). The average 28-day compressive strength for lab-cured cylinders was 5840 psi (40.3 MPa). Compressive strengths of field-cured cylinders were not measured.

Communication was poor between KU representatives, KDOT personnel, and the contractor. KDOT personnel were unwilling to require the contractor to adjust the mixture even though the concrete was continuously out of specification. KDOT technicians reported many slump measurements without careful inspection of the ruler, causing the measurements to often be reported as too low. The representative for the concrete supplier was difficult to locate when the concrete was determined to be out of specification. Communication worsened near the end of construction as the personnel became tired. It is important to understand that the LC-HPC specifications can only benefit cracking performance if the specifications are properly enforced.

Pumping was completed more efficiently for LC-HPC-6 than for LC-HPC-4, likely due to the high slumps. Two pumps were used for placement. The first pump, which completed three of four spans, did not have an air cuff or other means to control air loss. Air and slump losses through the first pump were checked on the

first truckload and were measured to be 2.9 percent and 2.0 in. (50 mm), respectively, by pumping to the ground with the boom positioned vertically. This method of pumping did not realistically represent actual pumping conditions and actual air and slump losses were likely lower than measured with the vertical boom. The first two truckloads were delivered with slumps and air contents above the allowable limit; however, they were accepted by KDOT based on the (likely erroneous) measured losses. The concrete placed from the first two truckloads likely had higher slumps and air contents than assumed by KDOT. Air content losses were checked on another two truckloads by pumping to the deck and were determined to be 1.4 and 1.0 percent, respectively. The air loss through the second pump, which had an air cuff, was measured at 0.6 percent.

Placement was slow at times due to limited access for the concrete trucks around the pumps. The pumps could only be accessed by a single truck, forcing each truck to wait until the previous truck unloaded and backed away from the pump. Several delays were caused by the pumps moving locations and slow concrete delivery. Fogging was used during delays of more than 10 minutes. The concrete was finished with a single-drum roller screed followed by two bullfloats. Despite having high slumps, the concrete did not finish as well as other placements and voids were observed in the surface. KDOT personnel did not appear to be concerned with the finish.

Burlap placement was completed efficiently for LC-HPC-6, with an average placement time of 7 minutes. Any delays in burlap placement were the result of slow concrete delivery and placement. Burlap placement was completed in the same manner as for LC-HPC-4. Placed burlap was kept wet using a spray hose.

Soaker hoses were placed in the middle of the deck during curing. The placement of the soaker hoses may have caused the upper portion of the superelevated deck to receive insufficient curing water. The crack survey results

shown later in Section 6.2.18 indicate that high cracking has been observed along this upper edge. The superelevated deck is shown in Figure 5.15. The deck and girders were wrapped and heated during the 14-day curing period (Figure 5.16) to maintain temperatures above 55° F (13° C).

5.3.13 LC-HPC Bridge 3

LC-HPC-3 is the westbound 103rd Street bridge over US-69 in Overland Park, KS and was the third LC-HPC bridge constructed under the contract that included LC-HPC-3, 4, 5, and 6. The eastbound bridge at the same location acts as Control 3. The two bridges are separate structures, but are in contact with a joint located in the median. LC-HPC-3 is a four-span, steel plate-girder bridge with non-integral end conditions and a skew of 6 degrees. The bridge is 380.2 ft (115.9 m) long with spans of 74.3, 115.8, 115.8, and 74.3 ft (22.6, 35.3, 35.3, and 22.6 m). The bridge is 49.9 ft (15.2 m) wide, which includes a 6-ft (2-m) sidewalk along the north edge protected by concrete barriers.

5.3.13.1 Concrete

The same mixture was used in LC-HPC-3 as was used in LC-HPC-6.

5.3.13.2 Qualification Batch

The qualification batch placed prior to construction of LC-HPC-4 served as the qualification batch for LC-HPC-3.

5.3.13.3 Qualification Slab

The qualification slab placed prior to construction of LC-HPC-4 served as the qualification slab for LC-HPC-3.

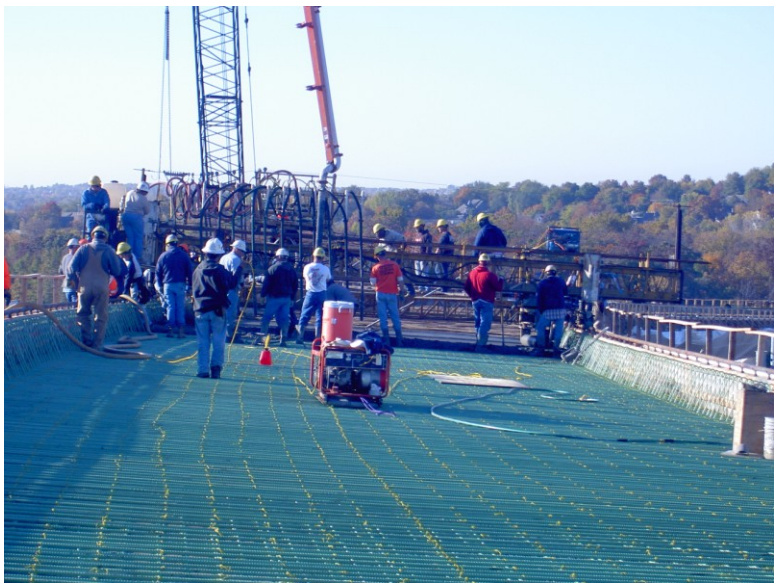

Figure 5.15 Superelevation of deck – LC-HPC-6

Figure 5.16 Girders wrapped for requirements of cold-weather curing – LC-HPC-6

5.3.13.4 LC-HPC-3 Placement

LC-HPC-3 was constructed in one placement beginning from the east abutment on November 13, 2007. The placement began at 2:00 a.m. and was completed by 9:30 a.m.

A clear strategy was established for concrete testing and acceptance as a result of the continuous placement of out-of-specification concrete in LC-HPC-6. The concrete was sampled and tested from the ready-mix truck to ensure that all concrete placed in the deck met the specifications. No concrete with a slump exceeding 4.0 in. (100 mm) or air content exceeding 9.5 percent could be placed in the deck. Truckloads that did not initially meet the specifications could be rejected or set aside and retested prior to placement in the deck.

The emphasis made on the concrete testing and acceptance was successful and all concrete placed in the deck met the specifications. The concrete test results are summarized in Table 5.23. Measured slumps ranged from 1.75 to 4.0 in. (45 to 100 mm) with an average of 3.25 in. (85 mm). Sixty-five percent of the slump values exceeded 3.0 in. (75 mm), 50 percent exceeded 3.5 in. (90 mm), and 26 percent were equal to 4.0 in. (100 mm). The air content ranged from 6.5 to 10.5 percent with an average of 8.7 percent. Truckloads that met the requirements for slump but had air contents exceeding 9.5 percent were retested for air content after pumping. Near the end of the placement, it was discovered that an aggregate correction factor was not taken into account for the air content measurements, indicating that the actual air contents were slightly lower than the recorded values. The concrete temperatures ranged from 52° to 62° F (11° to 17° C) with an average of 58° F (14° C). The average 28-day compressive strength for lab-cured cylinders was high at 5990 psi (41.3 MPa). Compressive strengths of field-cured cylinders were not measured.

The concrete was pumped adequately with two pumps, one located below each end of the bridge. The average air loss through the pumps was determined to be

Table 5.23 Concrete test results† – LC-HPC-3

KU Bridge Number	Slump	Air Content	Unit Weight	Concrete Temperature	28-Day Compressive Strength*
LC-HPC-3	**in. (mm)**	**%**	**lb/ft^3 (kg/m^3)**	**° F (° C)**	**psi (MPa)**
Average	3.25 (85)	8.7	Not Obtained	58 (14)	5990 (41.3)
Minimum	1.75 (45)	6.5		52 (11)	
Maximum	4.0 (100)	10.5		62 (17)	

Percentage of Slump Measurements			Percentage of Air Content Measurements	
> 3.0 in. (75 mm)	**≥ 3.5 in. (90 mm)**	**= 4.0 in. (100 mm)**	**> 6.5%**	**≥ 9.5%**
65%	50%	26%	0%	29%

* Lab-cured specimens, no data obtained for field-cured specimens
†Concrete tested from truck discharge

1.5 percent. The concrete was finished with a single-drum roller screed followed by two bullfloats. The contractor had difficulty properly sealing the surface during finishing. The workers wanted to use water as a finishing aid, but KDOT personnel required the surface to be finished as well as possible without the use of water. The finish of the deck surface appeared similar to the other LC-HPC decks. The contractor, however, did use water for finishing on the first 50 ft (15 m) of the sidewalk. The crack survey results, shown later in Section 6.2.21, do not indicate an increase in cracking in the sidewalk where the water was applied for finishing.

Finishing and burlap placement were often delayed by the slow placement of concrete. Although the contractor had constructed several LC-HPC decks to this point, a new crew placed the burlap on LC-HPC-3. Ten workers were used for burlap placement, including four workers placing the burlap from the work bridges, four workers pushing the work bridges along the deck, and two workers delivering the burlap to the work bridges. The time to burlap placement ranged from 9 to 25 minutes with an average of 15 minutes. The burlap covering the barrier steel blew off at two locations on the deck, leaving portions of concrete exposed. The workers were

directed to tie together overlapping portions of the burlap covering the barrier steel to prevent additional exposure. Fogging was not used during construction due to a low evaporation rate.

The sidewalk was unable to be struckoff and finished concurrently with the roadway due to the barrier steel obstructing the access of the screed. The sidewalk was hand-vibrated and screeded by hand with a 2 × 4 in. (50 × 100 mm) piece of lumber. The sidewalk surface was bullfloated and hand-troweled, followed by a broom finish.

Curing of the sidewalk in accordance with the LC-HPC specifications proved to be a challenge. The contractor refused to immediately cover the sidewalk with burlap after finishing because of the harm it would cause to the finish. The contractor suggested using a curing compound to delay the burlap placement; however, the use of curing compounds is not allowed by the specifications. KDOT personnel compromised with the contractor by allowing burlap placement to be delayed, but requiring water to be sprayed on the finished sidewalk surface every 10 minutes. The surface was required to maintain a shiny, wet appearance. The burlap was eventually placed on the east end approximately 2 hours after finishing. The rate of burlap placement increased to 20 to 30 minutes after finishing near the west end as placement was completed. As discussed in Section 6.2.21, the delayed burlap placement on the sidewalk did not contribute to increased cracking. To avoid damage to the sidewalk finish, the contractor hung the wet burlap over the barrier steel, minimizing contact between the burlap and a portion of the surface (Figure 5.17). The workers were instructed to tuck the burlap near the barrier steel after the concrete had set.

The finishing bridge was removed quickly from the deck and no delay in burlap placement occurred at the end of the deck because the non-integral end condition required no abutment to be filled.

Figure 5.17 Burlap hung over barrier steel to minimize contact between burlap and sidewalk surface – LC-HPC-3

Similar to LC-HPC-6, the deck and girders were wrapped and heated during the curing period to comply with the requirements for cold-weather concreting.

5.3.14 LC-HPC Bridge 5

LC-HPC-5 was the fourth and final LC-HPC bridge constructed under the contract that included LC-HPC-3, 4, 5, and 6. As previously stated, LC-HPC-5 and LC-HPC-6 make up the flyover bridge that connects southbound US-69 to westbound I-435 in Overland Park, KS. LC-HPC-5 is the southwest unit of the flyover bridge and connects to LC-HPC-6 on the northeast end and westbound I-435 on the west end. LC-HPC-6 is the portion of the bridge that connects to southbound US-69 and LC-HPC-5 is the portion that connects to I-435. An expansion joint separates LC-HPC-5 from LC-HPC-6.

Similar to LC-HPC-6, LC-HPC-5 is a four-span, superelevated, curved, steel-plate girder bridge with non-integral end conditions and no skew. LC-HPC-5 is 554.5 ft (169.0 m) long and 25.9 ft (7.9 m) wide, with span lengths of 96.4, 164.0, 164.0,

and 131.2 ft (29.4, 50.0, 50.0, and 40.0 m). The south edge of the deck is superelevated.

5.3.14.1 Concrete

The same mixture was used in LC-HPC-5 as was used in LC-HPC-4 Placement 2, except a high-range water reducer was used (similar to LC-HPC-3 and 6). The mixture included 13.0 percent manufactured sand, a 535 lb/yd^3 (317 kg/m^3) cement content, and a 0.42 water-cement ratio. As previously stated, a water-cement ratio of 0.45 was used for LC-HPC-3 and 6 to provide a more workable concrete. However, a qualification slab was successfully placed for another LC-HPC deck (designated as "OP Bridge" and summarized in a later section) the day before construction of LC-HPC-5 (November 13, 2007) using a mixture that contained a 0.42 water-cement ratio. Due to the success of this qualification slab and LC-HPC-4 Placement 2 and the fact that a lower paste content would be utilized, a 0.42 water-cement ratio was chosen for LC-HPC-5. It has since been recognized that a decrease in water-cement ratio at a fixed cement content does result in reduced shrinkage, but does not ultimately reduce cracking because the decrease in water-cement ratio increases strength, which can increase the modulus of elasticity and reduce the beneficial effects of creep of the concrete. The water-cement ratio was increased to 0.45 during placement of LC-HPC-5 to resolve pumping difficulties.

5.3.14.2 Qualification Batch

The qualification batch placed prior to construction of LC-HPC-4 served as the qualification batch for LC-HPC-5.

5.3.14.3 Qualification Slab

The qualification slab placed prior to construction of LC-HPC-4 served as the qualification slab for LC-HPC-5.

5.3.14.4 LC-HPC-5 Placement

LC-HPC-5 was constructed in one placement beginning from the west abutment on November 14, 2007, a day after construction of LC-HPC-3. The placement began at 2:00 a.m. and was completed by 10:00 a.m. for a total construction time of 8 hours.

As with LC-HPC-3, the concrete was tested from the truck discharge. The concrete test results are summarized in Table 5.24. Slumps ranged from 2.0 to 4.0 in. (50 to 100 mm) with an average of 3.0 in. (75 mm). Forty-six percent of the slumps exceeded 3.0 in. (75 mm), 27 percent exceeded or equaled 3.5 in. (90 mm), and 12 percent equaled 4.0 in. (100 mm). Air contents ranged from 6.8 to 10.3 percent with an average of 8.7 percent. The pump had a bladder valve to limit air loss. The air content was tested before and after pumping for the first truckload and the air loss was measured at 0.6 percent. Two out of the fifteen truckloads tested (13 percent) had concrete with air contents that exceeded the upper limit of 9.5 percent. The concrete temperature ranged from 57° to 64° F (14° to 18° C) with an average of 61° F (16° C). Lab-cured cylinders had a high average 28-day compressive strength at 6380 psi (44.0 MPa). Compressive strengths for field-cured cylinders were not measured. The concrete was delivered in a timely manner throughout the placement.

Pumping proved to be difficult during construction. The first pump seized up three times during the placement of the first seven truckloads, leading to its replacement. During the pump replacement, several truckloads sat on-site waiting for discharge for more than 45 minutes. Each of the truckloads that contributed to the seized pump had concrete with a water-cement ratio of 0.42. To improve pumpability, the concrete supplier began adding 0.5 gal/yd^3 (2.5 kg/m^3) of water to each of the next seven truckloads without notifying representatives from KDOT or KU representatives. After KDOT and KU representatives became aware of this additional water, the water-cement ratio was increased to 0.43 to provide

Table 5.24 Concrete test results† – LC-HPC-5

KU Bridge Number	Slump	Air Content	Unit Weight	Concrete Temperature	28-Day Compressive Strength*
LC-HPC-5	**in. (mm)**	**%**	**lb/ft^3 (kg/m^3)**	**° F (° C)**	**psi (MPa)**
Average	3.0 (75)	8.7	139.6 (2236)	61 (16)	6380 (44.0)
Minimum	2.0 (50)	6.8	136.1 (2181)	57 (14)	
Maximum	4.0 (100)	10.3	143.2 (2294)	64 (18)	

Percentage of Slump Measurements			Percentage of Air Content Measurements	
> 3.0 in. (75 mm)	**≥ 3.5 in. (90 mm)**	**= 4.0 in. (100 mm)**	**< 6.5%**	**≥ 9.5%**
46%	27%	12%	0%	13%

* Lab-cured specimens, no data obtained for field-cured specimens
†Concrete tested from truck discharge

documentation of the mixture used. The pumping problems persisted for the following nine truckloads and, as a result, the water-cement ratio was increased to 0.45. The efficiency of the pumping improved for the remainder of the placement. The crack survey results shown later in Section 6.2.24 indicate that less cracking has been observed near the east end of the deck, the region placed with improved pumping efficiency.

The concrete was finished with a single-drum roller screed followed by two bullfloats. The concrete was finished adequately for most of the placement. A few large voids were noted after bullfloating at the time of the pumping problems. Fogging was not used and the evaporation rate was not recorded during the placement.

Although the contractor had constructed several LC-HPC decks to this point, a new method of burlap placement was used for LC-HPC-5 that possibly negatively affected the cracking performance. For most LC-HPC decks, two pieces of burlap are placed transversely, covering the entire deck width. For LC-HPC-5, a single burlap piece was placed transversely from the northwest side to the southeast (superelevated)

side, leaving a 1 to 3 ft (0.3 to 0.9 m) concrete strip exposed along the superelevated edge. After placement of four to five widths of burlap along the deck length, an additional piece of burlap was longitudinally placed to cover the exposed strip. This placement method left an uncovered strip along the superelevated edge exposed for extended periods of time. To make matters worse, the soaker hoses were placed in the center of the deck (similar to LC-HPC-6), possibly contributing to the upper portion of the superelevated deck not receiving sufficient curing water. As shown in Section 6.2.24, the majority of cracks have propagated from the upper edge of the superelevated deck, likely a result of the increased exposure during delayed burlap placement and the lack of available curing water provided by the soaker hoses.

Similar to other bridges in the contract, the deck and girders were wrapped during the curing period to comply with the requirements for cold-weather concreting.

5.3.15 Control Bridges 3, 4, 5, and 6

Control bridges 3, 4, 5, and 6 were constructed under the same contract as LC-HPC-3, 4, 5, and 6 and are discussed together in this section. The placement dates of the four decks are shown in Table 5.25. A description of each bridge is presented in this section.

Control Bridge 3

Control 3 is the eastbound bridge on 103rd Street over US-69 in Overland Park, KS and is the control deck for LC-HPC-3, the westbound bridge at the same location. It is a four-span, steel plate-girder bridge with non-integral end conditions and a 6 degree skew. A 10-ft (3-m) sidewalk protected by concrete barriers is located along the south edge. The bridge is 380.3 ft (115.9 m) long, with spans of 72.9, 115.8, 115.8, and 72.9 ft (22.2, 35.5, 35.3, and 22.2 m). The total deck width is 53.8 ft (16.4 m), with a roadway width of 39.0 ft (11.9 m). Like most of the control decks, it was constructed in two phases, a subdeck and silica fume overlay.

Table 5.25 Placement dates of Control 3, 4, 5, and 6*

Bridge	Deck Section	Placement Date
Control 3	Subdeck	7/6/2007
	Overlay	7/17/2007
Control 4	Subdeck	10/20/2007
	Overlay	11/16/2007
Control 5	Subdeck - seq. 1 & 2	11/8/2008
	Subdeck - seq. 3, 5, & 6	11/13/2008
	Subdeck - seq. 4 & 7	11/17/2008
	Overlay - West Half	11/22/2008
	Overlay - East Half	11/25/2008
Control 6	Subdeck - seq. 1 & 2	9/16/2008
	Subdeck - seq. 3	9/18/2008
	Subdeck - seq. 5 & 6	9/23/2008
	Subdeck - seq. 4	9/26/2008
	Subdeck - seq. 7	9/30/2008
	Overlay - West 2/3	10/16/2008
	Overlay - East 1/3	10/20/2008

*seq. = placement sequence

Control Bridge 4

Control 4 is the bridge that connects Antioch Road to westbound I-435 in Overland Park, KS and is the comparative control deck for LC-HPC-4. It is a five-span, steel plate-girder bridge with non-integral end conditions and no skew. The bridge is 701.5 ft (213.8 m) long, with spans of 133.9, 167.3, 167.3, 131.2, and 99.4 ft (40.8, 51.0, 51.0, 40.0, and 30.3 m). The north edge of the deck, which supports a concrete barrier, cantilevers beyond the exterior girder. The total deck width is 40.8 ft (12.4 m). The deck was constructed in two phases with a silica fume overlay.

Control Bridge 5

Control 5 and 6 together constitute the flyover bridge that connects southbound US-69 to eastbound I-435 in Overland Park, KS. Control 5 is the

northwest unit of the flyover bridge and connects to Unit 2 of the LC-HPC-4 bridge on the north end and Control 6 on the southeast end. Control 5 is the portion of the bridge that connects to southbound US-69 and Control 6 is the portion that connects to eastbound I-435. Control 5 is a four-span, superelevated, curved, steel-plate girder bridge with non-integral end conditions and no skew. The bridge is 822.2 ft (250.6 m) long and 40.8 ft (12.4 m) wide, with spans of 149.6, 232.9, 232.9, and 206.7 ft (45.6, 71.0, 71.0, and 63.0 m). The deck was constructed in five phases, consisting of three subdecks and two silica fume overlays.

Control Bridge 6

Control 6 is the portion of the southbound US-69 to eastbound I-435 flyover bridge that connects to I-435. It is a four-span, superelevated, curved, steel plate-girder bridge with no skew, a non-integral end condition at the northwest abutment, and an integral end condition at the east abutment. The bridge is 882.2 ft (268.9 m) long and 40.8 ft (12.4 m) wide, with span lengths of 212.8, 239.5, 239.5, and 190.3 ft (64.9, 73.0, 73.0, and 58.0 m). Control 6 was constructed in seven phases, consisting of five subdecks and two silica fume overlays.

5.3.15.1 Concrete

The concrete mixtures for the subdecks and overlays met the KDOT specifications for the respective structures. A single mixture, which varied from the standard KDOT mixture, was used for all subdeck concrete. The subdeck mixture had 536 lb/yd^3 (318 kg/m^3) of cement, 133 lb/yd^3 (79 kg/m^3) of fly ash, and a water-cementitious material ratio (*w/cm*) of 0.40, resulting in a paste content of 29.0 percent. Additionally, a single mixture was used for each overlay. The overlays had a 7 percent weight replacement of portland cement with silica fume, 583 lb/yd^3 (346 kg/m^3) of Type I/II cement, a water-cementitious material ratio (*w/cm*) of 0.37, and a paste content of 26.0 percent. Granite was used as the coarse aggregate in the subdeck and overlay. Neither the subdeck nor overlay concrete met the LC-HPC

specifications for cement content or water-cement ratio. The concrete mixture information for the subdecks and overlays are shown in Table 5.26.

5.3.15.2 Deck Placements

The subdeck of Control 4 was the only placement of the four control decks observed by KU personnel. The concrete test results for placement of the subdecks and overlays are shown in Table 5.27. The measured slumps ranged from 5.75 to 9.25 in. (145 to 230 mm). Every subdeck and overlay of the four control decks had an average slump above the allowable upper limit [4.0 in. (100 mm)] in the LC-HPC specifications. Eleven of the sixteen placements (69 percent) had an average slump greater than or equal to 7.0 in. (180 mm). The average 28-day compressive strengths for the four control decks, ranging from 4950 to 8510 psi (34.1 to 58.7 MPa), were higher than for typical LC-HPC decks. The average air contents ranged from 5.5 to 8.1 percent. Five of the sixteen subdecks and overlays (31 percent) had average air contents below the allowable lower limit (6.5 percent) in the LC-HPC specifications. Five of the sixteen subdecks and overlays (31 percent) had average concrete temperatures above the allowable upper limit [75° F (24° C)] in the LC-HPC specifications.

5.3.16 LC-HPC Bridge 12

LC-HPC-12 and Control 12 constitute the two units of a steel plate-girder bridge on K-130 over the Neosho River near Hartford, KS, southeast of Emporia. LC-HPC-12 (Unit 2) includes the north three spans, while Control 12 (Unit 1) includes the south three spans. The contract for construction of both units was awarded to A. M. Cohron Construction. LC-HPC-12 and Control 12 were each constructed in two full-length, partial-width phases, with the east half constructed in the first phase and the west half constructed in the second phase. The entire bridge, consisting of LC-HPC-12 and Control 12, is 833.0-ft (254.0-m) long, with integral

Table 5.26 Concrete mixture information – Control 3, 4, 5, and 6

Deck Section	Cement Content	Water Content	Silica Fume Content	Class F Fly Ash Content	*w/cm**	Paste Content	Design Air Content	Coarse Agg. Type
	lb/yd^3 (kg/m^3)	lb/yd^3 (kg/m^3)	lb/yd^3 (kg/m^3)	lb/yd^3 (kg/m^3)		%	%	
Subdeck	536 (318)	268 (159)	-	133 (79)	0.40	29.0%	6.5%	Granite
Overlay	583 (346)	233 (133)	44 (26)	-	0.37	26.0%	6.5%	Granite

* *w/cm* = water-cementitious material ratio

Table 5.27 Concrete test results – Control 3, 4, 5, and 6*

Bridge	Deck Section	Average Slump	Average Air Content	Average Unit Weight	Average Concrete Temperature	Average 28-Day Compressive Strength
		in. (mm)	%	lb/ft^3 (kg/m^3)	° F (° C)	psi (MPa)
Control 3	Subdeck	6.75 (170)	5.8	140.5 (2251)	81 (27)	5690 (39.2)
	Overlay	7.25 (185)	7.3	140.4 (2249)	86 (30)	8350 (57.6)
Control 4	Subdeck	7.75 (195)	7.3	139.9 (2240)	73 (23)	6340 (43.7)
	Overlay	5.75 (145)	6.9	140.0 (2239)	68 (20)	7700 (53.0)
Control 5	Subdeck - seq. 1 & 2	7.75 (200)	5.6	142.2 (2278)	66 (19)	-
	Subdeck - seq. 3, 5, & 6	9.25 (230)	6.8	140.1 (2245)	68 (20)	-
	Subdeck - seq. 4 & 7	8.00 (205)	5.5	143.0 (2275)	63 (17)	-
	Overlay - West Half	6.00 (150)	7.6	140.5 (2250)	64 (18)	8510 (58.7)
	Overlay - East Half	9.00 (230)	6.6	141.2 (2262)	63 (17)	-
Control 6	Subdeck - seq. 1 & 2	8.00 (205)	7.4	139.7 (2238)	75 (24)	4950 (34.1)
	Subdeck - seq. 3	7.00 (180)	7.3	140.2 (2246)	70 (21)	-
	Subdeck - seq. 5 & 6	6.75 (175)	6.4	141.1 (2261)	88 (31)	-
	Subdeck - seq. 4	6.25 (160)	6.6	140.7 (2254)	86 (30)	-
	Subdeck - seq. 7	8.75 (225)	5.5	141.6 (2269)	79 (26)	-
	Overlay - West 2/3	7.00 (175)	7.7	141.0 (2258)	72 (22)	-
	Overlay - East 1/3	8.25 (210)	8.1	139.3 (2231)	72 (22)	7700 (53.1)

*seq. = placement sequence

abutments and no skew. LC-HPC-12 is 416.5 ft (127.0 m) long and 36.0 ft (11.0 m) wide, with span lengths of 142.5, 142.5, and 131.5 ft (43.4, 43.4, and 40.1 m). For LC-HPC-12 and Control 12, the first and second phase placements (Placements 1 and 2) were 18.0 ft (5.5 m) and 20 ft (6.1 m) wide, respectively. The proposed crown was located at the centerline of the roadway on Placement 2, approximately 1 ft (0.3 m) from the joint between the placements. The location of the crown and the orientation of the placements resulted in all of Placement 1 and the majority of Placement 2 to be sloped to the outer edges of the deck.

5.3.16.1 Concrete

The concrete for LC-HPC-12 was supplied by Builder's Choice Concrete in Emporia, a subsidiary of Concrete Supply of Topeka. The specifications for LC-HPC-12 required a maximum cement content of 535 lb/yd^3 (317 kg/m^3) and a water-cement ratio of 0.42; however, the cement content and water-cement ratio were increased to 540 lb/yd^3 (320 kg/m^3) and 0.44, respectively, for Placement 1 due to the pumping and finishing difficulties that occurred during the placement of previous decks with this specification. The mixture proportions for Placement 2 were slightly modified, consisting of a cement content of 535 lb/yd^3 (317 kg/m^3) and a water-cement ratio of 0.45. The aggregates used in the mixtures of both placements included two granite coarse aggregates and a natural river sand.

5.3.16.2 Qualification Batch – Placement 1

The qualification batch for Placement 1 of LC-HPC-12 was produced on March 25, 2008 in Emporia, KS with KU representatives in attendance. The concrete that was tested after a simulated haul time met the requirements for slump [4.0 in (100 mm)], air content (8.0 percent), and temperature [65° F (18° C)].

5.3.16.3 Qualification Slab – Placement 1

The qualification slab for Placement 1 was constructed on March 28, 2008. Unlike the construction of previous LC-HPC decks, buckets were chosen for concrete placement because flooding conditions at the bridge site made it impossible to position a pumping or conveyor system. Two buckets, with capacities of 0.75 and 1 yd^3 (0.57 and 0.76 m^3), were used for placement of the qualification slab. The contractor and KDOT personnel were satisfied with the placement rate of the slab using the buckets.

Measures to control the concrete temperature were unnecessary due to the low air temperatures during placement [around 40° F (4° C)]. The concrete in the first three truckloads had slumps of 4.25, 5.25, and 6.0 in. (110, 135, and 150 mm); all exceeding the upper limit of 4.0 in. (100 mm). These truckloads were set aside for 15 to 30 minutes and retested. The first truckload was used in the placement after the slump decreased to 3.75 in. (95 mm). The second and third truckloads were rejected as a result of the slumps remaining above the upper allowable limit after retesting. The second truckload was eventually placed in the slab to avoid delays in placement. The final two truckloads met the specifications for slump, with values of 2.75 and 3.25 in. (70 and 85 mm), respectively. All air content measurements met the requirements, with values ranging from 7.5 to 8.5 percent and an average of 7.9 percent. Delays in concrete delivery occurred due to the concrete supplier only batching new truckloads after the previous truckload was accepted.

A single-drum roller screed and a burlap drag attached to the screed were used to finish the qualification slab. Fogging equipment was not used on the slab, but was checked and appeared to be adequate. Burlap placement was completed efficiently with a maximum placement time of 10 minutes. Any delays in burlap placement were the result of delays in concrete delivery.

5.3.16.4 LC-HPC-12 Placement 1

Placement 1 was constructed on April 4, 2008. Construction began at the north abutment at 9:00 a.m. and lasted for approximately 6 hours. The concrete was placed using two crane buckets with the same capacities as those used on the qualification slab [0.75 and 1 yd^3 (0.57 and 0.76 m^3)]. A crane was positioned on the existing structure (west half of the bridge) that was to be replaced in Placement 2 and moved forward as construction progressed. The buckets were filled by concrete trucks on the existing structure and lifted by the crane to the placement site. The orientation of the equipment and method of placement are shown in Figure 5.18. One bucket deposited concrete on the deck as the second bucket was filled, allowing for continuous placement of concrete.

The concrete supplier produced concrete within the specifications throughout construction. In addition, no delays in concrete delivery occurred during placement. A portion of the mixture water was withheld in the first truckload, lowering the actual water-cement ratio to 0.42. The contractor was required to add the withheld water on-site to increase the water-cement ratio to the correct value of 0.44. No water was withheld in the remaining trucks and slumps were controlled using a mid-range water reducer. Testing was completed after the concrete was deposited on the deck with the buckets. The concrete test results are shown in Table 5.28. The slumps ranged from 1.75 to 3.5 in. (45 to 90 mm) with an average of 2.75 in. (70 mm). Three of the ten truckloads tested (30 percent) had slumps that exceeded 3.0 in. (75 mm), two truckloads (20 percent) had slumps that equaled 3.5 in. (90 mm), and no slumps exceeded 3.5 in. (90 mm). The air content ranged from 6.2 to 8.1 percent with an average of 7.4 percent. Concrete temperatures ranged from 53° to 67° F (12° to 20° C) with an average of 58° F (15° C). The average 28-day compressive strength of lab-cured cylinders was 4570 psi (31.5 MPa). Compressive strengths of field-cured cylinders were not measured.

Figure 5.18 Equipment orientation and placement method for LC-HPC-12 Placement 1

Table 5.28 Concrete test results† – LC-HPC-12 – Placement 1

KU Bridge Number	Slump	Air Content	Unit Weight	Concrete Temperature	28-Day Compressive Strength*
LC-HPC-12 Placement 1	**in. (mm)**	**%**	**lb/ft^3 (kg/m^3)**	**° F (° C)**	**psi (MPa)**
Average	2.75 (70)	7.4	141.0 (2259)	58 (15)	4570 (31.5)
Minimum	1.75 (45)	6.2	139.5 (2235)	53 (12)	
Maximum	3.5 (90)	8.1	143.5 (2299)	67 (20)	

Percentage of Slump Measurements			Percentage of Air Content Measurements	
> 3.0 in. (75 mm)	**= 3.5 in. (90 mm)**	**> 3.5 in. (90 mm)**	**< 6.5%**	**≥ 9.5%**
30%	20%	0%	10%	0%

*Lab-cured specimens, no data obtained for field-cured specimens
†Concrete tested on deck at discharge of buckets

The concrete was finished using a single-drum roller screed followed by a metal pan drag, rather than the burlap drag used in the qualification slab. Bullfloating was used only at the beginning and end of placement at locations where the pan drag could not be used. Crack survey results, shown in Section 6.2.27, indicate that bullfloating near the ends did not contribute to cracking. Fogging was not used due to a low evaporation rate [0.05 lb/ft^2/hr (0.24 kg/m^2/hr)].

The burlap was placed efficiently, with an average placement time of 7 minutes. The burlap placement remained approximately 4 ft (1.2 m) behind the finishing equipment throughout construction. The workers were able to place two layers of burlap on the deck simultaneously. The placed burlap was kept wet using spray hoses. The transverse slope of the deck contributed to ponding of the sprayed water along the outer edge. The crack survey results, discussed later in Section 6.2.27, suggest that this ponded water did not contribute to cracking.

Cold-weather curing provisions, which include heating the girders and deck during the 14-day curing period, were required for Placement 1 because the air temperatures dropped below 40° F (4° C) during the curing period. The provisions allow an alternate option that requires heating only within the first 72 hours of the curing period if the length of curing is increased an additional day beyond the original 14 days for every day that the air temperature drops below 40° F (4° C). A minimum air temperature of 50° F (10° C) is required for any additional day to be considered as part of the curing period. This alternate option was chosen for the cold-weather curing, although the procedure was not correctly followed by the contractor. The curing period was lengthened an additional 3 days; however, weather station data indicate that air temperatures dropped below 40° F (4° C) during 10 of the 14 days of the original curing period. Additionally, Days 15 and 16 of the extended curing period had air temperatures below the required 50° F (10° C). Furthermore, no measures were taken to heat the deck and girders during the first 72 hours of curing

even though air temperatures dropped below 40° F (4° C). Overall, the contractor did a poor job of executing the alternate provisions for cold-weather curing.

5.3.16.5 Qualification Batch – Placement 2

The qualification batch was produced for Placement 2 on March 12, 2009 in Emporia, KS with KU representatives in attendance. As previously stated, Placement 2 used a different mixture design with a cement content of 535 lb/yd^3 (317 kg/m^3) and a water-cement ratio of 0.45. The batch met the requirements for slump [3.75 in. (95 mm)], air content (7.0 percent), and concrete temperature [61° F (16° C)]. The concrete was tested after a simulated haul time of 25 minutes.

5.3.16.6 Qualification Slab – Placement 2

An additional qualification slab for Placement 2 was not required due to the previous experience of the contractor constructing Placement 1 and LC-HPC-8 and 10.

5.3.16.7 LC-HPC-12 Placement 2

Placement 2, the west half of the deck, was constructed on March 18, 2009. Construction began at the south end at 10:30 a.m. and lasted for approximately 9.5 hours. Two crane buckets were again used for placement. Placement 2 was constructed in a method similar to Placement 1, requiring the crane, buckets, and concrete trucks to be positioned on the newly-constructed Placement 1 (11.4 months of age) during construction (Figure 5.19). The movement of the crane during construction induced significant vertical deflections in both placements. The vertical deflections were estimated to be as large as 1.5 in. (38 mm) when the loaded bucket was in motion near the midspans. KDOT and KU representatives expressed concern over whether the significant deflections would contribute to early-age cracking in Placement 2. Additionally, the movement of the bucket induced stresses in

Figure 5.19 Construction equipment placed on newly-constructed Placement 1 during construction of LC-HPC-12 Placement 2

Placement 1. Prior to the construction of Placement 2, the contractor requested permission to use extended chutes to directly discharge the concrete from the trucks to the deck. This method of placement was not adopted because of concern over the low-slump concrete adequately flowing down the gradually-sloped chutes.

The concrete supplier had difficulty producing consistent concrete. The initial mixture, which had a cement content of 535 lb/yd^3 (317 kg/m^3) and a water-cement ratio of 0.45, exhibited high slumps without the addition of a water reducer. The supplier attempted to lower the slump by heating a portion of the mixture water. After six truckloads with slumps ranging from 3.5 to 5.75 in. (90 to 145 mm), the supplier was required to lower the water-cement ratio to 0.44. The crack survey results discussed in Section 6.2.27 indicate that the placement of this high-slump concrete did not appear to affect cracking in this region. It is possible that the cracking on this deck was primarily caused by effects from the loads induced during construction, not the placement of high-slump concrete. The reduction in water-cement ratio proved to be successful in controlling the slump. After the delivery of

four truckloads with adequate slumps, the contractor, without approval from KDOT or KU, switched the water-cement ratio back to 0.45. The following 10 truckloads with the higher water-cement ratio had slumps ranging from 3.5 to 5.0 in. (90 to 125 mm). The evaporation rate increased near the end of placement [up to 0.22 lb/ft^2/hr (1.07 kg/m^2/hr)] and, as a result, the contractor attempted to lower the concrete temperature. To avoid significantly increasing the slump of the lower-temperature concrete, the contractor chose to again lower the water-cement ratio to 0.44.

The concrete test results are shown in Table 5.29. Approximately half of the concrete samples were tested from the truck discharge and the other half were tested from the bucket discharge on the deck. The drop from the bucket discharge to the deck was only 3 ft (1 m) and likely did not significantly affect the plastic concrete properties. All concrete placed in the deck had a slump of 3.5 in. (90 mm) or higher. The slumps ranged from 3.5 to 5.75 in. (90 to 145 mm) with an average of 4.25 in. (110 mm). Air contents ranged from 6.3 to 9.0 percent with an average of 7.8 percent. One truckload had an air content of 6.3 percent, below the required limit of 6.5 percent. The concrete temperatures ranged from 61° to 72° F (16° to 22° C) with an average of 67° F (20° C). A set of cylinders was cast for each of the two water-cement ratios used in the placement (0.44 and 0.45). The average 28-day compressive strengths of lab-cured cylinders for the mixtures containing water-cement ratios of 0.44 and 0.45 were 4580 and 4180 psi (31.6 and 28.8 MPa), respectively. Compressive strengths of field-cured cylinders were not measured.

The first quarter of the deck appeared to be over-vibrated and the contractor was asked to correct this issue. Over-vibration causes the coarse aggregate to settle lower in the deck, increasing the paste content at the surface. This additional paste at the surface leaves the deck more susceptible to shrinkage cracking and freeze-thaw damage. The concrete finished well with a single-drum roller screed followed by a metal pan drag. Bullfloating was used at each end of the deck. The fogging system

Table 5.29 Concrete test results† – LC-HPC-12 – Placement 2

KU Bridge Number	Slump	Air Content	Unit Weight	Concrete Temperature	28-Day Compressive Strength
LC-HPC-12 Placement 2	in. (mm)	%	lb/ft^3 (kg/m^3)	° F (° C)	psi (MPa)
Average	4.25 (110)	7.8	140.1 (2258)	67 (20)	4580 (31.6)#
Minimum	3.5 (90)	6.3	138.0 (2210)	61 (16)	4180 (28.8)##
Maximum	5.75 (145)	9.0	143.2 (2294)	72 (22)	

Percentage of Slump Measurements			Percentage of Air Content Measurements	
> 3.0 in. (75 mm)	≥ 3.5 in. (90 mm)	≥ 4.0 in. (90 mm)	< 6.5%	≥ 9.5%
100%	100%	43%	8%	0%

†Approximately half of samples were tested at truck discharge and half tested at bucket discharge on deck

Average 28-day compressive strength for lab-cured specimens, *w/c* = 0.44, no data obtained for field-cured specimens

Average 28-day compressive strength for lab-cured specimens, *w/c* = 0.45, no data obtained for field-cured specimens

was not used because of low evaporation rates during construction. The burlap was placed efficiently, with an average time of 6 minutes. A long delay, about 50 minutes, occurred near the end of construction due to the need to back-order concrete. The contractor was required to cover all placed concrete with wet burlap during the delay. The contractor did not adequately soak the burlap, requiring it to be rewetted prior to placement. Although the workers were constantly instructed otherwise, dry burlap was occasionally placed. In-place burlap was rewetted periodically with a spray hose. The crack survey results, discussed later, indicate that cracking did not appear to be significantly affected by this delay.

The temperatures of the top girder flanges were monitored using an infrared thermometer (Fluke® 561) and air temperatures were checked with a weather meter (Kestrel® 3000) throughout construction. As explained in Section 1.2.2, temperature differences between the concrete and steel girders can contribute to the development of thermal stresses in the deck. The steel girder temperature was lower than the

ambient and concrete temperatures before 10:00 a.m. and after 5:30 p.m. During the majority of the day (between 10:00 a.m. and 5:30 p.m.), the steel girder temperature was above the ambient temperature and slightly above the concrete temperature.

Similar to Placement 1, the alternate option for cold-weather concrete curing was used for Placement 2. For this placement, however, the contractor was required to provide a record to account for the extended curing. The contractor noted 112 hours (totaling 4-2/3 days) during the initial 14-day curing period in which the temperature dropped below 40° F (4° C). An additional 15 days of curing were required after the initial 14-day curing period to counteract the curing time below 40° F (4° C).

5.3.17 Control Bridge 12

Control 12 is the first unit of the bridge on K-130 over the Neosho River near Hartford, KS and includes the three spans to the south of LC-HPC-12 (Unit 2). Both Control 12 and LC-HPC-12 were part of the same contract awarded to A. M. Cohron Construction. Construction included two full-length, partial-width phases, beginning on the east half of the deck. The phases of construction included a subdeck and silica fume overlay. The east and west portions of the deck are designated as Placements 1 and 2, respectively. The placement dates are shown in Table 5.30.

The entire bridge, including Control 12 and LC-HPC-12, is a six-span, steel plate-girder bridge with integral abutments and no skew. Control 12 has the same total length, span lengths, and width as LC-HPC-12. As with LC-HPC-12, the first (east) and second (west) placements were, respectively, 18.0 ft (5.5 m) and 20.0 ft (6.1 m) wide.

5.3.17.1 Concrete

The concrete mixture designs for both the subdeck and overlay met the KDOT specifications for this type of structure. Builder's Choice Concrete was the ready-mix

Table 5.30 Placement dates and concrete mixture information – Control 12

Placement Designation	Deck Section	Placement Date	Cement Content	Water Content	Silica Fume Content	*w/cm* *	Paste Content	Design Air Content	Coarse Agg. Type
			lb/yd^3 (kg/m^3)	lb/yd^3 (kg/m^3)	lb/yd^3 (kg/m^3)		%	%	
Placement 1	East Subdeck	3/11/2008	602 (357)	265 (157)	-	0.44	27.1%	6.5%	Limestone
	East Overlay	4/1/2008	581 (345)	231 (137)	44 (26)	0.37	25.8%	6.5%	Quartzite
Placement 2	West Subdeck	3/13/2009	602 (357)	265 (157)	-	0.44	27.1%	6.5%	Limestone
	West Overlay	4/14/2009	581 (345)	231 (137)	44 (26)	0.37	25.8%	6.5%	Quartzite

* *w/cm* = water-cementitious material ratio

supplier. The standard KDOT mixture was used in the subdeck, containing a cement content of 602 lb/yd^3 (357 kg/m^3) and a water-cement ratio of 0.44, resulting in a paste content of 27.1 percent. Limestone was used in the subdeck. The silica fume overlay included a 7 percent replacement of portland cement with silica fume, resulting in 44 lb/yd^3 (26 kg/m^3) of silica fume. The overlay had 581 lb/yd^3 (345 kg/m^3) of Type I/II cement, a water-cementitious material ratio (*w/cm*) of 0.37, and a paste content of 25.8 percent. Quartzite was used as the coarse aggregate in the overlay. The concrete mixture information is shown in Table 5.30.

5.3.17.2 Control 12 Placement

Construction of Control 12 was not observed by KU personnel. The concrete properties of the placements are presented in Table 5.31. The concrete in Control 12 had lower slumps than typically found in control decks, with average slumps of 4.25 and 4.5 in. (110 and 120 mm) in the two subdecks and average slumps of 2.25 and 3.75 in. (55 and 95 mm) in the two overlays. The average air content of the four phases ranged from 6.8 to 7.7 percent. The average 28-day compressive strengths were 5270 and 5010 psi (36.4 and 34.5 MPa) for the two subdecks and 6240 and 7710 psi (43.0 and 53.1 MPa) for the two overlays.

Table 5.31 Concrete test results – Control 12

Placement Designation	Deck Section	Average Slump	Average Air Content	Average Unit Weight	Average Concrete Temperature	Average 28-Day Compressive Strength
		in. (mm)	%	lb/ft^3 (kg/m^3)	° F (° C)	psi (Mpa)
Placement 1	East Subdeck	4.25 (110)	6.9	140.5 (2250)	72 (22)	5270 (36.4)
	East Overlay	3.75 (95)	6.8	140.7 (2254)	59 (15)	6240 (43.0)
Placement 2	West Subdeck	4.5 (120)	7.2	Not Obtained	72 (22)	5010 (34.5)
	West Overlay	2.25 (55)	7.7	Not Obtained	62 (17)	7710 (53.1)

The concrete was placed through a pipe line extending from a pump truck located on the approach slab of the bridge. The concrete supplier encountered problems with delays and the production of concrete with correct air contents when placing the silica fume overlay in Placement 1, with air contents ranging from 2.5 to 9.9 percent. The contractor encountered problems achieving proper depth during the subdeck placement in Placement 2. A number of areas with significantly shallow depths were noted in the placement, and at times, the finishing equipment made contact with the top reinforcement.

5.3.18 LC-HPC Bridge 13

LC-HPC-13 is the northbound bridge on US-69 over the BNSF railroad near Pleasanton in Linn County, KS. Control 13 is the southbound bridge at the same location. The contract that included LC-HPC-13 and Control 13 was awarded to Koss Construction. Construction of both bridges was subcontracted to Beachner Construction. LC-HPC-13 is a three-span, steel rolled-beam bridge with integral abutments and a 34.8 degree skew. The bridge is 295.6 ft (90.1 m) long and 40.0 ft (12.2 m) wide, with span lengths of 90.4, 114.8, and 90.4 ft (27.5, 35.0, and 27.5 m). The bridge was constructed in a single placement.

5.3.18.1 Concrete

The concrete for LC-HPC-13 was supplied by O'Brien Ready Mix. The specifications for LC-HPC-13 required a maximum cement content of 535 lb/yd^3 (317 kg/m^3) and a water-cement ratio of 0.42. The mixture design used in LC-HPC-13, however, was based on the LC-HPC-12 Placement 1 mixture and consisted of a cement content of 540 lb/yd^3 (320 kg/m^3) and a water-cement ratio of 0.44 to provide improved pumpability and workability. The cement content was later reduced to 535 lb/yd^3 (317 kg/m^3) after high slumps were observed during placement of the qualification slab. The mixture contained one granite coarse aggregate and two natural sands.

5.3.18.2 Qualification Batch

A qualification batch was not required due to the experience of the concrete supplier on LC-HPC-8 and 10.

5.3.18.3 Qualification Slab

The qualification slab for LC-HPC-13 was completed on April 16, 2008 on farm property. The slab required four truckloads and was placed using a pump with a bladder valve. This qualification slab was the first experience with low-cracking high-performance concrete (LC-HPC) for Beachner Construction.

Water was withheld [1.5 gal/yd^3 (7.5 L/m^3)] and a mid-range water reducer was added for the first two truckloads. These truckloads met the requirements for slump, but had low air contents (5.7 and 6.0 percent, respectively) below the specified lower limit of 6.5 percent. The concrete supplier was ordered to include all mixture water at the batch plant for the remaining truckloads to avoid the production of concrete with low water-cement ratios. The final truckloads had no water withheld or water reducer and had slumps averaging 4.25 in. (110 mm), exceeding the required upper limit of 4.0 in. (100 mm). In addition, the air contents of these truckloads

remained below the requirements of the specifications. No measures were taken to control the concrete temperature, resulting in temperatures approaching the upper allowable limit of 75° F (24° C). Following completion of the qualification slab, the cement content for the deck mixture was decreased to 535 lb/yd^3 (317 kg/m^3) to provide better management of the slump. In addition, the concrete supplier was instructed to prepare for cooling of the concrete during the deck placement.

Finishing was completed with a double-drum roller screed with one roller removed, followed by a metal pan drag and a bullfloat. The surface was given a smoother finish than the typical LC-HPC decks because the slab was to be used as a building floor after construction.

The qualification slab did not provide the contractor with realistic experience placing burlap because the width of the slab [42 ft (12.8 m)] was narrower than the proposed deck width [52 ft (15.9 m)]. Although a single burlap piece reached the full width of the qualification slab, two pieces would be required to cover the full deck width. There were concerns that the contractor would become accustomed to a procedure for burlap placement that would leave a strip of concrete at the deck edge uncovered for extended periods, similar to the burlap placement on LC-HPC-5. The workers initially placed two layers of burlap at a time on the slab, but were later instructed to cover the entire deck width with a single layer prior to placement of a second layer to avoid the potential exposure of a concrete strip at the edge during deck construction.

5.3.18.4 LC-HPC-13 Placement

The deck on LC-HPC-13 was constructed in a single placement on April 29, 2008. Placement began at the south abutment at 11:15 a.m. and was completed by 6:30 p.m.

The concrete was delivered in a timely manner throughout construction, except for a relatively long delay at the end of the placement due to backordered

concrete. In addition, most of the concrete met the specifications throughout the placement. The concrete test results are summarized in Table 5.32. Plastic concrete testing was completed on the deck at the pump discharge. The slumps ranged from 1.75 to 5.0 in. (45 to 125 mm) with an average of 3.0 in. (75 mm). Slumps for nine of the thirty-two truckloads tested (28 percent) exceeded 3.0 in. (75 mm), eight (25 percent) equaled or exceeded 3.5 in. (90 mm), and six (19 percent) equaled or exceeded 4.0 in. (100 mm), with two truckloads (6 percent) above 4.0 in. (100 mm). An improper testing technique was employed by one technician that possibly resulted in increased slump readings. The air contents ranged from 6.8 to 9.5 percent with an average of 8.1 percent. All measured air contents remained between the specified limits of 6.5 to 9.5 percent. The concrete temperatures ranged from 61° to 72° F (16° to 22° C) with an average of 69° F (20° C). The average 28-day compressive strength of the concrete was 4280 psi (29.5 MPa). Compressive strengths of field-cured cylinders were not measured.

Two pumps with bladder valves were positioned at opposite ends of the bridge for the placement. Concretes with slumps as low as 1.75 in. (45 mm) were pumped without trouble. Excluding a short delay of about 15 minutes as the pumps were switched, the concrete was continuously pumped throughout construction. Based on samples from three truckloads, the average air loss through the pump was 1.1 percent.

The surface was finished efficiently with a double-drum roller screed with one roller removed and a metal pan drag. Bullfloating was only used on the first half of the deck. As discussed in Section 6.2.30, greater cracking has been observed in the first half of the deck, possibly a result of the bullfloating bringing additional paste to the surface. Fogging equipment was mounted to the finishing bridge and worked well when used. Water continuously dripped from the equipment after it was shut off during the second half of the deck placement. The bulfloating was discontinued on the second half of the deck to avoid working this additional water into the surface.

Table 5.32 Concrete test results† – LC-HPC-13

KU Bridge Number	Slump	Air Content	Unit Weight	Concrete Temperature	28-Day Compressive Strength*
LC-HPC-13	**in. (mm)**	**%**	**lb/ft^3 (kg/m^3)**	**° F (° C)**	**psi (MPa)**
Average	3.0 (75)	8.1	141.5 (2266)	69 (20)	4280 (29.5)
Minimum	1.75 (45)	6.8	137.0 (2195)	61 (16)	
Maximum	5.0 (125)	9.5	144.6 (2317)	72 (22)	

Percentage of Slump Measurements			Percentage of Air Content Measurements	
> 3.0 in. (75 mm)	**≥ 3.5 in. (90 mm)**	**≥ 4.0 in. (90 mm)**	**< 6.5%**	**> 9.5%**
28%	25%	19%	0%	0%

* Lab-cured specimens, no data obtained for field-cured specimens
†Concrete tested at pump discharge

Burlap placement began slowly at the beginning of placement, but increased speed throughout construction. The time for burlap placement ranged from 2 to 24 minutes with an average of 12 minutes. The speed of burlap placement was greatly dependent on the speed of finishing throughout the placement. Two delays in burlap placement of 20 minutes each occurred near the end of construction due to an insufficient supply of concrete. The crack survey results discussed in Section 6.2.30 suggest that these delays did not significantly affect cracking. The burlap appeared to have partially dried before construction began, so the contractor sprayed it with water prior to placement on the deck. The contractor later re-soaked some of the burlap in a water tank and lifted it to the deck with a crane. The workers kept the burlap wet after placement using misting hoses. Ponding on the east side of the deck was observed and the workers were instructed to minimize use of the soaker hoses.

5.3.19 Control Bridge 13

Control 13 is the southbound bridge on US-69 over the BNSF railroad in Linn County, KS and is located alongside northbound LC-HPC-13. It was constructed under the same contract as LC-HPC-13 by Beachner Construction. As with LC-HPC-13, O'Brien Ready Mix supplied the concrete for Control 13.

Control 13 is a three-span, steel rolled-beam bridge with integral abutments and a 34.8 degree skew, with the same dimensions (length, width, and span length) as LC-HPC-13. As with most other control decks, the deck included the placement of a subdeck and silica fume overlay. The placement dates are shown in Table 5.33.

5.3.19.1 Concrete

The concrete mixture designs for both the subdeck and overlay met the KDOT specifications for this type of structure. The subdeck had 612 lb/yd^3 (363 kg/m^3) of cement, a water-cement ratio of 0.40, and a paste content of 26.0 percent. Limestone was used in the subdeck. The silica fume overlay included a 7 percent replacement of portland cement with silica fume, resulting in 44 lb/yd^3 (26 kg/m^3) of silica fume. The overlay had 590 lb/yd^3 (350 kg/m^3) of Type I/II cement, a water-cementitious material ratio (*w/cm*) of 0.37, and a paste content of 26.2 percent. Quartzite was used as the coarse aggregate in the overlay. Neither the subdeck nor overlay concrete met the LC-HPC specifications for cement content or water-cement ratio. The concrete mixture information is shown in Table 5.33.

5.3.19.2 Control 13 Placement

Construction of Control 13 was not observed by KU personnel. Concrete properties were recorded by KDOT personnel and are presented in Table 5.34. The subdeck concrete had an average slump of 3.5 in. (90 mm); a lower value than found in most control decks. The overlay concrete had an average slump of 5.25 in. (135 mm), more typical of control decks. The subdeck and overlay had average air

Table 5.33 Placement dates and concrete mixture information – Control 13

Deck Section	Placement Date	Cement Content	Water Content	Silica Fume Content	*w/cm**	Paste Content	Design Air Content	Coarse Agg. Type
		lb/yd^3 (kg/m^3)	lb/yd^3 (kg/m^3)	lb/yd^3 (kg/m^3)		%	%	
Subdeck	7/11/2008	612 (363)	244 (145)	-	0.40	26.0%	6.5%	Limestone
Overlay	7/25/2008	590 (350)	234 (139)	44 (26)	0.37	26.2%	6.5%	Quartzite

* *w/cm* = water-cementitious material ratio

Table 5.34 Concrete test results – Control 13

Deck Section	Average Slump	Average Air Content	Average Unit Weight	Average Concrete Temperature	Average 28-Day Compressive Strength
	in. (mm)	%	lb/ft^3 (kg/m^3)	° F (° C)	psi (Mpa)
Subdeck	3.5 (90)	5.8	141.7 (2271)	89 (32)	Not Obtained
Overlay	5.25 (135)	6.3	141.6 (2269)	91 (33)	8280 (57.1)

contents of 5.8 and 6.3 percent, respectively. The average concrete temperatures of 89° and 91° F (32° and 33° C) for the subdeck and overlay, respectively, were considerably higher than those allowed in the LC-HPC specifications. Compressive strength was not measured for the subdeck. The overlay had an average 28-day compressive strength of 8280 psi (57.1 MPa).

5.3.20 LC-HPC Bridge 9

LC-HPC-9 is the northbound bridge on US-69 over the Marais Des Cygnes River near Pleasanton in Linn County, KS. Control 9 is the southbound bridge at the same location. LC-HPC-9 and Control 9 were part of the same contract as LC-HPC-8, 10, and Contro1 8/10 that was awarded to Koss Construction. Construction of LC-HPC-9 and Control 9 was subcontracted to United Construction. LC-HPC-9 is a three-span, steel plate-girder bridge with non-integral abutments and an average skew of 24.4 degrees. The bridge is 431.9 ft (131.7 m) long and 40.0 ft (12.2 m) wide, with

spans of 134.0, 164.0, and 133.9 ft (40.8, 50.0, and 40.8 m). The bridge was constructed in a single phase.

5.3.20.1 Concrete

O'Brien Ready Mix supplied the concrete for the deck. The specifications for LC-HPC-9 required a maximum cement content of 535 lb/yd^3 (317 kg/m^3) and a water-cement ratio of 0.42. As with the other LC-HPC decks in the contract (LC-HPC-8 and 10), the mixture used in LC-HPC-9 was modified from the specified requirements to provide improved pumpability and workability. The mixtures had cement contents that varied between 535 and 540 lb/yd^3 (317 and 320 kg/m^3) and a water-cement ratio of 0.44. Two granite coarse aggregates and a natural sand were used in the mixtures.

5.3.20.2 Qualification Batch

The first batch produced for the second attempt of the qualification slab was considered as the qualification batch. The concrete had a cement content of 540 lb/yd^3 (320 kg/m^3) and a water-cement ratio of 0.44. The batch was tested out of the truck prior to placement in the qualification slab and met the specifications with a slump of 3.5 in. (90 mm), an air content of 9.2 percent, and a concrete temperature of 60° F (16° C).

5.3.20.3 Qualification Slab – Attempt 1

The first attempt at the qualification slab for LC-HPC-9 was made on March 23, 2009, just south of LC-HPC-9. The mixture had a cement content of 535 lb/yd^3 (317 kg/m^3) and a water-cement ratio of 0.44. The first truckload was tested prior to pumping and had a slump of 1.75 in. (45 mm), an air content of 7.4 percent, and a temperature of 78° F (26° C). Although the temperature was above the upper limit and a slump approaching the lower limit of the specifications, pumping was

attempted because the concrete appeared to be workable. The pump became clogged during the attempt and the qualification slab was cancelled before any concrete was placed.

5.3.20.4 Qualification Slab – Attempt 2

The second attempt at the qualification slab was made two days later, on March 25, 2009. The cement content was increased to 540 lb/yd^3 (320 kg/m^3) as a result of the problems associated with the first attempt at pumping. The first truckload met the specifications and appeared to be workable; therefore, an attempt was made to pump the concrete with the same pump used in the first attempt. The pump was initially lubricated with mortar prior to the pumping of the concrete. Once again, the pump was not able to handle the concrete and the qualification slab was cancelled before any concrete was placed. An investigation of the concrete discovered coarse aggregates as large as 1.5 and 2.0 in. (38 and 51 mm). Because the pump-hose diameter was only 4.5 in. (114 mm), it is possible that large aggregates became lodged in the pump hose and obstructed the flow of concrete.

5.3.20.5 Qualification Slab – Attempt 3

The third attempt at the qualification slab was completed on April 1, 2009. Two options to help increase the pumpability of the concrete included adjusting the mixture design by increasing the paste content or using a pump with a larger hose diameter. The contractor, however, elected to place the concrete with a conveyor system and avoid any additional pumping difficulties.

The concrete had a cement content of 540 lb/yd^3 (320 kg/m^3) and a water-cement ratio of 0.44. Concrete from the first truckload was tested out of the truck and had a slump of 4.0 in. (100 mm), an air content of 9.7 percent, and a temperature of 55° F (13° C). This concrete was tested again at the end of the conveyor belt and met the specifications, with a slump of 3.0 in. (75 mm), an air content of 7.6 percent, and

a temperature of 58° F (14° C). The drop from the end of the conveyor to the slab [approximately 15 ft (4.6 m)] exceeded the maximum drop height of 5 ft (1.5 m) allowed by the LC-HPC specifications. The second truckload was tested at the end of the conveyor and did not meet the specifications due to a high slump [4.75 in. (115 mm)] and air content (9.9 percent). The third truckload had an air content of 9.0 percent and appeared to have a high slump. The out-of-specification concrete was placed in the slab; however, the contractor and concrete supplier were notified that this would not be permitted during the deck placement.

Placement and finishing were completed efficiently, with help from the high-slump concrete. The concrete was finished with a double drum-roller screed with one roller removed, followed by a double pan drag. The burlap was placed in an average of 11 minutes.

5.3.20.6 LC-HPC-9 Placement

The deck for LC-HPC-9 was constructed on April 15, 2009 in a single placement. Placement began at the north abutment at 9:30 a.m. and the final burlap was placed by 6:20 p.m., for a total time of 8.8 hours. A delay at the end of the placement occurred when the contractor needed to backorder concrete. The crack survey results, shown in Section 6.2.33, do not indicate any increased cracking as a result of this delay. The start of placement was delayed due to the adoption of a new condition in the specifications regarding the air temperature during placement. This condition required that placement not begin until the ambient temperature exceeded 50° F (10° C) if the temperature during the day of placement was expected to exceed 60° F (16° C).

The concrete had a cement content of 540 lb/yd^3 and a water-cement ratio of 0.44. A portion of the mixture water was withheld from the first four truckloads, but was required to be added prior to placement. The concrete was tested at the discharge of the conveyor. The concrete test results are shown in Table 5.35. Slumps ranged

Table 5.35 Concrete test results† – LC-HPC-9

KU Bridge Number	Slump	Air Content	Unit Weight	Concrete Temperature	30-Day Compressive Strength*
LC-HPC-9	**in. (mm)**	**%**	**lb/ft^3 (kg/m^3)**	**° F (° C)**	**psi (MPa)**
Average	3.5 (90)	6.7	141.3 (2264)	64 (18)	4190 (28.9)
Minimum	2.25 (55)	5.7	139.6 (2237)	60 (16)	
Maximum	5.25 (135)	7.6	143.0 (2291)	69 (21)	

Percentage of Slump Measurements			Percentage of Air Content Measurements	
> 3.0 in. (75 mm)	**≥ 3.5 in. (90 mm)**	**≥ 4.0 in. (90 mm)**	**< 6.5%**	**> 9.5%**
58%	47%	32%	19%	0%

* 30-day compressive strength of lab-cured specimens, no data obtained for field-cured specimens
†Concrete tested at discharge end of conveyor

from 2.25 to 5.25 in. (55 to 135 mm) with an average of 3.5 in. (90 mm). The majority of the truckloads with high slumps were delivered early in the placement. As described in Section 6.2.33, it is not clear that the use of high-slump concrete early in the placement contributed to increased cracking. Fifty-eight percent of the slumps exceeded 3.0 in. (75 mm), 47 percent equaled or exceeded 3.5 in. (90 mm), and 32 percent equaled or exceeded 4.0 in. (100 mm). The air content ranged from 5.7 to 7.6 percent with an average of 6.7 percent. An additional dosage of air-entraining admixture was added on-site to the first truckload because the air content was below the required specifications. The dosage of air-entraining admixture was increased throughout the placement to adjust for low air contents. Nineteen percent of the air contents were below the required limit of 6.5 percent. The concrete temperatures ranged from 60° to 69° F (16° to 21° C) with an average of 64° F (18° C). The average compressive strength of lab-cured cylinders at 30 days was 4190 psi (28.9 MPa). Compressive strengths of field-cured cylinders were not measured.

Two conveyor belts were used to place the concrete. The first conveyor belt was positioned at the ends of the deck, while the second conveyor was located on the

adjacent, southbound bridge (Control 9). The height of the concrete drop to the deck from the first and second conveyor belts was estimated at 20 and 36 ft (6.1 and 11.0 m), respectively; significantly exceeding the allowable drop height of 5 ft (1.5 m). The height of the concrete drop from the second conveyor belt is shown in Figure 5.20.

Similar to the qualification slab, the concrete was finished with a double-drum roller screed with one roller removed, followed by two pan drags. Hand floating was used at locations where the pan drags could not reach. Fogging was not used due to a low evaporation rate throughout the placement.

Portions of the burlap were partially dry prior to placement. The partially-dry burlap is shown in Figure 5.21. The workers attempted to place the burlap in the dry condition and rewet it once it was placed on the deck; however, this action was ended quickly. The workers were unsuccessful in adequately wetting the dry burlap with spray hoses. Ponding was observed on the east side of the deck due to the use of the spray hoses. Holes were drilled through the forms to allow the ponded water to drain from the deck. The burlap was placed fairly quickly, with an average time to placement of 10 minutes. The two layers of the burlap were placed separately. Two overlapping strips of burlap were needed to cover the entire deck width. While waiting for the backordered concrete near the end of construction, the workers were required to cover the unfinished portions of the deck with wet burlap to prevent drying.

As with LC-HPC-12 Placement 2, the ambient and top girder flange temperatures were monitored throughout the construction. The steel girder temperatures increased at a greater rate than the ambient temperature during the placement, beginning below the ambient temperature prior to 10:30 a.m., rising to and remaining near ambient between 10:30 a.m. and 1:30 p.m., and increasing above ambient from 1:30 to 5:30 p.m. The greatest difference between the steel girder and

Figure 5.20 Height of concrete drop from second conveyor belt to deck – LC-HPC-9

Figure 5.21 Partially-dry burlap – LC-HPC-9

ambient temperature [16° F (9° C)] occurred between 1:30 and 3:30 p.m. due to heating from the sun. The concrete temperature closely matched the ambient temperature, gradually increasing from about 60° to 70° F (16° to 21° C) throughout the day.

Temperature distributions were monitored through the depth of the girders at locations in which concrete had and had not been placed. At locations in which concrete had not yet been placed, temperatures were greatest at the top flange and decreased through the girder depth to the bottom flange. The temperatures of the top flanges at approximately 4:00 p.m. were 88° and 86° F (31° and 30° C) at locations on the east and west girders, respectively, prior to concrete placement. The maximum temperature gradients between the top and bottom flanges prior to concrete placement were 30° and 38° F (17° and 21° C) for the east and west girders, respectively. At a location in which concrete had been placed five hours earlier, however, the temperature distribution was much more gradual from the top to the bottom flange. The temperature of the top flange at this location was 64° F (18° C), much lower than at the locations in which concrete had not yet been placed. The temperature difference between the top and bottom flange at this location after concrete placement was only 4° F (2° C).

5.3.21 Control Bridge 9

Control 9 is the southbound bridge on US-69 over the Marais Des Cygnes River in Linn County, KS and is located adjacent to LC-HPC-9 (the northbound bridge). Control 9 was part of the same contract as LC-HPC-8, 9, 10, and Control 8/10. As for LC-HPC-9, United Construction was the contractor and O'Brien Ready Mix was the concrete supplier. The bridge is a three-span, steel plate-girder bridge with non-integral abutments and an average skew of 23.9 degrees. The bridge is 431.9 ft (131.7 m) long and 40.0 ft (12.2 m) wide, with spans of 131.2, 164.0, and 131.2 ft (40.0, 50.0, 40.0 m). The deck was constructed in three phases, including

one subdeck and two silica fume overlays. The placement dates are shown in Table 5.36.

5.3.21.1 Concrete

The concrete mixtures for the subdeck and overlays met the KDOT specifications for this type of structure. The subdeck had 612 lb/yd^3 (363 kg/m^3) of cement, a water-cement ratio of 0.40, and a paste content of 26.0 percent. Limestone was used in the subdeck. The silica fume overlays had 590 lb/yd^3 (350 kg/m^3) of Type I/II cement and 44 lb/yd^3 (26 kg/m^3) of silica fume (7 percent replacement of cement by weight) and had a water-cementitious material ratio (*w/cm*) of 0.37 and a paste content of 26.2 percent. Quartzite was used as the coarse aggregate in the overlays. The concrete mixture information is shown in Table 5.36.

5.3.21.2 Control 9 Placement

Construction of Control 9 was not observed by KU personnel. The average concrete properties are presented in Table 5.37. The subdeck concrete had an average slump of 2.75 in. (60 mm), an average air content of 6.2 percent, an average temperature of 66° F (19° C), and an average 28-day compressive strength of 4850 psi (33.5 MPa). The silica fume overlay for the west half of the deck had an average slump of 3.5 in. (90 mm), an average air content of 5.6 percent, and an average 28-day compressive strength of 6380 psi (44.0 MPa). The overlay for the east half of the deck had an average slump of 5.0 in. (130 mm), an average air content of 6.2 percent, and an average 28-day compressive strength of 6170 psi (42.6 MPa). The average concrete temperatures were 77° and 71° F (25° and 22° C) for the west and east overlays, respectively.

Table 5.36 Placement dates and concrete mixture information – Control 9

Deck Section	Placement Date	Cement Content	Water Content	Silica Fume Content	*w/cm* *	Paste Content	Design Air Content	Coarse Agg. Type
		lb/yd^3 (kg/m^3)	lb/yd^3 (kg/m^3)	lb/yd^3 (kg/m^3)		%	%	
Subdeck	11/3/2007	612 (363)	244 (145)	-	0.40	26.0%	6.5%	Limestone
Overlay - West	5/21/2008	590 (350)	234 (139)	44 (26)	0.37	26.2%	6.5%	Quartzite
Overlay - East	5/28/2008	590 (350)	234 (139)	44 (26)	0.37	26.2%	6.5%	Quartzite

* *w/cm* = water-cementitious material ratio

Table 5.37 Concrete test results – Control 9

Deck Section	Average Slump	Average Air Content	Average Unit Weight	Average Concrete Temperature	Average Compressive Strength
	in. (mm)	%	lb/ft^3 (kg/m^3)	° F (° C)	psi (Mpa)
Subdeck	2.75 (65)	6.2	142.7 (2286)	66 (19)	4850 (33.5)
Overlay	3.5 (90)	5.6	142.4 (2282)	77 (25)	6380 (44.0)
Overlay	5.0 (130)	6.2	141.2 (2262)	71 (22)	6170 (42.6)

5.3.22 OP Bridge (LC-HPC-14)

The fourteenth bridge let under LC-HPC specifications in Kansas is located on Metcalf Avenue over Indian Creek in Overland Park, KS. The contract contained one bridge and was awarded to Pyramid Construction. Although the contract specified that the deck was to be constructed in accordance with the LC-HPC specifications, the contractor did not follow and the owner (the City of Overland Park) did not enforce many aspects of the specifications. For this reason, the bridge is designated as "OP Bridge" instead of "LC-HPC-14". This bridge provided valuable lessons regarding the importance of complying with all aspects of the LC-HPC specifications. As discussed in Section 6.2.39, the OP Bridge placements

experienced higher cracking than all LC-HPC decks and many control decks in the study.

The OP Bridge is a three-span, rolled steel-girder bridge with integral abutments and a skew of 18 degrees. The bridge is 217.6 ft (66.3 m) long with spans of 67.3, 83.0, and 67.3 ft (20.5, 25.3, and 20.5 m). The deck is 140.0 ft (42.7 m) wide to accommodate nine lanes of traffic and two sidewalks. The large deck width and the need to maintain traffic during construction required the deck to be completed in three placements. The first placement was a 60-ft (18.2-m) wide section in the center of the deck, while the second and third placements consisted, respectively, of a 47.5-ft (14.4-m) wide section on the west side and a 32.5-ft (9.9-m) wide section on the east side.

5.3.22.1 Concrete

The concrete supplier for the OP Bridge, Fordyce Concrete, also supplied the concrete for six LC-HPC decks (LC-HPC-1 through 6). Initially, the alternate mixture used in LC-HPC-4 and 5, which included a cement content of 535 lb/yd^3 (317 kg/m^3) and a water-cement ratio of 0.42, was to be used in the OP Bridge; however, the water-cement ratio was ultimately increased to 0.45 to counteract a number of difficulties that were encountered during construction. These difficulties are discussed in the following sections. Two granite coarse aggregates, a natural sand, and a manufactured sand were combined to provide an optimized gradation for the mixture design.

5.3.22.2 Qualification Batch

A qualification batch was not required for the OP Bridge because Fordyce Concrete was simultaneously supplying the concrete mixtures for LC-HPC-3 through 6 under a separate contract.

5.3.22.3 Qualification Slab

The qualification slab was placed on November 13, 2007 in approximately three hours. This slab provided the first opportunity for the contractor to work with concrete meeting the LC-HPC specifications. The qualification slab was 30 ft (9.1 m) wide, only half the width of the first deck placement.

A miscommunication at the ready-mix plant caused concrete with an incorrect water-cement ratio to be placed in the qualification slab. The concrete supplier for the qualification slab was supplying the same mixture (water-cement ratio = 0.42) for the deck placement of LC-HPC-3 on the same day. After the water-cement ratio for LC-HPC-3 was increased to 0.45 during construction, the concrete supplier began delivering concrete with the increased water-cement ratio to both LC-HPC-3 and the qualification slab, even though this modification had not been approved for use in the slab. The concrete with the higher water-cement ratio pumped and finished well. The slumps ranged from 2.75 to 3.75 in. (70 to 95 mm) with an average of 3.0 in. (90 mm). The air contents ranged from 7.4 to 8.5 percent with an average of 7.6 percent.

City officials and KU representatives decided to order one truckload with the correct water-cement ratio (0.42) to check if it was also pumpable and finishable. The new truckload had a slump of 3.0 in. (75 mm) and an air content of 7.4 percent and pumped and finished well. An additional concrete pumping test was performed three days later, on November 16, 2007, to alleviate concerns over the pumping of concrete with a water-cement ratio of 0.42. The concrete had a slump of 1.5 in. (40 mm) and an air content of 8.5 percent and pumped well, provided that the pumping was continuous. The contractor experienced some trouble restarting the pump after a delay occurred in the concrete supply. The contractor and city officials were satisfied with the performance and felt that the concrete would pump adequately, given that the concrete for the deck placement had slumps near 3.0 in. (90 mm). The mixture was chosen for use in the deck. The contractor stated that two pumps would be available

on-site for the deck placement, including the same pump as used in the qualification slab.

The contractor had the KU representatives clarify the LC-HPC specifications during placement of the qualification slab to resolve any issues prior to the placement of the deck. The contractor asked for clarification regarding the requirements for consolidation and demonstrated their typical consolidation procedures for the KU representatives. Upon examination, the contractor was instructed to vibrate the concrete for 2 to 3 seconds or until the coarse aggregate dropped below the concrete surface. The contractor also asked if bullfloating was recommended for use. The KU representatives advised the contractor to use a pan or burlap drag to minimize the time to burlap placement; however, a bullfloat could be used if necessary. Additionally, the contractor was instructed to not use water as a finishing aid. The contractor later asked if two layers of burlap could be placed simultaneously. They were told that this was acceptable as long as the burlap was placed within 10 minutes after strikeoff. The contractor was reminded that the same crew should be used for the burlap placement of the qualification slab and the deck. Due to the expected low air temperatures during curing, the contractor planned to wrap and heat the deck and girders to comply with the cold-weather curing requirements. The contractor asked if the heater could be turned off during the curing period if there was concern over overheating of the girders. They were told that the heater could be turned off in this situation.

5.3.22.4 OP Bridge Placement 1 – Attempt 1

The first attempt at Placement 1 of the OP Bridge made on November 19, 2007 was a failure. After placement of only 30 ft (9.1 m) of concrete, construction was stopped due to the concrete being both out of specification and not pumpable. The placement was cancelled after the pump became clogged and blew a gasket. The portion of the deck that was placed was eventually removed.

The placement began at 6:00 p.m. The first several truckloads delivered to the bridge had slumps and air contents that exceeded the allowable limits. These truckloads were set aside to allow for the slump and air to drop. Eventually, a large backup of trucks were waiting on-site to be placed. Some of these trucks were required to be rejected after the wait on-site became too long. When the truckloads were finally placed in the deck, the slumps had become very low and the concrete was difficult to pump and place. The pump was frequently stopped and restarted because of a narrow pathway that allowed only a single truck to reach the pump at a time. In addition, a slump loss of 1.0 in. (25 mm) and an air loss of approximately 2.0 percent were observed through the pump as no measures were taken to limit the air loss. The concrete eventually became umpumpable. Ultimately, the pump blew a gasket, and by the time the repairs were made, the line had become clogged. The placement was cancelled.

A meeting was held the following day, November 20, 2007, with representatives from the concrete supplier, the contractor, the City of Overland Park, the pumping company, the structural design firm, and KU in attendance. The contractor stated that they would tear out the concrete. It was decided that conveyor belts would be used for the second attempt. There was considerable discussion regarding the standard of accepting concrete, although no final decision was made.

5.3.22.5 OP Bridge Placement 1 – Attempt 2

The second attempt at Placement 1 was successfully completed on December 19, 2007. Placement began at the south abutment beginning at 9:00 a.m. and lasted for 7 hours. The concrete that was placed in the south abutment from the first attempt was retained.

The concrete mixture design was modified by increasing the water-cement ratio from 0.42 to 0.45. This additional paste was added to assist with the difficulties in placing and finishing encountered in the first attempt. The plastic concrete was

tested out of the truck, approximately 15 minutes before being placed in the deck. The concrete test results are shown in Table 5.38. The slumps ranged from 1.75 to 5.25 in. (45 to 135 mm) with an average of 3.75 in. (95 mm). Three-quarters of the concrete tested had slumps greater than or equal to 3.5 in. (90 mm) and half of the concrete tested had slumps greater than or equal to 4.0 in. (100 mm). Concrete with slumps up to 5 in. (125 mm) was allowed to be placed in the deck. One truckload with a slump of 5.25 in. (125 mm) was placed in the deck without retesting after the conveyor. Air contents ranged from 7.8 to 9.7 percent with an average of 8.7 percent. The drop from the conveyor discharge to the deck was 12 to 15 ft (3.7 to 4.6 m), resulting in an air loss of 2.0 to 2.5 percent. The concrete temperature ranged from 60° to 69° F (16° to 21° C) with an average of 65° F (18° C). The average 28-day compressive strength of lab-cured cylinders was 4440 psi (30.6 MPa). Compressive strengths of field-cured cylinders were not measured

The consolidation procedures used in Placement 1 did not adhere to the requirements of the specifications, even though the contractor was specifically instructed on the correct procedures during the qualification slab. Coarse aggregate remained visible on the surface after the vibrators were removed from the concrete. The vibrators were removed too abruptly from the concrete, leaving holes at each insertion point (Figure 5.22).

The deck was finished using a double-drum roller screed with one drum removed, followed by a metal pan drag and extensive bullfloating. Bullfloating and hand-finishing were completed by a subcontractor specialized in finishing slabs, which may explain the apparent desire to apply an extra smooth surface to the deck. The bullfloating was performed in the longitudinal direction, perpendicular to the work bridge (Figure 5.23). This method of bullfloating is slow and requires additional space between the work bridge and the finishing equipment, both of which

Table 5.38 Concrete test results† – OP Bridge – Placement 1

KU Bridge Number	Slump	Air Content	Unit Weight	Concrete Temperature	28-Day Compressive Strength*
OP Bridge Placement 1	**in. (mm)**	**%**	**lb/ft^3 (kg/m^3)**	**° F (° C)**	**psi (MPa)**
Average	3.75 (95)	8.7	139.7 (2237)	65 (18)	4440 (30.6)
Minimum	1.75 (45)	7.8	136.6 (2188)	60 (16)	
Maximum	5.25 (135)	9.7	142.0 (2274)	69 (21)	

Percentage of Slump Measurements			Percentage of Air Content Measurements	
> 3.0 in. (75 mm)	**≥ 3.5 in. (90 mm)**	**≥ 4.0 in. (90 mm)**	**< 6.5%**	**> 9.5%**
75%	75%	50%	0%	10%

* Lab-cured specimens, no data obtained for field-cured specimens
†Concrete tested at truck discharge

Figure 5.22 Holes left in concrete surface due to improper consolidation – OP Bridge Placement 1

Figure 5.23 Bullfloating completed in longitudinal direction, perpendicular to work bridge – OP Bridge Placement 1

increase the time to burlap placement. More effort was put into finishing than other LC-HPC decks, leaving much of the deck overfinished. The finishers performed additional bullfloating although most of the surface appeared to be adequately finished after the passing of the pan drag. This overfinishing likely contributed to plastic shrinkage cracking by providing an additional layer of paste at the surface of the deck. The paste at the surface was increased an even greater extent as water that accumulated from fogging was worked into the deck by the bullfloating. Many short cracks resembling those associated with plastic shrinkage have developed throughout the deck. A detailed description of the cracking in the deck is provided in Chapter 6.

The placement of burlap was slow throughout construction, with an average placement time of 28 minutes. At times, the burlap placement time exceeded 40 minutes. The rate of burlap placement increased throughout the placement as the workers began to develop a routine; however, no burlap was placed in less than 20 minutes. Crack survey results in Section 6.2.36 show that the increased rate of burlap placement on the north end of the deck may have contributed to reduced cracking.

The slow burlap placement was caused by a number of factors, including delays in concrete delivery and finishing and the large width of Placement 1. In addition, the burlap could not be placed immediately after strikeoff because one work bridge was used for bullfloating and two were used for the burlap placement, requiring two front work bridges to always be positioned ahead of the burlap. The large width of the placement required three pieces of burlap to cover the entire width.

Cold-weather concreting procedures were followed for Placement 1. The bridge was enclosed underneath and eight heaters (four at each end of the deck) were used to heat the air under the deck. The air temperature under the deck was measured prior to and periodically during the deck placement. The temperature began at 42° F (6° C) at 9:00 a.m. and increased to 80° F (27° C) later in the day. City officials reported that the temperature increased to 85° F (29° C) on the evening of placement, but remained within the required range of 55° to 70° F (13° to 21° C) throughout the remainder of the 14-day curing period. The high early temperatures likely increased the tensile strain in the weak concrete deck.

5.3.22.6 OP Bridge Placement 2

The second placement of the OP Bridge, the west portion, was constructed on May 2, 2008 in approximately 7 hours. Placement began at the south abutment at 9:15 a.m. The placement included a 7.5-ft (2.3-m) wide sidewalk along the west edge. As with Placement 1, the concrete had a cement content and water-cement ratio of 535 lb/yd^3 (317 kg/m^3) and 0.45, respectively, and was placed with a conveyor belt.

The concrete supplier consistently produced concrete with high slump and air content. Heavy rains from the previous night caused difficulty in determining the moisture content of the aggregates. Concrete testing was completed out of the truck, before placement on the deck; however, two truckloads were tested before and after placement on the deck, with slump losses of 0.75 and 0.5 in. (20 and 15 mm) and air

losses of 1.4 and 2.4 percent for the two truckloads, respectively. These slump and air losses were used as justification for placing out-of-specification concrete throughout construction.

The concrete test results are shown in Table 5.39. Slumps ranged from 2.5 to 6.0 in. (65 to 150 mm) with an average of 4.25 in. (110 mm). Ten of the eleven slumps (91 percent) were greater than or equal to 3.5 in. (90 mm), and eight of the eleven (73 percent) were greater than or equal to 4.0 in. (100 mm). Air contents ranged from 7.0 to 11.0 percent with an average of 9.8 percent. Nine of the twelve air content values (75 percent) exceeded the allowable upper limit of 9.5 percent. The concrete temperature ranged from 63° to 65° F (17° to 18° C) with an average of 64° F (18° C). The average 28-day compressive strength of lab-cured cylinders was 3710 psi (25.6 MPa). Compressive strengths of field-cured cylinders were not measured.

Throughout the placement, city officials were persuaded by the contractor to accept concrete that did not meet the specifications. Additionally, the city officials indicated that concrete with a slump of 4.5 in. (115 mm) and an air content of 10.0 to 10.5 percent was "perfect" for use. The placement of high-slump concrete renders the deck increasingly susceptible to settlement cracking. Ultimately, LC-HPC specifications cannot provide improved cracking performance if they are not enforced.

The second placement of the OP Bridge went smoothly, partly because the out-of-specification concrete was continuously placed in the deck rather than rejected. Delays occurred near the beginning and end of placement due to adjustments to the mixture and the slow ordering of concrete. Crack survey results, shown in Section 6.2.37, indicate that the delay in placement at the south abutment likely contributed to increased cracking. Two delays at the end of placement due to backordered concrete lasted 30 and 15 minutes. As with Placement 1, the contractor put considerable effort into finishing the concrete. The deck was finished with a double-drum roller screed

Table 5.39 Concrete test results† – OP Bridge – Placement 2

KU Bridge Number	Slump	Air Content	Unit Weight	Concrete Temperature	28-Day Compressive Strength*
OP Bridge Placement 2	**in. (mm)**	**%**	**lb/ft^3 (kg/m^3)**	**° F (° C)**	**psi (MPa)**
Average	4.25 (110)	9.8	138.1 (2213)	64 (18)	3710 (25.6)
Minimum	2.5 (65)	7.0	134.7 (2157)	63 (17)	
Maximum	6.0 (150)	11.0	142.6 (2284)	65 (18)	

Percentage of Slump Measurements			Percentage of Air Content Measurements	
> 3.0 in. (75 mm)	**≥ 3.5 in. (90 mm)**	**≥ 4.0 in. (90 mm)**	**< 6.5%**	**> 9.5%**
91%	91%	73%	0%	75%

* Lab-cured specimens, no data obtained for field-cured specimens
†Concrete tested at truck discharge

(Figure 5.24) with a metal pan drag, followed by bullfloating and a large burlap drag mounted to the first work bridge. The extra burlap drag, shown in Figure 5.25, extended the time to place the burlap by requiring additional space between the strikeoff equipment and burlap placement.

Placement 2 was the first time a double-drum roller screed was used on a bridge let in accordance with the LC-HPC specifications. Bullfloating was used extensively on the last 30 ft (9.1 m) of the deck (north end) due to difficulty finishing caused by delays in concrete delivery. A finishing aid was used at this location as well. Although the use of bullfloating increased on the north end, less cracking has been observed in this section compared to the balance of the placement (described in Section 6.2.37). During the delays, a portion of the concrete that was placed in the wing wall was transferred to the deck in an effort to complete the placement. The sidewalk portion of the deck was screeded with 2 × 4-in. lumber. The surface was then bullfloated and finished by hand.

Figure 5.24 Double drum-roller screed used for finishing on OP Bridge Placement 2

Figure 5.25 Burlap drag used for finishing on OP Bridge Placement 2

As with Placement 1, burlap was placed slowly on Placement 2, with an average time of 21 minutes. One layer of burlap was placed at a time. A delay in burlap placement of 74 minutes occurred near the end of the construction (on the north end) due to significant delays in concrete delivery. As shown in Section 6.2.37, this delay did not appear to increase cracking relative to the balance of the deck. The burlap placement on the sidewalk was completed even more slowly than on the roadway, with placements ranging from 20 to 50 minutes. Surprisingly, the crack survey results (Section 6.2.37) indicate that less cracking has been observed on the sidewalk than on the roadway portion of the placement. The burlap was placed longitudinally along the sidewalk, with one piece of burlap placed for every four pieces placed on the roadway. During the delays in placement, any concrete that had been placed but not screeded or finished was covered with wet burlap.

Fogging, with a hand fogger, was used only once during a delay in concrete delivery, on the north end of the deck. The hand fogging resulted in some ponding on the deck, mainly along the east edge. Some of this water was worked into the deck by bullfloating. As described in Section 6.2.37, the east edge of the placement has experienced significant cracking, but no higher than the balance of this placement.

5.3.22.7 OP Bridge Placement 3

The third placement, and east portion, of the OP Bridge was constructed on May 21, 2008, 19 days after the construction of Placement 2. Placement began at the south abutment at about 6:00 p.m. and lasted for approximately 3.5 hours. The placement included a 10.5-ft (3.2-m) wide sidewalk along the east edge. The same concrete mixture and method of placement (conveyor belt) were used for this placement as were used in Placements 1 and 2.

As with Placement 2, the city officials appeared to be influenced by the contractor to accept concrete with higher slumps and air contents and had little interest in enforcing the specifications requirements. The results from the concrete

tests conducted at the truck discharge, shown in Table 5.40, indicate that all of the concrete placed in the deck had high slump and air content. Ultimately, the average slump and air content increased with each placement as construction progressed from Placement 1 to 3. Slumps ranged from 4.25 to 6.5 in. (110 to 165 mm) with an average of 5.25 in. (130 mm). Every concrete sample in Placement 3 had a slump that exceeded the allowable limit of 4.0 in. (100 mm). To make matters worse, a city official indicated that the deck reinforcement was not adequately supported, leaving it susceptible to upward deflections, which likely contributed to settlement cracking. The air content ranged from 9.5 to 10.5 percent with an average of 9.9 percent. Two truckloads were tested before and after the conveyor belt to establish slump and air losses. The slump losses were 2.5 and 2.0 in. (65 and 50 mm), while the air losses were 0.5 and 1.4 percent, respectively. The concrete temperature ranged from 62° to 67° F (17° to 19° C) with an average of 65° F (18° C). The average 28-day compressive strength of lab-cured cylinders was 3830 psi (26.4 MPa). The compressive strengths of field-cured cylinders were not measured.

Similar to Placement 2, the deck was finished using a double-drum roller screed with a pan drag, followed by a burlap drag attached to the first work bridge. The sidewalk portion of the deck was finished using a broom/hydraulic pump mechanism. The concrete was easily finished, primarily due to the high-slump concrete. Fogging was not used due to a low evaporation rate during placement.

The burlap placement, although completed slightly faster than for Placements 1 and 2, was completed more slowly than for typical LC-HPC decks. The time to burlap placement ranged from 9 to 21 minutes with an average of 15 minutes. A portion of the burlap was partially dry when placed on the deck, but was later rewetted with a spray hose. Unlike on Placement 2, the burlap placement on the sidewalk was completed at the same rate as the roadway.

Table 5.40 Concrete test results† – OP Bridge – Placement 3

KU Bridge Number	Slump	Air Content	Unit Weight	Concrete Temperature	28-Day Compressive Strength*
OP Bridge Placement 3	**in. (mm)**	**%**	**lb/ft^3 (kg/m^3)**	**° F (° C)**	**psi (MPa)**
Average	5.25 (130)	9.9	137.1 (2195)	65 (18)	3830 (26.4)
Minimum	4.25 (110)	9.5	135.1 (2165)	62 (17)	
Maximum	6.5 (165)	10.5	138.3 (2215)	67 (19)	

Percentage of Slump Measurements			Percentage of Air Content Measurements	
> 3.0 in. (75 mm)	**≥ 3.5 in. (90 mm)**	**≥ 4.0 in. (90 mm)**	**< 6.5%**	**≥ 9.5%**
100%	100%	100%	0%	100%

* Lab-cured specimens, no data obtained for field-cured specimens
†Concrete tested at truck discharge

5.3.23 LC-HPC Bridge 16

The construction of LC-HPC-15, 16, and 17 was included in a contract that involved substantial roadway improvements along the K-7 Highway corridor in Shawnee, KS. The contract was awarded to Miles Excavating, Inc. Construction of the three LC-HPC decks was subcontracted to R. A. Knapp Construction. LC-HPC-16 was the first LC-HPC bridge constructed in the contract and is discussed first. LC-HPC-16 is the southbound bridge on K-7 over Johnson Drive in Shawnee, KS, while LC-HPC-15 is the northbound bridge at the same location. LC-HPC-17 is the bridge on Clear Creek Parkway over K-7, less than a mile south of LC-HPC-15 and 16. Geiger Ready Mix supplied the concrete for the three bridges. These decks provided the first opportunity for the contractor and concrete supplier to work with the LC-HPC specifications. No associated control decks were selected to match with these three LC-HPC decks.

LC-HPC-16 is a steel plate-girder bridge with non-integral abutments and no skew. The bridge is 352.5 ft (107.4 m) long and 40.0 ft (12.2 m) wide, with two 176.25-ft (53.7-m) spans. The bridge was constructed in a single placement.

5.3.23.1 Concrete

The concrete mixture proportions were modified a number of times to accommodate problems with pumping and producing in-specification concrete. The concrete supplier initially elected to provide concrete with a cement content of 500 lb/yd^3 (296 kg/m^3) and a water-cement ratio of 0.45, even though the LC-HPC specifications permitted a maximum cement content of 540 lb/yd^3 (320 kg/m^3). The mixture with 500 lb/yd^3 (296 kg/m^3) of cement was used in the qualification batch and slab; however, this mixture did result in some problems with pumping during placement of the qualification slab. Two cement contents [520 and 540 lb/yd^3 (308 and 320 kg/m^3)] and water-cement ratios (0.44 and 0.45) were used in the concrete placed in the deck. Two granite coarse aggregates and a natural sand were used in the mixtures.

5.3.23.2 Qualification Batch

The qualification batch for LC-HPC 15, 16, and 17 was produced on September 14, 2010 at the batching plant of Geiger in Olathe, KS. Initially, the KDOT personnel in attendance were not aware of the procedure for the qualification batch and had to be informed by the concrete supplier. In addition, the concrete supplier, not the KDOT personnel, completed all of the concrete testing.

The first batch had an air content of 9 percent and a temperature of 75° F (24° C). Slump was not measured for this batch. The concrete supplier decided to produce a second batch since the concrete temperature exceeded the allowable upper limit of 70° F (21° C). The second batch, with a slump of 3.5 in. (90 mm), an air content of 9.5 percent, and a temperature of 70° F (21° C), was accepted.

5.3.23.3 Qualification Slab

The qualification slab for LC-HPC-15, 16, and 17 was placed successfully by pumping on October 14, 2010. The slab was constructed to a length of 100 ft (30.5 m) instead of the typical 33 ft (10.1 m) to allow the contractor to use the slab for additional functions. The center 33 ft (10.1 m) of the slab was constructed in accordance with LC-HPC specifications.

The mixture had a cement content of 500 lb/yd^3 (296 kg/m^3) and a water-cement ratio of 0.45. The first truckload was used only for the portion of the slab that did not require compliance with the specifications and was not tested. The second truckload was intended for use in the LC-HPC portion of the slab. With a slump of 3.5 in. (90 mm), an air content of 11.0 percent, and a temperature of 69° F (21° C), it did not meet the specifications for air content. Water was added to the truckload [15 gal (57 L)] and the concrete was used in the non-LC-HPC portion of the slab. The third truckload, with a slump of 3.25 in. (85 mm) and an air content of 8.25 percent at the truck, was used in the LC-HPC portion of the slab. After pumping, the concrete had a slump of 2.25 in. (55 mm), an air content of 6.8 percent, and a temperature of 65° F (18° C).

The pump worked well when placing concrete with slumps of 2.75 to 3.5 in. (70 to 90 mm); however, concrete with slumps below 2.75 in. (70 mm) was difficult to pump. The pump had problems restarting after setting idle for extended periods of time while waiting for the arrival of concrete. A mid-range water reducer was added to low-slump concrete to aide in restarting the pump. Placement of the concrete was slow and portions of the slab were left uncovered for more than 20 minutes.

The concrete was finished with a double-drum roller screed with one roller removed, followed by two metal pan drags. This finishing equipment appeared to provide a good seal of the surface. Near the end of the LC-HPC section (south side), the concrete was not sealing well and a bullfloat was used. Water was used as a

finishing aid on portions of the slab, but the contractor guaranteed that this would not occur during the deck placement.

The burlap was soaked, cut, and rolled onto large spools before construction began. The spools were attached to the ends of three, manually-controlled work bridges that were tied together. This technique of burlap placement allowed two workers to easily unroll and place the pre-cut pieces of burlap (Figure 5.26). Because the workers had difficulty moving the work bridges along the slab, the contractor indicated that the movement of the work bridges would be automated during the deck placement. At the beginning of construction, only four workers were working on the burlap placement. As construction progressed, more workers began to help with the repositioning of the work bridges to speed up the process of placing burlap. Even with more workers, the time to burlap placement was around 20 minutes. The burlap placement times ranged from 19 to 25 minutes. Sections of the placed burlap began to dry out quickly; however, no measures were taken to rewet this burlap.

5.3.23.4 LC-HPC-16 Placement

LC-HPC-16 was placed on October 29, 2010 beginning from the north abutment. Construction began at 11:00 a.m. and the last concrete was placed at 9:30 p.m., for a total construction time of 10.5 hours. Wind breaks were set up on the west and north sides of the deck to prevent rapid evaporation as the result of windy conditions. Due to the pumping difficulties during the qualification slab, the concrete mixture was modified for the deck placement by initially increasing the cement content to 520 lb/yd^3 (308 kg/m^3). The concrete supplier used ice as a partial replacement of mixture water for temperature control.

Most of the concrete was tested from the pump discharge. The pump contained a bladder valve to limit air losses, but the pump operator did not want to use the bladder valve due to the potential for increased wear. The results from the concrete tests are shown in Table 5.41. The slumps ranged from 1.25 to 5.75 in. (30

Figure 5.26 Pre-cut, pre-rolled burlap placed on qualification slab for LC-HPC-16

Table 5.41 Concrete test results† – LC-HPC-16

KU Bridge Number	Slump	Air Content	Unit Weight	Concrete Temperature	28-Day Compressive Strength
LC-HPC-16	**in. (mm)**	**%**	**lb/ft^3 (kg/m^3)**	**° F (° C)**	**psi (MPa)**
Average	3.75 (95)	6.4	141.1 (2259)	59 (15)	5040 (34.7)*
Minimum	1.25 (30)	4.3	136.8 (2190)	52 (11)	4350 (30.0)**
Maximum	5.75 (145)	8.7	145.3 (2326)	68 (20)	

Percentage of Slump Measurements			Percentage of Air Content Measurements	
> 3.0 in. (75 mm)	**≥ 3.5 in. (90 mm)**	**≥ 4.0 in. (90 mm)**	**< 6.5%**	**≥ 9.5%**
75%	56%	44%	45%	0%

* Lab-cured specimens
** Field-cured specimens
†Concrete tested at pump discharge

to 145 mm) with an average of 3.75 in. (95 mm). Twelve of the sixteen slumps measured at the pump discharge (75 percent) exceeded 3.0 in. (75 mm), nine of the sixteen (56 percent) were greater than or equal to 3.5 in. (95 mm), and seven of the sixteen (44 percent) were greater than or equal to 4.0 in. (100 mm). The air content ranged from 4.3 to 8.7 percent with an average of 6.4 percent. Five of the eleven air contents measured from the pump discharge (45 percent) were less than the allowable limit of 6.5 percent. Three truckloads (Truckloads 1, 14, and 24) were tested for slump and two truckloads (Truckloads 1 and 24) were tested for air content before and after pumping to establish slump and air loss values. The three truckloads exhibited slump losses of 1.25, 0.75, and 2.0 in. (30, 20, and 50 mm), respectively, while the two truckloads, respectively, exhibited air losses of 2.0 and 1.8 percent. The concrete temperature ranged from 52° to 68° F (11° to 20° C) with an average of 59° F (15° C). The average 28-day compressive strengths of lab and field-cured cylinders were 5040 and 4350 psi (34.7 and 30.0 MPa), respectively.

Pumping difficulties developed early in the placement. The pump became clogged while placing the second truckload and, as a result, water was added to the hopper on the back of the pump to aid the pumping. The concrete with the additional water, however, was not placed in the deck. The following several truckloads had slumps around 3.0 to 4.0 in. (75 to 90 mm), but were also not able to be pumped without effort. On several occasions, the pump operator added water to the hopper to aid pumping and then placed the concrete in the deck and the north abutment (Figure 5.27). KU personnel instructed the pump operator that the concrete with extra water could not be placed in the deck; however, this concrete was only disposed of on one occasion. A better effort was made to discard concrete with extra water on the second half (south side) of the placement, yet the practice occasionally occurred. As shown in the crack survey results in Section 6.2.40, higher cracking has been observed on the north side of the deck, possibly a result of the excess water.

Figure 5.27 Water added to hopper to aid pumping – LC-HPC-16

Due to persisting pumping issues, the cement content was increased from 520 to 540 lb/yd^3 (308 to 320 kg/m^3) near the midspan of the bridge. This additional cement ultimately increased the concrete slumps from 4.0 to 6.0 in. (100 to 150 mm) near midspan. To combat the high slumps, the water-cement ratio was then lowered from 0.45 to 0.44. Additionally, the concrete supplier reduced the amount of ice added to the truckloads from 60 to 20 lb/yd^3 (36 to 12 kg/m^3) in an attempt to reduce the slump by increasing the concrete temperature. This mixture was used for the final one-third of the placement (south end). The slumps remained high [4.0 to 5.0 in. (100 to 125 mm)] for the first few truckloads after the modifications were made, although subsequent concrete had slumps within the specifications.

A second pump replaced the first pump when the modifications were made to the concrete mixture. As with the first pump, the second pump contained a bladder valve to limit air losses. The concrete was pumped much more efficiently with the second pump compared to the first. Crack survey results, shown in Section 6.2.40, indicate that the north span (primarily placed with the first pump) has higher cracking

than the south span. The first pump was relocated and used again for the final 50 ft (15.2 m) of the deck. As before, significant pumping difficulties were encountered with the first pump. KU personnel suspected that the first pump was not performing properly and the pumping difficulties could not be entirely blamed on the concrete.

As with the qualification slab, the concrete was finished with a double-drum roller screed with one roller removed, followed by two metal pan drags. The edges of the deck were not able to be reached by the screed and were finished by hand with wooden trowels. The deck finished well and no bullfloating was needed, partially due to the high-slump concrete.

Prior to the placement of concrete, it was noted that the contractor did not dampen the forms and reinforcement. The contractor stated that the reinforcement was cleaned on the previous day and the forms had been oiled. After about 30 ft (9.1 m) of placement, the contractor was instructed to dampen the bridge and clean dirt from the reinforcement. This task was carried out for about 30 ft (9.1 m) and then stopped.

Similar to the qualification slab, the burlap was soaked, cut, and rolled onto large spools attached to each work bridge prior to the construction. Three to five workers were assigned to place the burlap. The burlap placement was slow, with times ranging from 10 to 65 minutes with an average of 18 minutes; however, the long delays were a result of concrete placement problems, not inefficiencies in the process of burlap placement. No burlap was placed over the freshly-finished concrete during the delays. Two sprinklers were used to keep the burlap wet after placement. Some ponding from the sprinklers was noted along the deck edges near the pier and, as a result, the contractor was instructed to shut off one sprinkler. The crack survey results shown in Section 6.2.40 indicate that a number of cracks have been observed near the pier along the deck edges, possibly a result of the ponded water. Ponding was noted yet again with the use of one sprinkler, prompting the contractor to begin

wetting the burlap occasionally with a spray hose. At a few locations, the burlap was blown away from the deck, leaving the deck uncovered. The contractor repositioned this burlap. At times, the burlap was not properly tucked near the barrier reinforcement, leaving the concrete uncovered near the reinforcement (Figure 5.28).

The girders and deck were wrapped for the 14-day curing period in compliance with the specifications for cold weather concreting.

5.3.24 LC-HPC Bridge 15

LC-HPC-15 is the northbound bridge on K-7 over Johnson Drive in Shawnee, KS, located adjacent to LC-HPC-16 (southbound bridge). As previously stated, the construction of LC-HPC-15, 16, and 17 was included in a single contract.

LC-HPC-15 is a two-span, steel plate-girder bridge with non-integral abutments and no skew. The bridge has identical dimensions to that of LC-HPC-16 and was constructed in a single placement. As a result of the many difficulties encountered with pumping on LC-HPC-16, the contractor elected to place the deck using two crane buckets.

5.3.24.1 Concrete

The original mixture design accepted in the qualification batch and slab was used in LC-HPC-15 since crane buckets were used for placement. This mixture had a cement content of 500 lb/yd^3 (296 kg/m^3) and a water-cement ratio of 0.45. Two granite coarse aggregates and a natural sand were used in the mixture.

5.3.24.2 Qualification Batch

The qualification batch produced on September 14, 2010 served as the qualification batch for LC-HPC-15, 16, and 17.

Figure 5.28 Burlap improperly tucked near barrier reinforcement – LC-HPC-16

5.3.24.3 Qualification Slab

The qualification slab placed on October 14, 2010 served as the qualification slab for LC-HPC-15, 16, and 17.

5.3.24.4 LC-HPC-15 Placement

LC-HPC-15 was placed on November 10, 2010 beginning from the south abutment starting at 7:15 a.m. The placement was completed at approximately 8:40 p.m., for a total construction time of about 13.5 hours. Two cranes with two buckets each were used for the majority of the placement. A photo of a crane bucket placing concrete is shown in Figure 5.29. A fifth bucket was used near the ends of the deck to place the abutments.

The concrete was tested from the truck discharge. The results from the concrete tests are shown in Table 5.42. The slumps ranged from 1.5 to 6.0 in. (40 to

Figure 5.29 Concrete placed by crane bucket for LC-HPC-15

Table 5.42 Concrete test results† – LC-HPC-15

KU Bridge Number	Slump	Air Content	Unit Weight	Concrete Temperature	28-Day Compressive Strength
LC-HPC-15	**in. (mm)**	**%**	**lb/ft^3 (kg/m^3)**	**° F (° C)**	**psi (MPa)**
Average	3.25 (85)	9.0	137.4 (2200)	63 (17)	4440 (30.6)*
Minimum	1.5 (40)	7.0	134.8 (2158)	58 (14)	3980 (27.4)**
Maximum	6.0 (150)	10.6	139.2 (2229)	68 (20)	

Percentage of Slump Measurements			Percentage of Air Content Measurements	
> 3.0 in. (75 mm)	**≥ 3.5 in. (90 mm)**	**≥ 4.0 in. (90 mm)**	**< 6.5%**	**> 9.5%**
74%	52%	22%	0%	33%

* Lab-cured specimens
** Field-cured specimens
†Concrete tested at truck discharge

150 mm) with an average of 3.25 in. (85 mm). Seventy-four percent of the measured slumps exceeded 3.0 in. (75 mm), 52 percent were greater than or equal to 3.5 in. (90 mm), and 22 percent were greater than or equal to 4.0 in. (100 mm). The air content ranged from 7.0 to 10.6 percent with an average of 9.0 percent. Thirty-three percent of the measured air contents exceeded the upper allowable limit of 9.5 percent. The concrete temperature ranged from 58° to 68° F (14° to 20° C) with an average of 63° F (17° C). The average 28-day compressive strengths of lab and field-cured cylinders were 4440 and 3980 psi (30.6 and 27.4 MPa), respectively.

The first few truckloads had low slumps, ranging from 1.5 to 2.0 in. (40 to 50 mm). The concrete supplier, however, would occasionally add a mid-range water reducer after the slumps were measured. At the beginning of the placement, the concrete containing the additional water reducer was not retested. Eventually, the testing crew began testing the concrete after the water reducer was added. Four truckloads that were placed near the middle of the deck had high slumps, ranging from 4.0 to 6.0 in. (100 to 150 mm). Although these truckloads were eventually set aside to allow for the slump to drop, portions of the concrete had already been placed in the deck before placement was halted. As discussed in Section 6.2.41, increased cracking has been observed near the middle of the deck where this high-slump concrete was placed. Most of these truckloads were not retested before being placed in the deck. Ultimately, most of the concrete placed in the first half (south half) of the deck had a slump of 3.5 in. (90 mm) or more. The concrete placed in the second half (north half) of the deck had more consistent slumps, ranging from 3.25 to 3.5 in. (85 to 90 mm). As discussed in Section 6.2.41, somewhat higher cracking is observed in the north span, the region where the slumps were consistently lower. Several truckloads placed near the beginning of the second half of the deck had air contents above 10 percent.

Throughout the placement, two crane buckets simultaneously placed concrete on the deck. On one occasion, a crane bucket was dropped onto the reinforcing steel, bending some of the steel. The contractors were able to realign the reinforcement with a crane and new chairs were inserted beneath the bars.

As with LC-HPC-16, the deck finished well using a double-drum roller screed with one roller removed, followed by two metal pan drags. Hand-finishing was again used on the edges of the deck where the screed could not reach. Due to a delay in concrete placement, the first 45 ft (13.7 m) of the deck (south end) was exposed for about 30 minutes without burlap cover. The crack survey results indicate that this delay did not significantly affect cracking. The exposed concrete became difficult to finish and required the use of bullfloating. The remainder of the deck finished well after the first pan passed behind the screed. The contractor was able to adequately finish concrete with low slumps [approximately 2.0 in. (50 mm)]. The screeding equipment leaked a small amount of oil on the deck, but the contractor adequately plugged the leak with towels.

The same method of burlap placement used on LC-HPC-16 was also used on LC-HPC-15 (Figure 5.30). Throughout the entire placement, the burlap cover was completed immediately behind the screeding equipment. Any delays in burlap placement were the result of problems with concrete placement. Two sprinklers and, occasionally, spray hoses were used to keep the placed burlap wet. At one point, ponding was observed, and as a result, the contractor immediately stopped the use of the sprinklers. On one occasion, water ponded on the concrete in front of the burlap placement. This ponding was likely caused by water being sprayed on the deck as the burlap roll was rewetted. Afterward, rewetting of the burlap was completed using a spray hose pointing away from the uncovered concrete.

The evaporation rate remained below the limit of 0.2 lb/ft^2/hr (1.0 kg/m^2/hr) required by the specifications.

Figure 5.30 Burlap placement on LC-HPC-15

5.3.25 LC-HPC Bridge 17

LC-HPC-17 is the bridge on Clear Creek Parkway over K-7, less than a mile south of LC-HPC-15 and 16. The bridge is a two-span, steel plate-girder bridge with non-integral abutments and no skew. LC-HPC-17 is 302.5 ft (92.2 m) long with two span-lengths of 151.3 ft (46.1 m) each. The bridge has a roadway width of 30.0 ft (9.1 m) and contains a 6-ft (1.8-m) sidewalk on the north side and a 10-ft (3.0-m) "recreational trail" on the south side. The bridge is located within a vertical curve, with approaching roadway grades of 6 percent on each side, connecting to the bridge. The vertical curve is apparent in the photo in Figure 5.31. The deck was constructed in a single placement using two pumps.

The contractor and KDOT district representatives were reluctant to place the deck in accordance with the LC-HPC specifications for a number of reasons. First, the construction layout made pumping the most practical method of placement; however, pumping this deck concerned the contractor because of the many issues experienced while pumping LC-HPC-16. This construction layout prevented crane

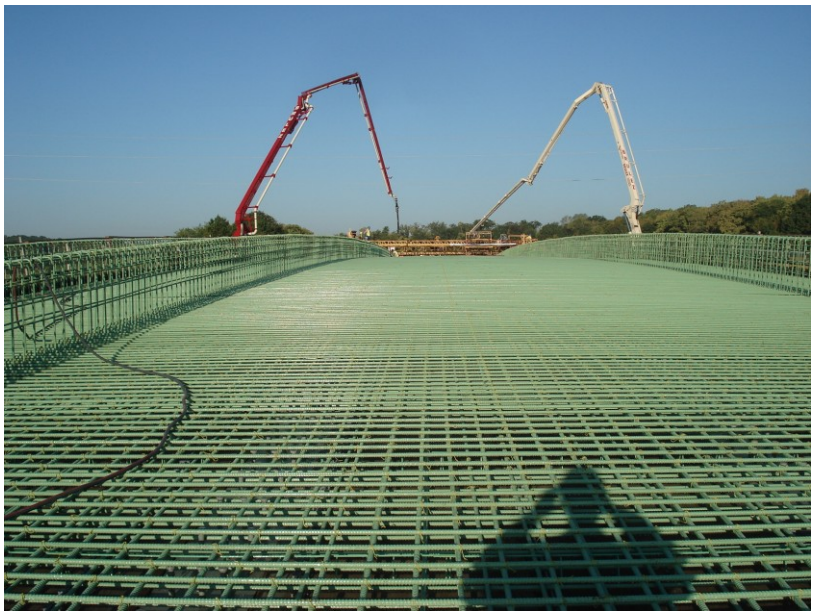

Figure 5.31 Vertical curve within LC-HPC-17

buckets or conveyors from being used due to open lanes of traffic below the deck on K-7 and the vertical curve within the bridge. In addition, the bridge design included unique characteristics that increased the difficulty of compliance with the LC-HPC requirements for curing. The sidewalk and recreational trail were separated from the roadway by barriers, preventing them from being finished with the equipment used on the roadway and, ultimately, extending the time to burlap placement. A photo of the recreational trail on the south edge prior to placement is shown in Figure 5.32. Furthermore, the sidewalk and recreational trail were specified as stamped colored and colored concrete, respectively, and the process of stamping and coloring the concrete would additionally increase the time to burlap placement.

After discussions with KDOT and KU representatives, the contractor agreed to construct the deck in accordance with the LC-HPC specifications under the condition that two deviations from the specifications were allowed. First, to ensure that pumping could be used, the contractor requested that additional redosing of water

Figure 5.32 Barrier between recreational trail and roadway contributed delays in finishing and curing – LC-HPC-17

reducer be allowed on-site. The specifications allowed for one redosing of water reducer on-site. Additionally, due to the increased time to burlap placement as a result of the unique requirements for the sidewalk, the contractor proposed that a monomolecular film be used to cover the exposed concrete prior to burlap placement to combat any delays in curing. All parties agreed to the deviations.

5.3.25.1 Concrete

The concrete supplier attempted to design a more pumpable mixture for LC-HPC-17 because of the many pumping issues experienced with LC-HPC-16. The new mixture had a cement content of 540 lb/yd^3 (297 kg/m^3), a water-cement ratio of 0.45, and an optimized gradation using four aggregates (two granite coarse aggregates, pea gravel, and natural sand).

5.3.25.2 Qualification Batch

Although the qualification batch produced on September 14, 2010 served for LC-HPC-15, 16, and 17, an additional batch that contained the new concrete mixture

was produced on September 14, 2011 to determine the pumpability of the mixture. No KU representatives were in attendance for this qualification batch. The test verified that the mixture was pumpable and placeable and that the slump and air content were controllable.

5.3.25.3 Qualification Slab

The qualification slab placed on October 14, 2010 served as the qualification slab for LC-HPC-15, 16, and 17.

5.3.25.4 LC-HPC-17 Placement

LC-HPC-17 was placed on September 28, 2011 beginning from the west abutment at 7:00 a.m. The placement was completed at 9:20 p.m., for a total construction time of about 14.5 hours. Overall, construction proceeded smoothly; however, many aspects of the LC-HPC specifications were not followed.

Plastic concrete was tested either at the truck or at the pump discharge; some concrete was tested at both locations. The results of the concrete tests are shown in Table 5.43. The test results, however, do not accurately represent the entire deck since few of the final 20 truckloads, representing approximately 100 ft (30.5 m) on the east end of the deck, were tested. The measured slumps ranged from 1.5 to 6.0 in. (40 to 150 mm) with an average of 3.25 in. (85 mm), mirroring the slumps on LC-HPC-15. Thirty-seven percent of the slumps were greater than or equal to 3.5 in. (90 mm) and 26 percent were greater than or equal to 4.0 in. (100 mm). The air content ranged from 5.5 to 9.0 percent with an average of 7.0 percent. Eighteen percent of the air contents were lower than the allowable limit of 6.5 percent. The concrete temperature ranged from 68° to 80° F (20° to 27° C) with an average of 72° F (22° C). The average 28-day compressive strength of the lab-cured cylinders was 5160 psi (35.6 MPa). The compressive strengths of field-cured cylinders were not measured.

Table 5.43 Concrete test results† – LC-HPC-17

KU Bridge Number	Slump	Air Content	Unit Weight	Concrete Temperature	28-Day Compressive Strength*
LC-HPC-17	**in. (mm)**	**%**	**lb/ft^3 (kg/m^3)**	**° F (° C)**	**psi (MPa)**
Average	3.25 (85)	7.0	141.2 (2261)	72 (22)	5160 (35.6)
Minimum	1.5 (40)	5.5	140.7 (2253)	68 (20)	
Maximum	6.0 (150)	9.0	141.5 (2266)	80 (27)	

Percentage of Slump Measurements			Percentage of Air Content Measurements	
> 3.0 in. (75 mm)	**≥ 3.5 in. (90 mm)**	**≥ 4.0 in. (90 mm)**	**< 6.5%**	**> 9.5%**
37%	37%	26%	18%	0%

* Lab-cured specimens, no data obtained for field-cured specimens
†Concrete tested at either truck or pump discharge

Slump and air losses were established by testing the first two truckloads at both the truck and pump discharge. The slump loss for the first two truckloads was 0.5 in. (15 mm) and the air loss of the first truckload was 1.5 percent. The first three truckloads had relatively low slumps [2.0 in. (50 mm) each] and were pumped without difficulty. This concrete was placed in the abutment. The first few truckloads placed in the deck had slumps of around 2.5 in. (65 mm) and experienced minor pumping issues. As a result, the concrete supplier increased the dosage of water reducer added at the plant. This increase in dosage improved the pumping performance, but also contributed to high slumps of 4.5 to 5.0 in. (115 to 125 mm) in Truckloads 7 through 10. This concrete was placed in the deck [approximately 60 ft (18 m) from the west abutment], but the concrete supplier was instructed to lower the slump in the following truckloads. The crack survey results shown in Section 6.2.42 indicate the region where the high-slump concrete was placed experienced higher cracking. The concrete supplier decreased the dosage of water reducer added at the plant and began to redose as needed on-site. This method was successful in lowering

the slump; however, the following truckloads with the decreased dosage of water reducer experienced some pumping difficulties (discussed below).

Starting with Truckload 15, the concrete supplier began replacing a portion of the mixture water with ice to aid in controlling the concrete temperature. Despite the addition of ice to the following truckloads, concrete temperatures were near the upper limit of 75° F (24° C) [values above 70° F (21° C) must be approved by the Engineer]. As a result, the concrete supplier increased the addition of ice from 8 to 16 lb/yd^3 (5 to 10 kg/m^3).

The frequency of testing was greatly reduced during placement of the final 20 truckloads. The majority of these truckloads were accepted based on visual inspection for slump and a check of concrete temperature with an infrared thermometer at the truck discharge. Visually, most of the truckloads appeared to have slumps between 3 and 4 in. (90 and 100 mm). Truckload 43 was rejected after the slump was visually-estimated to be 5 in. (125 mm). The final three truckloads that were tested from the truck discharge (Truckloads 27, 30, and 35) had air contents less than or equal to the lower allowable limit of 6.5 percent; therefore, it is possible that portions of the east side of the deck contain concrete with low air content.

As stated previously, two pumps were used to place the deck. The first pump was positioned near the west end of the bridge while the second pump was located near the middle of the bridge, in the grassy median of K-7 Highway. The first 90 ft (27 m) of the deck was placed with the first pump with little difficulty. The contractor switched to the second pump around noon and immediately began having pumping problems. After struggling with the second pump for more than an hour, the first pump was relocated and was used for much of the remainder of the deck. Once the second pump was repaired, both pumps simultaneously placed concrete. As shown in Section 6.2.42, the highest cracking in the deck was observed

approximately 60 to 120 ft (18 to 37 m) from the west abutment, near the location at which the pumping problems began.

The sidewalks and roadway were finished at the same time, but with separate equipment. The roadway was finished using a double-drum roller screed positioned to move in the transverse direction, followed by two metal pan drags. Excluding Placements 2 and 3 of the OP Bridge, LC-HPC-17 was the only case in which a double-drum roller screed was used on a deck let in accordance with the LC-HPC specifications. The sidewalks were struckoff with a single-drum roller screed oriented in the transverse direction that was moved manually in the longitudinal direction (Figure 5.33) and then hand-finished and broomed by workers. A monomolecular curing compound was sprayed on the finished deck surface prior to burlap placement to provide protection during extended periods of finishing. Bullfloating was used and was excessive on the driving lanes of the west half of the deck after the final pan passed and the curing compound was sprayed on the surface. According to the contractor, this high degree of bullfloating was performed to seal holes in the surface. These holes, however, were a result of delayed finishing. The contractor minimized bullfloating on the driving lanes of the east half of the bridge, but put considerable effort into finishing the concrete near the vertical barrier reinforcement. Crack survey results shown in Section 6.2.42 indicate that cracking was higher in the west span, the location in which the excessive bullfloating occurred, than in the east span. The extensive finishing slowed the initiation of curing and subjected the concrete to additional exposure to the environment. In some instances, the curing compound was sprayed on the unfinished concrete and then worked into the concrete by the pan drags. On occasion, the container holding the curing compound leaked on the north sidewalk, leaving small puddles. These puddles were later worked over with hand trowels. Any influences on cracking from the finishing

Figure 5.33 Single-drum roller screed used for strikeoff of sidewalks – LC-HPC-17

and curing techniques used on the sidewalks remain unclear because the coloring of this concrete has limited the ability to accurately survey these regions.

During delays in placement and finishing, the drum rollers continuously finished the surface even as the finishing equipment stopped moving forward. As a result, portions of the deck were overfinished. After the contractor was notified of this issue, the drum rollers on the roadway were shut off. The single-drum rollers on each sidewalk, however, continued to finish the surface and likely brought additional paste to the surface.

Throughout placement, application of the curing compound was delayed 15 to 30 minutes after strikeoff as a result of excessive bullfloating by the contractor. In addition, portions of the east side of the deck were not completely covered with the curing compound. A portion of the deck at the west end was left uncovered for approximately 1.5 hours, the same region in which pumping difficulties were encountered. The crack survey results, shown in Section 6.2.42, indicate the existence of high cracking in this exposed area at the west end. The entire east side of the deck was exposed for at least 30 minutes after strikeoff. The final 30 ft (9.1 m) of

the east side of the deck was left uncovered for about two hours, but the evaporation rate was well below the limit of 0.2 lb/ft^2/hr (1.0 kg/m^2/hr) throughout deck placement. The crack survey data indicate that cracking is minimal in this region. The burlap on the west end of the deck was partially dry when placed and, as a result, the contractor was instructed to immediately wet down the placed burlap. The contractor was hesitant to spray water on the dry burlap for fear that the water would flow onto the unfinished concrete due to the slope of the bridge. The roadway portion of the deck was covered with two layers of burlap, while the sidewalks were covered with a single layer. On the west end of the deck, the burlap was not properly tucked in at the barrier reinforcement, leaving the concrete exposed adjacent to the barriers. The contractor was notified and the burlap was properly tucked.

In the end, the contractor did have a number of difficulties with this deck, but those difficulties appeared to be largely due to a lack of planning, poor organization on the job site, and the inability to take advantage of the experience gained on LC-HPC-15 and 16. During construction, it often appeared that the deck was being constructed by a different company than had completed LC-HPC-15.

5.3.26 LC-HPC Bridge Deck Construction – Summary of Experiences and Proposed Methods of Improvement

The experiences gained during construction of the 17 bridge decks let in accordance with the LC-HPC specifications are summarized in this section. Many experiences were positive and construction of all but one of the 17 decks complied with the greater part of the specifications. Even so, similar missteps occurred during the construction of many decks. Lessons were learned from the construction of each deck to improve future LC-HPC construction. The matters that impacted construction in conjunction with proposed methods for improvement are documented in this section. An updated version of the LC-HPC specifications, provided in Appendix G,

has been created based on these methods for improvement and findings from the laboratory evaluation described in Chapter 4.

5.3.26.1 Concrete Placement

Successful construction in accordance with the LC-HPC specifications includes the design of a concrete mixture that offers beneficial cracking performance (low paste content, moderate strength, etc.) while also providing a workable and placeable concrete. Although concrete with a low paste content and slump will provide low cracking potential, it is important that it be placed quickly (most commonly using a pump). Delays in placement lead to subsequent delays in strikeoff, finishing, and curing, and allow the concrete to be exposed longer to the environment, contributing to plastic shrinkage cracking.

The construction observations in this study suggest that contractors are hesitant to place concrete in any way other than pumping. Many contractors feel that placement by conveyor or crane bucket is overly slow compared to placement by pump. Of the twenty-two placements in decks let in accordance with the LC-HPC specifications, fourteen were placed by pump, five were placed by conveyor, and three were placed using crane buckets.

LC-HPC mixtures with a water-cement ratio of 0.44 to 0.45 pumped well, while mixtures with a water-cement ratio of 0.42 were occasionally difficult to pump, likely due to the stickier paste and the lower total paste content. Thus, during the construction of a number of decks, the water-cement ratio was increased from 0.42 to 0.44 or 0.45 to increase the paste content to improve pumping performance. Current LC-HPC specifications require a water-cement ratio of 0.44 or 0.45. Occasionally, a portion of the mixture water was held out during the construction to achieve better control of the slump. This reduction in water often led to pumping difficulties. While a reduction in water reduces the paste content and improves shrinkage performance, it also lowers the water-cement ratio and increases strength. As

discussed in Chapter 1, an increase in compressive strength can lead to increased cracking by increasing the modulus of elasticity (increased stress for a given strain) and decreasing the beneficial effects of creep in the concrete. Withholding mixture water is now prohibited in LC-HPC specifications.

Pumping difficulties during the construction of several decks were attributed to characteristics of the aggregates. LC-HPC-4 and 5 and the OP Bridge experienced problems with pumping because angular, manufactured sand was used as part of the fine aggregate fraction in the concrete. More rounded, natural sand improves the pumpability of concrete. In fact, the concrete used in LC-HPC-8 and 10 pumped without difficulty while having the same cement content [535 lb/yd^3 (317 kg/m^3)] and water-cement ratio (0.42) as LC-HPC-4 and 5 and the OP Bridge but without manufactured sand. The concrete placed in the qualification slabs for LC-HPC-11 and 9 was difficult to pump due to the presence of excessively-elongated and overly-large coarse aggregate particles, respectively. An overestimation of the free surface moisture content of the fine aggregate contributed to pumping problems during Placement 1 of LC-HPC-4. This overestimation supplied the concrete with less water than was expected, lowering the water-cement ratio and paste content.

Different pumps used by the various contractors often had large variances in capability. For example, concretes with slumps as low as 1.5 in. (40 mm) were pumped at times with no trouble, while concretes with slumps as high as 4.0 in (100 mm) occasionally experienced pumping problems. During the construction of LC-HPC-16, one pump continuously experienced problems while the other pump on the job site placed the same concrete without trouble. These observations suggest that poorly-performing pumps contributed to a portion of the pumping difficulties. Two pumps should be available on-site to minimize any delays due to problems with pumping. Additionally, the second pump can continue the placement of concrete if the first pump must be relocated.

5.3.26.2 Qualification Batch and Slab

The qualification batch and slab contribute to successful LC-HPC construction by allowing the contractor and concrete supplier to become familiar with the LC-HPC specifications prior to deck placement. In many instances, the contractor was able to gain valuable knowledge during placement of the slab. The qualification slab was often waived when a contractor had recently constructed an LC-HPC deck; however, an additional qualification slab was occasionally required, as with LC-HPC-8, after the contractor had experienced a number of problems during construction of a previous LC-HPC deck. The additional qualification slab required prior to placement of LC-HPC-8 proved to be valuable as LC-HPC-8 was constructed much more efficiently than the previous LC-HPC deck, LC-HPC-10.

During the qualification slab, the contractor must accurately simulate the procedures planned for the deck placement. For example, during placement of the qualification slab for LC-HPC-11, the workers used the ground around the slab for burlap placement. This workspace was not accessible during the deck construction, and using it during construction of the qualification slab did not provide the workers with the appropriate experience. During construction of the qualification slabs for LC-HPC-13 and the OP Bridge, the slabs had different widths than the decks. Consequently, the workers were unable to become familiar with the number of pieces of burlap needed to cover the full width of the deck. The same workers should complete the same tasks on both the qualification slab and deck. For example, during placement of LC-HPC-3 and 7, a different crew completed the burlap placement on the deck and qualification slab. As a result, the burlap was placed on these decks by crews with no prior experience with LC-HPC construction.

The requirements of the qualification batch and slab must be enforced to verify the ability of the contractor and concrete supplier to comply with the specifications. During the qualification batch for LC-HPC-1 and 2, the concrete

supplier did not take actions to control the concrete temperature and, as a result, concrete was produced with a temperature of 89° F (32° C). The qualification batch was accepted because it was decided that the concrete temperature could be adequately controlled during construction. During the first attempt at placement of the qualification slab, however, the concrete supplier was unsuccessful in controlling the concrete temperature with chilled water, and as a result, the placement was cancelled.

5.3.26.3 Finishing and Burlap Placement

Excessive finishing was observed on a number of LC-HPC decks, most notably on the OP Bridge placements. Not only does excessive finishing work additional paste to the surface that can contribute to plastic shrinkage cracking, but the time taken for the additional finishing lengthens the time that the concrete is exposed to the environment, further contributing to plastic shrinkage cracking. Double-drum roller screeds with both rollers attached were used on just a few LC-HPC placements. The act of finishing with two rollers works additional paste to the surface, which can contribute to plastic shrinkage cracking. The use of two rollers is not needed for a well-proportioned concrete mixture and is prohibited in the current LC-HPC specifications.

The time from strikeoff to placement of burlap often exceeded the limit of 10 minutes indicated in the specifications. Many times, this delay was due to delays in concrete delivery, placement, or finishing. This observation reinforces the importance of delivering, placing, and finishing the concrete in a timely manner. Many decks experienced delays in burlap placement near the end of construction due to the insufficient availability of concrete, the placement of an abutment, or the removal of construction equipment from the deck. During the construction of LC-HPC-17, a portion of the deck near the end of construction was left uncovered for approximately two hours. During extended delays, all exposed concrete, including

concrete that is consolidated, unconsolidated, finished, or unfinished, must be covered with wet burlap.

An appropriate plan for burlap placement must be established by the contractor prior to construction. A placement sequence should be instituted with consideration for the width of the deck and the length of the burlap pieces. It is best to cover the entire width of the deck with burlap before continuing the burlap placement longitudinally along the deck. This method prevents strips of concrete from being exposed along the deck edges for extended periods of time. The number of burlap pieces required to cover the full width of the deck should be determined in advance. An alternate method of burlap placement was used for LC-HPC-5 that possibly contributed to increased cracking. For LC-HPC-5, single burlap pieces were placed transversely across a partial-width of the deck, leaving a concrete strip along the edge of the deck exposed for extended periods. A single burlap piece was eventually placed longitudinally over the exposed strip after the placement of four or five transverse pieces. A description of the cracking performance of this deck, provided in Chapter 6, shows that the region left exposed experienced increased cracking.

After the burlap is placed on the deck, it must be kept saturated throughout the construction and curing period. In addition, the burlap must be fully saturated prior to construction. The use of partially-dry burlap has the potential to be more detrimental than the use of no burlap because of its capability to draw water from the concrete and cause drying shrinkage cracking. In contrast, excessive water after burlap placement has the potential to pond water on the deck surface and increase the water-cement ratio of the paste on the upper surface. A number of times, the contractor became overly concerned with other aspects of construction and neglected to ensure that the burlap remained wet. A single worker should be designated to oversee the condition of the placed burlap during construction.

The transverse grade of the deck must be considered when determining the placement of soaker hoses for maintaining the saturation of burlap. During the placement of LC-HPC-5 and 6, soaker hoses were positioned on the burlap near the center of the decks. Due to the superelevation of the decks, the higher side of the deck did not receive sufficient water during the curing period. A description of cracking in these decks, provided in Chapter 6, shows that the upper edges experienced more cracking than the rest of the deck.

5.3.26.4 Concrete Acceptance and Testing

A strict concrete acceptance and testing plan must be established prior to construction. All parties involved, including the contractor, concrete supplier, and owner, must be in full agreement on implementing of this plan. As stated earlier, LC-HPC specifications cannot minimize cracking if concrete is accepted that does not comply with the specifications. A prime example of the negative effects of the acceptance of out-of-specification concrete is provided by the OP Bridge placements. Throughout construction of these placements, the owner did not enforce and the contractor did not comply with the LC-HPC specifications. The owner experienced significant pushback from the contractor throughout construction, especially after the first attempt of Placement 1 was torn out, the choice of the contractor, not the owner. Ultimately, high-slump concrete was accepted for all placements, and every concrete sample tested during the third placement had a slump above 4.0 in. (100 mm), the upper allowable limit of the specifications. At one point, a city official remarked that concrete with a slump of 4.5 in. (115 mm) and an air content of 10.0 to 10.5 percent was “perfect” for use. The poor cracking performance of the three placements of the OP Bridge is described in Chapter 6. As stated previously, these placements are not considered LC-HPC placements because of the many aspects of the specifications that were not followed.

A strict acceptance plan was established prior to placement of LC-HPC-3. During placement of LC-HPC-3, concrete was sampled and tested from the ready-mix trucks to ensure that all concrete placed in the deck met the specifications. No concrete with a slump exceeding 4.0 in. (100 mm) or an air content exceeding 9.5 percent was placed in the deck. Truckloads that did not initially meet the specifications were rejected or held and retested prior to placement in the deck. This plan proved to be successful given that all concrete placed in the deck met the specifications.

In spite of this, a majority of the LC-HPC decks involved the acceptance and placement of out-of-specification concrete. For example, high-slump concrete was frequently placed in LC-HPC-6 and LC-HPC-12 Placement 2, resulting in average slumps of 4.0 and 4.25 in. (100 and 110 mm), respectively. These average values, in addition to the average slump values for the OP Bridge Placements 2 and 3, are, in fact, higher than the average slumps for a number of the control decks. Occasionally, KDOT personnel were reluctant to reject concrete that did not meet the specifications, primarily near the end of a long day. During the construction of LC-HPC-6, 15, 16, and 17, KDOT personnel accepted out-of-specification concrete due to the lengthy construction periods and considerable pushback from the contractors and concrete suppliers.

A clear strategy for testing concrete must be implemented by the owner and testing technicians. It is good practice to test the first few truckloads for all properties, including slump, air content, temperature, and unit weight. This testing at the beginning of placement verifies that the concrete supplier has settled into a routine of producing acceptable concrete and sets a tone for what will be accepted during placement. The frequency of testing can be reduced later in the placement; however, if one truckload is found to not meet the specifications, successive truckloads should also be tested until the specifications are met. In addition, each

truckload should be visually-checked by an experienced inspector and any concrete suspected to not meet the specifications should be tested. Considering the very physical nature of concrete testing, retests of out-of-specification concrete should be made by concrete-supplier personnel under the supervision of the owner's inspectors.

It is acceptable to set aside truckloads with high slumps and/or air contents to provide an opportunity for the concrete properties to drop to within the specified ranges. Concrete not compliant with the specifications must be retested prior to use in the deck. During the placement of the LC-HPC decks, out-of-specification truckloads set aside in an attempt to allow slump and air content to drop into the specified range were occasionally placed in the decks without retesting. In addition, truckloads with low slumps that received an additional dose of water reducer on-site were occasionally not retested prior to placement in the deck.

Consideration must be given to the location where the concrete is initially evaluated and tested. Testing for some LC-HPC decks was completed primarily at the truck discharge, while testing of other decks occurred primarily on the deck. Evaluating at the truck prior to placement of any concrete, especially if an inspector can visually identify changes in the concrete, increases the probability that out-of-specification concrete will be rejected before it is placed in the deck. When concrete is not checked at the truck and is tested on the deck and only then deemed out-of-specification, a portion of this concrete is likely already placed in the deck before it is rejected. Testing alone at the truck will not prevent the placement of out-of-specification concrete in the deck because official tests are performed on the middle portion of the batch, after part of the batch has already been placed. If tested only at the truck, the effect of the placement method on the concrete properties should be considered. Thus, early in the placement, the concrete should be tested at both the truck and on the deck to establish a standard for air and slump losses from placement. These air and slump losses should be verified with more than one measurement. The

measured values of air and slump loss should not be used for justification to accept out-of-specification concrete. During the construction of LC-HPC-2 Placement 2, the air loss from pumping was measured at 2.0 percent in the first truckload. As a result, concrete with high air contents measured from the discharge of the trucks was to be placed in the deck. Measured values of air and slump loss were also used as justification for the placement of out-of-specification concrete during construction of the decks on LC-HPC-6, 15, 16, and 17 and the OP Bridge. Additionally, the measurement of air and slump losses should be completed in a manner that matches the actual placement conditions. For example, air and slump losses for LC-HPC-6 were established by pumping to the ground with the boom positioned vertically. This method of pumping likely produced higher values of air and slump loss than would have been measured had the concrete been pumped to the deck.

As a final word, testing, by itself, cannot ensure quality concrete construction – that can be attained only through the placement of quality concrete that is produced and placed in accordance with the plans and specifications. Achieving this goal depends on commitment by the contractor, concrete supplier, and owner.

5.3.26.5 Commitment from Contractor, Concrete Supplier, and Owner

For successful LC-HPC construction, the contractor, concrete supplier, and owner must be committed to producing bridge decks in compliance with the specifications. Naturally, the primary goal of the contractor and concrete supplier is often, instead, to complete construction in the most expeditious manner. This is often a primary goal of the owner's representatives. This point is demonstrated by the predominant use of pumps on LC-HPC placements, not a problem in itself, and the consistent use of slumps above those allowed by the specifications, a problem. Before the late 1980s, contractors regularly placed concretes with slumps below 3 in. (75 mm) (Schmitt and Darwin 1995, Miller and Darwin 2000, Lindquist et al. 2005). Since then, the bridge construction community has become accustomed to working

with high-slump concrete, and many believe that high slumps correlate with a more efficient placement.

During the construction of the LC-HPC decks in this study, contractors and concrete suppliers often used the allowable limit of 3.5 or 4.0 in. (90 or 100 mm) as the target slump, rather than attempting to consistently produce concrete within the specified limits. This behavior contributed to the placement of a great amount of high-slump concrete. Figures 5.34 and 5.35 show the percentage of slump tests greater than or equal to 3.5 and 4.0 in. (90 and 100 mm), respectively, for the 22 placements on decks that were let under LC-HPC specifications. For 12 of the 22 placements, at least half of the recorded slumps were greater than 3.5 in. (90 mm), and for 5 placements, at least half of the slumps were greater than or equal to 4.0 in. (100 mm). Two placements, LC-HPC-8 and LC-HPC-12 Placement 1, had no slumps above 3.75 in. (95 mm). Only a single placement, LC-HPC-8, had no slumps greater than 3.25 in. (85 mm). All of the slump measurements on LC-HPC-12 Placement 2 exceeded or equaled 3.5 in. (90 mm), and all of the slump measurements on OP Bridge Placement 3 exceeded 4.0 in. (100 mm). These results clearly show the tendency of the contractors and concrete suppliers to use the maximum allowable slump.

At this time, contractors and concrete suppliers have little motivation to produce low-cracking decks. The current method of selecting the lowest bidder for construction does not allow the owner to select a preferred contractor with experience in successfully constructing LC-HPC decks. After construction is completed, the contractors have little invested in the long-term cracking performance of the decks. In addition, extending the service life of decks through a reduction in cracking contributes to a less-frequent need for deck replacements. Contractors would have a greater motivation to produce low-cracking decks if incentives were associated with either meeting the specifications during construction or with cracking performance.

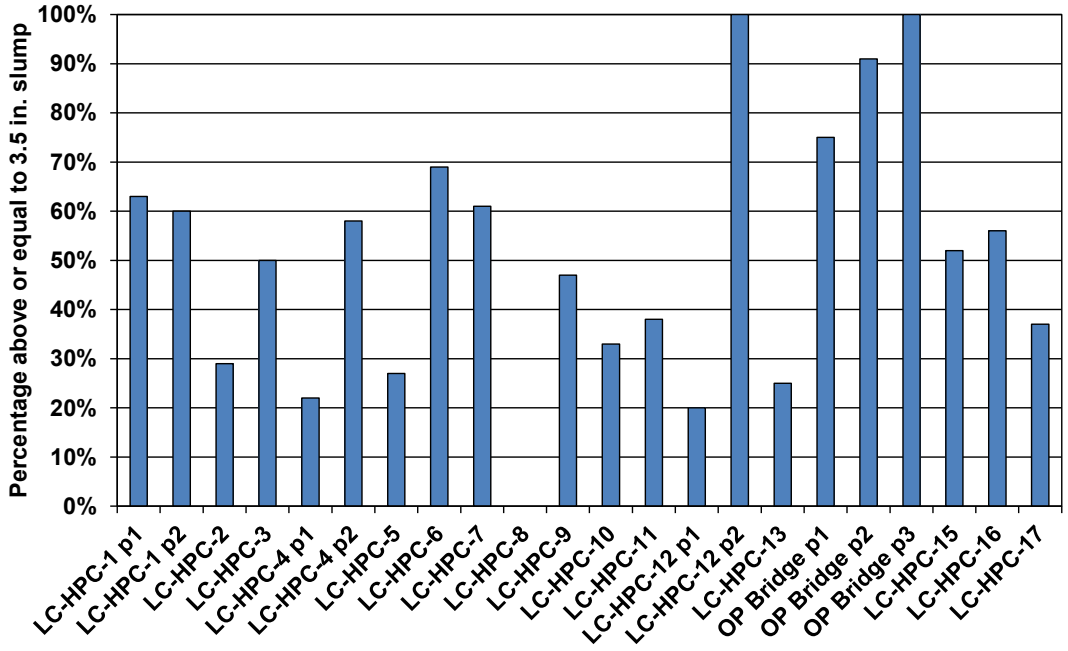

Figure 5.34 Percentage of slump tests greater than or equal to 3.5 in. (90 mm)

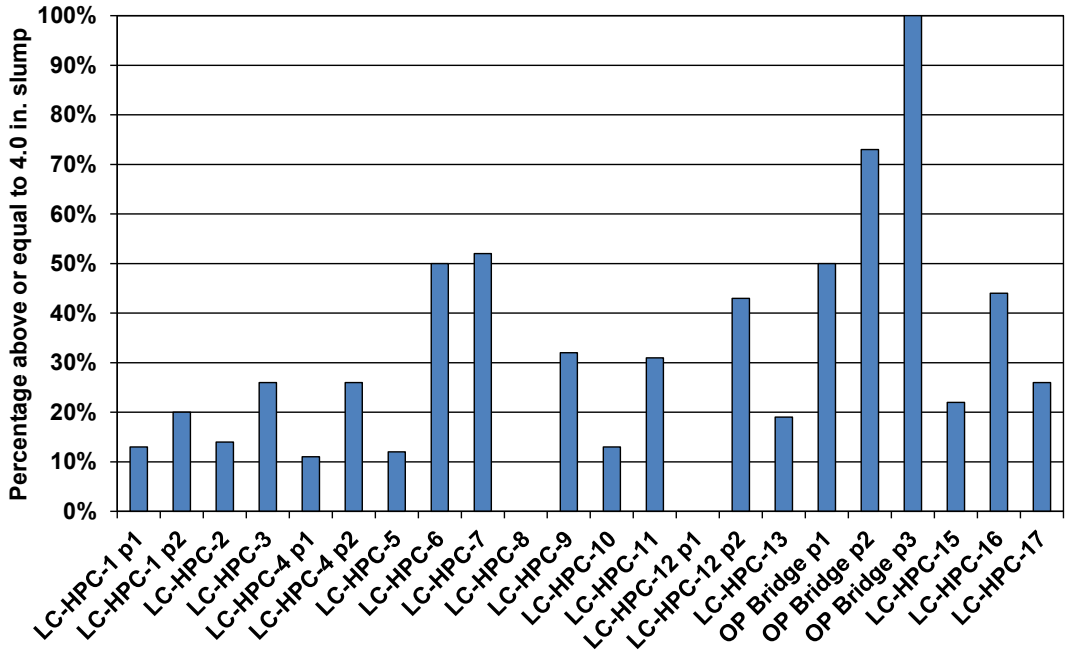

Figure 5.35 Percentage of slump tests greater than or equal to 4.0 in. (100 mm)

The type of incentive to provide to the contractors could be selected by the owner. For example, the contract could include penalties or bonuses depending on the percentage of test results that met the specifications. The owners could also establish a minimum level of cracking performance in terms of a specified crack density determined at a designated deck age, such as the first three years after placement. Cracking above the specified value would have to be repaired. Alternatively, or in conjunction with this requirement, the contractor could also be required to seal cracks wider than a given threshold [for example, 4 mils (0.10 mm)]. The large quantity of crack survey data accumulated in this study (discussed in Chapter 6) could be used to establish an acceptable level of cracking performance.

CHAPTER 6: EVALUATION OF CRACKING PERFORMANCE OF LOW-CRACKING HIGH-PERFORMANCE CONCRETE (LC-HPC) AND CONTROL BRIDGE DECKS AND FACTORS THAT AFFECT CRACKING

6.1 GENERAL

This chapter examines the cracking performance of the LC-HPC and associated control decks described in Chapter 5. Crack surveys (described in Section 2.7 and Appendix B) are completed annually on the bridge decks to quantitatively evaluate the cracking performance in terms of a crack density. Crack maps are created using the data from the crack surveys and display the distribution of the cracks throughout the decks. Crack survey results are discussed and the crack maps for the most recent crack surveys showing crack distribution, crack density, bridge location, dimensions, and construction date are presented in this chapter. Cracking performance of each LC-HPC deck is compared to that of the associated control deck to determine the effectiveness of the LC-HPC specifications. In addition, the cracking performance of the LC-HPC and control decks is compared with the performance of decks examined in three previous studies of older bridge decks by the University of Kansas (Schmitt and Darwin 1995, Miller and Darwin 2000, and Lindquist et al. 2005). A literature review summarizing the earlier studies is provided in Chapter 1. The cracking performance of each deck is compared with data collected and observations made during construction (discussed in Chapter 5) to evaluate the factors that influence cracking.

6.2 CRACK SURVEY RESULTS

The results of the crack surveys are summarized in this section. Crack maps from the most recent surveys are provided. Cracking performance over time is compared for each LC-HPC and associated control deck. Crack densities from the annual surveys are tabulated for the decks in Appendix F.

6.2.1 LC-HPC-1 Crack Survey Results

Seven crack surveys have been completed annually on LC-HPC-1 since construction in 2005. The crack map for the 2012 survey is shown in Figure 6.1. The deck was constructed in two placements, and both deck placements have performed well, exhibiting low crack densities. The crack density for Placement 1 (south placement) has increased from 0.012 m/m^2 at 5.9 months to 0.096 m/m^2 at 79.0 months. The crack density for Placement 2 (north placement) has increased from 0.003 m/m^2 at 5.3 months to 0.081 m/m^2 at 78.4 months. The majority of cracks in both placements are short and randomly positioned. An increased occurrence of short, map cracks have formed near the east end of Placement 1. These additional map cracks likely resulted due to finishing delays, excess bullfloating, and the use of partially-dry burlap during placement near the east end, discussed in Section 5.3.1.4. Map cracks are commonly caused by plastic shrinkage cracking due to drying out of the plastic concrete surface. Overfinishing, which was observed in the construction of both placements, can increase the paste content at the surface and lead to increased map cracking. No increase in cracking is observed in a region about 50 ft (15 m) from the east abutment on Placement 1 where a truckload with a slump of 6.5 in. (165 mm) was placed (discussed in Section 5.3.1.4). A few longer, transverse cracks have developed in Placement 1 over the middle pier (negative moment region). Flexural tensile stresses that develop in negative moment regions on deck surfaces are minimal compared to thermal and shrinkage stresses (Krauss and Rogalla 1996), but flexural tensile stresses can act in conjunction with thermal and shrinkage mechanisms resulting in increased tensile stresses and cracking. As is common on decks with integral abutments, short longitudinal cracks extend from each abutment due to the restraint provided by the abutments in the transverse direction (Schmitt and Darwin 1995, Miller and Darwin 2000, and Lindquist et al 2005).

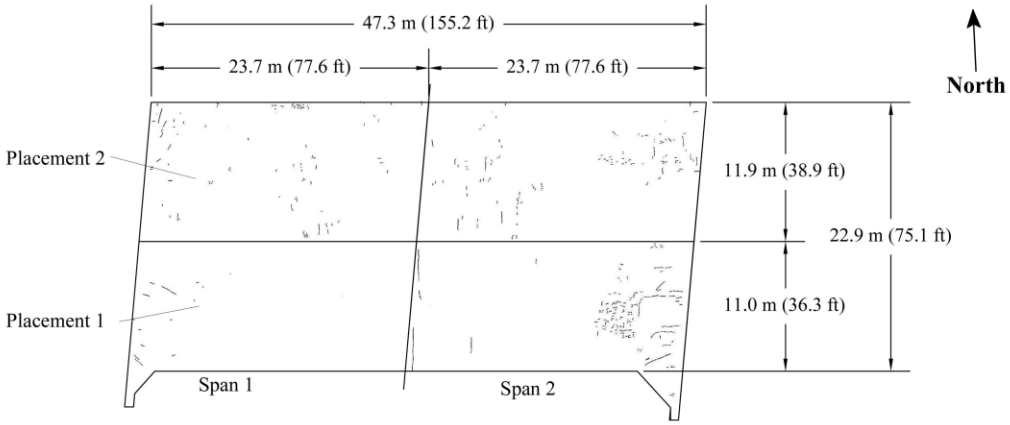

Bridge Number: 105-304 (LC-HPC-1)
Bridge Location: EB Parallel Pkwy over I-635
Construction Date:
Placement 1 (South): 10/14/2005
Placement 2 (North): 11/2/2005
Crack Survey Date: 5/16/2012

Bridge Length: 47.3 m (155.2 ft)
Bridge Width: 22.9 m (75.1 ft)
Skew: -5°
Number of Spans: 2
Span 1 (West): 23.7 m (77.6 ft)
Span 2 (East): 23.7 m (77.6 ft)
Number of Placements: 2

Bridge Age:
Placement 1: 79.0 months
Placement 2: 78.4 months
Crack Density: 0.085 m/m²
Placement 1: 0.096 m/m²
Placement 2: 0.081 m/m²
Span 1: 0.046 m/m²
Span 2: 0.124 m/m²

Figure 6.1 LC-HPC-1 crack map at 79.0 and 78.4 months (Placements 1 and 2, respectively)

6.2.2 LC-HPC-2 Crack Survey Results

Six crack surveys have been completed on LC-HPC-2 since construction in 2006. The crack map for the 2012 survey is shown in Figure 6.2. The deck had a low crack density for the first 45 months, increasing from 0.013 m/m^2 at 7.2 months to 0.059 m/m^2 at 44.5 months. The crack density then increased to 0.144 m/m^2 at 59.3 months and 0.197 m/m^2 at 68.1 months. As with LC-HPC-1, the majority of cracks are short and randomly positioned. The excessive bullfloating, use of additional water as a finishing aide, and improper wetting and placement of burlap observed during construction (described in Section 5.3.2.4) may have contributed to plastic shrinkage cracking. No increase in cracking is observed approximately 15 ft (4.6 m) from the west abutment, a location at which excess water was sprayed on the deck surface to aid in finishing. Long, transverse cracks have formed above the middle pier in the negative moment region. As described in Section 5.3.2.4, two truckloads with slumps of approximately 6 in. (150 mm) (based on visual inspection) were

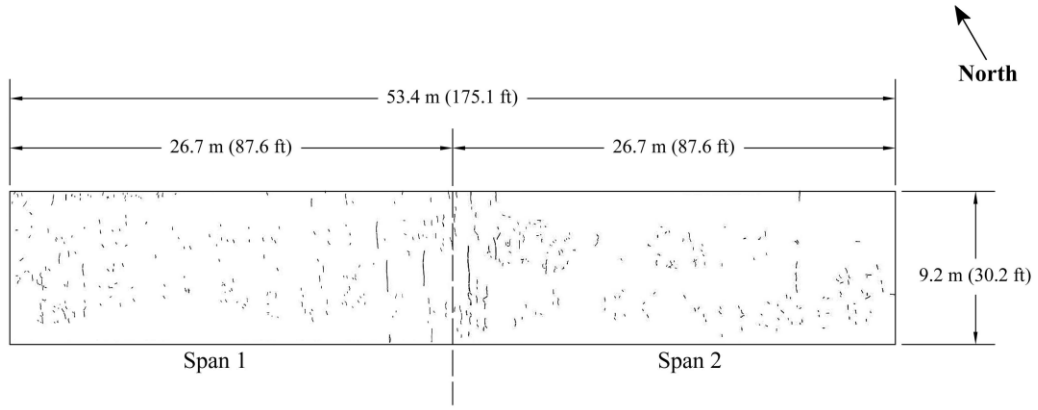

Bridge Number: 105-310 (LC-HPC-2)
Bridge Location: 34th St over I-635
Construction Date: 9/13/2006
Crack survey Date: 5/18/2012

Bridge Length: 53.4 m (175.1 ft)
Bridge Width: 9.2 m (30.2 ft)
Skew: 0°
Number of Spans: 2
Span 1 (West): 26.7 m (87.6 ft)
Span 2 (East): 26.7 m (87.6 ft)
Number of Placements: 1

Bridge Age: 68.1 months
Crack density: 0.197 m/m^2
Span 1 (West): 0.204 m/m^2
Span 2 (East): 0.191 m/m^2

Figure 6.2 LC-HPC-2 crack map at 68.1 months

placed near this point on the deck. None of the transverse cracks extend across the full deck width.

6.2.3 Control 1/2 Crack Survey Results

Seven crack surveys have been completed on Control 1/2 since construction in 2005. The crack map for the 2012 survey is shown in Figure 6.3. The deck exhibits low cracking and is the best-performing control deck in the study. The crack density of Placement 1 (north placement) increased from 0 m/m^2 at 6.1 months to 0.240 m/m^2 at 79.2 months. The crack density of Placement 2 (south placement) increased from 0 m/m^2 at 5.5 months to 0.161 m/m^2 at 78.6 months. As discussed in Section 5.3.3.2, the two subdeck placements had relatively low slumps, 4.25 and 3.25 in. (110 and 80 mm), respectively – values similar to many of the LC-HPC decks. Long, transverse cracks have formed near the middle pier in the negative moment region. Two longitudinal cracks, approximately 30 ft (9 m) in length, extend from each abutment near, and parallel to, a cold joint between placements. Many small, longitudinal cracks extend from each abutment along the full bridge width.

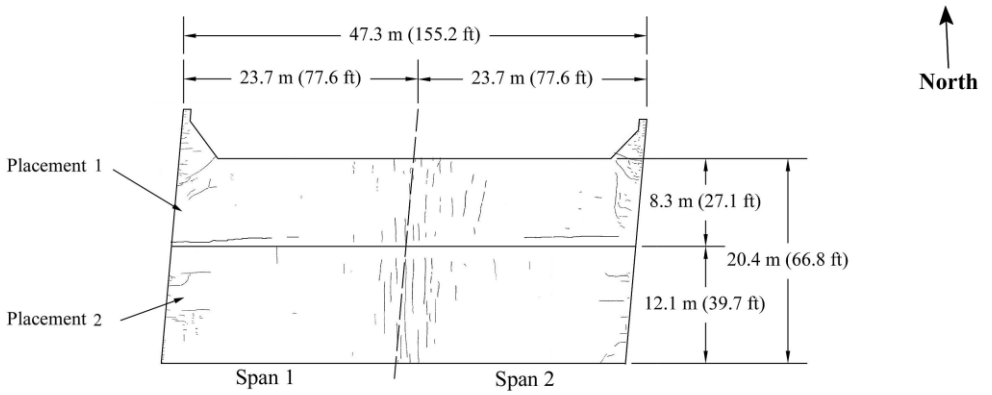

Bridge Number: 105-311 (Control-1/2)
Bridge Location: WB Parallel Pkwy over I-635
Construction Dates:
North Subdeck: 9/30/2005
North Overlay: 10/10/2005
South Subdeck: 10/18/2005
South Overlay: 10/28/2005
Crack Survey Date: 5/16/2012

Bridge Length: 47.3 m (155.2 ft)
Bridge Width: 20.7 m (67.8 ft)
Skew: -5°
Number of Spans: 2
Span 1 (West): 23.7 m (77.6 ft)
Span 2 (East): 23.7 m (77.6 ft)
Number of Placements: 2

Bridge Age:
Placement 1 (N): 79.2 months
Placement 2 (S): 78.6 months
Crack Density: 0.196 m/m²
Placement 1: 0.240 m/m²
Placement 2: 0.161 m/m²
Span 1: 0.166 m/m²
Span 2: 0.226 m/m²

Figure 6.3 Control 1/2 crack map at 79.2 and 78.6 months (Placements 1 and 2, respectively)

6.2.4 Cracking Performance of LC-HPC-1 and 2 and Control 1/2

Crack density is plotted as a function of age for both placements of LC-HPC-1, LC-HPC-2, and both placements of Control 1/2 in Figure 6.4. The placements of LC-HPC-1 have consistently performed better than the placements of Control 1/2 over a span of approximately 80 months and seven surveys each. The most recent crack surveys at about 80 months indicate that the crack densities of Placements 1 and 2 of LC-HPC-1 are approximately half of those of Control 1/2 Placement 2 and one-third of the crack density of Control 1/2 Placement 1.

LC-HPC-2 has regularly performed better than Control 1/2 Placement 1, but has experienced higher cracking than Placement 2 in the two most recent crack surveys at 59 and 68 months. The crack surveys completed in 2012 indicate that the crack density of LC-HPC-2 at 68 months is greater than the crack density of Control

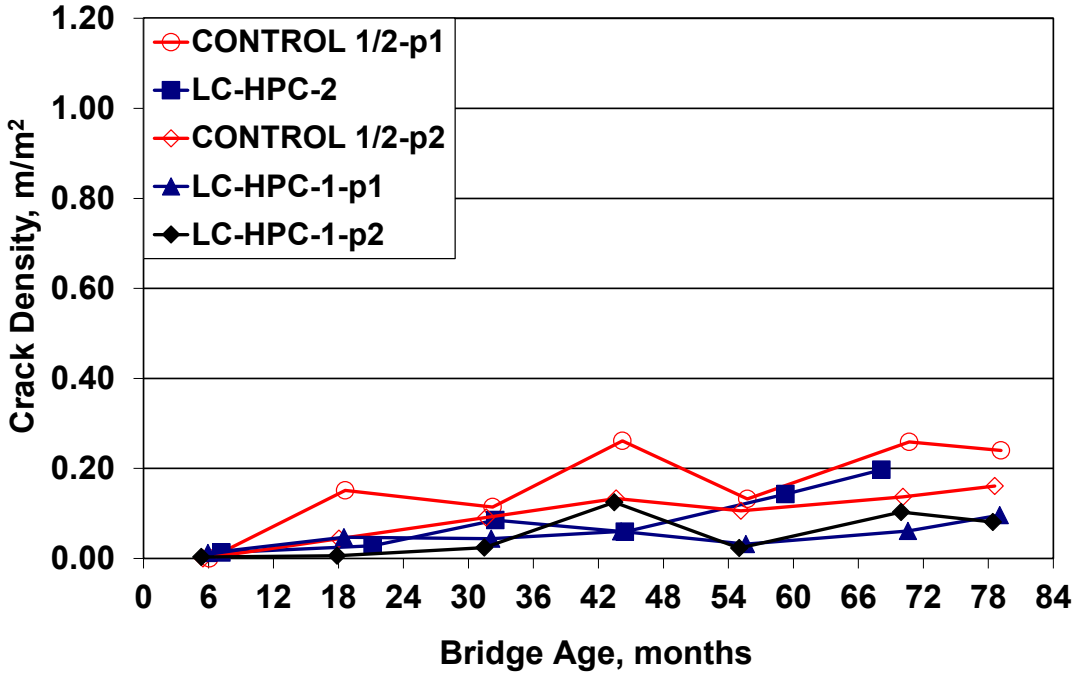

Figure 6.4 Crack density versus age for LC-HPC-1, 2, and Control 1/2

1/2 Placement 2 and less than the crack density of Control 1/2 Placement 1, both at 79 months.

As shown in Figure 6.4, crack densities generally increase for the decks over time, although a few decreases have been observed from year to year. These decreases in cracking result from a number of factors. First, the crack survey crews include several new members every year and any disparity in the ability of the crew members to find cracks can contribute to a variance in the crack density values. In addition, the nature of the cracks found in these three decks (many short, map cracks) makes it difficult to identify every crack. Nevertheless, the survey crews are typically led by the same graduate students from year to year to provide a level of consistency in the survey data. Second, the air temperature on the day of the survey can affect the size and, ultimately, the visibility of the cracks. The steel girders below the deck expand as air temperatures increase, widening the cracks in the deck. For example,

the crack surveys of LC-HPC-1 and Control 1/2 at approximately 44 months exhibited higher cracking than the surveys at about 55 months; the 44-month surveys were completed on a day with an average temperature of 7° F (4° C) higher than the 55-month surveys.

6.2.5 LC-HPC-7 Crack Survey Results

Six crack surveys have been completed on LC-HPC-7 since construction in 2006. The crack map for the 2012 survey is shown in Figure 6.5. LC-HPC-7 is the best performing deck examined in this study. The crack density has increased from 0.003 m/m^2 at 11.4 months to 0.065 m/m^2 at 71.3 months. The majority of the cracks are small and randomly positioned, developing in the westbound lane (north side of the deck). A few longitudinal cracks have propagated from the west abutment, likely due to the added restraint provided by the integral abutment and the exposure of the concrete during the construction delay discussed in Section 5.3.4.4.

6.2.6 Control 7 Crack Survey Results

Control 7 has been surveyed six times since construction in 2006 and has consistently been one of the highest-cracking decks examined in the study. The crack map for the 2012 survey is shown in Figure 6.6. Placement 1, which includes the eastern two-thirds of the deck, has exhibited significantly high cracking from an early age. The crack density of Placement 1 has increased from 0.293 m/m^2 at 16.4 months to 1.022 m/m^2 at 74.5 months. The crack density of Placement 2, which includes the western third of the deck, has increased from 0.030 m/m^2 at 10.8 months to 0.638 m/m^2 at 68.9 months. Transverse cracks have formed throughout Placement 1, but are more extensive near the pier. The transverse cracks appear to be located directly above the reinforcing steel. The use of high-slump concretes, such as used in this deck, increase the risk of settlement cracking directly above reinforcing steel, and the high paste content of the concrete increases the potential for drying shrinkage

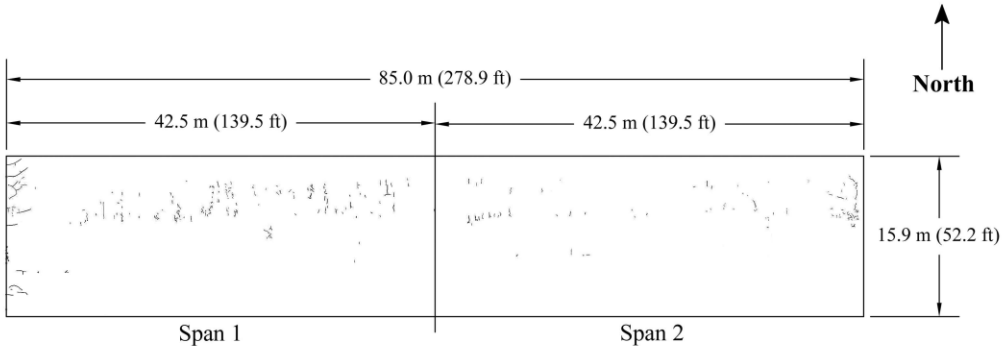

Bridge Number: 43-33 (LC-HPC-7)
Bridge Location: Co. Rd. 150 over US-75
Construction Date: 6/24/2006
Crack survey Date: 6/1/2012

Bridge Length: 85.0 m (278.9 ft)
Bridge Width: 15.9 m (52.2 ft)
Skew: 0°
Number of Spans: 2
Span 1 (West): 42.5 m (139.5 ft)
Span 2 (East): 42.5 m (139.5 ft)
Number of Placements: 1

Bridge Age: 71.3 months
Crack density: 0.065 m/m²
Span 1: 0.088 m/m²
Span 2: 0.036 m/m²

Figure 6.5 LC-HPC-7 crack map at 71.3 months

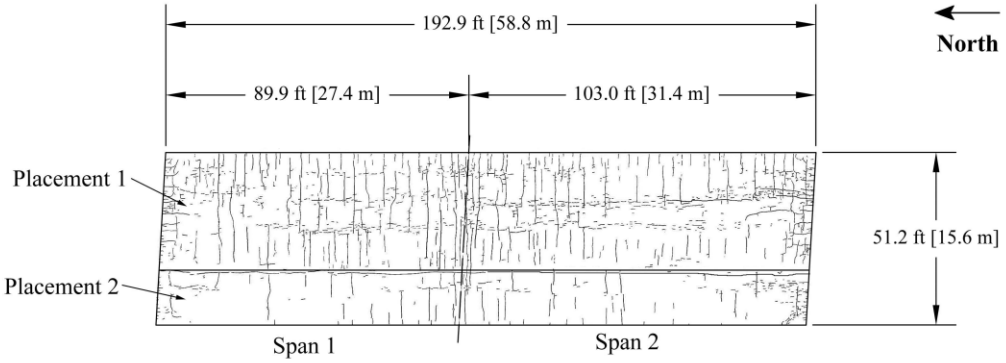

Bridge Number: 46-334 (Control-7)
Bridge Location: NB Antioch over I-435
Construction Date:
Placement 1 (East): 3/29/2006
Placement 2 (West): 9/15/2006
Crack survey Date: 6/12/2012

Bridge Length: 58.8 m (192.9 ft)
Bridge Width: 15.6 m (51.2 ft)
Skew: -3.3°
Number of Spans: 2
Span 1 (North): 27.4 m (89.9 ft)
Span 2 (South): 31.4 m (103.0 ft)
Number of Placements: 2

Bridge Age:
Placement 1: 74.5 months
Placement 2: 68.9 months
Crack density: 0.899 m/m²
Span 1: 0.904 m/m²
Span 2: 0.895 m/m²
Placement 1: 1.022 m/m²
Placement 2: 0.638 m/m²

Figure 6.6 Control 7 crack map at 74.5 and 68.9 months [Placement 1 (east) and 2 (west), respectively]

cracking. Smaller longitudinal cracks have developed at both abutments. Two partially-connected lines of small, longitudinal cracks have developed approximately 15 and 25 ft (4.5 and 7.6 m) from the eastern edge of Placement 1 and extend the majority of the deck length. In Placement 2, a single longitudinal crack extends the entire length of the bridge near, and parallel to, the cold joint between placements.

6.2.7 Cracking Performance of LC-HPC-7 and Control 7

Crack density is plotted as a function of age for LC-HPC-7 and both placements of Control 7 in Figure 6.7. LC-HPC-7 has performed significantly better than Control 7 over the course of the study. The most recent crack surveys at approximately 70 months indicate that the crack density of Control 7 Placement 1 is more than 15 times the crack density of LC-HPC-7, while the crack density of Control 7 Placement 2 is nearly 10 times the crack density of LC-HPC-7. The high cracking of Control 7 is likely a result of the high-slump, high-cement-paste-content concrete placed in the deck. With an average slump value of 9.25 in. (235 mm), the subdeck of Control 7 Placement 1 contains the highest average value of slump of any deck in the study. In addition, the techniques used by the different contractors that placed the two decks (discussed in Sections 5.3.4 and 5.3.5) may have contributed to the discrepancy in cracking performance.

Apart from the most recent surveys, the rate of increase in cracking has been considerably greater for Control 7 than for LC-HPC-7 throughout the study. The decrease in rate of cracking in the recent surveys of Control 7 is likely due to small cracks being overlooked by the survey crew. During surveys of decks with substantial cracking, such as Control 7, crew members occasionally miss small cracks as they mark longer cracks that continue over great lengths along the deck. After the marking of a long crack, the crew members are instructed to again inspect the deck from the location at which the crack marking began to prevent smaller cracks from being overlooked in the area.

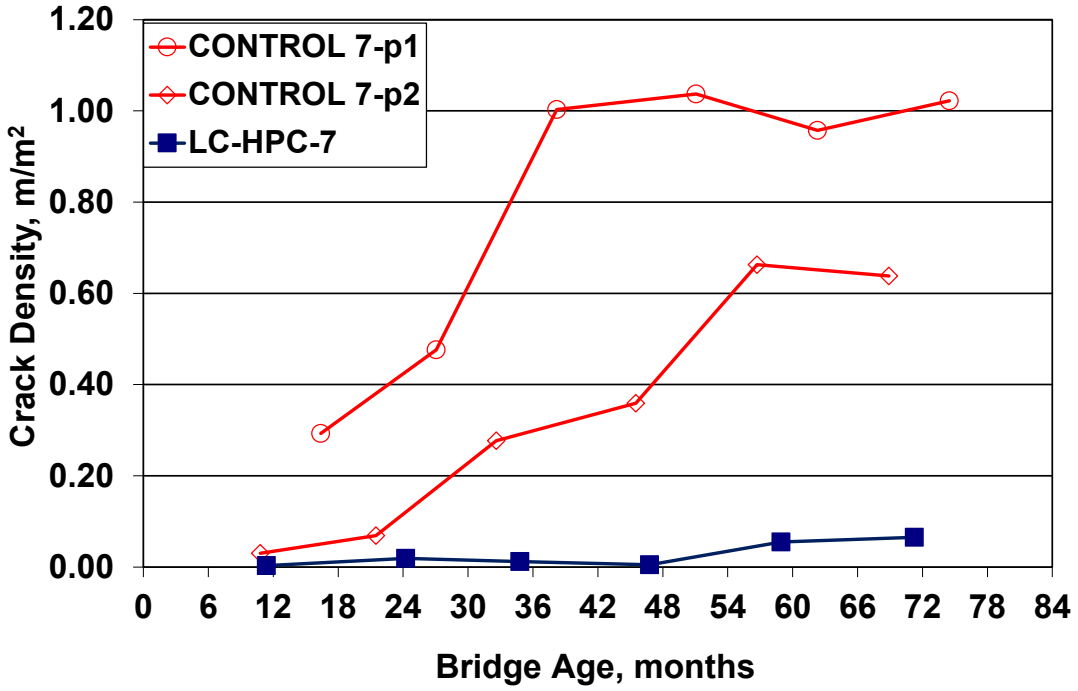

Figure 6.7 Crack density versus age for LC-HPC-7 and Control 7

6.2.8 LC-HPC-10 Crack Survey Results

Five crack surveys have been completed on LC-HPC-10 since construction in 2007. The first crack survey was completed 3.9 months after construction, before a grooved surface was placed on the deck, and yielded a relatively high crack density of 0.248 m/m^2. Since all other decks in the study contain grooved surfaces, the second survey was not completed until grooves were placed in the surface (at 25.4 months). The first survey of the grooved surface produced a crack density of 0.076 m/m^2. The crack map for the 2012 survey, which yielded a crack density of 0.125 m/m^2, is shown in Figure 6.8. The majority of cracks are long and propagate in the transverse direction. Higher cracking is observed near the eastern and western piers compared to the balance of the deck. The transverse cracks near the piers are parallel to the reinforcing steel, not parallel to the piers, demonstrating that flexural cracking is not

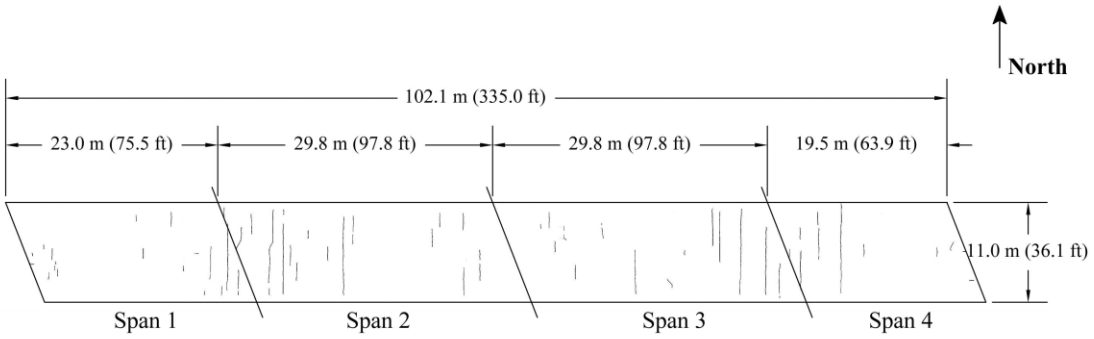

Bridge Number: 54-60 (LC-HPC-10)
Bridge Location: E1800Rd over US-69
Construction Date: 5/17/2007
Crack survey Date: 5/15/2012

Bridge Length: 102.1 m (335.0 ft)
Bridge Width: 11.0 m (36.1 ft)
Skew: 21.3°
Number of Spans: 4
Span 1 (West): 23.0 m (75.5 ft)
Span 2 (West): 29.8 m (97.8 ft)
Span 3 (East): 29.8 m (97.8 ft)
Span 4 (East) : 19.5 m (63.9 ft)
Number of Placements: 1

Bridge Age: 60.0 months
Crack density: 0.125 m/m²
Span 1 (West): 0.091 m/m²
Span 2 (West): 0.156 m/m²
Span 3 (East): 0.128 m/m²
Span 4 (East): 0.114 m/m²

Figure 6.8 LC-HPC-10 crack map at 60.0 months

the main contributor to this cracking. The placement of improperly-soaked burlap during construction, as discussed in Section 5.3.6.4, did not appear to contribute to plastic shrinkage cracking. In addition, the delays in placement, finishing, and curing that occurred approximately 140 ft (43 m) from the west abutment as a result of relocation of the pump did not appear to affect cracking.

6.2.9 LC-HPC-8 Crack Survey Results

Four crack surveys have been completed on LC-HPC-8 since construction in 2007. The crack map for the 2012 survey is shown in Figure 6.9. The first crack survey, completed 20.9 months after construction, was performed before the bridge was open to traffic, due to ongoing construction in the area. A crack survey scheduled less than 12 months after construction was canceled due to excessive mud on the deck surface from construction traffic. Cracking has increased for LC-HPC-8

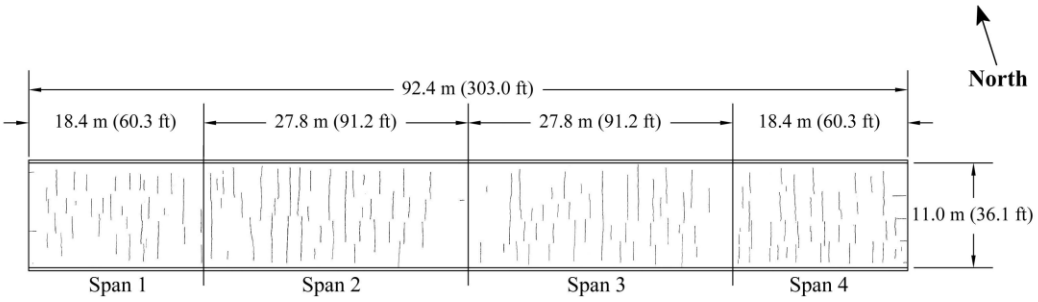

Bridge Number: 54-53 (LC-HPC-8)
Bridge Location: E 1350 Rd over US-69
Construction Date: 10/3/2007
Crack survey Date: 5/15/2012

Bridge Length: 92.4 m (303.0 ft)
Bridge Width: 11.0 m (36.1 ft)
Skew: 0^{o}
Number of Spans: 4
Span 1 (West): 18.4 m (60.3 ft)
Span 2 (West): 27.8 m (91.2 ft)
Span 3 (East): 27.8 m (91.2 ft)
Span 4 (East): 18.4 m (60.3 ft)
Number of Placements: 1

Bridge Age: 55.4 months
Crack density: 0.383 m/m^2
Span 1 (West): 0.341 m/m^2
Span 2 (West): 0.400 m/m^2
Span 3 (East): 0.357 m/m^2
Span 4 (East): 0.425 m/m^2

Figure 6.9 LC-HPC-8 crack map at 55.4 months

from 0.298 m/m^2 at 20.9 months to 0.383 m/m^2 at 55.4 months. LC-HPC-8 has exhibited high early-age cracking, but cracking has increased at a relatively slow rate. Long, transverse cracks have developed at 3 to 5-ft (0.9 to 1.5-m) increments along the entire bridge. The majority of the transverse cracks have developed in the positive moment regions of the spans. The cracking performance of LC-HPC-8 is possibly influenced by the prestressed girders, as will be discussed in Section 6.2.11. A few longitudinal cracks have propagated from the west abutment, likely a result of a delay in concrete delivery, discussed in Section 5.3.7.4.

6.2.10 Control 8/10 Crack Survey Results

Control 8/10 is the only monolithic control deck and the only control deck placed on prestressed girders in the study. The deck has been surveyed five times

since construction in 2007. The crack map for the 2012 survey is shown in Figure 6.10. Cracking has increased from 0.177 m/m^2 at 14.4 months to 0.425 m/m^2 at 61.6 months. The deck exhibited a decrease in cracking between the first and second surveys (0.177 m/m^2 at 14.4 months to 0.127 m/m^2 at 25.5 months). This decrease in cracking is possibly influenced by the prestressed girders, as discussed later in Section 6.2.11. The great majority of the cracks have developed in the two westernmost spans. Significant map cracking has developed near the west abutment. Many longitudinal cracks have propagated from the west abutment. Transverse cracks extending nearly across the full width of the deck have developed in the west, middle span. A few transverse cracks appear in the two east spans. Four short, longitudinal cracks have propagated from the east abutment.

6.2.11 Cracking Performance of LC-HPC-8 and 10 and Control 8/10

Crack density is plotted as a function of age for LC-HPC-8 and 10 and Control 8/10 in Figure 6.11. Throughout most of the study, Control 8/10 exhibited greater cracking than LC-HPC-10 and less cracking than LC-HPC-8. In the most recent surveys, however, both LC-HPC-8 and 10 have less cracking than Control 8/10.

LC-HPC-8 experienced high early-age cracking with a crack density of 0.298 m/m^2 at 20.9 months, with a more gradual increase since. As discussed in Section 6.2.9, the majority of the cracks in LC-HPC-8 developed transversely in the positive moment regions of the deck – uncommon locations for high cracking as these are sites where the deck surface is in compression. The high early-age cracking in the positive moment regions may result from the deck and girders being subjected to additional camber after deck placement. This additional camber may have induced tensile stresses in the deck surface at these locations, increasing the potential for cracking. LC-HPC-10 experienced a decrease in cracking between the surveys at 3.9 and 25.4 months and again between the surveys at 25.4 and 36.2 months. As explained in Section 6.2.8, at the time of the survey at 3.9 months, the deck surface

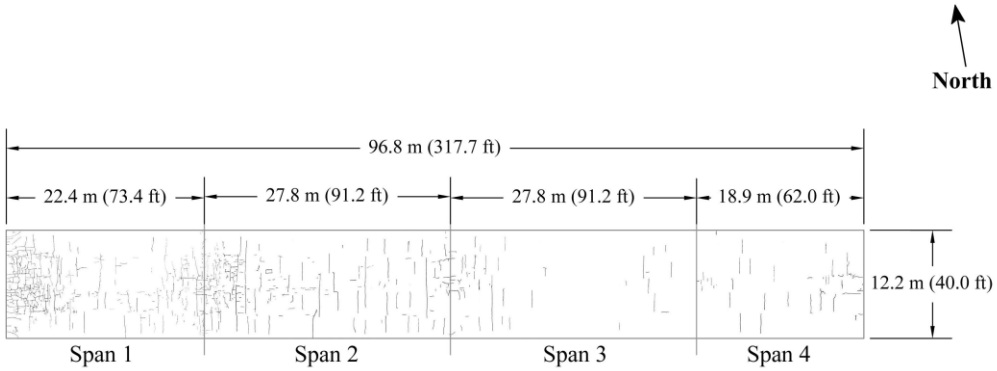

Bridge Number: 54-59 (Control-8/10)
Bridge Location: K-52 over US-69
Construction Date: 4/16/2007
Crack survey Date: 6/4/2012

Bridge Length: 96.8 m (317.7 ft)
Bridge Width: 12.2 m (40.0 ft)
Skew: 0°
Number of Spans: 4
Span 1: 22.4 m (73.4 ft)
Span 2: 27.8 m (91.2 ft)
Span 3: 27.8 m (91.2 ft)
Span 4: 18.9 m (62.0 ft)
Number of Placements: 1

Bridge Age: 61.6 months
Crack density: 0.425 m/m²
Span 1: 0.825 m/m²
Span 2: 0.522 m/m²
Span 3: 0.149 m/m²
Span 4: 0.193 m/m²

Figure 6.10 Control 8/10 crack map at 61.6 months

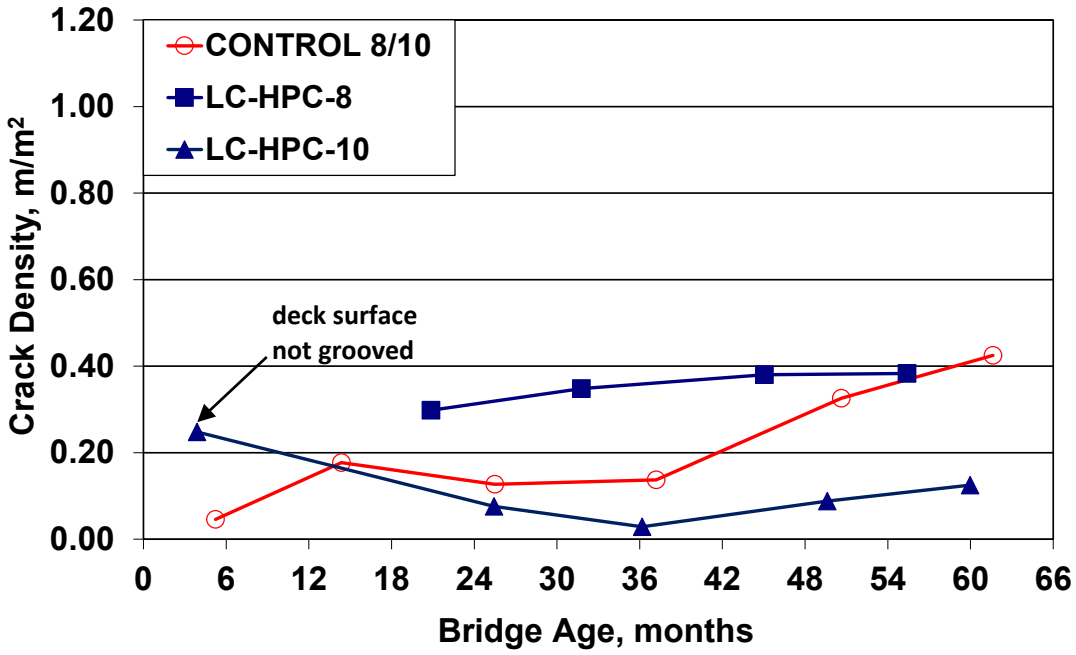

Figure 6.11 Crack density versus age for LC-HPC-8 and 10 and Control 8/10

had not yet been grooved and the un-grooved surface may have made the cracks more visible and contributed to the high crack density. It is also possible that the high crack density had no connection to the presence of the grooves. Similar to LC-HPC-10, Control 8/10 experienced a decrease in cracking between 14.4 and 25.5 months, followed by a very gradual increase in cracking between 25.5 and 37.2 months. These decreases in cracking may result from a reduction in the camber and shortening of the prestressed girders as a result, respectively, of relaxation of the prestressed steel and concrete creep. LC-HPC-10 and Control 8/10 have both experienced an increase in cracking in the two most recent surveys. Additional studies of prestressed girder bridges will be necessary to fully understand their cracking behavior.

6.2.12 LC-HPC-11 Crack Survey Results

Four crack surveys have been completed on LC-HPC-11 since construction in 2007. The crack map for the 2012 survey is shown in Figure 6.12. Cracking has increased from 0.059 m/m^2 at 23.4 months to 0.260 m/m^2 at 61.0 months. Longitudinal cracks have propagated from the west abutment along the full width of the bridge. Transverse and longitudinal cracks have developed at random locations throughout the deck. The majority of cracks have formed in the west span. This additional cracking in the west span cannot be explained by observations made during construction.

6.2.13 Control 11 Crack Survey Results

Control 11 has been surveyed six times since construction in 2006. The crack map for the 2012 survey is shown in Figure 6.13. Significant cracking developed on the deck at an early age, resulting in a crack density of 0.351 m/m^2 at 16.5 months after construction. The crack density increased to 0.923 m/m^2 at 62.9 months after construction, one of the highest crack densities observed in the study. Significant

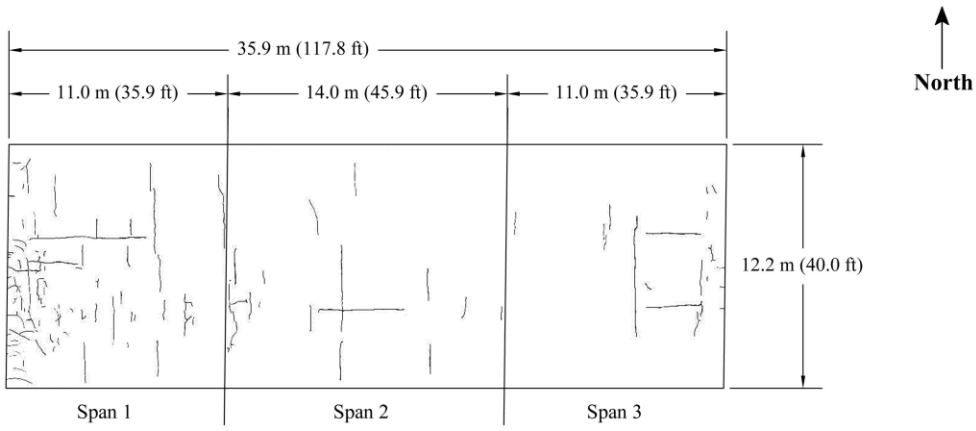

Bridge Number: 78-119 (LC-HPC-11)
Bridge Location: EB US-50 over K &ORR, Hutchinson, KS
Construction Date: 6/9/2007
Crack Survey Date:7/10/2012

Bridge Length: 35.9 m (117.8 ft)
Bridge Width: 12.2 m (40.0 ft)
Skew: -0.7°
Number of Spans: 3
Span 1: 11.0 m (35.9 ft)
Span 2: 14.0 m (45.9 ft)
Span 3: 11.0 m (35.9 ft)
Number of Placements: 1

Bridge Age: 61.0 months
Crack Density: 0.260 m/m²
Span 1: 0.476 m/m²
Span 2: 0.159 m/m²
Span 3: 0.160 m/m²

Figure 6.12 LC-HPC-11 crack map at 61.0 months

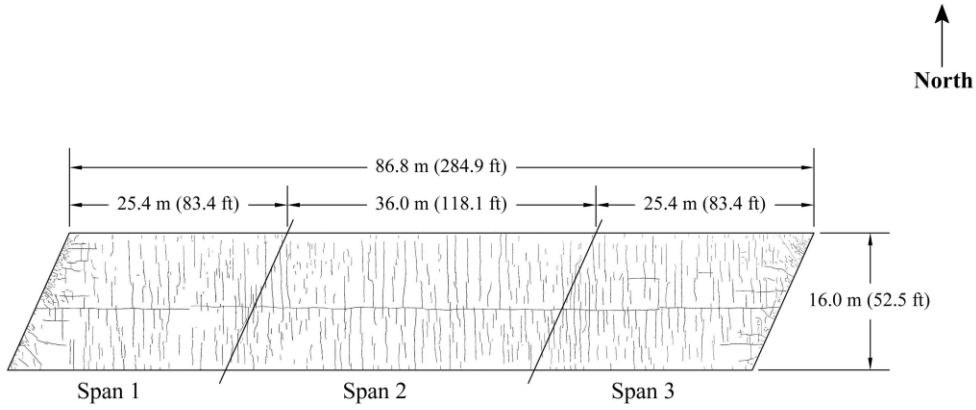

Bridge Number: 56-155 (Control-11)
Bridge Location: US-50 over BNSF Railroad, Emporia, KS
Construction Date: 3/28/2006
Crack Survey Date: 7/3/2012

Bridge Length: 86.8 m (284.9 ft)
Bridge Width: 16.0 m (52.5 ft)
Skew: -24.3°
Number of Spans: 3
Span 1: 25.4 m (83.4 ft)
Span 2: 36.0 m (118.1 ft)
Span 3: 25.4 m (83.4 ft)
Number of Placements: 1

Bridge Age: 75.2 months
Crack Density: 0.849 m/m²
Span 1: 0.830 m/m²
Span 2: 0.793 m/m²
Span 3: 0.945 m/m²

Figure 6.13 Control 11 crack map at 75.2 months

scaling has been observed annually during the crack surveys. The scaling obstructs the view of some cracks, making it difficult to accurately identify all cracks on the deck. Cracking is known to contribute to increased scaling by allowing moisture to penetrate the surface, which expands when frozen, weakening the concrete surface. The substantial cracking observed in the deck likely contributed to the scaling. Transverse cracks have formed at 1 to 3-ft (0.3 to 0.9-m) increments, extending nearly across the full width of the deck. The transverse cracks appear to be directly above and parallel to the reinforcing steel, not parallel to the skew of the bridge. Significant longitudinal cracking is observed near both abutments along the full width of the bridge. A single longitudinal crack that appears to be located directly above the construction joint between the two subdeck placements extends the entire length of the bridge near the centerline. Although not shown in Figure 6.13, crack densities based on the subdeck placements are shown in Table F.2 in Appendix F.

6.2.14 Cracking Performance of LC-HPC-11 and Control 11

Crack density is plotted as a function of age for LC-HPC-11 and Control 11 in Figure 6.14. LC-HPC-11 has experienced significantly less cracking than Control 11 at similar ages. At only 16.5 months, Control 11 exhibited nearly six times the cracking of LC-HPC-11 at 23.4 months. Furthermore, Control 11 at 61.0 months yielded nearly four times the cracking of LC-HPC-11 at 62.9 months (0.923 m/m^2 vs. 0.260 m/m^2). Some of the discrepancy in cracking performance between the two decks may have been influenced by the different contractors that placed the decks (as discussed in Sections 5.3.9 and 5.3.10); however, the higher average slump and strength of the concrete and the use of overlay on Control 11, also discussed in Sections 5.3.9 and 5.3.10, likely contributed to this discrepancy as well. The crack density of Control 11 decreased at 37.8, 50.2, and 75.2 months, likely due to surface scaling obstructing the view of many cracks. The crack density of Control 11 increased significantly between surveys at 50.2 and 62.9 months.

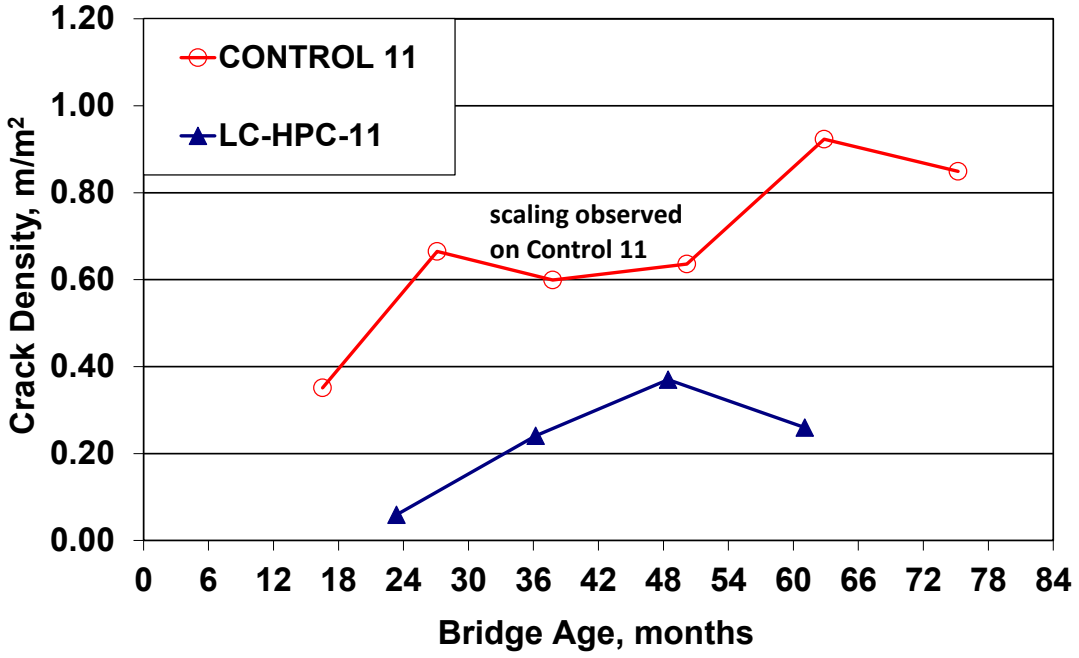

Figure 6.14 Crack density versus age for LC-HPC-11 and Control 11

6.2.15 LC-HPC-4 Crack Survey Results

Both placements of LC-HPC-4 have been surveyed five times since construction in 2007. The crack map for the 2012 survey is shown in Figure 6.15. Placement 1 has consistently exhibited twice the crack density of Placement 2, likely a result of the pumping difficulties and the continual production of out-of-specification concrete during construction of Placement 1 (discussed in Section 5.3.11.4). Cracking increased from 0.017 m/m^2 at 9.5 months to 0.184 m/m^2 at 56.0 months for Placement 1, while increasing from 0.004 m/m^2 at 9.4 months to 0.092 m/m^2 at 55.9 months for Placement 2. Nearly all cracks have formed in the transverse direction in both placements. Increased cracking is observed directly above the piers between Spans 1 and 2 and Spans 3 and 4 (see Figure 6.15). The majority of the cracking in Placement 1 developed in the positive moment region of Span 4. Although 25 ft (8 m) of deck at the west end was exposed with no burlap

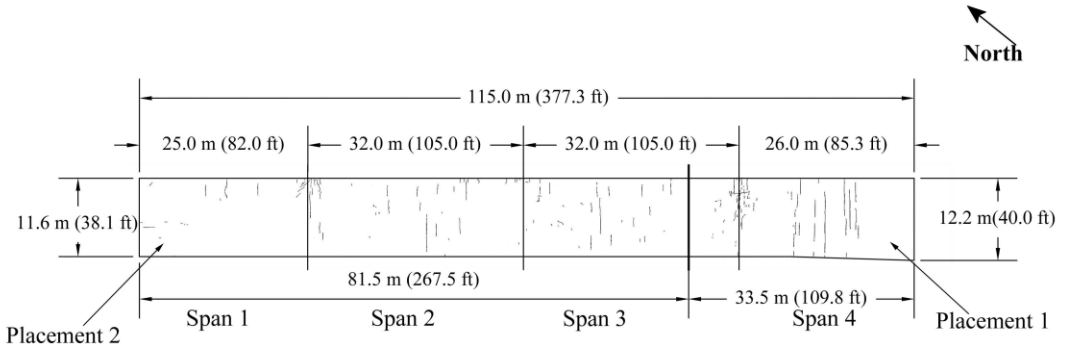

Bridge Number: 46-339 Unit 1 (LC-HPC-4)
Bridge Location: Flyover Ramp US-69S to I-435W
Construction Date:
Placement 1 (South): 9/29/2007
Placement 2 (North): 10/2/2007
Crack Survey Date: 5/30/2012

Bridge Length: 115.0 m (377.3 ft)
Bridge Width: 11.6 m (38.1 ft)
Skew: 0°
Number of Spans: 4
Span 1: 25.0 m (82.0 ft)
Span 2: 32.0 m (105.0 ft)
Span 3: 32.0 m (105.0 ft)
Span 4: 26.0 m (85.3 ft)
Number of Placements: 2

Bridge Age:
Placement 1: 56.0 months
Placement 2: 55.9 months
Crack Density: 0.120 m/m^2
Placement 1: 0.184 m/m^2
Placement 2: 0.092 m/m^2
Span 1: 0.054 m/m^2
Span 2: 0.110 m/m^2
Span 3: 0.124 m/m^2
Span 4: 0.188 m/m^2

Figure 6.15 LC-HPC-4 crack map at 56.0 months

cover or fogging for about 40 minutes, no increase in cracking is observed in this region.

6.2.16 Control 4 Crack Survey Results

Control 4 has been surveyed five times since construction in 2007. The crack map for the 2012 survey is shown in Figure 6.16. Control 4 experienced a large increase in cracking between the first and second crack survey, with the crack density increasing from 0.050 m/m^2 at 6.8 months to 0.366 m/m^2 at 19.7 months. Cracking increased steadily in subsequent surveys, resulting in a crack density of 0.669 m/m^2 at 54.9 months. The substantial cracking on Control 4 is likely the result of the use of concrete with high slump, strength, and paste content as well as the use of an overlay, discussed in Section 5.3.15. Significant transverse cracking is observed throughout the deck. Transverse cracks have developed every 1 to 3-ft (0.3 to 0.9-m) along most of the length of the deck. Many cracks have propagated from the edges of the deck in the form of concentric circles, directly above the pier between the second and third

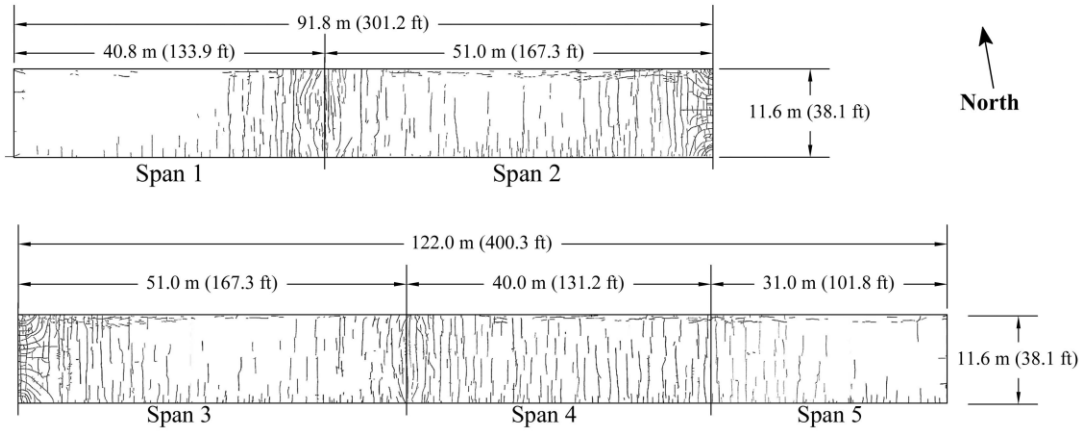

Figure 6.16 Control 4 crack map at 54.9 months

spans from the west (see Figure 6.16). Fewer transverse cracks are observed in the first 100 ft (30.5 m) at the west end of the deck than in the remainder of the deck. Longitudinal cracks have developed in a cantilevered portion of the deck (as described in Section 5.3.15), approximately 2 ft from the north edge. This cantilevered portion bears the weight of a concrete barrier located along the edge of the deck, which contributes to increased tensile stresses in the top surface. A few longitudinal cracks have propagated from the abutments.

6.2.17 Cracking Performance of LC-HPC-4 and Control 4

Crack density is plotted as a function of age for LC-HPC-4 and Control 4 in Figure 6.17. Both placements of LC-HPC-4 have exhibited less cracking than Control 4 at similar ages. LC-HPC-4 and Control 4 experienced similar low early-

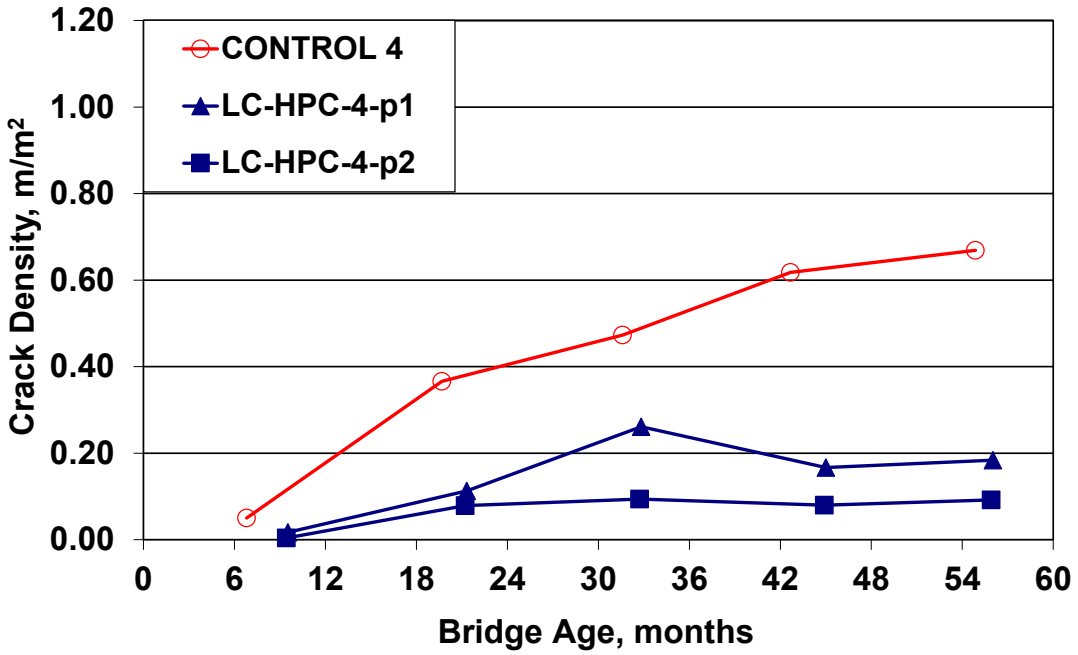

Figure 6.17 Crack density versus age for LC-HPC-4 and Control 4

age cracking around six to nine months; although, Control 4 experienced a greater rate of increase in cracking in the following four surveys. The higher cracking observed on Control 4 compared to LC-HPC-4 is likely due to the higher slump, strength, and paste content of the concrete used in the deck, discussed in Section 5.3.15. The most recent crack surveys at approximately 55 months indicate that the crack density of Control 4 is nearly four times the crack density of Placement 1 and more than seven times the crack density of Placement 2.

The two placements of LC-HPC-4 experienced similar early-age cracking at approximately 9 and 21 months; Placement 1, however, has displayed about twice the cracking of Placement 2 at 33, 45, and 56 months. The additional cracking in Placement 1 may be a result of the difficulties encountered during placement, discussed in Section 5.3.11.4. These difficulties include the possible placement of concrete with a water-cement ratio as low as 0.37, as well as extended delays in burlap placement.

6.2.18 LC-HPC-6 Crack Survey Results

LC-HPC-6 has been surveyed five times since construction in 2007. The crack map for the 2012 survey is shown in Figure 6.18. Cracking has increased from 0.063 m/m^2 at 6.5 months to 0.362 m/m^2 at 54.6 months. LC-HPC-6 is one of the highest cracking LC-HPC decks in the study. As described in Section 5.3.12.4, a significant amount of high-slump concrete was placed in this deck, which can lead to increased settlement cracking above the reinforcement. A majority of cracks have developed in the transverse direction, extending across most of the deck width. Many of the transverse cracks have propagated from the upper edge of this superelevated deck. The increased cracking along the upper edge may be a result of a lack of curing water provided by the soaker hoses. Crack density is low at the ends of the deck.

6.2.19 Control 6 Crack Survey Results

Control 6 has been surveyed four times since construction in 2008. The crack map for the 2012 survey is shown in Figure 6.19. Cracking has increased from 0.142 m/m^2 at 8.6 months to 0.539 m/m^2 at 43.0 months. Cracking doubled from 8.6 to 20.0 months (0.142 to 0.282 m/m^2) and nearly doubled again from 20.0 to 31.8 months (0.282 to 0.456 m/m^2). Significant transverse cracking has occurred in the two middle spans, often with the cracks extending across the full deck width. Cracking decreases in the outer 150 ft (45.7 m) at each end of the deck. A longitudinal crack approximately 60 ft (18.3 m) in length has developed near the deck centerline in the two easternmost spans. Longitudinal cracks have propagated from each abutment. The concrete placed in the deck had an average slump above 7 in. (180 mm) (discussed in Section 5.3.15), likely contributing to the significant cracking.

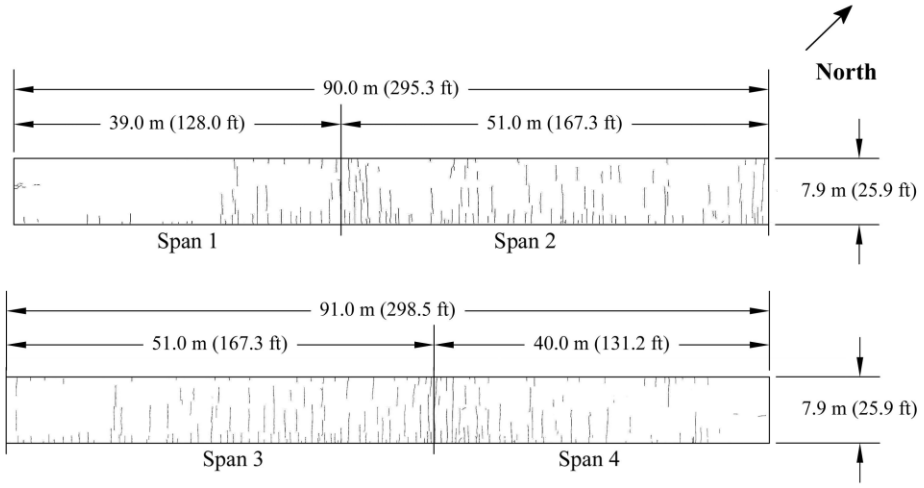

Bridge Number: 46-340 Unit 2 (LC-HPC-6)
Bridge Location: SB US-69 to WB I-435
Construction Date: 11/3/2007
Crack survey Date: 5/23/2012

Bridge Length: 181.0 m (593.8 ft)
Bridge Width: 7.9 m (25.9 ft)
Skew: 0°
Number of Spans: 4
Span 1: 39.0 m (128.0 ft)
Span 2: 51.0 m (167.3 ft)
Span 3: 51.0 m (167.3 ft)
Span 4: 40.0 m (131.2 ft)
Number of Placements: 1

Bridge Age: 54.6 months
Crack density: 0.362 m/m^2
Span 1: 0.168 m/m^2
Span 2: 0.451 m/m^2
Span 3: 0.418 m/m^2
Span 4: 0.365 m/m^2

Figure 6.18 LC-HPC-6 crack map at 54.6 months

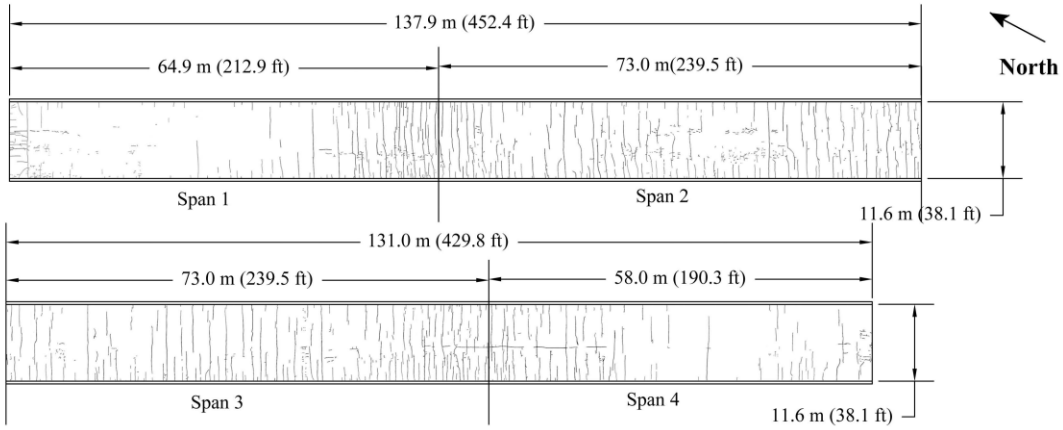

Bridge Number: 46-341 Unit 4 (Control-6)
Bridge Location: Flyover Ramp S-69 to I-435 E, Overland Park, KS
Construction Date: 10/20/2008
Crack survey Date: 5/30/2012

Bridge Length: 268.9 m (882.2 ft)
Bridge Width: 11.6 m (38.1 ft)
Skew: 0°
Number of Spans: 4
Span 1: 64.9 m (212.9 ft)
Span 2: 73.0 m (239.5 ft)
Span 3: 73.0 m (239.5 ft)
Span 4: 58.0 m (190.3 ft)
Number of Placements: 1

Bridge Age: 43.0 months
Crack density: 0.539 m/m^2
Span 1: 0.433 m/m^2
Span 2: 0.643 m/m^2
Span 3: 0.605 m/m^2
Span 4: 0.400 m/m^2

Figure 6.19 Control 6 crack map at 43.0 months

6.2.20 Cracking Performance of LC-HPC-6 and Control 6

Crack density is plotted as a function of age for LC-HPC-6 and Control 6 in Figure 6.20. At similar ages, LC-HPC-6 has exhibited less cracking than Control 6. At 43 months, LC-HPC-6 had nearly 40 percent less cracking than Control 6 (0.336 vs. 0.539 m/m^2). In the first two surveys, LC-HPC-6 and Control 6 experienced similar rates of increase in cracking. Since then, however, LC-HPC-6 has exhibited a lower rate of increase in cracking than Control 6. With a crack density of 0.362 m/m^2 at 54.6 months, LC-HPC-6 has more cracking than most other LC-HPC decks. This relatively high crack density may be a result of the high-slump concrete used in the placement [average of 4.0 in. (100 mm)] and the insufficient curing of the upper edge of the superelevated deck, discussed in Section 5.3.12.4.

6.2.21 LC-HPC-3 Crack Survey Results

LC-HPC-3 has been surveyed five times since construction in 2007. The crack map for the 2012 survey is shown in Figure 6.21. Cracking has increased from 0.028 m/m^2 at 6.5 months to 0.173 m/m^2 at 54.0 months. A crack survey was completed at 31.5 months, although an 18-ft (5.5-m) wide section along the north edge of the deck was covered with mud from construction in the area. The crack data for that survey represent only the uncovered portion of the deck. Two widely-spaced lines of small, longitudinal cracks have developed approximately 15 and 25 ft (4.5 and 7.6 m) from the north roadway barrier. Long, transverse cracks have developed above the east and west piers. Small, longitudinal cracks have propagated from both abutments. The delayed curing of the sidewalk, discussed in Section 5.3.13.4, does not appear to have increased cracking. In addition, no increase in cracking has been observed in the eastern 50 ft (15 m) of the sidewalk, a location at which water was used as a finishing aide. Small 1/2-in. (15-mm) maximum size voids in the surface are observed at locations that were not properly sealed during finishing, as discussed in Section 5.3.13.4. Although the requirements for slump and air content were met

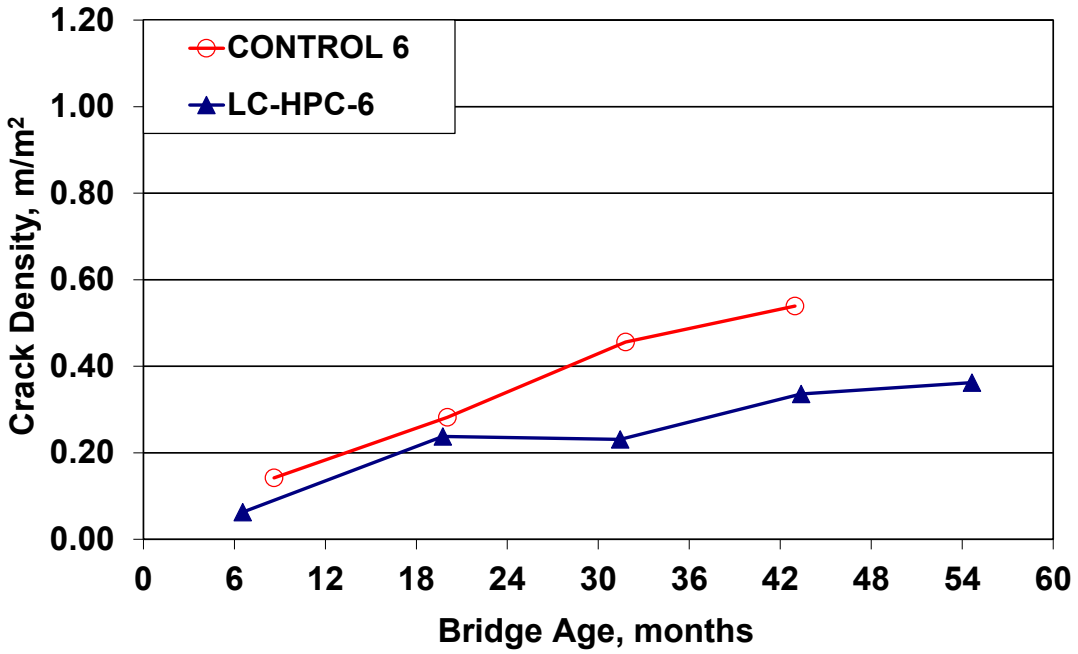

Figure 6.20 Crack density versus age for LC-HPC-6 and Control 6

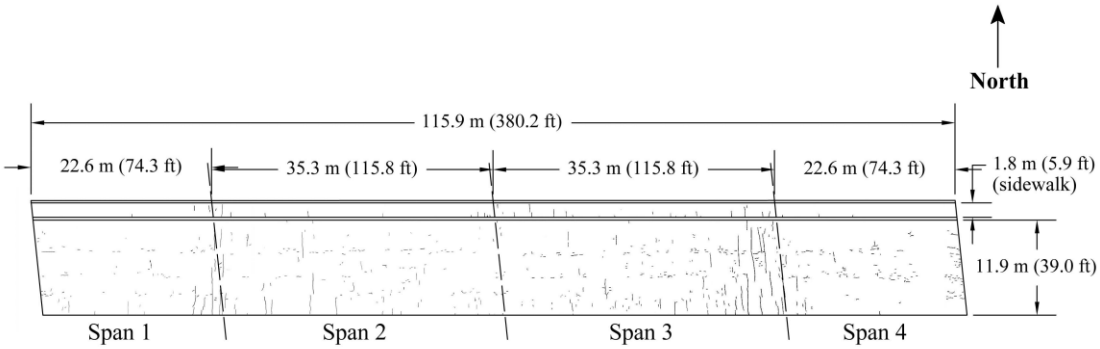

Bridge Number: 46-338 (LC-HPC-3)
Bridge Location: WB 103rd St over US 69
Construction Date: 11/13/2007
Crack survey Date: 5/14/2012

Bridge Length: 115.9 m (380.2 ft)
Bridge Width: 11.9 m (39.0 ft)
Skew: 6°
Number of Spans: 4
Span 1 : 22.6 m (74.3 ft)
Span 2 : 35.3 m (115.8 ft)
Span 3 : 35.3 m (115.8 ft)
Span 4 : 22.6 m (74.3 ft)
Number of Placements: 1

Bridge Age: 54.0 months
Crack density: 0.173 m/m²
Span 1 : 0.142 m/m²
Span 2 : 0.138 m/m²
Span 3 : 0.244 m/m²
Span 4 : 0.133 m/m²

Figure 6.21 LC-HPC-3 crack map at 54.0 months

continually during construction, the slow rate of concrete placement that resulted in delays in finishing and curing likely contributed to the cracking in the deck.

6.2.22 Control 3 Crack Survey Results

Control 3 has been surveyed five times since construction in 2007. The crack map for the 2012 survey is shown in Figure 6.22. The deck exhibited low cracking at an early age with a crack density of 0.037 m/m^2 at 10.4 months; however, the cracking significantly increased by the second survey at 22.6 months with a crack density of 0.216 m/m^2. Cracking has increased to 0.314 m/m^2 at 57.9 months. Transverse cracks have developed in every span along the deck. A portion of the transverse cracks have extended across the majority of the deck width. Similar transverse cracking is observed on the sidewalk. A few longitudinal cracks have propagated from each abutment. The cracking on this deck is likely due to the use of concrete with a high average slump [6.75 in. (170 mm)] and strength [5690 psi (39.2 MPa)] and the use of an overlay, as discussed in Section 5.3.15.

6.2.23 Cracking Performance of LC-HPC-3 and Control 3

Crack density is plotted as a function of age for LC-HPC-3 and Control 3 in Figure 6.23. Apart from a single crack survey at 42.6 months, LC-HPC-3 has continuously exhibited lower cracking than Control 3. The most recent crack surveys indicate that the crack density of LC-HPC-3 at 54.0 months is a little more than half the crack density of Control 3 at 57.9 months. Both decks exhibited low early-age cracking, but Control 3 underwent a greater rate of increase in cracking than LC-HPC-3 in subsequent surveys (excluding the survey of LC-HPC-3 at 42.6 months).

The crack survey of LC-HPC-3 at 42.6 months produced a high crack density that does not follow the trends of the preceding and following surveys. This abnormally high crack density may be due to the surveyors marking imperfections in surface finish as cracks. As discussed in Section 5.3.13.4, the contractor had

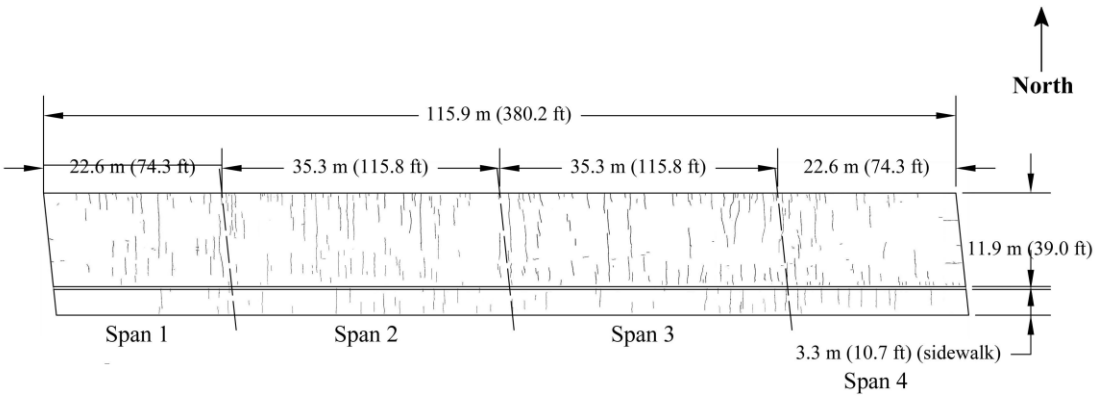

Bridge Number: 46-337 (Control-3)

Bridge Location: EB 103rd St. over US-69

Construction Date: 7/17/2007

Crack survey Date: 5/14/2012

Bridge Length: 115.9 m (380.2 ft)

Bridge Width: 11.9 m (39.0 ft)

Skew: 6°

Number of Spans: 4

Span 1: 22.6 m (74.3 ft)

Span 2: 35.3 m (115.8 ft)

Span 3: 35.3 m (115.8 ft)

Span 4: 22.6 m (74.3 ft)

Number of Placements: 1

Bridge Age: 57.9 months

Crack density: 0.314 m/m²

Span 1: 0.236 m/m²

Span 2: 0.346 m/m²

Span 3: 0.329 m/m²

Span 4: 0.306 m/m²

Figure 6.22 Control 3 crack map at 57.9 months

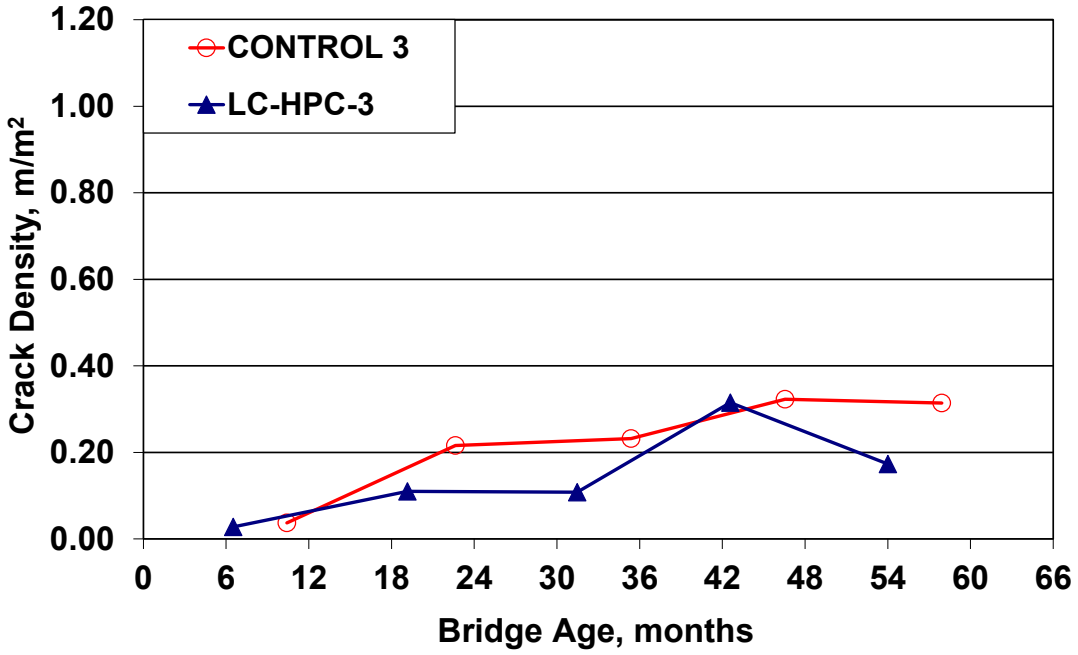

Figure 6.23 Crack density versus age for LC-HPC-3 and Control 3

difficulty properly sealing portions of the deck surface during finishing. A photo of an improperly-sealed portion of the surface is shown in Figure 6.24.

6.2.24 LC-HPC-5 Crack Survey Results

LC-HPC-5 has been surveyed five times since construction in 2007. The crack map for the 2012 survey is shown in Figure 6.25. Cracking increased from 0.059 m/m^2 at 8.0 months to 0.158 m/m^2 at 54.3 months. All cracks have developed in the transverse direction. The majority of cracks have propagated from the upper edge of the superelevated deck, likely a result of the increased exposure during delayed burlap placement and a lack of available curing water provided by the soaker hoses. Little to no cracking is observed at either end of the deck. The lowest cracking is observed at the east end of the deck – a region that experienced improved pumping efficiency compared to the remainder of the deck (discussed in Section 5.3.14.4).

6.2.25 Control 5 Crack Survey Results

Control 5 has been surveyed three times since construction in 2008, but surveys were terminated following the 2011 survey due to the placement of an overlay. The bridge exhibited the highest early-age cracking of any of the bridges in this study, with a crack density of 0.670 m/m^2 at 7.4 months. The crack map for the 2011 survey (age 30.6 months) is shown in Figure 6.26. The crack density was 0.738 m/m^2. Transverse cracks have developed every 1 to 3-ft (0.3 to 0.9-m) along the majority of the deck, extending across the full deck width at most locations. The transverse cracking is highest near the two outer piers. The transverse cracks appear to have formed directly above the reinforcing steel, likely a result of settlement cracking caused by the high [8.25 in. (210 mm)] slump concrete used for the subdecks and the use of the overlay. The cracking decreases near the ends of the deck. Longitudinal cracks have propagated from the abutments.

Figure 6.24 Improperly-sealed portions of deck surface – LC-HPC-3

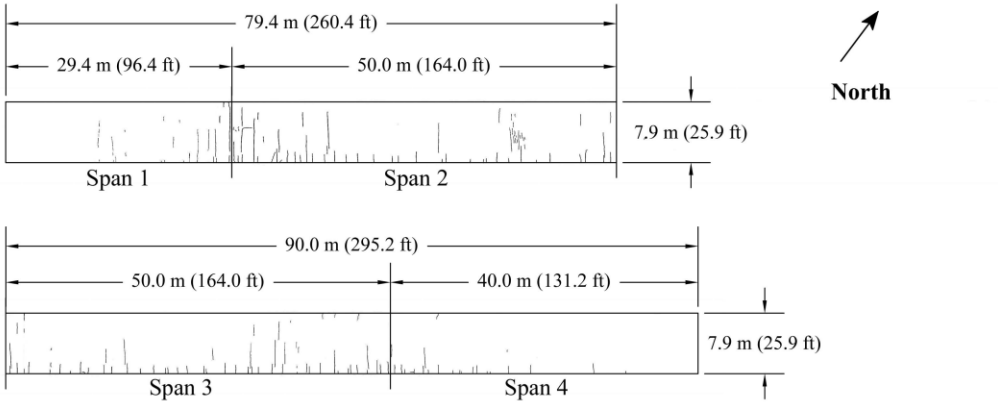

Bridge Number: 46-340 Unit 1 (LC-HPC-5)
Bridge Location: Flyover Ramp US-69 to I-435 W
Construction Date: 11/14/2007
Crack survey Date: 5/23/2012

Bridge Length: 169.4 m (555.7 ft)
Bridge Width: 7.9 m (25.9 ft)
Skew: 0°
Number of Spans: 4
Span 1: 29.4 m (96.4 ft)
Span 2: 50.0 m (164.0 ft)
Span 3: 50.0 m (164.0 ft)
Span 4: 40.0 m (131.2 ft)
Number of Placements: 1

Bridge Age: 54.3 months
Crack density: 0.158 m/m^2
Span 1: 0.131 m/m^2
Span 2: 0.231 m/m^2
Span 3: 0.175 m/m^2
Span 4: 0.045 m/m^2

Figure 6.25 LC-HPC-5 crack map at 54.3 months

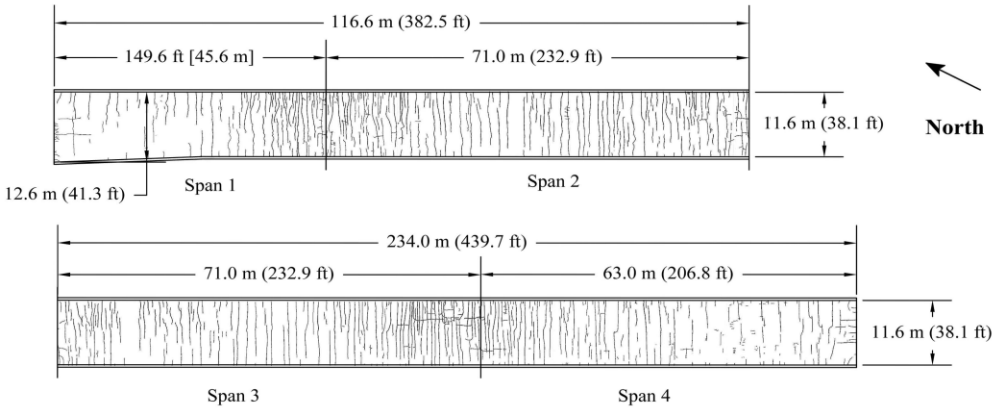

Bridge Number: 46-341 Unit 3 (Control-5)
Bridge Location: Flyover Ramp S-69 to I-435 E, Kansas City, KS
Construction Date: 11/25/2008
Crack survey Date: 6/15/2011

Bridge Length: 250.6 m (822.2 ft)
Bridge Width: 11.6 m (38.1 ft)
Skew: 0°
Number of Spans: 4
Span 1: 45.6 m (149.6 ft)
Span 2: 71.0 m (232.9 ft)
Span 3: 71.0 m (232.9 ft)
Span 4: 63.0 m (206.8 ft)
Number of Placements: 1

Bridge Age: 30.6 months
Crack density: 0.738 m/m^2
Span 1: 0.601 m/m^2
Span 2: 0.874 m/m^2
Span 3: 0.862 m/m^2
Span 4: 0.657 m/m^2

Figure 6.26 Control 5 crack map at 30.6 months

6.2.26 Cracking Performance of LC-HPC-5 and Control 5

Crack density is plotted as a function of age for LC-HPC-5 and Control 5 in Figure 6.27. LC-HPC-5 has exhibited significantly less cracking than Control 5. In the first surveys of the decks at about 8 months, Control 5 exhibited more than 11 times the early-age cracking of LC-HPC-5. Control 5 displayed the highest early-age cracking of any deck in the study, with a crack density of 0.670 m/m^2 at 7.4 months. At approximately 31 months, Control 5 had a crack density nearly six times that of LC-HPC-5. Other than Control 7 Placement 1, the Control 5 subdeck had a higher average slump than any deck in this study, with an average value of 8.25 in. (210 mm) for the seven subdeck placements. The 2011 survey will be the last available for Control 5. LC-HPC-5 exhibited low early-age cracking (0.059 m/m^2 at 8.0 months) and has since experienced a gradual increase in cracking.

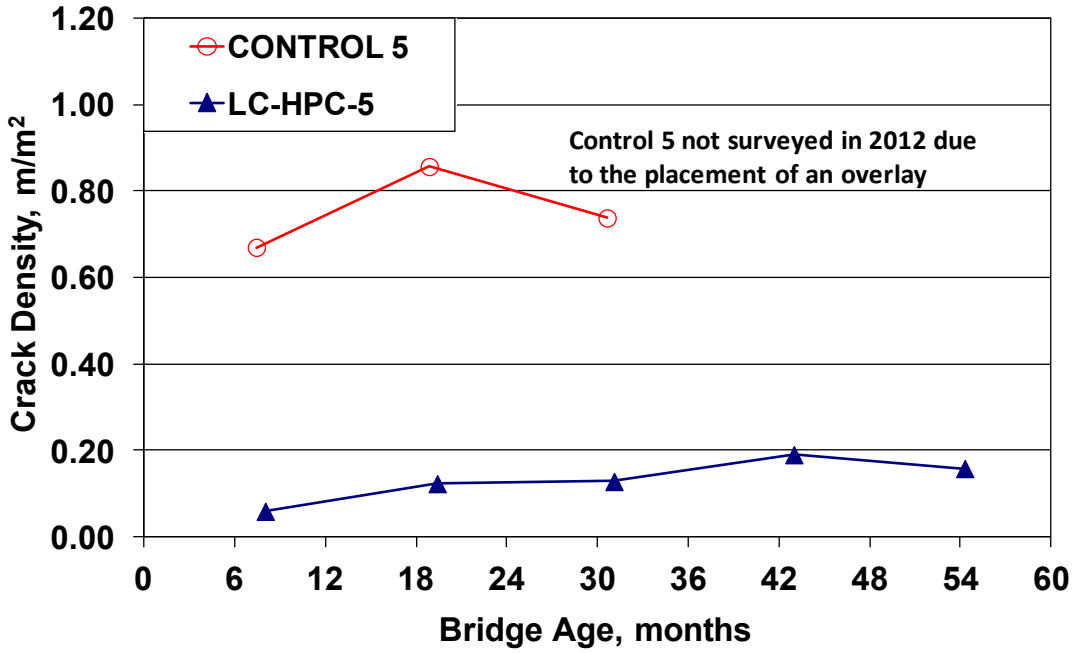

Figure 6.27 Crack density versus age for LC-HPC-5 and Control 5

6.2.27 LC-HPC-12 Crack Survey Results

Both placements of LC-HPC-12 have been surveyed four times since construction. The crack map for the 2012 survey is shown in Figure 6.28. The placements have exhibited the highest early-age cracking of any LC-HPC deck in the study. The atypical loading and significant vertical deflections caused by the positioning of the construction equipment (discussed in Section 5.3.16) likely contributed to the high early-age cracking. Placement 1 had a crack density of 0.271 m/m^2 at 16.3 months, while Placement 2 had a crack density of 0.254 m/m^2 at only 4.9 months. The crack density has increased to 0.450 m/m^2 in Placement 1 and 0.375 m/m^2 in Placement 2 at 49.5 and 38.1 months, respectively. Transverse cracks extend from both edges of the deck from the longitudinal construction joint. The crack density is highest in the middle of the center span; a location at which vertical deflections during construction would have been greatest. No increased cracking has occurred near the piers; locations at which vertical deflections during construction would have been minimal. The use of bullfloating near the ends of the deck,

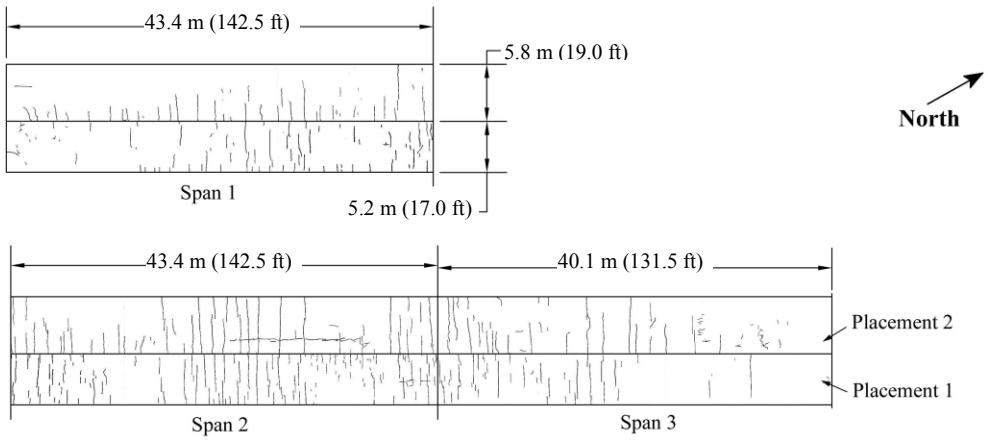

Bridge Number: 56-057 (LC-HPC-12)
Bridge Location: K-130 over Neosho Rv Unit 2
Construction Date:
Placement 1(east): 4/4/2008
Placement 2(west): 3/18/2009
Crack Survey Date: 5/21/2012

Bridge Length: 416.5' (126.95m)
Bridge Width: 36' (10.97m)
Skew: 0°
Number of Spans: 3
Span 1 (West): 142.5' (43.43m)
Span 2 (Mid): 142.5' (43.43m)
Span 3 (East): 131.5' (40.08m)
Number of Placements: 2

Bridge Age:
Placement 1: 49.5 months
Placement 2: 38.1 months
Crack Density: 0.410 m/m²
Placement 1: 0.450 m/m²
Placement 2: 0.375 m/m²
Span 1: 0.283 m/m²
Span 2: 0.604 m/m²
Span 3: 0.331 m/m²

Figure 6.28 LC-HPC-12 crack map at 49.5 and 38.1 months [Placements 1 (east) and 2 (west), respectively]

discussed in Section 5.3.16, did not appear to contribute to cracking. No increase in cracking is observed along the outer edges of the deck – regions at which water from spray hoses accumulated and ponded (discussed in Section 5.3.16). The placement of high-slump concrete on the south end of Placement 2 (discussed in Section 5.3.16.7) does not appear to have resulted in an increase in cracking in this region relative to the balance of the deck. A delay in concrete placement at the north end of Placement 2 does not appear to have significantly affected cracking.

6.2.28 Control 12 Crack Survey Results

Placement 1 (east half) of Control 12 has been surveyed four times and Placement 2 (west half) has been surveyed three times since construction. The crack map for the 2012 survey is shown in Figure 6.29. Apart from Control 5, both

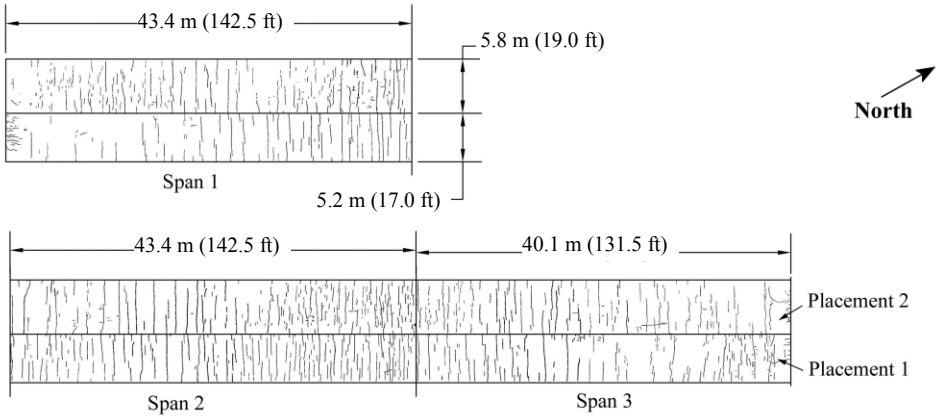

Bridge Number: 56-057 (Control-12)
Bridge Location: K-130 over Neosho Rv Unit 1
Construction Date:
Placement 1(east): 4/1/2008
Placement 2(west): 4/14/2009
Crack Survey Date: 5/21/2012

Bridge Length: 416.5' (126.95m)
Bridge Width: 36' (10.97m)
Skew: 0°
Number of Spans: 3
Span 1 (West): 142.5' (43.43m)
Span 2 (Mid): 142.5' (43.43m)
Span 3 (East): 131.5' (40.08m)
Number of Placements: 2

Bridge Age:
Placement 1: 49.6 months
Placement 2: 37.2 months
Crack Density: 0.843 m/m²
Placement 1: 0.857 m/m²
Placement 2: 0.831 m/m²
Span 1: 0.723 m/m²
Span 2: 1.015 m/m²
Span 3: 0.786 m/m²

Figure 6.29 Control 12 crack map at 49.6 and 37.2 months [Placements 1 (east) and 2 (west), respectively]

placements of Control 12 have exhibited the highest early-age cracking of any control deck in the study. Placements 1 and 2 have exhibited crack densities of 0.606 and 0.442 m/m^2 at only 16.4 and 14.5 months, respectively. In 2012, Placements 1 and 2 had crack densities of 0.857 and 0.831 m/m^2 at 49.6 and 37.2 months, respectively. Closely-spaced, transverse cracks, often extending across the full deck width, have developed along the full length of the deck. The transverse cracking decreases in the outer 75 ft (23 m) at the ends of the deck, especially in Placement 1 near the south abutment. Longitudinal cracks extend from the south abutment in the east half of the deck (Placement 1). Additional longitudinal cracks extend from the north end of the deck in both placements. The concrete used in this deck had a paste content above 27 percent – the value, when exceeded, observed by Schmitt and Darwin (1995, 1999) and Lindquist et al. (2005) to significantly increase cracking.

6.2.29 Cracking Performance of LC-HPC-12 and Control 12

Crack density is plotted as a function of age for the placements of LC-HPC-12 and Control 12 in Figure 6.30. The placements of LC-HPC-12 exhibit lower cracking than the placements of Control 12 at similar ages. At approximately 38 months, the LC-HPC-12 placements have less than half the cracking of the Control 12 placements. Control 12 may have exhibited higher cracking than LC-HPC-12 due to the use of concrete with a higher paste content (27.1 vs. 24.2 percent) and the use of the overlay. In addition, as shown in Sections 5.3.16 and 5.3.17, higher-strength concrete was used in Control 12 than in LC-HPC-12. LC-HPC-12 has experienced the highest early-age cracking of any LC-HPC deck in the study. Because of the high early-age cracking, this deck also exhibited high crack densities at later ages. The performance of this deck reinforces the importance of minimizing early-age cracking to achieve long-term benefits. In this case, the high early-age cracking likely results from the unusual load applied during construction. As discussed in Section 5.3.16.7, movement of the crane during construction of Placement 2 induced significant vertical deflections in both placements. The location that experienced the highest cracking in both placements of LC-HPC-12, the center of the middle span, is a location that would have experienced the largest deflections during construction. The extension of the bucket loads across to Placement 2 also likely induced stresses in Placement 1.

6.2.30 LC-HPC-13 Crack Survey Results

LC-HPC-13 has been surveyed four times since construction in 2008. The crack map for the 2012 survey is shown in Figure 6.31. The deck experienced low cracking at an early age (0.050 m/m^2 at 13.8 months), but cracking has increased significantly with values of 0.364 m/m^2 at 37.1 months and 0.342 m/m^2 at 49.0 months, the two most recent surveys. With the exception of a line of small cracks parallel to the bridge skew in the middle of the south span, most of the cracks have

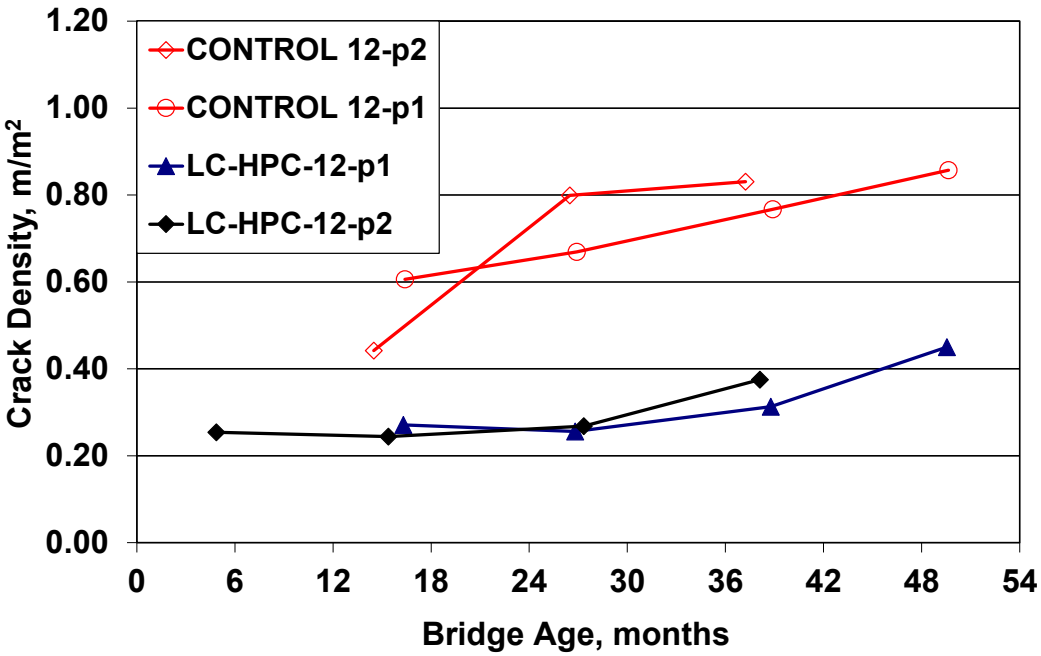

Figure 6.30 Crack density versus age for LC-HPC-12 and Control 12

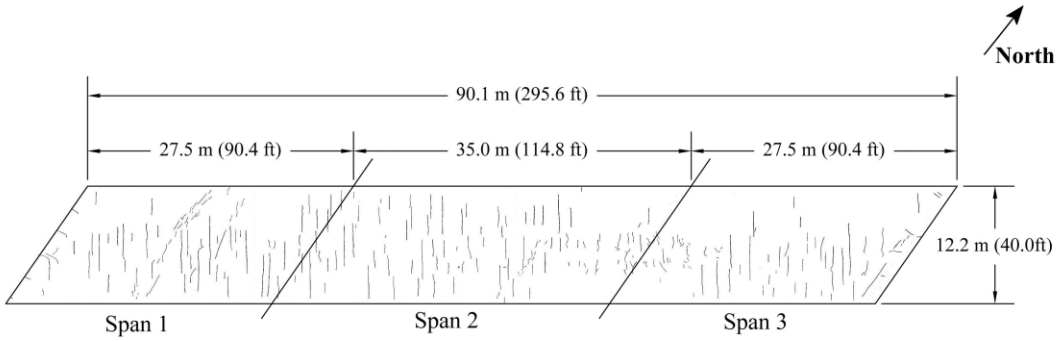

Bridge Number: 54-66 (LC-HPC-13)
Bridge Location: NB US-69 over BNSF RR, Linn County, KS
Construction Date: 4/29/2008
Crack survey Date: 5/29/2012

Bridge Length: 90.1 m (295.6 ft)
Bridge Width: 12.2 m (40.0 ft)
Skew: -34.8
Number of Spans: 3
Span 1 (West): 27.5 m (90.4 ft)
Span 2 (Middle): 35.0 m (114.8 ft)
Span 3 (East): 27.5 m (90.4 ft)
Number of Placements: 1

Bridge Age: 49.0 months
Crack density: 0.342 m/m²
Span 1 (West): 0.392 m/m²
Span 2 (middle): 0.342 m/m²
Span 3 (East): 0.291 m/m²

Figure 6.31 LC-HPC-13 crack map at 49.0 months

developed in the transverse direction, parallel to the reinforcement, not parallel to the skew of the bridge. Slightly more cracking has developed in the south half of the deck than in the north half, possibly due to an increased paste content at the surface due to bullfloating on the south half. No increase in cracking is observed on the east edge or the north end of the deck due to, respectively, the ponding of water or the relatively long delay at the end of placement due to backordered concrete (as discussed in Section 5.3.18.4).

6.2.31 Control 13 Crack Survey Results

Control 13 has been surveyed four times since construction in 2008. The crack map for the 2012 survey is shown in Figure 6.32. The deck exhibited low early-age cracking with a crack density of 0.028 m/m^2 at 11.0 months; however, by the third survey (34.4 months), the crack density had increased to 0.524 m/m^2. The most recent crack survey yielded a crack density of 0.543 m/m^2 at 46.1 months. Significantly more cracks have formed in the two outer spans compared to the center span. At 46.1 months, the crack density of the center span (0.268 m/m^2) was slightly more than half the crack density of the west span (0.494 m/m^2) and slightly more than a quarter the crack density of the east span (0.927 m/m^2). The significant cracking in the west span is focused in a 70-ft (21-m) section directly west of the pier. Many small, map cracks have developed in the two outer spans. As discussed in Section 5.3.19.2, the average concrete temperatures of the subdeck and overlay of Control 13 were 89° and 91° F (32° and 33° C), respectively; significantly higher values than allowed in the LC-HPC specifications. High concrete temperatures such as these increase the potential for plastic shrinkage cracking, which typically develop in the form of map cracks. Overfinishing can also contribute to map cracking by bringing additional paste to the surface. Many transverse cracks have also formed in the outer spans. A smaller number of transverse cracks have formed in the positive moment region of the center span. Small, longitudinal cracks extend from the abutments.

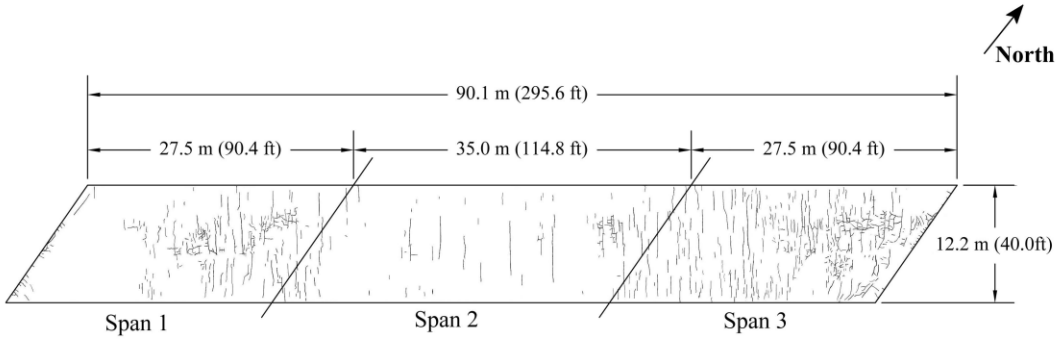

Bridge Number: 54-67 (Control-13)
Bridge Location: SB US-69 over BNSF RR, Linn County, KS
Construction Date: 7/25/2008
Crack survey Date: 5/29/2012

Bridge Length: 90.1 m (295.6 ft)
Bridge Width: 12.2 m (40.0 ft)
Skew: -34.8°
Number of Spans: 3
Span 1 (West): 27.5 m (90.4 ft)
Span 2 (Middle): 35.0 m (114.8 ft)
Span 3 (East): 27.5 m (90.4 ft)
Number of Placements: 1

Bridge Age: 46.1 months
Crack density: 0.543 m/m²
Span 1 (West): 0.494 m/m²
Span 2 (middle): 0.268 m/m²
Span 3 (East): 0.927 m/m²

Figure 6.32 Control 13 crack map at 46.1 months

6.2.32 Cracking Performance of LC-HPC-13 and Control 13

Crack density is plotted as a function of age for LC-HPC-13 and Control 13 in Figure 6.33. LC-HPC-13 has displayed less cracking than Control 13 at similar ages. At approximately 48 months, LC-HPC-13 has about 60 percent of the crack density of Control 13 (0.342 vs. 0.543 m/m^2). Both decks exhibited low early-age cracking at approximately 12 months. Control 13, however, has experienced a greater increase in cracking than LC-HPC-13 in later surveys. The average temperature of the concrete placed in Control 13 was 21° F (12° C) higher than that of the concrete placed in LC-HPC-13, likely contributing to the higher cracking. The significantly higher compressive strength of the Control 13 overlay compared to the LC-HPC-13 deck [8280 vs. 4280 psi (57.1 vs. 29.5 MPa)] (discussed in Sections 5.3.18 and 5.3.19) likely contributed to the higher cracking as well. Nonetheless, LC-HPC-13 has experienced greater cracking than most LC-HPC decks in the study.

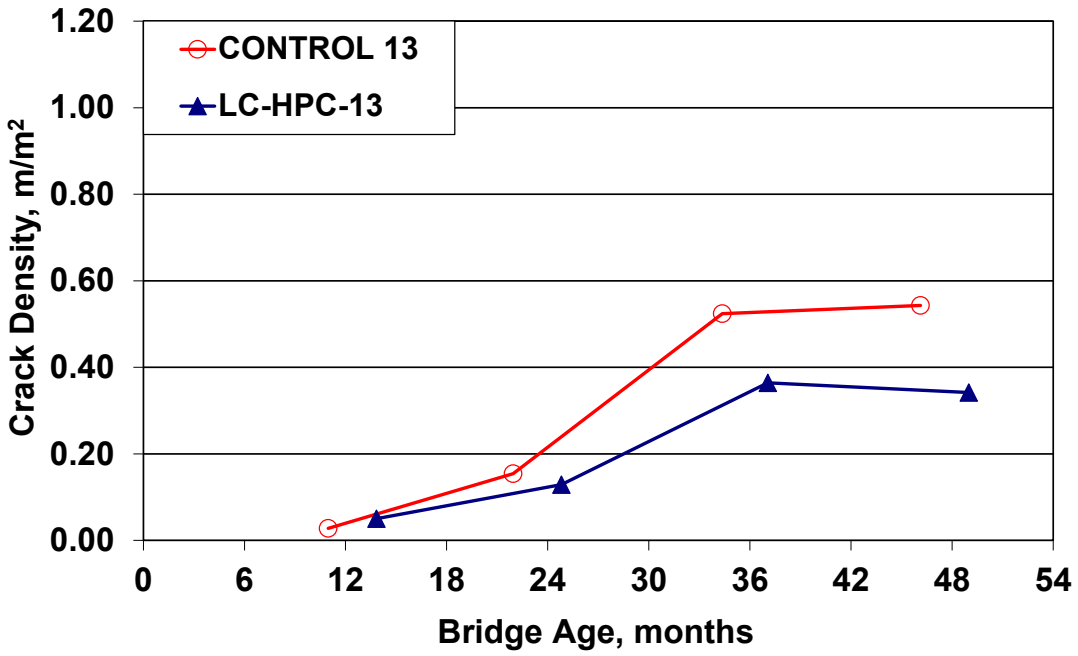

Figure 6.33 Crack density versus age for LC-HPC-13 and Control 13

6.2.33 LC-HPC-9 Crack Survey Results

LC-HPC-9 has been surveyed three times since construction in 2009. The crack map for the 2012 survey is shown in Figure 6.34. Cracking has increased from 0.130 m/m^2 at 13.6 months to 0.362 m/m^2 at 38.3 months. Transverse cracks have developed parallel to the reinforcement throughout most of the deck. Cracking decreases in the outer 50 ft (15.2 m) at each end of the deck and, unlike many of the decks in this study, no longitudinal cracks have formed at the abutments. The non-integral design of the abutments, described in Section 5.3.20, will not provide the same level of restraint to the deck ends as integral abutments, likely the primary reason no cracking was observed at the abutments. The delay in placement at the south abutment and the increased use of high-slump concrete placed near the north abutment (discussed in Section 5.3.20.6) do not appear to have contributed to cracking. It is not entirely clear why LC-HPC-9 has experienced such high cracking as the average slump and strength are both relatively low [3.5 in. (90 mm) and 4190

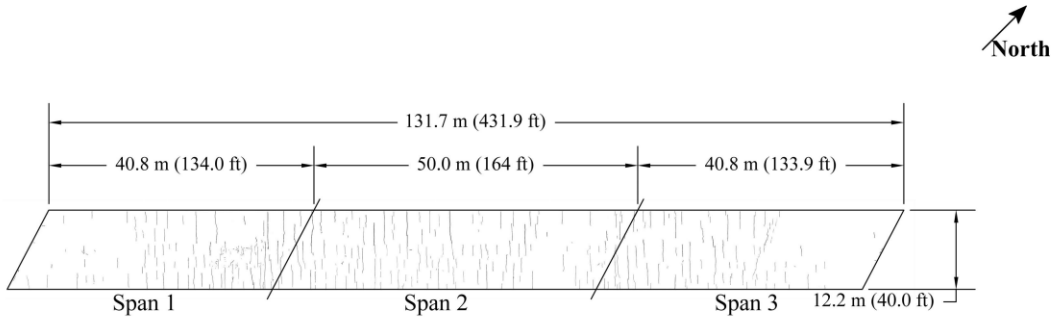

Bridge Number: 54-57 (LC-HPC-9)
Bridge Location: NB US-69 over Marair Des Cygnes Rv
Construction Date: 4/15/2009
Crack survey Date: 6/25/2012

Bridge Length: 131.7 m (431.9 ft)
Bridge Width: 12.2 m (40.0 ft)
Skew: -27.7°
Number of Spans: 3
Span 1 (South): 40.8 m (134.0 ft)
Span 2 (Middle): 50.0 m (164.0 ft)
Span 3 (North): 40.8 m (133.9 ft)
Number of Placements: 1

Bridge Age: 38.3 months
Crack density: 0.362 m/m²
Span 1 (South): 0.319 m/m²
Span 2 (Middle): 0.421 m/m²
Span 3 (North): 0.325 m/m²

Figure 6.34 LC-HPC-9 crack map at 38.3 months

psi (28.9 MPa), respectively] and the burlap was placed quickly after strikeoff. The effect of the relative difference between the concrete and ambient air temperature during construction (discussed in Section 6.4.2) may have contributed to the high cracking.

6.2.34 Control 9 Crack Survey Results

Control 9, with its two overlay placements, has been surveyed three times since construction in 2008. The crack map for the 2012 survey is shown in Figure 6.35. Placements 1 and 2 exhibited high early-age cracking with crack densities of 0.368 and 0.395 m/m^2 at 24.2 and 24.0 months, respectively. Transverse cracks extend nearly across the full deck width along the entire length of the deck. The transverse cracks increase somewhat near the piers and are highest between the midpoints of the two outside spans, including the full length of the center span. A few longitudinal cracks have developed on both sides of the longitudinal overlay placement joint,

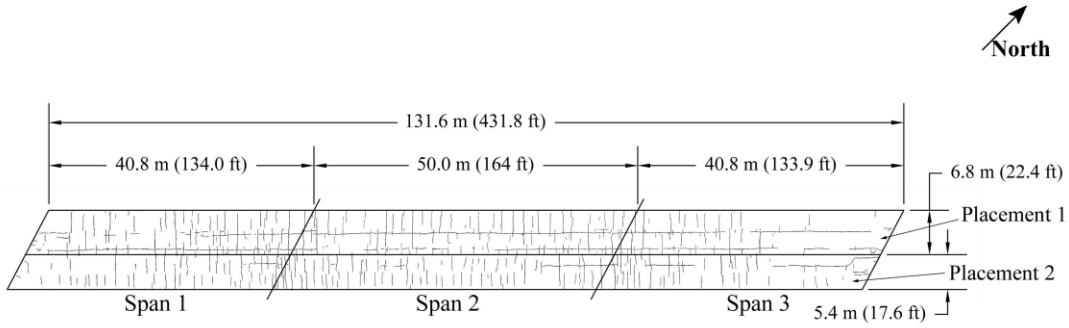

Bridge Number: 54-58 (Control-9)
Bridge Location: NB US-69 over Marair Des Cygnes Rv
Construction Date:
Placement 1 (West)**:** 5/21/2008
Placement 2 (East): 5/29/2008

Crack survey Date: 6/25/2012

Bridge Length: 131.6 m (431.8 ft)
Bridge Width: 12.2 m (40.0 ft)
Skew: -27.2 °
Number of Spans: 3
Span 1 (South): 40.8 m (134.0 ft)
Span 2 (Middle): 50.0 m (164.0 ft)
Span 3 (North): 40.8 m (133.8 ft)
Number of Placements: 2
Placement1(West): 6.8 m (22.4 ft)
Placement2 (East): 5.4 m (17.6 ft)

Bridge Age:
Placement 1: 49.1 months
Placement 2: 48.9 months
Crack density: 0.577 m/m²
Placement 1: 0.637 m/m²
Placement 2: 0.501 m/m²
Span 1 (South): 0.574 m/m²
Span 2 (Middle): 0.651 m/m²
Span 3 (North): 0.486 m/m²

Figure 6.35 Control 9 crack map at 49.1 and 48.9 months [Placements 1 (west) and 2 (east), respectively]

continuing nearly the entire length of the deck. Only a few longitudinal cracks have propagated from the abutments. Similar to LC-HPC-9, Control 9 has non-integral end conditions (discussed in Section 5.3.21) which provide less restraint to the deck near the abutments than integral end conditions. The two overlays of Control 9 had high compressive strengths, each exceeding 6000 psi (41.4 MPa), likely contributing to the cracking.

6.2.35 Cracking Performance of LC-HPC-9 and Control 9

Crack density is plotted as a function of age for LC-HPC-9 and the placements of Control 9 in Figure 6.36. To date, LC-HPC-9 has experienced better cracking performance than the placements of Control 9 at similar ages. At approximately 38 months, LC-HPC-9 has two-thirds the crack density of Control 9 at the same age. This higher cracking in Control 9 is likely due to the use of the overlays and the high

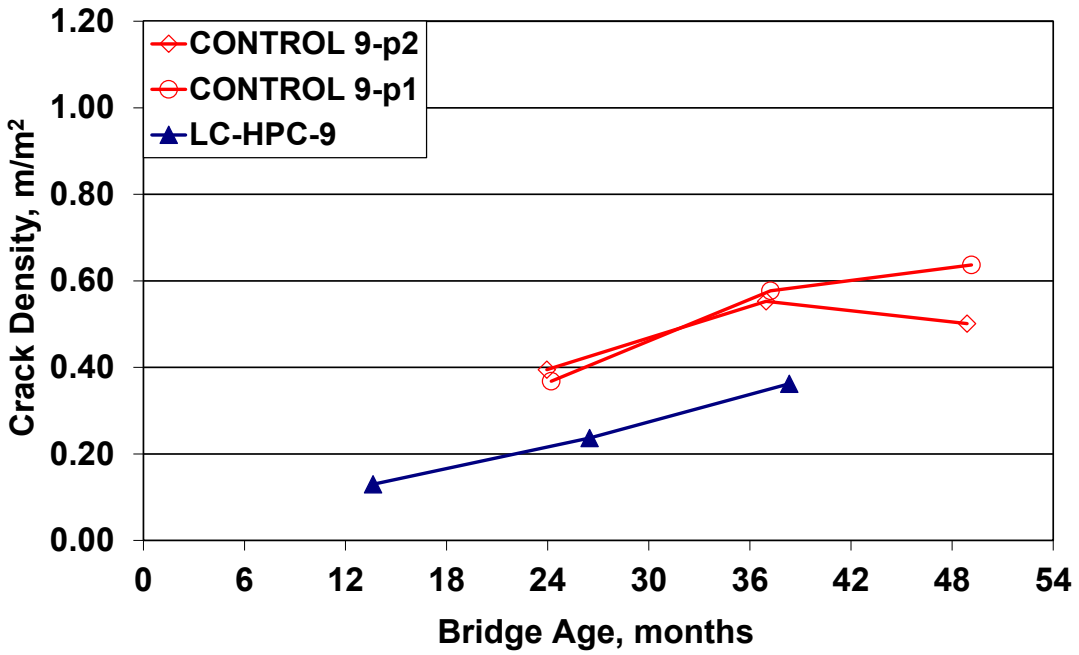

Figure 6.36 Crack density versus age for LC-HPC-9 and Control 9

strength of these overlays. At 0.130 m/m^2 at 13.6 months, LC-HPC-9 exhibited a higher early-age crack density than most LC-HPC decks in the study and continues to exhibit a relatively high rate of increase. As stated previously, this high cracking in LC-HPC-9 may be due to the effect of the relative difference in the concrete and air temperature during construction, discussed in Section 6.4.2.

6.2.36 OP Bridge – Placement 1 Crack Survey Results

Three surveys have been completed on Placement 1 of the OP Bridge since construction in 2007. This placement exhibited higher early-age cracking than any of the LC-HPC decks; however, the following two placements of the OP Bridge, which are discussed in the subsequent sections, exhibited even greater early-age cracking. Cracking trends were clearly established within the first 36 months after the construction of the OP Bridge, and therefore, a crack survey was not completed on the deck in 2012. The crack map for the 2011 survey is shown in Figure 6.37. Cracking increased from 0.341 m/m^2 at 18.3 months to 0.585 m/m^2 at 42.2 months. Most cracks are transverse with short longitudinal cracks developing at both

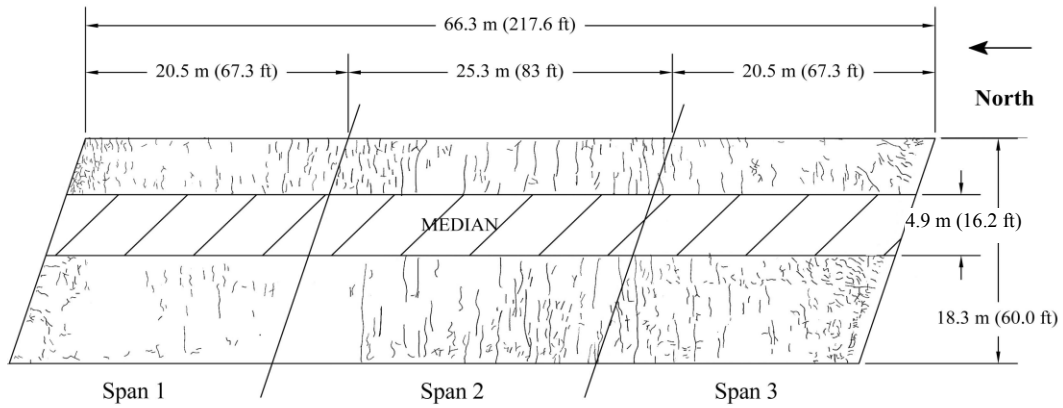

Bridge Number: 46-363 (OP Bridge - Placement 1)
Bridge Location: Metcalf Ave over Indian Creek, OP, Kansas
Construction Date: 12/19/2007
Crack Survey Date: 6/24/2011

Bridge Length: 66.3 m (217.6 ft)
Bridge Width: 18.3 m (60.0 ft)
Skew: -18°
Number of Spans: 3
Span 1: 20.5 m (67.3 ft)
Span 2: 25.3 m (83.0 ft)
Span 3: 20.5 m (67.3 ft)
Number of Placements: 1

Bridge Age: 42.2 months
Crack Density: 0.585 m/m^2
Span 1: 0.410 m/m^2
Span 2: 0.621 m/m^2
Span 3: 0.718 m/m^2

Figure 6.37 OP Bridge Placement 1 crack map at 42.2 months

abutments. A majority of the cracks are short, developing randomly throughout the deck. The short cracks appear to be associated with plastic shrinkage, which was likely caused by excessive paste at the surface from the overfinishing and drying out of the surface due to the delays in burlap placement. As discussed in Section 5.3.22.5, the placement of burlap was slow throughout placement, averaging 28 minutes from strikeoff to burlap placement. In addition, the consolidation procedures used during placement did not comply with the requirements of the specifications (discussed in Section 5.3.22.5) and likely contributed to the significant cracking. The placement of high-slump concrete [commonly greater than 4 in. (90 mm)] in all three placements of the OP Bridge (discussed in Section 5.3.22) increased the potential for settlement cracking. Less cracking is observed on the north end of the placement, possibly due to an increased rate of burlap placement in this region compared to the remainder of the deck (discussed in Section 5.3.22.5).

6.2.37 OP Bridge – Placement 2 Crack Survey Results

Three surveys have been completed on Placement 2 of the OP Bridge since construction in 2008. This placement has exhibited the highest early-age cracking of any deck let in accordance with the LC-HPC specifications and by the third survey (37.7 months) had a higher crack density than all but one other monolithic bridge deck in Kansas. Placement 2 exhibited nearly twice the early-age cracking of Placement 1, yielding a crack density of 0.640 m/m^2 at only 13.7 months. As previously stated, cracking trends in the OP Bridge were clearly established within the first 36 months after construction, and therefore, a crack survey was not completed in 2012. The crack map for the 2011 survey, which yielded a crack density of 1.304 m/m^2 at 37.7 months, is shown in Figure 6.38. Short, map cracks have developed extensively throughout the deck. As in Placement 1, the map cracking appears to be caused by plastic shrinkage – a result of the excessive finishing of the surface and extended time to burlap placement. The double-drum roller screed used in the placement, discussed in Section 5.3.22.6, likely contributed to the extensive map cracking by bringing additional cement paste to the surface. Increased cracking is observed near the south abutment, likely a result of the delay in placement due to backordered concrete discussed in Section 5.3.22.6. Long, transverse cracks are scattered between the map cracks, primarily in the middle span, but extending to the middle of the two outer spans. The cracks in the sidewalk portion of the deck are mainly transverse and often extend across the full width of the sidewalk. As discussed in Section 5.3.22.6, the concrete supplier consistently produced concrete with high values of slump, increasing the potential for settlement cracking. The transfer of concrete from a wing wall into the deck during a delay in placement at the north end likely affected the quality of concrete placed at this location. The increased use of bullfloating and a delay near the north end of the placement (discussed in Section 5.3.22.6) did not increase cracking in this section

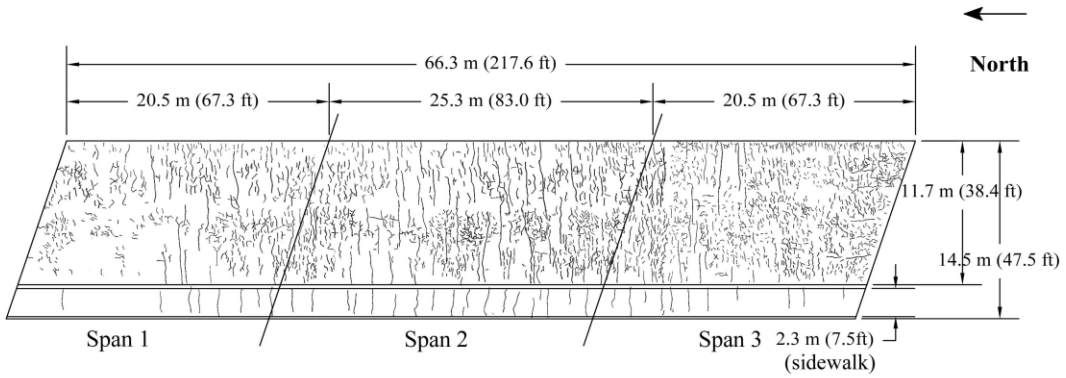

Bridge Number: 46-363 (OP Bridge - Placement 2)
Bridge Location: Metcalf Ave over Indian Creek, OP, Kansas
Construction Date: 5/2/2008
Crack Survey Date: 6/24/2011

Bridge Length: 66.3 m (217.6 ft)
Bridge Width: 14.5 m (47.5 ft)
Skew: -18°
Number of Spans: 3
Span 1: 20.5 m (67.3 ft)
Span 2: 25.3 m (83.0 ft)
Span 3: 20.5 m (67.3 ft)
Number of Placements: 1

Bridge Age: 37.7 months
Crack Density: 1.303 m/m^2
Span 1: 0.940 m/m^2
Span 2: 1.443 m/m^2
Span 3: 1.500 m/m^2

Figure 6.38 OP Bridge Placement 2 crack map at 37.7 months

relative to the balance of the placement. The slower rate of burlap placement on the sidewalk compared to the roadway portion of the placement did not contribute to increased cracking; in fact, the sidewalk has experienced less cracking than the roadway.

6.2.38 OP Bridge – Placement 3 Crack Survey Results

As with Placements 1 and 2, Placement 3 has exhibited higher early-age cracking than any of the LC-HPC decks previously constructed. The placement has been surveyed three times since construction in 2008. With a crack density of 0.421 m/m^2 at 13.3 months, Placement 3 has exhibited higher early-age cracking than Placement 1, but lower early-age cracking than Placement 2. The crack map for the 2011 survey is shown in Figure 6.39. At 37.1 months, the placement had a crack density of 0.678 m/m^2. The pattern of cracking in Placement 3 is similar to that of Placements 1 and 2. Significant map cracking has developed throughout the outer

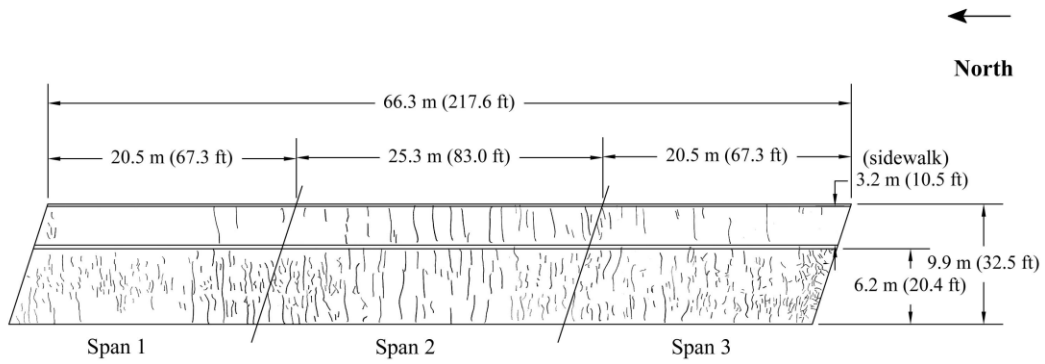

Bridge Number: 46-363 (OP Bridge - Placement 3)
Bridge Location: Metcalf Ave over Indian Creek, OP, Kansas
Construction Date: 5/21/2008
Crack Survey Date: 6/24/2011

Bridge Length: 66.3 m (217.6 ft)
Bridge Width: 9.9 m (32.5 ft)
Skew: -18°
Number of Spans: 3
Span 1: 20.5 m (67.3 ft)
Span 2: 25.3 m (83.0 ft)
Span 3: 20.5 m (67.3 ft)
Number of Placements: 1

Bridge Age: 37.1 months
Crack Density: 0.678 m/m^2
Span 1: 0.558 m/m^2
Span 2: 0.708m/m ^{2}
Span 3: 0.737 m/m^2

Figure 6.39 OP Bridge Placement 3 crack map at 37.1 months

spans and near the piers in the interior span. Long, transverse cracks extend nearly across the full width of the roadway and sidewalk in the middle span. As with Placements 1 and 2, the placement of high-slump concrete, discussed in Section 5.3.22.7, likely contributed to settlement cracking. The double-drum roller screed used during placement likely brought additional paste to the surface and contributed to plastic shrinkage cracking.

6.2.39 Cracking Performance of the OP Bridge

Crack density is plotted in Figure 6.40 as a function of time for the three placements of the OP Bridge along with those for LC-HPC steel girder bridges. This comparison of cracking performance demonstrates the importance of following all aspects of the LC-HPC specifications. The three OP Bridge placements have exhibited greater cracking than every LC-HPC placement at a similar age. The OP Bridge placements experienced considerably high early-age cracking, ranging from

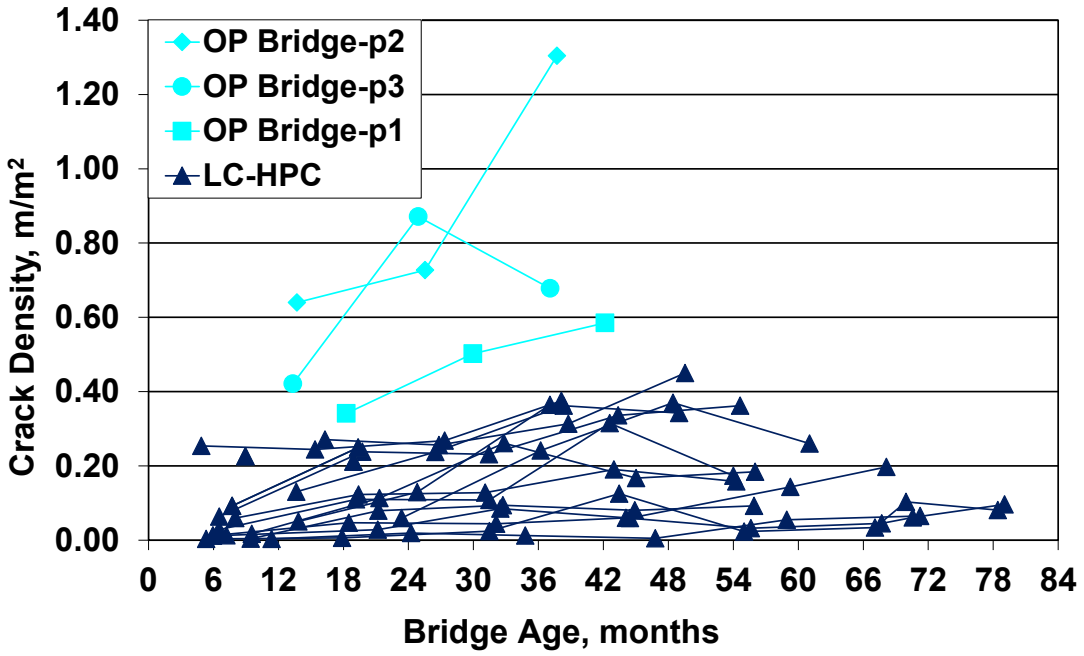

Figure 6.40 Crack density versus age for OP Bridge and LC-HPC decks constructed on steel girders

0.341 to 0.640 m/m^2, at ages between 12 and 18 months. In addition, each placement experienced a substantial increase in cracking between the first and second surveys. A decrease in cracking occurred for Placement 3 between 24.9 and 37.1 months. This is likely a result of small cracks being overlooked by the survey crew, as occurred with Control 7. As discussed in Section 5.3.22, a number of factors likely contributed to the poor cracking performance of the OP Bridge, including placement of out-of-specification high-slump concrete, improper consolidation, overfinishing, and delayed burlap placement.

6.2.40 LC-HPC-16 Crack Survey Results

LC-HPC-16 has been surveyed twice since construction in 2010. A 5-ft (1.5-m) section along the west edge of the deck was covered with construction materials and was unable to be inspected during the first survey at 7.7 months; however, this section was not considered in the calculation of the crack density for that survey. The crack map for the 2012 survey is shown in Figure 6.41. Cracking increased from

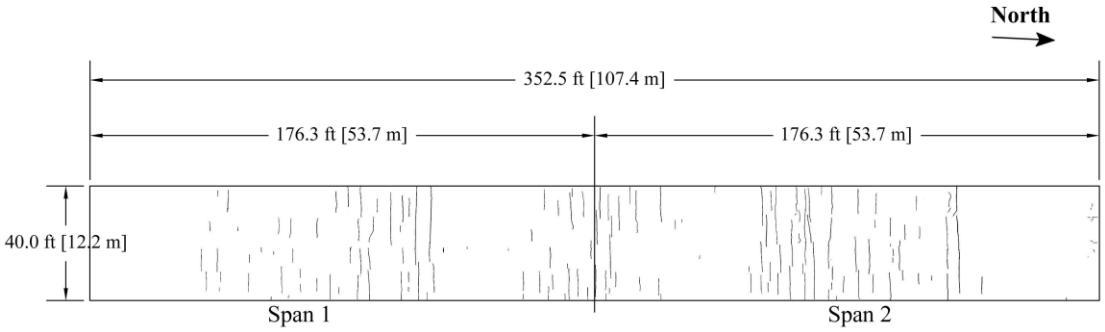

Bridge Number: 46-352 (LC-HPC-16)
Bridge Location: SB K-7 over Johnson Dr./55th St.
Construction Date: 10-28-2010
Crack Survey Date: 6-8-2012

Bridge Length: 352.5 ft (107.4 m)
Bridge Width: 40.0 ft(12.2 m)
Skew: 0°
Number of Spans: 2
Span 1: 176.25 ft (53.7 m)
Span 2: 176.25 ft (53.7 m)
Number of Placements: 1

Bridge Age: 19.4 months
Crack Density: 0.249 m/m²
Span 1: 0.204 m/m²
Span 2: 0.287 m/m²

Figure 6.41 LC-HPC-16 crack map at 19.4 months

0.092 m/m^2 at 7.7 months to 0.249 m/m^2 at 19.4 months. This level of cracking is relatively high for an LC-HPC deck at only 19 months. Nearly all cracking has developed in the transverse direction, focused near the middle of both spans and above the center pier. As discussed in Section 5.3.23.4, ponded water was noted during construction along the deck edges near the pier, where cracking is observed. Many of the transverse cracks in the middle of the spans extend across most of the deck width. Higher cracking is observed in the north span, possibly a result of the difficulties encountered using the first pump and the excess water that was occasionally added to the concrete to aide in pumping (both discussed in Section 5.3.23.4). Cracking is lower in the span with the higher cement content [520 lb/yd^3 (308 kg/m^3) in the north span vs. 540 lb/yd^3 (320 kg/m^3) in the south span]. Little to no cracking has developed in locations of low bending moment in the deck, including areas near the abutments, which are non-integral with the deck, and the inflection points. During the surveys, the survey crew noted abnormally-large deflections near

the middle of the spans as the bridge carried large truck traffic. It is possible that the construction equipment induced similar large deflections during placement, contributing to settlement cracking above the reinforcement in the center of the spans. Similar to LC-HPC-9 (discussed in Section 6.2.40), the relatively high cracking observed on LC-HPC-16 may have been contributed by the use of concrete with temperatures [average of 59º F (15º C)] that were higher than the air temperatures [average of 50º F (10º C) on the day of construction] during construction. A detailed explanation of this effect of temperature is presented in Section 6.4.2.

6.2.41 LC-HPC-15 Crack Survey Results

LC-HPC-15 has been surveyed once since construction in 2010. The crack map for the 2012 survey is shown in Figure 6.42. At 18.9 months after construction, LC-HPC-15 had a crack density of 0.211 m/m^2 – somewhat lower than that of LC-HPC-16 at a similar age (LC-HPC-16 had a crack density of 0.249 m/m^2 at 19.4 months). The crack patterns on LC-HPC-15 are similar to those of LC-HPC-16. Nearly all cracks have developed in the transverse direction, concentrated in the middle of both spans and above the center pier. The high cracking noted above the center pier is where, as discussed in Section 5.3.24.4, high-slump concrete was placed. Higher cracking is observed in the north span, although slumps were consistently lower in this half of the deck (discussed in Section 5.3.24.4). A delay in placement that left the first 45 ft (13.7 m) of the north end of the deck exposed for 30 minutes (discussed in Section 5.3.24.4) does not appear to have affected cracking in this region. As with LC-HPC-16, little to no cracking has developed in locations of low bending moment in the deck. Large deflections, similar to those on LC-HPC-16, were observed by the survey crew near the middle of the spans as the bridge carried large truck traffic. Again, large deflections such as these may have contributed to

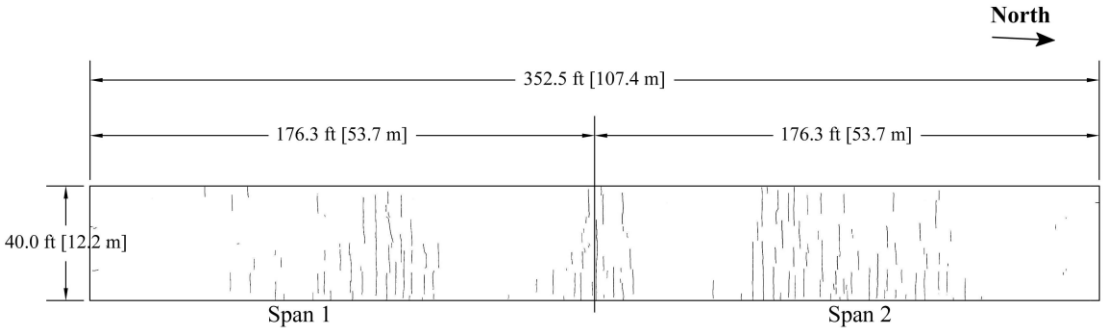

Bridge Number: 46-351 (LC-HPC-15)
Bridge Location: NB K-7 over Johnson Dr./55th St.
Construction Date: 11-10-10
Crack Survey Date: 6-8-2012

Bridge Length: 352.5 ft (118.2 m)
Bridge Width: 40.0 ft(12.2 m)
Skew: 0°
Number of Spans: 3
Span 1: 176.25 ft (36.7 m)
Span 2: 176.25 ft (44.8 m)
Number of Placements: 1

Bridge Age: 18.9 months
Crack Density: 0.211 m/m^2
Span 1: 0.183 m/m^2
Span 2: 0.236 m/m^2

Figure 6.42 LC-HPC-15 crack map at 18.9 months

settlement cracking a short time after placement. Apart from the possible effect of these large deflections, the reasons for the relatively high cracking of LC-HPC-15 (compared to other LC-HPC decks) are difficult to pinpoint since the concrete had an average slump [3.25 in. (85 mm)] and strength [4440 psi (30.6 MPa)] similar to other LC-HPC decks and the burlap was placed quickly after strikeoff.

6.2.42 LC-HPC-17 Crack Survey Results

LC-HPC-17 has been surveyed once since construction in 2011. The crack map for the 2012 survey is shown in Figure 6.43. Due to the coloring of the concrete sidewalk and recreational trail, discussed in Section 5.3.25, only the roadway portion of the deck is surveyed. At 8.9 months after construction, LC-HPC-17 exhibited a high early-age crack density of 0.226 m/m^2. The cracking patterns on LC-HPC-17 are similar to the patterns of LC-HPC-15 and 16. Cracks have primarily developed

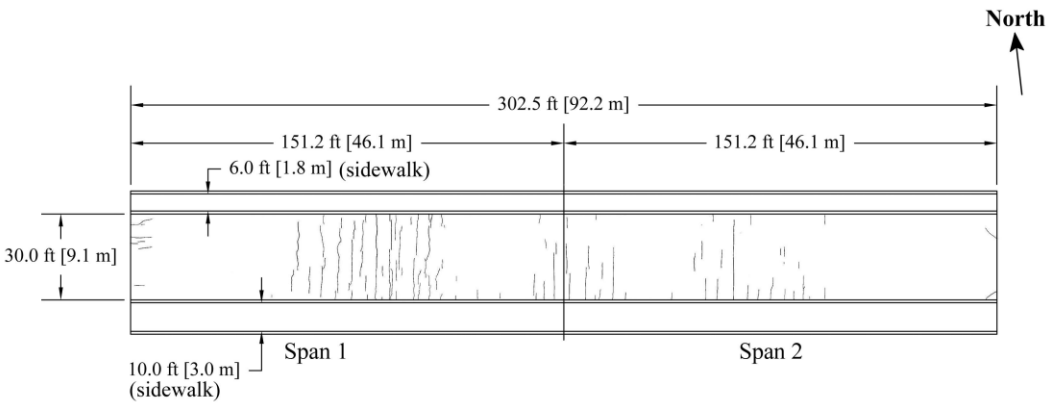

Bridge Number: 46-373 (LC-HPC-17)
Bridge Location: Clear Creek Parkway over K-7
Construction Date: 09-28-11
Crack Survey Date: 6-26-2012

Bridge Length: 302.5 ft (92.2 m)
Bridge Width: 48.0 ft(14.6 m)
Skew: 0°
Number of Spans: 2
Span 1: 151.25 ft (46.1 m)
Span 2: 151.25 ft (46.1 m)
Number of Placements: 1

Bridge Age: 8.94 months
Crack Density: 0.226 m/m²
Span 1: 0.302 m/m²
Span 2: 0.145 m/m²

Figure 6.43 LC-HPC-17 crack map at 8.9 months

transversely in the locations of greatest bending moment in the deck (middle of spans and above the center pier). The highest crack density is observed 60 to 120 ft (18 to 37 m) from the west abutment, approximately the location at which pumping difficulties and excessive bullfloating led to delayed curing (described in Section 5.3.25.4). In addition, high-slump concrete [4.5 to 5.0 in. (115 to 125 mm)] was placed in this region of high cracking. Minimal cracking is observed in the east end of the deck, even though this area was left exposed for about two hours prior to burlap placement (as discussed in Section 5.3.25.4). The crack survey crew did not observe the large deflections on this deck as were noted on LC-HPC-15 and 16; however, no large loads from truck traffic were placed on the deck during the survey. A few short longitudinal and diagonal cracks were observed extending from the west and east abutments, respectively, likely a result of a portion of the west end being left uncovered for approximately 1.5 hours. The non-integral end conditions of the abutments (discussed in Section 5.3.25) will provide less restraint to the deck than

would integral abutments, lowering the potential for longitudinal cracking at the ends of the deck.

6.2.43 Cracking Performance of LC-HPC-15, 16, and 17

Crack density is plotted as a function of time for LC-HPC-15, 16, and 17 in Figure 6.44. As stated previously, no control decks were selected for comparison with these three LC-HPC decks. The three decks have experienced higher early-age cracking than most LC-HPC decks. In addition, the only deck in this group surveyed more than once, LC-HPC-16, has exhibited a higher rate of increase in cracking than most LC-HPC decks. This high cracking observed on LC-HPC-16 may be partially due to the excessive use of high-slump concrete. As shown in Section 5.3.23.4, 44 percent of the slumps measured during placement of LC-HPC-16 were greater than or equal to 4.0 in. (100 mm) – a higher percentage than most LC-HPC decks. The pumping difficulties experienced during placement of LC-HPC-16 and 17 likely also contributed to cracking by delaying placement, finishing, and curing. As discussed in Sections 6.2.40 and 6.2.42, the highest crack densities in LC-HPC-16 and 17 are observed near the locations where the pumping difficulties occurred. In addition, the overfinishing and excessive delays in curing experienced during placement of LC-HPC-17 likely contributed to the high early-age cracking.

Similar cracking patterns are observed in LC-HPC-15, 16, and 17, with transverse cracks concentrated near the maximum moment regions (positive and negative moment) of the decks. In addition, substantial deflections caused by truck traffic were noted at the midspans during the crack surveys of LC-HPC-15 and 16. The high cracking observed in the positive moment regions may be a result of settlement cracking. As discussed earlier, vibrations induced by construction equipment may have caused enough vertical movement at the midspans to contribute

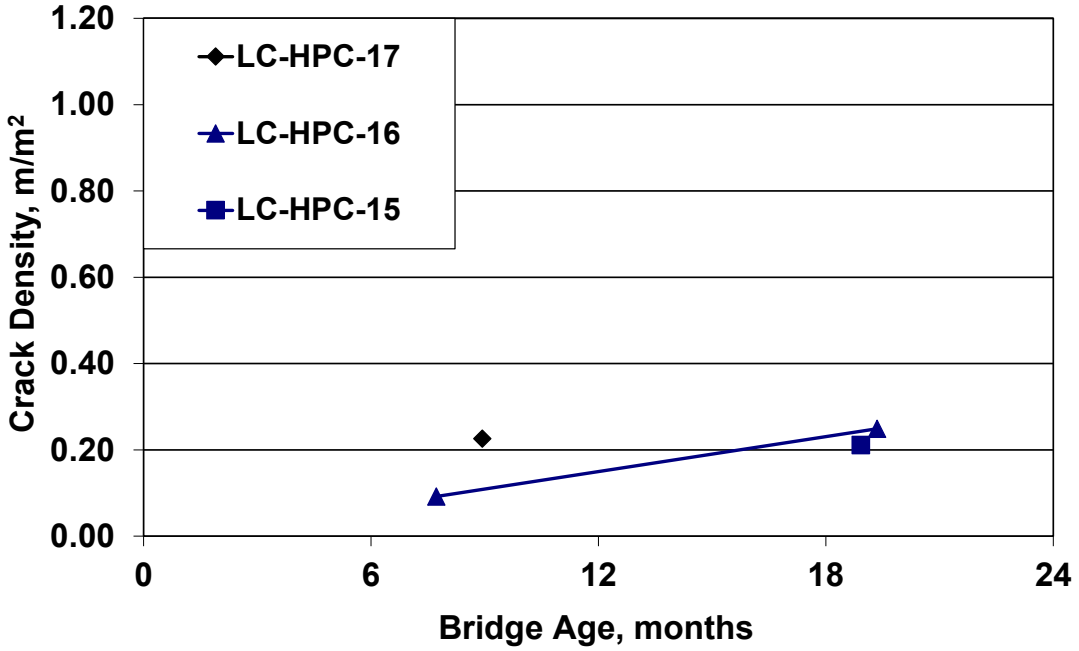

Figure 6.44 Crack density versus age for LC-HPC-15, 16, and 17

to settlement of the plastic concrete. Additional crack surveys will be needed to determine the long-term cracking performance of these decks.

6.2.44 Summary of Crack Survey Results

The survey results indicate that a great majority of the LC-HPC decks are performing better than the associated control decks. To date, 14 of the 16 LC-HPC placements matched with a control placement have better cracking performance than the control placement at a similar age. Of the two LC-HPC placements that do not have better cracking performance, one placement, LC-HPC-2, is matched with the lowest-cracking control placement in the study (Control 1/2 Placement 2) and the other placement, LC-HPC-8, would be expected to have lower cracking than its control deck in the next survey if current trends in cracking continue. The comparison between LC-HPC-2 and Control 1/2 Placement 2 is the only instance of an LC-HPC placement exhibiting greater cracking than a comparative control placement during the 2012 crack surveys. LC-HPC-8 is one of two LC-HPC decks

constructed on prestressed concrete girders, and as discussed in Section 6.2.11, creep, shrinkage, and camber of prestressed girders may influence cracking performance.

Table 6.1 shows the age and crack density of the LC-HPC and control placements from the most recent crack surveys, most of which were completed in 2012. OP Bridge and Control 5 were the only decks not surveyed in 2012. The LC-HPC placements range in age from 8.9 to 79.0 months with an average age of 50.0 months, while the control placements range in age from 30.6 to 79.2 months with an average age of 56.7 months. Excluding the three most recently constructed LC-HPC decks (LC-HPC-15, 16, and 17), the LC-HPC placements have an age of 36 months or more. In addition, the only control deck with an age less than 36 months at the time of the last crack survey was Control 5, which was not surveyed in 2012 and will not be surveyed again because an overlay was applied to the deck after the 2011 survey. For the LC-HPC placements, the average crack density from the most recent crack surveys is 0.217 m/m^2. In contrast, the average crack density for the control placements is nearly three times that value, at 0.610 m/m^2. A number of placements were omitted from the calculation of average age and crack density: The decks constructed on prestressed concrete girders (LC-HPC-8, 10 and Control 8/10) were omitted from the analysis to remove any effects that the prestressed girders have on cracking. Because of these effects, decks constructed on prestressed girders should be analyzed separately from those constructed on steel girders, when considering efforts to reduce bridge deck cracking. The OP Bridge placements were also excluded because of the many aspects of the LC-HPC specifications that were not followed during construction. Additionally, LC-HPC-4 Placement 1 was not included because of its unknown (possibly as low as 0.37) water-cement ratio and the many difficulties encountered during construction (discussed in Section 5.3.11.4). Finally, LC-HPC-12 Placement 1 was also excluded due to the abnormal loads placed on the

Table 6.1 Crack density and age determined from most recent crack survey

Bridge Deck	Placement	Age (months)	Crack Density (m/m^2)	Greatest Cracking
LC-HPC-1	Placement 1	79.0	0.096	Control 1/2 Placement 1
	Placement 2	78.4	0.081	
LC-HPC-2		68.1	0.197	
Control 1/2	Placement 1	79.2	0.240	
	Placement 2	78.6	0.161	
LC-HPC-3		54.0	0.173	Control 3
Control 3		57.9	0.314	
LC-HPC-4	Placement 1	56.0	0.184	Control 4
	Placement 2	55.9	0.092	
Control 4		54.9	0.669	
LC-HPC-5		54.3	0.158	Control 5
Control 5*		30.6	0.738	
LC-HPC-6		54.6	0.362	Control 6
Control 6		43.0	0.539	
LC-HPC-7		71.3	0.065	Control 7 Placement 1
Control 7	Placement 1	74.5	1.022	
	Placement 2	68.9	0.638	
LC-HPC-8		55.4	0.383	Control 8/10
LC-HPC-10		60.0	0.125	
Control 8/10		61.6	0.425	
LC-HPC-9		38.3	0.362	Control 9 Placement 1
Control 9	Placement 1	49.1	0.637	
	Placement 2	48.9	0.501	
LC-HPC-11		61.0	0.260	Control 11
Control 11		75.2	0.849	
LC-HPC-12	Placement 1	49.5	0.450	Control 12 Placement 1
	Placement 2	38.1	0.375	
Control 12	Placement 1	49.6	0.857	
	Placement 2	37.2	0.831	
LC-HPC-13		49.0	0.342	Control 13
Control 13		46.1	0.543	
OP Bridge*	Placement 1	42.2	0.585	No Comparison
	Placement 2	37.7	1.304	
	Placement 3	37.1	0.678	
LC-HPC-15		18.9	0.211	No Comparison
LC-HPC-16		19.4	0.249	
LC-HPC-17		8.9	0.226	
LC-HPC Placements				
Minimum		8.9		
Maximum		79.0		
Average**		50.0	0.217	
Control Placements				
Minumum		30.6		
Maximum		79.2		
Average**		56.7	0.610	

* Data from 2011crack survey

** OP Bridge placements, LC-HPC-4 Placement 1, LC-HPC-8, LC-HPC-10, Control 8/10, and LC-HPC-12 Placement 1 not included in average calculations

deck during the construction of LC-HPC-12 Placement 2 (discussed in Section 5.3.16.7). The placements listed above are also omitted from the analyses in Sections 6.3.1 and 6.3.2.

6.3 CRACK SURVEY EVALUATION

The cracking performance of the LC-HPC and associated control decks is evaluated in this section based on data collected from the crack surveys to determine the effectiveness of the LC-HPC specifications. In addition, the cracking performance of bridge decks examined in three previous studies at the University of Kansas (Schmitt and Darwin 1995, Miller and Darwin 2000, and Lindquist et al. 2005) is compared with the performance of the LC-HPC and control decks examined in this study. The crack densities obtained in surveys for the LC-HPC and control decks, as well as the decks in the previous studies, are provided in Tables F.1 to F.5 in Appendix F.

6.3.1 Cracking as a Function of Time

Crack density as a function of age is plotted for the LC-HPC and control decks in Figures 6.45 and 6.46, respectively. Data points connected by lines represent multiple surveys of a deck.

As shown in Figure 6.45, the LC-HPC decks generally exhibit low early-age cracking through the first 18 months and a gradual increase in cracking afterward. Conversely, the control decks (Figure 6.46) generally exhibit higher cracking than the LC-HPC decks within the first 18 months and undergo large increases in cracking in the following months. Crack densities for the LC-HPC decks ranged from 0.003 to 0.375 m/m^2 throughout the study, while the crack densities for the control decks ranged from 0 to 1.037 m/m^2. LC-HPC-12 Placement 2 has exhibited the highest cracking of the LC-HPC placements with a crack density of 0.375 m/m^2 at 38.1

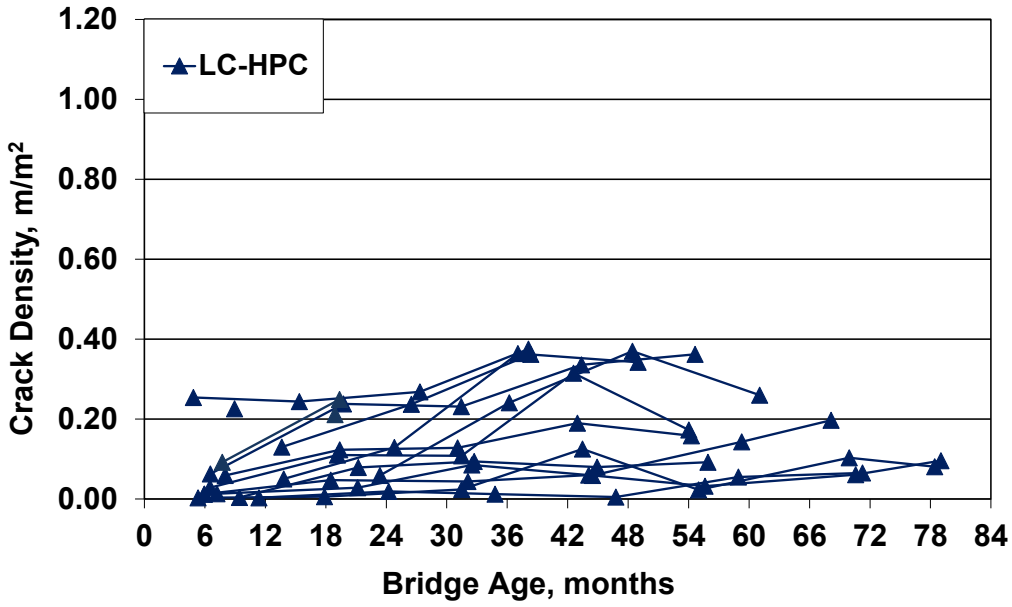

Figure 6.45 Crack density versus age for LC-HPC decks

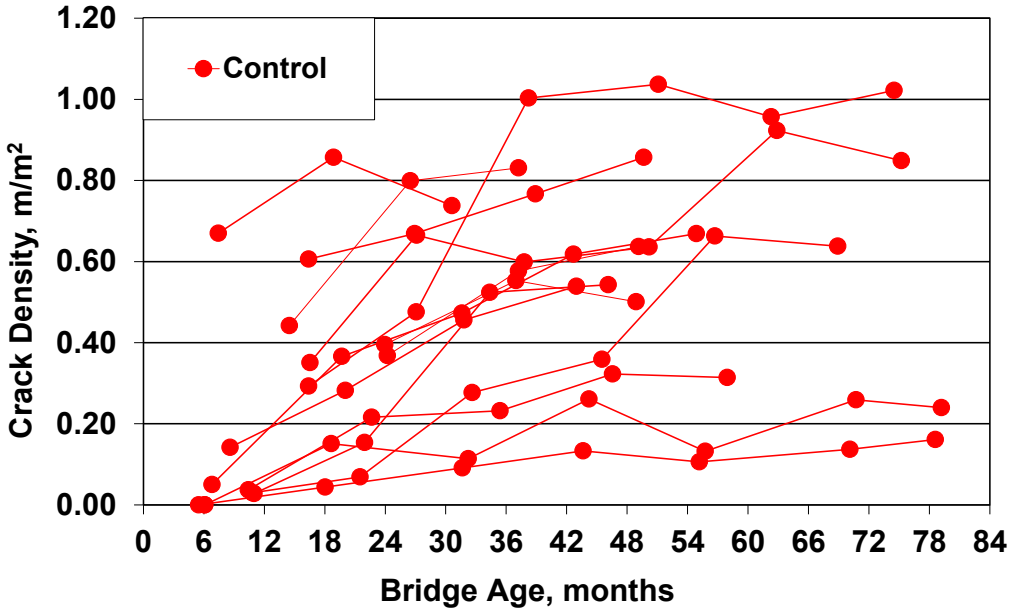

Figure 6.46 Crack density versus age for control decks

months. As discussed in Section 5.3.16, the atypical loading and significant vertical deflections caused by the positioning of the construction equipment likely contributed to this high cracking. Ultimately, 11 of the 14 control placements (79 percent) have crack densities greater than this value of 0.375 m/m^2. Five control placements (Control 5, Control 7 Placement 1, Control 12 Placement 1 and 2, and Control 11) have yielded crack densities above 0.800 m/m^2.

Table 6.2 and Figure 6.47 display the average crack density of the LC-HPC and control decks at three different ages: 12, 24, and 48 months. The three ages specify the ages of the decks at the time of the surveys. Average values of crack density are calculated using the survey data provided in Tables F.1 and F.2 in Appendix F. Crack densities at the specified ages (12, 24, and 48 months) are calculated using interpolation for decks surveyed both before and after a specified age. The crack densities of LC-HPC-1 Placement 2, Control 1/2 Placement 1, and LC-HPC-3 showed a substantial increase for a single survey, returning to a value more characteristic of the previous cracking trend in the following survey. For these placements, the abnormally-high crack densities are not considered and adjacent crack densities are used in the interpolation. For placements that were not surveyed both before and after a specified age, data from the two nearest surveys are linearly extrapolated to the desired age. Placements are not considered for extrapolation if the period between the nearest survey and the specified age is greater than 6 months. An exception is made for the 48-month crack density of Control 5, in which the crack density at 30.6 months is used because survey data are not available subsequent to 2011. Control 11 experienced decreases in crack density at 37.8 and 50.2 months because some cracks were obstructed by surface scaling. As a result, the crack density at 48 months for Control 11 is interpolated between the values at 27.1 and 62.9 months. Because the only survey for LC-HPC-15 was completed at 18.9 months, the 12-month crack density is interpolated between data from this survey and

Table 6.2 Average, maximum, and minimum crack densities for LC-HPC and control decks supported by steel girders at different ages: 12, 24, and 48 months

Age	Deck Type	Crack Density (m/m^2)			Standard Deviation
		Average	Max.	Min.	
12 Months	LC-HPC	0.076	0.247	0.004	0.071
	Control	0.224	0.745	0.023	0.212
24 Months	LC-HPC	0.112	0.261	0.014	0.085
	Control	0.388	0.805	0.065	0.231
48 Months	LC-HPC	0.163	0.365	0.010	0.140
	Control	0.550	1.029	0.123	0.259

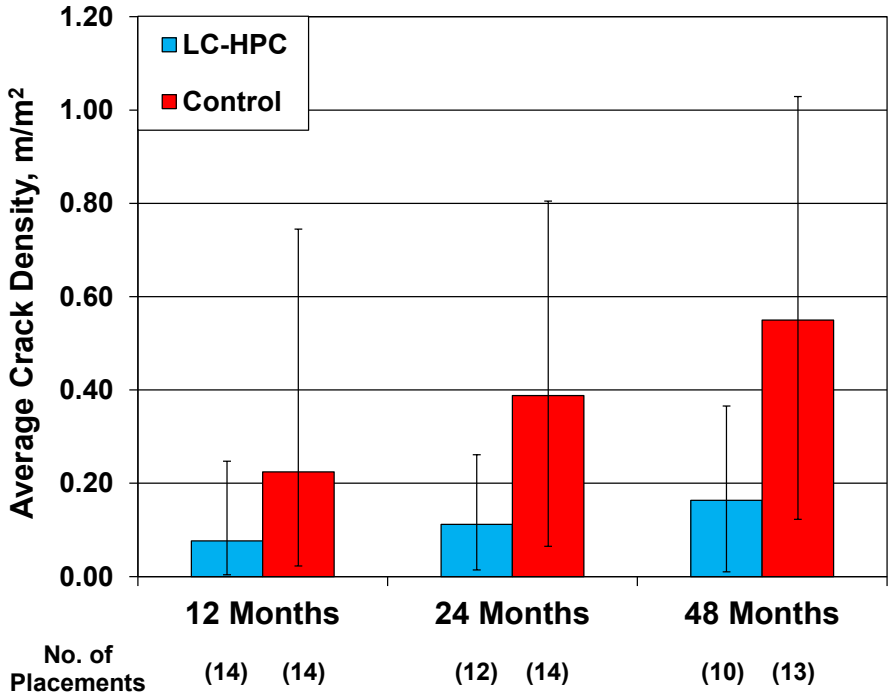

Figure 6.47 Average, maximum, and minimum crack densities for LC-HPC and control decks supported by steel girders at different ages: 12, 24, and 48 months

a crack density of 0 m/m^2 at 0 months. Due to the unknown water-cement ratio and the many difficulties encountered during construction of the first placement of LC-HPC-4 and the abnormal loads placed on the first placement of LC-HPC-12 during the construction of the second placement (discussed in Sections 5.3.11.4 and 5.3.16.7, respectively), these placements are excluded from the analysis.

Maximum and minimum values of crack density are displayed for LC-HPC and control decks in Figure 6.47 using error bars. The standard deviation σ of the crack densities at each age is calculated for the LC-HPC and control decks using the following equation:

$$\sigma = \sqrt{\frac{\Sigma(X - \mu)^2}{n - 1}} \tag{6.1}$$

where X is an individual crack density, μ is the mean of the crack densities in a given age range, and n is the number of crack densities in a given age range. The standard deviations are shown in Table 6.2.

The table and figure indicate that the average crack density increased over time for both the LC-HPC and control decks. The average crack density at 12 months is considerably higher for the control decks (0.224 m/m^2) than for the LC-HPC decks (0.076 m/m^2). In addition, the average crack density for the control decks increased at a faster rate over time than for the LC-HPC decks, as demonstrated by the greater increase in average crack density for the control decks between consecutive ages. The control decks exhibited approximately three times the cracking of the LC-HPC decks at each age. The greatest disparity in cracking performance occurred at the age of 24 months, where the LC-HPC and control decks exhibited average values of 0.112 and 0.388 m/m^2, respectively. The average crack density for the LC-HPC decks at 48 months (0.163 m/m^2) is, in fact, lower than the average crack density for the control decks at 12 months (0.224 m/m^2).

Table 6.2 and Figure 6.47 also demonstrate that the control decks exhibit a wider disparity in crack density than the LC-HPC decks at each age. The difference between maximum and minimum values of crack density is nearly three times greater for the control decks than for the LC-HPC decks at each age. In addition, the standard deviations for the control decks are two to three times greater than for the LC-HPC decks. Generally, the cracking performance of the control decks is inferior to and less predictable than the performance of the LC-HPC decks.

Three bridge deck cracking studies were completed at the University of Kansas prior to this study, by Schmitt and Darwin (1995), Miller and Darwin (2000), and Lindquist et al. (2005). These studies are summarized in Chapter 1. Four types of bridge decks were evaluated in the earlier studies, including decks with 5 and 7 percent silica fume overlays (SFO) and conventional high-density overlays (CO), as well as conventional monolithic (C-MONO) decks. The cracking performance of the conventional monolithic (C-MONO) decks examined in the earlier studies is plotted alongside the LC-HPC decks (also monolithic) in Figure 6.48. This comparison of monolithic decks eliminates the influence of overlays.

The conventional monolithic decks were generally older than the LC-HPC decks at the time of the first surveys, ranging from 12 to 240 months compared to 5 to 23 months for the LC-HPC decks, and the total range in age is greater for the conventional monolithic decks, ranging from 12 to 240 months of age compared to 5 to 79 months for the LC-HPC decks. The conventional monolithic decks were each surveyed one to three times, while all but three LC-HPC decks have been surveyed at least three times.

Figure 6.48 indicates that the conventional monolithic decks exhibited a wider variation in cracking performance than the LC-HPC decks. The crack densities of the conventional monolithic decks ranged from 0.012 to 0.760 m/m^2 in the age range of 0 to 72 months, while the LC-HPC decks have crack densities ranging from 0.003 to

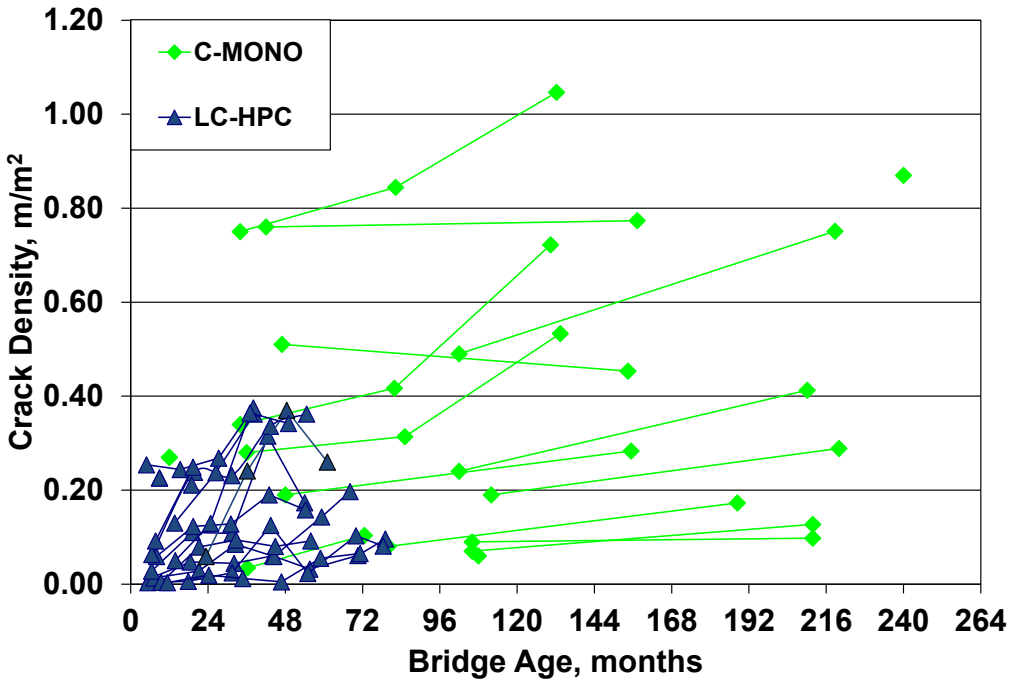

Figure 6.48 Crack density versus age for LC-HPC decks and conventional monolithic (C-MONO) decks examined by Schmitt and Darwin (1995), Miller and Darwin (2000), and Lindquist et al. (2005). All decks supported by steel girders.

0.375 m/m^2 for the same age range. In the first 72 months, the LC-HPC decks have performed better than or equal to the best performing monolithic decks at similar ages, indicating that the LC-HPC specifications have improved cracking performance.

The LC-HPC decks have experienced this lower cracking despite a number of circumstances that should have negatively affected their cracking performance compared to the older monolithic decks. First, construction data indicate that concrete placed in the older monolithic decks actually had lower values of slump than concrete placed in the LC-HPC decks, even though the LC-HPC specifications required the lower range of slump values. According to construction records provided by Miller and Darwin (2000), every conventional monolithic deck examined in the studies had an average slump below 3 in. (75 mm) and many of the decks had average slumps below 2 in. (50 mm). As discussed in Section 5.3.26.5, a large

percentage of the LC-HPC decks were constructed with concrete with slumps exceeding 3.5 and 4.0 in. (90 and 100 mm). Additionally, finer cement was likely used in the LC-HPC decks than in the older monolithic decks. As explained by Mindess et al. (2003), the fineness of cement has been steadily increasing over the past several decades. Concrete containing finer cement is at increased risk for cracking for a number of reasons. Increased water is absorbed on the surface of finer cement particles as a result of the increased particle surface area, decreasing the bleeding rate and increasing the potential for plastic shrinkage cracking. Finer cement undergoes an increased rate of hydration, increasing the early-age strength and modulus of elasticity – factors known to contribute to cracking. Finally, finer cement results in smaller capillaries within paste that contribute to increased surface tension of the capillary pore water, increasing the potential for drying shrinkage cracking. The lower cracking observed in the LC-HPC decks compared to the older monolithic decks confirms that the combined changes in concrete materials and construction procedures incorporated in the LC-HPC specifications improve cracking performance more than the aforementioned circumstances have hindered it.

While it is clear that the LC-HPC decks generally have lower cracking than the conventional monolithic decks within the first 72 months, limited long-term data on the LC-HPC decks prohibit comparisons to be made at later ages; for example, at 10 years and further after construction. Additional surveys of the LC-HPC decks will be required to compare the long-term cracking performance of the LC-HPC and conventional monolithic bridge decks.

6.3.2 Cracking Rate

The rates of increase in cracking over time, or cracking rates, of many of the LC-HPC and control decks in this study were reported earlier by Lindquist et al. (2008) and Yuan et al. (2011) using the results of successive crack surveys. While this method of determining cracking rate provides the exact increase in cracking

between two consecutive surveys, it does not take into account variances in survey data caused by the performance of different survey crews. The effect of these variances can be softened by considering the average cracking rate over multiple surveys rather than simply considering the rate between consecutive surveys. In this report, the cracking rates of the LC-HPC and control decks are examined for two time intervals: 0 to 36 months and after 36 months. The intervals typically encompass three or more surveys of a given deck. In a given time interval, the average cracking rate for a deck is determined by averaging the cracking rates of all consecutive surveys that fall within the time interval. For example, cracking rates calculated between hypothetical surveys at 10 and 22 months and 22 and 34 months would be averaged to determine the average cracking rate in the time interval of 0 to 36 months. Periods between surveys that span the 36-month boundary are considered in the time interval in which the majority of the period falls. For example, the cracking rate between the surveys of Control 7 Placement 1 at 27.1 and 38.2 months is considered for the time interval of 0 to 36 months. Because crack surveys are performed yearly, the cracking rates are weighted equally. The surveys of Control 11 at 37.8 and 50.2 months are not considered in the analysis because scaling of the deck surface have obstructed the view of cracks, resulting in inaccurate values of crack density.

Figure 6.49 displays crack densities over time for the LC-HPC and control decks in the two time intervals, 0 to 36 months and after 36 months. The average cracking rate for the LC-HPC and control decks surveyed within the time intervals is shown in the figure. As shown in the figure, the average cracking rate of the control decks is nearly two-and-a-half times that of the LC-HPC decks in the first 36 months (0.0139 vs. 0.0058 $m/m^2/mo$). At ages greater than 36 months, the cracking rates for both the LC-HPC and control decks are reduced to about one-third the rates in the

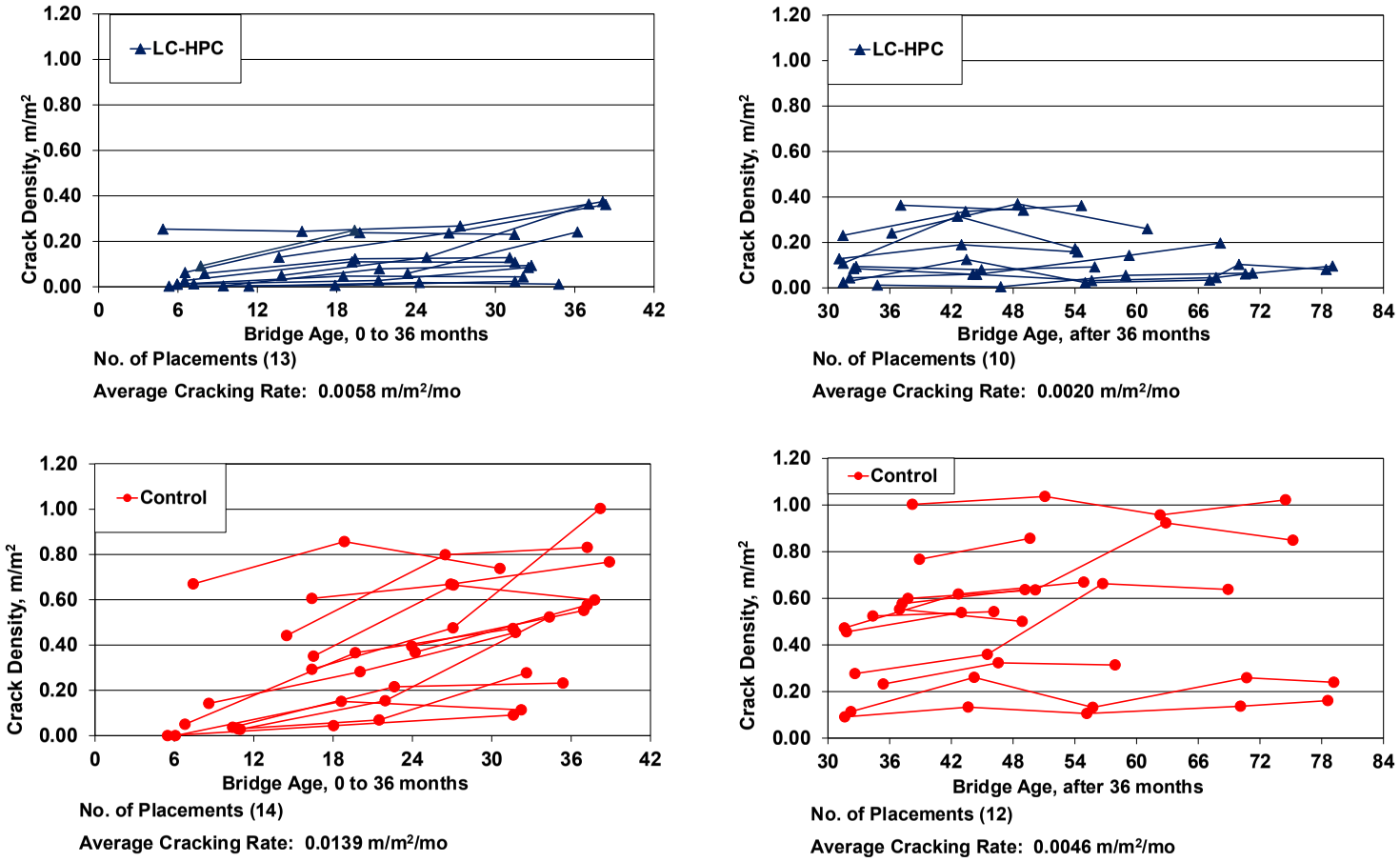

Figure 6.49 Average crack density versus time for different time increments for LC-HPC and control decks supported by steel girders: (a) cracking between 0 and 36 months; (b) cracking after 36 months

first 36 months. Even though the LC-HPC and control decks both experienced a reduction in cracking rate after 36 months, the control decks exhibited more than twice the cracking rate of the LC-HPC decks in this time interval (0.0046 vs. 0.0020 $m/m^2/mo$). The cracking rate shown in the figure for the control decks after 36 months is possibly lower than the actual cracking rate due to reduced cracking found in the 2011 survey of Control 7 Placement 1 and the 2012 surveys of Control 7 Placement 2 and Control 11. As explained in Section 6.2.7, survey crew members may have overlooked small cracks during the surveys of Control 7 in the process of marking longer cracks that continue over great lengths along the deck. Additionally, as discussed in Section 6.2.14, the severe scaling of the surface of Control 11 has likely obstructed the view of cracks and contributed to an erroneous reduction in crack density in the survey at 75.2 months (2012 survey). For comparative purposes, the average crack density of the control decks after 36 months, not including this survey data for Control 7 and 11, show that the average cracking rate after 36 months is 0.0053 $m/m^2/mo$, nearly three times the rate of the LC-HPC decks, rather than 0.0046 $m/m^2/mo$.

6.3.3 Crack Density at 42 Months

Direct comparisons of cracking performance of the decks in this study are challenging since they vary widely in age and, as discussed in Section 6.3.1, cracking increases continuously over time. To provide a fairer comparison, the variable of age can be removed from the analysis by characterizing cracking performance in terms of the crack density at 42 months of age. As discussed in Section 6.3.2, the rate of cracking is highest in both the LC-HPC and control decks within the first 36 months. This observation suggests that cracking performance can be fairly evaluated in terms of a crack density at or shortly after 36 months – an age of 42 months is selected for this study. Yuan et al. (2011) evaluated the decks in this study at an age of 36 months. Data from two additional annual crack surveys (24 months of additional

data) are now available for the decks beyond that available to Yuan et al. (2011). Therefore, data are available in this study for an evaluation at 60 months similar to the evaluation by Yuan et al. (2011) at 36 months. Crack densities at 42 months, rather than at 60 months, are employed, however, because a number of younger decks can be included in this evaluation that could not be included by Yuan et al. (2011).

The following procedure is used to determine crack density at 42 months for the LC-HPC and control decks. For decks surveyed both before and after 42 months, the crack density at 42 months is interpolated between the crack densities from contiguous crack surveys. For decks with ages between 36 and 42 months at the time of the most recent crack survey, the most recent crack survey is used as the crack density at 42 months. Decks younger than 36 months at the time of the last survey are omitted from the analysis. An exception is made for Control 5, for which the crack density at 30.6 months is used because survey data are not available subsequent to 2011. Because surveys of LC-HPC-1 Placement 2, Control 1/2 Placement 1, and LC-HPC-3 showed significant increases in crack density followed by a sharp reduction, the abnormally-high crack densities are not considered and the remaining values are used in the interpolation. Because the survey of Control 11 showed decreases in crack density at 37.8 and 50.2 months due to surface scaling, the crack density at 42 months for Control 11 is obtained by interpolation between the values at 27.1 and 62.9 months. This value is likely below the actual crack density at 42 months. The first placements for LC-HPC-4 and LC-HPC-12 are again excluded from the analysis for the reasons discussed in Sections 5.3.11.4 and 5.3.16.7, respectively.

The crack densities at 42 months are also determined for the decks examined by Schmitt and Darwin (1995), Miller and Darwin (2000), and Lindquist et al. (2005). As with the LC-HPC and control decks, these values are determined by interpolation in cases where surveys were completed both before and after 42 months. In many

cases, however, the first survey of these decks was not completed until after 42 months. If survey data prior to 42 months are not available, the 42-month crack density is linearly extrapolated based on the two consecutive surveys after 42 months, thus treating the cracking rate as constant after 42 months. For instances in which the crack density decreased after 42 months, the crack density between 42 and 48 months is used, if available. Decks subjected to a first survey after 48 months of age are excluded from the analysis. Decks surveyed only once are also excluded. The crack densities at 42 months for the decks evaluated in this study and previous studies are listed in Tables F.1 through F.5 in Appendix F.

Figure 6.50 shows the average crack density at 42 months for each deck type for the decks examined in this study and in the three previous studies. Maximum and minimum values of crack density at 42 months are displayed in the figure using error bars. The 7 percent silica fume overlay decks examined in the three previous studies are excluded from the figure because only one survey has been completed on each deck. The LC-HPC and control decks are grouped by those constructed on steel and prestressed (PS) girders. The LC-HPC decks, control decks constructed on prestressed girders, and the OP Bridge comprise of monolithic construction. The control decks constructed on steel girders are constructed with a 7 percent silica fume overlay.

As shown in Figure 6.50, the LC-HPC decks constructed on steel girders had the lowest average crack density of any deck type at 42 months (0.190 m/m^2). The associated control decks constructed on steel girders exhibited an average crack density of 0.524 m/m^2, nearly three times that of the LC-HPC decks. The LC-HPC and control decks constructed on prestressed girders exhibited 42-month crack densities slightly higher than the LC-HPC decks on steel girders, 0.214 and 0.205 m/m^2, respectively. Due to the small sample size of decks constructed on prestressed girders, definitive conclusions on cracking performance cannot be made. The OP

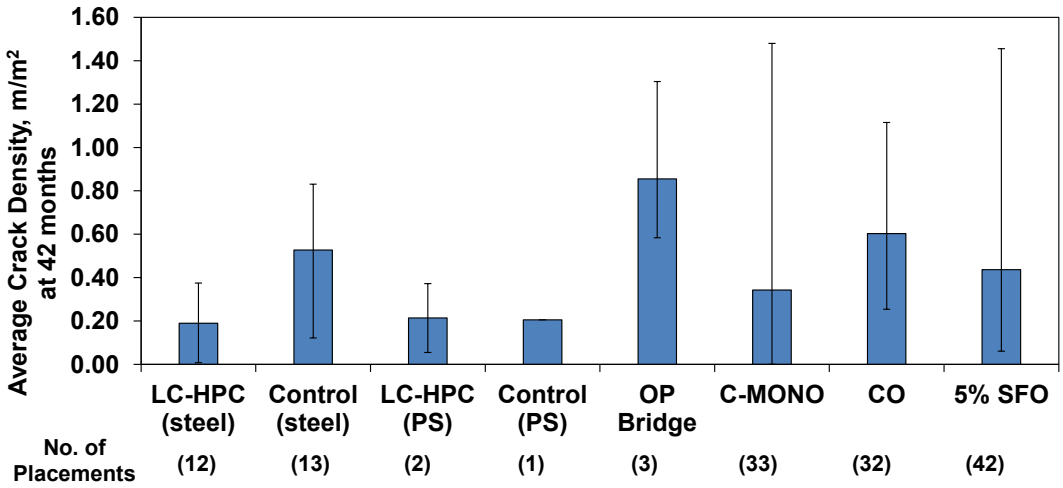

Figure 6.50 Crack density at 42 months for each deck type: LC-HPC, control, OP Bridge, conventional monolithic (C-MONO), conventional overlay (CO), and 5 percent silica fume overlay (5% SFO). Steel = steel girders, PS = precast, prestressed girders

Bridge had the highest crack density of all deck types at 42 months, 0.855 m/m^2. The conventional monolithic (C-MONO), conventional high-density overlay (CO), and 5 percent silica fume overly (5% SFO) decks examined in the earlier studies had crack densities of 0.343, 0.603, and 0.437 m/m^2, respectively, at 42 months. Excluding the OP Bridge, the monolithic decks had better cracking performance than decks with overlays. In addition, the LC-HPC decks on steel girders exhibited about half the crack density of the conventional monolithic decks at 42 months.

The maximum and minimum values shown in Figure 6.50 indicate that the LC-HPC decks have considerably less variation in crack density than the other deck types. For example, the conventional monolithic (C-MONO) decks collectively exhibited a lower average 42-month crack density (0.343 m/m^2) than any of the deck types with an overlay; however, an individual conventional monolithic placement, Bridge 99-076 Placement 2 (shown in Table F.3 in Appendix F from the earlier studies), had the highest 42-month crack density of any deck in the analysis (1.480 m/m^2). The standard deviation of the crack densities at 42 months can also be used to

examine the variation in cracking performance within each type of deck. These values are shown in Table 6.3.

As shown in Table 6.3, the LC-HPC decks supported by steel girders has the lowest standard deviation in 42-month crack density of all deck types, 0.145. The conventional monolithic (C-MONO) decks and OP Bridge have the highest standard deviations, 0.347 and 0.391, respectively. The control decks supported by steel girders (7% SFO) and decks with conventional and 5 percent silica fume overlays had similar standard deviations, between 0.205 and 0.259. The data suggest that the cracking performance of the LC-HPC decks is not only better, but more predictable than that of other deck types.

6.4 FACTORS AFFECTING BRIDGE DECK CRACKING

In this section, the data collected and observations made during the construction of each bridge deck are compared with cracking performance to determine the factors that contribute to cracking. Relationships between cracking and concrete material characteristics of the LC-HPC and associated control decks, including paste content, slump, air content, and compressive strength, are examined. The effects of ambient and concrete temperatures are also examined. The crack densities at 42 months, described in Section 6.3.3, are used to quantify the cracking performance of the decks in the analysis. A dummy variables regression analysis (Draper and Smith 1981) of the characteristics of the LC-HPC decks and OP Bridge and the conventional monolithic (C-MONO) decks included in the studies by Schmitt and Darwin (1995), Miller and Darwin (2000), and Lindquist et al. (2005) is performed to determine the influence of different factors on cracking. A similar analysis was completed for the monolithic decks by Yuan et al. (2011) based on crack densities at 36 months. The decks constructed on prestressed girders (LC-HPC-8, 10, and Control 8/10) and the first placements of LC-HPC-4 and LC-HPC-12 are excluded from the analyses in this section for the reasons discussed in Sections 5.3.11.4 and 5.3.16.7, respectively. In

Table 6.3 Average, maximum, minimum, and standard deviation of crack density at 42 months for each deck type: LC-HPC, control, OP Bridge, conventional monolithic (C-MONO), conventional overlay (CO), and 5 percent silica fume overlay (5% SFO). Steel = steel girders, PS = precast, prestressed girders

Deck Type	Crack Density (m/m^2)			Standard Deviation
	Average	Max.	Min.	
LC-HPC (steel)	0.190	0.375	0.008	0.145
Control (steel)	0.524	0.831	0.121	0.241
LC-HPC (PS)	0.214	0.373	0.055	0.225
Control (PS)	0.205	0.205	0.205	-
OP Bridge	0.855	1.304	0.584	0.391
C-MONO	0.343	1.480	0.000	0.347
CO	0.603	1.115	0.254	0.205
5% SFO	0.437	1.456	0.061	0.259

addition, LC-HPC-15, 16, and 17 are not included in the analyses because the decks were constructed too recently to determine crack densities at 42 months.

6.4.1 Material Factors Affecting Cracking

6.4.1.1 Paste Content

As discussed in Section 1.4.1, the volume of cement paste is a primary factor contributing to concrete shrinkage and cracking. In studies by Schmitt and Darwin (1995), Miller and Darwin (2000), and Lindquist et al. (2005), monolithic decks with paste volumes greater than 27 percent exhibited significantly greater cracking than decks with paste volumes below this value. The LC-HPC in this study had low paste contents, ranging from only 23.4 to 24.6 percent. The conventional monolithic decks examined by Schmitt and Darwin (1995), Miller and Darwin (2000), and Lindquist et al. (2005) had higher paste contents, ranging from 25.7 to 28.8 percent. The paste contents of the LC-HPC and conventional monolithic (C-MONO) decks are plotted versus crack density at 42 months in Figure 6.51. Figure 6.52 shows the average

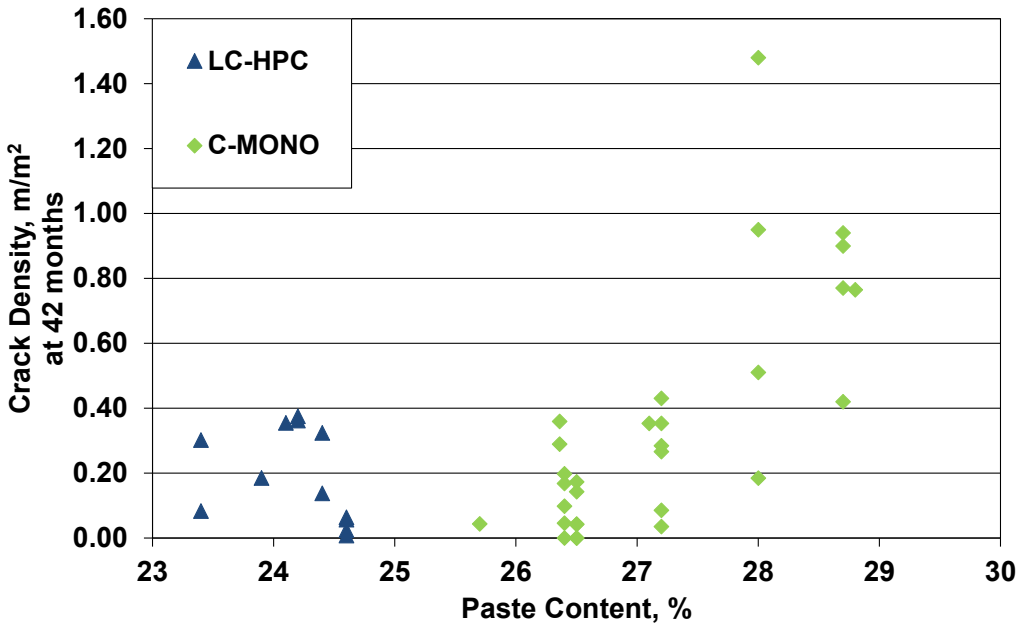

Figure 6.51 Crack density at 42 months as a function of paste content for LC-HPC and conventional monolithic (C-MONO) decks supported by steel girders

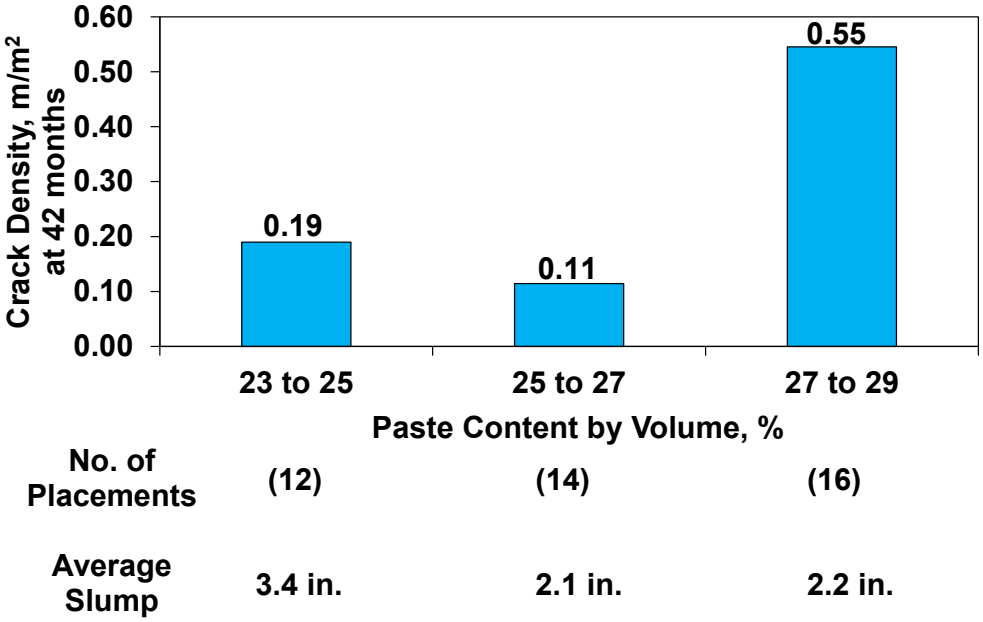

Note: 1 in. = 25.4 mm

Figure 6.52 Crack density at 42 months for LC-HPC and conventional monolithic (C-MONO) decks supported by steel girders as a function of paste content separated into three ranges: 23 to 25 percent, 25 to 27 percent, and 27 to 29 percent

crack density at 42 months for the monolithic decks within three ranges of paste content: 23 to 25 percent, 25 to 27 percent, and 27 to 29 percent. The LC-HPC and conventional monolithic decks are combined in Figure 6.52. The figure also shows the average slump of the decks in each range of paste content.

The figures indicate that cracking increases as paste content increases above 27 percent, supporting previous findings. No deck with a paste content below 27 percent had a crack density above 0.400 m/m^2 at 42 months (Figure 6.51). The five placements with the highest cracking have paste contents of 28 percent or above. Figure 6.52 shows that the average crack density at 42 months for the decks with paste contents of 27 to 29 percent is five times that of the decks with paste contents of 25 to 27 percent and nearly three times that of the decks with paste contents of 23 to 25 percent. The four placements with the lowest cracking have paste contents between 24.5 and 26.5 percent (Figure 6.51). The decks within the paste-content range of 25 to 27 percent, not 23 to 25 percent, have the lowest average crack density at 42 months, 0.11 m/m^2 (Figure 6.52). This observation suggests that other factors, such as slump, strength, and temperature, likely have a greater influence on cracking than paste content in decks with sufficiently-low amounts of paste.

When considering only the LC-HPC decks, the placements with paste contents of 24.6 percent, the top of the range for LC-HPC decks, experienced the lowest cracking (Figure 6.51). This observation may result from the following effects of low paste. First, the contractors occasionally had difficulty pumping the lower-paste concrete during construction of the LC-HPC decks (discussed in Chapter 5), often leading to subsequent delays in placement, finishing, and curing. Second, reductions in paste content for the LC-HPC decks were achieved through reductions in water content, not cement content. This modification to the constituent proportions resulted in a lower water-cement ratio (as low as 0.42 for some decks), likely increasing strength and, thus, the potential for cracking. The limited range of low paste contents

found in the LC-HPC decks makes it difficult to establish clear relationships between paste content and cracking. As discussed in Section 5.3.26.1, concrete that is highly-pumpable and contains sufficiently-low paste will likely experience low cracking, the former because it is likely to minimize placement time when a pump is used.

In Figure 6.52, no relationship is established between slump and paste content or slump and cracking. Decks within the highest range of paste contents (27 to 29 percent), which experienced the highest cracking, have similar or lower slumps than decks within the two lower ranges of paste contents. This observation suggests that low slump alone will not limit cracking. The influence of slump is addressed in the next section.

6.4.1.2 Slump

Increased cracking directly above reinforcing steel is often observed for concretes with increased slump, in all likelihood due to settlement cracking. In an evaluation of 31 monolithic decks, Darwin et al. (2004) and Lindquist et al. (2005) observed an increase in crack density of 0.11 m/m^2 as the average slump increased from 1.5 to 3 in. (40 to 75 mm). In addition, McLeod et al. (2009) and Yuan et al. (2011) observed increased overall cracking for bridge decks containing concretes with high slumps.

The average slumps of the LC-HPC decks in this study ranged from 2.0 to 4.25 in. (50 to 110 mm), while the slumps of the conventional monolithic decks evaluated in the three previous studies were lower, ranging from 1.5 to 3.0 in. (40 to 75 mm). The three placements of the OP Bridge had higher slumps than typical LC-HPC decks, with average values of 3.75, 4.25, and 5.25 in. (95, 110, and 130 mm), respectively.

Crack density at 42 months is plotted as a function of average slump for the LC-HPC, OP Bridge, and conventional monolithic (C-MONO) decks in Figure 6.53.

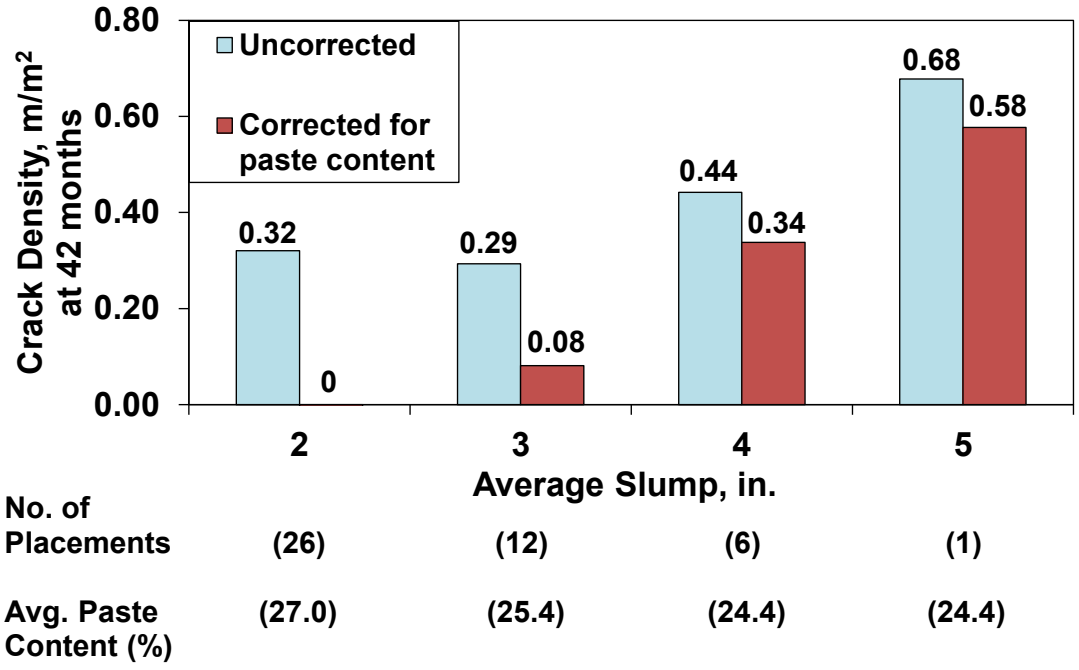

Note: 1 in. = 25.4 mm

Figure 6.53 Combined results of crack density at 42 months as a function of average slump for conventional monolithic (C-MONO), OP Bridge, and LC-HPC decks supported by steel girders.

For these decks, the results are presented in two ways – including (uncorrected) and removing (corrected) the influence of paste content. Based on the raw (uncorrected) data shown in Figure 6.53, the results indicate that the crack density increases from 0.29 to 0.44 m/m^2 as the slump increases from 3 to 4 in. (75 to 100 mm). In addition, a single placement with an average slump of 5.25 in. (135 mm) had a 42-month crack density of 0.68 m/m^2. The crack density decreases slightly from 0.32 to 0.29 m/m^2 as the slump increases from 2 to 3 in. (50 to 75 mm). These results are, however, influenced by paste content. The conventional monolithic decks were cast almost exclusively without water reducers, and therefore, a strong relationship exists between paste content and slump. Conversely, water reducers were commonly used to achieve a desired slump when casting the LC-HPC decks, and as a result, little correlation exists between paste content and slump. Although many of the LC-HPC

decks have higher slumps than the conventional monolithic decks, every LC-HPC deck has a lower paste content than the conventional monolithic decks. This trend is illustrated in a plot of average slump versus paste content in Figure 6.54. The paste contents ranged from 23.4 to 24.6 percent for the LC-HPC decks and the OP Bridge, while ranging from 25.7 to 28.8 percent for the conventional monolithic decks. By separating the effects of slump and paste content on cracking, the effect of settlement cracking is essentially isolated from the effect of shrinkage cracking.

The effects of slump and paste content on cracking were separated using the following procedure. First, by using linear regression analysis on the data points shown in Figure 6.51, Eq. (6.2) was established defining crack density at 42 months as a function of paste content for the LC-HPC and C-MONO decks.

$$CD_{42-month} = 0.1070 \times PC - 2.511 \tag{6.2}$$

In Eq. (6.2), $CD_{42-month}$ is the crack density at 42 months (m/m^2) and PC is the paste content (%). Data for the OP Bridge were not used to determine this equation because the many issues encountered during construction of these placements (discussed in Section 5.3.22) would likely have skewed the results. Second, the average paste content was determined for the decks in each range of slump shown in Figure 6.53. These average paste contents were used in the equation to establish a 42-month crack density due to paste content for each slump range. This crack density, which approximates the relative influence of paste content on cracking for each range of slump, was subtracted from the uncorrected crack density to isolate the effect of slump from paste content on cracking. The average paste contents and corresponding crack densities are shown in Table 6.4.

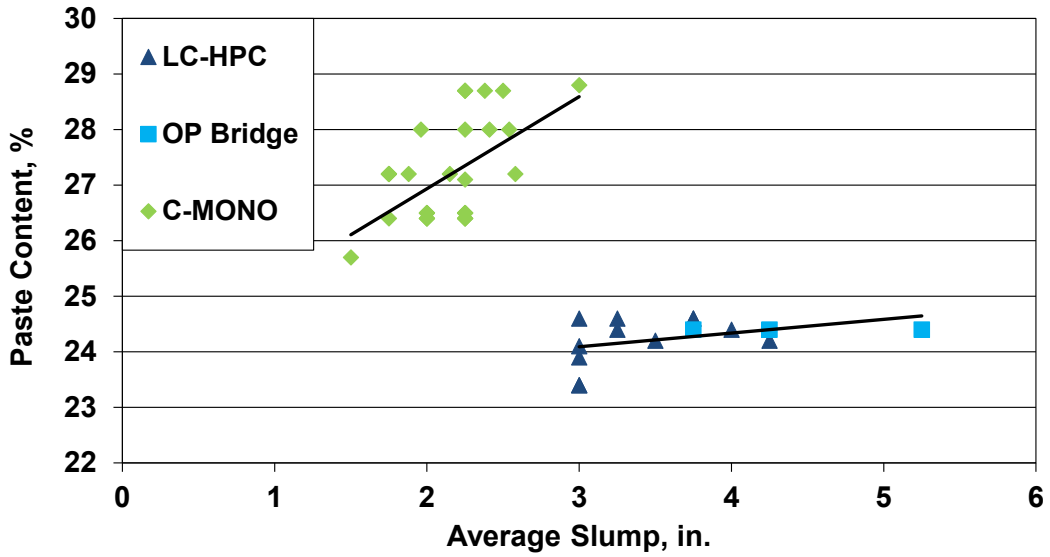

Note: 1 in. = 25.4 mm

Figure 6.54 Paste content as a function of average slump for LC-HPC, OP Bridge, and conventional monolithic (C-MONO) decks supported by steel girders

Table 6.4 Crack density at 42 months as a function of average slump, including (Uncorrected) and removing (Corrected for paste content) the effect of paste content, for conventional monolithic (C-MONO), OP Bridge, and LC-HPC decks supported by steel girders

Regression Analysis Equation‡: 42-month crack density = 0.1070 × paste content - 2.511					
Slump (in.)		**2**	**3**	**4**	**5**
No. of Placements		26	12	6	1
Avg. Paste Content (%)		27.0	25.4	24.4	24.4
Crack Density Uncorrected*	(m/m^2)	0.32	0.29	0.44	0.68
Crack Density Due to paste content†		0.38	0.21	0.10	0.10
Crack Density Corrected for paste content#		0	0.08	0.34	0.58

‡Regression Analysis Equation – Shown as Eq. (6.2) in the report. Determined by evaluating 42-month crack density of the LC-HPC and C-MONO decks as a function of paste content (this relationship is shown in Figure 6.51).

*Crack Density Uncorrected – 42-month crack density that includes the effects of both slump and paste content. Determined using 42-month crack densities shown in F.1 and F.3 in Appendix F.

†Crack Density Due to paste content – 42-month crack density that includes only the effect of paste content. Determined using the Regression Analysis Equation shown in this table.

#Crack Density Corrected for paste content – 42-month crack density that includes only the effect of slump. Determined by subtracting "Crack Density Due to paste content" from "Crack Density Uncorrected."

Note: 1 in. = 25.4 mm

As shown in Figure 6.53, when the relative influence of paste content is removed, cracking increases from 0.08 to 0.34 m/m^2 as the slump increases from 3 to 4 in. (75 to 100 mm); a shaper rate of increase than observed when the influence of paste content was considered. Crack density increases additionally to 0.58 m/m^2 as the slump increases to 5 in. (125 mm). For decks in the slump range of 2 in. (50 mm), paste content, not slump, is observed to be responsible for all cracking. The figure also shows that the average paste content of the decks decreased as the slump increased. These observations are as expected since the decks with lower slumps (typically C-MONO decks) generally had higher paste contents, which, therefore, had a greater influence, relative to slump, on cracking. The relative influence of paste content on cracking (Table 6.4), represented by the difference between the uncorrected and corrected crack densities, increases as the average paste content increases. Thus, cracking increases at a greater rate with increasing slump for the decks used in the analysis when the effect of paste content is removed than when the effect of paste content is ignored.

Average-slump data provide important information regarding the general plastic properties of the concrete; however, the data do not indicate the percentage of concrete in each deck that exceeded the specified requirements for slump. Figure 6.55 shows the crack density at 42 months for the LC-HPC decks and the OP Bridge as a function of the percentage of slump measurements greater than or equal to 4.0 in. (100 mm). The data are separated into three ranges: less than 30 percent, 30 to 60 percent, and more than 60 percent of slump measurements greater than or equal to 4.0 in. (100 mm). The crack densities displayed in Figure 6.55 are calculated by averaging the crack densities at 42 months for the decks that fall within a given range. The figure indicates that cracking increases as the percentage of slump measurements greater than or equal to 4.0 in. (100 mm) increases. The average crack density at 42 months increases by more than two times (0.13 to 0.33 m/m^2) as the percentage of

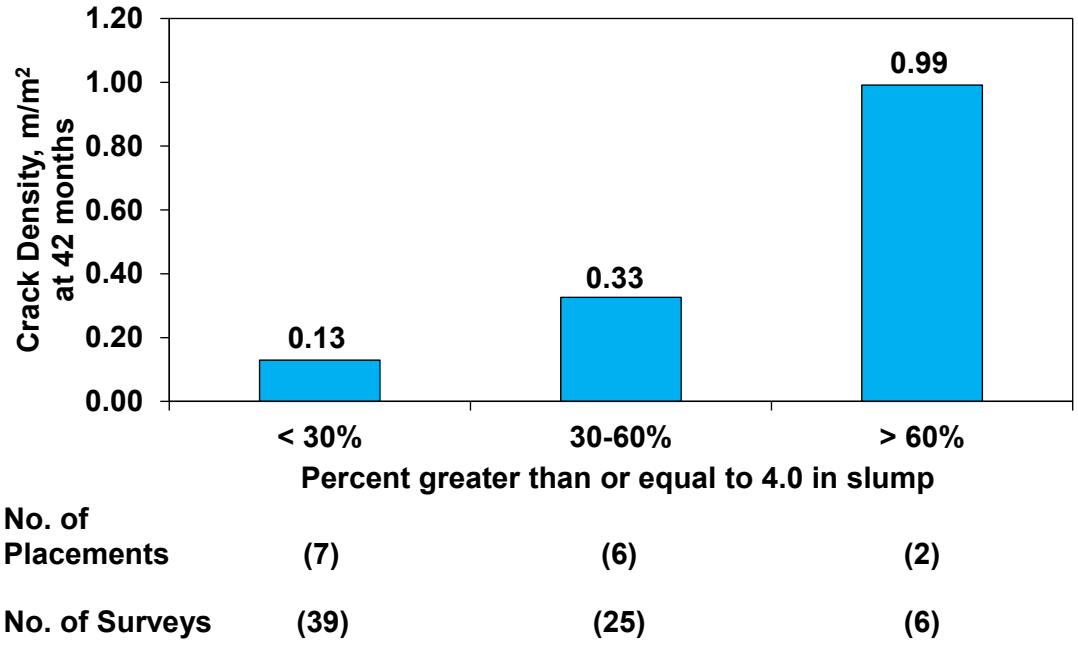

Figure 6.55 Crack density at 42 months for LC-HPC decks supported by steel girders and OP Bridge placements separated into three ranges: less than 30 percent, 30 to 60 percent, and more than 60 percent of slump measurements greater than or equal to 4.0 in. (100 mm)

values greater than or equal to 4.0 in. (100 mm) increases from below 30 percent to between 30 and 60 percent. The two placements with more than 60 percent of the slumps greater than or equal to 4.0 in. (100 mm), both for OP Bridge, have exhibited the poorest performance.

As discussed in Chapter 5, the OP Bridge placements each had at least 50 percent of slump measurements greater than or equal to 4.0 in. (100 mm) and exhibited higher cracking than any LC-HPC deck. In fact, every slump measurement for OP Bridge Placement 3 was greater than or equal to 4.0 in. (100 mm). Six of the seven lowest-cracking LC-HPC placements (LC-HPC-1 Placements 1 and 2, LC-HPC-2, LC-HPC-3, LC-HPC-4 Placement 2, and LC-HPC-5) had less than 30 percent of their slump values greater than or equal to 4.0 in. (100 mm).

6.4.1.3 Air Content

As discussed in Section 1.6.1.1, proper air entrainment improves the freeze-thaw durability of concrete by providing air voids within the cement paste for water to freeze (Mindess et al. 2003). In addition, entrained air is a constituent that improves the workability of concrete and does not contribute to shrinkage. American Concrete Institute (ACI) Committee 201 recommends air contents between 5 and 6 percent to achieve satisfactory freeze-thaw durability; however, the LC-HPC specifications require air contents above 6.5 percent for concrete to be accepted for placement. This requirement is based on observations by Schmitt and Darwin (1995), Miller and Darwin (2000), and Lindquist et al. (2005) that bridge decks placed with concretes with air contents below 6 percent exhibit an increase in cracking.

The LC-HPC decks in this study had average air contents ranging from 6.4 to 9.5 percent. The deck that contained an average air content of 6.4 percent, LC-HPC-16, was constructed in 2010 and is not considered in the analysis of crack densities at 42 months. The three OP Bridge placements contained average air contents of 8.7, 9.8, and 9.9 percent, respectively. OP Bridge Placements 2 and 3 contained average air contents that exceeded the upper limit of 9.5 percent allowed in the LC-HPC specifications. The conventional monolithic decks examined in the studies by Schmitt and Darwin (1995), Miller and Darwin (2000), and Lindquist et al. (2005) had average air contents ranging from 4.5 to 6.5 percent; significantly lower values than found in the LC-HPC decks. When considering the decks examined at 42 months, no overlap exists between the air content range of the LC-HPC decks and OP Bridge and the range of the conventional monolithic decks.

Crack density at 42 months is plotted as a function of average air content for the LC-HPC, OP Bridge, and conventional monolithic (C-MONO) decks in Figure 6.56. A trend line, shown in the figure, is fit to the data for the respective deck types using a least-squares linear regression. The figure indicates that air content had

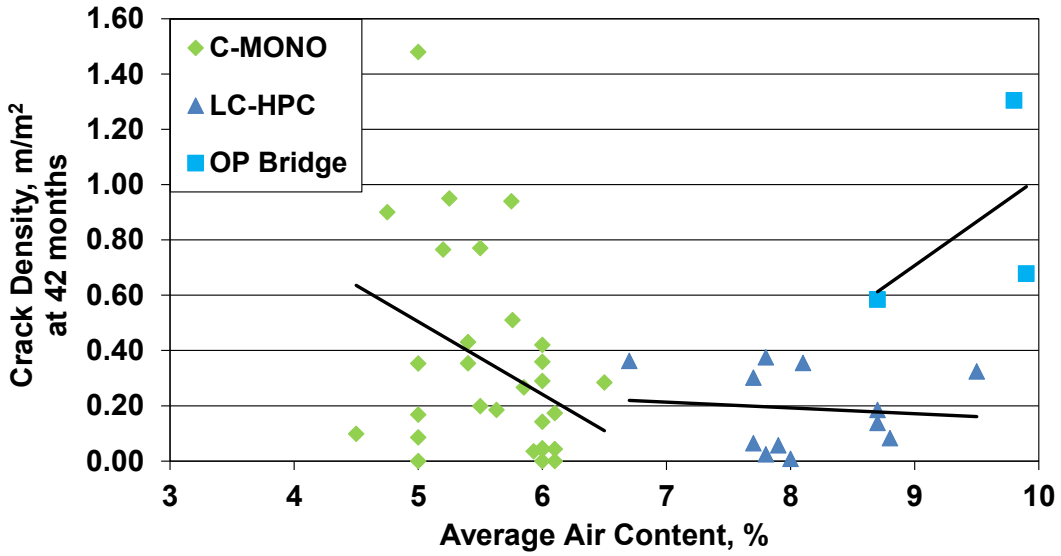

Figure 6.56 Crack density at 42 months plotted versus average air content for LC-HPC, OP Bridge, and conventional monolithic (C-MONO) decks supported by steel girders. Trend lines are fit to data for respective decks using a least-squares linear regression.

essentially no effect on cracking for the LC-HPC decks. The conventional monolithic decks, which had lower air contents than the LC-HPC decks or OP Bridge, experienced increased cracking with decreasing air content. The OP Bridge experienced increased cracking with increasing air content; however, only three placements are available to establish this relationship. The two placements with the highest cracking had average air contents of 5.0 percent (C-MONO Bridge 99-076 Placement 2) and 9.8 percent (OP Bridge Placement 2). The C-MONO deck with the highest cracking also had significantly high average compressive strength [7400 psi (51.0 MPa)] and paste content (28.0 percent), suggesting that factors other than air content also influenced cracking. In addition, the many issues experienced during construction of the OP Bridge (discussed in Section 5.3.22) likely had a greater influence on cracking than did air content. The four LC-HPC placements with the lowest cracking at 42 months (LC-HPC-1 Placements 1 and 2, LC-HPC-2, and LC-HPC-7) had air contents between 7.7 and 8.0 percent.

In Figure 6.57, the LC-HPC and conventional monolithic decks are separated into two ranges of average air content: less than 6.0 percent and greater than or equal to 6.0 percent. The figure shows that the decks with average air contents greater than or equal to 6.0 percent have an average crack density nearly three times less than the decks with average air contents less than 6.0 percent (0.17 vs. 0.47 m/m^2). As stated previously, the LC-HPC specifications require concrete to contain an air content between 6.5 and 9.5 percent to be accepted for placement.

6.4.1.4 Compressive Strength

Previous studies (Schmitt and Darwin 1995, Krauss and Rogalla 1996, Miller and Darwin 2000, Lindquist et al. 2005, Yuan et al. 2011) have observed increased cracking in bridge decks that contain concretes with higher compressive strengths. Increased compressive strengths reduce the beneficial effects of creep. Over time, decreased creep limits the mitigation of tensile stresses in the deck (Krauss and Rogalla 1996), increasing the potential for cracking. In the analysis of conventional monolithic bridge decks completed by Lindquist et al. (2005), an increase in crack density from 0.16 to 0.49 m/m^2 was observed as compressive strengths increased from 4500 to 6500 psi (31.0 to 44.8 MPa). Additionally, Yuan et al. (2011) analyzed the LC-HPC decks in this study and observed an increase in compressive strength from between 3500 and 5500 psi (24.1 and 37.9 MPa) to above 5500 psi (37.9 MPa) resulted in a doubling of the average crack density at 36 months from 0.08 to 0.16 m/m^2. The current LC-HPC specifications require 28-day compressive strengths between 3500 and 5500 psi (24.1 and 37.9 MPa); however, no upper limitation was included at the time of construction for LC-HPC decks 1 through 13 and the OP Bridge placements.

The 28-day compressive strengths of the LC-HPC decks ranged from 3790 to 6380 psi (26.1 to 44.0 MPa), while the compressive strengths of the control subdecks

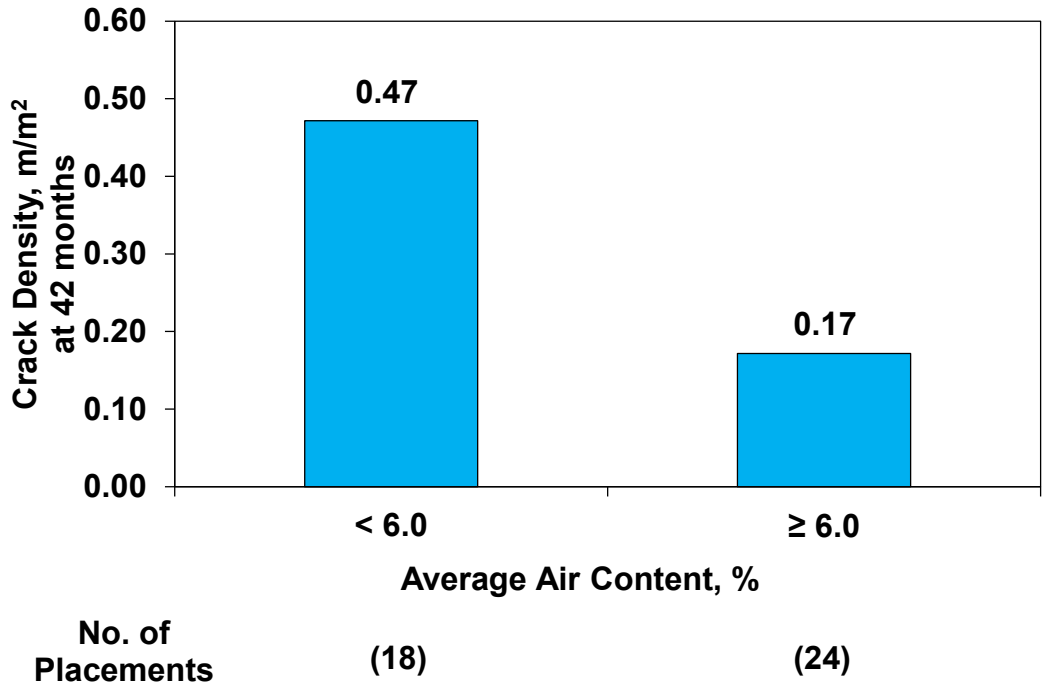

Figure 6.57 Crack density at 42 months for LC-HPC and conventional monolithic decks supported by steel girders separated into two ranges of average air content: less than 6.0 percent and greater than or equal to 6.0 percent

ranged from 4850 to 6340 psi (33.4 to 43.7 MPa). The crack densities at 42 months are plotted in terms of compressive strength for the LC-HPC decks and control subdecks in Figure 6.58. The LC-HPC and control decks are represented by "KU" and "C", respectively, in the figure due to space limitations. When considering the LC-HPC and control decks separately, a clear relationship between compressive strength and cracking is not evident from Figure 6.58; although, many of the decks that experienced high cracking had strengths above 5000 psi (34.5 MPa). The six placements that had crack densities at 42 months above 0.60 m/m^2 (Control 12 Placements 1 and 2, Control 11 Placements 1 and 2, Control 7 Placement 1, and Control 4) each contained concrete with an average compressive strength above 5000

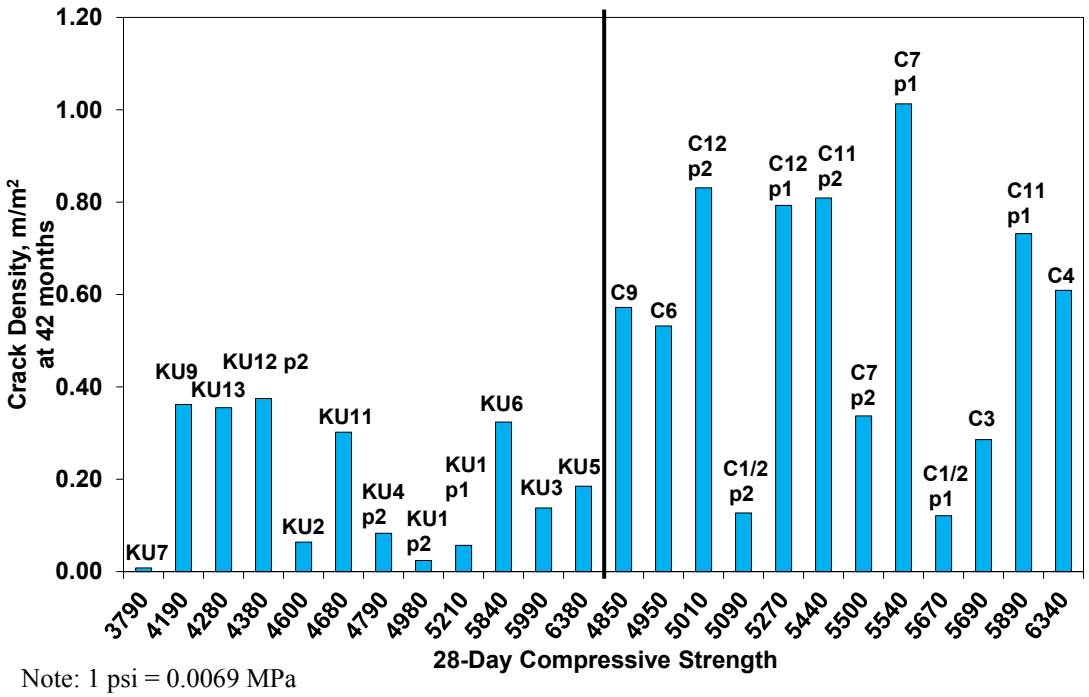

Note: 1 psi = 0.0069 MPa

Figure 6.58 Crack density at 42 months plotted versus 28-day compressive strength for LC-HPC decks and control subdecks supported by steel girders. LC-HPC and control decks are represented by "KU" and "C", respectively.

psi (34.5 MPa). In addition, the lowest-cracking deck in the study, LC-HPC-7, had the lowest average compressive strength [3790 psi (26.1 MPa)].

In Figure 6.59, the compressive strengths for the LC-HPC decks are separated into two ranges: average compressive strengths between 3500 and 5500 psi (24.1 and 37.9 MPa) and above 5500 psi (37.9 MPa). As shown in Figure 6.59, the average crack density at 42 months increases from 0.18 to 0.22 m/m^2 as the compressive strength increases from between 3500 and 5500 psi (24.1 and 37.9 MPa) to above 5500 psi (37.9 MPa). This observation supports the previous findings by Lindquist et al. (2005) and Yuan et al. (2011), although, the difference in cracking performance between the strength ranges is less pronounced in this comparison than in the previous studies.

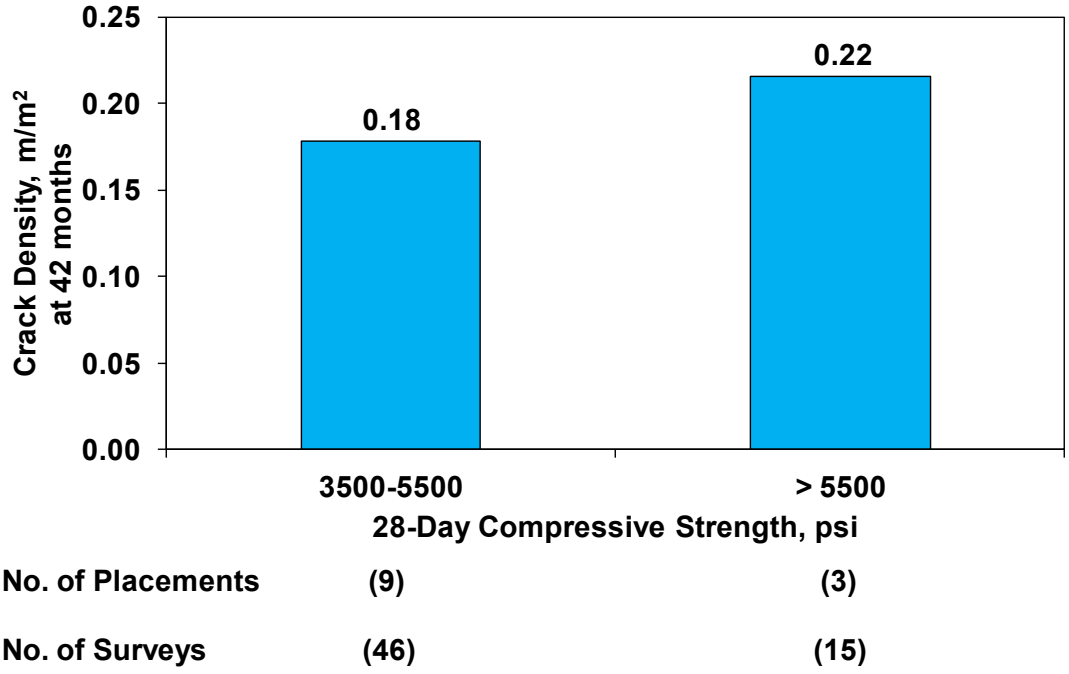

Note: 1 psi = 0.0069 MPa

Figure 6.59 Crack density at 42 months for LC-HPC decks supported by steel girders separated into two ranges: average compressive strength between 3500 and 5500 psi and above 5500 psi.

In Figure 6.60, compressive strengths for the conventional monolithic (C-MONO) decks are added to the LC-HPC strengths shown in Figure 6.59. The compressive strength data for the C-MONO decks are provided in Appendix F. The figure shows that the increase in cracking observed in decks with compressive strengths above 5500 psi (37.9 MPa) is more pronounced when the conventional monolithic decks are considered with LC-HPC decks. In this comparison, the crack density more than doubles, increasing from 0.23 to 0.50 m/m^2, as the average compressive strength increases from between 3500 and 5500 psi (24.1 and 37.9 MPa) to above 5500 psi (37.9 MPa).

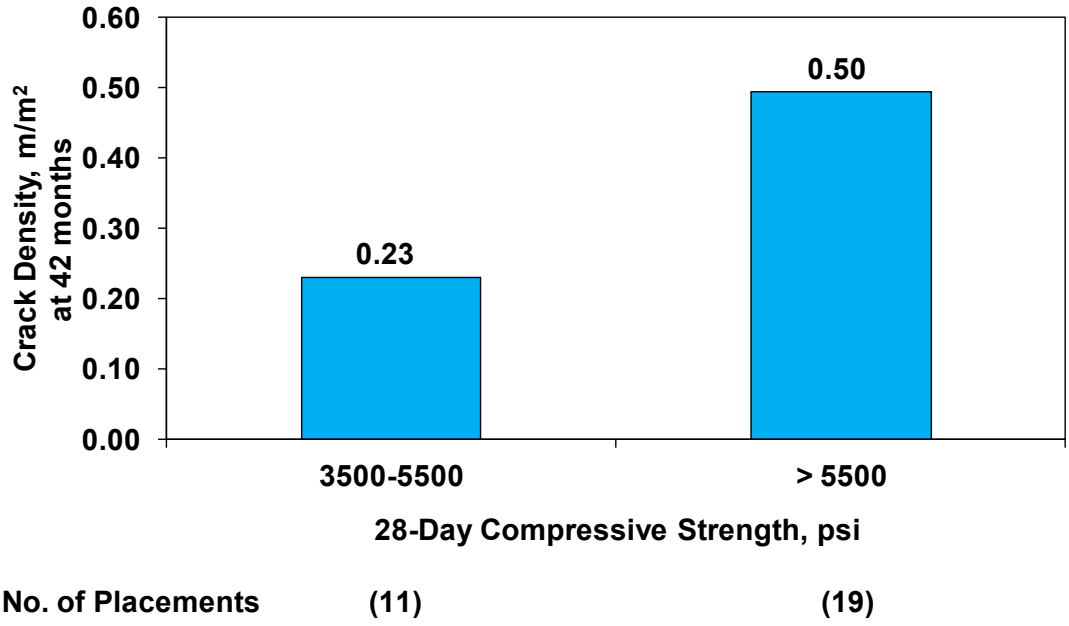

Note: 1 psi = 0.0069 MPa

Figure 6.60 Crack density at 42 months for LC-HPC and conventional monolithic (C-MONO) decks supported by steel girders separated into two ranges: average compressive strength between 3500 and 5500 psi and above 5500 psi

6.4.2 Temperature Factors Affecting Cracking

6.4.2.1 Concrete Temperature

The placement of higher-temperature concrete in bridge decks increases the potential for a number of cracking mechanisms. High concrete temperatures promote plastic shrinkage cracking by increasing the evaporation rate at the surface of the concrete, and the higher the initial temperature of concrete, the greater the heat of hydration and, subsequently, the greater the rise above the placement temperature; and the placement of higher-temperature concrete on cooler steel girders will induce thermal stresses as the restrained concrete contracts relative to the girders when temperatures normalize to ambient conditions. If the temperature of concrete is too low, however, slowing the hydration reaction may cause the concrete to remain in the

plastic condition longer and result in more settlement cracking, as well as slow strength gain.

LC-HPC specifications require bridge decks to be cast with concrete temperatures from 55° to 70° F (13° to 21° C), with a 5° F (3° C) adjustment outside of the range if approved by the Engineer. The average concrete temperatures of the LC-HPC decks ranged from 58° to 71° F (14° to 22° C), while the average concrete temperatures of the control subdecks ranged from 66° to 89° F (19° to 32° C).

The crack densities at 42 months for the LC-HPC decks are plotted as a function of average plastic concrete temperature in Figure 6.61. As shown in the figure, the average crack density of the LC-HPC decks decreases from 0.24 to 0.13 m/m^2 as the average concrete temperature increases from 60° to 70° F (16° to 21° C). Although these observations indicate that cracking decreases at higher concrete temperatures, the LC-HPC decks all had concrete temperatures within the range allowed by the LC-HPC specifications and, as other temperature effects investigated in this section will show, the concrete temperature alone is not the dominant factor for LC-HPC decks. These observations do, however, emphasize the importance of the early initiation of curing, as required on LC-HPC decks, which essentially eliminates the potential for plastic shrinkage cracking at all temperatures.

In Figure 6.62, the crack densities at 42 months are plotted as a function of plastic concrete temperature for the control subdecks. As stated previously, the control subdecks were placed with a much larger (and higher) range of concrete temperatures than the LC-HPC decks. The figure shows that in contrast with the observations from the LC-HPC decks, crack density at 42 months generally increases as the concrete temperature of the control subdecks increases, rising from 0.48 m/m^2 for concrete temperatures below 70º F (21º C) to 0.61 m/m^2 for concrete temperatures between 70º and 79º F (21º and 26º C). The average crack density decreases slightly, from 0.61 m/m^2 for concrete temperatures from between 70° and 79° F (21° and 26°

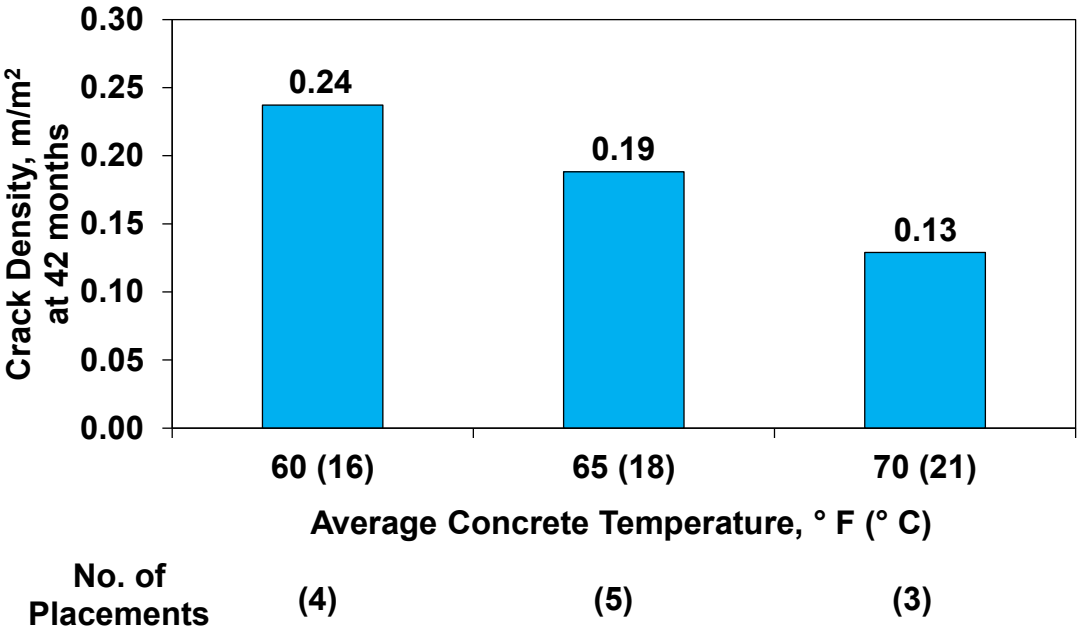

Figure 6.61 Crack density at 42 months as a function of average concrete temperature for LC-HPC decks supported by steel girders

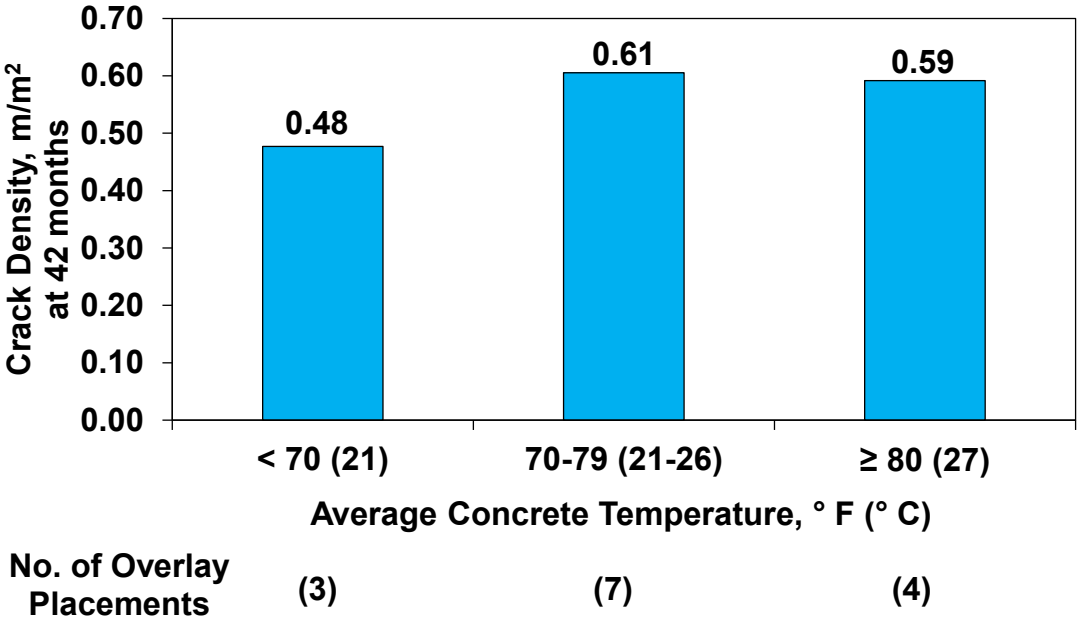

Figure 6.62 Crack density at 42 months as a function of average concrete temperature for control subdecks supported by steel girders

C) to 0.59 m/m^2 for temperatures of 80° F (27° C) and above. The concrete of the control subdeck with the highest cracking, Control 7 Placement 1, was placed at an average temperature of 80° F (27° C). Conversely, concrete of the lowest-cracking control subdeck, Control 1/2 Placement 1, was placed at an average temperature of 66° F (19° C); a value that would meet the requirement for an LC-HPC deck.

6.4.2.2 Temperature Differences between Concrete Deck and Steel Girders

As discussed in Section 1.2.2, large temperature differences between the concrete deck and the steel girders induce thermal stresses that can increase the potential for cracking. Where concrete temperatures are above the girder temperatures, the concrete contracts relative to the girders as temperatures normalize to ambient conditions. This relative contraction induces tensile stresses in the restrained concrete and increases the potential for cracking. Conversely, in instances where concrete temperatures are below the girder temperatures, the concrete expands relative to the girders as temperatures normalize to ambient conditions. This relative expansion places the restrained concrete in compression, lowering the potential for cracking.

This section examines the effects of differences between the concrete and air temperatures (used to estimate girder temperatures) at the time of concrete placement. Air temperature records for the construction of each deck are provided in Table F.6 in Appendix F. Yuan et al. (2011) examined the differences between ambient-air and steel-girder temperatures before and during the placement of LC-HPC-12 Placement 2. They observed that girder temperatures remained below the ambient temperature early in the day (before 10:00 a.m.), but increased above the ambient temperature later in the day (between 10:00 a.m. and 5:30 p.m.). Subramaniam and Agrawal (2009) measured temperature changes in the concrete decks and steel girders of bridges during construction. They observed that temperature changes over time occurred at similar rates for the ambient air and steel girders, demonstrating the close

relationship between the two. While the stresses induced in the concrete decks based on temperature differences with the steel girders cannot be quantified with the data available in this study, general trends in cracking performance can be observed while considering differences between concrete temperatures and ambient air temperatures on the day of construction.

In Figures 6.63 and 6.64, crack density at 42 months is plotted as a function of the difference between the average concrete temperature and the average air temperature on the day of construction for the LC-HPC decks and control subdecks, respectively. As shown in the figures, cracking increases as the average concrete temperature increases relative to the average air temperature. This observation suggests that as the concrete temperature increases relative to the girder temperature, there is greater potential for thermal tensile stresses to develop in the concrete, increasing the likelihood of cracking. The six placements with the highest cracking (Control 5, Control 7 Placement 1, Control 11 Placements 1 and 2, and Control 12 Placements 1 and 2) experienced the highest concrete temperatures relative to the average air temperature. Three of the four highest-cracking LC-HPC placements (LC-HPC-6, 12 Placement 2, and 13) had the three highest concrete temperatures relative to the average air temperature among the LC-HPC decks.

In Figure 6.65, crack density is compared based on differences between the average concrete temperatures and the average air temperature for the LC-HPC decks and control subdecks (displayed in Figures 6.63 and 6.64) for differences of less than or equal to 5° F (2° C), between 6° and 20° F (3° and 11° C), and greater than 20° F (11° C). As shown in Figure 6.65, cracking more than doubles in the LC-HPC decks (from 0.11 to 0.27 m/m^2) as the difference in average temperatures increases from a value less than or equal to 5° F (2° C) to a value between 6° and 20° F (3° and 11° C) above the average air temperature. No LC-HPC deck experienced an average concrete temperature greater than 20° F (11° C) above the average air temperature,

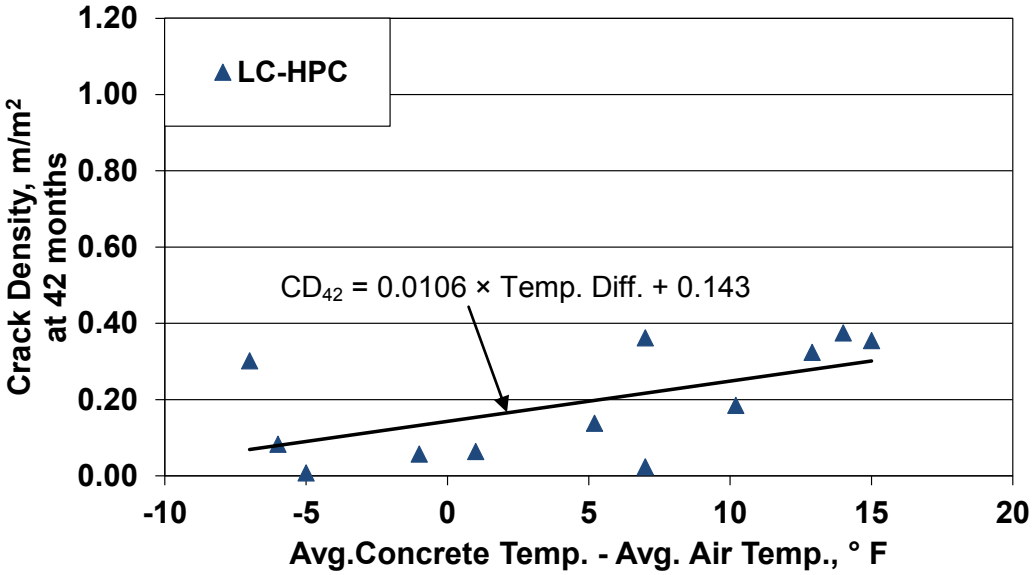

Note: CD_{42} = Crack density at 42 months (m/m^2)
Temp. Diff. = Difference between average concrete temperature and average air temperature on day of construction (° F)

Figure 6.63 Crack density at 42 months as a function of the difference between average concrete temperature and average air temperature on the day of construction for LC-HPC decks supported by steel girders. Air temperature data are provided in Table F.6 in Appendix F. Air temperature data were obtained from Weather Underground (www.weatherunderground.com).

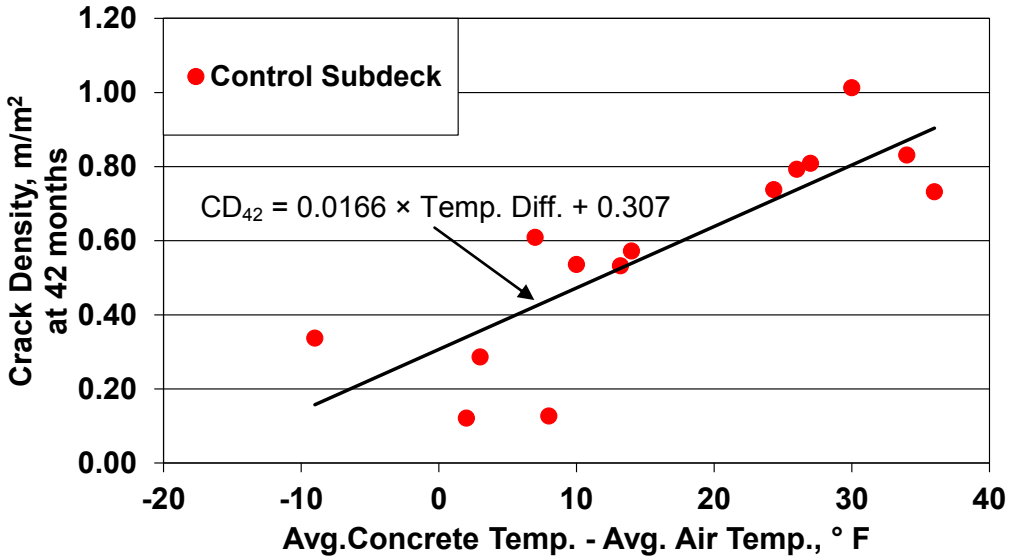

Note: CD_{42} = Crack density at 42 months (m/m^2)
Temp. Diff. = Difference between average concrete temperature and average air temperature on day of construction (° F)

Figure 6.64 Crack density at 42 months as a function of the difference between average concrete temperature and average air temperature on the day of construction for control subdecks supported by steel girders. Air temperature data are provided in Table F.6 in Appendix F. Air temperature data were obtained from Weather Underground (www.weatherunderground.com).

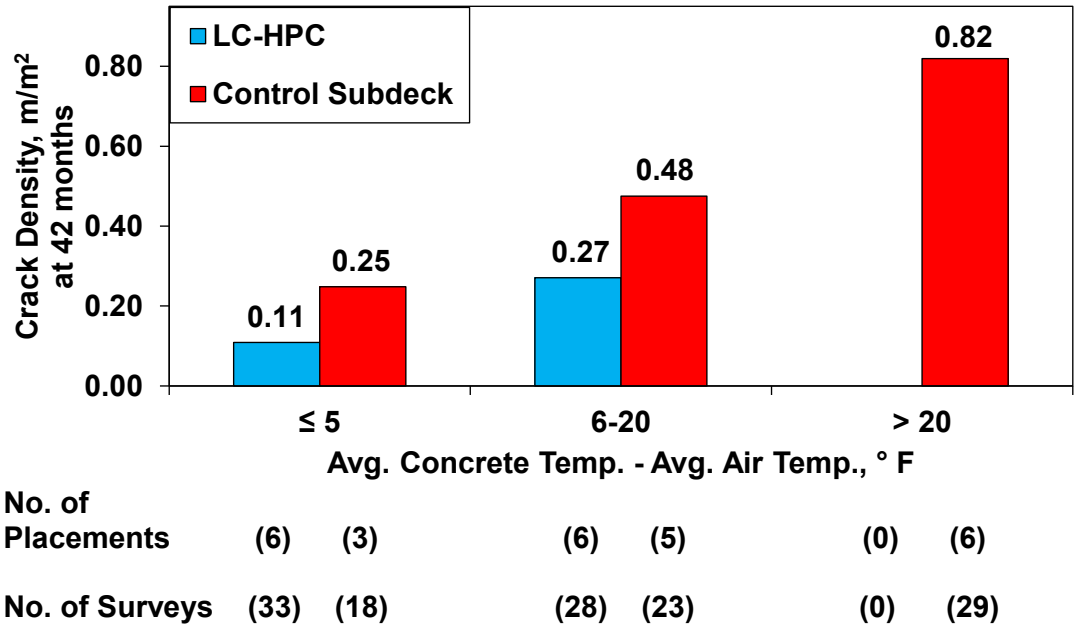

Figure 6.65 Crack density at 42 months for LC-HPC decks and control subdecks supported by steel girders separated into three ranges of difference between average concrete temperature and average air temperature: less than or equal to 5° F (2° C), between 6° and 20° F (3° and 11° C), and greater than 20° F (11° C). Air temperature data are provided in Table F.6 in Appendix F. Air temperature data were obtained from Weather Underground (www.weatherunderground.com).

likely due to the restrictions placed on concrete temperature and initiation of construction in cold weather. The latter prohibits placing concrete if there is a probability of the air temperature dropping more than 25° F (14° C) below the concrete temperature during the first 24 hours after placement unless insulation is provided for the deck and girders and delays the start of placement until the ambient temperature exceeds 50° F (10° C) if the temperature during the day of placement is expected to exceed 60° F (16° C) (Kansas Department of Transportation 2007c). Similar to the LC-HPC decks, cracking increases from 0.25 to 0.48 to 0.82 m/m^2 as the average temperature difference between the control subdecks and the air increases

from under 5° F (2° C) to between 6° and 20° F (3° and 11° C) and again from between 6° and 20° F (3° and 11° C) to over 20° F (11° C).

6.4.2.3 Air Temperature

Concrete placed during conditions of high ambient temperature experiences an increased risk for plastic shrinkage cracking and thermal cracking. As discussed in Section 1.2.1, increased ambient temperature along with increased concrete temperature and wind velocity and decreased relative humidity contribute to an increased evaporation rate of the surface water within the concrete. Lindquist et al. (2005) observed a sharp increase in cracking in conventional monolithic decks as the high temperature on the day of construction increased. Additionally, wide-ranging air temperatures on the day of placement increase the potential for thermal cracking as stresses are induced by thermal deformations in the deck and girders.

In Figures 6.66 and 6.67, crack density at 42 months is plotted as a function of the average air temperature on the day of construction for the LC-HPC and control subdecks, respectively. As stated previously, the air temperature records are provided in Table F.6 in Appendix F. As shown in Figures 6.66 and 6.67, cracking increases in decks constructed on days with lower average air temperatures. This observation suggests that any increase in cracking caused by high evaporation rates from high ambient temperatures is outweighed by decreases in thermal tensile stresses resulting from the placement of cooler concrete on warmer steel girders (shown in Figures 6.63 through 6.65). This trend is observed even for the control subdecks, which are subjected to less-stringent requirements for concrete temperature control and curing than are the LC-HPC decks. The six placements with the highest cracking at 42 months (Control 5, Control 7 Placement 1, Control 11 Placements 1 and 2, and Control 12 Placements 1 and 2) were constructed on days with average air temperatures of 50° F (10° C) or below. The five lowest-cracking LC-HPC

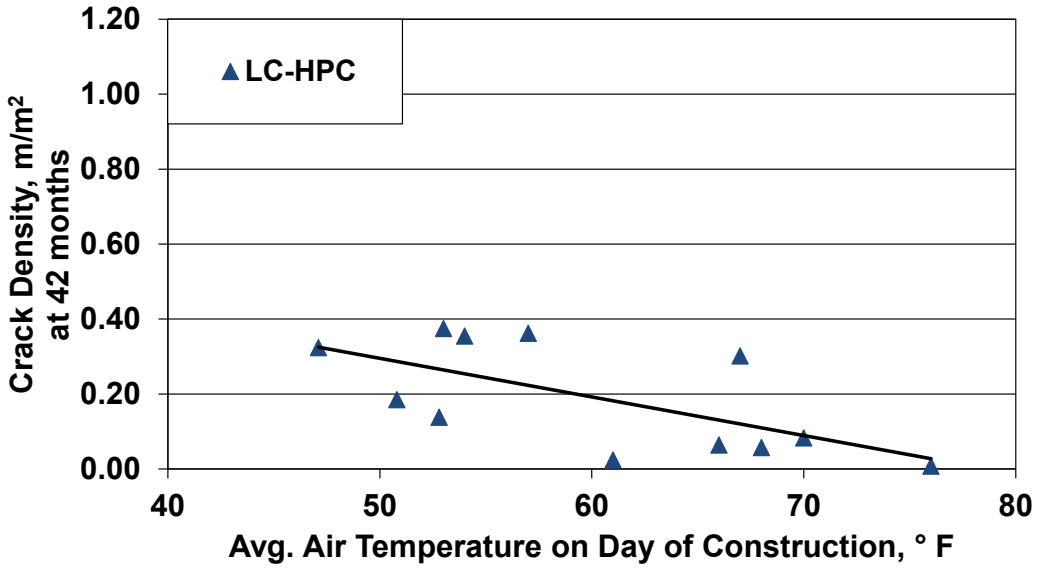

Figure 6.66 Crack density at 42 months as a function of the average air temperature on the day of construction for LC-HPC decks supported by steel girders. Air temperature data are provided in Table F.6 in Appendix F. Air temperature data were obtained from Weather Underground (www.weatherunderground.com).

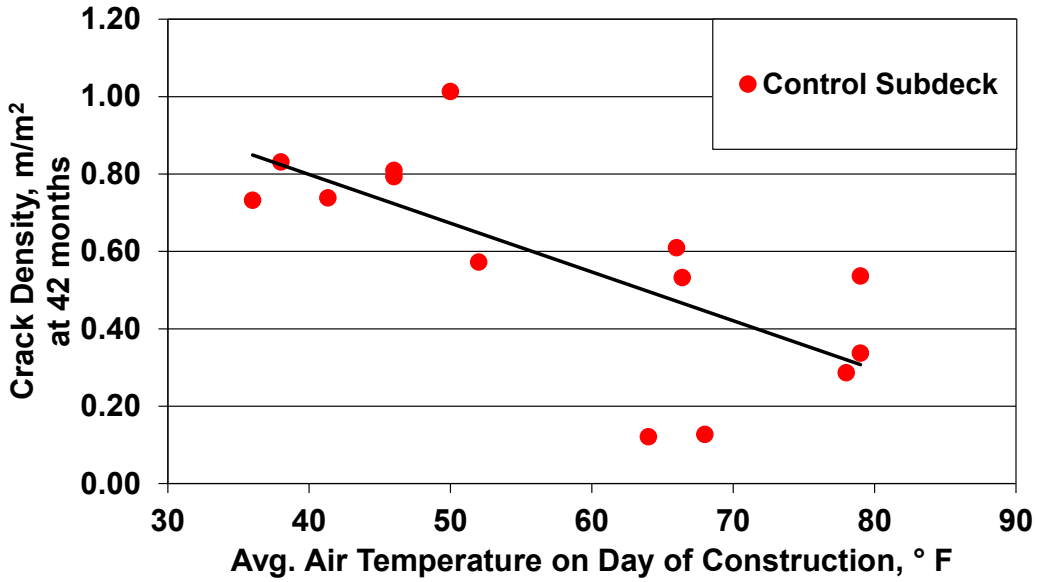

Figure 6.67 Crack density at 42 months as a function of the average air temperature on the day of construction for control subdecks supported by steel girders. Air temperature data are provided in Table F.6 in Appendix F. Air temperature data were obtained from Weather Underground (www.weatherunderground.com).

placements (LC-HPC-1 Placements 1 and 2, LC-HPC-2, LC-HPC-4 Placement 2, and LC-HPC-7) were constructed on days with average air temperatures above 60° F (16° C). The LC-HPC deck with the lowest cracking at 42 months, LC-HPC-7, was constructed on a day with the highest average temperature among the LC-HPC decks [76° F (24° C)].

Figures 6.68 and 6.69 show the crack density at 42 months as a function of high air temperature on the day of construction for the LC-HPC decks and control subdecks, respectively. As shown in the figures, decks constructed on days with greater high air temperatures exhibited less cracking at 42 months. The five lowest-cracking LC-HPC placements (LC-HPC-1 Placements 1 and 2, LC-HPC-2, LC-HPC-4 Placement 2, and LC-HPC-7) and the four lowest-cracking control subdeck placements (Control 1/2 Placements 1 and 2, Control 3, and Control 7 Placement 2) were constructed on days with high temperatures greater than or equal to 75° F (20° C).

In Figure 6.70, the data for high air temperature for the LC-HPC decks and control subdecks (shown in Figures 6.68 and 6.69) are separated into two ranges: decks constructed on days with high air temperatures of less than 75° F (24° C) and days with high air temperatures of 75° F (24° C) or more. As shown in the figure, the LC-HPC decks constructed on days with high temperatures of less than 75° F (24° C) experienced more than three times the cracking (0.29 vs. 0.09 m/m^2) of decks constructed on days with high temperatures of greater than or equal to 75° F (24° C). Control subdecks experienced more than two times the cracking when constructed on days with high temperatures of less than 75° F (24° C). Once again, this observation suggests that any negative effects on cracking caused by high evaporation rates from high ambient temperatures are outweighed by the reduced tensile stresses offered by the placement of cooler concrete on warmer steel girders. These results regarding the

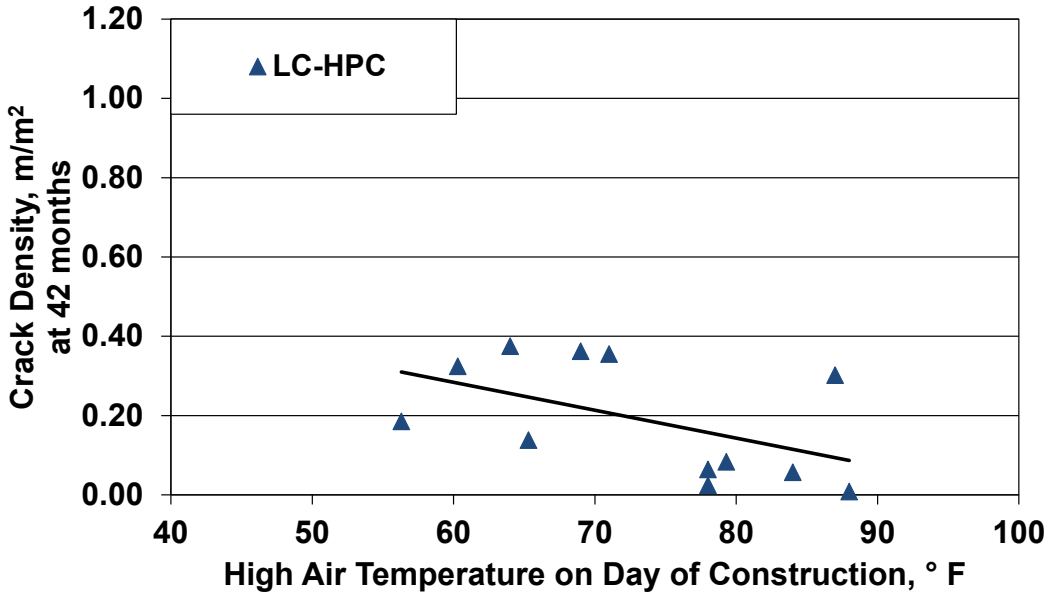

Figure 6.68 Crack density at 42 months as a function of the high air temperature on the day of construction for LC-HPC decks supported by steel girders. Air temperature data are provided in Table F.6 in Appendix F. Air temperature data were obtained from Weather Underground (www.weatherunderground.com).

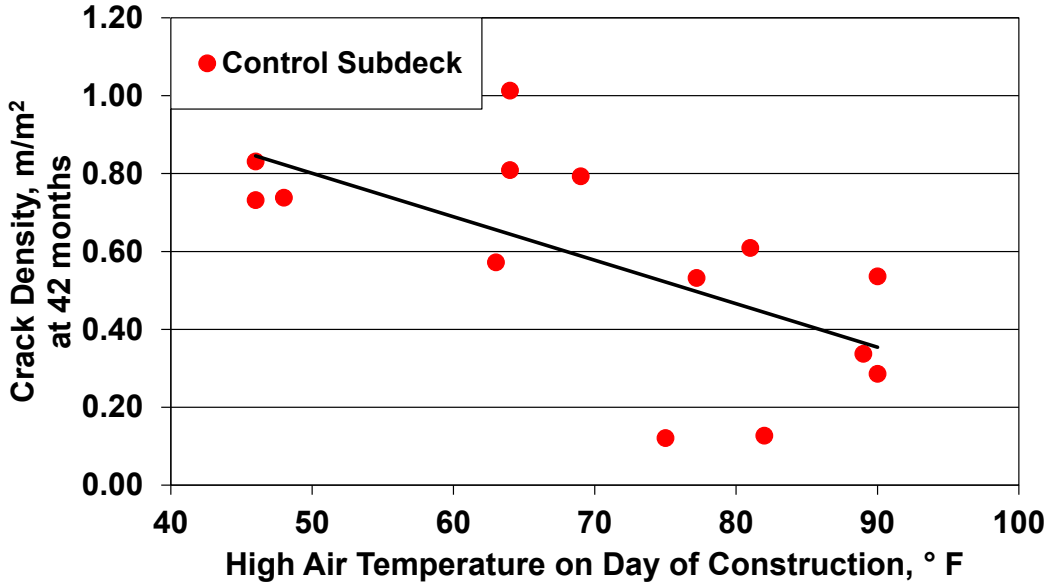

Figure 6.69 Crack density at 42 months as a function of the high air temperature on the day of construction for control subdecks supported by steel girders. Air temperature data are provided in Table F.6 in Appendix F. Air temperature data were obtained from Weather Underground (www.weatherunderground.com).

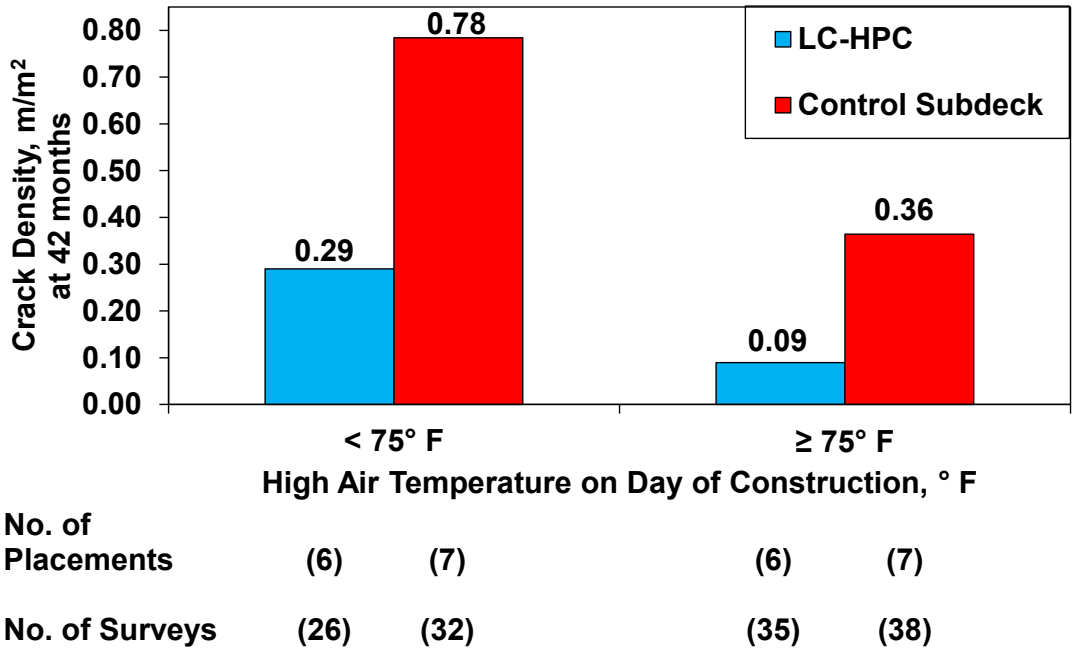

Figure 6.70 Crack density at 42 months for LC-HPC decks and control subdecks supported by steel girders separated into two ranges of high air temperature on the day of construction: less than 75° F (24° C) and greater than or equal to 75° F (24° C). Air temperature data are provided in Table F.6 in Appendix F. Air temperature data were obtained from Weather Underground (www.weatherunderground.com).

effects of average and high air temperatures on the day of construction contrast those observed in earlier studies.

Figure 6.71 shows the crack density at 42 months as a function of air temperature range on the day of construction for the LC-HPC decks and control subdecks. In the figure, the data are separated into two groups: air temperature range of less than or equal to 25° F (14° C) and greater than 25° F (14° C). As shown in the figure, the LC-HPC decks exhibited only slightly higher crack densities (0.18 vs. 0.20 m/m^2) as the range of air temperature on the day of construction increased from less than or equal to 25° F (14° C) to greater than 25° F (14° C). The control subdecks exhibited a greater increase in crack density than the LC-HPC decks, increasing from 0.52 to 0.68 m/m^2 as the air temperature range increased from less than or equal to

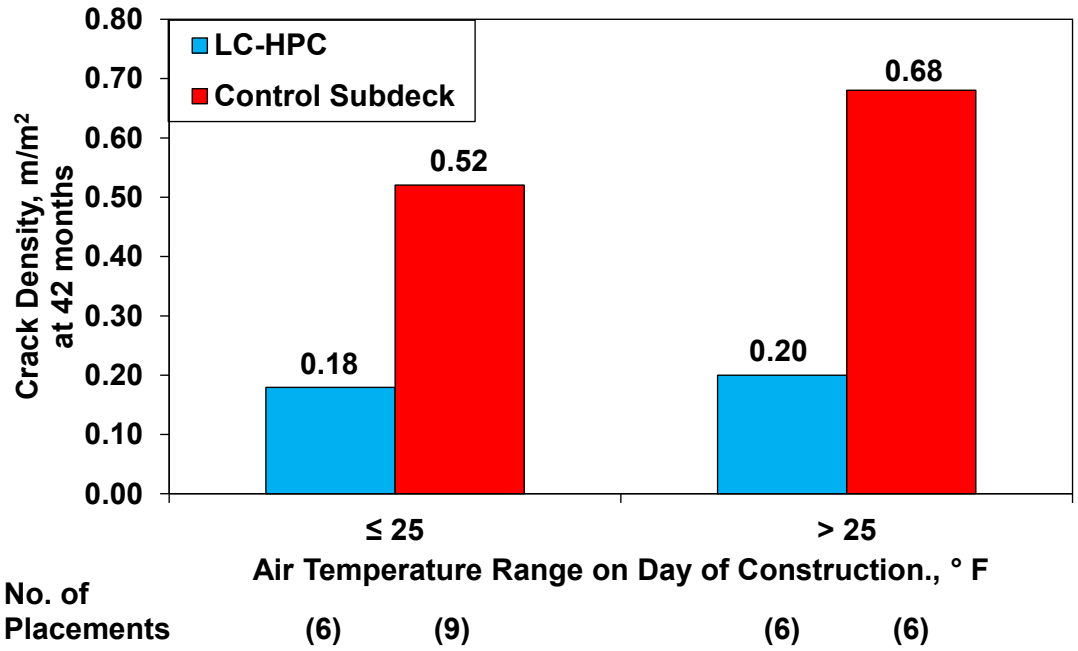

Figure 6.71 Crack density at 42 months for LC-HPC decks and control subdecks supported by steel girders separated into two groups of air temperature range on the day of construction: less than or equal to 25° F (14° C) and greater than 25° F (14° C). Air temperature data are provided in Table F.6 in Appendix F. Air temperature data were obtained from Weather Underground (www.weatherunderground.com).

25° F (14° C) to greater than 25° F (14° C). These observations suggest that stresses induced by thermal deformations in the deck and girders caused by air temperature fluctuations may influence cracking to some degree. However, the effect of temperature differences between the concrete deck and steel girders, discussed in Section 6.4.2.2, appear to have a greater influence on thermal cracking than the effect of air temperature range.

The trends observed in Sections 6.4.2.2 and 6.4.2.3 demonstrate that high ambient temperatures during construction may reduce cracking if concrete temperatures, plastic shrinkage, or both are controlled. Plastic shrinkage cracking is controlled in the LC-HPC decks by requiring limitations on concrete temperatures and rapid placement of burlap after strikeoff (within 10 minutes). The rapid

placement of burlap prevents the concrete from being exposed to high ambient temperatures for extended periods of time, minimizing the risk for plastic shrinkage cracking. If plastic shrinkage cracking is controlled by way of low concrete temperatures and rapid burlap placement, there is an apparent benefit in placing concrete decks during high ambient temperatures because of the mitigation of tensile thermal stresses induced on the deck due to the restraint provided by the girders. In fact, increased air temperatures during construction also appear to have led to decreased cracking in control subdecks, which are constructed to less-stringent requirements for concrete temperature control and burlap placement. Similar conclusions regarding the influence of air temperature on cracking cannot be made for decks supported by prestressed girders because of the higher thermal mass of concrete girders and a lack of data.

6.4.3 Regression Analyses of Monolithic Bridge Decks

6.4.3.1 Dummy Variables Analysis – Initial Analysis

A dummy variables regression analysis (Draper and Smith 1981) is performed on monolithic bridge decks constructed on steel girders to determine the factors that influence cracking. The decks used in the analysis include the LC-HPC decks and OP Bridge examined in this study and the conventional monolithic (C-MONO) decks examined by Schmitt and Darwin (1995), Miller and Darwin (2000), and Lindquist et al. (2005). An additional monolithic bridge deck (Bridge Number 56-49) that has been surveyed annually since 2006 is also included. In total, the analysis includes 26 bridge decks and 45 individual placements constructed by 10 different contractors. The crack density at 42 months, discussed in Section 6.3.3, is used to quantify cracking performance.

The analysis examines the influence of six factors on cracking, including paste content, slump, compressive strength, air content, and air temperature range and

difference between average concrete temperature and average air temperature on the day of construction. Average concrete temperatures are not available for the conventional monolithic decks, and as a result, the difference between concrete temperature and air temperature is evaluated as a factor only for the LC-HPC decks and OP Bridge. For the analysis to be executed, however, values for each factor must be included for all decks. For this reason, the mean value of the difference between concrete and air temperature for the LC-HPC decks and OP Bridge [6° F (4° C)] is assigned as the value for each C-MONO deck (Figure 6.72). The two trend lines in Figure 6.72 that, respectively, include and exclude the C-MONO crack densities are very close and are primarily contingent on the LC-HPC decks and OP Bridge. While necessary, this approach underestimates the effects of differences between concrete and air temperature. High and average air temperatures on the day of construction are omitted from the analysis because the effects of air temperature on cracking observed by Lindquist et al. (2005) for the C-MONO decks conflict with those observed in Section 6.4.2.3 for the LC-HPC decks. The effects on cracking of concrete temperature and high and average air temperature are evaluated separately for the LC-HPC and C-MONO decks in Section 6.4.3.3. The crack densities at 42 months and the values of the six factors are listed in Table F.7 in Appendix F. The cracking mechanisms associated with each factor have been discussed in depth in previous sections and are summarized below.

- **Paste Content** – Cement paste is the concrete constituent with the greatest shrinkage potential. An increased paste content increases the potential for drying shrinkage cracking.
- **Slump** – Increased slump increases the risk of settlement cracking. Settlement cracks occur directly above reinforcing steel, providing a direct path for corrosive agents to reach the steel.

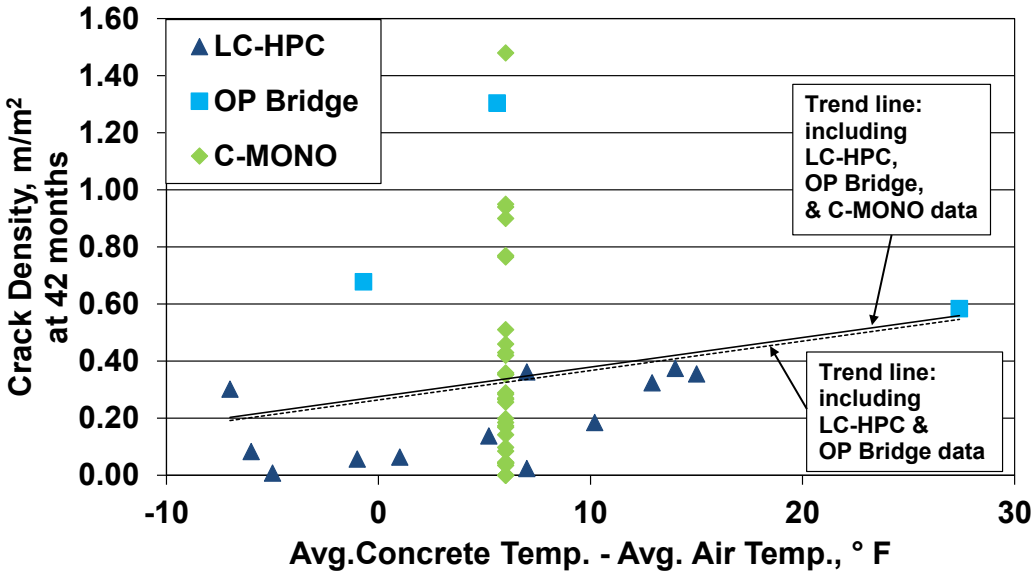

Note: Trend lines fit to data using least-squares linear regression.

Figure 6.72 Crack density at 42 months for LC-HPC and C-MONO decks and OP Bridge as a function of difference between average concrete temperature and average air temperature on the day of construction. C-MONO decks are assigned the mean value of temperature difference for the LC-HPC decks and OP Bridge. All decks supported by steel girders.

- **Compressive Strength** – Increased compressive strength reduces concrete creep. Creep, especially early-age creep, lowers the potential for cracking by relieving stresses in the concrete.
- **Air Content** – Entrained air is a workability agent and does not shrink.
- **Air Temperature Range** – An increased range of air temperatures on the day of construction increases the thermal deformations experienced in the deck and girders, increasing the risk for thermal stresses and cracking.
- **Difference between Concrete Temperature and Air Temperature** – Large temperature differences between the concrete deck and steel girders induce thermal stresses that can increase the potential for cracking. Where concrete temperatures are above girder temperatures, the concrete contracts relative to

the girders as temperatures normalize to ambient conditions, resulting in tensile stresses and increasing the potential for cracking.

The influence of each factor on cracking is determined by examining the crack densities at 42 months as a function of the six independent factors. A least-squares linear regression analysis is performed to determine a coefficient corresponding to each independent factor. The contractors involved with bridge construction are also included as a factor in the analysis, as previous findings suggest that construction methods influence cracking performance (Cady et al. 1971, Lindquist et al. 2005, Yuan et al. 2011). The dummy variables technique is used to evaluate the effect of each contractor on cracking. In the technique, a dummy variable (0 or 1) is assigned to each contractor for use in the regression analysis and a coefficient corresponding to each contractor is determined. Equation (6.2) is used in the dummy variables regression analysis.

$$Y = \gamma_1 X_1 + \gamma_2 X_2 \ldots + \gamma_n X_i + \beta_1 Z_1 + \beta_2 Z_2 \ldots \beta_{n-1} Z_{n-1} \quad (6.2)$$

where Y= dependent variable, crack density at 42 months in this analysis,

$X_1, X_2, \ldots X_i$= independent factors that may influence bridge deck cracking, including paste content, slump, compressive strength, air content, range of air temperature, and difference between average concrete temperature and average air temperature, respectively, in this analysis,

$\gamma_1, \gamma_2, \ldots \gamma_n$= coefficients corresponding to each independent variable,

$Z_1, Z_2, \ldots Z_{n-1}$= dummy variables assigned to each contractor,

= 1 for an individual contractor and 0 for the remaining contractors,

$\beta_1, \beta_2, \ldots \beta_{n-1}$= coefficients corresponding to each contractor associated with a given Z-value

The Student's t-test is used to determine the statistical significance α of the relationship established between a single independent factor and the crack density values by each coefficient γ. For example, a significance level of $\alpha = 0.10$ indicates that there is a 10 percent probability that the coefficient γ identifies as statistically significant a relationship between the corresponding independent factor and crack density when, in fact, there is no relationship. Detailed information regarding the Student's t-test is provided in Section 3.1.1. In addition, an F-test is performed to determine the probability that the correlation established between crack density and the entire group of independent factors occurs by chance.

The range of values of the independent factors for the 26 bridge decks (45 individual placements) are shown in Table 6.5. The coefficient corresponding to each independent factor derived from the regression analysis and the associated statistical data are shown in Table 6.6.

The analysis reveals an increase in paste content contributes to an increase in crack density at 42 months. Based on the analysis, an increase of 1 percent paste content increases crack density by 0.039 m/m^2 – this coefficient, however, does not estimate the relationship between paste content and crack density at a statistically significant level. This observation supports the findings of Section 6.4.1.1 that cracking increases in the LC-HPC and conventional monolithic decks with paste contents above 27 percent and is relatively stable at paste contents below 27 percent. Since cracking increases primarily at paste contents above 27 percent, the influence on cracking of higher paste contents is actually greater than that represented by this coefficient. An additional dummy variables analysis, described in Section 6.4.3.2, highlights the effect of higher paste contents. As shown in Table 6.6, slump has the greatest influence on cracking of the independent factors. A 1-in. (25-mm) increase in slump corresponds to a 0.132 m/m^2 increase in crack density, supporting previous

Table 6.5 Range of values of the independent factors for the 26 bridge decks (45 individual placements)

Factors	Paste Content %	Average Slump in.	Compressive Strength ksi	Air Content %	Air Temperature Range* ° F	Difference between Avg. Concrete Temp. & Avg. Air Temp.* ° F
Minimum	23.4	1.5	3.71	4.5	2	-7
Maximum	28.8	5.25	7.43	9.9	40	27
Average	26.2	2.50	5.41	6.5	24	6

*on day of construction
Note: 1 in. = 25.4 mm, temperature in °F = temperature in °C × 5/9 + 32, 1 psi = 0.0069 MPa
Values for Difference between Avg. Concrete Temp. & Avg. Air Temp. based only on LC-HPC decks and OP Bridge

Table 6.6 Correlation between crack density at 42 months and independent factors – first regression analysis

Factors	Paste Content %	Average Slump in.	Compressive Strength 1000 psi	Air Content %	Air Temperature Range* ° F	Difference between Avg. Concrete Temp. & Avg. Air Temp.* ° F
Coefficient γ	0.039	0.132	0.093	-0.016	0.004	0.001
T-Test Significance Level α	> 0.50	0.15	0.20	> 0.50	0.45	> 0.50
Coefficient of Determination (R^2)	0.732					
F-Test	0.0078%					

*on day of construction
T-Test Significance Level α: level of significance at which each coefficient estimates the relationship between the corresponding independent factor and crack density values.
F-Test: the probability that the observed correlation between the dependent and independent variables occurs by chance.
Note: Values for Difference between Avg. Concrete Temp & Avg Air Temp. based only on LC-HPC decks and OP Bridge

findings (Schmitt and Darwin 1995, Miller and Darwin 2000, Lindquist et al. 2005, Yuan et al. 2011). This coefficient estimates the relationship between slump and crack density at a significance level of $\alpha = 0.15$. In Section 6.4.1.2, the influence of slump on cracking in the LC-HPC decks was most apparent when cracking performance was evaluated based on the percentage of slump measurements over 4.0 in. (100 mm); however, individual slump measurements for the conventional monolithic decks were not available for use in the regression analysis. As shown in Table 6.6, an increase of 1000 psi (6.9 MPa) in compressive strength corresponds to an increase in crack density of 0.093 m/m^2. This coefficient estimates the relationship between compressive strength and crack density at a significance level of $\alpha = 0.20$. Compressive strength was determined as the greatest contributor to cracking in a regression analysis completed by Yuan et al. (2011) that included many of the decks used in the current analysis. The analysis indicates that an increase in air content of 1 percent contributes to a decrease in crack density of 0.016 m/m^2. As shown in Figure 6.56, the monolithic decks with average air contents below 6 percent exhibited high cracking, while those with air contents above 6 percent are relatively insensitive to air content. The observations from Figure 6.56 suggest that the coefficient for air content likely underestimates the effect of lower air contents on cracking. An increase in air temperature range on the day of construction of 10° F (6° C) results in an increase in crack density of 0.04 m/m^2, supporting Figure 6.71 and the understanding that increases in temperature range on the day of construction will induce additional thermal stresses in the deck. This coefficient, however, estimates the relationship between temperature range and crack density rather poorly, at a significance level of $\alpha = 0.45$. An increase in difference between average concrete temperature and average air temperature of 10° F (6° C) results in an increase in crack density of 0.01 m/m^2, supporting the findings of Section 6.4.2.2, which observed that cracking increased in LC-HPC decks as average concrete temperature increased

relative to the average air temperature on the day of construction. This coefficient, however, does not estimate the relationship between difference in temperature and crack density at a statistically significant level. As discussed earlier, this relationship is likely underestimated in the regression analysis as the result of assigning the average value of temperature difference for the LC-HPC decks and OP Bridge as the value for each C-MONO deck. An additional regression analysis that considers the effect of difference between concrete and air temperature for only the LC-HPC decks is performed in Section 6.4.3.3 to more effectively evaluate this influence on cracking. Although many of the coefficients did not estimate the relationship between the independent factors and crack density with great significance, the results of the F-test indicate that there is only a 0.0078 percent probability that the correlation established between the independent factors and crack density occurs by chance (Table 6.6).

The coefficients associated with each contractor, derived from the dummy variables analysis, are shown in Table 6.7, with Contractor Z10 acting as the reference contractor. A positive coefficient indicates that a bridge deck completed by the contractor is expected to experience greater cracking than one completed by the reference contractor, assuming all other factors are equal, while a negative coefficient indicates that a bridge deck completed by the contractor is expected to experience less cracking than one completed by the reference contractor. The coefficients range from -0.270 to 0.431 with units of m/m^2. Eight of the nine contractors have coefficients greater than that determined for slump, the independent factor with the greatest influence on cracking. These observations indicate that the method of construction used by a contractor can greatly influence cracking performance. Based on the coefficients, the crack density at 42 months, regardless of effects from the six independent factors, is expected to be, on average, 0.701 m/m^2 greater for Contractor

Table 6.7 Coefficient for dummy variable assigned to each contractor – first regression analysis

Contractor	Z1	Z2	Z3	Z4	Z5	Z6	Z7	Z8	Z9	Z10
Coefficient β	-0.232	-0.270	-0.202	-0.251	-0.254	-0.019	-0.178	0.431	0.308	-
T-Test Significance Level α	0.40	0.50	0.45	0.40	0.40	> 0.50	> 0.50	0.20	0.35	-

T-Test Significance Level α: level of significance at which each coefficient estimates the relationship between the corresponding independent factor and crack density values.

Z8 than for Contractor Z2 (determined by the difference between coefficients). The considerable influence of the contractors on cracking emphasizes the importance of having a contractor who is committed to producing a low-cracking bridge deck, as discussed in Section 5.3.26.5.

6.4.3.2 Dummy Variables Analysis – Second Analysis

Because the regression analysis in Section 6.4.3.1 established only a linear relationship between crack density and each independent factor, factors with non-linear relationships were likely not evaluated effectively. For example, Figure 6.51 in Section 6.4.1.1 shows that cracking increased significantly in decks with paste contents above 27 percent; however, decks with paste contents below 27 percent had similar levels of low cracking. Similarly, as shown in Figure 6.56, the influence of air content on cracking was significant only at values below 6 percent. Since single coefficients were used in the analysis to model these influences on cracking, the effect on cracking for decks with paste contents above 27 percent or air contents below 6 percent were greatly underestimated. Additionally, the single value assigned for the difference between the concrete and air temperature of the C-MONO decks potentially affected the correlations between the other independent factors and cracking. For these reasons, an additional dummy variables regression analysis is performed to more accurately determine the influence of the independent factors on cracking. In this analysis, a paste content of 26 percent is assigned to each deck with a paste content below this value. Similarly, an air content of 6.5 percent is assigned

to each deck with an air content above this value. These values were selected because paste contents below 26 percent and air contents above 6.5 percent do not appear to significantly affect cracking. By using this approach, the effect on cracking is focused on the decks with higher paste contents and lower air contents. Additionally, the difference between concrete temperature and air temperature is not considered as a factor in the second analysis to prevent the single value assigned to all C-MONO decks from potentially affecting the relationships between other factors and cracking. The coefficient corresponding to each independent factor derived from the regression analysis is shown in Table 6.8. The coefficients associated with each contractor are reported in Table 6.9.

As shown in Table 6.8, paste content and air content influence cracking to a higher degree after isolating the effects of higher paste contents and lower air contents. An increase of 1 percent paste content above 26 percent increases crack density at 42 months by 0.115 m/m^2; a significantly higher value than observed in the initial regression analysis (0.039 m/m^2). In addition, this coefficient estimates the relationship between paste content and crack density at a much higher level of significance than the coefficient determined from the first analysis ($\alpha = 0.10$ vs. $\alpha > 0.50$). An increase in air content of 1 percent *decreases* crack density at 42 months by 0.105 m/m^2; also a much higher value than observed in the initial regression analysis (0.016 m/m^2). Again, this coefficient estimates the relationship between air content and crack density at a higher level of significance than the coefficient determined from the first analysis ($\alpha = 0.25$ vs. $\alpha > 0.50$). The effect on cracking of slump and compressive strength are slightly decreased in the second analysis compared to the first, with the coefficients decreasing from 0.132 and 0.093 m/m^2 to 0.118 and 0.066 m/m^2, respectively. In addition, the coefficient determined for compressive strength in the second analysis estimates the relationship with crack

Table 6.8 Correlation between crack density at 42 months and independent factors – second regression analysis

Factors	Paste Content %	Average Slump in.	Compressive Strength 1000 psi	Air Content %	Air Temperature Range* ° F
Coefficient γ	0.115	0.118	0.066	-0.105	0.007
T-Test Significance Level α	0.10	0.15	0.30	0.25	0.15
Coefficient of Determination (R^2)	0.766				
F-Test	0.0004%				

*on day of construction

T-Test Significance Level α: level of significance at which each coefficient estimates the relationship between the corresponding independent factor and crack density values.

F-Test: the probability that the observed correlation between the dependent and independent variables occurs by chance.

Table 6.9 Coefficient for dummy variable assigned to each contractor – second regression analysis

Contractor	Z1	Z2	Z3	Z4	Z5	Z6	Z7	Z8	Z9	Z10
Coefficient β	-0.219	-0.328	-0.177	-0.302	-0.277	-0.136	-0.195	0.408	0.123	-
T-Test Significance Level α	0.35	0.35	0.50	0.25	0.25	> 0.50	0.45	0.15	> 0.50	-

T-Test Significance Level α: level of significance at which each coefficient estimates the relationship between the corresponding independent factor and crack density values.

density at a lower level of significance than the coefficient determined from the first analysis ($\alpha = 0.30$ vs. $\alpha = 0.20$). Air temperature range on the day of construction had a greater effect on cracking based on the second analysis than the first, with crack density increasing from 0.04 to 0.07 m/m^2 as the air temperature range increases by 10° F (6° C). The coefficient determined in the second analysis estimates the relationship between air temperature range and crack density at a higher level of significance than in the first analysis ($\alpha = 0.15$ vs. $\alpha > 0.50$). The F-test performed in the second analysis indicates that the correlation between crack density and the coefficients associated with the independent factors have just a 0.0004 percent probability of occurring by chance, lower than the probability determined by the F-test in the first analysis (0.0078 percent).

The coefficients associated with each contractor, derived from the second dummy variables analysis, are shown in Table 6.9. Tables 6.7 and 6.9 show that the coefficients for each contractor are similar in both analyses, ranging from -0.270 to 0.431 m/m^2 in the first analysis and ranging from -0.328 to 0.408 m/m^2 in the second analysis. Most of the coefficients from the second analysis estimate the relationship between contractor and crack density at a higher level of significance than those from the first analysis. In the second analysis, all eight contractors have coefficients greater than those for each of the six independent factors, emphasizing that the techniques used by contractors will greatly influence cracking performance.

6.4.3.3 Influence of Concrete and Ambient Air Temperatures on Cracking

As discussed earlier, high and average air temperatures on the day of construction were not included in the dummy variables regression analyses because these factors have been observed to influence the cracking performance of the LC-HPC and conventional monolithic decks differently. As shown in Section 6.4.2.3, cracking decreased in LC-HPC decks constructed on days with increasing high and average air temperatures. Conversely, Lindquist et al. (2005) observed a sharp

increase in cracking in the conventional monolithic decks as the high temperature on the day of construction increased. Due to the requirements for concrete temperature and burlap placement in the LC-HPC specifications, it is likely that construction during high temperatures did not negatively affect the cracking performance of the LC-HPC decks. In addition, the LC-HPC decks may have experienced the beneficial effects of placing cooler concrete on warmer girders (discussed in Section 6.4.2.2) that can occur during high ambient temperatures. The conventional monolithic decks, however, were not constructed in accordance with the strict requirements for concrete temperature and burlap placement and may have experienced problems with plastic shrinkage cracking as a result of high ambient temperatures.

To fairly examine the effects of temperature on cracking, two linear regression analyses are completed, separating the LC-HPC decks from the conventional monolithic decks. For the LC-HPC decks, crack density at 42 months is examined as a function of two independent factors, difference between average concrete temperature and average air temperature and high air temperature on the day of construction. Evaluating these two factors in a single regression analysis removes any effects of one factor on the other. For the conventional monolithic decks, crack density is examined as a function of one independent factor, high air temperature on the day of construction. The contractors are not included as dummy variables in these analyses. The range of factors and coefficients derived from the regression analyses for the LC-HPC and conventional monolithic decks are shown in Tables 6.10 and 6.11, respectively.

As shown in Table 6.10, a 10° F (6° C) increase in the difference between the average concrete temperature and the average air temperature increases the crack density at 42 months by 0.09 m/m^2 – this coefficient, however, estimates the relationship between difference in temperature and crack density relatively poorly, at a significance level of $\alpha = 0.35$, likely because other factors are not included in this

Table 6.10 Correlation between crack density at 42 months and difference between average concrete temperature and average air temperature and high air temperature and on the day of construction for the LC-HPC decks supported by steel girders.

Factor	Difference between Avg. Concrete Temp. & Avg. Air Temp.* ° F	High Air Temperature* ° F
Maximum	15	88
Minimum	-7	56
Average	4	73
Coefficient γ	0.009	-0.001
T-Test Significance Level α	0.35	> 0.50

*on day of construction
T-Test Significance Level α: level of significance at which each coefficient estimates the relationship between the corresponding independent factor and crack density values.

Table 6.11 Correlation between crack density at 42 months and high air temperature on the day of construction for the conventional monolithic decks. All decks supported by steel girders.

Factor	High Air Temperature* ° F
Maximum	97
Minimum	43
Average	66
Coefficient γ	0.007
T-Test Significance Level α	0.15

*on day of construction
T-Test Significance Level α: level of significance at which each coefficient estimates the relationship between the corresponding independent factor and crack density values.

analysis. This observation supports the findings in Section 6.4.2.2, that showed that cracking increased for LC-HPC decks as the average concrete temperature increased relative to the average air temperature. Conversely, Table 6.10 shows that high air temperature on the day of construction has little effect on cracking for the LC-HPC decks when these thermal effects are considered separately. As shown in the table, a 10° F (6° C) increase in high air temperature on the day of construction decreases the 42-month crack density by only 0.01 m/m^2. As discussed in Section 6.4.2.3, a decrease in cracking was noted in the LC-HPC decks constructed on days with greater high and average air temperatures. This decrease in cracking, however, is likely the result of decreased thermal tensile stresses due to the placement of cooler concrete on warmer girders, not the result of the higher temperatures alone. The fact that cracking did decrease, not increase, as high temperatures increased suggests that the requirements for concrete temperature and burlap placement in the LC-HPC specifications helped prevent plastic shrinkage cracking for decks constructed on days with high ambient temperatures.

Unlike the LC-HPC decks, the conventional monolithic decks exhibited increased cracking as the high air temperature increased on the day of construction, supporting the findings of Lindquist et al. (2005). As shown in Table 6.11, an increase in high temperature of 10° F (6° C) results in an increase in crack density of 0.07 m/m^2, suggesting that the conventional monolithic decks experienced problems with plastic shrinkage cracking as a result of high ambient temperatures. As stated previously, the conventional monolithic decks were not constructed in accordance with the requirements of the LC-HPC specifications for concrete temperature and burlap placement. These observations reinforce the importance of setting limits for concrete temperature and initiating rapid curing to lower the potential for plastic shrinkage cracking.

Ultimately, decks placed with consideration to the thermal effects caused by differences between the temperatures of the concrete and the steel girders, and also constructed with proper control of concrete temperature and rapid initiation of curing after strikeoff, have the potential to experience low levels of cracking.

CHAPTER 7: SUMMARY, OBSERVATIONS, CONCLUSIONS, AND RECOMMENDATIONS

7.1 SUMMARY

The problems associated with bridge deck cracking are well established and the factors responsible are generally recognized as a result of a number of studies focused on the subject. Cracking increases the potential for corrosion of the deck reinforcement by providing a direct path for water and other corrosive agents to penetrate the concrete and reach the steel. In addition, cracking increases the risk of freeze-thaw damage as water is able to more easily penetrate the deck surface and then expand when frozen, initiating tensile stresses and additional cracking. Although research concentrated on deck cracking has identified a number of contributing factors, few studies have taken the step to implement these findings through the construction of low-cracking bridge decks. In addition, new technologies developed to improve shrinkage and cracking performance that have gained momentum in the concrete industry in recent years have yet to be examined extensively with consideration of overall durability. This study is directed along two avenues to minimize bridge deck cracking: (1) laboratory evaluations of mixtures designed to reduce cracking while maintaining durability and (2) the construction and evaluation of low-cracking high-performance concrete bridge decks.

The laboratory portion of the study includes three programs (1, 2, and 3) comprising 53 concrete mixtures evaluated based on free shrinkage (ASTM C157), freeze-thaw durability (ASTM C666 and C215 and KDOT Test Method KTMR-22), scaling resistance (Quebec Test – BNQ NQ 2621-900), compressive strength (ASTM C39), and hardened air-void characteristics (ASTM C457). The mixtures employ technologies recognized to reduce shrinkage and cracking, including the addition of lightweight aggregate to provide a source of internal curing and the use of mineral and shrinkage-reducing admixtures. Programs 1 and 2 involve the evaluation of

mixtures containing different dosages (0, 0.5, 1.0, and 2.0 percent by weight of cement) of two shrinkage-reducing admixtures (SRAs) in combination with surfactant-based and polymer-based air-entraining admixtures (AEAs) and air contents ranging from 3.5 to 9 percent. Shrinkage-reducing admixtures and surfactant-based air-entraining admixtures function similarly by reducing the surface tension of water. When used in conjunction, the combined reduction in surface tension can decrease the stability of the air-void system and contribute to reduced freeze-thaw protection. Programs 1 and 2 assess the effects of SRAs on free shrinkage and determine the influence of the SRAs and AEAs on freeze-thaw durability, scaling resistance, and air-void stability. These findings are used to help establish a lower allowable limit for air content for mixtures containing SRAs. The mixtures in Program 2 contained only one type of SRA and the surfactant-based AEA. Program 3 includes an evaluation of mixtures with replacements of total aggregate with pre-wetted, intermediate-sized lightweight aggregate (0, 8, and 10 percent by volume), replacements of portland cement with Grade 100 slag cement (0 and 30 percent by volume), and replacements of portland cement with silica fume (0, 3, and 6 percent by volume). The pre-wetted lightweight aggregate provides a source of internal curing in the concrete, which has been observed to reduce free shrinkage. Previous studies have observed an additional reduction in shrinkage with the use of slag cement in conjunction with lightweight aggregate. The silica fume is predicted to reduce shrinkage even further when used in conjunction with internal curing and slag by lowering the permeability and, thus, slowing the rate of water loss during drying.

The second portion of the study involves the construction and evaluation of 16 bridge decks constructed in accordance with the LC-HPC specifications and 11 control decks constructed in accordance with standard specifications for state bridge construction in Kansas over a span of six years. Another deck bid under, but not

constructed in accordance with the LC-HPC specifications is also described. The LC-HPC specifications are summarized and subsequent modifications are noted. The design characteristics and construction experiences are described, the lessons learned during construction are summarized, and proposed methods of improvement are developed. Cracking performance of the decks is evaluated to determine the effectiveness of the LC-HPC specifications. Data collected during construction are related with cracking performance to evaluate the factors that affect cracking.

7.2 OBSERVATIONS AND CONCLUSIONS

The following observations and conclusions are based on the results and analyses presented in this report.

7.2.1 Evaluation of Mixtures Containing Two Air-Entraining Admixtures Used in Conjunction with Shrinkage-Reducing Admixtures (Program 1)

1. Both early-age and long-term shrinkage are reduced as shrinkage-reducing admixtures are added to the mixtures.
2. The reduction in shrinkage provided by the addition of a shrinkage-reducing admixture occurs primarily within the first 90 days of drying.
3. Mixtures with the highest dosage of shrinkage-reducing admixture (2.0 percent by weight of cement) exhibit the lowest shrinkage.
4. The type of shrinkage-reducing admixture has no apparent effect on early-age shrinkage; however, mixtures containing one of the SRAs experience lower long-term shrinkage than mixtures containing similar dosages of the other.
5. The type of air-entraining admixture (AEA) (surfactant-based or polymer-based) does not affect free shrinkage.
6. A majority of total shrinkage at one year is observed in the first 30 days of drying and more than 80 percent is observed in the first 90 days.

7. As observed in other studies, mixtures with increasing air-void spacing factors experience decreased freeze-thaw durability and scaling resistance, with significant decreases in durability observed for concrete with air-void spacing factors above 8×10^{-3} in. (0.20 mm).
8. Higher dosages of shrinkage-reducing admixture contribute to larger air-void spacing factors and greater decreases in air content between plastic and hardened concrete, leading to decreased freeze-thaw durability and scaling resistance.
9. When a shrinkage-reducing admixture is included, mixtures containing the polymer-based AEA exhibit much lower freeze-thaw durability and scaling resistance than mixtures containing the surfactant-based AEA. This is likely due to the larger air-void spacing factors observed in the mixtures containing the polymer-based AEA.

7.2.2 Durability Evaluation of Mixtures Containing Shrinkage-Reducing Admixtures with Air Contents below LC-HPC Requirements (Program 2)

1. Mixtures containing the surfactant-based air-entraining agent (AEA) used in this study with air contents of 7 percent or above, regardless of SRA dosage, had Durability Factors (DFs) above 95 in accordance with ASTM C666 and KDOT Test Method KTMR-22 and mass losses below the fail limit of 0.31 lb/ft^2 (1500 g/m^2) required by BNQ NQ 2621-900.
2. Mixtures with no SRA experienced the highest freeze-thaw durability and scaling resistance.
3. The reduction in freeze-thaw durability due to SRA dosage is most pronounced at dosages greater than 1.0 percent by weight of cement.
4. A reduction in air content from 8 to 4 percent did not affect the freeze-thaw durability or scaling resistance of mixtures containing the lowest dosage of SRA (0.5 percent by weight of cement) and the surfactant-based AEA.

7.2.3 Evaluation of Mixtures Containing Mineral Admixtures Used in Conjunction with Internal Curing (Program 3)

1. The replacement of a portion of total aggregate with pre-wetted lightweight aggregate (LWA) reduces both early-age and long-term shrinkage by providing a source of internal curing water.
2. Shrinkage is reduced additionally with the replacement of a portion of portland cement with slag cement in conjunction with the pre-wetted lightweight aggregate replacement.
3. Shrinkage is reduced further with the replacement of a portion of portland cement with silica fume in conjunction with the pre-wetted lightweight aggregate and slag cement replacements.
4. No significant difference in shrinkage is observed as the volume replacement of total aggregate with pre-wetted lightweight aggregate is increased from 8 to 10 percent.
5. No significant effect on shrinkage is obtained by increasing the replacement level of silica fume from 3 to 6 percent.
6. A greater percentage of the total shrinkage at 365 days is observed in the first 30 days of drying for mixtures without slag.
7. Additions of slag and silica fume contribute to reduced shrinkage primarily within the first 30 days of drying.
8. All mixtures evaluated in Program 3, regardless of replacement level of lightweight aggregate, slag, or silica fume, exhibited DFs above 95 in accordance with ASTM C666 and KDOT Test Method KTMR-22 and mass losses below the fail limit of 0.31 lb/ft^2 (1500 g/m^2) required by BNQ NQ 2621-900.
9. Small additions of lightweight aggregate, slag, or silica fume do not significantly affect freeze-thaw durability, scaling resistance, compressive strength, or air-void stability.

10. The addition of slag and silica fume decrease scaling resistance to a degree.

7.2.4 Construction and Evaluation of Low-Cracking High-Performance Concrete (LC-HPC) Bridge Decks

7.2.4.1 Construction Experiences

1. Successful construction in accordance with the LC-HPC specifications includes the use of a concrete with low-cracking characteristics (low paste, low slump, moderate strength) that is also highly workable and placeable.
2. LC-HPC mixtures with cement contents of 520 to 540 lb/yd^3 (309 to 320 kg/m^3) and water-cement ratios of 0.44 to 0.45 pumped well, while mixtures with a water-cement ratio of 0.42 were occasionally difficult to pump. These pumping difficulties were likely due to the lower total paste content of the mixtures with the lower water-cement ratio.
3. Pumping difficulties were occasionally caused by characteristics of the aggregates, such as the use of angular, manufactured sand and excessively-elongated or overly-large coarse aggregate particles.
4. Different pumps appeared to have different capabilities, and poorly-performing pumps likely contributed to a portion of pumping difficulties.
5. Accurately simulating the techniques required for LC-HPC construction during the qualification batch and slab provides the contractor and concrete supplier with experience employing the LC-HPC specifications prior to deck placement.
6. Excessive finishing was noted during placement of a number of LC-HPC decks, often delaying the initiating of curing.
7. The time from strikeoff to placement of burlap often exceeded the limit of 10 minutes required in the LC-HPC specifications. Delays in burlap placement, however, were often a result of delays in concrete delivery, placement, or finishing.

8. The method and sequence of burlap placement affects the length of time the deck is exposed to the environment.
9. The placement of partially-dry burlap may contribute to increased cracking by drawing water from the surface, drying out the concrete. Conversely, the placement of overly-wet burlap may increase the potential for cracking if excessive water is dripped onto the surface and then worked into the concrete through finishing, increasing the paste content.
10. Decks with superelevated edges may receive insufficient curing water if soaker hoses are not positioned to supply water to the entire deck.
11. Concrete that did not meet all aspects of the specifications was accepted and placed in the majority of the LC-HPC decks. Owners were occasionally reluctant to reject this concrete because of pushback from contractors and concrete suppliers.
12. Truckloads with out-of-specification concrete that were set aside or redosed with water reducer in an attempt to meet the specifications were occasionally not retested prior to placement in the deck.
13. Testing concrete at both the truck discharge and on the deck early in the placement establishes a standard for air and slump losses from placement.

7.2.4.2 Cracking Evaluation

1. Cracking increases over time for both the LC-HPC and control placements.
2. Fourteen of the sixteen LC-HPC placements matched with a control placement have lower cracking than the control placement at similar ages. On average, the control placements have approximately three times the cracking of the LC-HPC placements.
3. All LC-HPC placements had crack densities below 0.400 m/m^2, while 11 of the 14 control placements had crack densities above this value.

4. During the first 72 months, the LC-HPC decks have performed better than or equal to the best performing conventional monolithic placements examined by Schmitt and Darwin (1995), Miller and Darwin (2000), and Lindquist et al. (2005) at similar ages.
5. The average cracking rate of the control placements is nearly two-and-a-half times that of the LC-HPC placements in the first 36 months and more than twice that of the LC-HPC placements after 36 months.
6. The cracking rates after 36 months for both the LC-HPC and control placements decrease to approximately one-third of the rates in the first 36 months.
7. Based on the examination of 26 monolithic decks (including 45 individual placements) supported by steel girders, the factors that affect cracking include increased paste content, slump, compressive strength, and air temperature range on the day of construction, increases in concrete temperature relative to air temperature on the day of construction, and decreased air content.
8. Techniques used by contractors influence cracking.
9. For decks constructed in accordance with the LC-HPC specifications, crack densities are substantially higher for decks with 60 percent of the recorded slumps greater than or equal to 4 in. (100 mm) than for decks with less than 60 percent above this value.
10. For decks constructed in accordance with the LC-HPC specifications supported by steel girders, crack densities decrease as the maximum and average air temperatures on the day of construction increase. This decrease in cracking is likely the result of decreased thermal tensile stresses due to the placement of cooler concrete on warmer girders, not the result of the higher temperatures alone.

7.3 RECOMMENDATIONS

Based on the observations and conclusions presented in this report, the following recommendations are made to improve cracking and overall durability performance of concrete bridge decks.

1. Shrinkage-reducing admixtures (SRAs) may be used in bridge deck construction if there is assurance that only concrete with air contents of 7 percent or above would be placed. Restrictions on air content could be relaxed when low dosages of SRA (for example, 0.5 percent by weight of cement) are used.
2. Compatibility between air-entraining and shrinkage-reducing admixtures should be verified before use in construction.
3. Pre-wetted lightweight aggregate is recommended for use in bridge deck construction as a source of internal curing water. Volume replacements above 10 percent of total aggregate with lightweight aggregate should be evaluated before use in construction.
4. Additions of slag cement and silica fume in conjunction with pre-wetted lightweight aggregate are recommended for use in bridge deck construction if volume replacements of portland cement with slag and silica fume remain at 30 and 3 percent, respectively, or below.
5. A 3 percent volume replacement of portland cement with silica fume is recommended when used with pre-wetted lightweight aggregate and slag.
6. Concretes with water-cement ratios of 0.44 or 0.45 and cement contents between 520 and 540 lb/yd^3 (297 and 320 kg/m^3) are recommended for bridge deck construction.
7. The use of angular, manufactured sands should be avoided for concretes placed by pump.

8. If concrete is to be placed by pump, at least two pumps should be made available on-site during construction to minimize delays caused by pumping difficulties. A second pump can also continue placement if the first pump must be relocated.
9. During the qualification slab, the contractor should be required to accurately simulate all procedures planned for deck construction, using the same construction crew and equipment as to be used for the deck construction.
10. Excessive bullfloating and the use of double-drum roller screeds are not recommended for use in bridge deck construction.
11. An appropriate plan for burlap placement must be established by the contractor prior to construction. A placement sequence should be instituted with consideration for the width of the deck and the length of the burlap pieces.
12. The entire width of the deck should be covered with burlap before continuing the burlap placement longitudinally along the deck. This method prevents strips of concrete from being exposed along the deck edges for extended periods of time. The number of burlap pieces required to cover the entire deck width should be determined in advance.
13. A single worker should be designated to oversee the condition of the placed burlap during construction to prevent drying out or over-wetting.
14. The transverse grade of the deck must be considered when determining the placement of soaker hoses for maintaining the saturation of burlap.
15. A strict plan for concrete acceptance and testing must be established and agreed upon by the contractor, concrete supplier, and owner prior to construction.
16. As required by the LC-HPC specifications, the first few truckloads should be tested for slump, air content, temperature, and unit weight. The frequency of

testing can be reduced later in the placement. If a truckload is found to not comply with the LC-HPC specifications, successive truckloads should be tested until the specifications are met.

17. Each truckload should be visually-checked by an experienced inspector and any concrete suspected to not meet the specifications should be tested.
18. Truckloads with out-of-specification concrete may be set aside or redosed with water reducer in an attempt to fall within the specifications. This concrete, however, must be retested prior to placement in the deck. Retests should be completed by concrete-supplier/contractor personnel under the supervision of the owner's inspectors.
19. Early in placement, concrete should be tested at both the truck discharge and on the deck multiple times to establish a standard for air and slump losses from placement.
20. To provide motivation to contractors for successful construction of low-cracking decks, incentives should be implemented based on (1) contractor compliance with the LC-HPC specifications during construction or (2) cracking performance. The crack survey data accumulated in this study could be used to establish an acceptable level of cracking performance.

REFERENCES

ACI Committee 201. (1977). "Guide to Durable Concrete," *ACI Journal*, Vol. 74, No. 12, December, pp. 573-609.

ACI Committee 232. (2003). *Use of Fly Ash in Concrete,* ACI 232.2R-03, American Concrete Institute, Farmington Hills, Michigan.

ACI Committee 233. (2000). *Ground Granulated Blast-Furnace Slag as a Cementitious Constituent in Concrete,* ACI 233-95 (Reapproved 2000), American Concrete Institute, Farmington Hills, Michigan.

ACI Committee 234. (2000). *Guide for the Use of Silica Fume in Concrete,* ACI 234R-96 (Reapproved 2000), American Concrete Institute, Farmington Hills, Michigan.

ACI Committee 308, (1997). *Standard Practice for Curing Concrete,* ACI 308-92, American Concrete Institute, Farmington Hills, Michigan.

ACI Committee 345. (1991). *Guide for Concrete Highway Bridge Deck Construction,* ACI 345 R-91, American Concrete Institute, Detroit, Michigan.

Aitcin, P. C. and Vezina, D. (1984). "Resistance to Freezing and Thawing of Silica Fume Concrete," *Cement, Concrete, and Aggregates*, Vol. 6, No. 1, Summer, pp. 38-42.

ASTM C31-12 (2012). "*Standard Practice for Making and Curing Concrete Test Specimens in the Field*," ASTM International, West Conshocken, PA, 6 pp.

ASTM C39-12 (2012). "*Standard Test Method for Compressive Strength of Cylindrical Concrete Specimens*," ASTM International, West Conshocken, PA, 7 pp.

ASTM C70-13 (2013). "*Standard Test Method for Surface Moisture of Fine Aggregate*," ASTM International, West Conshocken, PA, 3 pp.

ASTM C127-12 (2012). "*Standard Test Method for Density, Relative Density (Specific Gravity), and Absorption of Coarse Aggregate*," ASTM International, West Conshocken, PA, 6 pp.

ASTM C143-12 (2012). "*Standard Test Method for Slump of Hydraulic-Cement Concrete*," ASTM International, West Conshocken, PA, 4 pp.

ASTM C173-10 (2010). "*Standard Test Method for Air Content of Freshly Mixed Concrete by the Volumetric Method*," ASTM International, West Conshocken, PA, 8 pp.

ASTM C173-12 (2012). "*Standard Test Method for Air Content of Freshly Mixed Concrete by the Volumetric Method*," ASTM International, West Conshocken, PA, 9 pp.

ASTM C192-12 (2012). "*Standard Practice for Making and Curing Concrete Test Specimens in the Laboratory*," ASTM International, West Conshocken, PA, 8 pp.

ASTM C457-12 (2012). "*Standard Test Method for Microscopical Determination of Parameters of the Air-Void System in Hardened Concrete*," ASTM International, West Conshocken, PA, 15 pp.

ASTM C490-11 (2011). "*Standard Practice for Use of Apparatus for the Determination of Length Change of Hardened Cement Paste, Mortar, and Concrete*," ASTM International, West Conshocken, PA, 5 pp.

ASTM C511-09 (2009). "*Standard Specification for Mixing Rooms, Moist Cabinets, Moist Rooms, and Water Storage Tanks Used in the Testing of Hydraulic Cements and Concretes*," ASTM International, West Conshocken, PA, 3 pp.

ASTM C618-12 (2012). "*Standard Specification for Coal Fly Ash and Raw or Calcined Natural Pozzolan for Use in Concrete,*" ASTM International, West Conshocken, PA, 3 pp.

ASTM C1064-12 (2012). "*Standard Test Method for Temperature of Freshly Mixed Hydraulic-Cement Concrete*," ASTM International, West Conshocken, PA, 3 pp.

ASTM C1761-12 (2012). "*Standard Specification for Lightweight Aggregate for Internal Curing of Concrete*," ASTM International. West Conshocken, PA, 8 pp.

Babaei, K. and Fouladgar, A. M. (1997). "Solutions to Concrete Bridge Deck Cracking," *Concrete International*, Vol. 19, No. 7, July, pp. 34-37.

Babaei, K. and Hawkins, N. M. (1987). "Evaluation of Bridge Deck Protective Strategies," *NCHRP Report* 297, Transportation Research Board, National Research Council, Washington, D.C., September.

Babaei, K. and Purvis, R. (1994a). "Prevention of Cracks in Concrete Bridge Decks: Report on Laboratory Investigation of Concrete Shrinkage," *Report,* Research Project No. 89-01, Pennsylvania Department of Transportation, Harrisburg, PA.

Babaei, K. and Purvis, R. (1994b). "Report on Surveys of Existing Bridges," *Wilbur Smith Associates Report,* PennDOT Project No. 89-01, Falls Church, VA.

Babaei, K. and Purvis, R. L. (1995). "Prevention of Cracks in Concrete Bridge Decks: Report on Surveys of Existing Bridges," *Report,* PA-FHWA-95-001+89-01, 100 pp.

Bakker, R. F. M. (1980). "On the Cause of Increased Resistance of Concrete Made from Blast-Furnace Cement to Alkali Reaction and to Sulfate Corrosion," *Thesis*, RWTH-Aachen, 118 pp.

Balogh, A. (1996). "New Admixture Combats Concrete Shrinkage," *Concrete Construction*, Vol. 41, No. 7, July, pp. 546-551.

Bentur, A., Goldman, A., and Cohen, M. D. (1988). "The Contributions of the Transition Zone to the Strength of High Quality Silica Fume Concretes," *Proceedings*, *Symposium on Bonding in Cementitious Composites*, Vol. 114, Materials Research Society, Pittsburgh, pp. 97-103.

Bentur, A., Igarashi, S., and Kovler, K. (2001). "Prevention of Autogenous Shrinkage in High-Strength Concrete by Internal Curing Using Wet Lightweight Aggregates," *Cement and Concrete Research*, Vol. 31, No. 11, July, pp. 1587-1591.

Bentz, D. P. and Snyder, K. A. (1999). "Protected Paste Volume in Concrete – Extension to Internal Curing Using Saturated Lightweight Fine Aggregate," *Cement and Concrete Research*, Vol. 29, No. 11, August, pp. 1863-1867.

Bentz, D. P., Jensen, O. M., Hansen, K. K., Olesen, J. F., Stang, H., and Haecker, C. J. (2001). "Influence of Cement Particle-Size Distribution on Early-Age Autogenous Strains and Stresses in Cement-Based Materials," *Journal of the American Ceramic Society*, Vol. 84, No. 1, January, pp. 129-135.

Bentz, D. P. (2005). "Curing with Shrinkage-Reducing Admixtures – Beyond Drying Shrinkage Reduction," *Concrete International*, Vol. 27, No. 10, October, pp. 55-60.

Bentz, D. P. (2009). "Influence of Internal Curing Using Lightweight Aggregates on Interfacial Transition Zone Percolation and Chloride Ingress in Mortars," *Cement and Concrete Composites*, Vol. 31, No. 5, March, pp. 285-289.

Berke, N. S., Dallaire, M. P., Hicks, M. C., and Kerkar, A. (1994). *Proceedings*, ACI International Conference on High Performance Concrete, Singapore, pp. 326-333.

Bickley, J., Hooten, R. D., and Hover, K. (2006). "Preparation of a Performance-Based Specification for Cast-In-Place Concrete," RMC Research Foundation, Silver Spring, MD, pp. 3-14 to 3-18.

Bilodeau, A. and Ludwig, H. M. (1992). "Deicing Salt Scaling Resistance of Concrete Incorporating Supplementary Cementing Materials: CANMET Research," *Freeze-Thaw Durability of Concrete*, New York, NY, pp. 247-258.

Bisschop, J. and Van Mier, J. G. M. (2000). "The Effect of Aggregates on Drying Shrinkage Microcracking in Cement-Based Materials," *UEF Conference 'Advances in Concrete and Cement'*, Mt. Tremblant, Canada, August, Published in Concrete Science and Technology.

Brown, M. D., Sellers, G., Folliard, K., Fowler, D. (2001). "Restrained Shrinkage Cracking of Concrete Bridge Decks: State-of-the-Art Review," *Report*, Research Project 0-4098, Texas Department of Transportation, 50 pp.

Browning, J., Darwin, D., Reynolds, D., and Pendergrass, B. (2011). "Lightweight Aggregate as Internal Curing Agent to Limit Concrete Shrinkage," *ACI Materials Journal*, Vol. 108, No. 6, November-December, pp. 638-644.

Byfors, K. (1987). "Influence of Silica Fume and Fly Ash on Chloride Diffusion and pH Values in Cement Paste," *Cement and Concrete Research*, Vol. 17, No. 1, January, pp. 115-130.

Chariton, T. and Weiss, W. J. (2002). "Using Acoustic Emission to Monitor Damage Development in Mortars Restrained from Volumetric Changes," *Concrete: Material Science to Application, A Tribute to Surendra P. Shah,* ACI SP-206, pp. 205-218.

Cong, X., Gong, S., Darwin, D., and McCabe, S. L. (1992). "Role of Silica Fume in Compressive Strength of Cement Paste, Mortar, and Concrete," *ACI Materials Journal*, Vol. 89, No. 4, July-August, pp. 375-387.

Cusson, D. and Hoogeveen, T. (2008). "Internal Curing of High-Performance Concrete with Pre-Soaked Fine Lightweight Aggregate for Prevention of Autogenous Shrinkage Cracking," *Cement and Concrete Research*, Vol. 38, No. 6, February, pp. 757-765.

Cusson, D. and Margeson, J. (2010). "Development of Low-Shrinkage High-Performance Concrete with Improved Durability," *6th International Conference on Concrete under Severe Conditions, Environment, and Loading*, Merida, Mexico, June 7-9, 8 pp.

Dakhil, F. H., Cady, P. D., and Carrier, R. E. (1975). "Cracking of Fresh Concrete as Related to Reinforcement," *ACI Journal, Proceedings*, Vol. 72, No. 8, August, pp. 421-428.

Darwin, D. and Slate, F. O. (1970). "Effect of Paste-Aggregate Bond Strength on Behavior Concrete," *Journal of Materials*, Vol. 5, No. 1, March., pp. 86-98.

Darwin, D., Browning, J., O'Reilly, M., Locke, C. E., and Virmani, Y. P. (2011). "Multiple Corrosion Protection Systems for Reinforced Concrete Bridge Components," Publication No. FHWA-HRT-11-060, Federal Highway Administration, also *SM Report* No. 101, University of Kansas Center for Research, Inc., Lawrence, KS, November, 255 pp.

Darwin, D., Browning, J., Lindquist, W. (2004). "Control of Cracking in Bridge Decks: Observations from the Field," *Cement, Concrete, and Aggregates*, Vol. 26, No. 2, December, pp. 148-154.

Deshpande, S., Darwin, D., and Browning, J. (2007). "Evaluating Free Shrinkage of Concrete for Control of Cracking in Bridge Decks," *SM Report* No. 89, University of Kansas Center for Research, Inc. Lawrence, KS, 290 pp.

Draper, N. R. and Smith, H. (1981). *Applied Regression Analysis*, second edition, Wiley, New York, 709 pp.

Durability of Concrete Bridge Decks – A Cooperative Study, Final Report. (1970). The state highway departments of California, Illinois, Kansas, Michigan, Minnesota, Missouri, New Jersey, Ohio, Texas, and Virginia; Bureau of Public Roads; and Portland Cement Association, 35 pp.

French, C., Eppers L., Le, Q., and Hajjar, J. F. (1999). "Transverse Cracking in Concrete Bridge Decks," *Transportation Research Record* 1688, Paper No. 99-0888, pp. 21-29.

Fulton, F. S. (1974). "The Properties of Portland Cement Containing Milled Granulated Blast-Furnace Slag," *Monograph*, Portland Cement Institute, Johannesburg, pp. 4-46.

Hansen, W. and Almudaiheem, J. A. (1987). "Ultimate Drying Shrinkage of Concrete – Influence of Major Parameters," *ACI Materials Journal*, Vol. 84, No. 3, May-June, pp. 39-46.

Hooton, R. D. (1993). "Influence of Silica Fume Replacement of Cement on Physical Properties and Resistance to Sulfate Attack, Freezing and Thawing, and Alkali Silica Reactivity," *ACI Materials Journal*, Vol. 90, No. 2, pp. 143-161.

Huang, C. and Feldman, R. F. (1985). "Hydration Reactions in Portland Cement-Silica Fume Blends," *Cement and Concrete Research*, Vol. 15, No. 4, pp. 585-592.

Geiker, M., Bentz, D. P., and Jensen, O. M. (2004). "Mitigating Autogenous Shrinkage by Internal Curing," *High-Performance Structural Lightweight Concrete*, ACI SP-218, American Concrete Institute, Farmington Hills, MI, pp. 143-154.

Gunter, M., Bier, T., and Hilsdorf, H. (1987). "Effect of Curing and Type of Cement on the Resistance of Concrete to Freezing in Deicing Salt Solutions." *Concrete Durability*, ACI SP-100, Detroit, MI, pp. 877-899.

Helmuth, R. A. and Turk, D. H. (1956). "The Reversible and Irreversible Drying Shrinkage of Hardened Portland Cement and Tricalcium Silicate Paste," *Journal of PCA Research and Development Laboratories*, Vol. 9, No. 2, pp. 8-21.

Hogan, F. J. and Meusel, J. W. (1981). "Evaluation for Durability and Strength Development of a Ground Granulated Blast Furnace Slag," *Cement, Concrete, and Aggregates*, Vol. 3, No. 1, pp. 40-52.

Holland, T. (2005). "Silica Fume User's Manual," *Technical Report* FHWA-IF-05-016, Federal Highway Administration, 193 pp.

Holm, T. A., Ooi, O. S., Bremner, T. W. (2003). "Moisture Dynamics in Lightweight Aggregate and Concrete," *Proceedings*, Theodore Bremner Symposium on High Performance Lightweight Concrete, 6th International Conference on Durability of Concrete, Thessalonika, Greece, pp. 167-184.

Holt, E. E. (2001). "Early Age Autogenous Shrinkage of Concrete," *Report*, Technical Research Centre of Finland, VTT Publications 446, 184 pp.

Horn, M. W., Stewart, C. F., and Boulware, R. L. (1972). "Factors Affecting the Durability of Concrete Bridge Decks: Normal vs. Thickened Deck," *Interim Report* No. 3, Bridge Department, California Division of Highways, CA-HY-4101-3-72-11, May.

Imamoto, K. and Arai, M. (2008). "Specific Surface Area of Aggregate and It's Relation to Concrete Drying Shrinkage," *Materials and Structures*, Vol. 41, No. 1, pp. 323-333.

Kansas Department of Transportation, (2007a). "Low-Cracking High-Performance Concrete – Aggregates," *Standard Specifications for State Road and Bridge Construction*, Topeka, KS.

Kansas Department of Transportation, (2007b). "Low-Cracking High-Performance Concrete," *Standard Specifications for State Road and Bridge Construction*, Topeka, KS.

Kansas Department of Transportation, (2007c). "Low-Cracking High-Performance Concrete – Construction," *Standard Specifications for State Road and Bridge Construction*, Topeka, KS.

Kansas Department of Transportation, (2007d). "Section 1102.2(a) Aggregates for Concrete," *Standard Specifications for State Road and Bridge Construction*, Topeka, KS.

Klieger, P. (1955). "Effect of Atmospheric Conditions During the Bleeding Period and Time of Finishing on the Scale Resistance of Concrete," *ACI Journal*, Vol. 27, No. 3, November, pp. 309-326.

Klieger, P. and Isberner, A. W. (1967). "Laboratory Studies of Blended Cement – Portland Blast-Furnace Slag Cements," *Journal*, Portland Cement Association Research and Development Department Laboratories, Vol. 9, No. 3, September, pp. 2-22.

Krauss, P. D. and Rogalla, E. A., (1996). "Transverse Cracking in Newly Constructed Bridge Decks," *National Cooperative Highway Research Program Report* 380, Transportation Research Board, Washington, D.C., 126 pp.

Lam, H. and Hooton, R. D. (2005). "Effects of Internal Curing Methods on Restrained Shrinkage and Permeability," *Proceedings*, 4th International Seminar on Self-Desiccation and It's Importance in Concrete Technology, pp. 210-228.

Larrard, de F. (1997). *Concrete,* E. & F.N. Spon, pp. 35-38.

Larson, T. D., Malloy, J J., and Price, J. T. (1967). "Durability of Bridge Concrete," *Report 4*, Vol. 1, Civil Engineering – Pennsylvania State University, University Park, PA, July, 211 pp.

Lindquist, W. D., Darwin, D., and Browning, J. (2005). "Cracking and Chloride Contents in Reinforced Concrete Bridge Decks," *SM Report* No. 78, University of Kansas Center for Research, Inc. Lawrence, KS, 482 pp.

Lindquist, W. D., Darwin, D,, Browning, J., Miller, G. (2006). "Effect of Cracking on Chloride Content in Concrete Bridge Decks," *ACI Materials Journal*, Vol. 103, No. 6, Nov., pp. 467-473.

Lindquist, W. D., Darwin, D., and Browning, J., (2008). "Development and Construction of Low-Cracking High-Performance Concrete (LC-HPC) Bridge Decks: Free Shrinkage, Mixture Optimization, and Concrete Production," *SM Report* No. 92, University of Kansas Center for Research, Inc., Lawrence, KS, 540 pp.

Lura, P. and van Breugel, K. (2000). "Moisture Exchange as a Basic Phenomenon to Understand the Volume Changes of Lightweight Aggregate Concrete at Early Age," *Shrinkage of Concrete – Shrinkage 2000*, RILEM Publications, pp. 533-546.

Luther, M. D. (1988). "Silica-Fume (Microsilica) Concrete in Bridges in the United States," *Portland Cement Concrete Modifiers*, Transportation Research Record 1204, Transportation Research Board, Washington D.C., pp. 11-20.

Maage, M. (1984). "Effect of Microsilica on the Durability of Concrete Structures," *SINTEF Report STF65 A84019*, Norwegian Cement and Concrete Research Institute, Trondheim.

Maage, M. and Sellevold, E. (1987). "Effect of Microsilica on the Durability of Concrete Structures," *Concrete International*, Vol. 9, No. 12, December, pp. 39-43.

Malhotra, V. M. (1986). "Mechanical Properties and Freezing and Thawing Resistance of Non-Air Entrained and Air Entrained Condensed Silica Fume Concrete Using ASTM Test C 666, Procedures A and B," *Proceedings,* CANMET/ACI Second International Conference on the Use of Fly Ash, Silica Fume, Slag, and Natural Pozzolans in Concrete, American Concrete Institute, Detroit, pp. 1069-1094.

Malhotra, V. M., Carette, G. G., and Bremmer, T. W. (1987). "Durability of Concrete Containing Supplementary Cementing Materials in Marine Environment," SP-100, American Concrete Institute, Detroit, pp. 1227-1258.

Mather, B. (1957). "Laboratory Tests of Portland Blast-Furnace Slag Cements," *Journal of the American Concrete Institute*, Vol. 54, No. 3, September, pp. 205-232.

McDonald, J. E. (1991). "The Potential for Cracking of Silica-Fume Concrete," *Repair, Evaluation, Maintenance, and Rehabilitation Bulletin*, Vol. 8, No. 3, August, pp. 8-11.

McLeod, H., Darwin, D., and Browning, J. (2009). "Development and Construction of Low-Cracking High-Performance Concrete Bridge Decks: Construction Methods, Temperature Effects, and Resistance to Chloride Ion Penetration," *SM Report* No. 94*,* University of Kansas Center for Research, Inc., Lawrence, KS, 848 pp.

Mehta, P. K. (1980). "Durability of Concrete in Marine Environment – A Review," *Performance of Concrete in Marine Environment*, ACI SP-65, American Concrete Institute, Detroit, pp. 1-20.

Merikallio, T., Mannonen, R., and Penttala, V. (1996). "Drying of Lightweight Concrete Produced from Crushed Expanded Clay Aggregates," *Cement and Concrete Research Journal*, Vol. 26, No. 9, September, pp. 1423-1433.

Meusel, J. W. and Rose, J. H. (1983). "Production of Granulated Blast Furnace Slag at Sparrows Point, and the Workability and Strength Potential of Concrete Incorporating the Slag," *Fly Ash, Silica Fume, Slag and Other Mineral By-Products in Concrete*, ACI SP-79, American Concrete Institute, Detroit, pp. 867-890.

Meyers, C. (1982). "Survey of Cracking on Underside of Classes B-1 and B-2 Concrete Bridge Decks in District 4," *Investigation 82-2*, Missouri Highway and Transportation Department, Division of Materials and Research, September.

Miller, G. G. and Darwin, D. (2000). "Performance and Constructability of Silica Fume Bridge Deck Overlays," *SM Report* No. 57, University of Kansas Center for Research, Inc., Lawrence, KS, 423 pp.

Mindess, S. (1988). "Bonding in Cementitious Composites: How Important is It?," *Proceedings*, Symposium on Bonding in Cementitious Composites, Vol. 114, Materials Research Society, Pittsburgh, pp. 3-10.

Mindess, S., Yound, F., and Darwin, D. (2003). *Concrete*, second edition, Prentice-Hall., Englewood Cliffs, NJ, 644 pp.

Mora-Ruacho, J., Gettu, R., and Aguado, A. (2009). "Influence of Shrinkage-Reducing Admixtures on the Reduction of Plastic Shrinkage Cracking in Concrete," *Cement and Concrete Research*, Vol. 39, No. 3, March, pp. 141-146.

Nassif, H. and Suksawang, N. (2002). "Effect of Curing Methods on Durability of High-Performance Concrete," *Transportation Research Record*, Paper No. 02-3305, Vol. 1798, pp. 31-38.

New York State Department of Transportation Specifications. (2008). Standard Specifications – Construction and Materials – Office of Engineering, New York State Department of Transportation.

Odman, S. T. A. (1968). "Effects of Variations in Volume, Surface Area Exposed to Drying, and Composition of Concrete Shrinkage," *RILEM/CEMBUREAU Intl. Colloquium on the Shrinkage of Hydraulic Concretes*, Madrid, Vol. 1, 1968, 20 pp.

Padron, I., Zollo, R. F., (1990). "Effect of Synthetic Fibers on Volume Stability and Cracking of Portland Cement and Mortar," *ACI Materials Journal*, Vol. 87, No. 4, July-August, pp. 327-332.

Parrott, L. J. (1989). "Modeling the Development of Microstructure," *Material Science of Concrete*, Vol. 1, The American Ceramic Society, Inc., Westerville, Ohio, pp. 181-195.

Pendergrass, B., Darwin, D., and Browning, J. (2011). "Crack Surveys of Low-Cracking High-Performance Concrete Bridge Decks in Kansas 2009-2010," *SL Report* No. 11-3, University of Kansas Center for Research, Lawrence, KS, 103 pp.

Perragaux, G. R. and Brewster, D. R. (1992). "In-Service Performance of Epoxy-Coated Steel Reinforcement in Bridge Decks – Final Report," *New York State Dept. of Transportation Technical Report 92-3*, June.

Philleo, R. E. (1986). "Freezing and Thawing Resistance of High Strength Concrete," *National Cooperative Highway Research Program (NCHRP) Synthesis 129*, Transportation Research Board, Washington, D.C., December, 38 pp.

Pickett, G. (1956). "Effect of Aggregate Shrinkage of Concrete and a Hypothesis Concerning Shrinkage," *ACI Journal*, Vol. 52, No. 5, January, pp. 581-590.

Pigeon, M., Pleau, R., and Aitcin, P. C. (1986). "Freeze-Thaw Durability of Concrete with and without Silica Fume in ASTM C 666 (Procedure A) Test Method: Internal Cracking vs. Scaling," *Cement, Concrete, and Aggregates*, Vol. 8, No. 2, January, pp. 76-85.

Pigeon, M., Perraton, D., and Pleau, R. (1987). "Scaling Tests of Silica Fume Concrete and the Critical Spacing Factor Concept," *Concrete Durability*, Proceedings of the Katharine and Bryant Mather International Conference, Vol. 2, American Concrete Institute, Detroit, pp. 1155-1182.

Popovic, P., Rewerts, T. L., and Sheahen, D. J. (1988). "Deck Cracking Investigation of the Hope Memorial Bridge," *Report,* Ohio Department of Transportation, January.

Poppe, J. B. (1981). "Factors Affecting the Durability of Concrete Bridge Decks," *Report* No. FHWA/CA/SD-81/2, California Dept. of Transportation, Division of Transportation Facilities Design, Sacramento, CA.

Powers, T. C. (1945). "A Working Hypothesis for Further Studies of Frost Resistance of Concrete," *ACI Journal*, Vol. 41, No. 4, February, pp. 245-272.

Powers, T.C. (1949). "The Air Requirement of Frost-Resistant Concrete," *Proceedings, Highway Research Board Annual Meeting*, National Academy of Sciences, Vol. 29, pp. 184-211.

Powers, T. C. and Brownyard, T. L. (1947). "Studies of the Physical Properties of Hardened Portland Cement Paste," *Proceedings,* American Concrete Institute, Vol. 43, 933 pp.

Powers, T. C. and Brownyard, T. L. (1948). "Studies of the Physical Properties of Hardened Portland Cement Paste," *Bulletin 22, Portland Cement Association*, Chicago, pp. 933-992.

Powers, T. C. and Helmuth, R. A. (1953). "Theory of Volume Changes in Hardened Portland-Cement Paste During Freezing," *Proceedings*, *Highway Research Board Annual Meeting*, National Academy of Science, pp. 285-297.

Pyc, W. A., Caldarone, M. A., Broton, D., and Reeves, D. (2008). "Internal Curing Study with Intermediate Lightweight Aggregate," ACI SP-256-2, American Concrete Institute, Farmington Hills, MI, October, pp. 13-33.

Ramachandran, V. S. (1995). *Concrete Admixtures Handbook*, second edition, Noyes Publications, Park Ridge, New Jersey, 1183 pp.

Ramey, G. E. and Wright, R. (1994). "Assessing and Enhancing the Durability/Longetivity Performances of Highway Bridges," *Final Report on Highway Research Center Project 2-13506*, Auburn University, Auburn, AL.

Ramey, G. E., Wright, R., and Wolff, A. (1996). "Guidelines for Enhancing the Durability/Longetivity of Concrete Bridges," *Final Report on Alabama Dept. of Trans. Research Project 930-313*, Auburn University, Auburn, AL.

Reynolds, D., Browning, D., and Darwin, D. (2009). "Lightweight Aggregates as an Internal Curing Agent for Low-Cracking High-Performance Concrete," *SM Report* No. 97, University of Kansas Center for Research, Lawrence, KS, 151 pp.

Roberts, J. (2004). "Internal Curing in Pavements, Bridge Decks and Parking Structures, Using Absorptive Aggregates to Provide Water to Hydrate Cement Not Hydrated by Mixing Water," 83rd Annual Meeting of the Transportation Research Board, Washington, DC, January.

Rose, J. H. (1987). "The Effects of Cementitious Blast-Furnace Slag on Chloride Permeability of Concrete," *Corrosion, Concrete, and Chlorides*, ACI SP-102, American Concrete Institute, Detroit, pp. 107-125.

Roy, D. M. and Idorn, G. M. (1983). "Hydration, Structure, and Properties of Blast Furnace Slag Cements, Mortars, and Concrete," *Proceedings*, ACI Journal, Vol. 79, No. 6, November-December, pp. 445-457.

Russell, H. G., Miller, R. A., Ozyildirim, H. C., and Tadros, M. K. (2003). "Compilation and Evaluation of Results from High Performance Concrete Bridge Projects – Final Report," *Proceedings, 3rd International Symposium on High Performance Concrete and PCI National Bridge Conference*, Orlando, FL, Oct. 19-22.

Russell, H. G., (2004). "Concrete Bridge Deck Performance," *National Cooperative Highway Research Program (NCHRP) Synthesis 333*, Transportation Research Board, Washington, D.C., 32 pp.

Sabir, B. B. and Kouyiali, K. (1991). "Freeze-Thaw Durability of Air-Entrained CSF Concrete," *Cement and Concrete Composites*, Vol. 13, No. 3, September, pp. 203-208.

Schmitt, T. R. and Darwin, D. (1995). "Cracking in Concrete Bridge Decks," *SM Report* No. 39, University of Kansas Center for Research, Inc., Lawrence, KS, 151 pp.

Schmitt, T. R. and Darwin, D. (1999). "Effect of Material Properties on Cracking in Bridge Decks," *Journal of Bridge Engineering*, ASCE, Vol. 4, No. 1, February, pp. 8-13.

Sellevold, E. J., Badger, d. h., Klitgaard, J. K., and Knudsen, T. (1982). "Silica Fume-Cement Pastes: Hydration and Pore Structure," *Condensed Silica Fume in Concrete*, Proceedings of the Nordic Research Seminar on Condensed Silica Fume Concrete, Norwegian Institute of Technology, Trondheim, Norway, pp. 19-50.

Shilstone, J. M., Sr. (1990). "Concrete Mixture Optimization," *Concrete International*, Vol. 12, No. 6, June, pp. 33-39.

Sorensen, E. V. (1983). "Freezing and Thawing Resistance of Condensed Silica Fume (Microsilica) Concrete Exposed to Deicing Chemicals," *Proceedings*, CANMET/ACI First International Conference on the Use of Fly Ash, Silica Fume, Slag, and Other Mineral By-products in Concrete, American Concrete Institute, Detroit, pp. 709-718.

Stark, J. and Ludwig H. (1997). "Freeze-Thaw and Freeze-Deicing Salt Resistance of Concretes Containing Cement Rich in Granulated Blast Furnace Slag," *ACI Materials Journal*, Vol. 94, No. 1, January, pp. 47-55.

Subramaniam, K. and Agrawal, A. K. (2009). "Concrete Deck Material Properties," *SPR Project* C-02-03, New York State Department of Transportation, 115 pp.

Suprenant, B. A. and Malisch, W. R. (1999). "The Fiber Factor – Lab Tests Show the Benefits of Using Synthetic Fibers to Limit Subsidence Cracking of Reinforced Concrete," *Concrete Construction*, October, 4 pp.

Therrien, J., Bissonnette, B., Cloutier, A. (2000). "Early-Age Evolution on the Mass Transfer Properties in Mortar and its Influence upon Ultimate Shrinkage," *Proceedings, RILEM Workshop on Shrinkage of Concrete*, Paris, France, pp. 247-270.

Thompson, N., Yunovich, M., and Dunmire, D J. (2005). "Corrosion Costs and Maintenance Strategies – A Civil/Industrial and Government Partnership," *Materials Performance*, Vol. 44, No. 9, pp. 16-20.

Tia, M., Liu, Y., Brown, D. (2005). "Modulus of Elasticity, Creep and Shrinkage of Concrete," *Final Report*, University of Florida Project No. 49104504973-12, RPWO No. 85, 165 pp.

Tomita, R. (1992). "A Study on the Mechanism of Drying Shrinkage Reduction Through the Use of an Organic Shrinkage Reducing Agent," *Concrete Library of JSCE*, No. 19, June, pp. 233-245.

Transportation Research Board, (1979). "Durability of Concrete Bridge Decks," *National Cooperative Highway Research Program (NCHRP) Synthesis 57,* Transportation Research Board, National Research Council, Washington, D.C., 61 pp.

Transportation Research Board. (1991). "Highway Deicing: Comparing Salt and Calcium Magnesium Acetate," *Special Report* 235, Transportation Research Board, National Research Council, Washington, D.C., 165 pp.

Tritsch, N., Darwin, D., and Browning, J. (2005). "Evaluating Shrinkage and Cracking Behavior of Concrete Using Restrained Ring and Free Shrinkage Test," *SM Report* No. 77, University of Kansas Center for Research, Inc., Lawrence, KS, 178 pp.

Valenza, J. J. and Scherer, G. W. (2006). "Mechanism for Salt Scaling," *Journal of the American Ceramic Society*, Vol. 89, No. 4, March, pp. 1161-1179.

Verbeck, G. J and Klieger, P. (1956). "Studies of 'Salt' Scaling of Concrete," *Highway Research Board Bulletin 150*, pp. 1-13.

Villarreal, V. H. and Crocker, D. A. (2007). "Better Pavements through Internal Hydration," *Concrete International*, Vol. 29, No. 2, February, pp. 32-36.

West, M., Darwin, D., and Browning, J. (2010). "Effect of Materials and Curing Period on Shrinkage of Concrete," *SM Report* No. 98, University of Kansas Center for Research, Inc., Lawrence, KS, 269 pp.

Whiting, D. and Detwiler, R. J. (1998). "Silica Fume Concrete for Bridge Decks," *National Cooperative Highway Research Program Report 410*, Transportation Research Board, Washington D.C., 110 pp.

Whiting, D. and Kuhlman, L. (1987). "Curing and Chloride Permeability," *Concrete International*, Vol. 9, No. 4, April, pp. 18-21.

Wood, K. (1981). "Twenty Years of Experience with Slag Cement," *Symposium on Slag Cement*, University of Alabama, Birmingham, AL.

Wood, S. L. (1992). "Evaluation of the Long-Term Properties of Concrete," *Research Development Bulletin RD102*, Portland Cement Association, pp. 14-15.

Yuan, J., Darwin, D., and Browning, J. (2011). "Development and Construction of Low-Cracking High-Performance Concrete Bridge Decks: Free Shrinkage Tests, Restrained Shrinkage Tests, Construction Experience, and Crack Survey Results," *SM Report* No. 103, University of Kansas Center for Research, Lawrence, KS, 505 pp.

Yunovich, M., Thompson, N. G., and Virmani, Y. P. (2005). "Corrosion Protection System for Construction and Rehabilitation of Reinforced Concrete Bridges," *International Journal of Materials and Product Technology*, Vol. 23, Nos. 3-4, pp. 269-285.

Zhutovsky, S., Kolver, K., and Bentur, A. (2002). "Efficiency of Lightweight Aggregates for Internal Curing of High Strength Concrete to Eliminate Autogenous Shrinkage," *Materials and Structures*, Vol. 35, No. 246, March, pp. 97-101.

APPENDIX A: MATERIAL INFORMATION AND CONCRETE MIXTURE PROPORTIONS

Table A.1 Cement Chemical Analysis

Sample No.	C1	C2	C3	C4	C5	C6†	C7†
Manufacturer	Ash Grove	Lafarge	Lafarge	Ash Grove	Lafarge	Ash Grove	Ash Grove
Specific Gravity	3.20	3.15	3.15	3.20	3.15	3.15	3.15
Blaine Fineness (cm^3/g)	3600	3890	3790	3740	3840	--	--
Oxides	Percentage by Weight						
Bogue Analysis							
C_3S	53	47	57	55	57	--	--
C_2S	19	22	12	13	12	--	--
C_3A	7	7	8	8	7	--	--
C_4AF	11	9	9	9	9	--	--
XRF							
SiO_2	20.50	20.97	20.03	20.00	20.26	--	--
Al_2O_3	4.97	4.82	4.91	5.00	4.81	--	--
Fe_2O_3	3.57	2.97	2.97	2.98	3.07	--	--
CaO	62.46	62.32	63.27	62.99	63.52	--	--
MgO	2.06	1.79	1.63	1.58	1.41	--	--
SO_3	2.49	2.87	3.02	2.94	2.78	--	--
Na_2O	0.35	0.19	0.16	0.17	0.24	--	--
K_2O	0.49	0.41	0.42	0.41	0.44	--	--
TiO_2	0.29	0.33	0.33	0.33	0.33	--	--
P_2O_5	0.11	0.16	0.13	0.13	0.14	--	--
Mn_2O_3	0.11	0.09	0.08	0.09	0.09	--	--
SrO	0.26	0.12	0.11	0.11	0.11	--	--
BaO	--	--	--	--	--	--	--
LOI	2.60	3.27	3.29	3.77	3.11	--	--
Total	100.25	100.31	100.35	100.50	100.31	--	--
Alkali Equivalent (EQV)	--	0.46	0.44	0.44	0.53	--	--

†Sample not obtained

Table A.2 Fine Aggregate Properties

	Sand					
Sample No.	S-1	S-2	S-3	S-4	S-5	S-6
Specific Gravity	2.61	2.61	2.62	2.62	2.62	2.62
Absorption (%)	0.92	0.77	0.75	0.72	--	--
Sieve Size	**Percent Retained on Each Sieve**					
1-1/2-in. (37.5-mm)	0	0	0	0	0	0
1-in. (25-mm)	0	0	0	0	0	0
3/4-in. (19-mm)	0	0	0	0	0	0
1/2-in. (12.5-mm)	0	0	0	0	0	0
3/8-in. (9.5-mm)	0	0	0	0	0	0
No. 4 (4.75-mm)	2.5	1.9	2.2	0.7	2.2	1.9
No. 8 (2.36-mm)	11.2	8.2	6.8	7.4	12.5	13.2
No. 16 (1.18-mm)	17.3	15.0	14.5	15.8	21.8	21.7
No. 30 (0.60-mm)	24.5	26.0	22.6	26.2	26.7	23.6
No. 50 (0.30-mm)	36.5	37.7	41.3	36.8	30.7	28.4
No. 100 (0.15-mm)	7.5	10.7	11.8	12.3	5.7	9.9
No. 200 (0.075-mm)	0.3	0.3	0.6	0.7	0.4	1.0
Pan	0.1	0.2	0.1	0.2	0.2	0.4

Table A.2 (Con't) Fine Aggregate Properties

	Sand					
Sample No.	S-7	S-8	S-9	S-10	S-11	S-12
Specific Gravity	2.62	2.61	2.62	2.62	2.62	2.62
Absorption (%)	--	--	--	0.86	0.69	0.69
Sieve Size	**Percent Retained on Each Sieve**					
1-1/2-in. (37.5-mm)	0	0	0	0	0	0
1-in. (25-mm)	0	0	0	0	0	0
3/4-in. (19-mm)	0	0	0	0	0	0
1/2-in. (12.5-mm)	0	0	0	0	0	0
3/8-in. (9.5-mm)	0	0	0	0	0	0
No. 4 (4.75-mm)	1.3	0.9	2.1	1.7	2.4	2.6
No. 8 (2.36-mm)	7.3	6.3	11.2	7.8	13.1	10.5
No. 16 (1.18-mm)	16.0	14.5	20.6	16.9	23.3	18.8
No. 30 (0.60-mm)	25.6	24.8	26.8	27.7	29.0	24.3
No. 50 (0.30-mm)	39.7	40.9	32.9	36.4	27.6	31.7
No. 100 (0.15-mm)	9.6	10.9	5.7	8.5	4.3	11.2
No. 200 (0.075-mm)	0.5	1.3	0.6	0.9	0.3	0.8
Pan	0.1	0.5	0.2	0.1	0.1	0.2

Table A.2 (Con't) Fine Aggregate Properties

	Pea Gravel				
Sample No.	PG-1	PG-2	PG-3	PG-4	PG-5
Specific Gravity	2.60	2.59	2.59	2.60	2.62
Absorption (%)	0.84	1.01	0.70	1.05	0.84
Sieve Size	**Percent Retained on Each Sieve**				
1-1/2-in. (37.5-mm)	0	0	0	0	0
1-in. (25-mm)	0	0	0	0	0
3/4-in. (19-mm)	0	0	0	0	0
1/2-in. (12.5-mm)	0	0	0	0	0
3/8-in. (9.5-mm)	0	0	0	0	0
No. 4 (4.75-mm)	14.9	4.0	16.1	11.5	14.0
No. 8 (2.36-mm)	54.7	46.8	53.9	50.2	59.1
No. 16 (1.18-mm)	25.9	36.3	25.4	31.5	24.4
No. 30 (0.60-mm)	3.1	9.2	3.4	5.1	2.1
No. 50 (0.30-mm)	0.6	2.7	0.6	1.2	0.3
No. 100 (0.15-mm)	0.4	0.6	0.3	0.3	0.1
No. 200 (0.075-mm)	0.1	0.2	0.1	0.1	0.0
Pan	0.2	0.3	0.2	0.2	0.1

Table A.3 Coarse Aggregate Properties

	Granite						
Sample No.	G-1	G-2	G-3	G-4	G-5	G-6	G-7
Source*	Geiger	Geiger	Geiger	Geiger	Geiger	Geiger	Geiger
Specific Gravity	2.61	2.61	2.61	2.61	2.59	2.59	2.59
Absorption (%)	0.63	0.81	--	--	--	0.70	0.83
Sieve Size	**Percent Retained on Each Sieve**						
1-1/2-in. (37.5-mm)	0	0	0	0	0	0	0
1-in. (25-mm)	7.9	0	20.3	0.1	0	7.0	0
3/4-in. (19-mm)	5.2	4.7	17.0	4.1	6.6	9.5	2.7
1/2-in. (12.5-mm)	21.0	27.0	24.2	31.6	38.5	20.4	27.4
3/8-in. (9.5-mm)	24.9	24.9	14.8	24.0	23.1	17.5	24.0
No. 4 (4.75-mm)	35.6	36.0	22.1	33.8	26.9	35.2	36.0
No. 8 (2.36-mm)	2.7	3.5	0.7	3.7	2.5	3.9	4.3
No. 16 (1.18-mm)	0	0	0	0	0	0	0
No. 30 (0.60-mm)	0	0	0	0	0	0	0
No. 50 (0.30-mm)	0	0	0	0	0	0	0
No. 100 (0.15-mm)	0	0	0	0	0	0	0
No. 200 (0.075-mm)	0	0	0	0	0	0	0
Pan	2.7	4.0	0.9	3.0	2.4	6.4	5.5

*Geiger denotes Geiger Ready Mix in Olathe, KS

Table A.3 (Con't) Coarse Aggregate Properties

	Granite						
Sample No.	G-8	G-9	G-10	G-11	G-12	G-13	G-14
Source*	Geiger	Geiger	Geiger	Geiger	Geiger	Geiger	Geiger
Specific Gravity	2.59	2.60	2.59	2.60	2.59	2.61	2.59
Absorption (%)	0.72	0.70	0.98	0.77	0.98	--	--
Sieve Size	**Percent Retained on Each Sieve**						
1-1/2-in. (37.5-mm)	0	0	0	0	0	0.3	0
1-in. (25-mm)	5.5	0	14.5	0	1.8	3.3	0
3/4-in. (19-mm)	11.9	6.9	19.6	4.9	9.6	5.4	3.5
1/2-in. (12.5-mm)	32.3	39.7	22.4	31.6	17.4	15.6	27.5
3/8-in. (9.5-mm)	19.6	26.5	15.4	25.9	24.5	28.4	25.7
No. 4 (4.75-mm)	26.4	24.9	24.9	28.2	35.5	44.3	38.2
No. 8 (2.36-mm)	1.4	1.2	1.6	2.4	3.7	1.5	3.8
No. 16 (1.18-mm)	0	0	0	0	0	0	0
No. 30 (0.60-mm)	0	0	0	0	0	0	0
No. 50 (0.30-mm)	0	0	0	0	0	0	0
No. 100 (0.15-mm)	0	0	0	0	0	0	0
No. 200 (0.075-mm)	0	0	0	0	0	0	0
Pan	2.9	0.7	1.6	7.0	7.6	1.2	1.4

*Geiger denotes Geiger Ready Mix in Olathe, KS

Table A.3 (Con't) Coarse Aggregate Properties

	Granite					
Sample No.	G-15	G-16	G-17	G-18	G-19A	G-19B
Source*	Geiger	Geiger	Geiger	Geiger	MCM	MCM
Specific Gravity	2.59	2.59	2.61	2.61	2.62	
Absorption (%)	--	0.71	0.93	--	0.79	
Sieve Size	**Percent Retained on Each Sieve**					
1-1/2-in. (37.5-mm)	0	0	0	0	0	0
1-in. (25-mm)	7.7	10.3	0	5.6	0	0
3/4-in. (19-mm)	6.0	10.3	8.5	6.7	5.9	0
1/2-in. (12.5-mm)	14.0	23.7	35.8	31.0	59.0	0
3/8-in. (9.5-mm)	20.0	29.7	27.4	28.0	33.1	2.7
No. 4 (4.75-mm)	35.0	22.7	26.1	26.1	1.7	91.5
No. 8 (2.36-mm)	13.3	2.8	1.0	0.8	0	4.6
No. 16 (1.18-mm)	0	0	0	0	0	0
No. 30 (0.60-mm)	0	0	0	0	0	0
No. 50 (0.30-mm)	0	0	0	0	0	0
No. 100 (0.15-mm)	0	0	0	0	0	0
No. 200 (0.075-mm)	0	0	0	0	0	0
Pan	4.1	0.5	1.2	1.9	0.3	1.2

*Geiger denotes Geiger Ready Mix in Olathe, KS
MCM denotes Midwest Concrete Materials in Lawrence, KS

Table A.4 Lightweight Aggregate Properties

	Lightweight Aggregate	
Sample No.	LWA-1	LWA-2
Specific Gravity*	1.15	1.15
Absorption (%)*	16	16
Sieve Size	**Percent Retained on Each Sieve**	
1-1/2-in. (37.5-mm)	0	0
1-in. (25-mm)	0	0
3/4-in. (19-mm)	0	0
1/2-in. (12.5-mm)	0	0
3/8-in. (9.5-mm)	0	0
No. 4 (4.75-mm)	22.1	22.0
No. 8 (2.36-mm)	75.9	75.9
No. 16 (1.18-mm)	1.5	1.5
No. 30 (0.60-mm)	0.1	0.1
No. 50 (0.30-mm)	0.0	0.0
No. 100 (0.15-mm)	0.0	0.0
No. 200 (0.075-mm)	0.0	0.0
Pan	0.4	0.4

* Values based on 24 hour absorption (ASTM C127 / C128)

Table A.5 Mineral Admixtures Chemical Composition

	GGBFS Grade 100	Silica Fume
Manufacturer	Holcim[1]	Euclid[2]
Specific Gravity	2.86	2.20
Oxides	**Percentage by Weight**	
XRF		
SiO_2	43.36	94.49
Al_2O_3	8.61	0.07
Fe_2O_3	0.37	0.10
CaO	31.13	0.53
MgO	12.50	0.62
SO_3	2.24	0.11
Na_2O	0.21	0.09
K_2O	0.40	0.54
TiO_2	0.32	--
P_2O_5	--	0.07
Mn_2O_3	0.35	0.02
SrO	0.04	0.01
Cl^-	--	0.05
LOI	0.37	3.21
Total	99.90	99.90
Alkali Equivalent (EQV)	0.47	0.45

Holcim[1] = GranChem® produced by Holcim Inc.
Euclid[2] = Eucon MSA produced by Euclid Chemical Company

Table A.6 Program 1: Material Sample Identification for Each Mixture

Batch Number	Mixture**	Material Sample No.				
		Cement	Sand	Pea Gravel	Coarse Aggregate	
					3/4 in.	1 in.
730	0% SRA-M	C-1	S-1	PG-1	G-4	G-3
754	0% SRA-M #2	C-1	S-2	PG-1	G-7	G-6
796	0% SRA-M #3	C-3	S-5	PG-3	G-11	G-12
769	0.5% SRA-M	C-2	S-3	PG-2	G-7	G-8
834	0.5% SRA-M #2	C-6	S-9	PG-4	G-17	G-16
722	1.0% SRA-M	C-1	S-1	PG-1	G-2	G-1
816	1.0% SRA-M #2	C-4	S-8	PG-3	G-14	G-15
727	2.0% SRA-M	C-1	S-1	PG-1	G-4	G-3
820	2.0% SRA-M #2	C-5	S-8	PG-3	G-14	G-15
732	0.5% CRA-M	C-1	S-1	PG-1	G-4	G-3
735	1.0% CRA-M	C-1	S-1	PG-1	G-5	G-3
843	1.0% CRA-M #2	C-7	S-10	PG-4	G-18*	G-16
845	2.0% CRA-M	C-7	S-10	PG-4	G-18*	G-16
772	0% SRA-T	C-2	S-4	PG-2	G-9	G-8
807	0% SRA-T #2	C-4	S-6	PG-3	G-11	G-13
781	0.5% SRA-T	C-2	S-4	PG-2	G-9	G-10
808	0.5% SRA-T #2	C-4	S-6	PG-3	G-11	G-13
782	1.0% SRA-T	C-2	S-4	PG-2	G-9	G-10
810	1.0% SRA-T #2	C-4	S-7	PG-3	G-14	G-15
786	2.0% SRA-T	C-3	S-5	PG-2	G-11	G-12
811	2.0% SRA-T #2	C-4	S-7	PG-3	G-14	G-15
789	0.5% CRA-T	C-3	S-5	PG-3	G-11	G-12
790	1.0% CRA-T	C-3	S-5	PG-3	G-11	G-12
794	2.0% CRA-T	C-3	S-5	PG-3	G-11	G-12

*1 in. max-size aggregate

**Mixture designation: *A*% *XXX*-*B* #*C*

A = Percent dosage of SRA or CRA by weight of cement

XXX = SRA for Tetraguard AS20, CRA for MasterLIFE CRA 007

B = M for Micro Air, T for Tough Air

C = 2 for first duplicate batch, 3 for second duplicate batch

Table A.7 Program 1: Constituent Proportions and Admixture Dosages

Batch Number	Mixture**	Cement	Water	Sand	Pea Gravel	Coarse Aggregate		Paste Content	SRA/CRA*	ToughAir Foam*	MicroAir*
						3/4 in.	1 in.				
		(lb/yd^3)	(lb/yd^3)	(lb/yd^3)	(lb/yd^3)	(lb/yd^3)		(% by volume)	($fl\ oz/yd^3$)	($fl\ oz/yd^3$)	($fl\ oz/yd^3$)
730	0% SRA-M	540$^{\$\$}$	238	1191††	539$^{\#\#}$	551††	953††	24.3	0	-	2.0
754	0% SRA-M #2	520$^{\$\$}$	234	1179††	335$^{\#\#}$	511$^{\#}$	971$^{\#}$	23.7	0	-	3.1
796	0% SRA-M #3	520$^{\$}$	234	944†	551$^{\#}$	565$^{\#\#}$	923$^{\#}$	23.7	0	-	2.9
769	0.5% SRA-M	540$^{\$}$	235	959†	278$^{\#}$	503$^{\#}$	1129$^{\#}$	24.3	41.9	-	1.4
834	0.5% SRA-M #2	540$^{\$}$	235	969†	354$^{\#\#}$	715$^{\#}$	941††	24.3	41.9	-	1.9
722	1.0% SRA-M	540$^{\$\$}$	232	1211††	404$^{\#\#}$	405††	1215††	24.3	83.7	-	1.4
816	1.0% SRA-M #2	540$^{\$\$}$	232	1074††	328$^{\#}$	558$^{\#}$	999$^{\#}$	24.3	83.7	-	1.4
727	2.0% SRA-M	540$^{\$\$}$	227	1191††	539$^{\#\#}$	551††	953††	24.3	167.4	-	2.7
820	2.0% SRA-M #2	540$^{\$}$	227	1077††	328$^{\#}$	558$^{\#}$	996$^{\#}$	24.3	167.4	-	3.0
732	0.5% CRA-M	540$^{\$\$}$	235	1193††	536$^{\#\#}$	554††	956††	24.3	41.9	-	1.5
735	1.0% CRA-M	540$^{\$\$}$	232	1193††	539$^{\#\#}$	551$^{\#}$	956††	24.3	83.7	-	6.8
843	1.0% CRA-M #2	520$^{\$}$	228	974†	358$^{\#\#}$	722$^{\#}$	954††	23.7	80.6	-	4.5
845	2.0% CRA-M	520$^{\$}$	222	974†	357$^{\#\#}$	721$^{\#}$	953††	23.7	161.1	-	20.3
772	0% SRA-T	520$^{\$}$	234	769†	649$^{\#}$	479$^{\#\#}$	1091$^{\#}$	23.7	0	93.9	-
807	0% SRA-T #2	520$^{\$\$}$	229	769†	650$^{\#}$	481$^{\#\#}$	1100††	23.4	0	93.9	-
781	0.5% SRA-T	520$^{\$}$	231	769†	650$^{\#}$	479$^{\#\#}$	1087$^{\#}$	23.7	40.3	422.7	-
808	0.5% SRA-T #2	520$^{\$\$}$	231	769†	650$^{\#}$	481$^{\#\#}$	1100††	23.7	40.3	845.4	-
782	1.0% SRA-T	520$^{\$}$	229	788†	680$^{\#}$	488$^{\#\#}$	1027$^{\#}$	23.7	80.6	493.1	-
810	1.0% SRA-T #2	520$^{\$\$}$	229	859†	640$^{\#}$	506$^{\#}$	983$^{\#}$	23.7	80.6	281.8	-
786	2.0% SRA-T	520$^{\$}$	224	904†	596$^{\#}$	600$^{\#\#}$	887$^{\#}$	23.7	161.1	469.6	-
811	2.0% SRA-T #2	520$^{\$\$}$	224	859†	640$^{\#}$	506$^{\#}$	983$^{\#}$	23.7	161.1	281.8	-
789	0.5% CRA-T	520$^{\$}$	231	1116†	383$^{\#}$	451$^{\#\#}$	1036$^{\#}$	23.7	40.3	681.0	-
790	1.0% CRA-T	520$^{\$}$	229	1115†	383$^{\#}$	450$^{\#\#}$	1034$^{\#}$	23.7	80.6	587.0	-
794	2.0% CRA-T	520$^{\$}$	224	1115†	383$^{\#}$	450$^{\#\#}$	1034$^{\#}$	23.7	161.1	2019.4	-

† Bulk specific gravity (SSD) = 2.62
†† Bulk specific gravity (SSD) = 2.61
# Bulk specific gravity (SSD) = 2.59
Bulk specific gravity (SSD) = 2.60
$ Cement specific gravity = 3.15
$$ Cement specific gravity = 3.20

Note: 1 lb/yd^3 = 0.5933 kg/m^3

*Dosage by volume
Specific gravity for Tetraguard AS20 (SRA) and MasterLIFE CRA 007 (CRA) = 0.99
Specific gravity for Micro Air = 1.01

**Mixture designation: *A% XXX-B #C*
A = Percent dosage of SRA or CRA by weight of cement
XXX = SRA for Tetraguard AS20, CRA for MasterLIFE CRA 007
B = M for Micro Air, T for Tough Air
C = 2 for first duplicate batch, 3 for second duplicate batch

Table A.8 Program 1: Concrete Mixture Properties

Batch Number	Mixture**	Slump in. (mm)	Air Content %	Batching Temperature °F (°C)	Unit Weight lb/ft^3 (kg/m^3)	28-Day Compressive Strength psi (MPa)
730	0% SRA-M	4.25 (108)	8.75	66 (19)	148.6 (2381)	4430 (30.5)
754	0% SRA-M #2	3 (76)	8.75	65 (18)	138.9 (2225)	4800 (33.1)
796	0% SRA-M #3	3 (76)	9.00	72 (22)		-
769	0.5% SRA-M	2 (51)	8.00	67 (19)	135.0 (2163)	4350 (30.0)
834	0.5% SRA-M #2	1.75 (44)	9.00	73 (23)	139.0 (2227)	4660 (32.2)
722	1.0% SRA-M	3 (76)	8.75	73 (23)	148.4 (2377)	4440 (30.6)#
816	1.0% SRA-M #2	3 (76)	7.75	72 (22)	138.2 (2214)	-
727	2.0% SRA-M	5 (127)	9.00	73 (23)	148.2 (2374)	3390 (23.4)
820	2.0% SRA-M #2	2.75 (70)	8.25	71 (22)	138.0 (2211)	4600 (31.7)*
732	0.5% CRA-M	2.5 (64)	8.00	73 (23)	148.7 (2382)	3970 (27.4)
735	1.0% CRA-M	3 (76)	8.50	72 (22)	148.6 (2381)	4230 (29.2)
843	1.0% CRA-M #2	3 (76)	9.00	61 (16)	139.1 (2229)	3980 (27.4)
845	2.0% CRA-M	3 (76)	9.00	66 (19)	138.8(2223)	3840 (27.2)
772	0% SRA-T	2 (51)	8.00	76 (24)	138.6 (2220)	-
807	0% SRA-T #2	2.25 (57)	7.75	75 (24)	138.9 (2225)	4690 (32.4)
781	0.5% SRA-T	3 (76)	8.25	69 (21)	138.4 (2217)	5210 (35.9)
808	0.5% SRA-T #2	2.5 (64)	8.75	76 (24)	138.9 (2225)	5190 (35.8)
782	1.0% SRA-T	2 (51)	7.75	73 (23)	138.2 (2214)	5270 (36.4)
810	1.0% SRA-T #2	3.5 (89)	7.75	75 (24)	138.4 (2217)	5050 (34.8)*
786	2.0% SRA-T	2.5 (64)	9.50	70 (21)	138.2 (2214)	4290 (29.6)
811	2.0% SRA-T #2	2.75 (70)	8.25	75 (24)	138.2 (2214)	5420 (37.3)#
789	0.5% CRA-T	2 (51)	8.50	73 (23)	138.4 (2217)	-
790	1.0% CRA-T	3 (76)	7.50	76 (24)	138.2 (2214)	4900 (33.8)
794	2.0% CRA-T	3 (76)	8.75	75 (24)	138.0 (2211)	4840 (33.4)

- Data not obtained
*33 day cylinder strength
37 day cylinder strength

**Mixture designation: *A*% *XXX*-*B* #*C*
A = Percent dosage of SRA or CRA by weight of cement
XXX = SRA for Tetraguard AS20, CRA for MasterLIFE CRA 007
B = M for Micro Air, T for Tough Air
C = 2 for first duplicate batch, 3 for second duplicate batch

Table A.9 Program 2: Material Sample Identification for Each Mixture

Batch Number	Mixture**	Material Sample No.				
		Cement	Sand	Pea Gravel	Coarse Aggregate	
					3/4 in.	1 in.
828	Control w/ 3.5% air	C-5	S-9	PG-4	G-17	G-16
839	Control w/ 6% air	C-6	S-9	PG-4	G-17	G-16
754	Control w/ 8.75% air	C-1	S-2	PG-1	G-7	G-6
796	Control w/ 9% air	C-3	S-5	PG-3	G-11	G-12
832	0.5% SRA w/ 4% air	C-6	S-9	PG-4	G-17	G-16
833	0.5% SRA w/ 7% air	C-6	S-9	PG-4	G-17	G-16
769	0.5% SRA w/ 8% air	C-2	S-3	PG-2	G-7	G-8
830	1% SRA w/ 5.25% air	C-6	S-9	PG-4	G-17	G-16
814	1% SRA w/ 6.75% air	C-4	S-8	PG-3	G-14	G-15
816	1% SRA w/ 7.75% air	C-4	S-8	PG-3	G-14	G-15
722	1% SRA w/ 8.75% air	C-1	S-1	PG-1	G-2	G-1
817	2% SRA w/ 3.5% air	C-5	S-8	PG-3	G-14	G-15
831	2% SRA w/ 3.75% air	C-6	S-9	PG-4	G-17	G-16
838	2% SRA w/ 4.75% air	C-6	S-9	PG-4	G-17	G-16
836	2% SRA w/ 7% air	C-6	S-9	PG-4	G-17	G-16
820	2% SRA w/ 8.25% air	C-5	S-8	PG-3	G-14	G-15

**Mixture designation: *Y*% SRA w/ *Z*% air
Control = no dosage of SRA
Y = Percent dosage of SRA by weight of cement
Z = Measured air content of mixture

Table A.10 Program 2: Constituent Proportions and Admixture Dosages

Batch Number	Mixture**	Cement (lb/yd^3)	Water (lb/yd^3)	Sand (lb/yd^3)	Pea Gravel (lb/yd^3)	Coarse Aggregate (lb/yd^3) 3/4 in.	Coarse Aggregate (lb/yd^3) 1 in.	Paste Content (% by volume)	SRA* (fl oz/yd^3)	MicroAir* (fl oz/yd^3)
828	Control w/ 3.5% air	520$	234	977†	357##	721#	950††	24.8	0	0.5
839	Control w/ 6% air	520$	234	1035†	378##	764#	1005††	23.2	0	1.0
754	Control w/ 8.75% air	520$$	234	1179††	335##	511#	971#	23.7	0	3.1
796	Control w/ 9% air	520$	234	944†	551#	565##	923#	23.7	0	2.9
832	0.5% SRA w/ 4% air	520$	231	1035†	378##	764#	1006††	23.7	40.3	0.5
833	0.5% SRA w/ 7% air	540$	235	969†	354##	715#	941††	24.5	41.9	1.5
769	0.5% SRA w/ 8% air	540$	235	959†	278#	503#	1129#	24.3	41.9	1.4
830	1% SRA w/ 5.25% air	520$	229	1034†	377##	763#	1005††	23.4	80.6	0.5
814	1% SRA w/ 6.75% air	540$$	232	1074††	328#	558#	999#	24.6	83.7	1.4
816	1% SRA w/ 7.75% air	540$$	232	1074††	328#	558#	999#	24.3	83.7	1.4
722	1% SRA w/ 8.75% air	540$$	232	1211††	404##	405††	1215††	24.3	83.7	1.4
817	2% SRA w/ 3.5% air	540$	227	1077††	328#	558#	996#	25.4	167.4	1.4
831	2% SRA w/ 3.75% air	520$	223	1035†	378##	764#	1006††	23.8	161.1	0.5
838	2% SRA w/ 4.75% air	520$	223	1035†	378##	764#	1006††	23.5	161.1	0.8
836	2% SRA w/ 7% air	520$	223	1035†	378##	764#	1006††	23.0	161.1	1.0
820	2% SRA w/ 8.25% air	540$	227	1077††	328#	558#	996#	24.3	167.4	3.0

† Bulk specific gravity (SSD) = 2.62
# Bulk specific gravity (SSD) = 2.59
$ Cement specific gravity = 3.15

†† Bulk specific gravity (SSD) = 2.61
Bulk specific gravity (SSD) = 2.60
$$ Cement specific gravity = 3.20

Note: 1 lb/yd^3 = 0.5933 kg/m^3

**Mixture designation: *Y*% SRA w/ *Z*% air
Control = no dosage of SRA
Y = Percent dosage of SRA by weight of cement
Z = Measured air content of mixture

*Dosage by volume
Specific gravity for Tetraguard AS20 (SRA) = 0.99
Specific gravity for Micro Air = 1.01

Table A.11 Program 2: Concrete Mixture Properties

Batch Number	Mixture**	Slump in. (mm)	Air Content %	Batching Temperature °F (°C)	Unit Weight lb/ft^3 (kg/m^3)	28-Day Compressive Strength psi (MPa)
828	Control w/ 3.5% air	1.5 (38)	3.50	69 (21)	148.0 (2371)	6700 (46.2)
839	Control w/ 6% air	2 (51)	6.00	69 (21)	142.8 (2288)	5360 (37.0)
754	Control w/ 8.75% air	3 (76)	8.75	65 (18)	138.9 (2225)	4800 (33.1)
796	Control w/ 9% air	3 (76)	9.00	72 (22)	-	-
832	0.5% SRA w/ 4% air	1.5 (38)	4.00	75 (24)	148.0 (2371)	5560 (38.3)
833	0.5% SRA w/ 7% air	2 (51)	7.00	70 (21)	143.3 (2296)	5190 (35.8)
769	0.5% SRA w/ 8% air	2 (51)	8.00	67 (19)	135.0 (2163)	4350 (30.0)
830	1% SRA w/ 5.25% air	1.75 (44)	5.25	66 (19)	145.3 (2328)	5860 (40.4)
814	1% SRA w/ 6.75% air	2.75 (70)	6.75	74 (23)	142.1 (2276)	-
816	1% SRA w/ 7.75% air	3 (76)	7.75	72 (22)	138.2 (2214)	-
722	1% SRA w/ 8.75% air	3 (76)	8.75	73 (23)	148.4 (2377)	4440 (30.6)#
817	2% SRA w/ 3.5% air	2.5 (64)	3.50	72 (22)	-	-
831	2% SRA w/ 3.75% air	1.75 (44)	3.75	65 (18)	146.7 (2350)	5970 (41.2)
838	2% SRA w/ 4.75% air	1.5 (38)	4.75	75 (24)	145.5 (2331)	5470 (37.7)
836	2% SRA w/ 7% air	2 (51)	7.00	64 (18)	142.0 (2275)	5170 (35.6)
820	2% SRA w/ 8.25% air	2.75 (70)	8.25	71 (22)	138.0 (2211)	4600 (31.7)*

- Data not obtained
*33 day cylinder strength
37 day cylinder strength

**Mixture designation: *Y*% SRA w/ *Z*% air
Control = no dosage of SRA
Y = Percent dosage of SRA by weight of cement
Z = Measured air content of mixture

Table A.12 Program 3: Material Sample Identification for Each Mixture

Batch Number	Mixture**	Material Sample No.					
		Cement	Sand	Pea Gravel	Coarse Aggregate		Lightweight Aggregate
					3/4 in.	1 in.	
754	Control	C-1	S-2	PG-1	G-7	G-6	--
756	8% LWA	C-1	S-2	PG-1	G-7	G-6	LWA-1
758	10% LWA	C-1	S-3	PG-2	G-7	G-6	LWA-1
759	10% LWA, 30% Slag	C-1	S-3	PG-2	G-7	G-6	LWA-1
764	10% LWA, 30% Slag, 3% SF	C-1	S-3	PG-2	G-7	G-8	LWA-1
767	10% LWA, 30% Slag, 6% SF	C-1	S-3	PG-2	G-7	G-8	LWA-1
796	Control	C-3	S-5	PG-3	G-11	G-12	--
798	8% LWA	C-3	S-6	PG-3	G-11	G-12	LWA-1
799	10% LWA	C-3	S-6	PG-3	G-11	G-12	LWA-1
801	10% LWA, 30% Slag	C-3	S-6	PG-3	G-11	G-13	LWA-1
802	10% LWA, 30% Slag, 3% SF	C-3	S-6	PG-3	G-11	G-13	LWA-1
803	10% LWA, 30% Slag, 6% SF	C-3	S-6	PG-3	G-11	G-13	LWA-1
827	8% LWA	C-5	S-9	PG-4	G-17	G-16	LWA-1
826	10% LWA	C-5	S-9	PG-4	G-14	G-16	LWA-1
821	10% LWA, 30% Slag	C-5	S-8	PG-4	G-14	G-15	LWA-1
823	10% LWA, 30% Slag, 3% SF	C-5	S-8	PG-4	G-14	G-16	LWA-1
822	10% LWA, 30% Slag, 6% SF	C-5	S-8	PG-4	G-14	G-15	LWA-1
876	Control	C-7	S-12	PG-5	G-19B*	G-19A*	--
873	10% LWA	C-7	S-11	PG-5	G-19B*	G-19A*	LWA-2
869	10% LWA, 30% Slag, 3% SF	C-7	S-11	PG-5	G-19B*	G-19A*	LWA-2
870	10% LWA, 30% Slag, 6% SF	C-7	S-11	PG-5	G-19B*	G-19A*	LWA-2

*Sample G-19 was separated into two portions. See Table A.3 for gradations of the two portions.
**Mixture designation: *X*% LWA, *Y*% Slag, *Z*% SF
Control = No addition of lightweight aggregate, slag, or silica fume
X = Percent replacement by volume of total aggregate with lightweight aggregate
Y = Percent replacement by volume of cement with GGBFS (Slag)
Z = Percent replacement by volume of cement with silica fume

Table A.13 Program 3: Constituent Proportions

Batch Number	Mixture**	Cement (lb/yd^3)	Slag‡ (lb/yd^3)	Silica Fume$^{\alpha}$ (lb/yd^3)	Water (lb/yd^3)	Sand (lb/yd^3)	Pea Gravel (lb/yd^3)
754	Control	520$^{\$\$}$	0	0	234	1179††	335$^{\#\#}$
756	8% LWA	520$^{\$\$}$	0	0	234	1174††	95$^{\#\#}$
758	10% LWA	520$^{\$\$}$	0	0	234	1034†	83$^{\#}$
759	10% LWA, 30% Slag	374$^{\$\$}$	146	0	234	1030†	83$^{\#}$
764	10% LWA, 30% Slag, 3% SF	359$^{\$\$}$	144	11	231	1033†	83$^{\#}$
767	10% LWA, 30% Slag, 6% SF	342$^{\$\$}$	146	22	230	1033†	83$^{\#}$
796	Control	520$^{\$}$	0	0	234	944†	551$^{\#}$
798	8% LWA	520$^{\$}$	0	0	234	927†	321$^{\#}$
799	10% LWA	520$^{\$}$	0	0	234	927†	271$^{\#}$
801	10% LWA, 30% Slag	374$^{\$}$	146	0	234	1098†	83$^{\#}$
802	10% LWA, 30% Slag, 3% SF	359$^{\$}$	144	11	231	1101†	83$^{\#}$
803	10% LWA, 30% Slag, 6% SF	342$^{\$}$	146	22	230	1144†	83$^{\#}$
827	8% LWA	520$^{\$}$	0	0	229	1044†	213$^{\#\#}$
826	10% LWA	520$^{\$}$	0	0	229	1044†	153$^{\#\#}$
821	10% LWA, 30% Slag	374$^{\$}$	146	0	229	1028††	84$^{\#\#}$
823	10% LWA, 30% Slag, 3% SF	359$^{\$}$	144	11	226	1031††	153$^{\#\#}$
822	10% LWA, 30% Slag, 6% SF	342$^{\$}$	146	22	224	1033††	153$^{\#\#}$
876	Control	520$^{\$}$	0	0	234	1033†	646†
873	10% LWA	520$^{\$}$	0	0	234	1082†	287†
869	10% LWA, 30% Slag, 3% SF	359$^{\$}$	145	11	231	1033†	287†
870	10% LWA, 30% Slag, 6% SF	341$^{\$}$	145	22	228	1083†	287†

† Bulk specific gravity (SSD) = 2.62
# Bulk specific gravity (SSD) = 2.59
$ Cement specific gravity = 3.15

†† Bulk specific gravity (SSD) = 2.61
Bulk specific gravity (SSD) = 2.60
$$ Cement specific gravity = 3.20

**Mixture designation: *X*% LWA, *Y*% Slag, *Z*% SF
Control = No addition of lightweight aggregate, slag, or silica fume
X = Percent replacement by volume of total aggregate with lightweight aggregate
Y = Percent replacement by volume of cement with GGBFS (Slag)
Z = Percent replacement by volume of cement with silica fume

‡ GranChem® produced by Holcim Inc., specific gravity = 2.86
α Eucon MSA produced by Euclid Chemical Company, specific gravity = 2.20

Note: 1 lb/yd^3 = 0.5933 kg/m^3

Table A.13 (Con't) Program 3: Constituent Proportions

Batch Number	Mixture**	Lightweight Aggregate[&] (lb/yd^3)	LWA Moisture Content (%)	Coarse Aggregate (lb/yd^3)		Paste Content (% by volume)	MicroAir* (fl oz/yd^3)	Water in Aggregate (lb/yd^3)
				3/4 in.	1 in.			
754	Control	0	-	511[#]	971[#]	23.7	3.1	22.9
756	8% LWA	142	26.56	511[#]	971[#]	23.7	3.1	58.6
758	10% LWA	177	27.32	565[#]	1012[#]	23.7	3.1	68.7
759	10% LWA, 30% Slag	177	26.35	562[#]	1008[#]	24.0	3.0	66.9
764	10% LWA, 30% Slag, 3% SF	177	27.87	564[#]	1015[#]	23.8	6.4	69.9
767	10% LWA, 30% Slag, 6% SF	177	28.42	564[#]	1016[#]	23.7	5.1	70.9
796	Control	0	-	565[##]	923[#]	23.7	2.9	-
798	8% LWA	142	20.59	565[##]	926[#]	23.7	3.0	-
799	10% LWA	177	25.22	565[##]	917[#]	23.7	3.0	-
801	10% LWA, 30% Slag	177	22.69	571[##]	939[††]	24.0	3.0	-
802	10% LWA, 30% Slag, 3% SF	177	22.20	573[##]	942[††]	23.8	3.0	-
803	10% LWA, 30% Slag, 6% SF	177	26.60	531[##]	942[††]	23.7	5.1	-
827	8% LWA	142	26.25	454[††]	1046[#]	23.4	2.0	-
826	10% LWA	177	23.54	454[#]	1046[#]	23.4	2.0	-
821	10% LWA, 30% Slag	177	24.51	454[#]	1110[#]	23.7	3.0	-
823	10% LWA, 30% Slag, 3% SF	177	23.24	454[#]	1045[#]	23.5	3.0	-
822	10% LWA, 30% Slag, 6% SF	177	21.37	456[#]	1047[#]	23.4	3.0	-
876	Control	0	-	398[Δ]	948[Δ]	23.7	2.0	23.2
873	10% LWA	178	20.31	359[Δ]	1002[Δ]	23.5	3.0	56.8
869	10% LWA, 30% Slag, 3% SF	177	24.12	359[Δ]	1000[Δ]	23.7	3.0	63.0
870	10% LWA, 30% Slag, 6% SF	178	25.46	360[Δ]	1003[Δ]	23.4	3.0	66.0

† Bulk specific gravity (SSD) = 2.62
# Bulk specific gravity (SSD) = 2.59
†† Bulk specific gravity (SSD) = 2.61
Bulk specific gravity (SSD) = 2.60

Note: 1 lb/yd^3 = 0.5933 kg/m^3

**Mixture designation: *X*% LWA, *Y*% Slag, *Z*% SF
Control = No addition of lightweight aggregate, slag, or silica fume
X = Percent replacement by volume of total aggregate with lightweight aggregate
Y = Percent replacement by volume of cement with GGBFS (Slag) *Dosage by volume
Z = Percent replacement by volume of cement with silica fume

& Lightweight aggregate bulk specific gravity (SSD) = 1.54
ΔG-20A and G-20B were used as two coarse aggregate portions
G-20 is 3/4 in. max-size aggregate w/ bulk specific gravity (SSD) = 2.62

Specific gravity for Micro Air = 1.01

Table A.14 Program 3: Concrete Mixture Properties

Batch Number	Mixture**	Slump in. (mm)	Air Content %	Batching Temperature °F (°C)	Unit Weight lb/ft^3 (kg/m^3)	28-Day Compressive Strength psi (MPa)
754	Control	3 (76)	8.75	65 (18)	138.9 (2225)	4800 (33.1)
756	8% LWA	3 (76)	8.50	75 (24)	-	4600 (31.7)
758	10% LWA	3 (76)	9.00	70 (21)	-	3740 (25.8)
759	10% LWA, 30% Slag	2.5 (64)	8.00	70 (21)	-	4860 (33.5)
764	10% LWA, 30% Slag, 3% SF	2 (51)	8.00	71 (22)	-	4050 (27.9)
767	10% LWA, 30% Slag, 6% SF	3 (76)	8.25	75 (24)	-	3620 (25.0)
796	Control	3 (76)	9.00	72 (22)	-	-
798	8% LWA	2.75 (70)	9.00	70 (21)	137.5 (2202)	-
799	10% LWA	3.25 (83)	9.00	74 (23)	135.3 (2168)	4300 (29.6)
801	10% LWA, 30% Slag	3 (76)	8.50	74 (23)	135.6 (2172)	4150 (28.6)
802	10% LWA, 30% Slag, 3% SF	3 (76)	8.50	77 (25)	136.0 (2179)	4210 (29.0)
803	10% LWA, 30% Slag, 6% SF	1.5 (38)	8.00	75 (24)	137.7 (2206)	5410 (37.3)
827	8% LWA	1.75 (44)	8.00	72 (22)	136.7 (2189)	5050 (34.8)
826	10% LWA	2.25 (57)	8.50	70 (21)	136.0 (2179)	4260 (29.4)
821	10% LWA, 30% Slag	3 (76)	8.75	69 (21)	-	4440 (30.6)
823	10% LWA, 30% Slag, 3% SF	1.5 (38)	8.00	69 (21)	134.0 (2147)	5660 (39.0)
822	10% LWA, 30% Slag, 6% SF	1.75 (44)	8.00	75 (24)	134.7 (2157)	5370 (37.0)
876	Control	2.5 (64)	7.00	68 (20)	145.9 (2337)	4290 (29.6)
873	10% LWA	2.75 (70)	8.25	72 (22)	138.5 (2219)	4980 (34.3)
869	10% LWA, 30% Slag, 3% SF	2.5 (64)	9.00	61 (16)	137.2 (2198)	4290 (29.6)
870	10% LWA, 30% Slag, 6% SF	2.25 (57)	8.00	62 (17)	138.7 (2221)	4720 (32.5)

- Data not obtained

**Mixture designation: *X*% LWA, *Y*% Slag, *Z*% SF

Control = No addition of lightweight aggregate, slag, or silica fume

X = Percent replacement by volume of total aggregate with lightweight aggregate

Y = Percent replacement by volume of cement with GGBFS (Slag)

Z = Percent replacement by volume of cement with silica fume

APPENDIX B: BRIDGE DECK SURVEY SPECIFICATIONS

1.0 DESCRIPTION.

This specification covers the procedures and requirements to perform bridge deck surveys of reinforced concrete bridge decks.

2.0 SURVEY REQUIREMENTS.

a. Pre-Survey Preparation.

(1) Prior to performing the crack survey, related construction documents need to be gathered to produce a scaled drawing of the bridge deck. The scale must be exactly 1 in. = 10 ft (for use with the scanning software), and the drawing only needs to include the boundaries of the deck surface.

NOTE 1 – In the event that it is not possible to produce a scaled drawing prior to arriving at the bridge deck, a hand-drawn crack map (1 in.= 10 ft) created on engineering paper using measurements taken in the field is acceptable.

(2) The scaled drawing should also include compass and traffic directions in addition to deck stationing. A scaled 5 ft by 5 ft grid is also required to aid in transferring the cracks observed on the bridge deck to the scaled drawing. The grid shall be drawn separately and attached to the underside of the crack map such that the grid can easily be seen through the crack map.

NOTE 2 – Maps created in the field on engineering paper need not include an additional grid.

(3) For curved bridges, the scaled drawing need not be curved, i.e., the curve may be approximated using straight lines.

(4) Coordinate with traffic control so that at least one side (or one lane) of the bridge can be closed during the time that the crack survey is being performed.

b. Preparation of Surface.

(1) After traffic has been closed, station the bridge in the longitudinal direction at ten feet intervals. The stationing shall be done as close to the centerline as possible. For curved bridges, the stationing shall follow the curve.

(2) Prior to beginning the crack survey, mark a 5 ft by 5 ft grid using lumber crayons or chalk on the portion of the bridge closed to traffic corresponding to the grid on the scaled drawing. Measure and document any drains, repaired areas, unusual cracking, or any other items of interest.

(3) Starting with one end of the closed portion of the deck, using a lumber crayon or chalk, begin tracing cracks that can be seen while bending at the waist. After beginning to trace cracks, continue to the end of the crack, even if this includes portions of the crack that were not initially seen while bending at the waist. Areas covered by sand or other debris need not be surveyed. Trace the cracks using a different color crayon than was used to mark the grid and stationing.

(4) At least one person shall recheck the marked portion of the deck for any additional cracks. The goal is not to mark every crack on the deck, only those cracks that can initially be seen while bending at the waist.

NOTE 3 – An adequate supply of lumber crayons or chalk should be on hand for the survey. Crayon or chalk colors should be selected to be readily visible when used to mark the concrete.

c. Weather Limitations.

(1) Surveys are limited to days when the expected temperature during the survey will not be below 60 °F.

(2) Surveys are further limited to days that are forecasted to be at least mostly sunny for a majority of the day.

(3) Regardless of the weather conditions, the bridge deck must be completely dry before the survey can begin.

3.0 BRIDGE SURVEY.

a. Crack Surveys.

Using the grid as a guide, transfer the cracks from the deck to the scaled drawing. Areas that are not surveyed should be marked on the scaled drawing. Spalls, regions of scaling, and other areas of special interest need not be included on the scale drawings but should be noted.

b. Delamination Survey.

At any time during or after the crack survey, bridge decks shall be checked for delamination. Any areas of delamination shall be noted and drawn on a separate drawing of the bridge. This second drawing need not be to scale.

c. Under Deck Survey.

Following the crack and delamination survey, the underside of the deck shall be examined and any unusual or excessive cracking noted.

APPENDIX C: DATA COLLECTED FROM FREEZE-THAW AND SCALING SPECIMENS IN PROGRAMS 1, 2, AND 3

Table C.1 Program 1 – Fundamental transverse frequency and mass data (ASTM C666 and C215)

Mixture: 0% SRA-M #2*

Cycles	0			32			65			106			152		
Specimen	754A	754B	754C	754A	754B	754C	754A	754B	754C	754A	754B	754C	754A	754B	754C
Frequency n [Hz]	*2185*	*2185*	*2192*	*2154*	*2157*	*2162*	*2158*	*2161*	*2170*	*2158*	*2161*	*2171*	*2166*	*2169*	*2180*
Mass M [g]	*7284.1*	*7297.9*	*7316*	*7293.7*	*7305.7*	*7320.5*	*7297.3*	*7309.7*	*7324.9*	*7298.9*	*7311.3*	*7326.6*	*7300.5*	*7312.8*	*7328.1*
Dynamic Modulus (Pa)	3.768E+10	3.776E+10	3.809E+10	3.667E+10	3.683E+10	3.708E+10	3.683E+10	3.699E+10	3.738E+10	3.683E+10	3.700E+10	3.742E+10	3.712E+10	3.728E+10	3.774E+10
Avg. Dy. Modulus (Pa)	3.784E+10			3.686E+10			3.706E+10			3.708E+10			3.738E+10		

Cycles	193			236			278			298			329		
Specimen	754A	754B	754C	754A	754B	754C	754A	754B	754C	754A	754B	754C	754A	754B	754C
Frequency n [Hz]	*2169*	*2163*	*2173*	*2169*	*2165*	*2181*	*2169*	*2168*	*2187*	*2172*	*2171*	*2185*	*2176*	*2176*	*2184*
Mass M [g]	*7299.7*	*7315.1*	*7327*	*7300.6*	*7316.4*	*7327.6*	*7301.9*	*7317.4*	*7328.2*	*7300.5*	*7317.2*	*7328.4*	*7299.7*	*7316.8*	*7328.5*
Dynamic Modulus (Pa)	3.721E+10	3.709E+10	3.749E+10	3.722E+10	3.716E+10	3.777E+10	3.723E+10	3.727E+10	3.798E+10	3.732E+10	3.737E+10	3.791E+10	3.745E+10	3.754E+10	3.788E+10
Avg. Dy. Modulus (Pa)	3.726E+10			3.738E+10			3.749E+10			3.754E+10			3.763E+10		

*Batch also designated as "Control w/ 8.75% air" in Program 2 and "Control" in Program 3, Series 1.

Mixture: 0% SRA-M #3*

Cycles	0			25			42			78			123		
Specimen	796A	796B	796C	796A	796B	796C	796A	796B	796C	796A	796B	796C	796A	796B	796C
Frequency n [Hz]	*2138*	*2117*	*2115*	*2133*	*2114*	*2106*	*2129*	*2110*	*2095*	*2126*	*2105*	*2092*	*2128*	*2109*	*2101*
Mass M [g]	*7342.9*	*7245.7*	*7191.9*	*7343.5*	*7247.4*	*7193.1*	*7344.7*	*7249.2*	*7194.6*	*7346.5*	*7251.4*	*7198.3*	*7342.9*	*7248*	*7194*
Dynamic Modulus (Pa)	3.637E+10	3.519E+10	3.486E+10	3.620E+10	3.510E+10	3.457E+10	3.607E+10	3.497E+10	3.422E+10	3.598E+10	3.482E+10	3.414E+10	3.603E+10	3.493E+10	3.441E+10
Avg. Dy. Modulus (Pa)	3.547E+10			3.529E+10			3.509E+10			3.498E+10			3.513E+10		

Cycles	157			191			220			249			274		
Specimen	796A	796B	796C	796A	796B	796C	796A	796B	796C	796A	796B	796C	796A	796B	796C
Frequency n [Hz]	*2128*	*2112*	*2102*	*2130*	*2118*	*2104*	*2127*	*2117*	*2102*	*2124*	*2115*	*2100*	*2126*	*2112*	*2106*
Mass M [g]	*7343.5*	*7249.7*	*7195.9*	*7344.7*	*7251.8*	*7197.1*	*7344.6*	*7251.9*	*7197.4*	*7344.4*	*7252*	*7198.3*	*7343.8*	*7251.8*	*7197.9*
Dynamic Modulus (Pa)	3.604E+10	3.504E+10	3.445E+10	3.611E+10	3.525E+10	3.452E+10	3.601E+10	3.522E+10	3.446E+10	3.590E+10	3.515E+10	3.440E+10	3.597E+10	3.505E+10	3.459E+10
Avg. Dy. Modulus (Pa)	3.518E+10			3.530E+10			3.561E+10			3.515E+10			3.521E+10		

Cycles	309		
Specimen	796A	796B	796C
Frequency n [Hz]	*2129*	*2110*	*2111*
Mass M [g]	*7343.5*	*7251.6*	*7197.6*
Dynamic Modulus (Pa)	3.607E+10	3.498E+10	3.476E+10
Avg. Dy. Modulus (Pa)	3.527E+10		

*Batch also designated as "Control w/ 9% air" in Program 2 and "Control" in Program 3, Series 2.

Mixture: 0.5% SRA-M*

Cycles	0			26			59			83			128		
Specimen	769A	769B	769C	769A	769B	769C	769A	769B	769C	769A	769B	769C	769A	769B	769C
Frequency n [Hz]	*2192*	*2221*	*2219*	*2189*	*2218*	*2214*	*2186*	*2215*	*2208*	*2160*	*2181*	*2186*	*2156*	*2182*	*2188*
Mass M [g]	*7337*	*7449.4*	*7370.7*	*7338.2*	*7449.8*	*7371.3*	*7338.7*	*7450.2*	*7371.8*	*7332.3*	*7446.2*	*7363.1*	*7331.5*	*7445.6*	*7362.7*
Dynamic Modulus (Pa)	3.820E+10	3.982E+10	3.933E+10	3.810E+10	3.971E+10	3.915E+10	3.800E+10	3.961E+10	3.895E+10	3.707E+10	3.838E+10	3.813E+10	3.693E+10	3.841E+10	3.820E+10
Avg. Dy. Modulus (Pa)	3.912E+10			3.899E+10			3.885E+10			3.786E+10			3.785E+10		

Cycles	164			210			247			279			304		
Specimen	769A	769B	769C	769A	769B	769C	769A	769B	769C	769A	769B	769C	769A	769B	769C
Frequency n [Hz]	*2152*	*2178*	*2185*	*2155*	*2179*	*2187*	*2160*	*2181*	*2189*	*2162*	*2182*	*2189*	*2163*	*2182*	*2189*
Mass M [g]	*7331*	*7443.6*	*7361.6*	*7330.2*	*7442.8*	*7361.7*	*7328*	*7441.9*	*7361.9*	*7328.5*	*7442.6*	*7361.7*	*7328.8*	*7443.4*	*7361.7*
Dynamic Modulus (Pa)	3.679E+10	3.826E+10	3.809E+10	3.689E+10	3.829E+10	3.816E+10	3.705E+10	3.836E+10	3.823E+10	3.712E+10	3.840E+10	3.823E+10	3.716E+10	3.840E+10	3.823E+10
Avg. Dy. Modulus (Pa)	3.771E+10			3.778E+10			3.788E+10			3.791E+10			3.793E+10		

*Batch also designated as "0.5% SRA w/ 8% air" in Program 2.

Table C.1 (Con't) Program 1 – Fundamental transverse frequency and mass data (ASTM C666 and C215)

Mixture: 0.5% SRA-M #2

Cycles	0			24			52			91			132		
Specimen	834A	834B	834C	834A	834B	834C	834A	834B	834C	834A	834B	834C	834A	834B	834C
Frequency n [Hz]	*2204*	*2242*	*2189*	*2207*	*2244*	*2190*	*2209*	*2245*	*2192*	*2211*	*2247*	*2195*	*2212*	*2250*	*2198*
Mass M [g]	*7422.5*	*7588.8*	*7360.9*	*7427.1*	*7594.5*	*7364.6*	*7431*	*7599.5*	*7369.3*	*7432.4*	*7600.6*	*7369.9*	*7433.5*	*7602*	*7370.6*
Dynamic Modulus (Pa)	3.907E+10	4.134E+10	3.822E+10	3.920E+10	4.144E+10	3.828E+10	3.929E+10	4.150E+10	3.837E+10	3.937E+10	4.158E+10	3.848E+10	3.941E+10	4.170E+10	3.859E+10
Avg. Dy. Modulus (Pa)	3.954E+10			3.964E+10			3.972E+10			3.981E+10			3.990E+10		

Cycles	154			182			221			257			300		
Specimen	834A	834B	834C	834A	834B	834C	834A	834B	834C	834A	834B	834C	834A	834B	834C
Frequency n [Hz]	*2213*	*2249*	*2195*	*2215*	*2248*	*2191*	*2215*	*2250*	*2195*	*2216*	*2252*	*2198*	*2216*	*2254*	*2202*
Mass M [g]	*7435.3*	*7603.7*	*7371.1*	*7437.3*	*7604.3*	*7372*	*7738.7*	*7604.1*	*7372.6*	*7739.3*	*7603.9*	*7373.1*	*7440*	*7603.9*	*7373.8*
Dynamic Modulus (Pa)	3.946E+10	4.168E+10	3.848E+10	3.954E+10	4.164E+10	3.835E+10	4.114E+10	4.172E+10	3.849E+10	4.118E+10	4.179E+10	3.860E+10	3.959E+10	4.186E+10	3.874E+10
Avg. Dy. Modulus (Pa)	3.987E+10			3.984E+10			4.045E+10			4.052E+10			4.007E+10		

Mixture: 1.0% SRA-M #2*

Cycles	0			37			74			111			155		
Specimen	816A	816B	816C	816A	816B	816C	816A	816B	816C	816A	816B	816C	816A	816B	816C
Frequency n [Hz]	*2233*	*2228*	*2236*	*2213*	*2206*	*2219*	*2216*	*2212*	*2220*	*2217*	*2212*	*2219*	*2210*	*2205*	*2190*
Mass M [g]	*7433.1*	*7560.9*	*7632.5*	*7449.5*	*7578.1*	*7649.3*	*7455.4*	*7581*	*7651.5*	*7456.3*	*7581*	*7652.3*	*7458.1*	*7582.3*	*7651.8*
Dynamic Modulus (Pa)	4.016E+10	4.067E+10	4.135E+10	3.953E+10	3.996E+10	4.081E+10	3.967E+10	4.020E+10	4.086E+10	3.971E+10	4.020E+10	4.083E+10	3.947E+10	3.995E+10	3.977E+10
Avg. Dy. Modulus (Pa)	4.073E+10			4.010E+10			4.024E+10			4.025E+10			3.973E+10		

Cycles	201			244			289			334		
Specimen	816A	816B	816C	816A	816B	816C	816A	816B	816C	816A	816B	816C
Frequency n [Hz]	*2219*	*2215*	*2209*	*2208*	*2212*	*2200*	*2204*	*2203*	*2186*	*2200*	*2197*	*2170*
Mass M [g]	*7464.5*	*7585.2*	*7659*	*7463.3*	*7586.2*	*7660.1*	*7464.7*	*7587.1*	*7660*	*7465.3*	*7588.1*	*7660*
Dynamic Modulus (Pa)	3.983E+10	4.033E+10	4.050E+10	3.943E+10	4.022E+10	4.018E+10	3.929E+10	3.990E+10	3.967E+10	3.915E+10	3.969E+10	3.909E+10
Avg. Dy. Modulus (Pa)	4.022E+10			3.994E+10			3.962E+10			3.931E+10		

*Batch also designated as "1.0% SRA w/ 7.75% air" in Program 2.

Mixture: 2.0% SRA-M #2*

Cycles	0			37			81			127			170		
Specimen	820A	820B	820C	820A	820B	820C	820A	820B	820C	820A	820B	820C	820A	820B	820C
Frequency n [Hz]	*2187*	*2227*	*2200*	*2162*	*2192*	*2168*	*2162*	*2182*	*2163*	*2160*	*2192*	*2168*	*2161*		*2175*
Mass M [g]	*7291.5*	*7411.5*	*7256.9*	*7297.1*	*7416.8*	*7261.7*	*7299.1*	*7418.7*	*7263.1*	*7303.5*	*7424.3*	*7267.3*	*7305.6*		*7269.4*
Dynamic Modulus (Pa)	3.779E+10	3.983E+10	3.806E+10	3.696E+10	3.862E+10	3.699E+10	3.697E+10	3.828E+10	3.682E+10	3.692E+10	3.866E+10	3.701E+10	3.697E+10	0	3.726E+10
Avg. Dy. Modulus (Pa)	3.856E+10			3.752E+10			3.736E+10			3.753E+10			3.712E+10		

Cycles	212			260			286			312		
Specimen	820A	820B	820C	820A	820B	820C	820A	820B	820C	820A	820B	820C
Frequency n [Hz]	*2159*		*2164*	*2156*		*2156*	*2151*		*2156*	*2145*		*2156*
Mass M [g]	*7306.7*		*7270.2*	*7308*		*7270.9*	*7308.4*		*7271.4*	*7308.8*		*7271.8*
Dynamic Modulus (Pa)	3.691E+10	0	3.689E+10	3.681E+10	0	3.662E+10	3.664E+10	0	3.663E+10	3.644E+10	0	3.663E+10
Avg. Dy. Modulus (Pa)	3.690E+10			3.672E+10			3.663E+10			3.653E+10		

*Batch also designated as "2.0% SRA w/ 8.25% air" in Program 2.

Note: Specimen 820B removed from testing after 127 cycles as a result of improper handling not in compliance with ASTM C666. Average dynamic modulus taken from Specimens 820A & 820C thereafter.

Table C.1 (Con't) Program 1 – Fundamental transverse frequency and mass data (ASTM C666 and C215)

Mixture: 1.0% CRA-M

Cycles	0			36			79			108			136		
Specimen	735A	735B	735C	735A	735B	735C	735A	735B	735C	735A	735B	735C	735A	735B	735C
Frequency n [Hz]	*2172*	*2109*	*2168*	*2135*	*2077*	*2131*	*2139*	*2085*	*2132*	*2141*	*2086*	*2135*	*2142*	*2088*	*2138*
Mass M [g]	*7427.2*	*7247.1*	*7382.9*	*7438*	*7256.8*	*7392.8*	*7440.2*	*7260*	*7399.2*	*7443.4*	*7264.1*	*7400.7*	*7446.9*	*7267.1*	*7402.1*
Dynamic Modulus (Pa)	3.797E+10	3.493E+10	3.760E+10	3.674E+10	3.392E+10	3.638E+10	3.689E+10	3.420E+10	3.645E+10	3.697E+10	3.425E+10	3.656E+10	3.702E+10	3.433E+10	3.666E+10
Avg. Dy. Modulus (Pa)	3.683E+10			3.568E+10			3.584E+10			3.593E+10			3.601E+10		

Cycles	173			201			242			266			293		
Specimen	735A	735B	735C	735A	735B	735C	735A	735B	735C	735A	735B	735C	735A	735B	735C
Frequency n [Hz]	*2140*	*2093*	*2138*	*2142*	*2088*	*2132*	*2138*	*2094*	*2130*	*2139*	*2092*	*2133*	*2140*	*2091*	*2135*
Mass M [g]	*7449.5*	*7270.5*	*7405.2*	*7451.6*	*7271.8*	*7406.3*	*7452.1*	*7272*	*7405.5*	*7452.4*	*7272.3*	*7405.7*	*7452.6*	*7272.5*	*7406*
Dynamic Modulus (Pa)	3.697E+10	3.451E+10	3.668E+10	3.705E+10	3.435E+10	3.648E+10	3.691E+10	3.455E+10	3.641E+10	3.695E+10	3.449E+10	3.651E+10	3.698E+10	3.446E+10	3.658E+10
Avg. Dy. Modulus (Pa)	3.605E+10			3.596E+10			3.596E+10			3.598E+10			3.601E+10		

Cycles	329		
Specimen	735A	735B	735C
Frequency n [Hz]	*2135*	*2096*	*2125*
Mass M [g]	*7452.8*	*7273.1*	*7410.1*
Dynamic Modulus (Pa)	3.681E+10	3.462E+10	3.626E+10
Avg. Dy. Modulus (Pa)	3.590E+10		

Mixture: 0% SRA-T

Cycles	0			25			52			77			122		
Specimen	772A	772B	772C	772A	772B	772C	772A	772B	772C	772A	772B	772C	772A	772B	772C
Frequency n [Hz]	*2227*	*2243*	*2206*	*2209*	*2213*	*2181*	*2214*	*2205*	*2188*	*2219*	*2205*	*2188*	*2205*	*2203*	*2189*
Mass M [g]	*7526.4*	*7587*	*7429.6*	*7535*	*7593.1*	*7438.2*	*7536.9*	*7595.2*	*7440.3*	*7538.9*	*7597.6*	*7443.3*	*7540.2*	*7599.4*	*7443.8*
Dynamic Modulus (Pa)	4.045E+10	4.136E+10	3.918E+10	3.984E+10	4.030E+10	3.834E+10	4.003E+10	4.002E+10	3.860E+10	4.023E+10	4.003E+10	3.861E+10	3.973E+10	3.997E+10	3.865E+10
Avg. Dy. Modulus (Pa)	4.033E+10			3.949E+10			3.955E+10			3.962E+10			3.945E+10		

Cycles	164			193			221			260			295		
Specimen	772A	772B	772C	772A	772B	772C	772A	772B	772C	772A	772B	772C	772A	772B	772C
Frequency n [Hz]	*2190*	*2202*	*2188*	*2189*	*2203*	*2189*	*2187*	*2203*	*2189*	*2167*	*2194*	*2182*	*2146*	*2185*	*2172*
Mass M [g]	*7541.3*	*7602.5*	*7444.8*	*7543.4*	*7603.2*	*7448.6*	*7545.1*	*7605*	*7448.8*	*7545.8*	*7604.4*	*7448.5*	*7546.4*	*7604*	*7448*
Dynamic Modulus (Pa)	3.919E+10	3.995E+10	3.862E+10	3.917E+10	3.999E+10	3.868E+10	3.911E+10	4.000E+10	3.868E+10	3.840E+10	3.967E+10	3.843E+10	3.766E+10	3.934E+10	3.807E+10
Avg. Dy. Modulus (Pa)	3.925E+10			3.928E+10			3.926E+10			3.883E+10			3.836E+10		

Cycles	324		
Specimen	772A	772B	772C
Frequency n [Hz]	*2132*	*2169*	*2162*
Mass M [g]	*7546.2*	*7604.8*	*7448.1*
Dynamic Modulus (Pa)	3.717E+10	3.877E+10	3.773E+10
Avg. Dy. Modulus (Pa)	3.789E+10		

Mixture: 0% SRA-T #2

Cycles	0			20			51			87			129		
Specimen	807A	807B	807C	807A	807B	807C	807A	807B	807C	807A	807B	807C	807A	807B	807C
Frequency n [Hz]	*2276*	*2241*	*2176*	*2254*	*2236*	*2173*	*2266*	*2228*	*2170*	*2263*	*2222*	*2165*	*2266*	*2223*	*2170*
Mass M [g]	*7569.8*	*7502.6*	*7353.5*	*7576.4*	*7509.7*	*7359.8*	*7585.5*	*7516.7*	*7369.5*	*7587.7*	*7519.9*	*7372.7*	*7592*	*7525*	*7376.5*
Dynamic Modulus (Pa)	4.249E+10	4.083E+10	3.773E+10	4.171E+10	4.069E+10	3.766E+10	4.221E+10	4.043E+10	3.760E+10	4.211E+10	4.023E+10	3.745E+10	4.224E+10	4.030E+10	3.764E+10
Avg. Dy. Modulus (Pa)	4.035E+10			4.002E+10			4.008E+10			3.993E+10			4.006E+10		

Cycles	165			203			240			277			321		
Specimen	807A	807B	807C	807A	807B	807C	807A	807B	807C	807A	807B	807C	807A	807B	807C
Frequency n [Hz]	*2257*	*2222*	*2163*	*2250*	*2220*	*2157*	*2254*	*2220*	*2152*	*2250*	*2215*	*2155*	*2242*	*2205*	*2130*
Mass M [g]	*7592.2*	*7525.1*	*7376.7*	*7592.5*	*7525.3*	*7376.8*	*7594*	*7527*	*7378.4*	*7596*	*7526.3*	*7379.4*	*7595.4*	*7527*	*7380.1*
Dynamic Modulus (Pa)	4.191E+10	4.026E+10	3.740E+10	4.165E+10	4.019E+10	3.719E+10	4.181E+10	4.020E+10	3.703E+10	4.167E+10	4.001E+10	3.714E+10	4.137E+10	3.966E+10	3.628E+10
Avg. Dy. Modulus (Pa)	3.986E+10			3.968E+10			3.968E+10			3.961E+10			3.910E+10		

Table C.1 (Con't) Program 1 – Fundamental transverse frequency and mass data (ASTM C666 and C215)

Mixture: 0.5% SRA-T

Cycles	0			20			57			94			131		
Specimen	781A	781B	781C	781A	781B	781C	781A	781B	781C	781A	781B	781C	781A	781B	781C
Frequency n [Hz]	*2248*	*2243*	*2283*	*2241*	*2219*	*2245*	*2202*	*2150*	*2193*	*2095*	*1997*	*2034*	*1915*	*1870*	*1860*
Mass M [g]	*7725.5*	*7429.6*	*7687.6*	*7735.6*	*7444.9*	*7699.6*	*7748.4*	*7462*	*7715.7*	*7755.1*	*7467.5*	*7721.3*	*7764.8*	*7473.8*	*7725.6*
Dynamic Modulus (Pa)	4.231E+10	4.050E+10	4.342E+10	4.210E+10	3.972E+10	4.205E+10	4.071E+10	3.738E+10	4.021E+10	3.688E+10	3.227E+10	3.462E+10	3.086E+10	2.832E+10	2.896E+10
Avg. Dy. Modulus (Pa)	4.208E+10			4.129E+10			3.943E+10			3.459E+10			2.938E+10		

Cycles	165		
Specimen	781A	781B	781C
Frequency n [Hz]	*1774*	*1731*	*1727*
Mass M [g]	*7767.6*	*7477.8*	*7732.3*
Dynamic Modulus (Pa)	2.649E+10	2.428E+10	2.499E+10
Avg. Dy. Modulus (Pa)	2.525E+10		

Mixture: 0.5% SRA-T #2

Cycles	0			20			51			67			96		
Specimen	808A	808B	808C	808A	808B	808C	808A	808B	808C	808A	808B	808C	808A	808B	808C
Frequency n [Hz]	*2262*	*2200*	*2315*	*2105*	*2063*	*2157*	*1779*	*1712*	*1869*	*1644*	*1569*	*1720*	*1345*	*1237*	*1417*
Mass M [g]	*7622.5*	*7489.9*	*7804.6*	*7645.4*	*7511.1*	*7806.1*	*7656.5*	*7525.1*	*7836.7*	*7661.9*	*7531.2*	*7841.6*	*7672.5*	*7543.7*	*7850.9*
Dynamic Modulus (Pa)	4.226E+10	3.928E+10	4.532E+10	3.671E+10	3.464E+10	3.936E+10	2.626E+10	2.390E+10	2.966E+10	2.244E+10	2.009E+10	2.514E+10	1.504E+10	1.251E+10	1.708E+10
Avg. Dy. Modulus (Pa)	4.229E+10			3.690E+10			2.661E+10			2.256E+10			1.488E+10		

Cycles	129		
Specimen	808A	808B	808C
Frequency n [Hz]	*1041*	*900*	*1120*
Mass M [g]	*7681.8*	*7552.3*	*7860.8*
Dynamic Modulus (Pa)	9.021E+09	6.629E+09	1.069E+10
Avg. Dy. Modulus (Pa)	8.778E+09		

Mixture: 1.0% SRA-T

Cycles	0			21			58			95		
Specimen	782A	782B	782C	782A	782B	782C	782A	782B	782C	782A	782B	782C
Frequency n [Hz]	*2289*	*2309*		*2141*	*2142*		*1845*	*1867*		*1320*	*1360*	
Mass M [g]	*7563.5*	*7690.4*		*7600*	*7731.4*		*7614.4*	*7743.2*		*7624.2*	*7754.8*	
Dynamic Modulus (Pa)	4.294E+10	4.443E+10	0	3.775E+10	3.844E+10	0	2.809E+10	2.925E+10	0	1.440E+10	1.554E+10	0
Avg. Dy. Modulus (Pa)	4.369E+10			3.810E+10			2.867E+10			1.497E+10		

Note: Specimen 782C not tested as a result of improper handling not in compliance with ASTM C666. Average dynamic modulus taken from Specimens 782A & 782B.

Mixture: 1.0% SRA-T #2

Cycles	0			16			41			78			116		
Specimen	810A	810B	810C	810A	810B	810C	810A	810B	810C	810A	810B	810C	810A	810B	810C
Frequency n [Hz]	*2311*	*2178*	*2210*	*2280*	*2144*	*2179*	*2245*	*2141*	*2171*	*2200*	*2139*	*2164*	*2098*	*2081*	*2093*
Mass M [g]	*7726.3*	*7309.6*	*7369.8*	*7743.1*	*7325.1*	*7386.4*	*7754.9*	*7335.2*	*7397.8*	*7764.1*	*7342.3*	*7404.6*	*7765.9*	*7345.2*	*7408.6*
Dynamic Modulus (Pa)	4.471E+10	3.757E+10	3.901E+10	4.362E+10	3.649E+10	3.800E+10	4.235E+10	3.644E+10	3.778E+10	4.072E+10	3.640E+10	3.757E+10	3.704E+10	3.447E+10	3.517E+10
Avg. Dy. Modulus (Pa)	4.043E+10			3.937E+10			3.886E+10			3.823E+10			3.556E+10		

Cycles	152			189			226			270			316		
Specimen	810A	810B	810C	810A	810B	810C	810A	810B	810C	810A	810B	810C	810A	810B	810C
Frequency n [Hz]	*2055*	*2027*	*2019*	*2038*	*2011*	*1988*	*1990*	*1980*	*1947*	*2000*	*1974*	*1977*	*1872*	*1930*	*1912*
Mass M [g]	*7767.8*	*7348.7*	*7411.5*	*7769.9*	*7350.5*	*7414.4*	*7772.2*	*7352.7*	*7415.8*	*7772.2*	*7354.3*	*7416.9*	*7779.6*	*7357.6*	*7422.2*
Dynamic Modulus (Pa)	3.555E+10	3.272E+10	3.274E+10	3.497E+10	3.221E+10	3.175E+10	3.335E+10	3.124E+10	3.046E+10	3.369E+10	3.105E+10	3.141E+10	2.954E+10	2.970E+10	2.940E+10
Avg. Dy. Modulus (Pa)	3.367E+10			3.298E+10			3.168E+10			3.205E+10			2.955E+10		

Mixture: 2.0% SRA-T

Cycles	0			20			51			76			103		
Specimen	786A	786B	786C	786A	786B	786C	786A	786B	786C	786A	786B	786C	786A	786B	786C
Frequency n [Hz]	*2245*	*2278*	*2290*	*1944*	*1965*	*1994*	*1449*	*1445*	*1690*	*1132*	*1120*	*1371*	*815*	*786*	*1047*
Mass M [g]	*7372.3*	*7563.3*	*7546*	*7395.1*	*7588.4*	*7567.7*	*7416.4*	*7605.7*	*7585.1*	*7429.7*	*7620.1*	*7594.5*	*7442.2*	*7631.8*	*7604.9*
Dynamic Modulus (Pa)	4.026E+10	4.253E+10	4.288E+10	3.028E+10	3.175E+10	3.261E+10	1.687E+10	1.721E+10	2.348E+10	1.032E+10	1.036E+10	1.547E+10	5.357E+09	5.109E+09	9.034E+09
Avg. Dy. Modulus (Pa)	4.189E+10			3.155E+10			1.919E+10			1.205E+10			6.500E+09		

Table C.1 (Con't) Program 1 – Fundamental transverse frequency and mass data (ASTM C666 and C215)

Mixture: 2.0% SRA-T #2

Cycles	0			25			62		
Specimen	811A	811B	811C	811A	811B	811C	811A	811B	811C
Frequency n [Hz]	*2300*	*2291*	*2216*	*1867*	*1854*	*1813*	*1260*	*1180*	*1338*
Mass M [g]	*7693*	*7757.7*	*7441.8*	*7703.3*	*7787.3*	*7471.2*	*7743.6*	*7809.9*	*7492.6*
Dynamic Modulus (Pa)	4.410E+10	4.412E+10	3.960E+10	2.910E+10	2.901E+10	2.661E+10	1.332E+10	1.178E+10	1.454E+10
Avg. Dy. Modulus (Pa)	4.261E+10			2.824E+10			1.321E+10		

Mixture: 0.5% CRA-T

Cycles	0			20			52		
Specimen	789A	789B	789C	789A	789B	789C	789A	789B	789C
Frequency n [Hz]	*2265*	*2252*		*2021*	*2062*		*1572*	*1770*	
Mass M [g]	*7708.7*	*7555.6*		*7732.3*	*7573.4*		*7755*	*7599.2*	
Dynamic Modulus (Pa)	4.285E+10	4.152E+10	0	3.422E+10	3.489E+10	0	2.077E+10	2.580E+10	0
Avg. Dy. Modulus (Pa)	4.219E+10			3.456E+10			2.328E+10		

Note: Specimen 789C not tested as a result of improper handling not in compliance with ASTM C666. Average dynamic modulus taken from Specimens 789A & 789B.

Mixture: 1.0% CRA-T

Cycles	0			20			52		
Specimen	790A	790B	790C	790A	790B	790C	790A	790B	790C
Frequency n [Hz]	*2260*	*2219*	*2279*	*2043*	*2011*	*2032*	*1578*	*1322*	*1436*
Mass M [g]	*7590.2*	*7467.4*	*7672.5*	*7610.4*	*7487.7*	*7697*	*7639.5*	*7519.4*	*7721.8*
Dynamic Modulus (Pa)	4.201E+10	3.984E+10	4.318E+10	3.442E+10	3.281E+10	3.444E+10	2.061E+10	1.424E+10	1.725E+10
Avg. Dy. Modulus (Pa)	4.168E+10			3.389E+10			1.737E+10		

Mixture: 2.0% CRA-T

Cycles	0			20			42			67			96		
Specimen	794A	794B	794C	794A	794B	794C	794A	794B	794C	794A	794B	794C	794A	794B	794C
Frequency n [Hz]	*2228*	*2252*	*2272*	*2098*	*2165*	*2233*	*1990*	*2078*	*2120*	*1861*	*1912*	*1947*	*1727*	*1740*	*1764*
Mass M [g]	*7394.9*	*7544.9*	*7655.7*	*7406.5*	*7553.1*	*7671*	*7429.9*	*7575.7*	*7691*	*7430.4*	*7576.4*	*7693.2*	*7431.1*	*7577.3*	*7694.5*
Dynamic Modulus (Pa)	3.978E+10	4.146E+10	4.282E+10	3.533E+10	3.836E+10	4.145E+10	3.188E+10	3.545E+10	3.746E+10	2.789E+10	3.001E+10	3.160E+10	2.402E+10	2.486E+10	2.595E+10
Avg. Dy. Modulus (Pa)	4.062E+10			3.838E+10			3.493E+10			2.983E+10			2.494E+10		

Cycles	100		
Specimen	794A	794B	794C
Frequency n [Hz]	*1712*	*1720*	*1739*
Mass M [g]	*7431.7*	*7577.9*	*7695.2*
Dynamic Modulus (Pa)	2.360E+10	2.429E+10	2.522E+10
Avg. Dy. Modulus (Pa)	2.437E+10		

Table C.2 Program 1 – Scaling mass loss data (BNQ NQ 2621-900 Annex B)

Mixture: 0% SRA-M

Specimen	Effective Area	Mass at 7 days		Mass at 21 days		Mass at 35 days		Mass at 56 days	
	in^2	g	lb/in^2	g	lb/in^2	g	lb/in^2	g	lb/in^2
A	85.06	2.3	6.21E-05	1.5	4.05E-05	0.5	1.35E-05	0.2	5.4E-06
B	84.26	2.1	5.72E-05	1.5	4.09E-05	0.5	1.36E-05	0.2	5.45E-06
C	84.55	1.9	5.16E-05	2	5.43E-05	1.3	3.53E-05	0.3	8.15E-06
Average	84.62		5.70E-05		4.52E-05		2.08E-05		6.33E-06
Cumulative mass loss (lb/ft^2)			**8.20E-03**		**1.47E-02**		**1.77E-02**		**1.86E-02**

Mixture: 0% SRA-M #2*

Specimen	Effective Area	Mass at 7 days		Mass at 21 days		Mass at 35 days		Mass at 56 days	
	in^2	g	lb/in^2	g	lb/in^2	g	lb/in^2	g	lb/in^2
A	82.60	2.1	5.84E-05	3.6	0.0001	0.2	5.56E-06	0	0
B	83.86	1	2.74E-05	2.4	6.57E-05	1.3	3.56E-05	0.3	8.21E-06
C	83.75	4.9	1.34E-04	4.4	0.000121	1	2.74E-05	0.1	2.74E-06
Average	83.40		7.34E-05		9.55E-05		2.29E-05		3.65E-06
Cumulative mass loss (lb/ft^2)			**1.06E-02**		**2.43E-02**		**2.76E-02**		**2.81E-02**

*Batch also designated as "Control w/ 8.75% air" in Program 2 and "Control in Program 3, Series 1.

Mixture: 0% SRA-M #3*

Specimen	Effective Area	Mass at 7 days		Mass at 21 days		Mass at 35 days		Mass at 56 days	
	in^2	g	lb/in^2	g	lb/in^2	g	lb/in^2	g	lb/in^2
A	83.57	1	2.75E-05	1.4	3.85E-05	0.8	2.2E-05	0.2	5.49E-06
B	84.08	1.8	4.91E-05	1.5	4.1E-05	1.1	3E-05	0.4	1.09E-05
C	84.44	0.3	8.16E-06	1.3	3.53E-05	0.9	2.45E-05	0.1	2.72E-06
Average	84.03		2.83E-05		3.83E-05		2.55E-05		6.38E-06
Cumulative mass loss (lb/ft^2)			**4.07E-03**		**9.58E-03**		**1.32E-02**		**1.42E-02**

*Batch also designated as "Control w/ 9% air" in Program 2 and "Control" in Program 3, Series 2 & 3.

Mixture: 0.5% SRA-M*

Specimen	Effective Area	Mass at 7 days		Mass at 21 days		Mass at 35 days		Mass at 56 days	
	in^2	g	lb/in^2	g	lb/in^2	g	lb/in^2	g	lb/in^2
A	84.01	1.5	4.10E-05	1.3	3.55E-05	7.4	0.000202	2.5	6.83E-05
B	84.39	0.5	1.36E-05	0.8	2.18E-05	1.8	4.9E-05	1.3	3.54E-05
C	83.74	0.4	1.10E-05	4.3	0.000118	10.6	0.000291	0.9	2.47E-05
Average	84.05		2.19E-05		5.84E-05		1.81E-04		4.28E-05
Cumulative mass loss (lb/ft^2)			**3.15E-03**		**1.16E-02**		**3.76E-02**		**4.37E-02**

*Batch also designated as "0.5% SRA w/ 8% air" in Program 2.

Table C.2 (Con't) Program 1 – Scaling mass loss data (BNQ NQ 2621-900 Annex B)

Mixture: 0.5% SRA-M #2

Specimen	Effective Area in^2	Mass at 7 days		Mass at 21 days		Mass at 35 days		Mass at 56 days	
		g	lb/in^2	g	lb/in^2	g	lb/in^2	g	lb/in^2
A	85.71	0.3	8.04E-06	0.2	5.36E-06	7.3	0.000196	4.4	0.000118
B	82.02	0.2	5.60E-06	0.1	2.8E-06	7.1	0.000199	5.2	0.000146
C	82.28	0.3	8.37E-06	0.4	1.12E-05	10.9	0.000304	17.8	0.000497
Average	83.34		7.33E-06		6.44E-06		2.33E-04		2.53E-04
Cumulative mass loss (lb/ft^2)			**1.06E-03**		**1.98E-03**		**3.55E-02**		**7.20E-02**

Mixture: 1.0% SRA-M*

Specimen	Effective Area in^2	Mass at 7 days		Mass at 21 days		Mass at 35 days		Mass at 56 days	
		g	lb/in^2	g	lb/in^2	g	lb/in^2	g	lb/in^2
A	82.49	0.1	2.78E-06	0.5	1.39E-05	2.2	6.12E-05	3.8	0.000106
B	83.06	2	5.53E-05	5.8	0.00016	5.9	0.000163	10.4	0.000287
C	82.95	0.2	5.54E-06	1.4	3.87E-05	1.7	4.7E-05	5	0.000138
Average	82.83		2.12E-05		7.10E-05		9.05E-05		1.77E-04
Cumulative mass loss (lb/ft^2)			**3.05E-03**		**1.33E-02**		**2.63E-02**		**5.18E-02**

*Batch also designated as "1.0% SRA w/ 8.75% air" in Program 2.

Mixture: 1.0% SRA-M #2*

Specimen	Effective Area in^2	Mass at 7 days		Mass at 21 days		Mass at 35 days		Mass at 56 days	
		g	lb/in^2	g	lb/in^2	g	lb/in^2	g	lb/in^2
A	85.28	2	5.38E-05	1.9	5.11E-05	3.5	9.42E-05	0.4	1.08E-05
B	85.12	2.6	7.01E-05	2.9	7.82E-05	3.1	8.36E-05	0.4	1.08E-05
C	82.81	1.4	3.88E-05	1.8	4.99E-05	1.4	3.88E-05	0.1	2.77E-06
Average	84.40		5.43E-05		5.98E-05		7.22E-05		8.11E-06
Cumulative mass loss (lb/ft^2)			**7.81E-03**		**1.64E-02**		**2.68E-02**		**2.80E-02**

*Batch also designated as "1.0% SRA w/ 7.75% air" in Program 2.

Mixture: 2.0% SRA-M

Specimen	Effective Area in^2	Mass at 7 days		Mass at 21 days		Mass at 35 days		Mass at 56 days	
		g	lb/in^2	g	lb/in^2	g	lb/in^2	g	lb/in^2
A	82.83	0.6	1.66E-05	0.8	2.22E-05	0.5	1.39E-05	0.2	5.54E-06
B	83.27	0.6	1.65E-05	0.6	1.65E-05	1.0	2.76E-05	0.7	1.93E-05
C	83.83	0.8	2.19E-05	0.8	2.19E-05	1.3	3.56E-05	1.0	2.74E-05
Average	83.31		1.84E-05		2.02E-05		2.57E-05		1.74E-05
Cumulative mass loss (lb/ft^2)			**2.64E-03**		**5.55E-03**		**9.25E-03**		**1.18E-02**

Table C.2 (Con't) Program 1 – Scaling mass loss data (BNQ NQ 2621-900 Annex B)

Mixture: 2.0% SRA-M #2*

Specimen	Effective Area	Mass at 7 days		Mass at 21 days		Mass at 35 days		Mass at 56 days	
	in^2	g	lb/in^2	g	lb/in^2	g	lb/in^2	g	lb/in^2
A	83.87	3.1	8.49E-05	0.6	1.64E-05	0.5	1.37E-05	0.1	2.74E-06
B	83.46	1.8	4.95E-05	0.5	1.38E-05	0.6	1.65E-05	0.1	2.75E-06
C	83.59	2.7	7.41E-05	0.5	1.37E-05	0.4	1.1E-05	0.1	2.75E-06
Average	83.64		6.95E-05		1.46E-05		1.37E-05		2.74E-06
Cumulative mass loss (lb/ft^2)			**1.00E-02**		**1.21E-02**		**1.41E-02**		**1.45E-02**

*Batch also designated as "2.0% SRA w/ 8.25% air" in Program 2.

Mixture: 0.5% CRA-M

Specimen	Effective Area	Mass at 7 days		Mass at 21 days		Mass at 35 days		Mass at 56 days	
	in^2	g	lb/in^2	g	lb/in^2	g	lb/in^2	g	lb/in^2
A	91.53	2.1	5.27E-05	2.5	6.27E-05	1.6	4.01E-05	0.7	1.76E-05
B	91.50	1.6	4.01E-05	2.3	5.77E-05	1.4	3.51E-05	1.1	2.76E-05
C	91.85	0.9	2.25E-05	1.4	3.5E-05	0.8	2E-05	0.7	1.75E-05
Average	91.63		3.84E-05		5.18E-05		3.18E-05		2.09E-05
Cumulative mass loss (lb/ft2)			**5.53E-03**		**1.30E-02**		**1.76E-02**		**2.06E-02**

Mixture: 1.0% CRA-M

Specimen	Effective Area	Mass at 7 days		Mass at 21 days		Mass at 35 days		Mass at 56 days	
	in^2	g	lb/in^2	g	lb/in^2	g	lb/in^2	g	lb/in^2
A	82.56	0.3	8.34E-06	1.4	3.89E-05	2.1	5.84E-05	0.9	2.5E-05
B	84.22	0.3	8.18E-06	0.4	1.09E-05	1.1	3E-05	1	2.73E-05
C	83.49	0.5	1.37E-05	0.9	2.47E-05	0.9	2.47E-05	0.5	1.37E-05
Average	83.42		1.01E-05		2.49E-05		3.77E-05		2.20E-05
Cumulative mass loss (lb/ft^2)			**1.45E-03**		**5.03E-03**		**1.05E-02**		**1.36E-02**

Mixture: 0% SRA-T

Specimen	Effective Area	Mass at 7 days		Mass at 21 days		Mass at 35 days		Mass at 56 days	
	in^2	g	lb/in^2	g	lb/in^2	g	lb/in^2	g	lb/in^2
A	84.91	1.1	2.97E-05	0.6	1.62E-05	0.9	2.43E-05	0.4	1.08E-05
B	86.36	0.3	7.98E-06	0.5	1.33E-05	1.3	3.46E-05	0.2	5.32E-06
C	86.65	1	2.65E-05	1.1	2.91E-05	1.1	2.91E-05	0.3	7.95E-06
Average	85.97		2.14E-05		1.96E-05		2.93E-05		8.03E-06
Cumulative mass loss (lb/ft^2)			**3.08E-03**		**5.90E-03**		**1.01E-02**		**1.13E-02**

Mixture: 0% SRA-T #2

Specimen	Effective Area	Mass at 7 days		Mass at 21 days		Mass at 35 days		Mass at 56 days	
	in^2	g	lb/in^2	g	lb/in^2	g	lb/in^2	g	lb/in^2
A	96.25	0.1	2.39E-06	0	0	0	0	0	0
B	82.20	0.4	1.12E-05	2.3	6.42E-05	3.8	0.000106	6.7	0.000187
C	83.26	0.8	2.21E-05	1.6	4.41E-05	1.7	4.69E-05	1.8	4.96E-05
Average	87.24		1.19E-05		5.42E-05		7.65E-05		1.18E-04
Cumulative mass loss (lb/ft^2)			**1.71E-03**		**9.51E-03**		**2.05E-02**		**3.76E-02**

Table C.2 (Con't) Program 1 – Scaling mass loss data (BNQ NQ 2621-900 Annex B)

Mixture: 0.5% SRA-T

Specimen	Effective Area in^2	Mass at 7 days		Mass at 21 days		Mass at 35 days		Mass at 56 days	
		g	lb/in^2	g	lb/in^2	g	lb/in^2	g	lb/in^2
A	82.33	1.5	4.18E-05	2.2	6.13E-05	1.1	3.07E-05	0.4	1.12E-05
B	83.47	2.9	7.98E-05	3.8	0.000105	2.2	6.05E-05	1.0	2.75E-05
C	82.23	2.1	5.86E-05	1.4	3.91E-05	0.6	1.68E-05	0.2	5.58E-06
Average	82.68		6.01E-05		6.83E-05		3.60E-05		1.47E-05
Cumulative mass loss (lb/ft^2)			**8.65E-03**		**1.85E-02**		**2.37E-02**		**2.58E-02**

Mixture: 0.5% SRA-T #2

Specimen	Effective Area in^2	Mass at 7 days		Mass at 21 days		Mass at 35 days		Mass at 56 days	
		g	lb/in^2	g	lb/in^2	g	lb/in^2	g	lb/in^2
A	82.72	6.3	1.75E-04	18.2	0.000505	110.7	0.003072	1	2.78E-05
B	82.32	8.4	2.34E-04	11.6	0.000323	126.3	0.003522	4.1	0.000114
C	80.59	3.9	1.11E-04	10.2	0.000291	121	0.003447	6.9	0.000197
Average	81.88		1.73E-04		3.73E-04		3.35E-03		1.13E-04
Cumulative mass loss (lb/ft^2)			**2.50E-02**		**7.87E-02**		**5.607E-01**		**5.769E-01**

Mixture: 1.0% SRA-T

Specimen	Effective Area in^2	Mass at 7 days		Mass at 21 days		Mass at 35 days		Mass at 56 days	
		g	lb/in^2	g	lb/in^2	g	lb/in^2	g	lb/in^2
A	83.01	9.0	2.49E-04	22.4	0.0006195	23.8	0.000658	37.6	0.00104
B	76.82	1.1	3.29E-05	11.3	0.0003377	14.7	0.000439	29.5	0.000882
C	77.14	6.8	2.02E-04	38.4	0.0011429	55	0.001637	101.6	0.003024
Average	78.99		1.61E-04		7.00E-04		9.11E-04		1.65E-03
Cumulative mass loss (lb/ft^2)			**2.32E-02**		**1.240E-01**		**2.553E-01**		**4.927E-01**

Mixture: 1.0% SRA-T #2

Specimen	Effective Area in^2	Mass at 7 days		Mass at 21 days		Mass at 35 days		Mass at 56 days	
		g	lb/in^2	g	lb/in^2	g	lb/in^2	g	lb/in^2
A	83.73	5.4	1.48E-04	5.4	0.000148	4.6	0.000126	3.9	0.000107
B	83.14	3.2	8.84E-05	3	8.28E-05	4.2	0.000116	1.5	4.14E-05
C	80.85	0.6	1.70E-05	2.7	7.67E-05	5.4	0.000153	1.8	5.11E-05
Average	82.58		8.45E-05		1.03E-04		1.32E-04		6.65E-05
Cumulative mass loss (lb/ft^2)			**1.22E-02**		**2.69E-02**		**4.59E-02**		**5.55E-02**

Mixture: 2.0% SRA-T

Specimen	Effective Area in^2	Mass at 7 days		Mass at 21 days		Mass at 35 days		Mass at 56 days	
		g	lb/in^2	g	lb/in^2	g	lb/in^2	g	lb/in^2
A	84.31	0.2	5.45E-06	7.7	0.00021	8.3	0.000226	37.0	0.001007
B	84.55	1.4	3.80E-05	2.6	7.06E-05	1.8	4.89E-05	8.4	0.000228
C	84.79	18.2	4.93E-04	60.6	0.001641	46.9	0.00127	72.7	0.001968
Average	84.55		1.79E-04		6.40E-04		5.15E-04		1.07E-03
Cumulative mass loss (lb/ft^2)			**2.57E-02**		**1.179E-01**		**1.921E-01**		**3.459E-01**

Table C.2 (Con't) Program 1 – Scaling mass loss data (BNQ NQ 2621-900 Annex B)

Mixture: 2.0% SRA-T #2

Specimen	Effective Area in^2	Mass at 7 days		Mass at 21 days		Mass at 35 days	
		g	lb/in^2	g	lb/in^2	g	lb/in^2
A	84.77	44.8	1.21E-03	18.4	0.000498	160.3	0.004341
B	84.76	19.8	5.36E-04	12.2	0.00033	150.2	0.004068
C	85.21	23.8	6.41E-04	12.1	0.000326	31.8	0.000857
Average	84.92		7.97E-04		3.85E-04		3.09E-03
Cumulative mass loss (lb/ft^2)			**1.148E-01**		**1.702E-01**		**6.149E-01**

Mixture: 0.5% CRA-T

Specimen	Effective Area in^2	Mass at 7 days		Mass at 21 days		Mass at 35 days		Mass at 56 days	
		g	lb/in^2	g	lb/in^2	g	lb/in^2	g	lb/in^2
A	82.35	28.6	7.97E-04	Not Tested		15.7	0.000438	2.1	5.85E-05
B	83.66	28.4	7.79E-04			9.4	0.000258	0.5	1.37E-05
C	83.61	40.3	1.11E-03			21.8	0.000599	1.5	4.12E-05
Average	83.21		8.94E-04		0.00E+00		4.31E-04		3.78E-05
Cumulative mass loss (lb/ft^2)			**1.288E-01**		**1.288E-01**		**1.909E-01**		**1.964E-01**

Mixture: 1.0% CRA-T

Specimen	Effective Area in^2	Mass at 7 days		Mass at 21 days		Mass at 35 days		Mass at 56 days	
		g	lb/in^2	g	lb/in^2	g	lb/in^2	g	lb/in^2
A	84.14	3.4	9.28E-05	4.5	0.000123	14.2	0.000387	26.5	0.000723
B	84.37	4.9	1.33E-04	6.2	0.000169	101.5	0.002762	177.8	0.004838
C	83.87	3.9	1.07E-04	5.7	0.000156	78.9	0.00216	59.0	0.001615
Average	84.13		1.11E-04		1.49E-04		1.77E-03		2.39E-03
Cumulative mass loss (lb/ft^2)			**1.60E-02**		**3.75E-02**		**2.923E-01**		**6.367E-01**

Mixture: 2.0% CRA-T

Specimen	Effective Area in^2	Mass at 7 days		Mass at 21 days		Mass at 35 days		Mass at 56 days	
		g	lb/in^2	g	lb/in^2	g	lb/in^2	g	lb/in^2
A	83.67	4.4	1.21E-04	4.2	1.15E-04	14.5	3.98E-04	29.2	0.000801
B	83.49	2.0	5.50E-05	1.7	4.67E-05	3.3	9.07E-05	Not Tested	
C	84.47	3.8	1.03E-04	3.7	1.01E-04	8.7	2.36E-04	7.2	0.000196
Average	83.88		9.30E-05		8.75E-05		2.42E-04		4.98E-04
Cumulative mass loss (lb/ft^2)			**1.34E-02**		**2.60E-02**		**6.08E-02**		**1.326E-01**

Note: Specimen B not tested at 56 days due to noncompliance with BNQ NQ 2621-900. Average cumulative mass loss taken from Specimens A & C.

Table C.3 Program 2 – Fundamental transverse frequency and mass data (ASTM C666 and C215)

Mixture: Control w/ 3.5% air

Cycles	0			20			46			89			134		
Specimen	828A	828B	828C	828A	828B	828C	828A	828B	828C	828A	828B	828C	828A	828B	828C
Frequency n [Hz]	*2353*	*2405*	*2302*	*2336*	*2394*	*2296*	*2329*	*2380*	*2286*	*2323*	*2382*	*2289*	*2310*	*2370*	*2259*
Mass M [g]	*7763.5*	*8024.3*	*7677.6*	*7769.3*	*8028.7*	*7683.1*	*7776.1*	*8034.7*	*7690.1*	*7779.6*	*8035.3*	*7692.9*	*7779.7*	*8032.4*	*7694.3*
Dynamic Modulus (Pa)	4.658E+10	5.029E+10	4.409E+10	4.594E+10	4.986E+10	4.389E+10	4.571E+10	4.932E+10	4.355E+10	4.549E+10	4.940E+10	4.368E+10	4.498E+10	4.889E+10	4.255E+10
Avg. Dy. Modulus (Pa)	4.699E+10			4.656E+10			4.619E+10			4.619E+10			4.547E+10		

Cycles	179			204			231			272			311		
Specimen	828A	828B	828C	828A	828B	828C	828A	828B	828C	828A	828B	828C	828A	828B	828C
Frequency n [Hz]	*2295*	*2360*	*2225*	*2287*	*2347*	*2215*	*2277*	*2336*	*2204*	*2239*	*2296*	*2179*	*2218*	*2260*	*2138*
Mass M [g]	*7779.6*	*8029.9*	*7696.2*	*7782*	*8030.4*	*7697.3*	*7784*	*8031*	*7698*	*7785.2*	*8033.1*	*7699.5*	*7785.8*	*8034*	*7700*
Dynamic Modulus (Pa)	4.440E+10	4.846E+10	4.129E+10	4.411E+10	4.793E+10	4.092E+10	4.373E+10	4.749E+10	4.052E+10	4.229E+10	4.589E+10	3.961E+10	4.151E+10	4.447E+10	3.814E+10
Avg. Dy. Modulus (Pa)	4.472E+10			4.432E+10			4.391E+10			4.260E+10			4.137E+10		

Mixture: Control w/ 6% air

Cycles	0			39			78			118			154		
Specimen	839A	839B	839C	839A	839B	839C	839A	839B	839C	839A	839B	839C	839A	839B	839C
Frequency n [Hz]	*2211*	*2270*	*2298*	*2205*	*2261*	*2290*	*2204*	*2268*	*2295*	*2202*	*2277*	*2306*	*2207*	*2274*	*2303*
Mass M [g]	*7403.6*	*7676.5*	*7725*	*7420.5*	*7691.8*	*7738.3*	*7424.2*	*7692.8*	*7740.4*	*7427*	*7694*	*7742.2*	*7427.7*	*7695.3*	*7744*
Dynamic Modulus (Pa)	3.922E+10	4.286E+10	4.421E+10	3.910E+10	4.261E+10	4.397E+10	3.908E+10	4.288E+10	4.418E+10	3.902E+10	4.323E+10	4.461E+10	3.920E+10	4.312E+10	4.451E+10
Avg. Dy. Modulus (Pa)	4.210E+10			4.189E+10			4.205E+10			4.229E+10			4.228E+10		

Mixture: 0.5% SRA w/ 4% air

Cycles	0			24			52			91			132		
Specimen	832A	832B	832C	832A	832B	832C	832A	832B	832C	832A	832B	832C	832A	832B	832C
Frequency n [Hz]	*2386*	*2332*	*2356*	*2382*	*2331*	*2352*	*2380*	*2330*	*2349*	*2379*	*2330*	*2349*	*2378*	*2330*	*2349*
Mass M [g]	*7921.3*	*7853.7*	*7787*	*7921.5*	*7855.3*	*7789.5*	*7921.3*	*7857.1*	*7790.6*	*7922.2*	*7858.3*	*7792.4*	*7922.9*	*7859*	*7794.3*
Dynamic Modulus (Pa)	4.887E+10	4.628E+10	4.684E+10	4.870E+10	4.625E+10	4.669E+10	4.862E+10	4.622E+10	4.658E+10	4.859E+10	4.623E+10	4.659E+10	4.855E+10	4.623E+10	4.660E+10
Avg. Dy. Modulus (Pa)	4.733E+10			4.722E+10			4.714E+10			4.714E+10			4.713E+10		

Cycles	177			221			261			300		
Specimen	832A	832B	832C	832A	832B	832C	832A	832B	832C	832A	832B	832C
Frequency n [Hz]	*2379*	*2324*	*2332*	*2372*	*2316*	*2315*	*2377*	*2307*	*2273*	*2383*	*2301*	*2231*
Mass M [g]	*7922.8*	*7861.2*	*7796.2*	*7923.8*	*7863.8*	*7799.7*	*7925.2*	*7869.6*	*7804.8*	*7925.2*	*7869.6*	*7804.8*
Dynamic Modulus (Pa)	4.859E+10	4.601E+10	4.594E+10	4.831E+10	4.571E+10	4.530E+10	4.852E+10	4.539E+10	4.370E+10	4.877E+10	4.515E+10	4.210E+10
Avg. Dy. Modulus (Pa)	4.685E+10			4.644E+10			4.587E+10			4.534E+10		

Mixture: 0.5% SRA w/ 7% air

Cycles	0			28			62			101			132		
Specimen	833A	833B	833C	833A	833B	833C	833A	833B	833C	833A	833B	833C	833A	833B	833C
Frequency n [Hz]	*2282*	*2255*	*2235*	*2254*	*2243*	*2224*	*2216*	*2232*	*2214*	*2215*	*2231*	*2214*	*2215*	*2231*	*2214*
Mass M [g]	*7622.3*	*7524.1*	*7460.9*	*7627.3*	*7526.4*	*7463.3*	*7630.3*	*7529*	*7466.1*	*7631.8*	*7529.3*	*7466.4*	*7633.3*	*7529*	*7466.6*
Dynamic Modulus (Pa)	4.301E+10	4.146E+10	4.039E+10	4.199E+10	4.103E+10	4.000E+10	4.060E+10	4.064E+10	3.966E+10	4.057E+10	4.061E+10	3.966E+10	4.058E+10	4.061E+10	3.966E+10
Avg. Dy. Modulus (Pa)	4.162E+10			4.101E+10			4.030E+10			4.028E+10			4.028E+10		

Cycles	177			221			260			300		
Specimen	833A	833B	833C	833A	833B	833C	833A	833B	833C	833A	833B	833C
Frequency n [Hz]	*2200*	*2230*	*2214*	*2195*	*2229*	*2210*	*2195*	*2231*	*2213*	*2195*	*2234*	*2217*
Mass M [g]	*7635.8*	*7529.2*	*7466.2*	*7638.2*	*7529.2*	*7467.5*	*7639.6*	*7529.6*	*7468.4*	*7641*	*7529.9*	*7469.5*
Dynamic Modulus (Pa)	4.005E+10	4.057E+10	3.966E+10	3.988E+10	4.054E+10	3.952E+10	3.989E+10	4.061E+10	3.963E+10	3.989E+10	4.072E+10	3.978E+10
Avg. Dy. Modulus (Pa)	4.009E+10			3.998E+10			4.004E+10			4.013E+10		

Table C.3 (Con't) Program 2 – Fundamental transverse frequency and mass data (ASTM C666 and C215)

Mixture: 1.0% SRA w/ 5.25% air

Cycles	0			22			43			88			133		
Specimen	830A	830B	830C	830A	830B	830C	830A	830B	830C	830A	830B	830C	830A	830B	830C
Frequency n [Hz]	*2307*	*2305*	*2305*	*2289*	*2278*	*2284*	*2268*	*2260*	*2272*	*2257*	*2229*	*2241*	*2245*	*2198*	*2210*
Mass M [g]	*7713.5*	*7631.4*	*7660.5*	*7718.7*	*7635.8*	*7669.2*	*7722.5*	*7638.6*	*7672.1*	*7726*	*7644.8*	*7676.2*	*7729.5*	*7651.6*	*7679.7*
Dynamic Modulus (Pa)	4.449E+10	4.394E+10	4.410E+10	4.382E+10	4.294E+10	4.335E+10	4.305E+10	4.228E+10	4.292E+10	4.265E+10	4.116E+10	4.177E+10	4.221E+10	4.006E+10	4.065E+10
Avg. Dy. Modulus (Pa)	4.418E+10			4.337E+10			4.275E+10			4.186E+10			4.097E+10		

Cycles	161			185			224			265			293		
Specimen	830A	830B	830C	830A	830B	830C	830A	830B	830C	830A	830B	830C	830A	830B	830C
Frequency n [Hz]	*2232*	*2176*	*2185*	*2210*	*2157*	*2150*	*2135*	*2068*	*2094*	*2055*	*1981*	*2035*	*2021*	*1945*	*1981*
Mass M [g]	*7732.3*	*7652.3*	*7683.7*	*7736.7*	*7653.9*	*7687.3*	*7741.5*	*7658.2*	*7690.5*	*7746.5*	*7662.4*	*7694.2*	*7747.6*	*7662.8*	*7694.8*
Dynamic Modulus (Pa)	4.174E+10	3.926E+10	3.975E+10	4.095E+10	3.859E+10	3.851E+10	3.824E+10	3.549E+10	3.654E+10	3.545E+10	3.258E+10	3.453E+10	3.429E+10	3.141E+10	3.272E+10
Avg. Dy. Modulus (Pa)	4.025E+10			3.935E+10			3.676E+10			3.419E+10			3.281E+10		

Cycles	315		
Specimen	830A	830B	830C
Frequency n [Hz]	*1971*	*1895*	*1946*
Mass M [g]	*7748.9*	*7662.6*	*7695.1*
Dynamic Modulus (Pa)	3.262E+10	2.982E+10	3.158E+10
Avg. Dy. Modulus (Pa)	3.134E+10		

Mixture: 1.0% SRA w/ 6.75% air

Cycles	0			37			74			111			155		
Specimen	814A	814B	814C	814A	814B	814C	814A	814B	814C	814A	814B	814C	814A	814B	814C
Frequency n [Hz]	*2256*	*2282*	*2226*	*2230*	*2252*	*2196*	*2231*	*2250*	*2198*	*2200*	*2200*	*2135*	*2147*	*2152*	*2090*
Mass M [g]	*7523.5*	*7531.7*	*7494.1*	*7541.8*	*7547.6*	*7512.4*	*7549.7*	*7556.8*	*7519.5*	*7556.4*	*7560.8*	*7524.5*	*7557*	*7561.7*	*7525.7*
Dynamic Modulus (Pa)	4.149E+10	4.250E+10	4.024E+10	4.064E+10	4.148E+10	3.926E+10	4.072E+10	4.146E+10	3.937E+10	3.963E+10	3.965E+10	3.717E+10	3.775E+10	3.795E+10	3.562E+10
Avg. Dy. Modulus (Pa)	4.141E+10			4.046E+10			4.051E+10			3.882E+10			3.711E+10		

Cycles	201			244			289			334		
Specimen	814A	814B	814C	814A	814B	814C	814A	814B	814C	814A	814B	814C
Frequency n [Hz]	*2098*	*2118*	*2050*	*2098*	*2100*	*2050*	*2018*	*2071*	*1982*	*1935*	*2036*	*1917*
Mass M [g]	*7564.8*	*7567.2*	*7530.4*	*7562.7*	*7565.9*	*7529.2*	*7565.8*	*7567.1*	*7531.7*	*7568.3*	*7568.3*	*7533.7*
Dynamic Modulus (Pa)	3.608E+10	3.678E+10	3.429E+10	3.607E+10	3.616E+10	3.429E+10	3.339E+10	3.517E+10	3.206E+10	3.071E+10	3.400E+10	3.000E+10
Avg. Dy. Modulus (Pa)	3.572E+10			3.551E+10			3.354E+10			3.157E+10		

Mixture: 2.0% SRA w/ 3.5% air

Cycles	0			37			74			111		
Specimen	817A	817B	817C	817A	817B	817C	817A	817B	817C	817A	817B	817C
Frequency n [Hz]	*2309*	*2290*	*2295*	*1982*	*2011*	*1967*	*1432*	*1528*	*1395*	*920*	*1100*	*950*
Mass M [g]	*7668.4*	*7646.1*	*7638.8*	*7698.1*	*7674*	*7671.9*	*7714.2*	*7692.2*	*7690*	*7734.8*	*7708.8*	*7709.2*
Dynamic Modulus (Pa)	4.430E+10	4.345E+10	4.360E+10	3.277E+10	3.363E+10	3.217E+10	1.714E+10	1.946E+10	1.622E+10	7.094E+09	1.011E+10	7.539E+09
Avg. Dy. Modulus (Pa)	4.378E+10			3.286E+10			1.761E+10			8.247E+09		

Mixture: 2.0% SRA w/ 3.75% air

Cycles	0			22			43			88			133		
Specimen	831A	831B	831C	831A	831B	831C	831A	831B	831C	831A	831B	831C	831A	831B	831C
Frequency n [Hz]	*2379*	*2352*	*2401*	*2267*	*2243*	*2278*	*2190*	*2120*	*2211*	*1315*	*1411*	*1391*	*425*	*640*	*560*
Mass M [g]	*7822.3*	*7859.9*	*7997.6*	*7836.1*	*7868.9*	*8004.2*	*7848.4*	*7884*	*8015.3*	*7866.3*	*7907.9*	*8041.1*	*7897.1*	*7936.3*	*8063.8*
Dynamic Modulus (Pa)	4.797E+10	4.712E+10	4.996E+10	4.364E+10	4.290E+10	4.501E+10	4.079E+10	3.840E+10	4.246E+10	1.474E+10	1.706E+10	1.686E+10	1.546E+09	3.523E+09	2.740E+09
Avg. Dy. Modulus (Pa)	4.835E+10			4.385E+10			4.055E+10			1.622E+10			2.603E+09		

Table C.3 (Con't) Program 2 – Fundamental transverse frequency and mass data (ASTM C666 and C215)

Mixture: 2.0% SRA w/ 4.75% air

Cycles	0			22			50			89			129		
Specimen	838A	838B	838C	838A	838B	838C	838A	838B	838C	838A	838B	838C	838A	838B	838C
Frequency n [Hz]	*2330*	*2304*	*2318*	*2271*	*2253*	*2262*	*2199*	*2192*	*2205*	*2000*	*2042*	*1990*	*1832*	*1904*	*1828*
Mass M [g]	*7729.7*	*7642.7*	*7771.3*	*7751.4*	*7662.7*	*7792.9*	*7751.4*	*7662.7*	*7792.9*	*7761.7*	*7672.2*	*7804*	*7763.9*	*7674.7*	*7808.4*
Dynamic Modulus (Pa)	4.547E+10	4.396E+10	4.525E+10	4.332E+10	4.215E+10	4.321E+10	4.062E+10	3.990E+10	4.106E+10	3.364E+10	3.467E+10	3.349E+10	2.824E+10	3.015E+10	2.827E+10
Avg. Dy. Modulus (Pa)	4.489E+10			4.289E+10			4.052E+10			3.393E+10			2.889E+10		

Cycles	168		
Specimen	838A	838B	838C
Frequency n [Hz]	*1660*	*1770*	*1660*
Mass M [g]	*7766.9*	*7677.9*	*7810.6*
Dynamic Modulus (Pa)	2.319E+10	2.607E+10	2.332E+10
Avg. Dy. Modulus (Pa)	2.419E+10		

Mixture: 2.0% SRA w/ 7% air

Cycles	0			40			80			104			130		
Specimen	836A	836B	836C	836A	836B	836C	836A	836B	836C	836A	836B	836C	836A	836B	836C
Frequency n [Hz]	*2292*	*2294*	*2240*	*2278*	*2281*	*2227*	*2261*	*2267*	*2211*	*2260*	*2263*	*2209*	*2260*	*2260*	*2206*
Mass M [g]	*7629.6*	*7715.1*	*7487.6*	*7632.2*	*7722.5*	*7492.1*	*7636.6*	*7728.6*	*7496.4*	*7637.5*	*7728.1*	*7497.6*	*7638.4*	*7727.6*	*7498.4*
Dynamic Modulus (Pa)	4.343E+10	4.400E+10	4.071E+10	4.292E+10	4.354E+10	4.026E+10	4.230E+10	4.304E+10	3.971E+10	4.227E+10	4.289E+10	3.965E+10	4.228E+10	4.277E+10	3.954E+10
Avg. Dy. Modulus (Pa)	4.271E+10			4.224E+10			4.169E+10			4.160E+10			4.153E+10		

Cycles	169			210			248			284			322		
Specimen	836A	836B	836C	836A	836B	836C	836A	836B	836C	836A	836B	836C	836A	836B	836C
Frequency n [Hz]	*2257*	*2266*	*2204*	*2254*	*2265*	*2207*	*2251*	*2265*	*2210*	*2239*	*2251*	*2207*	*2223*	*2243*	*2204*
Mass M [g]	*7640.5*	*7729.4*	*7500.3*	*7645.8*	*7729.5*	*7499.6*	*7645.8*	*7729.5*	*7499.6*	*7646.5*	*7731.7*	*7500*	*7647.5*	*7734.8*	*7503.2*
Dynamic Modulus (Pa)	4.218E+10	4.301E+10	3.948E+10	4.209E+10	4.297E+10	3.958E+10	4.198E+10	4.297E+10	3.969E+10	4.154E+10	4.245E+10	3.959E+10	4.095E+10	4.217E+10	3.950E+10
Avg. Dy. Modulus (Pa)	4.155E+10			4.155E+10			4.155E+10			4.119E+10			4.087E+10		

Table C.4 Program 2 – Scaling mass loss data (BNQ NQ 2621-900 Annex B)

Mixture: Control w/ 3.5% air

	Effective Area	Mass at 7 days		Mass at 21 days		Mass at 35 days		Mass at 56 days	
	in^2	g	lb/in^2	g	lb/in^2	g	lb/in^2	g	lb/in^2
A	82.55	1.5	4.17E-05	1.9	5.28E-05	1.1	3.06E-05	0.7	1.95E-05
B	82.57	1.3	3.61E-05	2.5	6.95E-05	0	0	0	0
C	82.00	1.9	5.32E-05	5.1	0.000143	1.6	4.48E-05	3.1	8.68E-05
Average	82.37		4.37E-05		8.84E-05		3.77E-05		5.31E-05
Cumulative mass loss (lb/ft^2)			**6.29E-03**		**1.90E-02**		**2.44E-02**		**3.21E-02**

Mixture: Control w/ 6% air

	Effective Area	Mass at 7 days		Mass at 21 days		Mass at 35 days		Mass at 56 days	
	in^2	g	lb/in^2	g	lb/in^2	g	lb/in^2	g	lb/in^2
A	79.63	0.2	5.77E-06	7	0.000202	0.2	5.77E-06	0.1	2.88E-06
B	78.79	0.5	1.46E-05	7.7	0.000224	0.6	1.75E-05	0.2	5.83E-06
C	78.09	0.5	1.47E-05	2.5	7.35E-05	0.8	2.35E-05	0.1	2.94E-06
Average	78.84		1.17E-05		1.67E-04		1.56E-05		3.88E-06
Cumulative mass loss (lb/ft^2)			**1.68E-03**		**2.57E-02**		**2.79E-02**		**2.85E-02**

Table C.4 (Con't) Program 2 – Scaling mass loss data (BNQ NQ 2621-900 Annex B)

Mixture: 0.5% SRA w/ 4% air

	Effective Area	Mass at 7 days		Mass at 21 days		Mass at 35 days		Mass at 56 days	
	in^2	g	lb/in^2	g	lb/in^2	g	lb/in^2	g	lb/in^2
A	81.44	1.9	5.36E-05	0.8	2.26E-05	1.1	3.1E-05	10.5	0.000296
B	80.47	3.6	1.03E-04	1.9	5.42E-05	2.6	7.42E-05	21	0.000599
C	79.28	2.4	6.95E-05	2.3	6.66E-05	2.2	6.37E-05	11.2	0.000324
Average	80.39		7.53E-05		4.78E-05		5.63E-05		4.06E-04
Cumulative mass loss (lb/ft^2)			**1.08E-02**		**1.77E-02**		**2.58E-02**		**8.44E-02**

Mixture: 0.5% SRA w/ 7% air

	Effective Area	Mass at 7 days		Mass at 21 days		Mass at 35 days		Mass at 56 days	
	in^2	g	lb/in^2	g	lb/in^2	g	lb/in^2	g	lb/in^2
A	85.98	0.8	2.14E-05	2.5	6.67E-05	3.8	0.000101	18.6	0.000497
B	81.96	0.9	2.52E-05	1.8	5.04E-05	3.4	9.52E-05	8.4	0.000235
C	82.38	0.8	2.23E-05	1.4	3.9E-05	3.3	9.2E-05	10.1	0.000281
Average	83.44		2.30E-05		5.21E-05		9.62E-05		3.38E-04
Cumulative mass loss (lb/ft^2)			**3.31E-03**		**1.08E-02**		**2.47E-02**		**7.33E-02**

Mixture: 1.0% SRA w/ 5.25% air

	Effective Area	Mass at 7 days		Mass at 21 days		Mass at 35 days		Mass at 56 days	
	in^2	g	lb/in^2	g	lb/in^2	g	lb/in^2	g	lb/in^2
A	82.55	4.4	1.22E-04	7.8	0.000217	3.4	9.46E-05	22	0.000612
B	82.57	3.9	1.08E-04	10.8	0.0003	3.9	0.000108	38.2	0.001062
C	82.00	3.6	1.01E-04	6.2	0.000174	1.6	4.48E-05	27.1	0.000759
Average	82.37		1.11E-04		2.30E-04		8.26E-05		8.11E-04
Cumulative mass loss (lb/ft^2)			**1.59E-02**		**4.91E-02**		**6.10E-02**		**1.78E-01**

Mixture: 1.0% SRA w/ 6.75% air

	Effective Area	Mass at 7 days		Mass at 21 days		Mass at 35 days		Mass at 56 days	
	in^2	g	lb/in^2	g	lb/in^2	g	lb/in^2	g	lb/in^2
A	84.99	3.4	9.18E-05	4	0.000108	5.2	0.00014	2.6	7.02E-05
B	85.40	3.2	8.60E-05	5.6	0.000151	4.6	0.000124	2	5.38E-05
C	85.25	4	1.08E-04	6.3	0.00017	5	0.000135	2.1	5.66E-05
Average	85.21		9.52E-05		1.43E-04		1.33E-04		6.02E-05
Cumulative mass loss (lb/ft^2)			**1.37E-02**		**3.43E-02**		**5.34E-02**		**6.21E-02**

Mixture: 2.0% SRA w/ 3.5% air

	Effective Area	Mass at 7 days		Mass at 21 days	
	in^2	g	lb/in^2	g	lb/in^2
A	79.30	23.5	6.80E-04	136.2	0.003943
B	80.91	22.3	6.33E-04	125.4	0.003558
C	79.84	31	8.91E-04	173.6	0.004991
Average	80.02		7.35E-04		4.16E-03
Cumulative mass loss (lb/ft^2)			**1.06E-01**		**7.05E-01**

Table C.4 (Con't) Program 2 – Scaling mass loss data (BNQ NQ 2621-900 Annex B)

Mixture: 2.0% SRA w/ 3.75% air

	Effective Area	Mass at 7 days		Mass at 21 days	
	in^2	g	lb/in^2	g	lb/in^2
A	82.00	7.2	2.02E-04	8.5	0.000238
B	82.98	6.2	1.72E-04	106.9	0.002957
C	82.02	6.7	1.88E-04	109.3	0.003059
Average	82.33		1.87E-04		3.01E-03
Cumulative mass loss (lb/ft^2)			**2.69E-02**		**4.60E-01**

Mixture: 2.0% SRA w/ 4.75% air

	Effective Area	Mass at 7 days		Mass at 21 days		Mass at 35 days		Mass at 56 days	
	in^2	g	lb/in^2	g	lb/in^2	g	lb/in^2	g	lb/in^2
A	78.05	0.3	8.82E-06	13.5	0.000397	12.1	0.000356	13.3	0.000391
B	77.04	0.1	2.98E-06	17.6	0.000524	19	0.000566	16.9	0.000504
C	73.64	0.2	6.23E-06	4.1	0.000128	2.7	8.42E-05	0.5	1.56E-05
Average	76.25		6.01E-06		3.50E-04		3.35E-04		3.03E-04
Cumulative mass loss (lb/ft^2)			**8.66E-04**		**5.12E-02**		**9.95E-02**		**1.43E-01**

Mixture: 2.0% SRA w/ 7% air

	Effective Area	Mass at 7 days		Mass at 21 days		Mass at 35 days		Mass at 56 days	
	in^2	g	lb/in^2	g	lb/in^2	g	lb/in^2	g	lb/in^2
A	84.74	0.2	5.42E-06	0.5	1.35E-05	9.2	0.000249	3.8	0.000103
B	82.00	0.1	2.80E-06	0.6	1.68E-05	24.2	0.000678	6.6	0.000185
C	81.19	0.1	2.83E-06	0.4	1.13E-05	10.9	0.000308	2.3	6.5E-05
Average	82.64		3.68E-06		1.39E-05		4.12E-04		1.18E-04
Cumulative mass loss (lb/ft^2)			**5.30E-04**		**2.53E-03**		**6.18E-02**		**7.87E-02**

Table C.5 Program 3 – Fundamental transverse frequency and mass data (ASTM C666 and C215)

Mixture: 8% LWA - Series 1

Cycles	0			41			87			128			168		
Specimen	756A	756B	756C	756A	756B	756C	756A	756B	756C	756A	756B	756C	756A	756B	756C
Frequency n [Hz]	*2078*	*2061*	*2093*	*2068*	*2059*	*2085*	*2084*	*2070*	*2098*	*2082*	*2069*	*2100*	*2087*	*2070*	*2101*
Mass M [g]	*7036.6*	*6987.9*	*7087*	*7064.8*	*7017.7*	*7116.2*	*7070.2*	*7023.3*	*7122.1*	*7078.3*	*7030.6*	*7128.4*	*7080.7*	*7032.2*	*7130.8*
Dynamic Modulus (Pa)	3.293E+10	3.216E+10	3.364E+10	3.274E+10	3.224E+10	3.352E+10	3.327E+10	3.261E+10	3.397E+10	3.325E+10	3.261E+10	3.407E+10	3.342E+10	3.265E+10	3.411E+10
Avg. Dy. Modulus (Pa)	3.291E+10			3.283E+10			3.329E+10			3.331E+10			3.339E+10		

Cycles	213			237			279			323		
Specimen	756A	756B	756C	756A	756B	756C	756A	756B	756C	756A	756B	756C
Frequency n [Hz]	*2092*	*2070*	*2101*	*2094*	*2074*	*2107*	*2095*	*2080*	*2110*	*2091*	*2078*	*2107*
Mass M [g]	*7082.5*	*7034.7*	*7132.4*	*7081.9*	*7033.2*	*7130.6*	*7081.9*	*7033.2*	*7130.6*	*7080.8*	*7032.7*	*7129.4*
Dynamic Modulus (Pa)	3.359E+10	3.266E+10	3.412E+10	3.365E+10	3.278E+10	3.430E+10	3.368E+10	3.297E+10	3.440E+10	3.355E+10	3.291E+10	3.430E+10
Avg. Dy. Modulus (Pa)	3.346E+10			3.358E+10			3.369E+10			3.358E+10		

Table C.5 (Con't) Program 3 – Fundamental transverse frequency and mass data (ASTM C666 and C215)

Mixture: 10% LWA - Series 1

Cycles	0			27			51			87			130		
Specimen	758A	758B	758C	758A	758B	758C	758A	758B	758C	758A	758B	758C	758A	758B	758C
Frequency n [Hz]	*2081*	*2055*	*2052*	*2074*	*2051*	*2047*	*2064*	*2046*	*2042*	*2061*	*2035*	*2041*	*2060*	*2044*	*2039*
Mass M [g]	*6873.8*	*6874.3*	*6905.1*	*6884.1*	*6886.3*	*6913.9*	*6894*	*6895.4*	*6924.6*	*6895*	*6892.9*	*6925.4*	*6897.8*	*6894.3*	*6927.8*
Dynamic Modulus (Pa)	3.226E+10	3.146E+10	3.151E+10	3.209E+10	3.139E+10	3.139E+10	3.183E+10	3.128E+10	3.129E+10	3.174E+10	3.093E+10	3.126E+10	3.172E+10	3.121E+10	3.121E+10
Avg. Dy. Modulus (Pa)	3.174E+10			3.162E+10			3.146E+10			3.131E+10			3.138E+10		

Cycles	172			217			256			282			306		
Specimen	758A	758B	758C	758A	758B	758C	758A	758B	758C	758A	758B	758C	758A	758B	758C
Frequency n [Hz]	*2059*	*2051*	*2038*	*2068*	*2051*	*2048*	*2067*	*2050*	*2048*	*2067*	*2050*	*2049*	*2053*	*2048*	*2039*
Mass M [g]	*6900.5*	*6898.3*	*6930.7*	*6900.7*	*6899.8*	*6932.3*	*6900.5*	*6899.4*	*6932.2*	*6900.2*	*6899.1*	*6932.2*	*6901.7*	*6900*	*6934.3*
Dynamic Modulus (Pa)	3.170E+10	3.145E+10	3.119E+10	3.198E+10	3.145E+10	3.151E+10	3.195E+10	3.142E+10	3.151E+10	3.195E+10	3.142E+10	3.154E+10	3.152E+10	3.136E+10	3.124E+10
Avg. Dy. Modulus (Pa)	3.145E+10			3.148E+10			3.162E+10			3.163E+10			3.137E+10		

Mixture: 10% LWA, 30% Slag - Series 1

Cycles	0			36			77			121			163		
Specimen	759A	759B	759C	759A	759B	759C	759A	759B	759C	759A	759B	759C	759A	759B	759C
Frequency n [Hz]	*2149*	*2158*	*2169*	*2127*	*2132*	*2150*	*2124*	*2134*	*2147*	*2122*	*2134*	*2145*	*2132*	*2142*	*2152*
Mass M [g]	*7089.8*	*7143.4*	*7194*	*7092.1*	*7146.4*	*7194.8*	*7094.4*	*7147.8*	*7195.7*	*7096.1*	*7149.6*	*7197.7*	*7096.5*	*7150.5*	*7195.3*
Dynamic Modulus (Pa)	3.548E+10	3.605E+10	3.667E+10	3.477E+10	3.520E+10	3.604E+10	3.468E+10	3.527E+10	3.594E+10	3.463E+10	3.528E+10	3.589E+10	3.495E+10	3.555E+10	3.611E+10
Avg. Dy. Modulus (Pa)	3.607E+10			3.534E+10			3.530E+10			3.526E+10			3.554E+10		

Cycles	200			231			255			300		
Specimen	759A	759B	759C	759A	759B	759C	759A	759B	759C	759A	759B	759C
Frequency n [Hz]	*2133*	*2141*	*2150*	*2132*	*2140*	*2149*	*2121*	*2122*	*2142*	*2111*	*2125*	*2140*
Mass M [g]	*7096.3*	*7150.2*	*7194.9*	*7096.5*	*7150.2*	*7194.8*	*7098.3*	*7149.4*	*7194.9*	*7099.1*	*7150.1*	*7196.4*
Dynamic Modulus (Pa)	3.499E+10	3.552E+10	3.604E+10	3.495E+10	3.548E+10	3.601E+10	3.460E+10	3.489E+10	3.577E+10	3.428E+10	3.499E+10	3.571E+10
Avg. Dy. Modulus (Pa)	3.551E+10			3.548E+10			3.509E+10			3.499E+10		

Mixture: 10% LWA, 30% Slag, 3% SF - Series 1

Cycles	0			24			59			83			128		
Specimen	764A	764B	764C	764A	764B	764C	764A	764B	764C	764A	764B	764C	764A	764B	764C
Frequency n [Hz]	*2129*	*2095*	*2118*	*2124*	*2091*	*2115*	*2119*	*2087*	*2114*	*2115*	*2072*	*2095*	*2112*	*2070*	*2097*
Mass M [g]	*7058.8*	*7008.5*	*7065.5*	*7060.2*	*7009.7*	*7066.8*	*7063.1*	*7010.2*	*7068.4*	*7059*	*7009.8*	*7066*	*7060.7*	*7011.4*	*7067.6*
Dynamic Modulus (Pa)	3.467E+10	3.333E+10	3.435E+10	3.451E+10	3.321E+10	3.425E+10	3.437E+10	3.309E+10	3.423E+10	3.422E+10	3.261E+10	3.361E+10	3.413E+10	3.256E+10	3.368E+10
Avg. Dy. Modulus (Pa)	3.412E+10			3.399E+10			3.389E+10			3.348E+10			3.345E+10		

Cycles	165			210			247			279			304		
Specimen	764A	764B	764C	764A	764B	764C	764A	764B	764C	764A	764B	764C	764A	764B	764C
Frequency n [Hz]	*2103*	*2072*	*2100*	*2104*	*2076*	*2100*	*2106*	*2079*	*2101*	*2107*	*2076*	*2100*	*2107*	*2075*	*2100*
Mass M [g]	*7062*	*7012.1*	*7067.1*	*7061.8*	*7011.7*	*7067.5*	*7061.5*	*7011.4*	*7067.8*	*7061.8*	*7012.1*	*7067.9*	*7062.3*	*7012.6*	*7068*
Dynamic Modulus (Pa)	3.384E+10	3.262E+10	3.377E+10	3.388E+10	3.275E+10	3.377E+10	3.394E+10	3.284E+10	3.381E+10	3.397E+10	3.275E+10	3.378E+10	3.397E+10	3.272E+10	3.378E+10
Avg. Dy. Modulus (Pa)	3.341E+10			3.347E+10			3.353E+10			3.350E+10			3.349E+10		

Mixture: 10% LWA, 30% Slag, 6% SF - Series 1

Cycles	0			27			59			83			128		
Specimen	767A	767B	767C	767A	767B	767C	767A	767B	767C	767A	767B	767C	767A	767B	767C
Frequency n [Hz]	*2102*	*2102*	*2114*	*2098*	*2098*	*2111*	*2094*	*2092*	*2107*	*2079*	*2073*	*2083*	*2078*	*2072*	*2085*
Mass M [g]	*7196.9*	*7063.9*	*7065*	*7197.5*	*7064.4*	*7065.7*	*7198.1*	*7064.9*	*7066.2*	*7194.8*	*7062.1*	*7064.2*	*7196.8*	*7063.9*	*7065.2*
Dynamic Modulus (Pa)	3.446E+10	3.382E+10	3.421E+10	3.433E+10	3.370E+10	3.412E+10	3.420E+10	3.350E+10	3.399E+10	3.370E+10	3.289E+10	3.321E+10	3.368E+10	3.286E+10	3.328E+10
Avg. Dy. Modulus (Pa)	3.416E+10			3.405E+10			3.390E+10			3.327E+10			3.327E+10		

Cycles	160			184			210			247			276		
Specimen	767A	767B	767C	767A	767B	767C	767A	767B	767C	767A	767B	767C	767A	767B	767C
Frequency n [Hz]	*2086*	*2079*	*2088*	*2085*	*2079*	*2088*	*2084*	*2079*	*2088*	*2082*	*2078*	*2089*	*2083*	*2079*	*2090*
Mass M [g]	*7196.3*	*7063.7*	*7065.9*	*7196.4*	*7063.4*	*7065.6*	*7196.2*	*7063.5*	*7065.7*	*7196.1*	*7063.4*	*7065.4*	*7197.2*	*7064.6*	*7065.9*
Dynamic Modulus (Pa)	3.393E+10	3.308E+10	3.338E+10	3.390E+10	3.308E+10	3.338E+10	3.387E+10	3.308E+10	3.338E+10	3.380E+10	3.305E+10	3.341E+10	3.384E+10	3.309E+10	3.345E+10
Avg. Dy. Modulus (Pa)	3.347E+10			3.345E+10			3.344E+10			3.342E+10			3.346E+10		

Cycles	304		
Specimen	767A	767B	767C
Frequency n [Hz]	*2084*	*2081*	*2092*
Mass M [g]	*7197.7*	*7065.1*	*7066.3*
Dynamic Modulus (Pa)	3.387E+10	3.315E+10	3.351E+10
Avg. Dy. Modulus (Pa)	3.351E+10		

Table C.5 (Con't) Program 3 – Fundamental transverse frequency and mass data (ASTM C666 and C215)

Mixture: 8% LWA - Series 2

Cycles	0			22			45			79			113		
Specimen	798A	798B	798C	798A	798B	798C	798A	798B	798C	798A	798B	798C	798A	798B	798C
Frequency n [Hz]	*2032*	*2048*	*2070*	*2024*	*2035*	*2055*	*2013*	*2027*	*2049*	*2022*	*2035*	*2055*	*2034*	*2051*	*2073*
Mass M [g]	*7007.9*	*7064.2*	*7115.2*	*7015.3*	*7070.4*	*7123.8*	*7021.7*	*7078.3*	*7129.6*	*7024.3*	*7081.4*	*7132.3*	*7028.6*	*7086.9*	*7137.7*
Dynamic Modulus (Pa)	3.136E+10	3.211E+10	3.304E+10	3.114E+10	3.173E+10	3.260E+10	3.083E+10	3.151E+10	3.244E+10	3.112E+10	3.178E+10	3.264E+10	3.151E+10	3.230E+10	3.324E+10
Avg. Dy. Modulus (Pa)	3.217E+10			3.182E+10			3.159E+10			3.185E+10			3.235E+10		

Cycles	142			185			231			268			296		
Specimen	798A	798B	798C	798A	798B	798C	798A	798B	798C	798A	798B	798C	798A	798B	798C
Frequency n [Hz]	*2031*	*2051*	*2070*	*2028*	*2052*	*2065*	*2042*	*2050*	*2074*	*2042*	*2054*	*2074*	*2043*	*2057*	*2074*
Mass M [g]	*7030.3*	*7088.7*	*7139.6*	*7034.4*	*7094.7*	*7142.2*	*7038.8*	*7097.3*	*7145.2*	*7040*	*7100.9*	*7148.4*	*7042.2*	*7102.3*	*7150.9*
Dynamic Modulus (Pa)	3.142E+10	3.231E+10	3.315E+10	3.135E+10	3.237E+10	3.300E+10	3.180E+10	3.232E+10	3.331E+10	3.181E+10	3.246E+10	3.332E+10	3.185E+10	3.256E+10	3.333E+10
Avg. Dy. Modulus (Pa)	3.230E+10			3.224E+10			3.248E+10			3.253E+10			3.258E+10		

Cycles	335		
Specimen	798A	798B	798C
Frequency n [Hz]	*2043*	*2060*	*2074*
Mass M [g]	*7043.8*	*7104.7*	*7152.5*
Dynamic Modulus (Pa)	3.186E+10	3.267E+10	3.334E+10
Avg. Dy. Modulus (Pa)	3.262E+10		

Mixture: 10% LWA - Series 2

Cycles	0			29			72			118			155		
Specimen	799A	799B	799C	799A	799B	799C	799A	799B	799C	799A	799B	799C	799A	799B	799C
Frequency n [Hz]	*2069*	*1980*	*2052*	*2062*	*1976*	*2049*	*2055*	*1972*	*2047*	*2070*	*1972*	*2051*	*2071*	*1981*	*2050*
Mass M [g]	*6988.3*	*6763.6*	*6993.5*	*6991.4*	*6769*	*6997.7*	*6996.9*	*6775.1*	*7000.7*	*7000.9*	*6779.8*	*7005.2*	*7004.5*	*6783.2*	*7008.1*
Dynamic Modulus (Pa)	3.242E+10	2.873E+10	3.191E+10	3.221E+10	2.864E+10	3.184E+10	3.202E+10	2.855E+10	3.179E+10	3.251E+10	2.857E+10	3.193E+10	3.255E+10	2.885E+10	3.191E+10
Avg. Dy. Modulus (Pa)	3.102E+10			3.090E+10			3.079E+10			3.100E+10			3.111E+10		

Cycles	189			222			265			308		
Specimen	799A	799B	799C	799A	799B	799C	799A	799B	799C	799A	799B	799C
Frequency n [Hz]	*2072*	*1983*	*2054*	*2073*	*1985*	*2058*	*2073*	*1988*	*2058*	*2074*	*1990*	*2058*
Mass M [g]	*7005.9*	*6784.8*	*7004.6*	*7007*	*6785.9*	*7001.3*	*7008.4*	*6787.4*	*7009.2*	*7009.7*	*6789.2*	*7013.8*
Dynamic Modulus (Pa)	3.259E+10	2.891E+10	3.202E+10	3.263E+10	2.897E+10	3.213E+10	3.264E+10	2.907E+10	3.217E+10	3.267E+10	2.913E+10	3.219E+10
Avg. Dy. Modulus (Pa)	3.118E+10			3.125E+10			3.129E+10			3.133E+10		

Mixture: 10% LWA, 30% Slag - Series 2

Cycles	0			20			60			99			131		
Specimen	801A	801B	801C	801A	801B	801C	801A	801B	801C	801A	801B	801C	801A	801B	801C
Frequency n [Hz]	*2071*	*2092*	*2078*	*2066*	*2088*	*2073*	*2059*	*2085*	*2069*	*2058*	*2087*	*2072*	*2063*	*2089*	*2074*
Mass M [g]	*6983.1*	*7051.5*	*6957.8*	*6992.5*	*7067.3*	*6970*	*7009.5*	*7078.3*	*6984.6*	*7015.1*	*7081.9*	*6989.2*	*7016.6*	*7082.9*	*6990.6*
Dynamic Modulus (Pa)	3.246E+10	3.344E+10	3.256E+10	3.234E+10	3.339E+10	3.246E+10	3.220E+10	3.334E+10	3.240E+10	3.220E+10	3.343E+10	3.252E+10	3.236E+10	3.349E+10	3.258E+10
Avg. Dy. Modulus (Pa)	3.282E+10			3.273E+10			3.265E+10			3.271E+10			3.281E+10		

Cycles	164			207			250			275			301		
Specimen	801A	801B	801C	801A	801B	801C	801A	801B	801C	801A	801B	801C	801A	801B	801C
Frequency n [Hz]	*2068*	*2090*	*2076*	*2069*	*2091*	*2084*	*2071*	*2093*	*2090*	*2072*	*2092*	*2091*	*2072*	*2092*	*2093*
Mass M [g]	*7017.8*	*7084*	*6991.4*	*7017.8*	*7084*	*6987.6*	*7018*	*7084.1*	*6985.9*	*7018.3*	*7085*	*6973.6*	*7018*	*7085.5*	*6962*
Dynamic Modulus (Pa)	3.252E+10	3.353E+10	3.265E+10	3.255E+10	3.356E+10	3.289E+10	3.262E+10	3.363E+10	3.307E+10	3.265E+10	3.360E+10	3.304E+10	3.265E+10	3.360E+10	3.305E+10
Avg. Dy. Modulus (Pa)	3.290E+10			3.300E+10			3.310E+10			3.310E+10			3.310E+10		

Mixture: 10% LWA, 30% Slag, 3% SF - Series 2

Cycles	0			20			60			99			140		
Specimen	802A	802B	802C	802A	802B	802C	802A	802B	802C	802A	802B	802C	802A	802B	802C
Frequency n [Hz]	*2075*	*2128*	*2120*	*2069*	*2123*	*2111*	*2063*	*2119*	*2102*	*2067*	*2116*	*2112*	*2067*	*2116*	*2110*
Mass M [g]	*6926.6*	*7045.5*	*7060.8*	*6936.9*	*7063.5*	*7073.1*	*6949.9*	*7070*	*7085.5*	*6953*	*7073.4*	*7089.4*	*6953.5*	*7074*	*7090.9*
Dynamic Modulus (Pa)	3.232E+10	3.457E+10	3.439E+10	3.218E+10	3.450E+10	3.416E+10	3.205E+10	3.440E+10	3.392E+10	3.219E+10	3.432E+10	3.427E+10	3.219E+10	3.432E+10	3.421E+10
Avg. Dy. Modulus (Pa)	3.376E+10			3.361E+10			3.346E+10			3.359E+10			3.358E+10		

Cycles	164			207			244			273			301		
Specimen	802A	802B	802C	802A	802B	802C	802A	802B	802C	802A	802B	802C	802A	802B	802C
Frequency n [Hz]	*2067*	*2118*	*2110*	*2068*	*2120*	*2111*	*2069*	*2122*	*2112*	*2066*	*2119*	*2111*	*2065*	*2118*	*2109*
Mass M [g]	*6954.1*	*7075.5*	*7091.9*	*6955.4*	*7075.6*	*7091.9*	*6956.1*	*7075.8*	*7091.9*	*6956.4*	*7076.2*	*7092.9*	*6956.7*	*7077*	*7094.2*
Dynamic Modulus (Pa)	3.220E+10	3.439E+10	3.421E+10	3.223E+10	3.446E+10	3.425E+10	3.227E+10	3.453E+10	3.428E+10	3.218E+10	3.443E+10	3.425E+10	3.215E+10	3.440E+10	3.419E+10
Avg. Dy. Modulus (Pa)	3.360E+10			3.365E+10			3.369E+10			3.362E+10			3.358E+10		

Table C.5 (Con't) Program 3 – Fundamental transverse frequency and mass data (ASTM C666 and C215)

Mixture: 10% LWA, 30% Slag, 6% SF - Series 2

Cycles	0			20			57			104			147		
Specimen	803A	803B	803C	803A	803B	803C	803A	803B	803C	803A	803B	803C	803A	803B	803C
Frequency n [Hz]	*2203*	*2130*	*2204*	*2197*	*2123*	*2199*	*2190*	*2117*	*2197*	*2190*	*2122*	*2200*	*2191*	*2124*	*2200*
Mass M [g]	*7240.6*	*7020.8*	*7247*	*7244.5*	*7024.3*	*7249.5*	*7248.7*	*7027.9*	*7252.1*	*7251.5*	*7029.5*	*7254.1*	*7251.4*	*7029.9*	*7254.7*
Dynamic Modulus (Pa)	3.808E+10	3.452E+10	3.815E+10	3.789E+10	3.431E+10	3.799E+10	3.767E+10	3.413E+10	3.793E+10	3.769E+10	3.430E+10	3.805E+10	3.772E+10	3.437E+10	3.805E+10
Avg. Dy. Modulus (Pa)	3.691E+10			3.673E+10			3.658E+10			3.668E+10			3.671E+10		

Cycles	190			220			241			277			319		
Specimen	803A	803B	803C	803A	803B	803C	803A	803B	803C	803A	803B	803C	803A	803B	803C
Frequency n [Hz]	*2192*	*2126*	*2199*	*2194*	*2123*	*2198*	*2194*	*2122*	*2198*	*2192*	*2119*	*2193*	*2193*	*2121*	*2198*
Mass M [g]	*7251.1*	*7030.7*	*7254.8*	*7250.8*	*7029.8*	*7255.5*	*7250.5*	*7029.6*	*7255.4*	*7248.5*	*7027.4*	*7253.3*	*7248.8*	*7028.5*	*7253.9*
Dynamic Modulus (Pa)	3.775E+10	3.444E+10	3.802E+10	3.782E+10	3.433E+10	3.798E+10	3.782E+10	3.430E+10	3.798E+10	3.774E+10	3.419E+10	3.780E+10	3.778E+10	3.426E+10	3.798E+10
Avg. Dy. Modulus (Pa)	3.673E+10			3.671E+10			3.670E+10			3.658E+10			3.667E+10		

Table C.6 Program 3 – Scaling mass loss data (BNQ NQ 2621-900 Annex B)

Mixture: 8% LWA - Series 1

	Effective Area	Mass at 7 days		Mass at 21 days		Mass at 35 days		Mass at 56 days	
	in^2	g	lb/in^2	g	lb/in^2	g	lb/in^2	g	lb/in^2
A	83.52	2.2	6.05E-05	2.4	6.6E-05	0.8	2.2E-05	0.5	1.37E-05
B	84.08	2.3	6.28E-05	2.7	7.37E-05	1.4	3.82E-05	1.1	3E-05
C	83.61	2.8	7.69E-05	1.6	4.39E-05	0.8	2.2E-05	0.2	5.49E-06
Average	83.74		6.67E-05		6.12E-05		2.74E-05		1.64E-05
Cumulative mass loss (lb/ft^2)			**9.61E-03**		**1.84E-02**		**2.24E-02**		**2.47E-02**

Mixture: 10% LWA - Series 1

	Effective Area	Mass at 7 days		Mass at 21 days		Mass at 35 days		Mass at 56 days	
	in^2	g	lb/in^2	g	lb/in^2	g	lb/in^2	g	lb/in^2
A	83.56	1.2	3.30E-05	1.4	3.85E-05	1.2	3.3E-05	0.8	2.2E-05
B	83.48	0.5	1.38E-05	1	2.75E-05	0.8	2.2E-05	1	2.75E-05
C	83.20	1.3	3.59E-05	1.3	3.59E-05	1.4	3.86E-05	0.8	2.21E-05
Average	83.41		2.75E-05		3.39E-05		3.12E-05		2.39E-05
Cumulative mass loss (lb/ft^2)			**3.96E-03**		**8.85E-03**		**1.33E-02**		**1.68E-02**

Mixture: 10% LWA, 30% Slag - Series 1

	Effective Area	Mass at 7 days		Mass at 21 days		Mass at 35 days		Mass at 56 days	
	in^2	g	lb/in^2	g	lb/in^2	g	lb/in^2	g	lb/in^2
A	79.90	5	1.44E-04	14.1	0.000405	2.9	8.33E-05	9.1	0.000261
B	80.43	3.3	9.42E-05	21	0.000599	4	0.000114	2.1	5.99E-05
C	80.05	7.2	2.06E-04	16.2	0.000465	3.9	0.000112	7.6	0.000218
Average	80.13		1.48E-04		4.90E-04		1.03E-04		1.80E-04
Cumulative mass loss (lb/ft^2)			**2.13E-02**		**9.18E-02**		**1.07E-01**		**1.33E-01**

Table C.6 (Con't) Program 3 – Scaling mass loss data (BNQ NQ 2621-900 Annex B)

Mixture: 10% LWA, 30% Slag, 3% SF - Series 1

	Effective Area	Mass at 7 days		Mass at 21 days		Mass at 35 days		Mass at 56 days	
	in^2	g	lb/in^2	g	lb/in^2	g	lb/in^2	g	lb/in^2
A	83.83	7.2	1.97E-04	27.1	0.000742	24.3	0.000665	18.5	0.000507
B	84.21	8.4	2.29E-04	20.3	0.000553	28.5	0.000777	10	0.000273
C	84.70	7.3	1.98E-04	16.2	0.000439	39.5	0.001071	17.5	0.000474
Average	84.25		2.08E-04		5.78E-04		8.38E-04		4.18E-04
Cumulative mass loss (lb/ft^2)			**3.00E-02**		**1.13E-01**		**2.34E-01**		**2.94E-01**

Mixture: 10% LWA, 30% Slag, 6% SF - Series 1

	Effective Area	Mass at 7 days		Mass at 21 days		Mass at 35 days		Mass at 56 days	
	in^2	g	lb/in^2	g	lb/in^2	g	lb/in^2	g	lb/in^2
A	84.78	15.7	4.25E-04	21.9	0.000593	1.5	4.06E-05	15.7	0.000425
B	84.25	20.5	5.59E-04	21.3	0.00058	22.3	0.000608	13.2	0.00036
C	84.51	26.3	7.14E-04	19.6	0.000532	26.2	0.000712	15.1	0.00041
Average	84.51		5.66E-04		5.69E-04		4.53E-04		3.98E-04
Cumulative mass loss (lb/ft^2)			**8.15E-02**		**1.63E-01**		**2.29E-01**		**2.86E-01**

Mixture: 8% LWA - Series 2

	Effective Area	Mass at 7 days		Mass at 21 days		Mass at 35 days		Mass at 56 days	
	in^2	g	lb/in^2	g	lb/in^2	g	lb/in^2	g	lb/in^2
A	83.45	0.8	2.20E-05	0.5	1.38E-05	0.4	1.1E-05	0.3	8.25E-06
B	83.78	0.8	2.19E-05	1	2.74E-05	0.3	8.22E-06	0.3	8.22E-06
C	81.96	0.7	1.96E-05	0.4	1.12E-05	0.5	1.4E-05	0.6	1.68E-05
Average	83.06		2.12E-05		1.75E-05		1.11E-05		1.11E-05
Cumulative mass loss (lb/ft^2)			**3.05E-03**		**5.56E-03**		**7.16E-03**		**8.76E-03**

Mixture: 10% LWA - Series 2

	Effective Area	Mass at 7 days		Mass at 21 days		Mass at 35 days		Mass at 56 days	
	in^2	g	lb/in^2	g	lb/in^2	g	lb/in^2	g	lb/in^2
A	83.88	0.9	2.46E-05	1.3	3.56E-05	0.3	8.21E-06	0.6	1.64E-05
B	82.73	1.8	5.00E-05	2.1	5.83E-05	0.6	1.67E-05	0.9	2.5E-05
C	83.85	1.5	4.11E-05	2.6	7.12E-05	0.4	1.1E-05	0.4	1.1E-05
Average	83.49		3.86E-05		5.50E-05		1.19E-05		1.74E-05
Cumulative mass loss (lb/ft^2)			**5.55E-03**		**1.35E-02**		**1.52E-02**		**1.77E-02**

Mixture: 10% LWA, 30% Slag - Series 2

	Effective Area	Mass at 7 days		Mass at 21 days		Mass at 35 days		Mass at 56 days	
	in^2	g	lb/in^2	g	lb/in^2	g	lb/in^2	g	lb/in^2
A	82.89	2.5	6.92E-05	8.1	0.000224	4.3	0.000119	7.9	0.000219
B	78.00	0.9	2.65E-05	3.6	0.000106	2.2	6.48E-05	5.3	0.000156
C	78.38	0.6	1.76E-05	3.2	9.37E-05	1.9	5.57E-05	4	0.000117
Average	79.75		3.78E-05		1.41E-04		7.98E-05		1.64E-04
Cumulative mass loss (lb/ft^2)			**5.44E-03**		**2.58E-02**		**3.73E-02**		**6.09E-02**

Table C.6 (Con't) Program 3 – Scaling mass loss data (BNQ NQ 2621-900 Annex B)

Mixture: 10% LWA, 30% Slag, 3% SF - Series 2

	Effective Area	Mass at 7 days		Mass at 21 days		Mass at 35 days		Mass at 56 days	
	in^2	g	lb/in^2	g	lb/in^2	g	lb/in^2	g	lb/in^2
A	78.77	6.3	1.84E-04	12.7	0.00037	4.9	0.000143	13.1	0.000382
B	80.73	8.4	2.39E-04	12.5	0.000355	6.3	0.000179	23.2	0.00066
C	80.73	3.9	1.11E-04	4.2	0.000119	2.8	7.96E-05	0	0
Average	80.07		1.78E-04		2.82E-04		1.34E-04		5.21E-04
Cumulative mass loss (lb/ft^2)			**2.56E-02**		**6.62E-02**		**8.54E-02**		**1.60E-01**

Mixture: 10% LWA, 30% Slag, 6% SF - Series 2

	Effective Area	Mass at 7 days		Mass at 21 days		Mass at 35 days		Mass at 56 days	
	in^2	g	lb/in^2	g	lb/in^2	g	lb/in^2	g	lb/in^2
A	77.63	3.3	9.76E-05	16.3	0.000482	18.8	0.000556	19.5	0.000577
B	79.42	1.4	4.05E-05	17.5	0.000506	16.8	0.000486	19.4	0.000561
C	78.80	11.6	3.38E-04	18.8	0.000548	11.4	0.000332	24.1	0.000702
Average	78.61		1.59E-04		5.12E-04		4.58E-04		6.13E-04
Cumulative mass loss (lb/ft^2)			**2.28E-02**		**9.66E-02**		**1.62E-01**		**2.51E-01**

Mixture: 8% LWA - Series 3

	Effective Area	Mass at 7 days		Mass at 21 days		Mass at 35 days		Mass at 56 days	
	in^2	g	lb/in^2	g	lb/in^2	g	lb/in^2	g	lb/in^2
A	81.37	1.9	5.36E-05	2.1	5.92E-05	0.1	2.82E-06	2	5.64E-05
B	82.52	1.7	4.73E-05	1.8	5.01E-05	0.1	2.78E-06	2.3	6.4E-05
C	82.57	1.6	4.45E-05	1.8	5E-05	0.2	5.56E-06	0.8	2.22E-05
Average	82.15		4.85E-05		5.31E-05		3.72E-06		4.76E-05
Cumulative mass loss (lb/ft^2)			**6.98E-03**		**1.46E-02**		**1.52E-02**		**2.20E-02**

Mixture: 10% LWA - Series 3

	Effective Area	Mass at 7 days		Mass at 21 days		Mass at 35 days		Mass at 56 days	
	in^2	g	lb/in^2	g	lb/in^2	g	lb/in^2	g	lb/in^2
A	85.42	0.2	5.37E-06	3.4	9.14E-05	0.1	2.69E-06	1.9	5.11E-05
B	83.59	1	2.75E-05	1.6	4.39E-05	0.3	8.24E-06	1	2.75E-05
C	84.81	0.6	1.62E-05	4.4	0.000119	0.3	8.12E-06	2.3	6.23E-05
Average	84.61		1.64E-05		8.48E-05		6.35E-06		4.69E-05
Cumulative mass loss (lb/ft^2)			**2.36E-03**		**1.46E-02**		**1.55E-02**		**2.22E-02**

Mixture: 10% LWA, 30% Slag - Series 3

	Effective Area	Mass at 7 days		Mass at 21 days		Mass at 35 days		Mass at 56 days	
	in^2	g	lb/in^2	g	lb/in^2	g	lb/in^2	g	lb/in^2
A	86.90	2.4	6.34E-05	4.4	0.000116	3.9	0.000103	1.3	3.43E-05
B	84.97	2.3	6.21E-05	3.2	8.65E-05	7.7	0.000208	1.9	5.13E-05
C	85.10	2.3	6.20E-05	4.3	0.000116	6.2	0.000167	1	2.7E-05
Average	85.66		6.25E-05		1.06E-04		1.59E-04		3.76E-05
Cumulative mass loss (lb/ft^2)			**9.00E-03**		**2.43E-02**		**4.73E-02**		**5.27E-02**

Table C.6 (Con't) Program 3 – Scaling mass loss data (BNQ NQ 2621-900 Annex B)

Mixture: 10% LWA, 30% Slag, 3% SF - Series 3

	Effective Area	Mass at 7 days		Mass at 21 days		Mass at 35 days		Mass at 56 days	
	in^2	g	lb/in^2	g	lb/in^2	g	lb/in^2	g	lb/in^2
A	82.81	9.3	2.58E-04	11	0.000305	4.2	0.000116	5.5	0.000152
B	82.67	7.4	2.06E-04	22.2	0.000617	9.1	0.000253	5.6	0.000156
C	82.28	7	1.95E-04	16	0.000446	7.6	0.000212	8.3	0.000232
Average	82.59		2.20E-04		4.56E-04		1.94E-04		1.80E-04
Cumulative mass loss (lb/ft^2)			**3.16E-02**		**9.73E-02**		**1.25E-01**		**1.51E-01**

Mixture: 10% LWA, 30% Slag, 6% SF - Series 3

	Effective Area	Mass at 7 days		Mass at 21 days		Mass at 35 days		Mass at 56 days	
	in^2	g	lb/in^2	g	lb/in^2	g	lb/in^2	g	lb/in^2
A	84.86	4.1	1.11E-04	7.3	0.000197	6.5	0.000176	11.9	0.000322
B	83.33	4.4	1.21E-04	13	0.000358	6.8	0.000187	11.4	0.000314
C	85.76	3.5	9.37E-05	11.4	0.000305	5.7	0.000153	13	0.000348
Average	84.65		1.09E-04		2.87E-04		1.72E-04		3.28E-04
Cumulative mass loss (lb/ft^2)			**1.56E-02**		**5.70E-02**		**8.17E-02**		**1.29E-01**

APPENDIX D: LOW-CRACKING HIGH-PERFORMANCE CONCRETE (LC-HPC) SPECIFICATIONS – AGGREGATES, CONCRETE, AND CONSTRUCTION

KANSAS DEPARTMENT OF TRANSPORTATION
SPECIAL PROVISION TO THE
STANDARD SPECIFICATIONS, 2007 EDITION

Add a new SECTION to DIVISION 1100:

LOW-CRACKING HIGH-PERFORMANCE CONCRETE – AGGREGATES

1.0 DESCRIPTION

This specification is for coarse aggregates, fine aggregates, and mixed aggregates (both coarse and fine material) for use in bridge deck construction.

2.0 REQUIREMENTS

a. Coarse Aggregates for Concrete.

(1) Composition. Provide coarse aggregate that is crushed or uncrushed gravel, chat, or crushed stone. (Consider calcite cemented sandstone, rhyolite, basalt and granite as crushed stone

(2) Quality. The quality requirements for coarse aggregate for bridge decks are in **TABLE 1-1:**

TABLE 1-1: QUALITY REQUIREMENTS FOR COARSE AGGREGATES FOR BRIDGE DECK				
Concrete Classification	**Soundness (min.)**	**Wear (max.)**	**Absorption (max.)**	**Acid Insol. (min.)**
Grade 3.5 (AE) (LC-HPC) [1]	0.90	40	0.7	55

[1] Grade 3.5 (AE) (LC-HPC) – Bridge Deck concrete with select coarse aggregate for wear and acid insolubility.

(3) Product Control.

(a) Deleterious Substances. Maximum allowed deleterious substances by weight are:

- Material passing the No. 200 sieve (KT-2)..... 2.5%
- Shale or Shale-like material (KT-8)..... 0.5%
- Clay lumps and friable particles (KT-7) 1.0%
- Sticks (wet) (KT-35)..... 0.1%
- Coal (AASHTO T 113)..... 0.5%

(b) Uniformity of Supply. Designate or determine the fineness modulus (grading factor) according to the procedure listed in the Construction Manual Part V, Section 17 before delivery, or from the first 10 samples tested and accepted. Provide aggregate that is within ±0.20 of the average fineness modulus.

(4) Do not combine siliceous fine aggregate with siliceous coarse aggregate if neither meet the requirements of **subsection 2.0c.(2)(a)**. Consider such fine material, regardless of proportioning, as a Basic Aggregate that must conform to **subsection 2.0c**.

(5) Handling Coarse Aggregates.

(a) Segregation. Before acceptance testing, remix all aggregate segregated by transportation or stockpiling operations.

(b) Stockpiling.

- Stockpile accepted aggregates in layers 3 to 5 feet thick. Berm each layer so that aggregates do not "cone" down into lower layers.
- Keep aggregates from different sources, with different gradings, or with a significantly different specific gravity separated.
- Transport aggregate in a manner that insures uniform gradation.
- Do not use aggregates that have become mixed with earth or foreign material.
- Stockpile or bin all washed aggregate produced or handled by hydraulic methods for 12 hours (minimum) before batching. Rail shipment exceeding 12 hours is acceptable for binning provided the car bodies permit free drainage.

- Provide additional stockpiling or binning in cases of high or non-uniform moisture.

b. Fine Aggregates for Basic Aggregate in MA for Concrete.

(1) Composition.

(a) Type FA-A. Provide either singly or in combination natural occurring sand resulting from the disintegration of siliceous or calcareous rock, or manufactured sand produced by crushing predominately siliceous materials.

(b) Type FA-B. Provide fine granular particles resulting from the crushing of zinc and lead ores (Chat).

(2) Quality.

(a) Mortar strength and Organic Impurities. If the District Materials Engineer determines it is necessary, because of unknown characteristics of new sources or changes in existing sources, provide fine aggregates that comply with these requirements:

- Mortar Strength (Mortar Strength Test, KTMR-26). Compressive strength when combined with Type III (high early strength) cement:
  - At age 24 hours, minimum……...100%*
  - At age 72 hours, minimum……...100%*

  *Compared to strengths of specimens of the same proportions, consistency, cement and standard 20-30 Ottawa sand.
- Organic Impurities (Organic Impurities in Fine Aggregate for Concrete Test, AASHTO T 21). The color of the supernatant liquid is equal to or lighter than the reference standard solution.

(b) Hardening characteristics. Specimens made of a mixture of 3 parts FA-B and 1 part cement with sufficient water for molding will harden within 24 hours. There is no hardening requirement for FA-A.

(3) Product Control.

(a) Deleterious Substances.

- Type FA-A: Maximum allowed deleterious substances by weight are:
  - Material passing the No. 200 sieve (KT-2)……..……. 2.0%
  - Shale or Shale-like material (KT-8) ……. 0.5%
  - Clay lumps and friable particles (KT-7)……..……. 1.0%
  - Sticks (wet) (KT-35)……...…… 0.1%
- Type FA-B: Provide materials that are free of organic impurities, sulfates, carbonates, or alkali. Maximum allowed deleterious substances by weight are:
  - Material passing the No. 200 sieve (KT-2)…….…….…..... 2.0%
  - Clay lumps & friable particles (KT-7)……. 0.25%

(c) Uniformity of Supply. Designate or determine the fineness modulus (grading factor) according to the procedure listed in the Construction Manual Part V, Section 17 before delivery, or from the first 10 samples tested and accepted. Provide aggregate that is within ±0.20 of the average fineness modulus.

(4) Proportioning of Coarse and Fine Aggregate. Use a proven optimization method such as the Shilstone Method or the KU Mix Method.

Do not combine siliceous fine aggregate with siliceous coarse aggregate if neither meet the requirements of **subsection 2.0c.(2)(a)**. Consider such fine material, regardless of proportioning, as a Basic Aggregate and must conform to the requirements in **subsection 2.0c**.

(5) Handling and Stockpiling Fine Aggregates.

- Keep aggregates from different sources, with different gradings or with a significantly different specific gravity separated.
- Transport aggregate in a manner that insures uniform grading.
- Do not use aggregates that have become mixed with earth or foreign material.
- Stockpile or bin all washed aggregate produced or handled by hydraulic methods for 12 hours (minimum) before batching. Rail shipment exceeding 12 hours is acceptable for binning provided the car bodies permit free drainage.
- Provide additional stockpiling or binning in cases of high or non-uniform moisture.

c. Mixed Aggregates for Concrete.

(1) Composition.

(a) Total Mixed Aggregate (TMA). A natural occurring, predominately siliceous aggregate from a single source that meets the Wetting & Drying Test (KTMR-23) and grading requirements.

(b) Mixed Aggregate. A combination of basic and coarse aggregates that meet **TABLE 1-2**.

- Basic Aggregate (BA). Singly or in combination, a natural occurring, predominately siliceous aggregate that does not meet the grading requirements of Total Mixed Aggregate.

(c) Coarse Aggregate. Granite, crushed sandstone, chat, and gravel. Gravel that is not approved under **subsection 2.0c.(2)** may be used, but only with basic aggregate that meets the wetting and drying requirements of TMA.

(2) Quality.

(a) Total Mixed Aggregate.

- Soundness, minimum (KTMR-21) ……..……0.90
- Wear, maximum (KTMR-25) ……..……50%
- Wetting and Drying Test (KTMR-23) for Total Mixed Aggregate
  Concrete Modulus of Rupture:
  - At 60 days, minimum……..550 psi
  - At 365 days, minimum…..……..……550 psi

  Expansion:
  - At 180 days, maximum……..…….0.050%
  - At 365 days, maximum……..…….0.070%

  Aggregates produced from the following general areas are exempt from the Wetting and Drying Test:
  - Blue River Drainage Area.
  - The Arkansas River from Sterling, west to the Colorado state line.
  - The Neosho River from Emporia to the Oklahoma state line.

(b) Basic Aggregate.

- Retain 10% or more of the BA on the No. 8 sieve before adding the Coarse Aggregate. Aggregate with less than 10% retained on the No. 8 sieve is to be considered a Fine Aggregate described in **subsection 2.0b**. Provide material with less than 5% calcareous material retained on the ⅜" sieve.
- Soundness, minimum (KTMR-21)…….0.90
- Wear, maximum (KTMR-25)……..……50%
- Mortar strength and Organic Impurities. If the District Materials Engineer determines it is necessary, because of unknown characteristics of new sources or changes in existing sources, provide mixed aggregates that comply with these requirements:
  - Mortar Strength (Mortar Strength Test, KTMR-26). Compressive strength when combined with Type III (high early strength) cement:
    - At age 24 hours, minimum……..100%*
    - At age 72 hours, minimum……..100%*
      *Compared to strengths of specimens of the same proportions, consistency, cement and standard 20-30 Ottawa sand.
  - Organic Impurities (Organic Impurities in Fine Aggregate for Concrete Test, AASHTO T 21). The color of the supernatant liquid is equal to or lighter than the reference standard solution.

(3) Product Control.

(a) Size Requirement. Provide mixed aggregates that comply with the grading requirements in **TABLE 1-2**.

TABLE 1-2: GRADING REQUIREMENTS FOR MIXED AGGREGATES FOR CONCRETE BRIDGE DECKS

Type	Usage	Percent Retained on Individual Sieves - Square Mesh Sieves										
		1½"	1"	3/4"	1/2"	3/8"	No. 4	No. 8	No. 16	No. 30	No. 50	No. 100
MA-4	Optimized for LC-HPC Bridge Decks*	0	2-6	5-18	8-18	8-18	8-18	8-18	8-18	8-15	5-15	0-5

*Use a proven optimization method, such as the Shilstone Method or the KU Mix Method.

Note: Manufactured sands used to obtain optimum gradations have caused difficulties in pumping, placing or finishing. Natural coarse sands and pea gravels used to obtain optimum gradations have worked well in concretes that were pumped.

(b) Deleterious Substances. Maximum allowed deleterious substances by weight are:

- Material passing the No. 200 sieve (KT-2)……..….. 2.5%
- Shale or Shale-like material (KT-8)……..……. 0.5%
- Clay lumps and friable particles (KT-7)…… 1.0%
- Sticks (wet) (KT-35)……..…… 0.1%
- Coal (AASHTO T 113)…..……..……. 0.5%

(c) Uniformity of Supply. Designate or determine the fineness modulus (grading factor) according to the procedure listed in the Construction Manual Part V, Section 17 before delivery, or from the first 10 samples tested and accepted. Provide aggregate that is within ±0.20 of the average fineness modulus.

(4) Handling Mixed Aggregates.

(a) Segregation. Before acceptance testing, remix all aggregate segregated by transit or stockpiling.

(b) Stockpiling.

- Keep aggregates from different sources, with different gradings or with a significantly different specific gravity separated.
- Transport aggregate in a manner that insures uniform grading.
- Do not use aggregates that have become mixed with earth or foreign material.
- Stockpile or bin all washed aggregate produced or handled by hydraulic methods for 12 hours (minimum) before batching. Rail shipment exceeding 12 hours is acceptable for binning provided the car bodies permit free drainage.
- Provide additional stockpiling or binning in cases of high or non-uniform moisture.

3.0 TEST METHODS

Test aggregates according to the applicable provisions of **SECTION 1117**.

4.0 PREQUALIFICATION

Aggregates for concrete must be prequalified according to **subsection 1101.2**.

5.0 BASIS OF ACCEPTANCE

The Engineer will accept aggregates for concrete base on the prequalification required by this specification, and **subsection 1101.4**.

KANSAS DEPARTMENT OF TRANSPORTATION
SPECIAL PROVISION TO THE
STANDARD SPECIFICATIONS 2007 EDITION

Add a new SECTION to DIVISION 400:

LOW-CRACKING HIGH-PERFORMANCE CONCRETE

1.0 DESCRIPTION

Provide the grades of low-cracking high-performance concrete (LC-HPC) specified in the Contract Documents.

2.0 MATERIALS

Coarse, Fine & Mixed Aggregate..... **07-PS0165, latest version**
Admixtures..... **DIVISION 1400**
Cement ..... **DIVISION 2000**
Water ..... **DIVISION 2400**

3.0 CONCRETE MIX DESIGN

a. General. Design the concrete mixes specified in the Contract Documents.

Provide aggregate gradations that comply with **07-PS0165, latest version** and Contract Documents.

If desired, contact the DME for available information to help determine approximate proportions to produce concrete having the required characteristics on the project.

Take full responsibility for the actual proportions of the concrete mix, even if the Engineer assists in the design of the concrete mix.

Submit all concrete mix designs to the Engineer for review and approval. Submit completed volumetric mix designs on KDOT Form No. 694 (or other forms approved by the DME).

Do not place any concrete on the project until the Engineer approves the concrete mix designs. Once the Engineer approves the concrete mix design, do not make changes without the Engineer's approval.

Design concrete mixes that comply with these requirements:

b. Air-Entrained Concrete for Bridge Decks. Design air-entrained concrete for structures according to **TABLE 1-1**.

TABLE 1-1: AIR ENTRAINED CONCRETE FOR BRIDGE DECKS

Grade of Concrete Type of Aggregate (SECTION 1100)	lb of Cementitious Material per cu yd of Concrete, min/max	lb of Water per lb of Cementitious Material*	Designated Air Content Percent by Volume**	Specified 28-day Compressive Strength Range, psi
Grade 3.5 (AE) (LC-HPC)				
MA-4	500 / 540	0.44 – 0.45	8.0 ± 1.0	3500 – 5500

*Limits of lb. of water per lb. of cementitious material. Includes free water in aggregates, but excludes water of absorption of the aggregates. With approval of the Engineer, may be decreased to 0.43 on-site.

**Concrete with an air content less than 6.5% or greater than 9.5% shall be rejected. The Engineer will sample concrete for tests at the discharge end of the conveyor, bucket or if pumped, the piping.

c. Portland Cement. Select the type of portland cement specified in the Contract Documents. Mineral admixtures are prohibited for Grade 3.5 (AE) (LC-HPC) concrete.

d. Design Air Content. Use the middle of the specified air content range for the design of air-entrained concrete.

e. Admixtures for Air-Entrainment and Water Reduction. Verify that the admixtures used are compatible and will work as intended without detrimental effects. Use the dosages recommended by the admixture

manufacturers to determine the quantity of each admixture for the concrete mix design. Incorporate and mix the admixtures into the concrete mixtures according to the manufacturer's recommendations.

Set retarding or accelerating admixtures are prohibited for use in Grade 3.5 (AE) (LC-HPC) concrete. These include Type B, C, D, E, and G chemical admixtures as defined by ASTM C 494/C 494M – 08. Do not use admixtures containing chloride ion (CL) in excess of 0.1 percent by mass of the admixture in Grade 3.5 (AE) (LC-HPC) concrete.

(1) Air-Entraining Admixture. If specified, use an air-entraining admixture in the concrete mixture. If another admixture is added to an air-entrained concrete mixture, determine if it is necessary to adjust the air-entraining admixture dosage to maintain the specified air content. Use only a vinsol resin or tall oil based air-entraining admixture.

(2) Water-Reducing Admixture. Use a Type A water reducer or a dual rated Type A water reducer – Type F high-range water reducer, when necessary to obtain compliance with the specified fresh and hardened concrete properties.

Include a batching sequence in the concrete mix design. Consider the location of the concrete plant in relation to the job site, and identify the approximate quantity, when and at what location the water-reducing admixture is added to the concrete mixture.

The manufacturer may recommend mixing revolutions beyond the limits specified in **subsection 5.0**. If necessary and with the approval of the Engineer, address the additional mixing revolutions (the Engineer will allow up to 60 additional revolutions) in the concrete mix design.

Slump control may be accomplished in the field only by redosing with a water-reducing admixture. If time and temperature limits are not exceeded, and if at least 30 mixing revolutions remain, the Engineer will allow redosing with up to 50% of the original dose.

(3) Adjust the mix designs during the course of the work when necessary to achieve compliance with the specified fresh and hardened concrete properties. Only permit such modifications after trial batches to demonstrate that the adjusted mix design will result in concrete that complies with the specified concrete properties.

The Engineer will allow adjustments to the dose rate of air entraining and water-reducing chemical admixtures to compensate for environmental changes during placement without a new concrete mix design or qualification batch.

f. Designated Slump. Designate a slump for each concrete mix design within the limits in **TABLE 1-2**.

TABLE 1-2: DESIGNATED SLUMP*

Type of Work	Designated Slump (inches)
Grade 3.5 (AE) (LC-HPC)	1 ½ - 3

* The Engineer will obtain sample concrete at the discharge end of the conveyor, bucket or if pumped, the piping.

If potential problems are apparent at the discharge of any truck, and the concrete is tested at the truck discharge (according to **subsection 6.0**), the Engineer will reject concrete with a slump greater than 3 ½ inches at the truck discharge, 3 inches if being placed by a bucket.

4.0 REQUIREMENTS FOR COMBINED MATERIALS

a. Measurements for Proportioning Materials.

(1) Cement. Measure cement as packed by the manufacturer. A sack of cement is considered as 0.04 cubic yards weighing 94 pounds net. Measure bulk cement by weight. In either case, the measurement must be accurate to within 0.5% throughout the range of use.

(2) Water. Measure the mixing water by weight or volume. In either case, the measurement must be accurate to within 1% throughout the range of use.

(3) Aggregates. Measure the aggregates by weight. The measurement must be accurate to within 0.5% throughout the range of use.

(4) Admixtures. Measure liquid admixtures by weight or volume. If liquid admixtures are used in small quantities in proportion to the cement as in the case of air-entraining agents, use readily adjustable mechanical dispensing equipment capable of being set to deliver the required quantity and to cut off the flow automatically when this quantity is discharged. The measurement must be accurate to within 3% of the quantity required.

b. Testing of Aggregates. Testing Aggregates at the Batch Site. Provide the Engineer with reasonable facilities at the batch site for obtaining samples of the aggregates. Provide adequate and safe laboratory facilities at the batch site allowing the Engineer to test the aggregates for compliance with the specified requirements.

KDOT will sample and test aggregates from each source to determine their compliance with specifications. Do not batch the concrete mixture until the Engineer has determined that the aggregates comply with the specifications. KDOT will conduct sampling at the batching site, and test samples according to the Sampling and Testing Frequency Chart in Part V. For QC/QA Contracts, establish testing intervals within the specified minimum frequency.

After initial testing is complete and the Engineer has determined that the aggregate process control is satisfactory, use the aggregates concurrently with sampling and testing as long as tests indicate compliance with specifications. When batching, sample the aggregates as near the point of batching as feasible. Sample from the stream as the storage bins or weigh hoppers are loaded. If samples can not be taken from the stream, take them from approved stockpiles, or use a template and sample from the conveyor belt. If test results indicate an aggregate does not comply with specifications, cease concrete production using that aggregate. Unless a tested and approved stockpile for that aggregate is available at the batch plant, do not use any additional aggregate from that source and specified grading until subsequent sampling and testing of that aggregate indicate compliance with specifications. When tests are completed and the Engineer is satisfied that process control is again adequate, production of concrete using aggregates tested concurrently with production may resume.

c. Handling of Materials.

(1) Aggregate Stockpiles. Approved stockpiles are permitted only at the batch plant and only for small concrete placements or for the purpose of maintaining concrete production. Mark the approved stockpile with an "Approved Materials" sign. Provide a suitable stockpile area at the batch plant so that aggregates are stored without detrimental segregation or contamination. At the plant, limit stockpiles of tested and approved coarse aggregate and fine aggregate to 250 tons each, unless approved for more by the Engineer. If mixed aggregate is used, limit the approved stockpile to 500 tons, the size of each being proportional to the amount of each aggregate to be used in the mix.

Load aggregates into the mixer so no material foreign to the concrete or material capable of changing the desired proportions is included. When 2 or more sizes or types of coarse or fine aggregates are used on the same project, only 1 size or type of each aggregate may be used for any one continuous concrete placement.

(2) Segregation. Do not use segregated aggregates. Previously segregated materials may be thoroughly re-mixed and used when representative samples taken anywhere in the stockpile indicated a uniform gradation exists.

(3) Cement. Protect cement in storage or stockpiled on the site from any damage by climatic conditions which would change the characteristics or usability of the material.

(4) Moisture. Provide aggregate with a moisture content of ± 0.5% from the average of that day. If the moisture content in the aggregate varies by more than the above tolerance, take whatever corrective measures are necessary to bring the moisture to a constant and uniform consistency before placing concrete. This may be accomplished by handling or manipulating the stockpiles to reduce the moisture content, or by adding moisture to the stockpiles in a manner producing uniform moisture content through all portions of the stockpile.

For plants equipped with an approved accurate moisture-determining device capable of determining the free moisture in the aggregates, and provisions made for batch to batch correction of the amount of water and the weight of aggregates added, the requirements relative to manipulating the stockpiles for moisture control will be waived. Any procedure used will not relieve the producer of the responsibility for delivery of concrete meeting the specified water-cement ratio and slump requirements.

Do not use aggregate in the form of frozen lumps in the manufacture of concrete.

(5) Separation of Materials in Tested and Approved Stockpiles. Only use KDOT Approved Materials. Provide separate means for storing materials approved by KDOT. If the producer elects to use KDOT Approved Materials for non-KDOT work, during the progress of a project requiring KDOT Approved Materials, inform the Engineer and agree to pay all costs for additional materials testing.

Clean all conveyors, bins and hoppers of unapproved materials before beginning the manufacture of concrete for KDOT work.

5.0 MIXING, DELIVERY, AND PLACEMENT LIMITATIONS

a. Concrete Batching, Mixing, and Delivery. Batch and mix the concrete in a central-mix plant, in a truck mixer, or in a drum mixer at the work site. Provide plant capacity and delivery capacity sufficient to maintain

continuous delivery at the rate required. The delivery rate of concrete during concreting operations must provide for the proper handling, placing and finishing of the concrete.

Seek the Engineer's approval of the concrete plant/batch site before any concrete is produced for the project. The Engineer will inspect the equipment, the method of storing and handling of materials, the production procedures, and the transportation and rate of delivery of concrete from the plant to the point of use. The Engineer will grant approval of the concrete plant/batch site based on compliance with the specified requirements. The Engineer may, at any time, rescind permission to use concrete from a previously approved concrete plant/batch site upon failure to comply with the specified requirements.

Clean the mixing drum before it is charged with the concrete mixture. Charge the batch into the mixing drum so that a portion of the water is in the drum before the aggregates and cementitious. Uniformly flow materials into the drum throughout the batching operation. Add all mixing water in the drum by the end of the first 15 seconds of the mixing cycle. Keep the throat of the drum free of accumulations that restrict the flow of materials into the drum.

Do not exceed the rated capacity (cubic yards shown on the manufacturer's plate on the mixer) of the mixer when batching the concrete. The Engineer will allow an overload of up to 10% above the rated capacity for central-mix plants and drum mixers at the work site, provided the concrete test data for strength, segregation and uniform consistency are satisfactory, and no concrete is spilled during the mixing cycle.

Operate the mixing drum at the speed specified by the mixer's manufacturer (shown on the manufacturer's plate on the mixer).

Mixing time is measured from the time all materials, except water, are in the drum. If it is necessary to increase the mixing time to obtain the specified percent of air in air-entrained concrete, the Engineer will determine the mixing time.

If the concrete is mixed in a central-mix plant or a drum mixer at the work site, mix the batch between 1 to 5 minutes at mixing speed. Do not exceed the maximum total 60 mixing revolutions. Mixing time begins after all materials, except water, are in the drum, and ends when the discharge chute opens. Transfer time in multiple drum mixers is included in mixing time. Mix time may be reduced for plants utilizing high performance mixing drums provided thoroughly mixed and uniform concrete is being produced with the proposed mix time. Performance of the plant must comply with Table A1.1, of ASTM C 94, Standard Specification for Ready Mixed Concrete. Five of the six tests listed in Table A1.1 must be within the limits of the specification to indicate that uniform concrete is being produced.

If the concrete is mixed in a truck mixer, mix the batch between 70 and 100 revolutions of the drum or blades at mixing speed. After the mixing is completed, set the truck mixer drum at agitating speed. Unless the mixing unit is equipped with an accurate device indicating and controlling the number of revolutions at mixing speed, perform the mixing at the batch plant and operate the mixing unit at agitating speed while traveling from the plant to the work site. Do not exceed 350 total revolutions (mixing and agitating).

If a truck mixer or truck agitator is used to transport concrete that was completely mixed in a stationary central mixer, agitate the concrete while transporting at the agitating speed specified by the manufacturer of the equipment (shown on the manufacturer's plate on the equipment). Do not exceed 250 total revolutions (additional re-mixing and agitating).

Provide a batch slip including batch weights of every constituent of the concrete and time for each batch of concrete delivered at the work site, issued at the batching plant that bears the time of charging of the mixer drum with cementitious and aggregates. Include quantities, type, product name and manufacturer of all admixtures on the batch ticket.

If non-agitating equipment is used for transportation of concrete, provide approved covers for protection against the weather when required by the Engineer.

Place non-agitated concrete within 30 minutes of adding the cement to the water.

Do not use concrete that has developed its initial set. Regardless of the speed of delivery and placement, the Engineer will suspend the concreting operations until corrective measures are taken if there is evidence that the concrete can not be adequately consolidated.

Adding water to concrete after the initial mixing is prohibited. Add all water at the plant. If needed, adjust slump through the addition of a water reducer according to **subsection 3.0e.(2)**.

b. Placement Limitations.

(1) Concrete Temperature. Unless otherwise authorized by the Engineer, the temperature of the mixed concrete immediately before placement is a minimum of 55°F, and a maximum of 70°F. With approval by the Engineer, the temperature of the concrete may be adjusted 5°F above or below this range.

(2) Qualification Batch. For Grade 3.5 (AE) (LC-HPC) concrete, qualify a field batch (one truckload or at least 6 cubic yards) at least 35 days prior to commencement of placement of the bridge decks. Produce the qualification batch from the same plant that will supply the job concrete. Simulate haul time to the jobsite prior to discharge of the concrete for testing. Prior to placing concrete in the qualification slab and on the job, submit documentation to the Engineer verifying that the qualification batch concrete meets the requirements for air content, slump, temperature of plastic concrete, compressive strength, unit weight and other testing as required by the Engineer.

Before the concrete mixture with plasticizing admixture is used on the project, determine the air content of the qualification batch. Monitor the slump, air content, temperature and workability at initial batching and estimated time of concrete placement. If these properties are not adequate, repeat the qualification batch until it can be demonstrated that the mix is within acceptable limits as specified in this specification.

(3) Placing Concrete at Night. Do not mix, place or finish concrete without sufficient natural light, unless an adequate and artificial lighting system approved by the Engineer is provided.

(4) Placing Concrete in Cold Weather. Unless authorized otherwise by the Engineer, mixing and concreting operations shall not proceed once the descending ambient air temperature reaches 40°F, and may not be initiated until an ascending ambient air temperature reaches 40°F. The ascending ambient air temperature for initiating concreting operations shall increase to 45°F if the maximum ambient air temperature is expected to be between 55°F and 60°F during or within 24 hours of placement and to 50°F if the ambient air temperature is expected to equal or exceed 60°F during or within 24 hours of placement.

If the Engineer permits placing concrete during cold weather, aggregates may be heated by either steam or dry heat before placing them in the mixer. Use an apparatus that heats the weight uniformly and is so arranged as to preclude the possible occurrence of overheated areas which might injure the materials. Do not heat aggregates directly by gas or oil flame or on sheet metal over fire. Aggregates that are heated in bins, by steam-coil or water-coil heating, or by other methods not detrimental to the aggregates may be used. The use of live steam on or through binned aggregates is prohibited. Unless otherwise authorized, maintain the temperature of the mixed concrete between 55°F to 70°F at the time of placing it in the forms. With approval by the Engineer, the temperature of the concrete may be adjusted up to 5°F above or below this range. Do not place concrete when there is a probability of air temperatures being more than 25°F below the temperature of the concrete during the first 24 hours after placement unless insulation is provided for both the deck and the girders. Do not, under any circumstances, continue concrete operations if the ambient air temperature is less than 20°F.

If the ambient air temperature is 40°F or less at the time the concrete is placed, the Engineer may permit the water and the aggregates be heated to at least 70°F, but not more than 120°F.

Do not place concrete on frozen subgrade or use frozen aggregates in the concrete.

(5) Placing Concrete in Hot Weather. When the ambient temperature is above 90°F, cool the forms, reinforcing steel, steel beam flanges, and other surfaces which will come in contact with the mix to below 90°F by means of a water spray or other approved methods. For Grade 3.5 (AE) (LC-HPC) concrete, cool the concrete mixture to maintain the temperature immediately before placement between 55°F and 70°F. With approval by the Engineer, the temperature of the concrete may be up to 5°F below or above this range.

Maintain the temperature of the concrete at time of placement within the specified temperature range by any combination of the following:

- Shading the materials storage areas or the production equipment
- Cooling the aggregates by sprinkling with potable water.
- Cooling the aggregates or water by refrigeration or replacing a portion or all of the mix water with ice that is flaked or crushed to the extent that the ice will completely melt during mixing of the concrete.
- Liquid nitrogen injection.

6.0 INSPECTION AND TESTING

The Engineer will test the first truckload of concrete by obtaining a sample of fresh concrete at truck discharge and by obtaining a sample of fresh concrete at the discharge end of the conveyor, bucket or if pumped, the piping. The Engineer will obtain subsequent sample concrete for tests at the discharge end of the conveyor, bucket or if pumped, the discharge end of the piping. If potential problems are apparent at the discharge of any truck, the Engineer will test the concrete at truck discharge prior to deposit on the bridge deck.

The Engineer will cast, store, and test strength test specimens in sets of 5. See **TABLE 1-3**.

KDOT will conduct the sampling and test the samples according to **SECTION 2500** and **TABLE 1-3**. The Contractor may be directed by the Engineer to assist KDOT in obtaining the fresh concrete samples during the placement operation.

A plan will be finalized prior to the construction date as to how out-of-specification concrete will be handled.

TABLE 1-3: SAMPLING AND TESTING FREQUENCY CHART

Tests Required (Record to)	Test Method	CMS	Verification Samples and Tests	Acceptance Samples and Tests
Slump (0.25 inch)	KT-21	a	Each of first 3 truckloads for any individual placement, then 1 of every 3 truckloads	
Temperature (1°F)	KT-17	a	Every truckload, measured at the truck discharge, and from each sample made for slump determination.	
Mass (0.1 lb)	KT-20	a	One of every 6 truckloads	
Air Content (0.25%)	KT-18 or KT-19	a	Each of first 3 truckloads for any individual placement, then 1 of every 6 truckloads	
Cylinders (1 lbf; 0.1 in; 1 psi)	KT-22 and AASHTO T 22	VER	Make at least 2 groups of 5 cylinders per pour or major mix design change with concrete sampled from at least 2 different truckloads evenly spaced throughout the pour, with a minimum of 1 set for every 100 cu yd. Include in each group 3 test cylinders to be cured according to KT-22 and 2 test cylinders to be field-cured. Store the field-cured cylinders on or adjacent to the bridge. Protect all surfaces of the cylinders from the elements in as near as possible the same way as the deck concrete. Test the field-cured cylinders at the same age as the standard-cured cylinders.	
Density of Fresh Concrete (0.1 lb/cu ft or 0.1% of optimum density)	KT-36	ACI		b,c: 1 per 100 cu yd for thin overlays and bridge deck surfacing.

Note a: "Type Insp" must = "ACC" when the assignment of a pay quantity is being made. "ACI" when recording test values for additional acceptance information.
Note b: Normal operation. Minimum frequency for exceptional conditions may be reduced by the DME on a project basis, written justification shall be made to the Chief of the Bureau of Materials and Research and placed in the project documents. (Multi-Level Frequency Chart (see page 17, Appendix A of Construction Manual, Part V).
Note c: Applicable only when specifications contain those requirements.

The Engineer will reject concrete that does not comply with specified requirements.

The Engineer will permit occasional deviations below the specified cementitious content, if it is due to the air content of the concrete exceeding the designated air content, but only up to the maximum tolerance in the air content. Continuous operation below the specified cement content for any reason is prohibited.

As the work progresses, the Engineer reserves the right to require the Contractor to change the proportions if conditions warrant such changes to produce a satisfactory mix. Any such changes may be made within the limits of the Specifications at no additional compensation to the Contractor.

KANSAS DEPARTMENT OF TRANSPORTATION
SPECIAL PROVISION TO THE
STANDARD SPECIFICATIONS, 2007 EDITION

Add a new SECTION to DIVISION 700:

LOW-CRACKING HIGH-PERFORMANCE CONCRETE – CONSTRUCTION

1.0 DESCRIPTION

Construct the low-cracking high-performance concrete (LC-HPC) structures according to the Contract Documents and this specification.

BID ITEMS	UNITS
Qualification Slab	Cubic Yard
Concrete (*) (AE) (LC-HPC)	Cubic Yard
*Grade of Concrete	

2.0 MATERIALS

Provide materials that comply with the applicable requirements.

LC-HPC ..... **07-PS0166, latest version**
Concrete Curing Materials ..... **DIVISION 1400**

3.0 CONSTRUCTION REQUIREMENTS

a. Qualification Batch and Slab. For each LC-HPC bridge deck, produce a qualification batch of LC-HPC that is to be placed in the deck and complies with **07-PS0166, latest version**, and construct a qualification slab that complies with this specification to demonstrate the ability to handle, place, finish and cure the LC-HPC bridge deck.

After the qualification batch of LC-HPC complies with **07-PS0166, latest version**, construct a qualification slab 15 to 45 days prior to placing LC-HPC in the bridge deck. Construct the qualification slab to comply with the Contract Documents, using the same LC-HPC that is to be placed in the deck and that was approved in the qualification batch. Submit the location of the qualification slab for approval by the Engineer. Place, finish and cure the qualification slab according to the Contract Documents, using the same personnel, methods and equipment (including the concrete pump, if used) that will be used on the bridge deck.

A minimum of 1 day after construction of the qualification slab, core 4 full-depth 4 inch diameter cores, one from each quadrant of the qualification slab, and forward them to the Engineer for visual inspection of degree of consolidation.

Do not commence placement of LC-HPC in the deck until approval is given by the Engineer. Approval to place concrete on the deck will be based on satisfactory placement, consolidation, finishing and curing of the qualification slab and cores, and will be given or denied within 24 hours of receiving the cores from the Contractor. If an additional qualification slab is deemed necessary by the Engineer, it will be paid for at the contract unit price for Qualification Slab.

b. Falsework and Forms. Construct falsework and forms according to **SECTION 708**.

c. Handling and Placing LC-HPC.

(1) Quality Control Plan (QCP). At a project progress meeting prior to placing LC-HPC, discuss with the Engineer the method and equipment used for deck placement. Submit an acceptable QCP according to the Contractor's Concrete Structures Quality Control Plan, Part V. Detail the equipment (for both determining and controlling the evaporation rate and LC-HPC temperature), procedures used to minimize the evaporation rate, plans for maintaining a continuous rate of finishing the deck without delaying the application of curing materials within the time specified in **subsection 3.0f.**, including maintaining a continuous supply of LC-HPC throughout the placement with an

adequate quantity of LC-HPC to complete the deck and filling diaphragms and end walls in advance of deck placement, and plans for placing the curing materials within the time specified in **subsection 3.0f**. In the plan, also include input from the LC-HPC supplier as to how variations in the moisture content of the aggregate will be handled, should they occur during construction.

(2) Use a method and sequence of placing LC-HPC approved by the Engineer. Do not place LC-HPC until the forms and reinforcing steel have been checked and approved. Before placing LC-HPC, clean all forms of debris.

(3) Finishing Machine Setup. On bridges skewed greater than 10º, place LC-HPC on the deck forms across the deck on the same skew as the bridge, unless approved otherwise by State Bridge Office (SBO). Operate the bridge deck finishing machine on the same skew as the bridge, unless approved otherwise by the SBO. Before placing LP-HPC, position the finish machine throughout the proposed placement area to allow the Engineer to verify the reinforcing steel positioning.

(4) Environmental Conditions. Maintain environmental conditions on the entire bridge deck so the evaporation rate is less than 0.2 lb/sq ft/hr. The temperature of the mixed LC-HPC immediately before placement must be a minimum of 55°F and a maximum of 70°F. With approval by the Engineer, the temperature of the LC-HPC may be adjusted 5°F above or below this range. This may require placing the deck at night, in the early morning or on another day. The evaporation rate (as determined in the American Concrete Institute Manual of Concrete Practice 305R, Chapter 2) is a function of air temperature, LC-HPC temperature, wind speed and relative humidity. The effects of any fogging required by the Engineer will not be considered in the estimation of the evaporation rate (**subsection 3.0c.(5)**).

Just prior to and at least once per hour during placement of the LC-HPC, the Engineer will measure and record the air temperature, LC-HPC temperature, wind speed, and relative humidity on the bridge deck. The Engineer will take the air temperature, wind, and relative humidity measurements approximately 12 inches above the surface of the deck. With this information, the Engineer will determine the evaporation rate using KDOT software or **FIGURE 710-1**.

When the evaporation rate is equal to or above 0.2 $lb/ft^2/hr$, take actions (such as cooling the LC-HPC, installing wind breaks, sun screens etc.) to create and maintain an evaporation rate less than 0.2 $lb/ft^2/hr$ on the entire bridge deck.

(5) Fogging of Deck Placements. Fogging using hand-held equipment may be required by the Engineer during unanticipated delays in the placing, finishing or curing operations. If fogging is required by the Engineer, do not allow water to drip, flow or puddle on the concrete surface during fogging, placement of absorptive material, or at any time before the concrete has achieved final set.

(6) Placement and Equipment. Place LC-HPC by conveyor belt or concrete bucket. Pumping of LC-HPC will be allowed if the Contractor can show proficiency when placing the approved mix during construction of the qualification slab using the same pump as will be used on the job. Placement by pump will also be allowed with prior approval of the Engineer contingent upon successful placement by pump of the approved mix, using the same pump as will be used for the deck placement, at least 15 days prior to placing LC-HPC in the bridge deck. To limit the loss of air, the maximum drop from the end of a conveyor belt or from a concrete bucket is 5 feet and pumps must be fitted with an air cuff/bladder valve. Do not use chutes, troughs or pipes made of aluminum.

Place LC-HPC to avoid segregation of the materials and displacement of the reinforcement. Do not deposit LC-HPC in large quantities at any point in the forms, and then run or work the LC-HPC along the forms.

Fill each part of the form by depositing the LC-HPC as near to the final position as possible.

The Engineer will obtain sample LC-HPC for tests and cylinders at the discharge end of the conveyor, bucket, or if pumped, the piping.

(7) Consolidation.

- Accomplish consolidation of the LC-HPC on all span bridges that require finishing machines by means of a mechanical device on which internal (spud or tube type) concrete vibrators of the same type and size are mounted (**subsection 154.2**).
- Observe special requirements for vibrators in contact with epoxy coated reinforcing steel as specified in **subsection 154.2**.
- Provide stand-by vibrators for emergency use to avoid delays in case of failure.
- Operate the mechanical device so vibrator insertions are made on a maximum spacing of 12 inch centers over the entire deck surface.
- Provide a uniform time per insertion of all vibrators of 3 to 15 seconds, unless otherwise designated by the Engineer.

- Provide positive control of vibrators using a timed light, buzzer, automatic control or other approved method.
- Extract the vibrators from the LC-HPC at a rate to avoid leaving any large voids or holes in the LC-HPC.
- Do not drag the vibrators horizontally through the LC-HPC.
- Use hand held vibrators (**subsection 154.2**) in inaccessible and confined areas such as along bridge rail or curb.
- When required, supplement vibrating by hand spading with suitable tools to provide required consolidation.
- Reconsolidate any voids left by workers.

Continuously place LC-HPC in any floor slab until complete, unless shown otherwise in the Contract Documents.

d. Construction Joints, Expansion Joints and End of Wearing Surface (EWS) Treatment. Locate the construction joints as shown in the Contract Documents. If construction joints are not shown in the Contract Documents, submit proposed locations for approval by the Engineer.

If the work of placing LC-HPC is delayed and the LC-HPC has taken its initial set, stop the placement, saw the nearest construction joint approved by the Engineer, and remove all LC-HPC beyond the construction joint.

Construct keyed joints by embedding water-soaked beveled timbers of a size shown on the Contract Documents, into the soft LC-HPC. Remove the timber when the LC-HPC has set. When resuming work, thoroughly clean the surface of the LC-HPC previously placed, and when required by the Engineer, roughen the key with a steel tool. Before placing LC-HPC against the keyed construction joint, thoroughly wash the surface of the keyed joint with clean water.

e. Finishing. Strike off bridge decks with a vibrating screed or single-drum roller screed, either self-propelled or manually operated by winches and approved by the Engineer. Use a self-oscillating screed on the finish machine, and operate or finish from a position either on the skew or transverse to the bridge roadway centerline. See **subsection 3.0c.(3)**. Do not mount tamping devices or fixtures to drum roller screeds; augers are allowed.

Irregular sections may be finished by other methods approved by the Engineer and detailed in the required QCP. See **subsection 3.0c.(1)**.

Finish the surface by a burlap drag, metal pan or both, mounted to the finishing equipment. Use a float or other approved device behind the burlap drag or metal pan, as necessary, to remove any local irregularities. Do not add water to the surface of LC-HPC. Do not use a finishing aid.

Tining of plastic LC-HPC is prohibited. All LC-HPC surfaces must be reasonably true and even, free from stone pockets, excessive depressions or projections beyond the surface.

Finish all top surfaces, such as the top of retaining walls, curbs, abutments and rails, with a wooden float by tamping and floating, flushing the mortar to the surface and provide a uniform surface, free from pits or porous places. Trowel the surface producing a smooth surface, and brush lightly with a damp brush to remove the glazed surface.

f. Curing and Protection.

(1) General. Cure all newly placed LC-HPC immediately after finishing, and continue uninterrupted for a minimum of 14 days. Cure all pedestrian walkway surfaces in the same manner as the bridge deck. Curing compounds are prohibited during the 14 day curing period.

(2) Cover With Wet Burlap. Soak the burlap a minimum of 12 hours prior to placement on the deck. Rewet the burlap if it has dried more one hour before it is applied to the surface of bridge deck. Apply 1 layer of wet burlap within 10 minutes of LC-HPC strike-off from the screed, followed by a second layer of wet burlap within 5 minutes. Do not allow the surface to dry after the strike-off, or at any time during the cure period. In the required QCP, address the rate of LC-HPC placement and finishing methods that will affect the period between strike-off and burlap placement. See **subsection 3.0c.(1)**. During times of delay expected to exceed 10 minutes, cover all concrete that has been placed, but not finished, with wet burlap.

Maintain the wet burlap in a fully wet condition using misting hoses, self-propelled, machine-mounted fogging equipment with effective fogging area spanning the deck width moving continuously across the entire burlap-covered surface, or other approved devices until the LC-HPC has set sufficiently to allow foot traffic. At that time,

place soaker hoses on the burlap, and supply running water continuously to maintain continuous saturation of all burlap material to the entire LC-HPC surface. For bridge decks with superelevation, place a minimum of 1 soaker hose along the high edge of the deck to keep the entire deck wet during the curing period.

(3) Waterproof Cover. Place white polyethylene film on top of the soaker hoses, covering the entire LC-HPC surface after soaker hoses have been placed, a maximum of 12 hours after the placement of the LC-HPC. Use as wide of sheets as practicable, and overlap 2 feet on all edges to form a complete waterproof cover of the entire LC-HPC surface. Secure the polyethylene film so that wind will not displace it. Should any portion of the sheets be broken or damaged before expiration of the curing period, immediately repair the broken or damaged portions. Replace sections that have lost their waterproof qualities.

If burlap and/or polyethylene film is temporarily removed for any reason during the curing period, use soaker hoses to keep the entire exposed area continuously wet. Replace saturated burlap and polyethylene film, resuming the specified curing conditions, as soon as possible.

Inspect the LC-HPC surface once every 6 hours for the entirety of the 14 day curing period, so that all areas remain wet for the entire curing period and all curing requirements are satisfied.

(4) Documentation. Provide the Engineer with a daily inspection set that includes:

- documentation that identifies any deficiencies found (including location of deficiency);
- documentation of corrective measures taken;
- a statement of certification that the entire bridge deck is wet and all curing material is in place;
- documentation showing the time and date of all inspections and the inspector's signature.
- documentation of any temporary removal of curing materials including location, date and time, length of time curing was removed, and means taken to keep the exposed area continuously wet.

(5) Cold Weather Curing. When LC-HPC is being placed in cold weather, also adhere to **07-PS0166, latest version**.

When LC-HPC is being placed and the ambient air temperature may be expected to drop below 40ºF during the curing period or when the ambient air temperature is expected to drop more than 25°F below the temperature of the LC-HPC during the first 24 hours after placement, provide suitable measures such as straw, additional burlap, or other suitable blanketing materials, and/or housing and artificial heat to maintain the LC-HPC and girder temperatures between 40ºF and 75ºF as measured on the upper and lower surfaces of the LC-HPC. Enclose the area underneath the deck and heat so that the temperature of the surrounding air is as close as possible to the temperature of LC-HPC and between 40ºF and 75ºF. When artificial heating is used to maintain the LC-HPC and girder temperatures, provide adequate ventilation to limit exposure to carbon dioxide if necessary. Maintain wet burlap and polyethylene cover during the entire 14 day curing period. Heating may be stopped after the first 72 hours if the time of curing is lengthened to account for periods when the ambient air temperature is below 40ºF. For every day the ambient air temperature is below 40ºF, an additional day of curing with a minimum ambient air temperature of 50ºF will be required. After completion of the required curing period, remove the curing and protection so that the temperature of the LC-HPC during the first 24 hours does not fall more than 25°F.

(6) Curing Membrane. At the end of the 14-day curing period remove the wet burlap and polyethylene and within 30 minutes, apply 2 coats of an opaque curing membrane to the LC-HPC. Apply the curing membrane when no free water remains on the surface but while the surface is still wet. Apply each coat of curing membrane according to the manufacturer's instructions with a minimum spreading rate per coat of 1 gallon per 80 square yards of LC-HPC surface. If the LC-HPC is dry or becomes dry, thoroughly wet it with water applied as a fog spray by means of approved equipment. Spray the second coat immediately after and at right angles to the first application. Protect the curing membrane against marring for a minimum of 7 days. Give any marred or disturbed membrane an additional coating. Should the curing membrane be subjected to continuous injury, the Engineer may limit work on the deck until the 7-day period is complete. Because the purpose of the curing membrane is to allow for slow drying of the bridge deck, extension of the initial curing period beyond 14 days, while permitted, shall not be used to reduce the 7-day period during which the curing membrane is applied and protected.

(7) Construction Loads. Adhere to **TABLE 710-2**.

If the Contractor needs to drive on the bridge before the approach slabs can be placed and cured, construct a temporary bridge from the approach over the EWS capable of supporting the anticipated loads. Do not bend the reinforcing steel which will tie the approach slab to the EWS or damage the LC-HPC at the EWS. The method of bridging must be approved by the Engineer.

TABLE 710-2: CONCRETE LOAD LIMITATIONS ON BRIDGE DECKS		
Days after concrete is placed	**Element**	**Allowable Loads**
1*	Subdeck, one-course deck or concrete overlay	Foot traffic only.
3*	One-course deck or concrete overlay	Work to place reinforcing steel or forms for the bridge rail or barrier.
7*	Concrete overlays	Legal Loads; Heavy stationary loads with the Engineer's approval.***
10 (15)**	Subdeck, one-course deck or post-tensioned haunched slab bridges**	Light truck traffic (gross vehicle weight less than 5 tons).****
14 (21)**	Subdeck, one-course deck or post-tensioned haunched slab bridges**	Legal Loads; Heavy stationary loads with the Engineer's approval.***Overlays on new decks.
28	Bridge decks	Overloads, only with the State Bridge Engineer's approval.***

*Maintain a 7 day wet cure at all times (14-day wet cure for decks with LC-HPC).
** Conventional haunched slabs.
*** Submit the load information to the appropriate Engineer. Required information: the weight of the material and the footprint of the load, or the axle (or truck) spacing and the width, the size of each tire (or track length and width) and their weight.
****An overlay may be placed using pumps or conveyors until legal loads are allowed on the bridge.

g. Grinding and Grooving. Correct surface variations exceeding 1/8 inch in 10 feet by use of an approved profiling device, or other methods approved by the Engineer after the curing period. Perform grinding on hardened LC-HPC after the 7 day curing membrane period to achieve a plane surface and grooving of the final wearing surface as shown in the Contract Documents.

Use a self-propelled grinding machine with diamond blades mounted on a multi-blade arbor. Avoid using equipment that causes excessive ravels, aggregate fractures or spalls. Use vacuum equipment or other continuous methods to remove grinding slurry and residue.

After any required grinding is complete, give the surface a suitable texture by transverse grooving. Use diamond blades mounted on a self-propelled machine that is designed for texturing pavement. Transverse grooving of the finished surface may be done with equipment that is not self-propelled providing that the Contractor can show proficiency with the equipment. Use equipment that does not cause strain, excessive raveling, aggregate fracture, spalls, disturbance of the transverse or longitudinal joint, or damage to the existing LC-HPC surface. Make the grooving approximately 3/16 inch in width at 3/4 inch centers and the groove depth approximately 1/8 inch. For bridges with drains, terminate the transverse grooving approximately 2 feet in from the gutter line at the base of the curb. Continuously remove all slurry residues resulting from the texturing operation.

h. Post Construction Conference. At the completion of the deck placement, curing, grinding and grooving for a bridge using LC-HPC, a post-construction conference will be held with all parties that participated in the planning and construction present. The Engineer will record the discussion of all problems and successes for the project.

i. Removal of Forms and Falsework. Do not remove forms and falsework without the Engineer's approval. Remove deck forms approximately 2 weeks (a maximum of 4 weeks) after the end of the curing period (removal of burlap), unless approved by the Engineer. The purpose of 4 week maximum is to limit the moisture gradient between the bottom and the top of the deck.

For additional requirements regarding forms and falsework, see **SECTION 708**.

4.0 MEASUREMENT AND PAYMENT

The Engineer will measure the qualification slab and the various grades of (AE) (LC-HPC) concrete placed in the structure by the cubic yard. No deductions are made for reinforcing steel and pile heads extending into the LP-HPC. The Engineer will not separately measure reinforcing steel in the qualification slab.

Payment for the "Qualification Slab" and the various grades of "(AE) (LC-HPC) Concrete" at the contract unit prices is full compensation for the specified work.

FIGURE 710-1: STANDARD PRACTICE FOR CURING CONCRETE

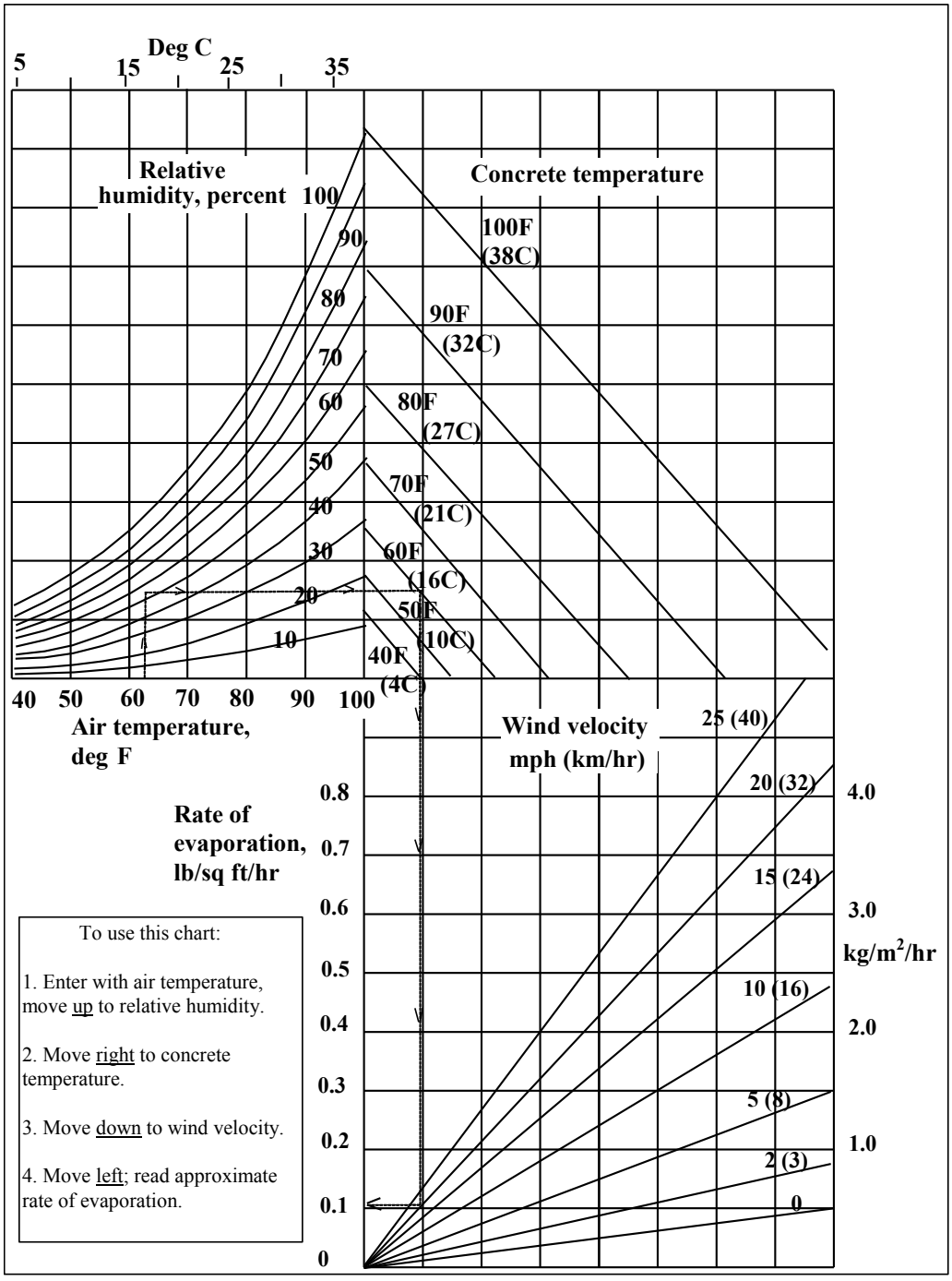

Effect of concrete and air temperatures, relative humidity, and wind velocity on the rate of evaporation of surface moisture from concrete. This chart provides a graphic method of estimating the loss of surface moisture for various weather conditions. To use the chart, follow the four steps outlined above. When the evaporation rate exceeds 0.2 lb/ft^2/hr (1.0 kg/ m^2/hr), measures shall be taken to prevent excessive moisture loss from the surface of unhardened concrete; when the rate is less than 0.2 lb/ft^2/hr (1.0 kg/m^2/hr) such measures may be needed. When excessive moisture loss is not prevented, plastic cracking is likely to occur.

APPENDIX E: PLASTIC CONCRETE TEST RESULTS AND MIXTURE DESIGN INFORMATION FOR BRIDGE DECKS

Table E.1 Individual plastic concrete test results for LC-HPC decks

LC-HPC-1 Placement 1				
Truck	**Slump (in.)**	**Air Content (%)**	**Concrete Temp. (° F)**	**Notes:**
1	3.75	7.5	64	Air Temp. = 52° F
2	3.25	6.2	61	Air Temp. = 54° F
3	2.5	8.0	72	Air Temp. = 55° F
7	3.75	9.0	66	Air Temp. = 57° F
10	6.5	11.5	66	Air Temp. = 57° F
11	3.5	6.0	68	Air Temp. = 59° F
15	3.5	7.5	72	Air Temp. = 59° F
21	3.25	7.4	72	Air Temp. = 59° F

LC-HPC-1 Placement 2				
Truck	**Slump (in.)**	**Air Content (%)**	**Concrete Temp. (° F)**	**Notes:**
1	4.25	7	66	Air Temp. = 52° F
2	3	6.5	68	Air Temp. = 52° F
3	2.5	3	68	Air Temp. = 54° F
4	3.75	9	66	Air Temp. = 55° F
8	3.5	9	69	Air Temp. = 57° F
12	2.5	8	66	Air Temp. = 59° F
16	4	8.5	68	Air Temp. = 68° F
20	3.5	9	66	Air Temp. = 55° F
24	2.75	9	69	Air Temp. = 57° F
26	3.5	8.5	68	Air Temp. = 68° F

LC-HPC-2				
Truck	**Slump (in.)**	**Air Content (%)**	**Concrete Temp. (° F)**	**Notes:**
-	4	7	66	
-	3.75	8.5	69	
-	3.25	7.2	68	
-	3.25	7.2	67	
-	3.25	7.5	61	
-	2.5	8	69	
-	1.5	8.5	66	

Note: 1 in. = 25.4 mm

° C × 9/5 + 32 = ° F

Table E.1 (con't) Individual plastic concrete test results for LC-HPC decks

LC-HPC-3				
Truck	**Slump (in.)**	**Air Content (%)**	**Concrete Temp. † (° F)**	**Notes:**
1	5.25	9.1	59	Held and retested
1	2.5	-	-	Retest
2	1.75	7.8	56	Air content 6% after pump, 1.8% loss
3	2	8.2	60	
5	3	-	59	
7	2.5	9.1	61	
9	3.25	-	62	
11	2.75	7	59	
13	2.75	-	59	
15	-	9.2	55	Retested-initially 12% air and 4 in. slump
16	-	9	60	
17	3.25	-	59	
19	2.25	6.5	59	
23	4	9.5	56	Air content 8.4% after pump, 1.1% loss
25	4	-	58	
27	3.75	-	59	Retested-initially 9% air and 4.75 in. slump
29	4	-	52	
31	2.75	8	56	
33	3.75	-	57	
35	3.5	7.8	60	
37	3.5	-	60	Retested-initially 8.2% air and 5.25 in. slump
39	4	-	60	
40	4	-	58	
41	3.5	-	59	
43	3.5	9.5	60	
45	3.25	-	57	
47	3.25	10.5	60	Air content 8.4% after pump, 1.5% loss
49	3.5	-	58	
51	3.75	10	60	

Note: 1 in. = 25.4 mm

° C × 9/5 + 32 = ° F

† Infrared measurement of concrete surface temperature

Table E.1 (con't) Individual plastic concrete test results for LC-HPC decks

LC-HPC-4 Placement 1				
Truck	**Slump (in.)**	**Air Content (%)**	**Concrete Temp. (° F)**	**Notes:**
1	1.25	7	-	Tested after pump
1	2.25	7.6	-	Tested after water reducer added
1	1.25	7.8	-	Tested from truck
2	0.75	6.8	-	
3	4	10.4	-	Rejected - high air
4	2	6.8	-	
6	1.5	-	-	
8	0.75	7.4	-	
10	0.75	-	-	
12	3.75	11.4	-	Rejected - high air
15	2.25	-	-	
17	4.25	11.6	-	Accepted to reach header
18	-	8.8	-	
19	3.5	10.6	-	Accepted to reach header

LC-HPC-4 Placement 2				
Truck	**Slump (in.)**	**Air Content (%)**	**Concrete Temp. † (° F)**	**Notes:**
1	2.5	8.8	65	Tested from truck
1	2.5	6.8	62	Tested from pump
2	1.5	7.2	63	
3	1.75	8.1	-	
5	1.5	-	63	
7	3.25	10.4	64	
9	3.5	-	64	
11	4	9.5	59	
13	4	-	62	
15	3.5	9.8	62	
17	2.25	-	62	
19	4	9.6	60	
21	4	-	63	
23	3.5	8.8	65	
25	3	-	64	
27	3.75	8.4	71	
29	4	-	66	
30	3.5	9.3	64	
32	3.75	-	65	
34	1.5	8.3	65	

Note: 1 in. = 25.4 mm

° C × 9/5 + 32 = ° F

† Infrared measurement of concrete surface temperature

Table E.1 (con't) Individual plastic concrete test results for LC-HPC decks

LC-HPC-5				
Truck	**Slump (in.)**	**Air Content (%)**	**Concrete Temp. (° F)**	**Notes:**
1	5.5	11	64	Held b/c of high slump & air
1	2.75	8	-	Retested
2	3.5	7	59	Tested from truck
2	2.5	7.4	-	Tested after pumping
3	3	9.5	61	
5	2.25	-	63	
7	2	8.7	64	
9	2.5	-	61	Slow pumping
11	2.25	9	63	
13	2.25	-	62	
15	2.25	9	62	
16	2.5	8.5	60	Switched from 0.42 to 0.43 w/c
17	4	-	58	
19	4	10.3	61	
21	5.5	-	61	Held b/c of high slump
21	4	8.5	61	Retested
22	3.75	-	61	
25	2.5	-	61	
27	2.25	6.8	61	Switched from 0.43 to 0.45 w/c
29	3.25	-	62	
31	4	9	62	
33	3.25	-	57	
35	3	8.8	61	
37	3.75	-	61	
39	3.25	9	60	
41	3.75	-	61	
43	3.25	8.5	58	
45	3	-	62	
47	3.25	10.2	63	
48	2.75	-	63	

Note: 1 in. = 25.4 mm

° C × 9/5 + 32 = ° F

Table E.1 (con't) Individual plastic concrete test results for LC-HPC decks

LC-HPC-6				
Truck	**Slump (in.)**	**Air Content (%)**	**Concrete Temp. † (° F)**	**Notes:**
1	4.25	9.9	55	Tested from truck
1	2.25	7.5	-	Tested after pumping
2	4.75	11.5	52	
5	3.25	-	60	
7	3	8.4	56	
9	2.25	-	55	
11	2.75	9.1	57	
13	2.75	-	60	
15	4	10.5	58	
17	4	-	54	
19	4.25	10.2	61	
21	3.25	-	62	
23	3.5	7.5	62	
25	4.25	-	63	Held for 40 min. then placed in deck w/o retesting
27	3.25	9.3	60	
29	4.25	-	64	
31	4	10.1	61	
33	4.25	-	60	
35	5	10.5	61	
37	4.75	-	62	
39	5	12.5	62	Rejected - high air
40	3.5	8.4	61	
41	6	-	59	
43	3.25	9.6	60	
45	4.25	-	60	
47	3.75	8.5	62	
49	3.75	-	62	
51	3.75	-	63	

Note: 1 in. = 25.4 mm

° C × 9/5 + 32 = ° F

† Infrared measurement of concrete surface temperature

Table E.1 (con't) Individual plastic concrete test results for LC-HPC decks

LC-HPC-7				
Truck	**Slump (in.)**	**Air Content (%)**	**Concrete Temp. † (° F)**	**Notes:**
-	2.75	7.5	73	
-	4	9	75	
-	5	8	75	
-	5.25	7.5	73	
-	2.5	6.5	73	
-	3	-	74	
-	2.75	6.5	71	
-	3.5	-	73	
-	3.5	8.5	71	
-	2.5	-	72	
-	4	8.5	72	
-	2.5	-	69	
-	4	8.5	69	
-	4	-	71	
-	6	8.5	70	
-	2.5	-	73	
-	2.5	7	73	
-	2.25	-	69	
-	4	9	69	
-	4	-	71	
-	4	-	70	
-	5.25	10.5	68	
-	6	7	69	

Note: 1 in. = 25.4 mm

° C × 9/5 + 32 = ° F

† Infrared measurement of concrete surface temperature

Table E.1 (con't) Individual plastic concrete test results for LC-HPC decks

LC-HPC-8					
Truck	**Slump (in.)**	**Air Content (%)**	**Concrete Temp. (° F)**	**Notes:**	**Location of Sample**
1	2.5	8.1	-		Truck
1	2.75	7.5	59		Deck
2	1.75	6.9	64		Deck
3	1.75	-	-		Truck
3	1	5.7	63		Deck
5	2	9	60		Truck
5	-	7.7	-		Deck
7	3.25	-	62		Truck
7	2.25	7.7	60		Deck
9	1.5	7.3	69		Deck
11	1.75	7.7	66		Deck
13	1.5	9	64		Deck
15	2	8.2	70		Deck
17	2.25	9	65		Deck
19	1.5	8.4	64		Deck
21	1.75	8.2	69		Deck
23	2	8	72		Deck
25	2.5	8.4	69		Deck
27	1.5	7	68		Deck
29	1.5	7.2	69		Deck
31	1.5	7.2	71		Deck
33	1.5	7.7	69		Deck
35	2.25	6.9	72		Deck
37	2.75	9.8	72		Truck
38	-	8.2	-		Truck
39	3	-	71		Deck
41	2.5	8.8	66		Deck
46	-	6.2	73		Deck
47	3.25	-	67		Truck
48	2	8.2	67		Deck
50	2.75	7.7	68		Deck
53	3	10.2	64		Deck
55	-	9.7	-		Deck

Note: 1 in. = 25.4 mm

° C × 9/5 + 32 = ° F

Table E.1 (con't) Individual plastic concrete test results for LC-HPC decks

LC-HPC-10				
Truck	**Slump (in.)**	**Air Content (%)**	**Concrete Temp. (° F)**	**Notes:**
1	2.75	5.5	64	Placed in abutment
2	2.25	4.9	65	Remixed with added AEA
2	1.75	5.1	65	Retested & Rejected
3	High	-	-	Rejected
4	3.75	7.2	65	Placed in abutment
5	3.25	-	65	Placed in abutment
7	4	6.1	65	
9	2.25	-	64	
11	2.5	6.5	68	
15	2.75	6.7	66	
16	2.25	-	65	
17	3.5	7.7	65	
18	3.25	6.3	65	
19	3	-	65	
20	3	8.2	65	
23	3.25	-	66	
25	3.25	8.1	65	
26	3.25	-	64	
28	3.5	8.1	65	
29	4	-	60	
31	3.25	7.5	60	
33	3	-	65	
35	5	9.2	65	Held, lost slump, then placed
37	3.25	8.5	65	
39	3.5	-	66	
42	3	7.8	66	
44	3	8.2	67	
47	2.25	7.3	67	
50	4.25	-	70	
55	3.25	7.7	70	
57	3.5	-	72	Placed in deck & abutment

Note: 1 in. = 25.4 mm

° C × 9/5 + 32 = ° F

Table E.1 (con't) Individual plastic concrete test results for LC-HPC decks

LC-HPC-9					
Truck	**Slump (in.)**	**Air Content (%)**	**Concrete Temp. (° F)**	**Notes:**	**Location of Sample**
1	2.75	6.7	60	Added AEA & remixed. Water held	Truck
1	2.25	5.9	60	Added remaining water & remixed	Deck
1	4	6.5	60		Deck
3	5.25	8	60	All water added. Held for slump to drop	Truck
3	3.25	6.7	60		Deck
5	5.25	7.1	60		Deck
6	4	6.9	60		Truck
9	3	-	60		Deck
12	3.75	7.5	64		Deck
15	2.25	-	68		Deck
18	3	6.5	62		Deck
21	3.25	5.9	64		Deck
24	3.5	7.1	64		Deck
27	3.5	6.5	66		Deck
30	2.5	7.1	66		Deck
33	4	-	66		Deck
36	3	7.6	68		Deck
39	4	-	69		Deck
42	2.5	5.7	66		Deck
43	-	6.1	66		Deck
46	3	6.7	66		Deck
47	3	6.1	66		Deck
49	4	-	68		Deck

LC-HPC-11					
Truck	**Slump (in.)**	**Air Content (%)**	**Concrete Temp. (° F)**	**Notes:**	**Location of Sample**
1	2.25	7	60		Truck
2	2.75	7.8	59	Placed out of chute	Truck
3	2.25	6	60	Placed out of chute	Truck
4	1.75	5.4	61	Rejected - low air	Truck
5	2.75	6.8	59	Placed w/ conveyor	-
7	4	7	59	Placed w/ conveyor	-
9	3	7.8	61	Held to lower slump	-
11	5.5	8.6	60	Held to lower slump	-
11	4.75	-	-	Held to lower slump	-
11	4	-	-		-
13	2.5	8.5	60		-
15	2.5	7.8	63		-
17	3.75	8.4	60		-
19	4	9	60		Chute
19	-	6.6	-		Conveyor
21	4	9.2	62		-
23	3.25	-	64		-
23	-	7.5	-		-

Note: 1 in. = 25.4 mm

° C × 9/5 + 32 = ° F

Table E.1 (con't) Individual plastic concrete test results for LC-HPC decks

LC-HPC-12 Placement 1					
Truck	**Slump (in.)**	**Air Content (%)**	**Concrete Temp. (° F)**	**Notes:**	**Location of Sample**
1	1.5	6.2	58	Initially, 0.42 w/c	-
1	1.75	6.2	59	Water added - w/c = 0.44	-
2	1.75	5.7	59		-
2	1.75	6.8	-		-
3	3.25	8.3	-		Deck
4	2.75	7.4	-		Deck
6	2.5	7.9	-		Deck
8	2.5	-	-		-
9	2.75	7.4	60		Deck
10	3.25	-	-		Deck
11	3.25	-	-		Deck
13	3	7.8	-		Deck
15	2.75	-	61		Deck
16	3.25	8.4	-		Deck
19	2.75	-	-		Deck
21	3.5	8	-		Deck
23	3	-	-		Deck
25	2.75	7.4	62		Deck

LC-HPC-12 Placement 2					
Truck	**Slump (in.)**	**Air Content (%)**	**Concrete Temp. (° F)**	**Notes:**	**Location of Sample**
1	2.75	6.3	71	0.45 w/c, Rejected	Truck
2	4.25	7	70		Truck
3	3.5	6.3	69		Truck
3	-	8.4	-	Redosed w/ AEA	-
4	5.75	9	66	Held for slump to drop. Not retested before placed.	Truck
6	5.5	-	61		Truck
7	3.5	7.9	69		Truck
8	4	8.9	69	New mix design, 0.44 w/c	Truck
11	3.5	7.7	71		Deck
13	4.75	-	71	Back to mix design w/ 0.45 w/c	Deck
15	3.5	6.3	72		Deck
16	-	8.9	-		Truck
17	-	8.4	-	Test by concrete supplier	-
18	3.5	8.1	71		Deck
20	5	-	64		Deck
23	3.5	7.9	63	Back to mix design w/ 0.44 w/c	Deck
25	5.25	-	-		Truck
26	6.25	-	-	Placed in N. abutment	Truck
27	3.5	6.6	62		Truck

Note: 1 in. = 25.4 mm

° C × 9/5 + 32 = ° F

Table E.1 (con't) Individual plastic concrete test results for LC-HPC decks

LC-HPC-13					
Truck	**Slump (in.)**	**Air Content (%)**	**Concrete Temp. (° F)**	**Notes:**	**Location of Sample**
1	3	8.3	61		Truck
1	3.25	7.5	-		Deck
2	4	9.5	62		Truck
2	3	9	-		Deck
3	4	9.5	62		Truck
3	3	9.5	-		Deck
5	2.25	-	68		Deck
8	2	6.8	70		Deck
12	3	7	68		Deck
14	3.75	7.3	70		Deck
16	2.5	-	71		Deck
18	4	8	71		Deck
22	1.75	6.8	71		Deck
26	2.5	7	70		Deck
30	3	7.7	70		Deck
34	2.75	8.7	70		Deck
36	4	-	69		Deck
38	4.25	9.2	69		Deck
40	4	-	70		Deck
42	3	8.9	69		Deck
44	5	-	69		Deck
45	2.75	-	-		Truck
46	3	8.7	70		Deck
48	3	-	69		Deck
50	3.75	9.2	69		Deck
52	2.75	-	68		Deck
54	2.75	7.9	67		Deck
56	1.75	-	69		Deck
58	2.25	7.5	72		Deck
60	2.75	-	70		Deck

Note: 1 in. = 25.4 mm

° C × 9/5 + 32 = ° F

Table E.1 (con't) Individual plastic concrete test results for LC-HPC decks

OP Bridge Placement 1					
Truck	**Slump (in.)**	**Air Content (%)**	**Concrete Temp. (° F)**	**Notes:**	**Location of Sample**
-	2.5	8.8	65		-
-	1.75	7.9	64		-
-	2	-	66		-
-	4	7.8	69	Water added	-
-	3.75	7.8	65		-
-	3.5	9.2	65		-
-	5.25	9.1	66		-
-	5.25	8.7	67		-
-	4	-	-		-
-	5	-	-		-
-	3.75	9	63		-
-	4	9.7	60		-
-	4.25	7.7	65		-

OP Bridge Placement 2					
Truck	**Slump (in.)**	**Air Content (%)**	**Concrete Temp. (° F)**	**Notes:**	**Location of Sample**
1	4.25	11	65		-
2	5	10.4	63		-
3	6	10.9	64		-
4	5.25	8.7	64		Truck
4	4.5	7	-		Deck
8	4	11	65		-
8	-	10.7	-	Retest	-
13	4.25	10.5	64		-
16	3.5	10.4	-		-
17	4	10.5	65		-
22	4.5	10.4	65		Truck
22	4	8.4	-		Deck
28	2.5	7.9	64		-
31	3.5	8.4	64		-

OP Bridge Placement 3					
Truck	**Slump (in.)**	**Air Content (%)**	**Concrete Temp. (° F)**	**Notes:**	**Location of Sample**
-	5.25	10.5	67	Air Temp. = 77° F	Truck
-	6.5	10.5	65	Air Temp. = 76° F	Truck
-	6	9.9	64	Air Temp. = 76° F	Truck
-	4.75	9.7	62	Air Temp = 74° F	Truck
-	4.25	9.5	66		Deck
-	4.75	9.5	67		Truck
-	5.25	9.6	67		Truck
-	5	9.8	66		Truck
-	4.75	9.7	63		Truck

Note: 1 in. = 25.4 mm

° C × 9/5 + 32 = ° F

Table E.1 (con't) Individual plastic concrete test results for LC-HPC decks

LC-HPC-15					
Truck	**Slump (in.)**	**Air Content (%)**	**Concrete Temp. (° F)**	**Notes:**	**Location of Sample**
1	1.75	9	62	Tested before water reducer was added	Truck
2	2	9	62	Tested before water reducer was added	Truck
3	1.5	9	68	Tested before water reducer was added	Truck
6	2	8.3	63	Tested before water reducer was added	Truck
8	2.25	-	58		Truck
9	4	8.5	63	Truck held after half placed in deck to allow slump to drop. Never retested.	Truck
10	3.5	-	63	Tested after water reducer was added	Truck
12	2	-	63		Truck
14	3.5	-	62		Truck
15	6	8.7	64	Four buckets placed before rejected	Truck
18	3.5	-	64		Truck
20	4.5	-	62	Two buckets placed, then held to allow slump to drop. Never retested.	Truck
21	4.75	8.8	64	One bucket placed, then held to allow slump to drop. Never retested.	Truck
24	5.25	-	64	Two buckets placed, then held to allow slump to drop. Never retested.	Truck
26	3.5	8.4	64		Truck
28	3.5	-	64		Truck
30	3.5	-	64		Truck
33	3.25	10	67		Truck
36	3.25	-	64		Truck
39	3.25	10.5	64		Truck
42	-	10	64	Rejected-high air, portion of load already placed	Truck
43	-	10.6	64	Rejected-high air, portion of load already placed	Truck
44	-	10	-	Rejected-high air, portion of load already placed	Truck
46	-	7	63		Truck
50	3.5	7.6	64		Truck
51	3.25	-	63		Truck
52	3.25	-	63		Truck

Note: 1 in. = 25.4 mm

° C × 9/5 + 32 = ° F

Table E.1 (con't) Individual plastic concrete test results for LC-HPC decks

LC-HPC-16					
Truck	**Slump (in.)**	**Air Content (%)**	**Concrete Temp. (° F)**	**Notes:**	**Location of Sample**
1	2.5	6.5	53	Air Temp. = 40° F	Truck
1	1.25	4.5	52	Air Temp. = 41° F	Deck
2	0.75	4.3	60	Water added & placed in abutment, Air Temp. = 42° F	Deck
2	1.75	-	-	Air Temp. = 42° F	Truck
3	2.75	-	-	Water added & placed in deck	-
4	2.25	-	58		-
5	6.25	-	57	Rejected before placement	Truck
6	3	6	57	Air Temp = 47° F	Deck
9	3.75	6.7	65		Deck
14	4.5	-	-	Air Temp = 49° F	Truck
14	3.75	-	-		Deck
16	4.75	-	-		Truck
16	5.25	-	-		Truck
17	3.25	-	-		Deck
20	3.25	7	-		Deck
21	5.25	-	-		Deck
22	4.5	-	-		Truck
24	6	7	53	Mixture design switched to 540 lb cement	Truck
24	4	5.7	58	Air Temp. = 60° F	Deck
25	5.5	-	56	Air Temp. = 59° F	Deck
27	5.25	-	-	Air Temp. = 58° F	Deck
29	5	6.6	63	Mixture design switched to 0.44 w/c	Deck
32	4	8.7	64	Air Temp. = 58° F	Deck
35	3.25	7.9	63	Air Temp. = 58° F	Deck
37	2.75	-	62	Air Temp. = 57° F	Deck
42	5.75	7.2	-	Air Temp. = 51° F	Deck
45	1.75	5.7	68	Air Temp. = 50° F	Deck

Note: 1 in. = 25.4 mm

° C × 9/5 + 32 = ° F

Table E.1 (con't) Individual plastic concrete test results for LC-HPC decks

LC-HPC-17					
Truck	**Slump (in.)**	**Air Content (%)**	**Concrete Temp. (° F)**	**Notes:**	**Location of Sample**
1	2	9	70		Truck
1	1.5	7.5	70		Deck
2	2.5	-	69		Truck
2	2	7.3	-		Deck
3	2	7	71		Deck
6	2.5	-	71		Deck
9	5	6	71		Truck
9	4.5	7	70		Deck
10	5	-	-		Truck
12	2.5	-	-		-
13	-	-	75	Ice to be added to next truck	-
15	3.5	7	73	Ice added	Deck
17	6	-	75	Held & retested	Truck
19	-	-	74		-
20	-	-	75	Visual slump of 2 in.	-
21	-	-	-	Visual slump of 6 in.	-
23	2.5	8.5	73		-
25	2.75	-	-	Pumping issues	-
27	-	6.5	-	water reduced aded on site	Deck
28	2.75	-	76	Second pump used	-
30	1.5	6.5	80	Visually 4 in. slump from truck	Deck
33	4.75	-	71		-
34	-	-	-	Visually 5 in. slump from truck	-
35	3	5.5	69		Deck
36	-	-	72	Visually 4 in. slump from truck	-
39	-	-	75	Visually 3.5 in. slump from truck	-
40	-	-	70	Visually 4.5 in. slump from truck	-
41	-	-	68	Visually 4.5 in. slump from truck	-
43	-	-	69	Visually 5 in. slump from truck	-
45	-	-	72	Visually 3.5 in. slump from truck	-
46	-	-	71	Visually 3 in. slump, pumping issues, added water reducer	-
48	-	-	73	Visually 4 in. slump from truck	-
50	-	-	75	Visually 3 in. slump from truck	-
54	-	-	71	Visually 4 in. slump from truck	-

Note: 1 in. = 25.4 mm

° C × 9/5 + 32 = ° F

Table E.2 Mixture design information – LC-HPC bridge decks

Bridge	Cement (lb/yd^3)	Water (lb/yd^3)	*w/c*	Fine Aggregate (lb/yd^3)		Coarse Aggregate Max Size Agg. (lb/yd^3)			Design Air Content (%)	Paste Content (% by volume)
				#1	#2	3/4 in. (CA-5)	1-1/2 in. (CA-6)	3/8 in. (CA-7)		
LC-HPC-1 p1	540	243	0.45	1246*	-	565	890	266	8.0	24.6
LC-HPC-1 p2										
LC-HPC-2										
LC-HPC-3	535	241	0.45	1071*	387†	862	654	-	8.0	24.4
LC-HPC-4 p1	535	225	0.42	526*	1001†	774	723	-	8.0	23.4
LC-HPC-4 p2	535	225	0.42	1089*	393†	877	665	-	8.0	23.4
LC-HPC-5	535	225	0.42	1089*	393†	877	665	-	8.0	23.4
LC-HPC-6	535	241	0.45	1071*	387†	862	654	-	8.0	24.4
LC-HPC-7	540	243	0.45	1407**	-	599	988	-	8.0	24.6
LC-HPC-8	535	223	0.42	465*	1122$	745	707	-	8.0	23.4
LC-HPC-9‡	535	235	0.44	1419$	-	1189	373	-	8.0	24.1
LC-HPC-10	535	223	0.42	465*	1122$	745	707	-	8.0	23.4
LC-HPC-11	535	225	0.42	1467##	-	312††	312	1030	8.0	23.4
LC-HPC-12 p1	540	238	0.44	1438**	-	360	1199	-	8.0	24.3
LC-HPC-12 p2	535	239	0.45	1415**	-	855	805	-	8.0	24.2
LC-HPC-13	535	235	0.44	415*	1059$	-	1510	-	8.0	24.1
OP p1	535	241	0.45	974**	392†	875	745	-	8.0	24.4
OP p2										
OP p3										
LC-HPC-15	500	225	0.45	1472##	-	1166	429‡‡	-	8.0	22.8
LC-HPC-16#	500	225	0.45	1472##	-	1166	429‡‡	-	8.0	22.8
LC-HPC-17	540	243	0.45	1470##	220$$	789	497‡‡	-	8.0	24.6

Note: 1 lb/yd^3 = 0.5933 kg/m^3, 1 in. = 25 mm, granite used for all coarse aggregate
‡ Cement content increased to 540 lb/yd^3 for deck placement
# Cement content increased to 520 and 540 lb/yd^3 for deck placement
*Fine aggregate designated as FA-A
**Fine aggregate designated as MA-2
Fine aggregate designated as MA-3
$ Fine aggregate designated at BD-2
† Manufactured sand
$$ Pea Gravel
†† Coarse aggregate designated as CA-1
‡‡ Coarse aggregate designated as MA-4

Table E.3 Mixture design information – control bridge decks

Bridge	Deck Section	Cement (lb/yd^3)	Class F Fly Ash (lb/yd^3)	Silica Fume (lb/yd^3)	Water (lb/yd^3)	*w/cm* †	Fine Aggregate (FA-A) (lb/yd^3)	Coarse Aggregate (lb/yd^3)			Design Air Content (%)	Paste Content (% by volume)
								CA-5	CA-7	Type		
Control 1/2 p1	Subdeck	602	-	-	241	0.40	1493	1493	-	Limestone	6.5	25.6
	Overlay	583	-	44	233	0.37	1488	-	1488	Granite	6.5	26.0
Control 1/2 p2	Subdeck	605	-	-	241	0.40	1493	1493	-	Limestone	6.5	25.7
	Overlay	583	-	44	233	0.37	1488	-	1488	Granite	6.5	26.0
Control 3	Subdeck	536	133	-	268	0.40	Not Available			Granite	6.5	29.0
	Overlay	583	-	44	233	0.37	Not Available			Granite	6.5	26.0
Control 4	Subdeck	536	133	-	268	0.40	Not Available			Granite	6.5	29.0
	Overlay	583	-	44	233	0.37	Not Available			Granite	6.5	26.0
Control 5	Subdeck	536	133	-	268	0.40	Not Available			Granite	6.5	29.0
	Overlay	583	-	44	233	0.37	Not Available			Granite	6.5	26.0
Control 6	Subdeck	536	133	-	268	0.40	Not Available			Granite	6.5	29.0
	Overlay	583	-	44	233	0.37	Not Available			Granite	6.5	26.0
Control 7 p1	Subdeck	536	133	-	268	0.40	1419	1419	-	Granite	6.5	29.0
	Overlay	583	-	44	233	0.37	1488	-	1488	Granite	6.5	26.0
Control 7 p2	Subdeck	536	133	-	268	0.40	1419	1419	-	Granite	6.5	29.0
	Overlay	583	-	44	233	0.37	1488	-	1488	Granite	6.5	26.0
Control 8/10	Monolithic	612	-	-	244	0.40	Not Available			Limestone	6.5	26.0
Control 9	Subdeck	612	-	-	244	0.40	1478	1478	-	Limestone	6.5	26.0
	West Overlay	590	-	44	234	0.37	1485	-	1485	Quartzite	6.5	26.2
	East Overlay											
Control 11	North Subdeck	602	-	-	241	0.40	1508	1478	-	Limestone	6.5	25.6
	South Subdeck	602	-	-	241	0.40	1508	1478	-	Limestone	6.5	25.6
	Overlay	583	-	44	233	0.37	1490	-	1490	Quartzite	6.5	26.0
Control 12 p1	Subdeck	602	-	-	265	0.44	1455	1455	-	Limestone	6.5	27.1
	Overlay	581	-	44	231	0.37	1475	-	1475	Quartzite	6.5	25.8
Control 12 p2	Subdeck	602	-	-	265	0.44	1455	1455	-	Limestone	6.5	27.1
	Overlay	581	-	44	231	0.37	1475	-	1475	Quartzite	6.5	25.8
Control 13	Subdeck	612	-	-	244	0.40	1478	1478	-	Limestone	6.5	26.0
	Overlay	590	-	44	234	0.37	1485	-	1485	Quartzite	6.5	26.2

lb/yd^3 = 0.5933 kg/m^3

† *w/cm* = water-cementitious material ratio

APPENDIX F: DATA FOR EVALUATION OF BRIDGE DECK CRACKING PERFORMANCE

Table F.1 Crack densities for LC-HPC and OP Bridge placements obtained from annual crack surveys and interpolated crack densities at 42 months

Bridge Number	Bridge & Placement		Survey Age (months)	Crack Density (m/m^2)	Interpolated Crack Density at 42 months (m/m^2)
105-304	LC-HPC-1	Full Bridge	5.6	0.007	Not Used in Analysis
			18.2	0.027	
			31.8	0.034	
			43.8	0.093	
			55.3	0.027	
			70.3	0.082	
			78.7	0.085	
		Placement 1	5.9	0.012	0.057
			18.5	0.047	
			32.1	0.044	
			44.1	0.060	
			55.6	0.032	
			70.6	0.061	
			79.0	0.096	
		Placement 2	5.3	0.003	0.024
			17.9	0.006	
			31.5	0.024	
			43.5	0.125	
			55.0	0.023	
			69.9	0.103	
			78.4	0.081	
105-310	LC-HPC-2		7.2	0.013	0.064
			21.2	0.028	
			32.5	0.085	
			44.5	0.059	
			59.3	0.143	
			68.1	0.197	
46-338	LC-HPC-3		6.5	0.028	0.138
			19.2	0.110	
			31.5	0.108	
			42.6	0.315	
			54.0	0.173	

Table F.1 (con't) Crack densities for LC-HPC and OP Bridge placements obtained from annual crack surveys and interpolated crack densities at 42 months

Bridge Number	Bridge & Placement		Survey Age (months)	Crack Density (m/m^2)	Interpolated Crack Density at 42 months (m/m^2)
46-339	LC-HPC-4	Full Bridge	9.5	0.008	Not Included in Analysis
			21.3	0.090	
			32.8	0.146	
			45.0	0.107	
			56.0	0.120	
		Placement 1	9.5	0.017	Not Included in Analysis
			21.3	0.113	
			32.8	0.261	
			45.0	0.167	
			56.0	0.184	
		Placement 2	9.4	0.004	0.083
			21.2	0.079	
			32.7	0.094	
			44.9	0.080	
			55.9	0.092	
46-340 #1	LC-HPC-5		8.0	0.059	0.185
			19.4	0.123	
			31.1	0.128	
			43.0	0.190	
			54.3	0.158	
46-340 #2	LC-HPC-6		6.5	0.063	0.324
			19.7	0.238	
			31.4	0.231	
			43.4	0.336	
			54.6	0.362	
43-33	LC-HPC-7		11.4	0.003	0.008
			24.2	0.019	
			34.8	0.012	
			46.8	0.005	
			58.9	0.055	
			71.3	0.065	
54-53	LC-HPC-8		20.9	0.298	0.373
			31.8	0.348	
			45.0	0.380	
			55.4	0.383	
54-57	LC-HPC-9		13.6	0.130	0.362
			26.5	0.237	
			38.3	0.362	

Table F.1 (con't) Crack densities for LC-HPC and OP Bridge placements obtained from annual crack surveys and interpolated crack densities at 42 months

Bridge Number	Bridge & Placement		Survey Age (months)	Crack Density (m/m^2)	Interpolated Crack Density at 42 months (m/m^2)
54-60	LC-HPC-10		3.9 25.4 36.2 49.6 60.0	0.248 0.076 0.029 0.088 0.125	0.055
78-119	LC-HPC-11		23.4 36.2 48.4 61.0	0.059 0.241 0.370 0.260	0.302
56-57	LC-HPC-12	Full Bridge	10.6 21.1 33.1 43.8	0.262 0.250 0.289 0.410	Not Included in Analysis
		Placement 1	16.3 26.8 38.8 49.5	0.271 0.256 0.315 0.450	Not Included in Analysis
		Placement 2	4.9 15.4 27.3 38.1	0.254 0.244 0.268 0.375	0.375
54-66	LC-HPC-13		13.8 24.8 37.1 49.0	0.050 0.129 0.364 0.342	0.355
46-363	OP Bridge	Placement 1	18.3 30.0 42.2	0.341 0.502 0.585	0.584
		Placement 2	13.7 25.5 37.7	0.640 0.727 1.304	1.304
		Placement 3	13.3 24.9 37.1	0.421 0.871 0.678	0.678
46-351	LC-HPC-15		18.9	0.211	Not Included in Analysis
46-352	LC-HPC-16		7.7 19.4	0.092 0.249	Not Included in Analysis
46-373	LC-HPC-17		8.9	0.226	Not Included in Analysis

Table F.2 Crack densities for control placements obtained from annual crack surveys and interpolated crack densities at 42 months

Bridge Number	Bridge & Placement		Survey Age (months)	Crack Density (m/m^2)	Interpolated Crack Density at 42 months (m/m^2)
105-311	Control 1/2	Full Bridge	5.8	0.000	Not Included in Analysis
			18.3	0.089	
			31.9	0.099	
			43.9	0.184	
			55.5	0.115	
			70.4	0.190	
			78.9	0.196	
		Placement 1	6.1	0.000	0.121
			18.6	0.151	
			32.2	0.114	
			44.2	0.261	
			55.8	0.132	
			70.7	0.259	
			79.2	0.240	
		Placement 2	5.5	0.000	0.127
			18.0	0.044	
			31.6	0.091	
			43.6	0.133	
			55.2	0.106	
			70.1	0.137	
			78.6	0.161	
46-337	Control 3		10.4	0.037	0.286
			22.6	0.216	
			35.4	0.232	
			46.6	0.323	
			57.9	0.314	
46-347	Control 4		6.8	0.050	0.609
			19.7	0.366	
			31.6	0.473	
			42.7	0.618	
			54.9	0.669	
46-341 #3	Control 5		7.4	0.670	0.738
			18.9	0.857	
			30.6	0.738	
46-341 #4	Control 6		8.6	0.142	0.532
			20.0	0.282	
			31.8	0.456	
			43.0	0.539	

Table F.2 (con't) Crack densities for control placements obtained from annual crack surveys and interpolated crack densities at 42 months

Bridge Number	Bridge & Placement		Survey Age (months)	Crack Density (m/m^2)	Interpolated Crack Density at 42 months (m/m^2)
46-334	Control 7	Full Bridge	13.6	0.205	Not Included in Analysis
			24.3	0.346	
			35.4	0.772	
			48.3	0.819	
			59.5	0.856	
			71.7	0.899	
		Placement 1	16.4	0.293	1.013
			27.1	0.476	
			38.2	1.003	
			51.1	1.037	
			62.3	0.957	
			74.5	1.022	
		Placement 2	10.8	0.030	0.337
			21.5	0.069	
			32.6	0.277	
			45.5	0.359	
			56.7	0.663	
			68.9	0.638	
54-59	Control 8/10		5.2	0.046	0.205
			14.4	0.177	
			25.5	0.127	
			37.2	0.137	
			50.6	0.326	
			61.6	0.425	
54-58	Control 9	Full Bridge	24.1	0.383	0.572
			37.1	0.568	
			49.0	0.577	
		Placement 1	24.2	0.368	0.601
			37.2	0.577	
			49.1	0.637	
		Placement 2	24.0	0.395	0.531
			37.0	0.553	
			48.9	0.501	

Table F.2 (con't) Crack densities for control placements obtained from annual crack surveys and interpolated crack densities at 42 months

Bridge Number	Bridge & Placement		Survey Age (months)	Crack Density (m/m^2)	Interpolated Crack Density at 42 months (m/m^2)
56-155	Control 11	Full Bridge	16.5	0.351	0.773
			27.1	0.665	
			37.8	0.599	
			50.2	0.636	
			62.9	0.923	
			75.2	0.849	
		Subdeck Placement 1 (North)	18.3	0.253	0.732
			28.8	0.599	
			39.5	0.596	
			51.9	0.583	
			64.6	0.918	
			76.9	0.788	
		Subdeck Placement 2 (South)	17.9	0.436	0.809
			28.5	0.722	
			39.2	0.611	
			51.5	0.682	
			64.2	0.931	
			76.6	0.901	
56-57	Control 12	Full Bridge	20.7	0.548	Not Included in Analysis
			32.7	0.788	
			43.4	0.843	
		Placement 1	16.4	0.606	0.793
			26.9	0.669	
			38.9	0.767	
			49.6	0.857	
		Placement 2	14.5	0.442	0.831
			26.5	0.799	
			37.2	0.831	
54-67	Control 13		11.0	0.028	0.536
			21.9	0.154	
			34.4	0.524	
			46.1	0.543	

Table F.3 Crack densities and interpolated crack densities at 42 months for conventional monolithic (C-MONO) placements in previous studies (Schmitt and Darwin 1995, Miller and Darwin 2000, Lindquist et al. 2005)

Bridge Number	Placement	Survey Age (months)	Crack Density (m/m^2)	Interpolated Crack Density at 42 months (m/m^2)
3-046	East Deck	210 102	0.53 0.42	0.359
	West Deck	210 102	0.40 0.33	0.289
	Ctr. Deck	210 102	0.34 0.15	0.044
75-044	Deck	155 48	0.28 0.19	0.185
75-045	Deck	154 47	0.45 0.51	0.510
89-204	Deck	132 82 34	1.05 0.84 0.75	0.765
3-045	West Deck	223 112	0.43 0.12	0.000
	East Deck	223 112	0.39 0.21	0.098
	W. Ctr. Deck	223 112	0.20 0.18	0.168
	Ctr. Deck	220 112	0.28 0.23	0.198
	E. Ctr. Deck	220 112	0.31 0.15	0.046
56-142	North End	188 80	0.04 0.00	0.000
	N. + Moment	189 80	0.35 0.22	0.173
	S. + Moment	189 80	0.19 0.08	0.043
	N. Pier	188 80	0.07 0.02	0.000
	Ctr. Pier	188 80	0.36 0.20	0.142
	S. Pier	188 80	0.07 0.05	0.042
56-148	Deck	133 36 85	0.53 0.28 0.31	0.284

Table F.3 (con't) Crack densities and interpolated crack densities at 42 months for conventional monolithic (C-MONO) placements in previous studies (Schmitt and Darwin 1995, Miller and Darwin 2000, Lindquist et al. 2005)

Bridge Number	Placement	Survey Age (months)	Crack Density (m/m^2)	Interpolated Crack Density at 42 months (m/m^2)
70-095	Deck	212 106	0.13 0.07	0.035
70-103	Right	219 102	0.66 0.40	0.266
	Left	219 102	0.84 0.57	0.430
70-104	Deck	212 106	0.10 0.09	0.085
70-107	Deck	130 34 82	0.72 0.34 0.42	0.353
99-076	Placement 4	163 42	0.93 0.94	0.940
	Placement 5	163 42	0.74 0.90	0.900
	North (West Ln.)	161 42	0.57 0.77	0.770
	North (East Ln.)	157 42	0.55 0.42	0.420
	Placement 2	165 42	1.04 1.48	1.480
	Placement 3	164 42	0.81 0.95	0.950
	South End	42	0.46	0.460
89-208	Deck	73 36	0.11 0.03	0.353
105-000	Deck	42	0.27	0.270
56-49	Deck	12.0 25.8 36.8 47.5 60.7 72.7 85.0	0.077 0.230 0.219 0.265 0.316 0.358 0.395	0.256

Table F.4 Crack densities and interpolated crack densities at 42 months for conventional overlay (CO) placements in previous studies (Schmitt and Darwin 1995, Miller and Darwin 2000, Lindquist et al. 2005)

Bridge Number	Placement	Survey Age (months)	Crack Density (m/m^2)	Interpolated Crack Density at 42 months (m/m^2)
81-49	BDWS 12' Rt. of CL	133 76.0	1.060 0.803	0.651
75-1	BDWS Rt. of CL	139 82.5	0.581 0.391	0.254
89-196	BDWS Lt. Side	124 75.2	0.431 0.404	0.387
81-49	BDWS Rt. 22'	134 76.2	0.686 0.577	0.512
46-289	Outside 20'	118 71.4	0.653 0.635	0.624
89-186	Outside	130 94.3 42	0.695 0.755 0.450	0.450
89-183	BDWS Rt. Side	142 94.0	0.564 0.439	0.304
46-290	Inside 24'	118 71.7	0.748 0.656	0.598
46-301	BDWS Rt. CL 24' to 38' West	95 48.8 74	0.780 0.432 0.080	0.381
	BDWS Lt. CL 24'	94 48.5	0.833 0.566	0.528
89-186	Inside	130 94.4 42	0.790 0.688 0.560	0.560
89-200	Left	133 83.5 33	0.510 0.437 0.450	0.448

Table F.4 (con't) Crack densities and interpolated crack densities at 42 months for conventional overlay (CO) placements in previous studies (Schmitt and Darwin 1995, Miller and Darwin 2000, Lindquist et al. 2005)

Bridge Number	Placement	Survey Age (months)	Crack Density (m/m^2)	Interpolated Crack Density at 42 months (m/m^2)
46-299	Rt. Of CL 22'	95 48.7	0.665 0.686	0.686
89-183	BDWS Lt. Side	142 93.9	0.641 0.577	0.508
89-201	Right	133 83.6 34	0.688 0.659 0.590	0.601
89-185	Inside	145 97.1 41	0.631 0.568 0.950	0.943
46-289	Inside 24'	118 71.7	0.748 0.655	0.596
46-299	Lt. Of CL 18'	95 48.6	0.999 1.115	1.115
89-196	BDWS Rt. Side	124 75.3	0.758 0.664	0.599
89-201	Left	133 83.5 34	0.729 0.593 0.770	0.741
75-1	BDWS Lt. of CL	139 82.5	0.409 0.348	0.304
89-200	Right	133 83.6 33	0.771 0.672 0.570	0.588
89-185	Outside	145 97.2 41	0.955 0.806 0.600	0.604
46-301	BDWS Rt.CL 24'	95 48.6	0.719 0.976	0.976
	BDWS Lt.CL 24' to 38'	95 48.8	1.117 0.922	0.893
89-198	Right	133 83.3 33	0.510 0.412 0.400	0.402
	Left	133 83.4 33	0.445 0.356 0.700	0.638

Table F.4 (con't) Crack densities and interpolated crack densities at 42 months for conventional overlay (CO) placements in previous studies (Schmitt and Darwin 1995, Miller and Darwin 2000, Lindquist et al. 2005)

Bridge Number	Placement	Survey Age (months)	Crack Density (m/m^2)	Interpolated Crack Density at 42 months (m/m^2)
89-199	Left	133 83.4 35	0.674 0.750 0.640	0.656
	Right	133 83.3 35	0.729 0.543 0.710	0.686
46-300	BDWS 18' Rt. of CL	72 36.1	0.682 0.981	0.932
	BDWS 22' Lt. of CL	72 36.0	0.629 0.491	0.514

Table F.5 Crack densities and interpolated crack densities at 42 months for 5 percent silica fume overlay (SFO) placements in previous studies (Schmitt and Darwin 1995, Miller and Darwin 2000, Lindquist et al. 2005)

Bridge Number	Placement	Survey Age (months)	Crack Density (m/m^2)	Interpolated Crack Density at 42 months (m/m^2)
87-453	South 18'	15 61	0.32 0.92	0.669
46-317	SFO 12'	26 73	0.07 0.19	0.109
81-50	SFO Lt. Unit #2	32 78	0.70 1.28	0.823
46-302	Lt. 1/2 SFO	28 75	0.43 0.71	0.513
	Rt. 1/2 SFO	28 75	0.56 0.85	0.643
87-454	Right of CL	24 70	0.82 0.93	0.862
89-245	Lt. 1/2 Unit 1 SFO	9 68	0.03 0.47	0.276
89-234	SFO Center 12'	24 87	0.51 0.57	0.523
89-245	Lt. 1/2 Unit 2 SFO	9 68	0.03 0.54	0.318
89-244	SFO Lt.	8 67	0.00 0.15	0.090
23-85	West 1/2 SFO	28 76	0.37 0.59	0.431
46-317	SFO 16'	26 72	0.08 0.39	0.188
89-234	SFO North 18'	24 87	0.23 0.24	0.232
89-240	Rt. 22' SFO	11 68	0.01 0.10	0.061
89-244	SFO Rt.	9 67	0.03 0.45	0.269
89-245	Rt. 1/2 Unit 2 SFO	9 68	0.05 0.45	0.279
89-246	West 1/2 SFO	10 61	0.06 0.29	0.207

Table F.5 (con't) Crack densities and interpolated crack densities at 42 months for 5 percent silica fume overlay (SFO) placements in previous studies (Schmitt and Darwin 1995, Miller and Darwin 2000, Lindquist et al. 2005)

Bridge Number	Placement	Survey Age (months)	Crack Density (m/m^2)	Interpolated Crack Density at 42 months (m/m^2)
81-50	SFO Rt. Unit #2	33 78	0.67 0.90	0.718
89-247	Rt. 26' SFO	14 72	0.52 0.51	0.516
89-207	Right	27 86	0.39 0.45	0.403
89-234	SFO South 20'	25 88	0.17 0.18	0.176
89-245	Rt. 1/2 Unit 1 SFO	9 68	0.09 0.35	0.235
87-454	Left of CL	25 71	0.66 0.80	0.713
89-235	SFO Right 18'	14 77	0.38 0.21	0.307
89-240	Lt. 22' SFO	11 68	0.41 0.32	0.361
46-309	Lt. 1/2 SFO	33 81	0.38 0.56	0.413
87-453	North 22'	15 61	0.19 0.71	0.490
89-206	Left	33 91	0.27 0.48	0.305
89-210	Right	32 70	0.17 0.62	0.286
89-206	Right	33 91	0.58 0.41	0.552
89-246	East 1/2 SFO	10 61	0.08 0.37	0.263

Table F.5 (con't) Crack densities and interpolated crack densities at 42 months for 5 percent silica fume overlay (SFO) placements in previous studies (Schmitt and Darwin 1995, Miller and Darwin 2000, Lindquist et al. 2005)

Bridge Number	Placement	Survey Age (months)	Crack Density (m/m^2)	Interpolated Crack Density at 42 months (m/m^2)
89-248	Eastbound Lane	4 62	0.03 0.55	0.366
46-309	Rt. 1/2 SFO	34 81	0.32 0.50	0.349
89-247	Lt. 13' SFO	14 72	0.47 0.62	0.542
89-207	Left	33 91	0.33 0.40	0.342
89-248	Westbound Lane	4 62	0.02 0.48	0.317
23-85	East 1/2 SFO	29 76	0.37 0.54	0.415
89-210	Left	32 70	0.15 0.55	0.257
89-184	Inside	39 94 142	0.68 0.94 0.90	0.694
	Outside	39 94 142	0.70 1.06 0.88	0.719
89-187	Inside	41 97 133	1.46 1.21 0.99	1.456
	Outside	41 97 132	0.65 0.79 0.83	0.652

Table F.6 Temperature data for LC-HPC and Control subdeck placements‡

Bridge & Placement		42-month Crack Density (m/m^2)	Avg. Concrete Temp. ° F (° C)	Avg. Air Temp. during construction ° F (° C)	Avg. Concrete Temp. - Avg. Air Temp. during construction† ° F (° C)
LC-HPC-1	Placement 1	0.057	67 (20)	57 (14)	10 (6)
	Placement 2	0.024	68 (20)	56 (13)	12 (7)
LC-HPC-2		0.064	67 (19)	58 (14)	9 (5)
LC-HPC-3		0.138	58 (14)	44 (7)	14 (7)
LC-HPC-4	Placement 2	0.083	64 (18)	64 (18)	0 (0)
LC-HPC-5		0.185	61 (16)	51 (11)	10(5)
LC-HPC-6		0.324	60 (15)	44 (7)	16 (8)
LC-HPC-7		0.008	71 (22)	67 (19)	4 (3)
LC-HPC-9		0.362	64 (18)	63 (17)	1 (1)
LC-HPC-11		0.302	60 (16)	65 (18)	-5 (-2)
LC-HPC-12	Placement 2	0.375	67 (20)	58 (14)	9 (6)
LC-HPC-13		0.355	69 (20)	66 (19)	3 (1)
OP Bridge	Placement 1	0.584	65 (18)	50 (10)	15 (8)
	Placement 2	1.304	64 (18)	57 (14)	7 (4)
	Placement 3	0.678	65 (18)	68 (20)	-3 (-2)
Control 1/2	Placement 1	0.121	66 (19)	Not Available	Not Available
	Placement 2	0.127	76 (25)		
Control 3		0.286	81 (27)		
Control 4		0.609	73 (23)		
Control 5*		0.738	66 (19)		
Control 6*		0.532	75 (24)		
Control 7	Placement 1	1.013	80 (27)		
	Placement 2	0.337	70 (21)		
Control 9**	Placement 1	0.601	66 (19)		
	Placement 2	0.531	66 (19)		
Control 11	Placement 1	0.732	72 (22)		
	Placement 2	0.809	73 (23)		
Control 12	Placement 1	0.793	72 (22)		
	Placement 2	0.831	72 (22)		
Control 13		0.536	89 (32)		

* Temperature data for Control 5 and 6 based on average values from each subdeck

**Control 9 includes one subdeck and two overlay placements. 42-month Crack Density of Control 9 subdeck = 0.572 m/m^2, shown in Table F.2. Temperature data shown represents values recorded during subdeck construction.

† Represents difference between average concrete temperature and average air temperature during construction

‡ Air temperature data obtained from Weather Underground (weatherunderground.com)

Table F.6 (con't) Temperature data for LC-HPC and Control subdeck placements‡

Bridge & Placement		Air Temperature on day of construction			
		High ° F (° C)	Average ° F (° C)	Low ° F (° C)	Range ° F (° C)
LC-HPC-1	Placement 1	84 (29)	68 (20)	51 (11)	33 (18)
	Placement 2	78 (26)	61 (16)	43 (6)	35 (20)
LC-HPC-2		78 (26)	66 (19)	53 (12)	25 (14)
LC-HPC-3		65 (18)	53 (12)	39 (4)	26 (14)
LC-HPC-4	Placement 2	79 (26)	70 (21)	59 (15)	20 (11)
LC-HPC-5		56 (13)	51 (11)	41 (5)	15 (8)
LC-HPC-6		60 (16)	47 (8)	34 (1)	26 (15)
LC-HPC-7		88 (31)	76 (24)	63 (17)	25 (14)
LC-HPC-9		69 (21)	57 (14)	44 (7)	25 (14)
LC-HPC-11		87 (31)	67 (19)	48 (9)	39 (22)
LC-HPC-12	Placement 2	64 (18)	53 (12)	44 (7)	20 (11)
LC-HPC-13		71 (22)	54 (12)	37 (3)	34 (19)
OP Bridge	Placement 1	51 (11)	38 (3)	26 (-3)	25 (14)
	Placement 2	68 (20)	58 (14)	50 (10)	18 (10)
	Placement 3	78 (26)	65 (18)	50 (10)	28 (16)
Control 1/2	Placement 1	75 (24)	64 (18)	52 (11)	23 (13)
	Placement 2	82 (28)	68 (20)	53 (12)	29 (16)
Control 3		90 (32)	78 (26)	69 (21)	21 (11)
Control 4		81 (27)	66 (19)	51 (11)	30 (16)
Control 5*		48 (9)	41 (5)	34 (1)	14 (8)
Control 6*		77 (25)	66 (19)	56 (13)	21 (12)
Control 7	Placement 1	64 (18)	50 (10)	35 (2)	29 (16)
	Placement 2	89 (32)	79 (26)	69 (21)	20 (11)
Control 9**	Placement 1	63 (17)	52 (11)	41 (5)	22 (12)
	Placement 2	63 (17)	52 (11)	41 (5)	22 (12)
Control 11	Placement 1	46 (8)	36 (2)	24 (-4)	22 (12)
	Placement 2	64 (18)	46 (8)	28 (-2)	36 (20)
Control 12	Placement 1	69 (21)	46 (8)	25 (-4)	44 (25)
	Placement 2	46 (8)	38 (3)	30 (-1)	16 (9)
Control 13		90 (32)	79 (26)	69 (21)	21 (11)

* Temperature data for Control 5 and 6 is based on average values from each subdeck

** Control 9 includes one subdeck and two overlay placements. Temperature data shown represents values recorded during subdeck construction.

‡ Air temperature data obtained from Weather Underground (weatherunderground.com)

Table F.6 (con't) Temperature data for LC-HPC and Control subdeck placements‡

Bridge & Placement		Avg. Concrete Temp. - High Air Temp. on day of construction† ° F (° C)	Avg. Concrete Temp. - Avg. Air Temp. on day of construction# ° F (° C)
LC-HPC-1	Placement 1	-17 (-9)	-1 (-1)
	Placement 2	-10 (-6)	7 (4)
LC-HPC-2		-11 (-7)	1 (1)
LC-HPC-3		-7 (-4)	5 (2)
LC-HPC-4	Placement 2	-15 (-8)	-6 (-3)
LC-HPC-5		5 (3)	10 (5)
LC-HPC-6		0 (0)	13 (8)
LC-HPC-7		-17 (-9)	-5 (-2)
LC-HPC-9		-5 (-3)	7 (4)
LC-HPC-11		-27 (-15)	-7 (-3)
LC-HPC-12	Placement 2	3 (2)	14 (8)
LC-HPC-13		-2 (-1)	15 (9)
OP Bridge	Placement 1	14 (7)	27 (15)
	Placement 2	-4 (-2)	6 (4)
	Placement 3	-13 (-7)	-1 (-1)
Control 1/2	Placement 1	-9 (-5)	2 (1)
	Placement 2	-6 (-3)	8 (5)
Control 3		-9 (-5)	3 (1)
Control 4		-8 (-4)	7 (4)
Control 5*		18 (10)	25 (14)
Control 6*		3 (2)	14 (8)
Control 7	Placement 1	16 (9)	30 (17)
	Placement 2	-19 (-11)	-9 (-5)
Control 9**	Placement 1	3 (2)	14 (8)
	Placement 2	3 (2)	14 (8)
Control 11	Placement 1	26 (14)	36 (20)
	Placement 2	9 (5)	27 (15)
Control 12	Placement 1	3 (2)	26 (14)
	Placement 2	26 (14)	34 (19)
Control 13		-1 (-1)	10 (6)

* Temperature data for Control 5 and 6 is based on average values from each subdeck

** Control 9 includes one subdeck and two overlay placements. Temperature data shown represents values recorded during subdeck construction.

† Represents difference between average concrete temperature and high air temperature on the day of construction

Represents difference between average concrete temperature and average air temperature on the day of construction

‡ Air temperature data obtained from Weather Underground (weatherunderground.com)

Table F.7 Raw data used in dummy variables regression analysis

Bridge Number	Placement	Crack Density at 42 months m/m^2	Contractor	Paste Content %	Average Slump in. (mm)
56-142	N. + Moment	0.173	#1	26.5	2 (50)
	S. + Moment	0.043		26.5	2 (50)
	N. Pier	0.000		26.5	2.25 (60)
	Ctr. Pier	0.142		26.5	2.25 (60)
	S. Pier	0.042		26.5	2.25 (60)
75-044	Deck	0.185		27.9	2.5 (65)
75-045	Deck	0.510		27.9	2.5 (65)
LC-HPC-12 p2		0.375		24.2	4.25 (110)
89-208	Deck	0.353	#2	27.1	2.25 (60)
3-045	West Deck	0.000	#3	26.4	2 (50)
	East Deck	0.098		26.4	2.25 (60)
	W. Ctr. Deck	0.168		26.4	2 (50)
	Ctr. Deck	0.198		26.4	2.25 (60)
	E. Ctr. Deck	0.046		26.4	1.75 (45)
3-046	West Deck	0.289		26.4	2 (50)
	East Deck	0.359		26.4	2.25 (60)
	Ctr. Deck	0.044		25.6	1.5 (40)
LC-HPC-13		0.355		24.1	3 (75)
LC-HPC-7		0.008	#4	24.6	3.75 (95)
70-095	Deck	0.035		27.2	1.75 (45)
70-104	Deck	0.085		27.2	1.75 (45)
89-204	Deck	0.765	#5	28.8	3 (75)
LC-HPC-1 p1		0.057		24.6	3.75 (95)
LC-HPC-1 p2		0.024		24.6	3.25 (85)
LC-HPC-2		0.064		24.6	3 (75)
LC-HPC-3		0.138		24.4	3.25 (85)
LC-HPC-4 p2		0.083		23.4	3 (75)
LC-HPC-5		0.185		23.9	3 (75)
LC-HPC-6		0.324		24.4	4 (100)

Table F.7 (con't.) Raw data used in dummy variables regression analysis

Bridge Number	Placement	28-Day Compressive Strength psi (MPa)	Average Air Content %	Air Temperature Range ° F (° C)	Diff. between Avg. Concrete Temp & Avg. Air Temp. ° F (° C)	Max. Air Temperature ° F (° C)
56-142	N. + Moment	4760 (32.8)	6.1	34 (19)	6 (4)*	78 (26)
	S. + Moment	4760 (32.8)	6.1	34 (19)	6 (4)*	78 (26)
	N. Pier	5130 (35.4)	6.0	24 (13)	6 (4)*	65 (18)
	Ctr. Pier	5130 (35.4)	6.0	24 (13)	6 (4)*	65 (18)
	S. Pier	5130 (35.4)	6.0	24 (13)	6 (4)*	65 (18)
75-044	Deck	6430 (44.3)	5.6	4 (2)	6 (4)*	66 (19)
75-045	Deck	5640 (38.9)	5.8	22 (12)	6 (4)*	88 (31)
LC-HPC-12 p2		4380 (30.2)	7.8	20 (11)	14 (8)	64 (18)
89-208	Deck	7430 (51.2)	5.0	21 (12)	6 (4)*	89 (32)
3-045	West Deck	4790 (33.0)	5.0	18 (10)	6 (4)*	46 (8)
	East Deck	6190 (42.7)	4.5	16 (9)	6 (4)*	49 (9)
	W. Ctr. Deck	5640 (38.9)	5.0	13 (7)	6 (4)*	62 (17)
	Ctr. Deck	6140 (42.3)	5.5	19 (10)	6 (4)*	54 (12)
	E. Ctr. Deck	6270 (43.2)	6.0	31 (17)	6 (4)*	61 (16)
3-046	West Deck	5260 (36.3)	6.0	15 (8)	6 (4)*	43 (6)
	East Deck	5760 (39.7)	6.0	16 (9)	6 (4)*	52 (11)
	Ctr. Deck	5630 (38.8)	6.0	24 (13)	6 (4)*	50 (10)
LC-HPC-13		4280 (29.5)	8.1	34 (19)	15 (9)	71 (22)
LC-HPC-7		3790 (26.1)	8.0	25 (14)	-5 (-2)	88 (31)
70-095	Deck	5510 (38.0)	5.9	18 (10)	6 (4)*	57 (14)
70-104	Deck	4170 (28.8)	5.0	2 (1)	6 (4)*	73 (23)
89-204	Deck	6370 (43.9)	5.2	21 (12)	6 (4)*	77 (25)
LC-HPC-1 p1		5210 (35.9)	7.9	33 (18)	-1 (-1)	84 (29)
LC-HPC-1 p2		4980 (34.3)	7.8	35 (20)	7 (4)	78 (26)
LC-HPC-2		4600 (31.7)	7.7	25 (14)	1 (1)	78 (26)
LC-HPC-3		5990 (41.3)	8.7	26 (14)	5 (2)	65 (18)
LC-HPC-4 p2		4790 (33.0)	8.8	20 (11)	-6 (-3)	79 (26)
LC-HPC-5		6380 (44.0)	8.7	15 (8)	10 (5)	56 (13)
LC-HPC-6		5840 (40.3)	9.5	26 (14)	13 (8)	60 (16)

*Average value of difference between average concrete temperature and average air temperature on the day of construction for LC-HPC decks and OP Bridge inserted as value for each C-MONO deck

Table F.7 (con't.) Raw data used in dummy variables regression analysis

Bridge Number	Placement	Crack Density at 42 months m/m^2	Contractor	Paste Content %	Average Slump in. (mm)
70-103	Right	0.266	#6	27.2	1.75 (45)
	Left	0.430		27.2	1.75 (45)
56-148	Deck	0.284	#7	27.2	2.5 (65)
70-107	Deck	0.353		27.2	2.25 (60)
LC-HPC-11		0.302		23.4	3 (75)
56-49	Deck	0.256		25.7	3 (75)
OP Bridge p1		0.584	#8	24.4	3.75 (95)
OP Bridge p2		1.304		24.4	4.25 (110)
OP Bridge p3		0.678		24.4	5.25 (135)
99-076	Placement 2	1.480	#9	27.9	2 (50)
	Placement 3	0.950		27.9	2.25 (60)
	Placement 4	0.940		28.7	2.25 (60)
	Placement 5	0.900		28.7	2.25 (60)
	North (West Ln.)	0.770		28.7	2.5 (65)
	North (East Ln.)	0.420		28.7	2.25 (60)
LC-HPC-9		0.362	#10	24.2	3.5 (90)

Table F.7 (con't.) Raw data used in dummy variables regression analysis

Bridge Number	Placement	28-Day Compressive Strength psi (MPa)	Average Air Content %	Air Temperature Range ° F (° C)	Diff. between Avg. Concrete Temp & Avg. Air Temp. ° F (° C)	Max. Air Temperature ° F (° C)
70-103	Right	5110 (35.2)	5.9	31 (17)	6 (4)*	61 (16)
	Left	4750 (32.8)	5.4	31 (17)	6 (4)*	70 (21)
56-148	Deck	6170 (42.5)	6.5	23 (13)	6 (4)*	97 (36)
70-107	Deck	6820 (47.0)	5.4	21 (12)	6 (4)*	57 (14)
LC-HPC-11		4680 (32.3)	7.7	39 (22)	-7 (-3)	87 (31)
56-49	Deck	5510 (38.0)	5.9	22 (12)	6 (4)*	79 (26)
OP Bridge p1		4440 (30.6)	8.7	25 (14)	27 (15)	51 (11)
OP Bridge p2		3710 (25.6)	9.8	18 (10)	6 (4)	68 (20)
OP Bridge p3		3830 (26.4)	9.9	28 (16)	-1 (-1)	78 (26)
99-076	Placement 2	7400 (51.0)	5.0	38 (21)	6 (4)*	82 (28)
	Placement 3	6700 (46.2)	5.3	40 (22)	6 (4)*	88 (31)
	Placement 4	6100 (42.1)	5.8	34 (19)	6 (4)*	62 (17)
	Placement 5	6250 (43.1)	4.8	25 (14)	6 (4)*	53 (12)
	North (West Ln.)	5750 (39.6)	5.5	18 (10)	6 (4)*	55 (13)
	North (East Ln.)	5750 (39.6)	6.0	18 (10)	6 (4)*	60 (16)
LC-HPC-9		4190 (28.9)	6.7	25 (14)	7 (4)	69 (21)

*Average value of difference between average concrete temperature and average air temperature on the day of construction for LC-HPC decks and OP Bridge inserted as value for each C-MONO deck

APPENDIX G: REVISED LOW-CRACKING HIGH-PERFORMANCE CONCRETE (LC-HPC) SPECIFICATIONS

KANSAS DEPARTMENT OF TRANSPORTATION
SPECIAL PROVISION TO THE
STANDARD SPECIFICATIONS, 2007 EDITION

Add a new SECTION to DIVISION 1100:

LOW-CRACKING HIGH-PERFORMANCE CONCRETE – AGGREGATES

1.0 DESCRIPTION

This specification is for coarse aggregates, fine aggregates, mixed aggregates (both coarse and fine material), and lightweight aggregates (for the purpose of internal curing) for use in bridge deck construction.

2.0 REQUIREMENTS

a. Coarse Aggregates for Concrete.

(1) Composition. Provide coarse aggregate that is crushed or uncrushed gravel, chat, or crushed stone. (Consider calcite cemented sandstone, rhyolite, basalt and granite as crushed stone

(2) Quality. The quality requirements for coarse aggregate for bridge decks are in **TABLE 1-1**:

TABLE 1-1: QUALITY REQUIREMENTS FOR COARSE AGGREGATES FOR BRIDGE DECK

Concrete Classification	Soundness (min.)	Wear (max.)	Absorption (max.)	Acid Insol. (min.)
Grade 3.5 (AE) (LC-HPC) [1]	0.90	40	0.7	55

[1] Grade 3.5 (AE) (LC-HPC) – Bridge Deck concrete with select coarse aggregate for wear and acid insolubility.

(3) Product Control.

(a) Deleterious Substances. Maximum allowed deleterious substances by weight are:

- Material passing the No. 200 sieve (KT-2)..... 2.5%
- Shale or Shale-like material (KT-8)..... 0.5%
- Clay lumps and friable particles (KT-7) 1.0%
- Sticks (wet) (KT-35)..... 0.1%
- Coal (AASHTO T 113)..... 0.5%

(b) Uniformity of Supply. Designate or determine the fineness modulus (grading factor) according to the procedure listed in the Construction Manual Part V, Section 17 before delivery, or from the first 10 samples tested and accepted. Provide aggregate that is within ±0.20 of the average fineness modulus.

(4) Do not combine siliceous fine aggregate with siliceous coarse aggregate if neither meet the requirements of **subsection 2.0c.(2)(a)**. Consider such fine material, regardless of proportioning, as a Basic Aggregate that must conform to **subsection 2.0c**.

(5) Handling Coarse Aggregates.

(a) Segregation. Before acceptance testing, remix all aggregate segregated by transportation or stockpiling operations.

(b) Stockpiling.

- Stockpile accepted aggregates in layers 3 to 5 feet thick. Berm each layer so that aggregates do not "cone" down into lower layers.
- Keep aggregates from different sources, with different gradings, or with a significantly different specific gravity separated.
- Transport aggregate in a manner that insures uniform gradation.
- Do not use aggregates that have become mixed with earth or foreign material.

- Stockpile or bin all washed aggregate produced or handled by hydraulic methods for 12 hours (minimum) before batching. Rail shipment exceeding 12 hours is acceptable for binning provided the car bodies permit free drainage.
- Provide additional stockpiling or binning in cases of high or non-uniform moisture.

b. Fine Aggregates for Basic Aggregate in MA for Concrete.

(1) Composition.

(a) Type FA-A. Provide either singly or in combination natural occurring sand resulting from the disintegration of siliceous or calcareous rock, or manufactured sand produced by crushing predominately siliceous materials.

(b) Type FA-B. Provide fine granular particles resulting from the crushing of zinc and lead ores (Chat).

(2) Quality.

(a) Mortar strength and Organic Impurities. If the District Materials Engineer determines it is necessary, because of unknown characteristics of new sources or changes in existing sources, provide fine aggregates that comply with these requirements:

- Mortar Strength (Mortar Strength Test, KTMR-26). Compressive strength when combined with Type III (high early strength) cement:
  - At age 24 hours, minimum……...100%*
  - At age 72 hours, minimum……...100%*

  *Compared to strengths of specimens of the same proportions, consistency, cement and standard 20-30 Ottawa sand.
- Organic Impurities (Organic Impurities in Fine Aggregate for Concrete Test, AASHTO T 21). The color of the supernatant liquid is equal to or lighter than the reference standard solution.

(b) Hardening characteristics. Specimens made of a mixture of 3 parts FA-B and 1 part cement with sufficient water for molding will harden within 24 hours. There is no hardening requirement for FA-A.

(3) Product Control.

(a) Deleterious Substances.

- Type FA-A: Maximum allowed deleterious substances by weight are:
  - Material passing the No. 200 sieve (KT-2)……..……. 2.0%
  - Shale or Shale-like material (KT-8) ……. 0.5%
  - Clay lumps and friable particles (KT-7)……..……. 1.0%
  - Sticks (wet) (KT-35)……...…… 0.1%
- Type FA-B: Provide materials that are free of organic impurities, sulfates, carbonates, or alkali. Maximum allowed deleterious substances by weight are:
  - Material passing the No. 200 sieve (KT-2)…….…….…..... 2.0%
  - Clay lumps & friable particles (KT-7)……. 0.25%

(c) Uniformity of Supply. Designate or determine the fineness modulus (grading factor) according to the procedure listed in the Construction Manual Part V, Section 17 before delivery, or from the first 10 samples tested and accepted. Provide aggregate that is within ±0.20 of the average fineness modulus.

(4) Proportioning of Coarse and Fine Aggregate. Use a proven optimization method such as the Shilstone Method or the KU Mix Method.

Do not combine siliceous fine aggregate with siliceous coarse aggregate if neither meet the requirements of **subsection 2.0c.(2)(a)**. Consider such fine material, regardless of proportioning, as a Basic Aggregate and must conform to the requirements in **subsection 2.0c**.

(5) Handling and Stockpiling Fine Aggregates.

- Keep aggregates from different sources, with different gradings or with a significantly different specific gravity separated.
- Transport aggregate in a manner that insures uniform grading.
- Do not use aggregates that have become mixed with earth or foreign material.

- Stockpile or bin all washed aggregate produced or handled by hydraulic methods for 12 hours (minimum) before batching. Rail shipment exceeding 12 hours is acceptable for binning provided the car bodies permit free drainage.
- Provide additional stockpiling or binning in cases of high or non-uniform moisture.

c. Mixed Aggregates for Concrete.

(1) Composition.

(a) Total Mixed Aggregate (TMA). A natural occurring, predominately siliceous aggregate from a single source that meets the Wetting & Drying Test (KTMR-23) and grading requirements.

(b) Mixed Aggregate. A combination of basic and coarse aggregates that meet **TABLE 1-2**.

- Basic Aggregate (BA). Singly or in combination, a natural occurring, predominately siliceous aggregate that does not meet the grading requirements of Total Mixed Aggregate.

(c) Coarse Aggregate. Granite, crushed sandstone, chat, and gravel. Gravel that is not approved under **subsection 2.0c.(2)** may be used, but only with basic aggregate that meets the wetting and drying requirements of TMA.

(2) Quality.

(a) Total Mixed Aggregate.

- Soundness, minimum (KTMR-21) …….……0.90
- Wear, maximum (KTMR-25) ……..……50%
- Wetting and Drying Test (KTMR-23) for Total Mixed Aggregate
  Concrete Modulus of Rupture:
  - At 60 days, minimum…….550 psi
  - At 365 days, minimum…..……..……550 psi

  Expansion:
  - At 180 days, maximum…….……0.050%
  - At 365 days, maximum…….…….0.070%
  - Aggregates produced from the following general areas are exempt from the Wetting and Drying Test:
  - Blue River Drainage Area.
  - The Arkansas River from Sterling, west to the Colorado state line.
  - The Neosho River from Emporia to the Oklahoma state line.

(b) Basic Aggregate.

- Retain 10% or more of the BA on the No. 8 sieve before adding the Coarse Aggregate. Aggregate with less than 10% retained on the No. 8 sieve is to be considered a Fine Aggregate described in **subsection 2.0b**. Provide material with less than 5% calcareous material retained on the ⅜" sieve.
- Soundness, minimum (KTMR-21)…….0.90
- Wear, maximum (KTMR-25)…….……50%
- Mortar strength and Organic Impurities. If the District Materials Engineer determines it is necessary, because of unknown characteristics of new sources or changes in existing sources, provide mixed aggregates that comply with these requirements:
  - Mortar Strength (Mortar Strength Test, KTMR-26). Compressive strength when combined with Type III (high early strength) cement:
    - At age 24 hours, minimum……..100%*
    - At age 72 hours, minimum……..100%*

      *Compared to strengths of specimens of the same proportions, consistency, cement and standard 20-30 Ottawa sand.
  - Organic Impurities (Organic Impurities in Fine Aggregate for Concrete Test, AASHTO T 21). The color of the supernatant liquid is equal to or lighter than the reference standard solution.

(3) Product Control.

(a) Size Requirement. Provide mixed aggregates that comply with the grading requirements in **TABLE 1-2**.

TABLE 1-2: GRADING REQUIREMENTS FOR MIXED AGGREGATES FOR CONCRETE BRIDGE DECKS												
Type	**Usage**	**Percent Retained on Individual Sieves - Square Mesh Sieves**										
		1½"	**1"**	**3/4"**	**1/2"**	**3/8"**	**No. 4**	**No. 8**	**No. 16**	**No. 30**	**No. 50**	**No. 100**
MA-4	Optimized for LC-HPC Bridge Decks*	0	2-6	5-18	8-18	8-18	8-18	8-18	8-18	8-15	5-15	0-5

*Use a proven optimization method, such as the Shilstone Method or the KU Mix Method.

Note: Manufactured sands used to obtain optimum gradations have caused difficulties in pumping, placing or finishing. Natural coarse sands and pea gravels used to obtain optimum gradations have worked well in concretes that were pumped.

(b) Deleterious Substances. Maximum allowed deleterious substances by weight are:

- Material passing the No. 200 sieve (KT-2)……..….. 2.5%
- Shale or Shale-like material (KT-8)……..……. 0.5%
- Clay lumps and friable particles (KT-7)…… 1.0%
- Sticks (wet) (KT-35)……..…… 0.1%
- Coal (AASHTO T 113)…..……..……. 0.5%

(c) Uniformity of Supply. Designate or determine the fineness modulus (grading factor) according to the procedure listed in the Construction Manual Part V, Section 17 before delivery, or from the first 10 samples tested and accepted. Provide aggregate that is within ±0.20 of the average fineness modulus.

(4) Handling Mixed Aggregates.

(a) Segregation. Before acceptance testing, remix all aggregate segregated by transit or stockpiling.

(b) Stockpiling.

- Keep aggregates from different sources, with different gradings or with a significantly different specific gravity separated.
- Transport aggregate in a manner that insures uniform grading.
- Do not use aggregates that have become mixed with earth or foreign material.
- Stockpile or bin all washed aggregate produced or handled by hydraulic methods for 12 hours (minimum) before batching. Rail shipment exceeding 12 hours is acceptable for binning provided the car bodies permit free drainage.
- Provide additional stockpiling or binning in cases of high or non-uniform moisture.

d. Lightweight Aggregates for Concrete.

This specification covers lightweight aggregate used to provide internal curing water for concrete. The requirements of ASTM C1761 and C330 shall apply except as modified in this specification.

(1) Product Control

(a) Size Requirement. Entire portion of lightweight aggregate shall pass 3/8 in. sieve.

(2) Proportioning.

(a) Volume of lightweight aggregate added to a mixture shall not exceed 10 percent of total aggregate volume. If lightweight aggregate is used as a replacement for normalweight aggregate, the replacement shall be made on a volume basis.

(3) Pre-wetting.

(a) Lightweight aggregate shall be pre-wetted prior to adding at the time of batching. Recommendations for pre-wetting made by the lightweight aggregate supplier shall be followed to ensure that the lightweight aggregate has achieved an acceptable absorbed moisture content at the

time of batching. Mixture proportions shall not be adjusted based on the absorbed water in the lightweight aggregate.

(4) Handling and Stockpiling Lightweight Aggregates.

(a) Lightweight aggregates shall be handled and stockpiled in accordance with the requirements for fine aggregates in subsection 2.0b.(5)

3.0 TEST METHODS

Test aggregates according to the applicable provisions of **SECTION 1117**.

4.0 PREQUALIFICATION

Aggregates for concrete must be prequalified according to **subsection 1101.2**.

5.0 BASIS OF ACCEPTANCE

The Engineer will accept aggregates for concrete base on the prequalification required by this specification, and **subsection 1101.4**.

01-27-14 BP DD

KANSAS DEPARTMENT OF TRANSPORTATION
SPECIAL PROVISION TO THE
STANDARD SPECIFICATIONS 2007 EDITION

Add a new SECTION to DIVISION 400:

LOW-CRACKING HIGH-PERFORMANCE CONCRETE

1.0 DESCRIPTION

Provide the grades of low-cracking high-performance concrete (LC-HPC) specified in the Contract Documents.

2.0 MATERIALS

Coarse, Fine & Mixed Aggregate.....**07-PS0165, latest version**
Admixtures.....**DIVISION 1400**
Cement .....**DIVISION 2000**
Water .....**DIVISION 2400**

3.0 CONCRETE MIX DESIGN

a. General. Design the concrete mixes specified in the Contract Documents.

Provide aggregate gradations that comply with **07-PS0165, latest version** and Contract Documents.

If desired, contact the DME for available information to help determine approximate proportions to produce concrete having the required characteristics on the project.

Take full responsibility for the actual proportions of the concrete mix, even if the Engineer assists in the design of the concrete mix.

Submit all concrete mix designs to the Engineer for review and approval. Submit completed volumetric mix designs on KDOT Form No. 694 (or other forms approved by the DME).

Do not place any concrete on the project until the Engineer approves the concrete mix designs. Once the Engineer approves the concrete mix design, do not make changes without the Engineer's approval.

Design concrete mixes that comply with these requirements:

b. Air-Entrained Concrete for Bridge Decks. Design air-entrained concrete for structures according to **TABLE 1-1**.

TABLE 1-1: AIR ENTRAINED CONCRETE FOR BRIDGE DECKS

Grade of Concrete Type of Aggregate (SECTION 1100)	lb of Cementitious Material per cu yd of Concrete, min/max	lb of Water per lb of Cementitious Material*	Designated Air Content Percent by Volume**	Specified 28-day Compressive Strength Range, psi
Grade 3.5 (AE) (LC-HPC)				
MA-4	500 / 540	0.44 – 0.45	8.0 ± 1.0	3500 – 5500

*Limits of lb. of water per lb. of cementitious material. Includes free water in aggregates, but excludes water of absorption of the aggregates. With approval of the Engineer, may be decreased to 0.43 on-site.

**Concrete with an air content less than 6.5% or greater than 9.5% shall be rejected. The Engineer will sample concrete for tests at the discharge end of the conveyor, bucket or if pumped, the piping.

c. Portland Cement. Select the type of portland cement specified in the Contract Documents. Portions of portland cement may be replaced with slag cement or slag cement and silica fume if used in conjunction with

internal curing using pre-wetted lightweight aggregate (see 07-PS0165 subsection 2.0d.). The replacements of portland cement are limited to 30% by volume with slag cement and 3% by volume with silica fume.

d. Design Air Content. Use the middle of the specified air content range for the design of air-entrained concrete.

e. Admixtures for Air-Entrainment and Water Reduction. Verify that the admixtures used are compatible and will work as intended without detrimental effects. Use the dosages recommended by the admixture manufacturers to determine the quantity of each admixture for the concrete mix design. Incorporate and mix the admixtures into the concrete mixtures according to the manufacturer's recommendations.

Set retarding or accelerating admixtures are prohibited for use in Grade 3.5 (AE) (LC-HPC) concrete. These include Type B, C, D, E, and G chemical admixtures as defined by ASTM C 494/C 494M – 08. Do not use admixtures containing chloride ion (CL) in excess of 0.1 percent by mass of the admixture in Grade 3.5 (AE) (LC-HPC) concrete.

(1) Air-Entraining Admixture. If specified, use an air-entraining admixture in the concrete mixture. If another admixture is added to an air-entrained concrete mixture, determine if it is necessary to adjust the air-entraining admixture dosage to maintain the specified air content. Use only a vinsol resin or tall oil based air-entraining admixture.

(2) Water-Reducing Admixture. Use a Type A water reducer or a dual rated Type A water reducer – Type F high-range water reducer, when necessary to obtain compliance with the specified fresh and hardened concrete properties.

Include a batching sequence in the concrete mix design. Consider the location of the concrete plant in relation to the job site, and identify the approximate quantity, when and at what location the water-reducing admixture is added to the concrete mixture.

The manufacturer may recommend mixing revolutions beyond the limits specified in **subsection 5.0**. If necessary and with the approval of the Engineer, address the additional mixing revolutions (the Engineer will allow up to 60 additional revolutions) in the concrete mix design.

Slump control may be accomplished in the field only by redosing with a water-reducing admixture. If time and temperature limits are not exceeded, and if at least 30 mixing revolutions remain, the Engineer will allow redosing with up to 50% of the original dose. The redosed concrete shall be retested for slump prior to deposit on the bridge deck.

(3) Adjust the mix designs during the course of the work when necessary to achieve compliance with the specified fresh and hardened concrete properties. Only permit such modifications after trial batches to demonstrate that the adjusted mix design will result in concrete that complies with the specified concrete properties.

The Engineer will allow adjustments to the dose rate of air entraining and water-reducing chemical admixtures to compensate for environmental changes during placement without a new concrete mix design or qualification batch.

f. Designated Slump. Designate a slump for each concrete mix design within the limits in **TABLE 1-2**.

TABLE 1-2: DESIGNATED SLUMP*

Type of Work	Designated Slump (inches)
Grade 3.5 (AE) (LC-HPC)	1 ½ - 3

* The Engineer will obtain sample concrete at the discharge end of the conveyor, bucket or if pumped, the piping.

If potential problems are apparent at the discharge of any truck, and the concrete is tested at the truck discharge (according to **subsection 6.0**), the Engineer will reject concrete with a slump greater than 3 ½ inches at the truck discharge, 3 inches if being placed by a bucket.

4.0 REQUIREMENTS FOR COMBINED MATERIALS

a. Measurements for Proportioning Materials.

(1) Cement. Measure cement as packed by the manufacturer. A sack of cement is considered as 0.04 cubic yards weighing 94 pounds net. Measure bulk cement by weight. In either case, the measurement must be accurate to within 0.5% throughout the range of use.

(2) Water. Measure the mixing water by weight or volume. In either case, the measurement must be accurate to within 1% throughout the range of use.

(3) Aggregates. Measure the aggregates by weight. The measurement must be accurate to within 0.5% throughout the range of use.

(4) Admixtures. Measure liquid admixtures by weight or volume. If liquid admixtures are used in small quantities in proportion to the cement as in the case of air-entraining agents, use readily adjustable mechanical dispensing equipment capable of being set to deliver the required quantity and to cut off the flow automatically when this quantity is discharged. The measurement must be accurate to within 3% of the quantity required.

b. Testing of Aggregates. Testing Aggregates at the Batch Site. Provide the Engineer with reasonable facilities at the batch site for obtaining samples of the aggregates. Provide adequate and safe laboratory facilities at the batch site allowing the Engineer to test the aggregates for compliance with the specified requirements.

KDOT will sample and test aggregates from each source to determine their compliance with specifications. Do not batch the concrete mixture until the Engineer has determined that the aggregates comply with the specifications. KDOT will conduct sampling at the batching site, and test samples according to the Sampling and Testing Frequency Chart in Part V. For QC/QA Contracts, establish testing intervals within the specified minimum frequency.

After initial testing is complete and the Engineer has determined that the aggregate process control is satisfactory, use the aggregates concurrently with sampling and testing as long as tests indicate compliance with specifications. When batching, sample the aggregates as near the point of batching as feasible. Sample from the stream as the storage bins or weigh hoppers are loaded. If samples can not be taken from the stream, take them from approved stockpiles, or use a template and sample from the conveyor belt. If test results indicate an aggregate does not comply with specifications, cease concrete production using that aggregate. Unless a tested and approved stockpile for that aggregate is available at the batch plant, do not use any additional aggregate from that source and specified grading until subsequent sampling and testing of that aggregate indicate compliance with specifications. When tests are completed and the Engineer is satisfied that process control is again adequate, production of concrete using aggregates tested concurrently with production may resume.

c. Handling of Materials.

(1) Aggregate Stockpiles. Approved stockpiles are permitted only at the batch plant and only for small concrete placements or for the purpose of maintaining concrete production. Mark the approved stockpile with an "Approved Materials" sign. Provide a suitable stockpile area at the batch plant so that aggregates are stored without detrimental segregation or contamination. At the plant, limit stockpiles of tested and approved coarse aggregate and fine aggregate to 250 tons each, unless approved for more by the Engineer. If mixed aggregate is used, limit the approved stockpile to 500 tons, the size of each being proportional to the amount of each aggregate to be used in the mix.

Load aggregates into the mixer so no material foreign to the concrete or material capable of changing the desired proportions is included. When 2 or more sizes or types of coarse or fine aggregates are used on the same project, only 1 size or type of each aggregate may be used for any one continuous concrete placement.

(2) Segregation. Do not use segregated aggregates. Previously segregated materials may be thoroughly re-mixed and used when representative samples taken anywhere in the stockpile indicated a uniform gradation exists.

(3) Cement. Protect cement in storage or stockpiled on the site from any damage by climatic conditions which would change the characteristics or usability of the material.

(4) Moisture. Provide aggregate with a moisture content of ± 0.5% from the average of that day. If the moisture content in the aggregate varies by more than the above tolerance, take whatever corrective measures are

necessary to bring the moisture to a constant and uniform consistency before placing concrete. This may be accomplished by handling or manipulating the stockpiles to reduce the moisture content, or by adding moisture to the stockpiles in a manner producing uniform moisture content through all portions of the stockpile.

For plants equipped with an approved accurate moisture-determining device capable of determining the free moisture in the aggregates, and provisions made for batch to batch correction of the amount of water and the weight of aggregates added, the requirements relative to manipulating the stockpiles for moisture control will be waived. Any procedure used will not relieve the producer of the responsibility for delivery of concrete meeting the specified water-cement ratio and slump requirements.

Do not use aggregate in the form of frozen lumps in the manufacture of concrete.

(5) Separation of Materials in Tested and Approved Stockpiles. Only use KDOT Approved Materials. Provide separate means for storing materials approved by KDOT. If the producer elects to use KDOT Approved Materials for non-KDOT work, during the progress of a project requiring KDOT Approved Materials, inform the Engineer and agree to pay all costs for additional materials testing.

Clean all conveyors, bins and hoppers of unapproved materials before beginning the manufacture of concrete for KDOT work.

5.0 MIXING, DELIVERY, AND PLACEMENT LIMITATIONS

a. Concrete Batching, Mixing, and Delivery. Batch and mix the concrete in a central-mix plant, in a truck mixer, or in a drum mixer at the work site. Provide plant capacity and delivery capacity sufficient to maintain continuous delivery at the rate required. The delivery rate of concrete during concreting operations must provide for the proper handling, placing and finishing of the concrete.

Seek the Engineer's approval of the concrete plant/batch site before any concrete is produced for the project. The Engineer will inspect the equipment, the method of storing and handling of materials, the production procedures, and the transportation and rate of delivery of concrete from the plant to the point of use. The Engineer will grant approval of the concrete plant/batch site based on compliance with the specified requirements. The Engineer may, at any time, rescind permission to use concrete from a previously approved concrete plant/batch site upon failure to comply with the specified requirements.

Clean the mixing drum before it is charged with the concrete mixture. Charge the batch into the mixing drum so that a portion of the water is in the drum before the aggregates and cementitious. Uniformly flow materials into the drum throughout the batching operation. Add all mixing water in the drum by the end of the first 15 seconds of the mixing cycle. Keep the throat of the drum free of accumulations that restrict the flow of materials into the drum.

Do not exceed the rated capacity (cubic yards shown on the manufacturer's plate on the mixer) of the mixer when batching the concrete. The Engineer will allow an overload of up to 10% above the rated capacity for central-mix plants and drum mixers at the work site, provided the concrete test data for strength, segregation and uniform consistency are satisfactory, and no concrete is spilled during the mixing cycle.

Operate the mixing drum at the speed specified by the mixer's manufacturer (shown on the manufacturer's plate on the mixer).

Mixing time is measured from the time all materials, except water, are in the drum. If it is necessary to increase the mixing time to obtain the specified percent of air in air-entrained concrete, the Engineer will determine the mixing time.

If the concrete is mixed in a central-mix plant or a drum mixer at the work site, mix the batch between 1 to 5 minutes at mixing speed. Do not exceed the maximum total 60 mixing revolutions. Mixing time begins after all materials, except water, are in the drum, and ends when the discharge chute opens. Transfer time in multiple drum mixers is included in mixing time. Mix time may be reduced for plants utilizing high performance mixing drums provided thoroughly mixed and uniform concrete is being produced with the proposed mix time. Performance of the plant must comply with Table A1.1, of ASTM C 94, Standard Specification for Ready Mixed Concrete. Five of the six tests listed in Table A1.1 must be within the limits of the specification to indicate that uniform concrete is being produced.

If the concrete is mixed in a truck mixer, mix the batch between 70 and 100 revolutions of the drum or blades at mixing speed. After the mixing is completed, set the truck mixer drum at agitating speed. Unless the mixing unit is equipped with an accurate device indicating and controlling the number of revolutions at mixing

speed, perform the mixing at the batch plant and operate the mixing unit at agitating speed while traveling from the plant to the work site. Do not exceed 350 total revolutions (mixing and agitating).

If a truck mixer or truck agitator is used to transport concrete that was completely mixed in a stationary central mixer, agitate the concrete while transporting at the agitating speed specified by the manufacturer of the equipment (shown on the manufacturer's plate on the equipment). Do not exceed 250 total revolutions (additional re-mixing and agitating).

Provide a batch slip including batch weights of every constituent of the concrete and time for each batch of concrete delivered at the work site, issued at the batching plant that bears the time of charging of the mixer drum with cementitious and aggregates. Include quantities, type, product name and manufacturer of all admixtures on the batch ticket.

If non-agitating equipment is used for transportation of concrete, provide approved covers for protection against the weather when required by the Engineer.

Place non-agitated concrete within 30 minutes of adding the cement to the water.

Do not use concrete that has developed its initial set. Regardless of the speed of delivery and placement, the Engineer will suspend the concreting operations until corrective measures are taken if there is evidence that the concrete can not be adequately consolidated.

Adding water to concrete after the initial mixing is prohibited. Add all water at the plant. If needed, adjust slump through the addition of a water reducer according to **subsection 3.0e.(2)**.

b. Placement Limitations.

(1) Concrete Temperature. Unless otherwise authorized by the Engineer, the temperature of the mixed concrete immediately before placement is a minimum of 55°F, and a maximum of 70°F. With approval by the Engineer, the temperature of the concrete may be adjusted 5°F above or below this range.

(2) Qualification Batch. For Grade 3.5 (AE) (LC-HPC) concrete, qualify a field batch (one truckload or at least 6 cubic yards) at least 35 days prior to commencement of placement of the bridge decks. Produce the qualification batch from the same plant that will supply the job concrete. Simulate haul time to the jobsite prior to discharge of the concrete for testing. Prior to placing concrete in the qualification slab and on the job, submit documentation to the Engineer verifying that the qualification batch concrete meets the requirements for air content, slump, temperature of plastic concrete, compressive strength, unit weight and other testing as required by the Engineer.

Before the concrete mixture with plasticizing admixture is used on the project, determine the air content of the qualification batch. Monitor the slump, air content, temperature and workability at initial batching and estimated time of concrete placement. If these properties are not adequate, repeat the qualification batch until it can be demonstrated that the mix is within acceptable limits as specified in this specification.

(3) Placing Concrete at Night. Do not mix, place or finish concrete without sufficient natural light, unless an adequate and artificial lighting system approved by the Engineer is provided.

(4) Placing Concrete in Cold Weather. Unless authorized otherwise by the Engineer, mixing and concreting operations shall not proceed once the descending ambient air temperature reaches 40°F, and may not be initiated until an ascending ambient air temperature reaches 40°F. The ascending ambient air temperature for initiating concreting operations shall increase to 45°F if the maximum ambient air temperature is expected to be between 55°F and 60°F during or within 24 hours of placement and to 50°F if the ambient air temperature is expected to equal or exceed 60°F during or within 24 hours of placement.

If the Engineer permits placing concrete during cold weather, aggregates may be heated by either steam or dry heat before placing them in the mixer. Use an apparatus that heats the weight uniformly and is so arranged as to preclude the possible occurrence of overheated areas which might injure the materials. Do not heat aggregates directly by gas or oil flame or on sheet metal over fire. Aggregates that are heated in bins, by steam-coil or water-coil heating, or by other methods not detrimental to the aggregates may be used. The use of live steam on or through binned aggregates is prohibited. Unless otherwise authorized, maintain the temperature of the mixed concrete between 55°F to 70°F at the time of placing it in the forms. With approval by the Engineer, the temperature of the concrete may be adjusted up to 5°F above or below this range. Do not place concrete when there is a probability of air temperatures being more than 25°F below the temperature of the concrete

during the first 24 hours after placement unless insulation is provided for both the deck and the girders. Do not, under any circumstances, continue concrete operations if the ambient air temperature is less than 20°F.

If the ambient air temperature is 40°F or less at the time the concrete is placed, the Engineer may permit the water and the aggregates be heated to at least 70°F, but not more than 120°F.

Do not place concrete on frozen subgrade or use frozen aggregates in the concrete.

(5) Placing Concrete in Hot Weather. When the ambient temperature is above 90°F, cool the forms, reinforcing steel, steel beam flanges, and other surfaces which will come in contact with the mix to below 90°F by means of a water spray or other approved methods. For Grade 3.5 (AE) (LC-HPC) concrete, cool the concrete mixture to maintain the temperature immediately before placement between 55°F and 70°F. With approval by the Engineer, the temperature of the concrete may be up to 5°F below or above this range.

Maintain the temperature of the concrete at time of placement within the specified temperature range by any combination of the following:

- Shading the materials storage areas or the production equipment.
- Cooling the aggregates by sprinkling with potable water.
- Cooling the aggregates or water by refrigeration or replacing a portion or all of the mix water with ice that is flaked or crushed to the extent that the ice will completely melt during mixing of the concrete.
- Liquid nitrogen injection.

6.0 INSPECTION AND TESTING

The Engineer will test the first truckload of concrete by obtaining a sample of fresh concrete at truck discharge and by obtaining a sample of fresh concrete at the discharge end of the conveyor, bucket or if pumped, the piping. The Engineer will obtain subsequent sample concrete for tests at the discharge end of the conveyor, bucket or if pumped, the discharge end of the piping. If potential problems are apparent at the discharge of any truck, the Engineer will test the concrete at truck discharge prior to deposit on the bridge deck. If a truckload is redosed with an admixture on-site or set aside to allow for concrete properties to meet the required specifications, the truckload shall be retested prior to deposit on the bridge deck. All retesting shall be performed by the Contractor or Concrete Supplier under the supervision of the Engineer.

The Engineer will cast, store, and test strength test specimens in sets of 5. See **TABLE 1-3**.

KDOT will conduct the sampling and test the samples according to **SECTION 2500** and **TABLE 1-3**. The Contractor may be directed by the Engineer to assist KDOT in obtaining the fresh concrete samples during the placement operation.

A plan will be finalized prior to the construction date as to how out-of-specification concrete will be handled.

TABLE 1-3: SAMPLING AND TESTING FREQUENCY CHART

Tests Required (Record to)	Test Method	CMS	Verification Samples and Tests	Acceptance Samples and Tests
Slump (0.25 inch)	KT-21	a	Each of first 3 truckloads for any individual placement, then 1 of every 3 truckloads	
Temperature (1°F)	KT-17	a	Every truckload, measured at the truck discharge, and from each sample made for slump determination.	
Mass (0.1 lb)	KT-20	a	One of every 6 truckloads	
Air Content (0.25%)	KT-18 or KT-19	a	Each of first 3 truckloads for any individual placement, then 1 of every 6 truckloads	

TABLE 1-3: SAMPLING AND TESTING FREQUENCY CHART				
Tests Required (Record to)	**Test Method**	**CMS**	**Verification Samples and Tests**	**Acceptance Samples and Tests**
Cylinders (1 lbf; 0.1 in; 1 psi)	KT-22 and AASHTO T 22	VER	Make at least 2 groups of 5 cylinders per pour or major mix design change with concrete sampled from at least 2 different truckloads evenly spaced throughout the pour, with a minimum of 1 set for every 100 cu yd. Include in each group 3 test cylinders to be cured according to KT-22 and 2 test cylinders to be field-cured. Store the field-cured cylinders on or adjacent to the bridge. Protect all surfaces of the cylinders from the elements in as near as possible the same way as the deck concrete. Test the field-cured cylinders at the same age as the standard-cured cylinders.	
Density of Fresh Concrete (0.1 lb/cu ft or 0.1% of optimum density)	KT-36	ACI		b,c: 1 per 100 cu yd for thin overlays and bridge deck surfacing.

Note a: "Type Insp" must = "ACC" when the assignment of a pay quantity is being made. "ACI" when recording test values for additional acceptance information.
Note b: Normal operation. Minimum frequency for exceptional conditions may be reduced by the DME on a project basis, written justification shall be made to the Chief of the Bureau of Materials and Research and placed in the project documents. (Multi-Level Frequency Chart (see page 17, Appendix A of Construction Manual, Part V).
Note c: Applicable only when specifications contain those requirements.

The Engineer will reject concrete that does not comply with specified requirements. If a truckload is found not to comply with the specified requirements, successive truckloads must be tested until the requirements are met.

The Engineer will permit occasional deviations below the specified cementitious content, if it is due to the air content of the concrete exceeding the designated air content, but only up to the maximum tolerance in the air content. Continuous operation below the specified cement content for any reason is prohibited.

As the work progresses, the Engineer reserves the right to require the Contractor to change the proportions if conditions warrant such changes to produce a satisfactory mix. Any such changes may be made within the limits of the Specifications at no additional compensation to the Contractor.

01-27-14 BP DD

KANSAS DEPARTMENT OF TRANSPORTATION
SPECIAL PROVISION TO THE
STANDARD SPECIFICATIONS, 2007 EDITION

Add a new SECTION to DIVISION 700:

LOW-CRACKING HIGH-PERFORMANCE CONCRETE – CONSTRUCTION

1.0 DESCRIPTION

Construct the low-cracking high-performance concrete (LC-HPC) structures according to the Contract Documents and this specification.

BID ITEMS	**UNITS**
Qualification Slab	Cubic Yard
Concrete (*) (AE) (LC-HPC)	Cubic Yard
*Grade of Concrete	

2.0 MATERIALS

Provide materials that comply with the applicable requirements.

LC-HPC .....**07-PS0166, latest version**
Concrete Curing Materials .....**DIVISION 1400**

3.0 CONSTRUCTION REQUIREMENTS

a. Qualification Batch and Slab. For each LC-HPC bridge deck, produce a qualification batch of LC-HPC that is to be placed in the deck and complies with **07-PS0166, latest version**, and construct a qualification slab that complies with this specification to demonstrate the ability to handle, place, finish and cure the LC-HPC bridge deck.

After the qualification batch of LC-HPC complies with **07-PS0166, latest version**, construct a qualification slab 15 to 45 days prior to placing LC-HPC in the bridge deck. Construct the qualification slab to comply with the Contract Documents, using the same LC-HPC that is to be placed in the deck and that was approved in the qualification batch. Submit the location of the qualification slab for approval by the Engineer. Place, finish and cure the qualification slab according to the Contract Documents, using the same personnel, methods and equipment (including the concrete pump, if used) that will be used on the bridge deck.

A minimum of 1 day after construction of the qualification slab, core 4 full-depth 4 inch diameter cores, one from each quadrant of the qualification slab, and forward them to the Engineer for visual inspection of degree of consolidation.

Do not commence placement of LC-HPC in the deck until approval is given by the Engineer. Approval to place concrete on the deck will be based on satisfactory placement, consolidation, finishing and curing of the qualification slab and cores, and will be given or denied within 24 hours of receiving the cores from the Contractor. If an additional qualification slab is deemed necessary by the Engineer, it will be paid for at the contract unit price for Qualification Slab.

b. Falsework and Forms. Construct falsework and forms according to **SECTION 708**.

c. Handling and Placing LC-HPC.

(1) Quality Control Plan (QCP). At a project progress meeting prior to placing LC-HPC, discuss with the Engineer the method and equipment used for deck placement. Submit an acceptable QCP according to the Contractor's Concrete Structures Quality Control Plan, Part V. Detail the equipment (for both determining and controlling the evaporation rate and LC-HPC temperature), procedures used to minimize the evaporation rate, plans

for maintaining a continuous rate of finishing the deck without delaying the application of curing materials within the time specified in **subsection 3.0f.**, including maintaining a continuous supply of LC-HPC throughout the placement with an adequate quantity of LC-HPC to complete the deck and filling diaphragms and end walls in advance of deck placement, and plans for placing the curing materials within the time specified in **subsection 3.0f**. In the plan, also include input from the LC-HPC supplier as to how variations in the moisture content of the aggregate will be handled, should they occur during construction.

(2) Use a method and sequence of placing LC-HPC approved by the Engineer. Do not place LC-HPC until the forms and reinforcing steel have been checked and approved. Before placing LC-HPC, clean all forms of debris.

(3) Finishing Machine Setup. On bridges skewed greater than 10º, place LC-HPC on the deck forms across the deck on the same skew as the bridge, unless approved otherwise by State Bridge Office (SBO). Operate the bridge deck finishing machine on the same skew as the bridge, unless approved otherwise by the SBO. Before placing LP-HPC, position the finish machine throughout the proposed placement area to allow the Engineer to verify the reinforcing steel positioning.

(4) Environmental Conditions. Maintain environmental conditions on the entire bridge deck so the evaporation rate is less than 0.2 lb/sq ft/hr. The temperature of the mixed LC-HPC immediately before placement must be a minimum of 55°F and a maximum of 70°F. With approval by the Engineer, the temperature of the LC-HPC may be adjusted 5°F above or below this range. This may require placing the deck at night, in the early morning or on another day. The evaporation rate (as determined in the American Concrete Institute Manual of Concrete Practice 305R, Chapter 2) is a function of air temperature, LC-HPC temperature, wind speed and relative humidity. The effects of any fogging required by the Engineer will not be considered in the estimation of the evaporation rate (**subsection 3.0c.(5)**).

Just prior to and at least once per hour during placement of the LC-HPC, the Engineer will measure and record the air temperature, LC-HPC temperature, wind speed, and relative humidity on the bridge deck. The Engineer will take the air temperature, wind, and relative humidity measurements approximately 12 inches above the surface of the deck. With this information, the Engineer will determine the evaporation rate using KDOT software or **FIGURE 710-1**.

When the evaporation rate is equal to or above 0.2 lb/ft^2/hr, take actions (such as cooling the LC-HPC, installing wind breaks, sun screens etc.) to create and maintain an evaporation rate less than 0.2 lb/ft^2/hr on the entire bridge deck.

(5) Fogging of Deck Placements. Fogging using hand-held equipment may be required by the Engineer during unanticipated delays in the placing, finishing or curing operations. If fogging is required by the Engineer, do not allow water to drip, flow or puddle on the concrete surface during fogging, placement of absorptive material, or at any time before the concrete has achieved final set.

(6) Placement and Equipment. Place LC-HPC by conveyor belt or concrete bucket. Pumping of LC-HPC will be allowed if the Contractor can show proficiency when placing the approved mix during construction of the qualification slab using the same pump as will be used on the job. Placement by pump will also be allowed with prior approval of the Engineer contingent upon successful placement by pump of the approved mix, using the same pump as will be used for the deck placement, at least 15 days prior to placing LC-HPC in the bridge deck. To limit the loss of air, the maximum drop from the end of a conveyor belt or from a concrete bucket is 5 feet and pumps must be fitted with an air cuff/bladder valve. Do not use chutes, troughs or pipes made of aluminum.

Place LC-HPC to avoid segregation of the materials and displacement of the reinforcement. Do not deposit LC-HPC in large quantities at any point in the forms, and then run or work the LC-HPC along the forms.

Fill each part of the form by depositing the LC-HPC as near to the final position as possible.

The Engineer will obtain sample LC-HPC for tests and cylinders at the discharge end of the conveyor, bucket, or if pumped, the piping.

(7) Consolidation.

- Accomplish consolidation of the LC-HPC on all span bridges that require finishing machines by means of a mechanical device on which internal (spud or tube type) concrete vibrators of the same type and size are mounted (**subsection 154.2**).
- Observe special requirements for vibrators in contact with epoxy coated reinforcing steel as specified in **subsection 154.2**.
- Provide stand-by vibrators for emergency use to avoid delays in case of failure.

- Operate the mechanical device so vibrator insertions are made on a maximum spacing of 12 inch centers over the entire deck surface.
- Provide a uniform time per insertion of all vibrators of 3 to 15 seconds, unless otherwise designated by the Engineer.
- Provide positive control of vibrators using a timed light, buzzer, automatic control or other approved method.
- Extract the vibrators from the LC-HPC at a rate to avoid leaving any large voids or holes in the LC-HPC.
- Do not drag the vibrators horizontally through the LC-HPC.
- Use hand held vibrators (**subsection 154.2**) in inaccessible and confined areas such as along bridge rail or curb.
- When required, supplement vibrating by hand spading with suitable tools to provide required consolidation.
- Reconsolidate any voids left by workers.

Continuously place LC-HPC in any floor slab until complete, unless shown otherwise in the Contract Documents.

d. Construction Joints, Expansion Joints and End of Wearing Surface (EWS) Treatment. Locate the construction joints as shown in the Contract Documents. If construction joints are not shown in the Contract Documents, submit proposed locations for approval by the Engineer.

If the work of placing LC-HPC is delayed and the LC-HPC has taken its initial set, stop the placement, saw the nearest construction joint approved by the Engineer, and remove all LC-HPC beyond the construction joint.

Construct keyed joints by embedding water-soaked beveled timbers of a size shown on the Contract Documents, into the soft LC-HPC. Remove the timber when the LC-HPC has set. When resuming work, thoroughly clean the surface of the LC-HPC previously placed, and when required by the Engineer, roughen the key with a steel tool. Before placing LC-HPC against the keyed construction joint, thoroughly wash the surface of the keyed joint with clean water.

e. Finishing. Strike off bridge decks with a vibrating screed or single-drum roller screed, either self-propelled or manually operated by winches and approved by the Engineer. Use a self-oscillating screed on the finish machine, and operate or finish from a position either on the skew or transverse to the bridge roadway centerline. See **subsection 3.0c.(3)**. Do not mount tamping devices or fixtures to drum roller screeds; augers are allowed.

Irregular sections may be finished by other methods approved by the Engineer and detailed in the required QCP. See **subsection 3.0c.(1)**.

Finish the surface by a burlap drag, metal pan or both, mounted to the finishing equipment. Use a float or other approved device behind the burlap drag or metal pan, as necessary, to remove any local irregularities. Do not add water to the surface of LC-HPC. Do not use a finishing aid.

Tining of plastic LC-HPC is prohibited. All LC-HPC surfaces must be reasonably true and even, free from stone pockets, excessive depressions or projections beyond the surface.

Finish all top surfaces, such as the top of retaining walls, curbs, abutments and rails, with a wooden float by tamping and floating, flushing the mortar to the surface and provide a uniform surface, free from pits or porous places. Trowel the surface producing a smooth surface, and brush lightly with a damp brush to remove the glazed surface.

f. Curing and Protection.

(1) General. Cure all newly placed LC-HPC immediately after finishing, and continue uninterrupted for a minimum of 14 days. Cure all pedestrian walkway surfaces in the same manner as the bridge deck. Curing compounds are prohibited during the 14 day curing period.

(2) Cover With Wet Burlap. Soak the burlap a minimum of 12 hours prior to placement on the deck. Rewet the burlap if it has dried more than one hour before it is applied to the surface of bridge deck. Apply 1

layer of wet burlap within 10 minutes of LC-HPC strike-off from the screed, followed by a second layer of wet burlap within 5 minutes. Do not allow the surface to dry after the strike-off, or at any time during the cure period. In the required QCP, address the rate of LC-HPC placement and finishing methods that will affect the period between strike-off and burlap placement. See **subsection 3.0c.(1)**. During times of delay expected to exceed 10 minutes, cover all concrete that has been placed, but not finished, with wet burlap.

Maintain the wet burlap in a fully wet condition using misting hoses, self-propelled, machine-mounted fogging equipment with effective fogging area spanning the deck width moving continuously across the entire burlap-covered surface, or other approved devices until the LC-HPC has set sufficiently to allow foot traffic. At that time, place soaker hoses on the burlap, and supply running water continuously to maintain continuous saturation of all burlap material to the entire LC-HPC surface. For bridge decks with superelevation, place a minimum of 1 soaker hose along the high edge of the deck to keep the entire deck wet during the curing period.

(3) Waterproof Cover. Place white polyethylene film on top of the soaker hoses, covering the entire LC-HPC surface after soaker hoses have been placed, a maximum of 12 hours after the placement of the LC-HPC. Use as wide of sheets as practicable, and overlap 2 feet on all edges to form a complete waterproof cover of the entire LC-HPC surface. Secure the polyethylene film so that wind will not displace it. Should any portion of the sheets be broken or damaged before expiration of the curing period, immediately repair the broken or damaged portions. Replace sections that have lost their waterproof qualities.

If burlap and/or polyethylene film is temporarily removed for any reason during the curing period, use soaker hoses to keep the entire exposed area continuously wet. Replace saturated burlap and polyethylene film, resuming the specified curing conditions, as soon as possible.

Inspect the LC-HPC surface once every 6 hours for the entirety of the 14 day curing period, so that all areas remain wet for the entire curing period and all curing requirements are satisfied.

(4) Documentation. Provide the Engineer with a daily inspection set that includes:

- documentation that identifies any deficiencies found (including location of deficiency);
- documentation of corrective measures taken;
- a statement of certification that the entire bridge deck is wet and all curing material is in place;
- documentation showing the time and date of all inspections and the inspector's signature.
- documentation of any temporary removal of curing materials including location, date and time, length of time curing was removed, and means taken to keep the exposed area continuously wet.

(5) Cold Weather Curing. When LC-HPC is being placed in cold weather, also adhere to **07-PS0166, latest version**.

When LC-HPC is being placed and the ambient air temperature may be expected to drop below 40ºF during the curing period or when the ambient air temperature is expected to drop more than 25°F below the temperature of the LC-HPC during the first 24 hours after placement, provide suitable measures such as straw, additional burlap, or other suitable blanketing materials, and/or housing and artificial heat to maintain the LC-HPC and girder temperatures between 40ºF and 75ºF as measured on the upper and lower surfaces of the LC-HPC. Enclose the area underneath the deck and heat so that the temperature of the surrounding air is as close as possible to the temperature of LC-HPC and between 40ºF and 75ºF. When artificial heating is used to maintain the LC-HPC and girder temperatures, provide adequate ventilation to limit exposure to carbon dioxide if necessary. Maintain wet burlap and polyethylene cover during the entire 14 day curing period. Heating may be stopped after the first 72 hours if the time of curing is lengthened to account for periods when the ambient air temperature is below 40ºF. For every day the ambient air temperature is below 40ºF, an additional day of curing with a minimum ambient air temperature of 50ºF will be required. After completion of the required curing period, remove the curing and protection so that the temperature of the LC-HPC during the first 24 hours does not fall more than 25°F.

(6) Curing Membrane. At the end of the 14-day curing period remove the wet burlap and polyethylene and within 30 minutes, apply 2 coats of an opaque curing membrane to the LC-HPC. Apply the curing membrane when no free water remains on the surface but while the surface is still wet. Apply each coat of curing membrane according to the manufacturer's instructions with a minimum spreading rate per coat of 1 gallon per 80 square yards of LC-HPC surface. If the LC-HPC is dry or becomes dry, thoroughly wet it with water applied as a fog spray by means of approved equipment. Spray the second coat immediately after and at right angles to the first application.

Protect the curing membrane against marring for a minimum of 7 days. Give any marred or disturbed membrane an additional coating. Should the curing membrane be subjected to continuous injury, the Engineer may limit work on the deck until the 7-day period is complete. Because the purpose of the curing membrane is to allow for slow drying of the bridge deck, extension of the initial curing period beyond 14 days, while permitted, shall not be used to reduce the 7-day period during which the curing membrane is applied and protected.

(7) Construction Loads. Adhere to **TABLE 710-2**.

If the Contractor needs to drive on the bridge before the approach slabs can be placed and cured, construct a temporary bridge from the approach over the EWS capable of supporting the anticipated loads. Do not bend the reinforcing steel which will tie the approach slab to the EWS or damage the LC-HPC at the EWS. The method of bridging must be approved by the Engineer.

TABLE 710-2: CONCRETE LOAD LIMITATIONS ON BRIDGE DECKS

Days after concrete is placed	Element	Allowable Loads
1*	Subdeck, one-course deck or concrete overlay	Foot traffic only.
3*	One-course deck or concrete overlay	Work to place reinforcing steel or forms for the bridge rail or barrier.
7*	Concrete overlays	Legal Loads; Heavy stationary loads with the Engineer's approval.***
10 (15)**	Subdeck, one-course deck or post-tensioned haunched slab bridges**	Light truck traffic (gross vehicle weight less than 5 tons).****
14 (21)**	Subdeck, one-course deck or post-tensioned haunched slab bridges**	Legal Loads; Heavy stationary loads with the Engineer's approval.***Overlays on new decks.
28	Bridge decks	Overloads, only with the State Bridge Engineer's approval.***

*Maintain a 7 day wet cure at all times (14-day wet cure for decks with LC-HPC).

** Conventional haunched slabs.

*** Submit the load information to the appropriate Engineer. Required information: the weight of the material and the footprint of the load, or the axle (or truck) spacing and the width, the size of each tire (or track length and width) and their weight.

****An overlay may be placed using pumps or conveyors until legal loads are allowed on the bridge.

g. Grinding and Grooving. Correct surface variations exceeding 1/8 inch in 10 feet by use of an approved profiling device, or other methods approved by the Engineer after the curing period. Perform grinding on hardened LC-HPC after the 7 day curing membrane period to achieve a plane surface and grooving of the final wearing surface as shown in the Contract Documents.

Use a self-propelled grinding machine with diamond blades mounted on a multi-blade arbor. Avoid using equipment that causes excessive ravels, aggregate fractures or spalls. Use vacuum equipment or other continuous methods to remove grinding slurry and residue.

After any required grinding is complete, give the surface a suitable texture by transverse grooving. Use diamond blades mounted on a self-propelled machine that is designed for texturing pavement. Transverse grooving of the finished surface may be done with equipment that is not self-propelled providing that the Contractor can show proficiency with the equipment. Use equipment that does not cause strain, excessive raveling, aggregate fracture, spalls, disturbance of the transverse or longitudinal joint, or damage to the existing LC-HPC surface. Make the grooving approximately 3/16 inch in width at 3/4 inch centers and the groove depth approximately 1/8 inch. For bridges with drains, terminate the transverse grooving approximately 2 feet in from the gutter line at the base of the curb. Continuously remove all slurry residues resulting from the texturing operation.

h. Post Construction Conference. At the completion of the deck placement, curing, grinding and grooving for a bridge using LC-HPC, a post-construction conference will be held with all parties that participated in the planning and construction present. The Engineer will record the discussion of all problems and successes for the project.

i. Removal of Forms and Falsework. Do not remove forms and falsework without the Engineer's approval. Remove deck forms approximately 2 weeks (a maximum of 4 weeks) after the end of the curing period (removal of burlap), unless approved by the Engineer. The purpose of 4 week maximum is to limit the moisture gradient between the bottom and the top of the deck.

For additional requirements regarding forms and falsework, see **SECTION 708**.

4.0 MEASUREMENT AND PAYMENT

The Engineer will measure the qualification slab and the various grades of (AE) (LC-HPC) concrete placed in the structure by the cubic yard. No deductions are made for reinforcing steel and pile heads extending into the LP-HPC. The Engineer will not separately measure reinforcing steel in the qualification slab.

Payment for the "Qualification Slab" and the various grades of "(AE) (LC-HPC) Concrete" at the contract unit prices is full compensation for the specified work.

FIGURE 710-1: STANDARD PRACTICE FOR CURING CONCRETE

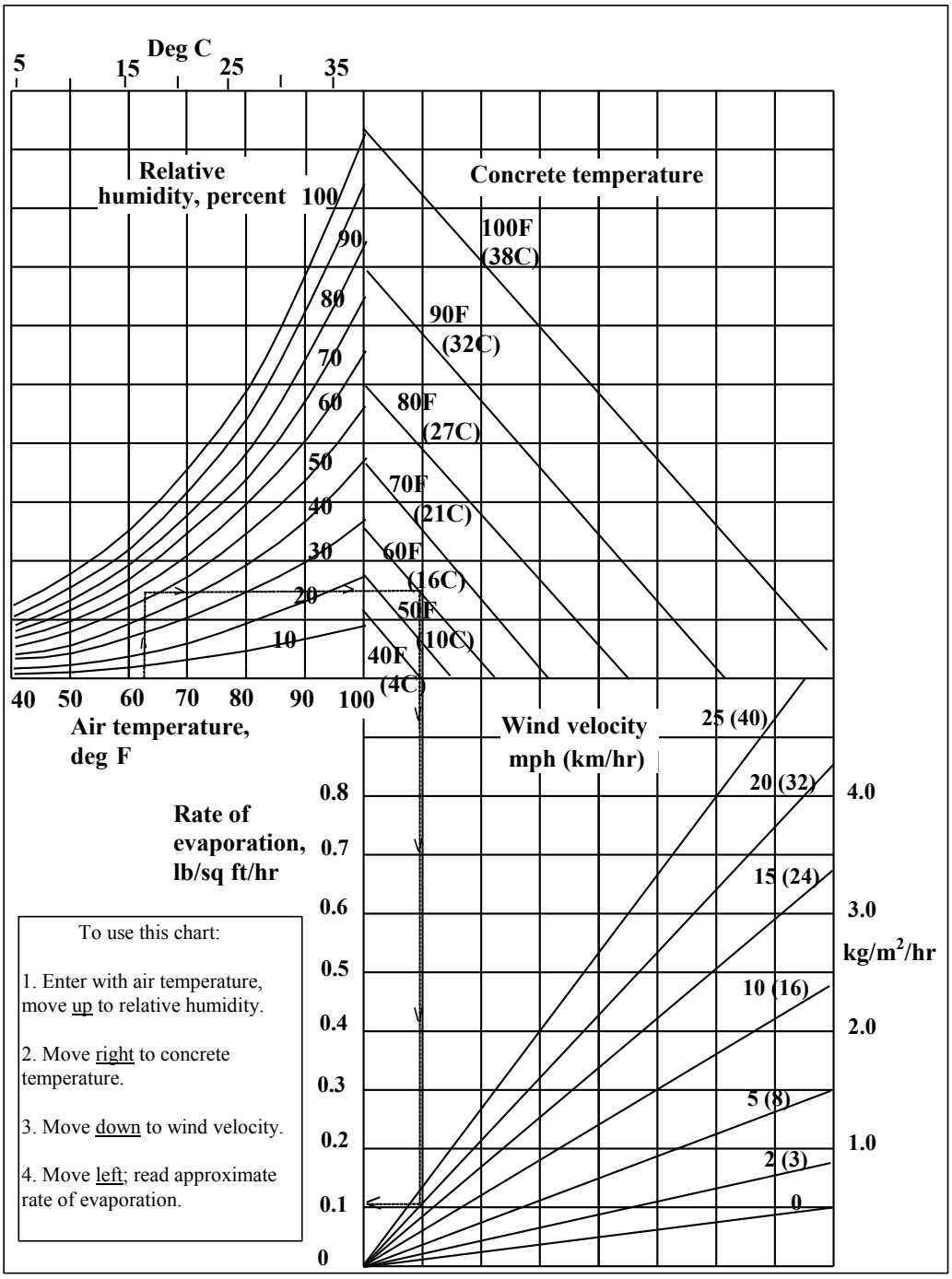

Effect of concrete and air temperatures, relative humidity, and wind velocity on the rate of evaporation of surface moisture from concrete. This chart provides a graphic method of estimating the loss of surface moisture for various weather conditions. To use the chart, follow the four steps outlined above. When the evaporation rate exceeds 0.2 lb/ft^2/hr (1.0 kg/ m^2/hr), measures shall be taken to prevent excessive moisture loss from the surface of unhardened concrete; when the rate is less than 0.2 lb/ft^2/hr (1.0 kg/m^2/hr) such measures may be needed. When excessive moisture loss is not prevented, plastic cracking is likely to occur.